

Lecture Notes in Civil Engineering

Han Ay Lie · Monty Sutrisna ·
Joewono Prasetijo ·
Bonaventura H.W. Hadikusumo ·
Leksmono Suryo Putranto *Editors*

Proceedings of the Second International Conference of Construction, Infrastructure, and Materials

ICCIM 2021, 26 July 2021, Jakarta,
Indonesia

 Springer

Lecture Notes in Civil Engineering

Volume 216

Series Editors

Marco di Prisco, Politecnico di Milano, Milano, Italy

Sheng-Hong Chen, School of Water Resources and Hydropower Engineering,
Wuhan University, Wuhan, China

Ioannis Vayas, Institute of Steel Structures, National Technical University of
Athens, Athens, Greece

Sanjay Kumar Shukla, School of Engineering, Edith Cowan University, Joondalup,
WA, Australia

Anuj Sharma, Iowa State University, Ames, IA, USA

Nagesh Kumar, Department of Civil Engineering, Indian Institute of Science
Bangalore, Bengaluru, Karnataka, India

Chien Ming Wang, School of Civil Engineering, The University of Queensland,
Brisbane, QLD, Australia

Lecture Notes in Civil Engineering (LNCE) publishes the latest developments in Civil Engineering—quickly, informally and in top quality. Though original research reported in proceedings and post-proceedings represents the core of LNCE, edited volumes of exceptionally high quality and interest may also be considered for publication. Volumes published in LNCE embrace all aspects and subfields of, as well as new challenges in, Civil Engineering. Topics in the series include:

- Construction and Structural Mechanics
- Building Materials
- Concrete, Steel and Timber Structures
- Geotechnical Engineering
- Earthquake Engineering
- Coastal Engineering
- Ocean and Offshore Engineering; Ships and Floating Structures
- Hydraulics, Hydrology and Water Resources Engineering
- Environmental Engineering and Sustainability
- Structural Health and Monitoring
- Surveying and Geographical Information Systems
- Indoor Environments
- Transportation and Traffic
- Risk Analysis
- Safety and Security

To submit a proposal or request further information, please contact the appropriate Springer Editor:

- Pierpaolo Riva at pierpaolo.riva@springer.com (Europe and Americas);
- Swati Meherishi at swati.meherishi@springer.com (Asia - except China, and Australia, New Zealand);
- Wayne Hu at wayne.hu@springer.com (China).

All books in the series now indexed by Scopus and EI Compindex database!

More information about this series at <https://link.springer.com/bookseries/15087>

Han Ay Lie · Monty Sutrisna ·
Joewono Prasetijo ·
Bonaventura H.W. Hadikusumo ·
Leksmono Suryo Putranto
Editors


Proceedings of the Second International Conference of Construction, Infrastructure, and Materials

ICCIM 2021, 26 July 2021, Jakarta, Indonesia


Editors

Han Ay Lie 
Department of Civil Engineering
Diponegoro University
Semarang, Indonesia

Monty Sutrisna 
School of Built Environment
Massey University
Auckland, New Zealand

Joewono Prasetyo 
Department of Transportation Engineering
Technology
Universiti Tun Hussein Onn Malaysia
Panchor, Malaysia

Bonaventura H.W. Hadikusumo
Department of Construction, Engineering
and Infrastructure Management
Asian Institute of Technology
Klong Luang, Thailand

Leksmono Suryo Putranto 
Civil Engineering Department
Universitas Tarumanagara
Jakarta Barat, Indonesia

ISSN 2366-2557

ISSN 2366-2565 (electronic)

Lecture Notes in Civil Engineering

ISBN 978-981-16-7948-3

ISBN 978-981-16-7949-0 (eBook)

<https://doi.org/10.1007/978-981-16-7949-0>

© The Editor(s) (if applicable) and The Author(s), under exclusive license to Springer Nature Singapore Pte Ltd. 2022

This work is subject to copyright. All rights are solely and exclusively licensed by the Publisher, whether the whole or part of the material is concerned, specifically the rights of translation, reprinting, reuse of illustrations, recitation, broadcasting, reproduction on microfilms or in any other physical way, and transmission or information storage and retrieval, electronic adaptation, computer software, or by similar or dissimilar methodology now known or hereafter developed.

The use of general descriptive names, registered names, trademarks, service marks, etc. in this publication does not imply, even in the absence of a specific statement, that such names are exempt from the relevant protective laws and regulations and therefore free for general use.

The publisher, the authors and the editors are safe to assume that the advice and information in this book are believed to be true and accurate at the date of publication. Neither the publisher nor the authors or the editors give a warranty, expressed or implied, with respect to the material contained herein or for any errors or omissions that may have been made. The publisher remains neutral with regard to jurisdictional claims in published maps and institutional affiliations.

This Springer imprint is published by the registered company Springer Nature Singapore Pte Ltd. The registered company address is: 152 Beach Road, #21-01/04 Gateway East, Singapore 189721, Singapore

Organization

Steering Committee

Prof. Han Ay Lie, Diponegoro University, Indonesia

Prof. Buntara Sthenly Gan, Nihon University, Japan

Dr. Najid, Universitas Tarumanagara, Indonesia

Dr. Widodo Kushartomo, Universitas Tarumanagara, Indonesia

International Scientific Committee

Prof. Leksmono Suryo Putranto, Universitas Tarumanagara, Indonesia

Prof. Buntara Sthenly Gan, Nihon University, Japan

Dr. Dimas Bayu Endrayana Dharmowijoyo, Universiti Teknologi Petronas, Malaysia

Dr. Bashar S. Mohammed, Universiti Teknologi Petronas, Malaysia

Dr. Andri Setiawan, Ecole Polytechnique Federale de Lausanne, Switzerland

Dr. Fadhilah Muslim, Universitas Indonesia, Indonesia; Technical University of Munich, Germany

Prof. Han Ay Lie, Universitas Diponegoro, Indonesia

Prof. Chaidir Anwar Makarim, Universitas Tarumanagara, Indonesia

Prof. Dewa Made Priyantha Wedagama, Universitas Udayana, Indonesia

Prof. Sofyan M. Saleh, Universitas Syiah Kuala, Indonesia

Prof. Eng. Joni Arliansyah, Universitas Sriwijaya, Indonesia

Prof. Sakti Adji Adisasmita, Universitas Hassanuddin, Indonesia

Prof. Siti Malkhamah, Universitas Gadjah Mada, Indonesia

Prof. Krishna Mochtar, Institut Teknologi Indonesia, Indonesia

Prof. Ade Sjafruddin, Institut Teknologi Bandung, Indonesia
Prof. Ludfi Djakfar, Universitas Brawijaya, Indonesia
Prof. Wimpy Santosa, Universitas Parahyangan, Indonesia
Prof. Antonius, Universitas Islam Sultan Agung, Indonesia
Prof. Erika Buchari, Universitas Sriwijaya, Indonesia
Prof. Ria Asih Aryani Soemitro, Institut Teknologi Sepuluh November, Indonesia
Prof. I Nyoman Arya Thanaya, Universitas Udayana, Indonesia
Dr. Hermawan, Universitas Katolik Soegijapranata, Indonesia
Dr. Maria Wahyuni, Universitas Katolik Soegijapranata, Indonesia
Dr. Djoko Suwarno, Universitas Katolik Soegijapranata, Indonesia
Dr. Bayu Martanto Adji, Universitas Andalas, Indonesia
Dr. Aine Kusumawati, Institut Teknologi Bandung, Indonesia
Dr. Bagus Hario Setiadji, Universitas Diponegoro, Indonesia
Dr. Basuki Anondho, Universitas Tarumanagara, Indonesia
Dr. Widodo Kushartomo, Universitas Tarumanagara, Indonesia
Dr. Najid, Universitas Tarumangara, Indonesia
Dr. Dewanti Marsoyo, Universitas Gadjah Mada, Indonesia
Dr. Wati A. Pranoto, Universitas Tarumanagara, Indonesia
Dr. Noor Mahmudah, Universitas Muhammadiyah Yogyakarta, Indonesia
Dr. Eng. Muhammad Isran Ramli, Universitas Hassanuddin, Indonesia
Dr. Eng. Imam Muthohar, Universitas Gadjah Mada, Indonesia
Dr. Achmad Wicaksono, Universitas Brawijaya, Indonesia
Dr. Caroline A. Sutandi, Universitas Parahyangan, Indonesia
Dr. Hera Widyastuti, Institut Teknologi Sepuluh November, Indonesia
Dr. R. Sony Sulaksono Wibowo, Institut Teknologi Bandung, Indonesia
Dr. Resdiansyah, Universitas Pembangunan Jaya, Indonesia
Dr. Yosritzal, Universitas Andalas, Indonesia
Dr. M. Asad Abdurrahman, Universitas Hassanuddin, Indonesia
Dr. Eng. M. Zudhy Irawan, Universitas Gadjah Mada, Indonesia
Dr. Ir. Hitapriya Suprayitno, M.Eng., Institut Teknologi Sepuluh November, Indonesia
Dr. Ani Hairani, Universitas Muhammadiyah Yogyakarta, Indonesia
Dr. Hendy Setiawan, Universitas Gadjah Mada, Indonesia
Dr. Alfred Jonathan Susilo, Universitas Tarumanagara, Indonesia
Dr. Aksan Kawanda, Universitas Trisakti, Indonesia
Dr. Nurul Fajar Januriyadi, Universitas Pertamina, Indonesia
Dr. Neil Andika, Universitas Gadjah Mada, Indonesia
Dr. Faizal Immaddudin Wira Rohmat, Institut Teknologi Bandung, Indonesia
Dr. Usman Wijaya, Universitas Kristen Krida Wacana, Indonesia
Dr. Leni Sagita Riantini, Universitas Indonesia, Indonesia
Dr. Hendrik Sulistio, Universitas Tarumanagara, Indonesia
Dr. Jane Sekarsari, Universitas Trisakti, Indonesia

Local Organizing Committee

Chairman

Prof. Chaidir Anwar Makarim, Universitas Tarumanagara, Indonesia

Vice Chairwoman

Anissa Noor Tajudin, Universitas Tarumanagara, Indonesia

Members

Prof. Leksmono Suryo Putranto, Universitas Tarumanagara, Indonesia

Yenny Untari, Universitas Tarumanagara, Indonesia

Dewi Linggasari, Universitas Tarumanagara, Indonesia

Vittorio Kurniawan, Universitas Tarumanagara, Indonesia

Aniek Prihatiningsih, Universitas Tarumanagara, Indonesia

Arif Sandjaya, Universitas Tarumanagara, Indonesia

Abdul Roji, Universitas Tarumanagara, Indonesia

Slamet Riyadi, Universitas Tarumanagara, Indonesia

Daniel Christianto, Universitas Tarumanagara, Indonesia

Arianti Sutandi, Universitas Tarumanagara, Indonesia

Ni Luh Putu Shinta Eka Setyarini, Universitas Tarumanagara, Indonesia

Anugerah Tiffanyputri, Universitas Tarumanagara, Indonesia

Matthew Ephraim, Universitas Tarumanagara, Indonesia

Saskia Calysta Zetira, Universitas Tarumanagara, Indonesia

Channy Saka, Universitas Tarumanagara, Indonesia

Jessica Clarita, Universitas Tarumanagara, Indonesia

Prem Singh, Universitas Tarumanagara, Indonesia

Federick Luanga, Universitas Tarumanagara, Indonesia

Preface

This new volume of Lecture Notes in Civil Engineering contains the proceedings of the Second International Conference of Construction, Infrastructure, and Materials (ICCIM 2021). This book presents the latest development in civil engineering on a global scale. It highlights the conference scopes, such as Structural Engineering, Construction Materials, Geotechnical Engineering, Transportation System and Engineering, Constructions Management, Water Resources Engineering, and Infrastructure Development. The 55 articles published in this book went through peer-review processes double-blindly and plagiarism check. Manuscript assessments by the expert reviewers were based on the organizer's technical criteria, including technical criteria, quality criteria, and presentation criteria.

The Second International Conference of Construction, Infrastructure, and Materials (ICCIM 2021) was hosted by the Civil Engineering Undergraduate Study Program of Universitas Tarumanagara, Indonesia, on 26 July 2021. The conference brought together national and international experts to share their researches, knowledge, and experiences. ICCIM 2021 carried the theme "Research and Technology in Civil Engineering to Enhance the Sustainability of the Built Environment".

Due to the global COVID-19 pandemic, which has impacted all activities globally, ICCIM 2021 was held as an online conference. ICCIM 2021 online conference aimed to capture a broader range of participants. The Conference was also expected to facilitate researchers, practitioners, and students in their respective fields of expertise to share information and exchange ideas about the current state of civil engineering development.

ICCIM 2021 was supported by Massey University, New Zealand; Universiti Tun Hussein Onn Malaysia, Malaysia; Nihon University, Japan; fib Indonesia; Diponegoro University, Indonesia; Soegijapranata Catholic University, Indonesia; Universitas Sebelas Maret, Indonesia; and Universitas Atma Jaya Yogyakarta, Indonesia.

ICCIM 2021 has received papers from various countries, such as Indonesia, Japan, Thailand, the United Kingdom, the United States of America, the

Philippines, India, Nigeria, and Bangladesh. More than 600 researchers, practitioners, and students from all over the world registered to attend the Conference.

We are likewise grateful to the keynote speakers for bringing the exciting topics to ICCIM 2021: Prof. Roesdiman Soegiarso (Universitas Tarumanagara, Indonesia); Prof. Monty Sutrisna (Massey University, New Zealand); Dr.-Ing. Joewono Prasetijo (Universiti Tun Hussein Onn Malaysia, Malaysia); and Dr. Tam Chat Tim (National University of Singapore, Singapore).

We would also like to extend our appreciation to the supporting institutions. Secondly, thank you to the sponsors for the utmost support and kind contribution: PT. Waskita Karya (Persero) Tbk, PT. Pamapersada Nusantara, and PT. Bank Negara Indonesia Tbk.

Many people have worked very hard for the organization of this Conference. Special thanks are needed to the Organizing Committee, Steering Committee, Editorial Board, and Scientific Committee. All of whom have generously worked to make this Conference rich in content and pleasant for the attendees. We would also like to thank all the authors who have contributed to the success of this Conference.

Semarang, Indonesia
Auckland, New Zealand
Panchor, Malaysia
Klong Luang, Thailand
Jakarta Barat, Indonesia

Han Ay Lie
Monty Sutrisna
Joewono Prasetijo
Bonaventura H. W. Hadikusumo
Leksmono Suryo Putranto

Contents

Additional Horizontal Movement of the Single Pile Foundation with Combined Loads	1
Sumiyati Gunawan, Niken Silmi Surjandari, Bambang Setiawan, and Yusep Muslih Purwana	
The Combined Effects of Terraces Slope Model and Geotextile Reinforcement Design in Sendangmulyo, Wonogiri	13
Siti Nurlita Fitri and Niken Silmi Surjandari	
Erosion and Distribution of Total Suspended Sediment (TSS) Using Landsat-8 in Krueng Pase Watershed	23
Ichwana Ramli, Ashfa Achmad, Hairul Basri, and Atika Izzaty	
Shoreline Change Cause of Abrasion in Bantan District Bengkalis Island as the Outstanding Beach Area	35
H. Tampubolon	
Nonlinear Effect of Fluid–Structure Interaction Modeling in the Rock-Fill Dam Jatiluhur	49
Albert Sulaiman, Wati A. Pranoto, Tati Zera, and Mouli De Rizka Dewantoro	
Assessment of Flooding Event in the Upper Sunter Watershed, Jakarta, Indonesia	59
Anasya Arsita Laksmi, Anthony Harly Sasono Putro, Wisnu Setia Dharma, Pungky Dharma Saputra, Nina Purwanti, and Muhammad Hamzah Fansuri	
Modeling of Flood Propagation in the Lower Citarum River Using a Coupled 1D-2D HEC-RAS Model	77
Angga Prawirakusuma, Sri Legowo Wignyo Darsono, and Arno Adi Kuntoro	

Review: Effects of Climate on the Geochemical Properties of Volcanic Rocks 85
 Novi Asniar, Yusep Muslih Purwana, Niken Silmi Surjandari,
 and Bambang Setiawan

Analysis of the Utilization of the Embung Klampeyan, Tlogoadi Village, Mlati District, Sleman Regency, Indonesia 93
 Edy Sriyono

Analysis of Shift Pile Foundation on Mall and Hotel Projects in Bontang, East Kalimantan 105
 Nicholas Joshua and Alfred Jonathan Susilo

Analysis of Diaphragm Wall Stability with Dewatering and Ground Freezing Treatment 117
 Eduard Teja and Aniek Prihatiningsih

Analysis of Hollow Concrete Column with CFRP Wrapping Using Finite Element Method 129
 William Supardjo and Sunarjo Leman

The Use of Fly Ash in Pervious Concrete Containing Plastic Waste Aggregate for Sustainable Green Infrastructure 141
 Steve W. M. Supit and Priyono

Artificial Aggregate Made from Expanded Polystyrene Beads Coated with Cement Kiln Dust—An Experimental Trial 153
 A. P. Wibowo, M. Saidani, and M. Khorami

Load Transfer Shear Wall to Pile Cap Modelling Partially for Group Precast Pile 165
 Daud Rahmat Wiyono, Roi Milyardi, Yosafat Aji Pranata,
 Asriwiyanti Desiani, Ginardi Husada, and Maria Christine Sutandi

Effect of Cement–Water Ratio on the Mechanical Properties of Reactive Powder Concrete with Marble Powder as Constituent Materials 177
 Widodo Kushartomo, Henny Wiyanto, and Daniel Christianto

Structural Analysis Using Matched Acceleration Time Histories 187
 Windu Partono

Non-linear Analysis of Steel Shear Key at Epoxy Joint 199
 Khairunnisa Masturoh, Nuraziz Handika, and Heru Purnomo

On-Field Testing of the Monolith Joint of the Full Slab on a Slab-on-Pile Bridge 213
 Ahmad Zaki Risadi, Josia Irwan Rastandi, Bastian Okto Bangkit Sentosa,
 and Nuraziz Handika

Seismic Design Load Comparison of Reinforced Concrete Special Moment Frame and Dual Systems Based on SNI 1726:2019 231
 Suradjin Sutjipto and Indrawati Sumeru

Analysis of Asphalt Damping Ratio on Shear Test 239
 Sunarjo Leman, Maria Kevinia Sutanto, Elizabeth Ivana Harsono, Vryscilia Marcella, Anugerah Tiffanyputri, and Yuskar Lase

Analysis of the Sand Grains Influence on Damping Ratio Using Shear Test 247
 Daniel Christianto, Vryscilia Marcella, Channy Saka, Alvira Nathania Tanika, and Yuskar Lase

Parametric Study on Neutral Axis Growth of Concrete Beams Reinforced with Fiber-Reinforced Polymer and Steel Bars 255
 Ahmad Zaki and Rendy Thamrin

Dr. Saharjo Road Condition Audit Using IRAP Method to Achieve 3 Star Rating 265
 Ni Luh Putu Shinta Eka Setyarini and Garry Edison

Analyzing Zones and Accessibility of Public Senior High School in Makassar City 277
 Ardiansyah, Syafruddin Rauf, and Sumarni Hamid Aly

Evaluation Readiness of Contractor and Government in Implementing the Road Preservation Program: Case Study National Road in Indonesia 289
 Maharani Pasha Umar, Ayomi Dita Rarasati, and R. Jachrizal Sumabrata

Analysis of Travel Behavior Under Flooding Condition Based on Probe Data in Ubon Ratchathani City, Thailand 303
 Noriyasu Tsumita, Kohga Miyamura, Sittha Jaensirisak, and Atsushi Fukuda

Modeling Movement of Rice Commodities Between Provinces in Indonesia 317
 Dwi Novi Wulansari, Saskia Kanisaa Puspanikan, and Zafir Istawa Pramoeodya

Single Tariff System to Provide Incentive for Longer Distance Users and to Keep Efficient Toll Gates Operations 329
 Apta Sampoerna and Leksmono Suryo Putranto

Analysis of Transportation Accessibility in Shopping Areas in Makassar City 341
 Jefryanto Londongsalu, Syafruddin Rauf, and Sumarni Hamid Aly

Priority of Sustainable Transport Policy Implementation in Expert Perspective	353
Nindyo Cahyo Kresnanto, Ricko Nasrianda Sinaga, Risdiyanto, and Wika Harisa Putri	
Prioritizing District Road Maintenance Using AHP Method	363
Nindyo Cahyo Kresnanto	
Overview of Side Friction Factors for Evaluation of Capacity Calculation at Indonesian Highway Capacity Manual	373
Najid and Tamara Marlianny	
Thickness Pavement Design Based on Heavy Vehicle Loads	385
Anita Rahmawati, Emil Adly, and Wahyu Widodo	
Performance of Polymer Modified Asphalt Mixture Using Gypsum Filler	399
Rindu Twidi Bethary, Dwi Esti Intari, and Siti Asyiah	
Resistance of Modified Concrete-Wearing Course Mixture Using LDPE Polymer Against Damage Due to Water Immersion	411
Indah Handayasari, Dyah Pratiwi Kusumastuti, and Arief Suardi Nur Chairat	
Experimental Study on the Self-healing Ability of Wearing Course-Asphalt Concrete Mixes Reinforced with Steel Particles	421
Anissa Noor Tajudin, Arif Sandjaya, Daniel Christianto, and M. Bagas Haris Kurniawan	
The Use of Gauss-Jordan Elimination Method in Determining the Proportion of Aggregate Gradation	431
Bagus Hario Setiadji, Supriyono, and Amelia Kusuma Indriastuti	
Conceptual System Model Dynamic OSH Performance Improvement of Building Construction Projects	441
Feri Harianto, Nadjadji Anwar, I Putu Artama Wiguna, and Erma Suryani	
Experiment the Effect of Providing Monetary Incentives and Safety Patrols on Work Safety Behavior in Construction Project Implementation	449
Feri Harianto, Nadjadji Anwar, I Putu Artama Wiguna, and Erma Suryani	
Development of Activity-Based Safety Plan for Precast Parapet Panel Work in Elevated Construction	459
Pungky Dharma Saputra, Anasya Arsita Laksmi, Nina Purwanti, and Muhammad Hamzah Fansuri	

Game Theory Approach for Risk Allocation in Public Private Partnership 471
 Adhika Nandi Wardhana, Farida Rachmawati, and Erwin Widodo

Analysis of Change Orders Based on the Type of Road Construction 479
 Mega Waty and Hendrik Sulistio

Implementation of Occupational Safety and Health Management Systems During COVID-19 Pandemic on High-Rise Building Construction Projects 489
 Aleksander Martin and Mega Waty

Developing Knowledge Management Strategy to Improve Project Communication in Construction of Coal Mining Infrastructure: A Conceptual Study 497
 Alfandias Seysna Putra, Leni Sagita Riantini, and Mohammad Ichsan

Portable Structure for Post-disaster Temporary Shelter 511
 Bayu Ariaji Wicaksono, Dalhar Susanto, and Emirhadi Suganda

Concrete Damage Risk Rating Examination to Existing Buildings 523
 Henny Wiyanto, Reagen Yocom, and Glen Thenaka

A Literature Review of Life Cycle Costing of Dam Asset Management 533
 Ismi Astuti Anggraini, Ayomi Dita Rarasati, and R. Jachrizal Sumabrata

An Explorative Study to Public Rental Housing’s Tenants Using Importance Performance Analysis 543
 Indira Surya Kumala and Farida Rachmawati

Modeling of Conceptual Framework to Understand Stakeholders’ Awareness in Construction Industry in Thailand Affected by the 3rd Wave of COVID-19 Pandemic 557
 Nattasit Chaisaard and Grit Ngowtanasuwan

A Literature Review on Healthy Buildings Based on Various Perspectives 567
 Louferinio Royanto Amatkasmin, Mohammed Ali Berawi, and Mustika Sari

Analysis of Dominant Influence Factors of the Application of the Incentive Plan Model on the Material Waste 585
 Triongko Agatha Bayuaji and Basuki Anondho

Accuracy of Schedule Performance Calculation with ES Method and EV Method 597
 Cangga Kristiandi and Basuki Anondho

Analysis of Dominant External Factors on Construction Project Overhead Costs	609
Hendi Wijaya and Basuki Anondho	
A Competency Model of Thai Small-Medium Enterprise Contractors for Owner Satisfaction in Construction Projects	619
Grit Ngowtanasuwan	

About the Editors

Prof. Dr. Han Ay Lie is working as Professor in the Department of Civil Engineering, Diponegoro University, Indonesia. At present, she is also Chairwoman of the International Federation of Structural Concrete Indonesia (fib-Indonesia). She has also taken the role of external examiner and is Advisor for many national and international universities. Her research interests include graded concrete, fibre-reinforced plastics for concrete, retrofitting and external reinforcing, modeling, and finite element analysis.

Prof. Dr. Monty Sutrisna is Professor of Construction and Project Management at Massey University, New Zealand. He is currently Head of the School of Built Environment at the same institution. His expertise includes Construction and Engineering Management, Construction Productivity, Construction Procurement and Contracts, Construction IT and other Advanced Technologies applied in Construction, Construction Project Management, Decision Making Modelling/Support, and Knowledge-Based Systems and Artificial Intelligence.

Dr.-Ing. Joewono Prasetyo teaches in the Department of Transportation Engineering Technology at Universiti Tun Hussein Onn Malaysia (UTHM), Malaysia. He has been Head of the Industry Center of Excellence—Railway (ICoE Rel) of Universiti Tun Hussein Onn Malaysia (UTHM) since 2020. He is professionally certified as Permanent Way Inspection: CO2 Track Maintenance Works (2019) and Professional Technologist (2020). His research interests include land transportation engineering, transportation safety, and rail technology.

Prof. Dr. Bonaventura H. W. Hadikusumo is Professor at the School of Engineering and Technology, Asian Institute of Technology, Thailand. His key expertise and interests encompass the area of safety management, system dynamics, project visualization, intelligent agent system, knowledge management tools, IT applications like building information modeling (BIM) and simulation in construction site improvement, and Web-based project management.

Prof. Dr. Leksmono Suryo Putranto is Professor in the Department of Civil Engineering, Universitas Tarumangara, Indonesia. He has been actively involved in a leading role in research conferences as organizing and scientific committees. He currently acts as Chief of Research and Development Commission in Jakarta Transportation Council. Social psychology, safety engineering, and transportation engineering are some of his areas of expertise and interest.

Additional Horizontal Movement of the Single Pile Foundation with Combined Loads



Sumiyati Gunawan , Niken Silmi Surjandari, Bambang Setiawan, and Yusep Muslih Purwana

Abstract Pile-foundation support the upper structure to the subgrade, it generally supports vertical loads, occasionally when the horizontal loads are found to be more dominant, it becomes an important consideration in the design. Pile foundations with combined loads are generally analyzed separately, however on the site, the two loads work simultaneously. In-Indonesia, particularly, loading tests do not performed once. Therefore, it does not account for the additional vertical displacement and lateral deflection. Therefore, this research was conducted to investigate and analyze, effect of horizontal loads or displacement on a single pile foundation in order to determine the impact of combined loads. It was also used to determine their relationship which is expected to be used as a reference in analyzing additional horizontal displacement through independent loading test. The process was in three stages with the first being the preliminary analysis through 2D Finite Element Method (2D-FEM) Plaxis2D8.6 while the second was an experimental test in the laboratory, and third, being the analysis through 3D-FEM Plaxis3DFoundation1.1 for validation with soil data and loading test on several projects in the field and the results showed the horizontal deflection increased significantly after reaching $(Pu.D)/(Hu.L.E) \geq 2.5 \times 10^{-6}$. This increment is required to be considered in the design.

Keywords Combined-load · Single-pile · Horizontal-displacement

1 Introduction

The foundation supports structural loads and transmits to the subgrade, usually using pile foundations, not only supporting axial loads, horizontal loads are dominant in some other structures. This means it is very important to calculate the

S. Gunawan (✉) · N. S. Surjandari · B. Setiawan · Y. M. Purwana
Department of Civil Engineering, Sebelas Maret University, Surakarta, Indonesia
e-mail: sumiyatig07@gmail.com

S. Gunawan
Department of Civil Engineering, Atma Jaya Yogyakarta University, Sleman, Indonesia

© The Author(s), under exclusive license to Springer Nature Singapore Pte Ltd. 2022
H. A. Lie et al. (eds.), *Proceedings of the Second International Conference of Construction, Infrastructure, and Materials*, Lecture Notes in Civil Engineering 216, https://doi.org/10.1007/978-981-16-7949-0_1

horizontal loads in pile foundations [1]. Combined loads are seldomly analyzed in simultaneity. This involves calculating the axial load first to determine the axial carrying capacity and vertical displacement followed by determining the lateral load to evaluate the lateral bearing capacity and deflection. Meanwhile, the two loads work simultaneously on the site [2]. In Indonesia, these loading tests are not usually conducted simultaneously, and this means the additional lateral deflection due to the combined loads is not considered in construction as required by the ASTM D3966-07 [3].

Previous studies reported the reduction of lateral deflection in pile foundation under combined loads due to axial loads [4], while lateral loading was discovered not to be causing any vertical movement but has the ability to increase the movement in combined loads [5]. A study also showed lateral bearing was reducing as the embedded part of the pile decreased while lateral deflections reduced with the increase in vertical load on the pile head [6]. Three-dimensional finite element analysis was also conducted to determine the influence of combined axial and lateral loads on homogeneous clay and sandy soils. The results showed a significant increase in the effect of axial load on the lateral bearing capacity in sandy soil and a slight decrease in clay soil, but a substantial influence of axial load was recorded for sandy soils, even for piles with 30D, D = Diameter in length, and a less significant impact was found with clay soils for piles above 15D in length [7].

Another test on poorly graded sand with variations in the pile and loading also showed an increase in the lateral bearing capacity as the vertical load was increased [8]. Numerical study analysis of pile-soil interactions which were subjected to axial and lateral loads simultaneously using LPILE, a finite element (FE) model with Abaqus/Cae and SAP 2000, showed an increase in axial load caused a reduction in the induced bending moment and lateral deflection and this subsequently increased its capacity to withstand lateral forces [9]. It was also discovered in another research that the influence of axial loads on the lateral bearing capacity pile increased significantly in sandy soils but less significant in loamy soils [10].

Vertical loads were also reported to have less effect on lateral resistance in sandy soils, but the progression was observed to be increasing as the soil density increased [11, 12]. Moreover, the influence of axial load on lateral bearing capacity significantly increased in sandy soils and slightly in clay soils while the square-shaped pile was found to have the ability to withstand 1.3 times more load than the round pile [13]. The numerical analysis also showed the effects of combined loads are beneficial, but the interactions were very complex and, depending on the load conditions, there is a possibility of a contrary effect on system rigidity and max load [14]. Limited experimental research discovered the application of a static axial load has a minimal effect on the lateral behavior of micropiles fixed in rigid clay soil [15]. Furthermore, some studies also provided evidence that lateral loads were decreased in combined loads even though deflection was reduced by axial loads due to their presence.

The initial analysis using FEM with several load combinations, pile dimensions, and soil types (homogeneous and non-homogeneous, submerged or drained) showed that by comparing the lateral forces, vertical forces, pile dimensions, and a

certain modulus of soil elasticity, the horizontal deflection increases significantly at a certain point until the period of collapse due to combined forces. Therefore, this research was conducted to investigate the effects of simultaneous axial and lateral loading on a horizontal deflection in a single pile foundation. It was also intended to obtain the axial-lateral load relationship which can be used as a reference to analyze additional horizontal deflection due to simultaneous loading through the use of an independent loading test. The process was divided into three stages, with the first being the analysis conducted using the Finite Element Method Plaxis2D approach, the second was the Laboratory Model Experimentation test. The model used was a $150 \times 150 \times 120$ cm box filled with silty-sand soil, pile foundation steels at 50 and 60 cm lengths and 1.5 and 2 cm diameters, load variations, and combined loads and the third with being the analysis conducted using the Finite Element Method Plaxis3D approach based on the results of loading tests in several projects in the field.

2 Research Method

The process was divided into three stages.

2.1 *Stage I: Analysis Using Finite Element Method 2D*

The analysis was conducted using the 2D Finite Element Method (2D-FEM) with Plaxis2D8.6, and this involved modeling a single pile foundation with the axisymmetry menu on the FEM. The variables used include the axial, lateral, and combined loadings, lengths and diameters of the pile, and soil types (soft, medium, or dense, homogeneous or layered, submerged or drained). The variations of the soil parameters are presented in Tables 1 and 2.

2.2 *Stage II: Laboratory Model Experimental Test*

The model was a $1.5 \times 1.5 \times 1.5$ m³ test box filled with silty-sand soil obtained from Berbah District, Sleman City, Yogyakarta. The pile foundations were modeled using steel bars with 0.5 and 0.6 m lengths and 0.015 and 0.02 m diameters and subjected to axial, horizontal, and combined loads. The model is presented in Fig. 1 and the differences in foundations' lengths and diameters and combined loads (loading rate every 10 min with interval load 2500 g for vertical load and 500 g for lateral load, the addition of the load is carried out after the decreasing speed is less than 0.05 mm/10 min (<0.0125 mm/2.5 min)), are indicated in Table 3.

Table 1 Variations of soil parameters

Name	T3		T5	T6				Pile
	Lyr. 1	Lyr. 2	Lyr. 1	Lyr. 1	Lyr. 2	Lyr. 3	Lyr. 4	
Material	MC	MC	MC	MC	MC	MC	MC	LE
Condition	D	D	D	D	D	D	D	NP
γ_k (kN/m ³)	16	17	16.5	11.86	12.22	12.86	13.57	24
γ_{sat} (kN/m ³)	20	21	20	17.5	18.03	17.67	17.83	25.33
E (kN/m ²)	1.2×10^5	1.2×10^5	8×10^4	1.6×10^6	1.6×10^6	1.6×10^6	1.6×10^6	0.3
Poisson ratio (μ)	0.3	0.3	0.3	0.3	0.3	0.3	0.3	
Cohesion (kN/m ²)	1	1	1	2.05	2.3	0.05	0.02	
ϕ (°)	30	33	31	30	30	35	40	
R_{inter}	1	0.7	1	0.4	0.35	0.7	0.7	1

D Drained, NP nonporous, MC Mohr Coulomb, LE linear elastic

Table 2 Variation of the load on FEM 2D

Type of soil	Pile dimensions		Load (kN), until it collapses		
	D (m)	L (m)	Lateral	Axial	Combined
T5	0.65	17	OK	OK	OK
T5	0.65	30	OK	OK	OK
T3	0.65	22	OK	OK	OK
T3	0.65	26	OK	OK	OK
T3	0.65	30	OK	OK	OK
T6	0.6	17	OK	OK	OK

T5 soft soil, T3 medium soil, T6 hard soil

2.3 Stage III: Analysis Using Finite Element Method 3D

The analysis was carried out using the Finite Element Method (FEM) with 3D Plaxis, and this involved modeling a single pile foundation with soil data from several projects in the field, namely: Citarum Bridge, South Jakarta Cikampek II; Dompok Bridge, Tanjung Pinang, Riau; PLTU Batang, Central Java, The variables used include axial, lateral, and combined loads until it collapses, presented in Table 4.

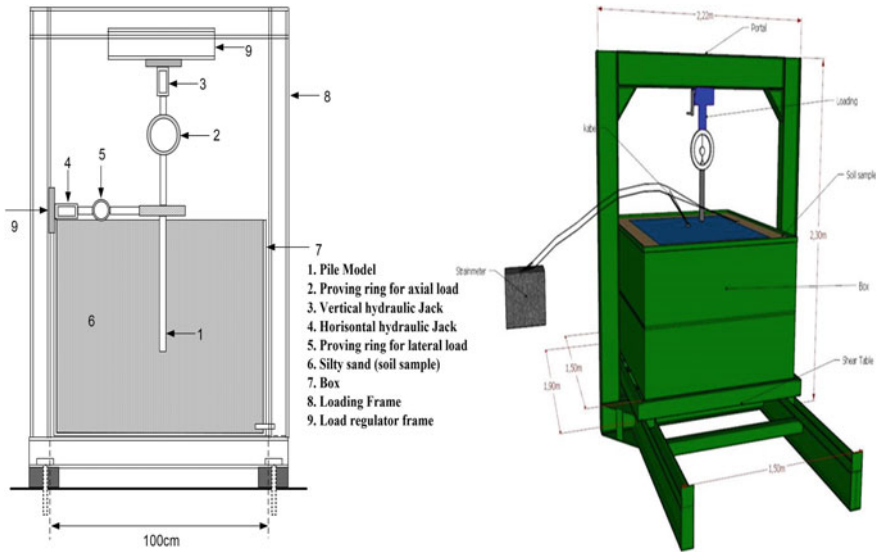


Fig. 1 Laboratory test model

Table 3 Variation of loads

Type of soil	Pile dimensions		Load (g) (until collapsed)		
	D (m)	L (m)	Lateral	Axial	Combined
Silty sand	0.015	0.5	OK	OK	OK
Silty sand	0.02	0.6	OK	OK	OK

Table 4 Variation of the load on FEM 3D

Project	Pile dimensions		Load (kN), until it collapses		
	D (m)	L (m)	Lateral	Axial	Combined
Citarum bridge	1.20	20	OK	OK	OK
Dompok bridge	1.00	18	OK	OK	OK
PLTU	0.60	17	OK	OK	OK

3 Results and Discussion

3.1 Result

Analysis with 2D-FEM, with axial loading, lateral loading, combined loads (axial and lateral), variation of length and diameter of the pile, soft soil type, medium and dense, homogeneous soil and layered, submerged and not submerged in water, illustrates movement at the head of the pile due to axial and lateral loading as shown in Fig. 2, from the initial research, it is obtained as shown in Fig. 3, one inflection point of the increase in lateral deflection for each soil density is at $(Pu.D)/(Hu.L)$ and Fig. 4 shows the same inflection point after taking into account the soil density factor (elastic modulus of soil) is at $(Pu.D)/(Hu.LE) \geq 2.5 \times 10^{-6}$.

Experimental tests of laboratory scale models, with silty sand as a description of conditions in the field, using the single pile foundation of steel with a length of 0.5 and 0.6 m, the diameter of 0.015 and 0.02 m, and the movement at the head of the pile with variations in axial loads and lateral loads are presented in Fig. 5. While the horizontal movement because of the combination of loads is shown in Fig. 6.

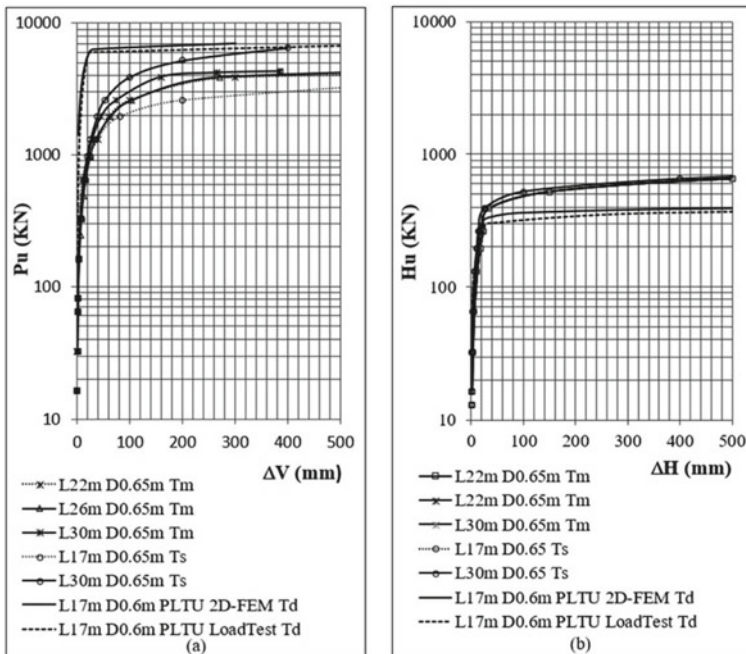


Fig. 2 Movement at the head of the pile (FEM 2D). a Displacement vertical without lateral load, b deflection horizontal without axial load

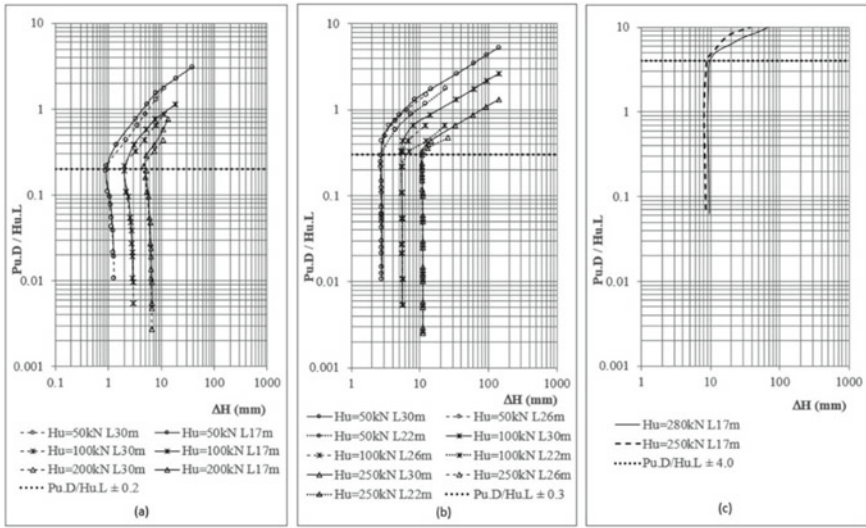


Fig. 3 Horizontal deflection at the head of the pile (FEM 2D). **a** Horizontal deflection for T5 (soft soil), **b** horizontal deflection for T3 (medium density soil), **c** horizontal deflection for T6 (dense soil)

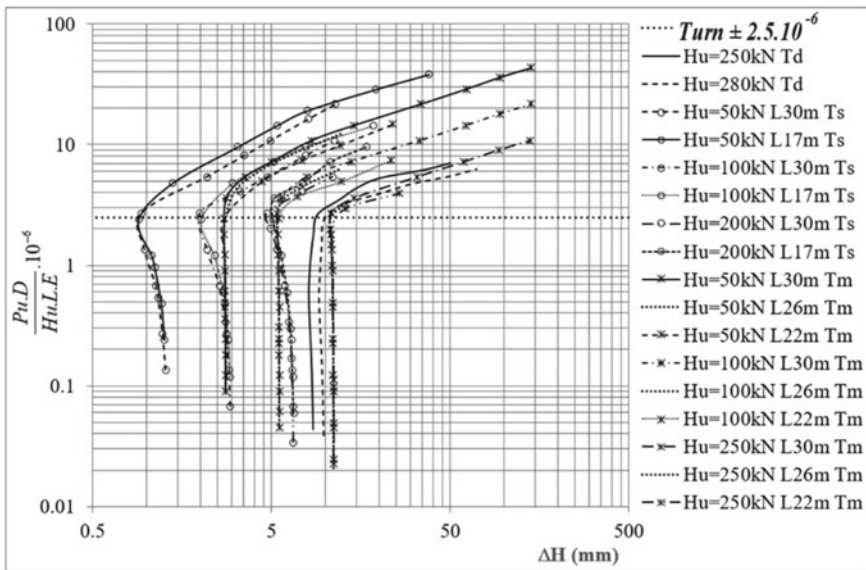


Fig. 4 Horizontal deflection at the head of the pile based (FEM 2D)

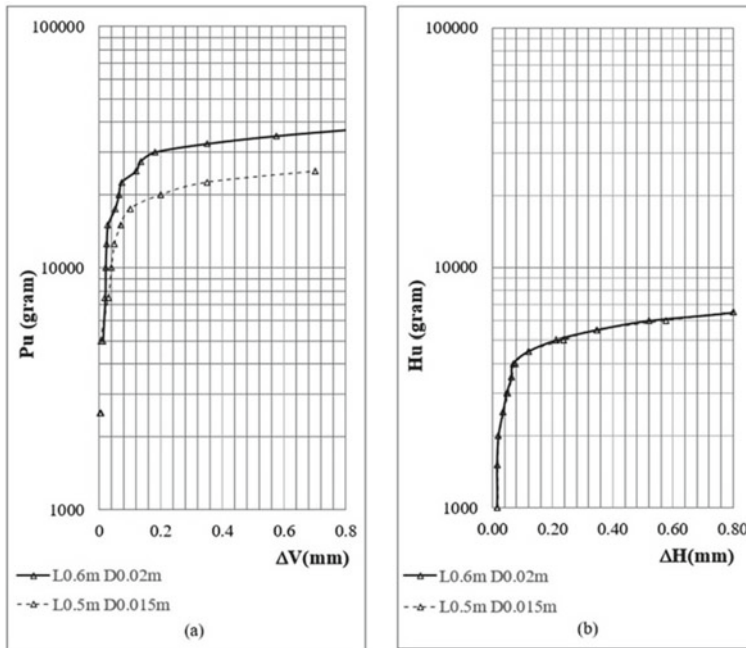


Fig. 5 Movement at the head of the pile (laboratory test). **a** Displacement vertical without lateral load, **b** deflection horizontal without axial load

Analysis with FEM 3D, with axial loading, lateral loading, combined loads (axial and lateral), based on soil data from several projects in the field, movement at the head of the pile due to axial and lateral loading are shown in Figs. 7 and 8.

3.2 Discussion

The lateral loads were observed to have increased the vertical downward movement while the vertical loads increased the lateral load capacity in all slenderness ratios for the combined loads, as previously stated. There was also no limit on how much the combined load ratio affected the vertical subsidence and lateral deflection on the pile foundation. Moreover, something new was found with the FEM 2D analysis and this was that the horizontal deflection started to increase significantly after reaching the load $(P_u.D)/(H_u.LE) \geq 2.5 \times 10^{-6}$ up to the moment it collapsed

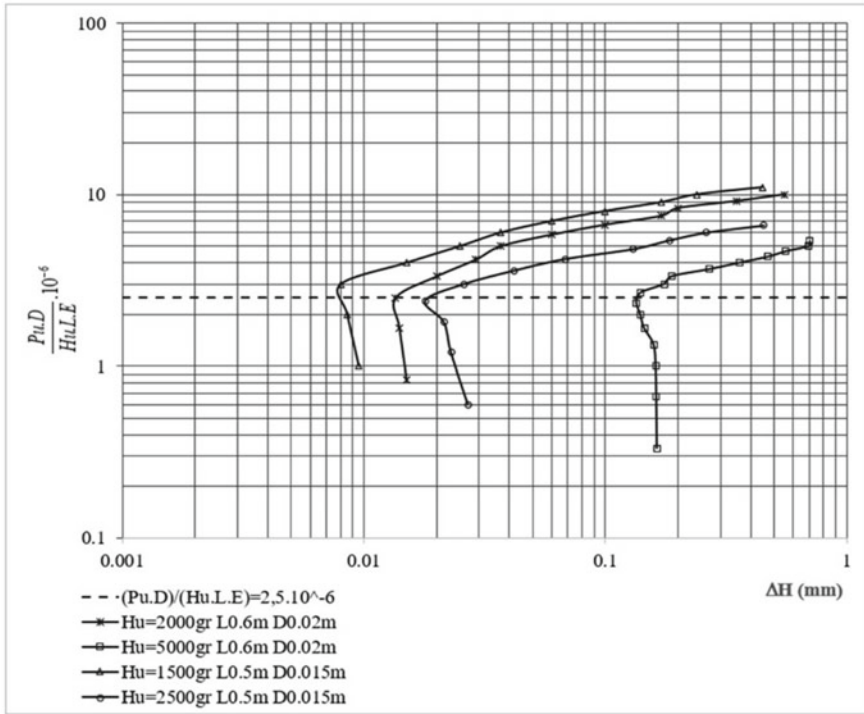


Fig. 6 Horizontal deflection at the head of the pile (laboratory test)

when combined axial and lateral loads acted on the pile foundation, where P_u is axial load (kN, g), D = Diameter of the pile (m), H_u = lateral load (kN, g), L = length of the pile (m) and E = modulus elastic of silty sand (kN/m^2 , g/cm^2).

Following up on the preliminary FEM 2D analysis test above, the research was continued with a scale-3D experimental test in the laboratory and validation by modeling the FEM 3D using 3D based on loading test data on several projects in the field. The test results for scale-3D experimental test in the laboratory and validation by modeling the FEM 3D not much different from FEM 2D, that horizontal deflection was increased significantly at $(P_u D)/(H_u L E) \geq 2.5 \times 10^{-6}$, to the period of collapse due to axial forces.

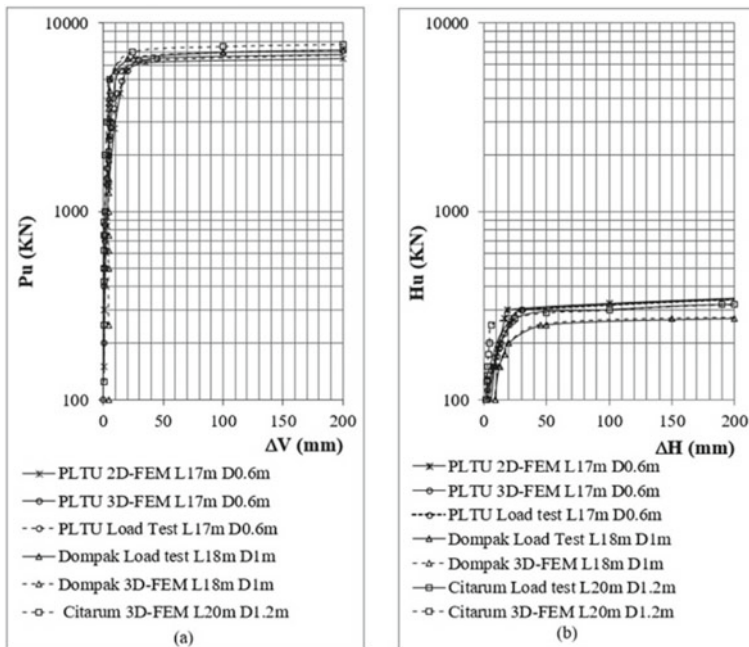


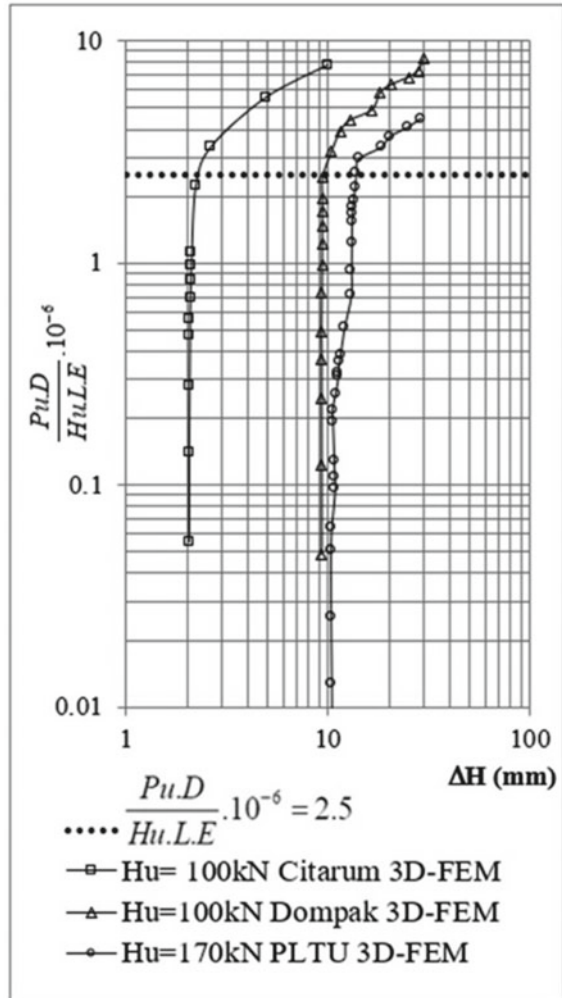
Fig. 7 Movement at the head of the pile (FEM 3D). a Displacement vertical without lateral load, b deflection horizontal without axial load

4 Conclusion

This research focused on investigating the effect of combined loads on the horizontal displacement of single pile foundations through analyses and laboratory experiments. It was also used to determine the relationship to be used as a reference to analyze additional horizontal displacement on a single pile foundation. A preliminary 2D-FEM analysis was first conducted, and this was followed by the laboratory experiment and further validated with a 3D-FEM model using loading test data from several field projects.

The results from the experiments and 3D-FEM modeling were observed not to be much different from those obtained from the 2D-FEM for single pile foundation that on $(P_u.D)/(H_u.L.E) \geq 2.5 \times 10^{-6}$. The horizontal displacement was observed to have increased significantly due to the combined load.

Fig. 8 Horizontal deflection at the head of the pile (FEM 3D)



This, therefore, needs to be considered in calculating and planning the pile foundations' bearing capacity. The layered soil was also observed to have different young modulus and shear modulus values and this means the horizontal deflection added was not linear. Therefore, further research is required to determine the average curvature of the line and the curve equation for the increase in lateral deflection in order to estimate the horizontal deflection added and Full-scale models also need to be verified through further studies to obtain satisfactory results.

References

1. Brown DA, Morrison C, Reese LC (1988) Lateral load behavior of pile group in sand. *J Geotech Eng* 114(11):1261–1276
2. Mandolini A, Russo G, Viggiani C (2005) Pile foundations: experimental investigations, analysis and design. In: Proceedings of the international conference on soil mechanics and geotechnical engineering, vol 16, no 1. AA Balkema Publishers, p 177
3. ASTM (2007) Standard test methods for deep foundations under lateral load. ASTM, United States. <https://doi.org/10.1520/d3966-07>
4. Ibrahim SF, Al-Soud MS, Al-Asadi FI (2018) Performance of a single pile under combined axial and lateral loads in layered sandy soil. *J Eng Sustain Dev* 22(1):121–136
5. Anagnostopoulos C, Georgiadis M (1993) Interaction of axial and lateral pile responses. *J Geotech Eng* 119(4):793–798
6. Zhu MX, Zhang Y, Gong WM, Wang L, Dai GL (2017) Generalized solutions for axially and laterally loaded piles in multilayered soil deposits with transfer matrix method. *Int J Geomech* 17(4):04016104
7. Karthigeyan S, Ramakrishna V, Rajagopal K (2007) Numerical investigation of the effect of vertical load on the lateral response of piles. *J Geotech Geoenviron Eng* 133(5):512–521
8. Nugroho SA (2016) Pengaruh Beban Vertikal terhadap Daya Dukung Lateral Pondasi Tiang. Dissertation, Riau University
9. Khodair Y, Abdel-Mohit A (2014) Numerical analysis of pile-soil interaction under axial and lateral loads. *Int J Concr Struct Mater* 8(3):239–249
10. Rajagopal K, Karthigeyan S (2008) Influence of combined vertical and lateral loading on the lateral response of piles. *Int Assoc Comput Methods Adv Geomech (IACMAG)* 3272–3282
11. Hazzar L, Hussien MN, Karray M (2016) Investigation of the influence of vertical loads on the lateral response of pile foundations in sands and clays 2. *J Rock Mech Geotech Eng*
12. Hazzar L, Hussien MN, Karray M (2017) Influence of vertical loads on lateral response of pile foundations in sands and clays. *J Rock Mech Geotech Eng* 9(2):291–304
13. Abbas JM, Chik Z, Taha MR (2018) Modelling and assessment of a single pile subjected to lateral load. *Studia Geotechnica et Mechanica* 40(1):65–78
14. Achmus M, Thieken K (2010) On the behavior of piles in non-cohesive soil under combined horizontal and vertical loading. *Acta Geotech* 5(3):199–210
15. Kershaw KA, Luna R (2014) Full-scale field testing of micropiles in stiff clay subjected to combined axial and lateral loads. *J Geotech Geoenviron Eng* 140(1):255–261

The Combined Effects of Terraces Slope Model and Geotextile Reinforcement Design in Sendangmulyo, Wonogiri



Siti Nurlita Fitri and Niken Silmi Surjandari

Abstract Several areas in Wonogiri Regency are vulnerable to natural disasters, particularly landslides. This is due to the hilly and steep contours and the high rainfall. In addition, the potential probability due to earthquake hazards leads to landslides. Soil improvement using geotextile and terracing is an alternative that can be used to protect slopes. This research aims to find the relationship between the number of geotextiles needed with various models of terracing in Wonogiri in post-rain conditions, as well as with external load, pseudo-static-earthquake, and traffic load. The number of geotextiles required uses the moment of resistance resulting from the analysis of the limit equilibrium method. The results of this study generated the terraces model affect the number of geotextiles; increasing the number of terraces steps reduces the quantity of geotextiles. The terraces slope with five steps of total height provided the fewest number of geotextile layers. The results of this study can be a reference in the form of the required number of geotextiles installed in the slopes for various terracing variations to prevent landslides.

Keywords Terraces · Landslide · Geotextile · Limit equilibrium · Slope

1 Introduction

Landslides are the most natural disaster that occurs in Wonogiri. The topography of some areas in Wonogiri dominated with the steep and abrupt slope are a major factor that caused the landslide. The damage of this case gave the high fatalities, people, cost, and material. The Indonesian National Disaster Management Agency

S. N. Fitri (✉) · N. S. Surjandari
Department of Civil Engineering, Sebelas Maret University, Ir. Sutami No. 36, Kentingan,
Jebres, Surakarta, Central Java 57126, Indonesia
e-mail: sitinurlitafitri@staff.uns.ac.id

N. S. Surjandari
e-mail: nikensilmisurjandari@staff.uns.ac.id

Table 1 Landslide case in Wonogiri based on BNPB data (2014–2018)

No	District	Landslide	No	District	Landslide	No	District	Landslide
1	Pracimantoro	1	9	Baturetno	1	17	Jatiroto	6
2	Paranggupito	2	10	Eromoko	3	18	Kismantoro	6
3	Giritontro	0	11	Wuryantoro	0	19	Purwantoro	2
4	Giriwoyo	5	12	Manyaran	2	20	Bulukerto	3
5	Batuwarno	2	13	Selogiri	6	21	Puhpelem	0
6	Karangtengah	5	14	Wonogiri	1	22	Slogohimo	1
7	Tirtomoyo	6	15	Ngadirojo	2	23	Jatipurno	7
8	Nguntoronadi	5	16	Sidoharjo	1	24	Girimarto	5

(BNPB) discovered the landslides phenomenon appeared in many areas of Wonogiri in Table 1.

Table 1 describes the landslide case from 2014 to 2018. The 72 landslides had detected in Wonogiri. The zero accident of landslide was just found in 3 districts of Wonogiri. Others arise maximal in 7 events in 4 years. As a result, the landslide is one of the major problems that must be addressed.

There is much reinforcement to manage the landslide. In the previous study [1], the slope improvement was design by terracing. The method successfully increases the stability of the slope in traffic load conditions [2]. The terracing model is the suitable method to protect the Sendangmulyo slope and many areas because the method also avoids erosion, is moderate, and is able to protect slopes safely [3, 4]. Moreover, the terrace variation is the requirement for a technology that stabilizes bench terraces that is simple, successful, and economically viable and minimizes soil erosion by absorbing rainfall, slowing runoff velocity, and sediment loss [5, 6]. Besides of terraces method, geotextile is one of the soil improvement methods which commonly use to protect natural or manmade slopes. The successful design of geotextile to prevent the landslide in many bridges approach and highway embankment project in Central Java of Indonesia have been carried out in other studies [7–10]. Whereas the research of natural slope reinforcement has been performed in [11–13]. The design of the geotextile model is appropriate with the natural angle of slope. Recently, there is very few research in slope stability mitigation toward landslide in Indonesia that particularly incorporates terracing configuration and the use of geotextiles. Although the combination of bronjong and terracing has been studied previously [14].

This study aims to know the behavior of the geotextile reinforcement model combines with terraces design. The simulation condition uses post-rain analysis of the groundwater table. Furthermore, the external load model with traffic and earthquake load as a result of the location of the case study must be conversant as the dynamic prone area including connecting zone between East Java, Central Java, and the Special Region of Yogyakarta.

2 Method

This research started with the collection of secondary data from previous studies to learn about the soil properties of slope in Sendangmulyo Village, Wonogiri Regency. As a crucial consequence of the earlier findings, the natural angle slope is 60 and 30 degrees. After rainfall, the simulation model is used, along with ten variations of the terraces model. This study assumes homogeneous and isotropic soil. According to other studies, the use of the model analysis in rainfall conditions perception gives the best impact on the simulation result [15–17]. The calculation has accumulated with earthquakes load and traffic load. The traffic load was simulated with the load of two vehicles in different paths and pavement. While the pseudo-static analysis was carried out based on the new earthquake map [18], Sendangmulyo has the $a_d = 0.9$. The values were considered in Eq. 1.

$$kh = \frac{a_d}{g} \quad (1)$$

with

kh horizontal earthquake coefficient

a_d bedrock acceleration (cm/s^2)

g gravity acceleration (cm/s^2)

2.1 Soil Parameter and Model

The ten terraces model, soil properties, and traffic load were adopted from [1]. Data on soil parameters were collected in Sendangmulyo Village is $\gamma_b = 17.81 \text{ kN/m}^3$, $\gamma_{\text{saturated}} = 19.15 \text{ kN/m}^3$, $\varphi = 37.47^\circ$, and $c = 0 \text{ kN/m}^2$. The variation model of the terrace was analyzed with an initial divided height of slope in many models of step; 1/2 until 1/5 of existing height and the combination of 1/2–1/5 of total initial height. Traffic load simulated with the weight of pavement and addition of trucks in 2 way. Furthermore, the other external load as a dynamic load was conducted based on [19] in the pseudo-static simulation model.

2.2 Research Analysis Model

The ten models of terraces were simulated in the Limit Equilibrium Method (LEM) to conducted the landslide parameter; Safety Factor (SF), circle radius of landslide (R), and resistance moment (Mr). Additionally, the result of landslide simulation was carried out to calculated the number of geotextile reinforcements. The formula to predict the number of geotextiles was adopted by the geotextile's allowable stress factors.

2.3 The Geotextile's Allowable Stress Factors

The stress of geotextile reinforcement was corrected with the external factor as chemical, creep, installation, and environment depend on the engineer perception of the geotextile area installation. This study was constructed with ultimate stress of geotextile (T_{ult}) = 52 kN/m and divided by factor in 1–1.5 values. The formula is given in Eq. 2.

$$\sigma_{all} = \sigma_{ult} = \left(\frac{1}{f_d \times f_{env} \times f_m \times f_c} \right) \quad (2)$$

- σ_{all} geotextile's allowable stress (kN/m²)
- σ_{ult} geotextile's ultimate stress (kN/m²)
- f_d biological factor (1–1.5)
- f_{env} environment factor (1–1.5)
- f_m installation factor (1–1.5)
- f_c creep factor (1–1.5).

2.4 The Geotextile's Reinforcement Analysis

The factor of stability, which has a minimum value of 1.2, is an overall calculation that accounts for all uncertainty in problems involving geometry, soil variability, and applied loads. The slope reinforcement, SF, becomes one after the overall factor of stability is taken into account in the stability analyses. A solution for the variable of safety was found by applying the Bishop method in Eq. 3 [20].

$$SF = \left(\frac{Mr}{Md} \right)_{unreinforced} + \frac{\Sigma Tall \times R}{Md} \quad (3)$$

- Mr resistance moment (kNm)
- Md overturning moment (kNm)
- $Tall$ geotextile's allowable stress (kN/m²)
- R Radius of circle landslide.

Based on Eq. 2, the Tall was considered with the distance of circle radius of landslide. This means the spacing of geotextile is required to analyze the number of geotextile reinforcements. This study was carried out with a 0.5 m range of geotextile. The combination model of many terraces and geotextile reinforcement is described in Figs. 1 and 2.

Figures 1 and 2 illustrates ten different models examined in this article. In several models of terraces step, the four others are combined with each variation model; 1/2 with 1/3, 1/4, 1/5 respectively from the initial height. Variation 1 has

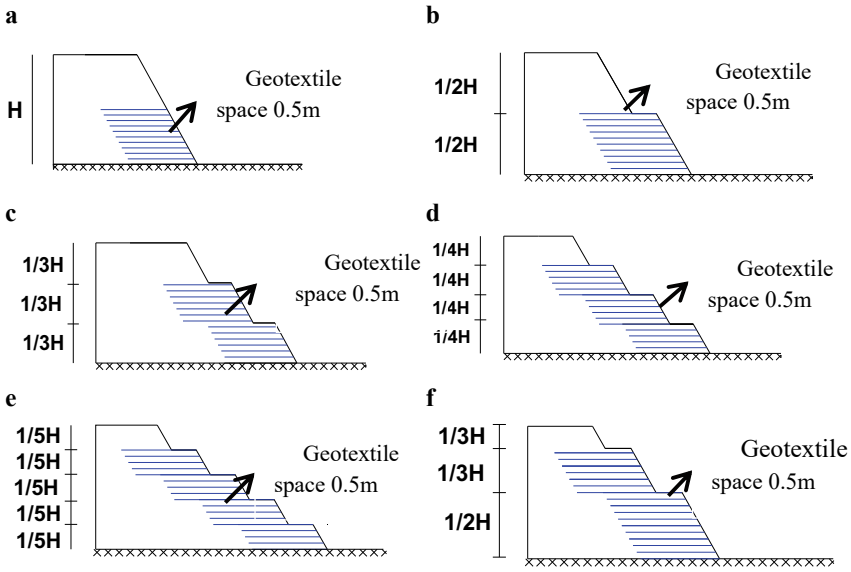


Fig. 1 The simulation combination model of terraces and geotextile reinforcement, a existing model, b variation 1, c variation 2, d variation 3, e variation 4, f variation 5

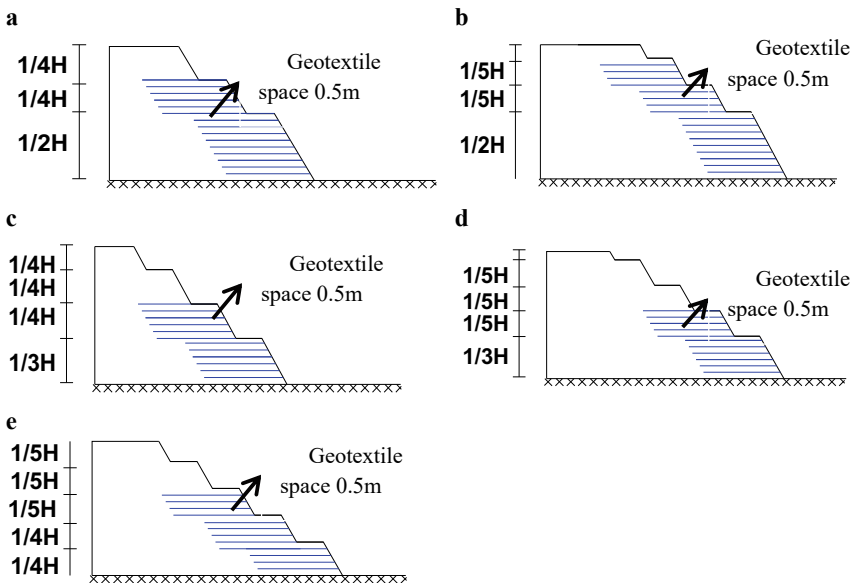


Fig. 2 The simulation combination model of terraces and geotextile reinforcement, a variation 6, b variation 7, c variation 8, d variation 9, e variation 10

two terrace steps, variations 2, 6, 5 has three terrace steps, variation 3, 7, 8 has four terrace steps, and variation 4, 9, 10 has five terrace steps. The detail of the terraces model is based on the past study [21].

3 Result and Discussion

The landslide variable result of this study shows in Figs. 3, 4, 5 and 6. The first parameter is the resistance moment illustrates in Fig. 3.

The relationship between the moment of resistance and various terraces models is depicted in Fig. 3. With traffic and earthquake pseudo-static load study, the result was simulated in different degrees of the slope; 30°, and 60°. In the pseudo-static model. 60 E load means the models of terraces with 60° angles of slope and addition of earthquake load, while 30 E load has different slope angle (30°) with earthquake load. 60 traffic means the 60-degree slope with the simulation of traffic load in two ways path. The lowest value is in a 60-degree slope. In contrast, a slope with 30° with traffic load has the highest rate in resistance of moment.

The other factor of the landslide simulation result is the circle radius of the landslide and was explained in Fig. 4. Based on this outcome, the positions of

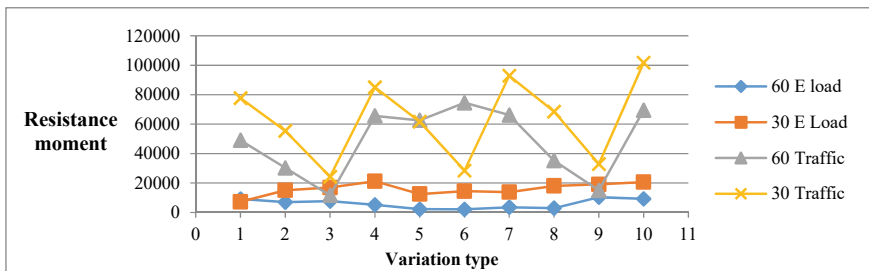


Fig. 3 The result of resistance moment (Mr) in various model

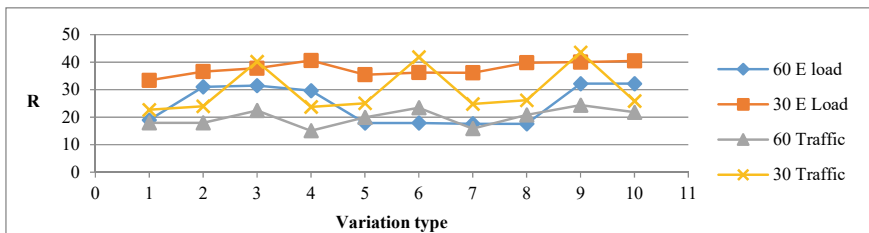


Fig. 4 The result of radius of circle landslide (R) in various model

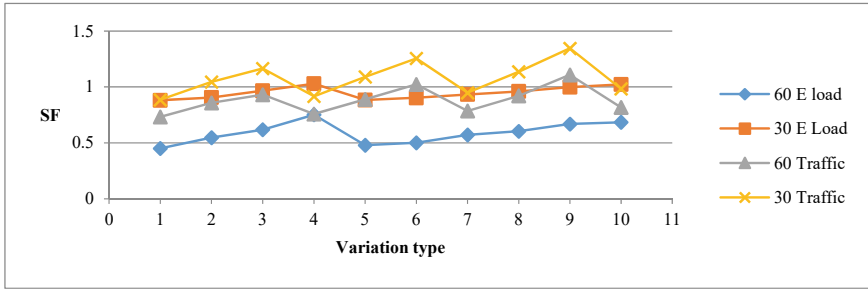


Fig. 5 The result of factor of safety (SF) in various model

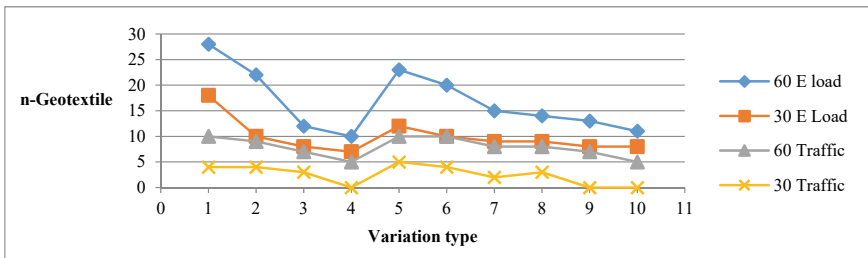


Fig. 6 The result of n geotextile of safety in various model

radius in the similar model (30 and 60 degrees, respectively) are not exactly in the related coordinate.

The last result of the simulation model is the Safety Factor (SF). In this research, The SF values are illustrated in Fig. 5. The Safety factor ranged between 0.4 and 0.68 in earthquake simulation and varied between 0.75 and 1.2 when traffic load is applied. All the condition in post-rain simulation describes the similar trend in variation of terraces model. The value rose in the first until the fourth variation, yet directly fall at the next model of terraces in all the conditions of the slope model. The highest SF is in model 4, the initial slope divided into five steps; 2 m for each number of steps. The lowest value is model 5, which is related to the first model, as a result of the cutting of the slope in 2 and 3 parts, respectively.

The number of geotextiles reinforcement is one of the simulation’s goals. The variable that will be determined to obtain the number of geotextiles will be all of the landslide data from the LEM process. The final calculation is shown in Fig. 6.

According to Fig. 6, The maximum number of geotextiles is dominated in models 1 and 5. Otherwise, the minimum is shown in variations 4 and 10. The result indicates the relationship in the SF factor. However, the Factor of safety is not only the variable that given an effect on the outcome, but also other parameters such as landslide geometric, the correction factor, and tensile strength of geotextiles.

The actual number of geotextiles is not always interpreted by the minimum SF. According to the findings of the previous report, the lowest landslide Safety Factor does not result in the greatest amount of reinforcement requirements [22]. The terraces model that dividing the slope in half part (model 1) obtains a high number of geotextiles. Otherwise, the few numbers found in models 4, 9, and 10 (five steps on terraces slope). This result is appropriated with the previous study [21]. If the number of steps is increased, SF will rise. However, as step height rises, the SF value decreases.

4 Conclusion

From the result and discussion shows that the terraces model of geotextile design does not influence by SF all the time, but other external variables are also contributed, such as the slope models, resistance moment, and circle radius of the slope. The terraces model is contributing to the number of geotextiles, if the number of terraces steps is increase, the number of geotextiles will decrease. The lowest number of geotextile layers was obtained in this study, which the terraces slope with five steps of total height generates; variation $4(1/5H)$, $9(1/3H)$ and $1(5H)$, and $10(1/4H)$ and $1(5H)$.

References

1. Pramudo LTH (2016) Slope stability analysis with terrace at Sendangmulyo Village, Tirtomoyo. Thesis, Universitas Sebelas Maret, Wonogiri
2. Surjandari NS, Fitri SN, Purwana YM, Setiawan B, Prakosa BB, Djarwanti N (2021) Penggunaan teraseing pada lereng yang menerima beban lalu lintas. Media Sains Indonesia, Banten
3. Berčić T, Ažman-Momirski L (2020) Parametric terracing as optimization of controlled slope intervention. Water 12(3). <https://doi.org/10.3390/w12030634>
4. Sumiyanto S, Patria AN (2010) Pengaruh pembuatan terasering pada lereng terhadap potensi longsor. Dinamika Rekayasa 6(2):50–55
5. Teixeira Guerra AJ, Rodrigues Bezerra JF, da Mota Lima LD, Silva Mendonça JK, Vieira Souza UD, Teixeira Guerra T (2009) Rehabilitation of degraded area by erosion, using soil bioengineering techniques in Bacanga river basin, Sao Luis City-Maranhao State, Brazil. In: EGU general assembly conference abstracts, p 3478
6. Anil KR, Rani G, Adoor P, Rani OPR (2012) Monetary considerations on use of coir geotextiles for soil and water conservation in varying slopes. In: 43rd international erosion control association annual conference 2012
7. Fitri SN (2021) Perkuatan oprit jembatan kali jubang jalan tol pejanggan-brebes timur menggunakan geotekstil. BENTANG: Jurnal Teoritis dan Terapan Bidang Rekayasa Sipil 9 (1):37–46
8. Sekarti DNA (2018) Analisis stabilitas timbunan di jalan tol semarang-solo ruas salatiga-kartasura (Analysis of embankment stability on semarang-solo road segment salatiga-kartasura). Universitas Islam Indonesia, Thesis

9. Ismanti S (2012) Analisis perilaku timbunan dengan perkuatan geosintetik menggunakan software plaxis. Universitas Gajah Mada, Thesis
10. Prakoso A, Mukhlisin M, Junaidi J, Rahardjo P (2019) Analisis penurunan timbunan tanah silt pada proyek jalan ruas giriwoyo-duwet wonogiri. *Wahana Teknik Sipil: Jurnal Pengembangan Teknik Sipil* 24(2):153–165
11. Fauzi IM, Hamdhan IN (2019) Analisis stabilitas lereng dengan perkuatan geotekstil woven akibat pengaruh termal menggunakan metode elemen hingga. *RekaRacana: Jurnal Teknol Sipil* 5(2):61. <https://doi.org/10.26760/rekaracana.v5i2.61>
12. Prasetyo I, Setiawan B, Dananjaya RH (2017) Analisis stabilitas lereng bertingkat dengan perkuatan geotekstil menggunakan metode elemen hingga. *Matriks Teknik Sipil* 5(3)
13. Famungkas F, Suyadi W, Zaika Y (2015) Analisis stabilitas lereng memakai perkuatan geotekstil dengan bantuan perangkat lunak (studi kasus pada sungai parit raya). *Jurnal Mahasiswa Jurusan Teknik Sipil* 1(3):1065
14. Saputro CD, Djarwanti N, Purwana YM (2017) Analisis stabilitas lereng dengan terasering dan perkuatan bronjong di desa sendangmulyo, tirtomoyo, wonogiri. *Matriks Teknik Sipil* 5(1)
15. Chen L, Young MH (2006) Green-Ampt infiltration model for sloping surfaces. *Water Resour Res* 42(7). <https://doi.org/10.1029/2005WR004468>
16. Sauffisseau R, Ahangar Asr A (2018) Numerical investigation of unloading effects due to excavation of geometrically non-homogeneous stratified rock masses using finite element analysis. In: 6th European conference on computational mechanics (ECCM 6)
17. Tang GP, Zhao LH, Li L, Yang F (2015) Stability charts of slopes under typical conditions developed by upper bound limit analysis. *Comput Geotech* 65:233–240. <https://doi.org/10.1016/j.compgeo.2014.12.008>
18. Nasional PSG (2017) Peta Sumber dan Bahaya Gempa Indonesia Tahun 2017. Pus. Litbang Perumahan. dan Pemukiman, Bandung
19. Irsyam M, Cummins PR, Asrurifak M et al (2020) Development of the 2017 national seismic hazard maps of Indonesia. *Earthq Spectra* 36(1_suppl):112–136
20. AASHTO (1990) Design guidelines for use of extensible reinforcements (geosynthetic) for mechanically stabilized earth walls in permanent applications. AASHTO, Washington
21. Surjandari NS, Fitri SN, Purwana YM et al (2021) Slope stability analysis in various Terraces model (case study: Sendangmulyo, Tirtomulyo District, Wonogiri Regency). *J Phys Conf Ser* 1858(1):012005 (IOP Publishing) <https://doi.org/10.1088/1742-6596/1858/1/012005>
22. Sari PTK, Lastiasih Y (2018) A general formulation to describe the empirical prediction of the critical area of a landslide. *J Eng Sci Technol* 13(8):2379–2394

Erosion and Distribution of Total Suspended Sediment (TSS) Using Landsat-8 in Krueng Pase Watershed



Ichwana Ramli¹, Ashfa Achmad², Hairul Basri³, and Atika Izzaty

Abstract Damage and loss of land resources due to improper land management tend to increase erosion. It will affect the production, ecological, and hydrological functions in the upstream watershed area. However, sedimentation that occurs due to erosion often affects the practical life of the dams. The purpose of this research is to estimate erosion and the distribution of Total Suspended Sediments (TSS) geospatially from Landsat-8 imagery data in 2015 and 2019 for Krueng Pase Watershed. The considerable erosion that occurred in 2014 was 117,987.71 tons. While the erosion that occurred in January 2015 was 18,624.45 tons, and the erosion in August 2019 was 6,672.06 tons. The results of the TSS distribution using algorithms in 2015 obtained the largest total suspended sediment with a value >17.15 mg/l found on the coastal, riverbanks and the smallest TSS with a value of ≤ 12.73 mg/l found on the upstream area. The TSS were found on the coastal with a value of >16.05 mg/l, and the smallest TSS >12.92 mg/l found on the upstream area in 2019. Information on the distribution of total sediment is a

I. Ramli (✉)

Agricultural Engineering Department, Universitas Syiah Kuala, 23111 Banda Aceh, Indonesia

e-mail: ichwana.ramli@unsyiah.ac.id

A. Achmad

Architecture and Planning Department, Universitas Syiah Kuala, 23111 Banda Aceh, Indonesia

H. Basri

Department of Soil Science, Faculty of Agriculture, Universitas Syiah Kuala, 23111 Banda Aceh, Indonesia

A. Izzaty

Geomatics Engineering Department, Institut Teknologi Sepuluh Nopember, 60111 Surabaya, Indonesia

I. Ramli

Research Center for Environmental and Natural Resources, Universitas Syiah Kuala, 23111 Banda Aceh, Indonesia

Department of Environmental Master's Program, Universitas Syiah Kuala, 23111 Banda Aceh, Indonesia

© The Author(s), under exclusive license to Springer Nature Singapore Pte Ltd. 2022

H. A. Lie et al. (eds.), *Proceedings of the Second International Conference of Construction, Infrastructure, and Materials*, Lecture Notes in Civil Engineering 216, https://doi.org/10.1007/978-981-16-7949-0_3

consideration in the application of the eco-hydrology concept as a short-term solution in water management.

Keywords Erosion · Total suspended sediment · Landsat-8

1 Introduction

The issue of soil erosion and sediment loads in watersheds is one of the hot spots that are currently of concern. River sediment loads are influenced by changes in land cover due to climate change in the watershed in an integrated manner [1]. If the sedimentation in the river is high, it can cause the river's capacity to decrease in terms of discharge. Several studies have stated that the most prominent natural factors include meteorology, geology, topography, the composition of the earth's surface and vegetation cover, as well as human activities that play a positive and negative role in soil erosion. Human activities change the hydrological cycle through land use change, the construction of dams and reservoirs, and the withdrawal of surface and groundwater [2]. The Krueng Pase watershed experiences flooding every year, there is a change in land use due to an increase in population, migration, and this has resulted in the expansion of the built-up area and reducing the area of vegetation [3]. Soil erosion and sediment transport at the watershed scale can be estimated using water and sediment balance models that take into account topography, soil properties, land cover, and land use [4, 5].

Sediment measurements can be carried out directly by measuring sediment deposits in rivers. However, direct measurements are sometimes difficult to do due to various constraints, such as limited tools. Advances in earth observation satellite technology for monitoring natural resources and for monitoring environmental quality. This is a change in human work that is expected to be realized as the implementation of government programs through industrial technology 4.0. With increasingly sophisticated spectral sensors and algorithms that are constantly being developed, detection of environmental quality parameters. Therefore, this study aims to estimate the erosion with the Modified Universal Soil Loss Equation (MUSLE) method and distribution of total suspended sediment using Landsat-8 image data and algorithms.

2 Methods

This research was conducted in the Krueng Pase Watershed (Fig. 1). It is located between 5°09'12"–4°49'25" North Latitude and 96°51'27"–97°14'55" East Longitude. The Krueng Pase watershed is located in Lhokseumawe city, Aceh Utara district, and Bener Meriah district. The types of data used are secondary data and primary data. Secondary data, which is needed is rainfall, watershed

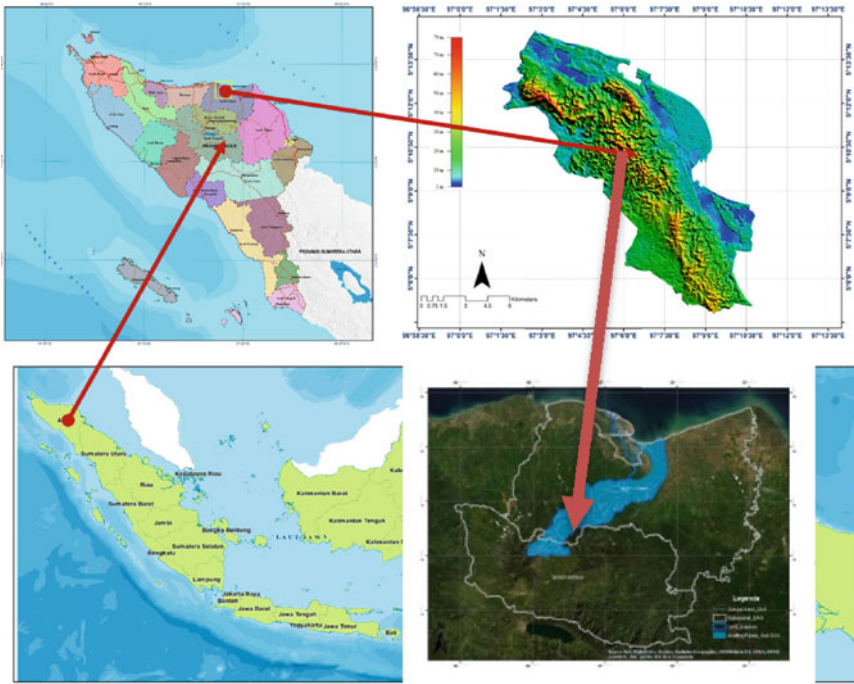


Fig. 1 Location of the research. *Source* <http://portal.ina-sdi.or.id/home/>; <http://tides.big.go.id/DEMNAS/>

characteristics, types of resistance, land use. Primary data in the form of Landsat Satellite Imagery for 2015 and 2019, obtained at <http://earthexplorer.usgs.gov/>. This year’s selection is based more on the availability of images that have less than 5% cloud.

2.1 Stage of Calculating Erosion

The analysis of the erosion’s amount in the Krueng Pase watershed uses the MUSLE equation (Eq. 1) [6].

$$Y = 11.8(Q \times Qp)^{0.56}(K \times C \times P \times LS) \tag{1}$$

where

- Y the resulting erosion (ton);
- Q surface runoff;
- Qp peak discharge;

- K soil erodibility factor;
 C land cover factor;
 P land management factors;
 LS slope factor;

The determination of surface run-off based on the SCS method (Soil Conservation Services method) is shown in Eq. 2.

$$Q = \frac{(P - Ia)^2}{(P - Ia) + S} \quad (2)$$

The Ia value can also vary according to soil conditions and land cover types, although the Ia value varies for each region. In general, the Ia value for $P \geq Ia$ is $Ia = 0.2S$. According to [7], S value is the maximum potential water retention (potential maximum retention) as calculated in Eq. 3.

$$S = \frac{25400}{CN} - 254 \quad (3)$$

where

- Q runoff volume (mm);
 P rainfall (mm);
 S maximum potential water retention (mm/year);
 CN *curve number*.

Determining the value of the peak discharge using the rational method [8] is shown in Eq. 4.

$$Qp = 0.278 \times C \times I \times A \quad (4)$$

where

- Qp Peak discharge (m^3/s);
 C flow coefficient;
 I Maximum rain intensity (mm/h);
 A Watershed area (km^2).

2.2 Steps to Calculate Total Suspended Sediment

- 1 The corrections made to Landsat images are radiometric corrections consisting of radiometric calibration and atmospheric correction. Radiometric calibration is an improvement due to errors in the optical system, errors due to interference

from electromagnetic radiation energy in the atmosphere, and errors due to the influence of the sun's elevation angle.

- 2 Atmospheric correction aims to derive the object reflectance from the total radiance ToA (Top of Atmosphere) after normalizing the lighting conditions and eliminating atmospheric effects. This stage produces surface reflectance value data from Landsat 8 images. Radiometric calibration is done by converting the Digital Number (DN) to a Radian value and or a ToA reflectance value.
- 3 After the satellite imagery data is corrected for atmospheric correction to get the corrected reflectance value, then the separation between land and sea is carried out using the land water algorithm [9]. To determine the separation boundary between the oceans, in this study, the NDWI (Normalized Difference Water Index) algorithm was used. This is done by dividing the image data into 2 pixel values. If the NDWI value is > 0 , then the area is land and if $NDWI < 0$, the area is water. Band 3 (Green) and band 5 (Near-Infrared) are used to produce the correct NDWI value based on Landsat-8 satellite imagery. With the separation between the land and the sea, it can be seen the identified part of the occurrence of sediment.
- 4 Calculating TSS is calculated spatially from Landsat-8 image data. The processed data is Landsat-8 image data which is a subset according to the area. The sensor type is changed from radiance to reflectance using Band Math on Bands 5, 4, 3, 2. As a representation of the band that has been converted into reflectance, it is used the following algorithm with $(\log_{10} (rrs_band_2))/(\log_{10} (rrs_band_4))$.

Algorithm formula used [10] is shown in Eq. 5.

$$TSS = \left(31.42 \left(\frac{\text{Log}(\text{band } 3)}{\text{Log}(\text{band } 4)} \right) \right) - 12.719 \quad (5)$$

3 Results and Discussion

In general, the soil conditions of the Krueng Pase watershed have moderate to good ability to withstand erosion, and soil types were obtained from Bappeda in 2019. There are four types of soil in the Krueng Pase watershed, namely inceptisol (30.01%) andisol (1.49%), Entisol-inceptisol (0.1%), and ultisol (68.4%). Each type of soil has a different erodibility (K), which indicates the soil's ability to withstand erosion. The higher the K value, the easier the soil will be eroded. Based on the K value, the types of soil that are easily eroded are inceptisol and andisol. While the types of soil that are not easily eroded are ultisol.

The slopes of 0–8% generally have a flat surface relief with an area of 14.31%. This area is an area that is used as land for agricultural development, urban development. Slopes 8–15% with an area of 10.67%. The area with this sloping condition is to be used as a location for the development of plantation cultivation.

Slopes 15–25% with an area of 1.23%. This area is a primary dryland forest area dan built-up area. Slope 25–40% with an area of 73.8%. Areas and areas with this slope are hilly areas or primary dryland forest areas.

3.1 Erosion

Overlay data on land use, rainfall, slope, and soil type resulted in potential erosion occurring in the Krueng Pase watershed. In this research, land use is classified into six types, namely forest, built-up area, agriculture, mixed agriculture, wetland, and water body. Land use based on the 2019 image classification consisting of forest 53.13%, built-up area (4.17%), agriculture (36.92%), mixed agriculture (2.18%), wetland (1.9%), and water body (1.69%). Land use agriculture category including areas being utilized by cropland, rice fields, livestock land, grasslands. Built-up areas including urban, residential, industrial, road, and other made structures. Mix agriculture, including land covered by more than one type of perennials and is not uniform. Water body includes seas and rivers, whereas wetland includes fish ponds and land that is saturated with water.

Run off is an important element in the water cycle and one of the causes of erosion. The calculation of run-off uses Eq. 2, where the parameters needed are rainfall and retention values. The retention value uses Eq. 3. The calculation of the retention value requires the curve number value parameter. The highest run off occurred in 2014 at 31,754.94 mm.

One of the other parameters in calculating erosion using the MUSLE method is peak discharge. Peak discharge using a rational method which is influenced by the watershed area, rainfall intensity, and run-off coefficient. The run-off coefficient obtained is 0.19. This means that the run-off water in the watershed is 19%, while 81% becomes groundwater storage. Each land use in the Krueng Pase watershed has a different coefficient value for agricultural land (0.4), settlement (0.6), forest (0.02), mixed garden (0.1), the body of water (0.05), and wetland (0.15).

The increase and decrease in surface run-off every year is due to the high and low rainfall that occurs. This results in a different intensity of rainfall each year. The peak discharge (Eq. 4) that occurred between 2011 and 2020 varied between 40 m³/s (in 2019) and 810.21 m³/s (2014). Meanwhile, the peak discharge in 2015 was 262.48 m³/s. The decrease and increase in erosion are influenced by surface run-off, peak discharge, soil erodibility, slope and land cover, and land management.

Erosion and run-off that occurred in 2011–2020 can be seen in Table 1. From the results of the analysis using the MUSLE formula, erosion that occurred as the highest is upstream. The highest erosion occurred in 2014 at 117,987.71 tons with a run-off of 31,754.94 mm at an annual average rainfall of 145 mm/year. In this study, Land use 2019 is used to calculate run-off in erosion analysis from 2011 to 2020. The size of the erosion was different each year depending on the rainfall.

Table 1 Erosion and run off that occurred in 2011–2020

Year	Erosion (ton)	Average annual rainfall (mm/year)	Run off (mm)
2011	32,701.26	135.92	27,854.56
2012	34,902.59	115.75	22,781.17
2013	31,409.37	109.67	19,084.75
2014	117,987.71	145.17	31,754.94
2015	42,343.85	110.50	20,867.80
2016	16,185.23	91.50	15,837.70
2017	49,596.43	148.92	29,976.94
2018	34,902.59	119.67	23,005.87
2019	6,869.98	80.83	12,076.86
2020	78,438.54	123.58	26,143.50

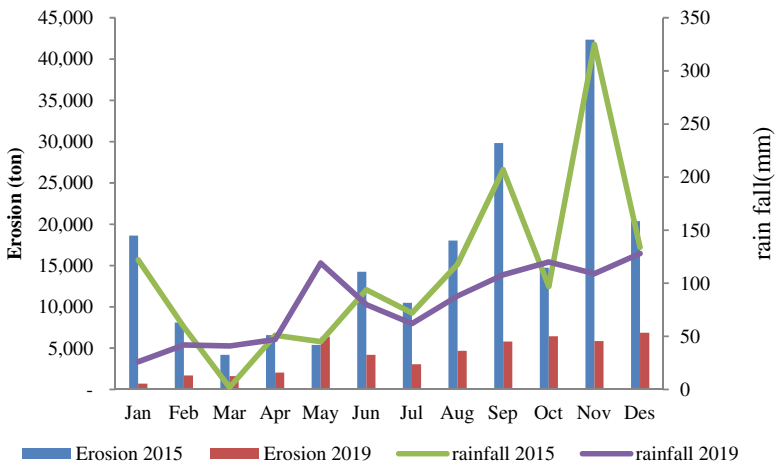


Fig. 2 Comparison of monthly rainfall erosion in 2015 and 2019

Figure 2 shows the difference in erosion between 2015 and 2019. The selection of the period is adjusted to the image to estimate cementation. When compared to the erosion that occurred between 2015 and 2019 (according to the image for sedimentation analysis, the largest erosion, which amounted to 42,343.85 tons, occurred in 2015, while the erosion in August 2019 was 6,869.98 tons. There was a decrease in the amount of erosion from the two observation periods. During the period 2011–2020, the lowest erosion occurred in 2019 as shown in Table 1.

Erosion is influenced by different land uses, the relationship between run-off, erosion on various land uses can be seen in Fig. 3. The largest run-off occurs on agricultural land and the smallest on the wetland. The increase and decrease in a surface run-off in various land use are influenced by different rainfall and curve

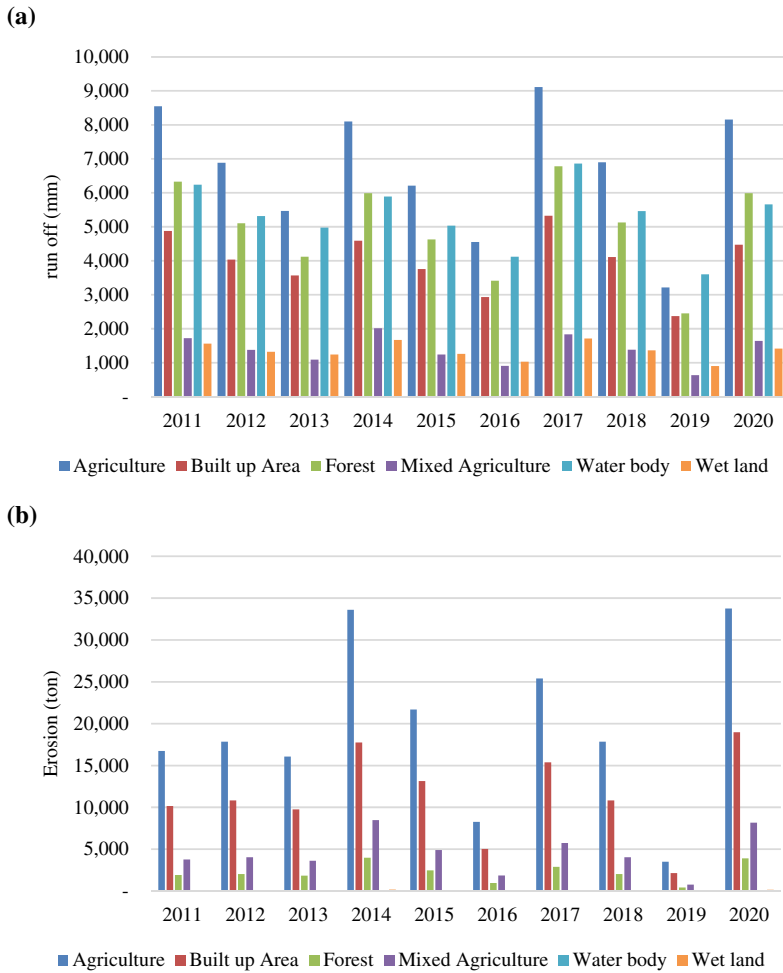


Fig. 3 a Surface run-off on land use from 2011 to 2020, b erosion based on land use from 2011 to 2020

number values. The erosion occurs based on land use. The highest erosion occurred on agricultural land, built-up areas, and mixed gardens. While the highest run-off occurs on agricultural land, which is on a slope less than 8% (11,289.52 ha) and 8–15% (2210.07 ha) with inceptisol soil types that are easily eroded.

3.2 Sedimentation

Sediment is the result of the process of erosion. Eroded soil will settle in one place. Sediment is influenced by all watershed biophysics, namely land use, the slope of soil type, surface run-off, and peak discharge. Damage to land resources, especially in the upstream part of the watershed, will reduce land productivity, affect production functions, ecological functions, and watershed hydrological functions [11].

NDWI can detect the extent of surface water areas and is useful in understanding the dynamics of surface water in basins and is effectively used in water resource management [12, 13]. NDWI is an indicator of moisture content in vegetation and land surface temperature [14]. Water index derived from satellite data is an effective use in the management of water resources. As a result of erosion and subsequent sedimentation can cause water quality to exceed the quality standard.

Based on the results of the application of the algorithm on the reflectance data of Landsat 8 images in the Kreung Pase watershed (Fig. 4), in 2015, the largest total suspended sediment with a value >17.15 mg/l was found on the coast and riverbanks and the smallest suspended sediment with a value of <12.73 mg/l upstream of the Krueng Pase watershed. The results of suspended sediment in 2019 also contained the largest suspended coast with a value of >16.05 mg/l and the smallest suspended with a value of <12.92 mg/l in the upstream part of the Krueng Pase watershed. Although the image used on January 8, 2015, when the rainfall in January 2015 was 122 mm, while the image in August 2019 when the rainfall in August 2019 was 88 mm. The results of the sedimentation calculation above use [12] and there are several other logarithms that can calculate TSS from the image and need to be tested for validation from water samples.

One of the important indicators for determining the damage of a watershed is its hydrological condition which is characterized by erosion, landslides, sedimentation, and unbalanced flow distribution (flood and drought). Another indicator can be seen

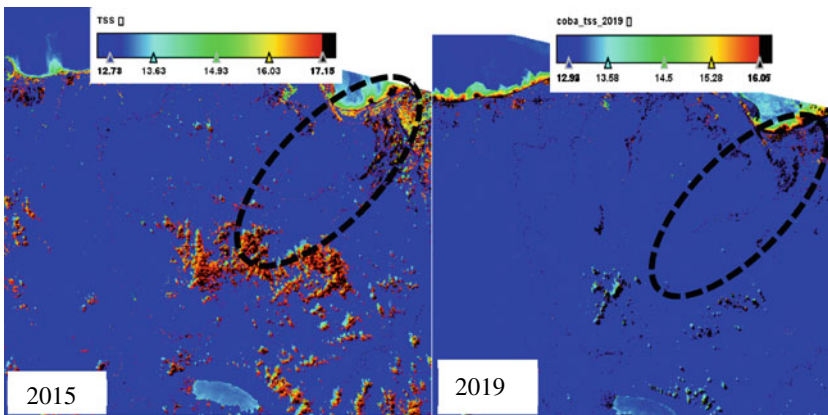


Fig. 4 Sediment distribution in January 2015 and August 2019 at the study location

from the shrinking of forest areas and damage to land, especially the protected areas around the watershed. This is due to the increasing population, which increases the intensity of land and water use [15]. Watersheds that are characterized by dry and semi-arid water will be eroded and sediment transport which can cause soil fertility to gradually decline. In addition, clogged sedimentation in waterways also allows the transfer of pollutants to agricultural land and dams so that it can interfere with the quality of drinking water and irrigation water as well as the age of the water building [16].

TSS is a reflection of the dynamics of changes in the ecology of waters and land. TSS is also an early indicator of the possibility of sedimentation in water areas. A high TSS value will indicate a high level of pollution. TSS concentration can be caused by various things, namely the level of turbidity in the waters and the level of sedimentation brought about by the flow of water that empties into the location of these waters. It can be said that suspended solids content is an early indicator of signs of sedimentation in waters, so that the concept of eco-hydrology becomes a consideration in land and water management.

4 Conclusion

1. The highest erosion occurred in 2014 of 117,987.71 tons with a run-off of 31,754.94 mm at an average annual rainfall of 145.17 mm/year, and in agricultural land use, erosion and run-off are highest.
2. Total suspended sediment in Kreung Pase watershed using Landsat 8 image, which was observed in January 2015 rainfall of 122 mm was > 17.15 mg/l was found on the coast and riverbanks and the smallest suspended sediment with a value of < 12.73 m/l upstream of the Krueng Pase watershed.
3. The results of suspended sediment in august 2019 with rainfall of 88 mm, also contained the largest suspended coast with a value of > 16.05 mg/l and the smallest suspended with a value of < 12.92 mg/l in the upstream part of the Krueng Pase watershed. With 88 mm of rainfall. Sedimentation distribution can be obtained from the image using the logarithm, but there needs to be validation from the sample in the field to get the TSS value.

Acknowledgements The authors thanks to BAPPEDA and BMKG Indrapuri Aceh for supporting this research. Also thanks to Universitas Syiah Kuala for funding this research with contract number 167/UN11/SPK/PNBP/2021 tanggal 19 Februari 2021.

References

1. Pijl A, Brauer CC, Sofia G, Teuling AJ, Tarolli P (2018) Hydrologic impacts of changing land use and climate in the Veneto lowlands of Italy. *Anthropocene* 22:20–30. <https://doi.org/10.1016/j.ancene.2018.04.001>
2. Nasution Z (2013) Determining groundwater recharge from stream flow with seasonal recession method. *Aceh Int J Sci Technol* 2(1):8–16
3. Achmad A, Ramli I, Irwansyah M (2020) The impacts of land use and cover changes on ecosystem services value in urban highland areas. *IOP Conf Ser Earth Environ Sci* 447 (1):012047 (IOP Publishing)
4. Bisantino T, Bingner R, Chouaib W, Gentile F, Trisorio Liuzzi G (2015) Estimation of runoff, peak discharge and sediment load at the event scale in a medium-size Mediterranean watershed using the AnnAGNPS model. *Land Degrad Dev* 26(4):340–355. <https://doi.org/10.1002/ldr.2213>
5. Yüce Mİ, Eşit M, Ercan B (2018) A relationship between flow discharge, sediment discharge and sub-basin areas in Ceyhan catchment. In: 13th international congress on advances in civil engineering, Izmir/TURKEY
6. Williams JR (1975) Sediment routing for agricultural watersheds 1. *JAWRA J Am Water Resour Assoc* 11(5):965–974
7. Schwab GO, Frevert RK, Edminster TW, Barnes KK (1981) *Soil and water conservation engineering: (3th edn)*. Wiley, New York, p 525. ISBN 0–471–03078–3
8. Chow VT, Maidment DR, Larry W (1988) *Mays. Applied hydrology*, International edition. MacGraw-Hill, Inc., United States
9. Guo Q, Pu R, Li J, Cheng J (2017) A weighted normalized difference water index for water extraction using Landsat imagery. *Int J Remote Sens* 38(19):5430–5445
10. Lailia NL, Arafah F, Jaelani A, Pamungkas AD (2015) Development of water quality parameter retrieval algorithms for estimating total suspended solids and chlorophyll-A concentration using Landsat-8 imagery at Poteran island water. *Remote Sens Spat Inf Sci* 2(2)
11. Nerantzaki SD, Giannakis GV, Efstathiou D, Nikolaidis NP, Sibetheros IA, Karatzas GP, Zacharias I (2015) Modeling suspended sediment transport and assessing the impacts of climate change in a Karstic Mediterranean watershed. *Sci Total Environ* 538:288–297. <https://doi.org/10.1016/j.scitotenv.2015.07.0929>
12. Campos JC, Sillero N, Brito JC (2012) Normalized difference water indexes have dissimilar performances in detecting seasonal and permanent water in the Sahara-Sahel transition zone. *J Hydrol* 464:438–446. <https://doi.org/10.1016/j.jhydrol.2012.07.042>
13. Ashtekar AS, Mohammed-Aslam MA, Moosvi AR (2019) Utility of normalized difference water index and GIS for mapping surface water dynamics in sub-upper Krishna Basin. *J Indian Soc Remote Sens* 47(8):1431–1442. <https://doi.org/10.1007/s12524-019-01013-60123>
14. Achmad A, Muftiadi M (2019) The relationship between land surface temperature and water index in the urban area of a tropical city. *IOP Conf Ser Earth Environ Sci* 365(1):012013 (IOP Publishing). <https://doi.org/10.1088/1755-1315/365/1/012013>
15. Basuki TM (2017) Water and sediment yields from two catchments with different land cover areas. *J Degraded Min Lands Manag* 4(4):853
16. Murtadha S, Yussof I, Fauzi R, Ramli I (2017) Analysis of groundwater quality for irrigation purposes in shallow aquifers: a case study from West Aceh, Indonesia. *Singapore J Trop Geogr* 38(2):185–200

Shoreline Change Cause of Abrasion in Bantan District Bengkalis Island as the Outstanding Beach Area



H. Tampubolon

Abstract This research is located in Bengkalis Regency, which is directly opposite the Malacca Strait, and cannot be separated from the problem of coastal abrasion. This abrasion is thought because by the impact of ocean waves and the conversion of land which was originally mangroves into oil palm plantations. The purpose of the study is to determine the characteristics and problems that exist in the coastal area and causes of changes in the coastline, both technically and non-technically which have an impact on reducing the boundaries of the sovereignty of the State of Indonesia. The methodology based on visual observations and primary data such as bathymetry, tides, wave height, wave direction, wave period and wind. Bantan District is flat to wavy, the type of soil in Bantan District very susceptible to abrasion, if this is allowed to result in land loss around the coast, agricultural crops and community land. This condition is triggered by high waves which are estimated to be as high as 3 m and erode the land. The placement of breakwater structures and hybrid engineering have been carried out for coastal protection after there is sediment deposition to overcome the problem of abrasion.

Keywords Shoreline • Abrasion • Bantan

1 Introduction

Indonesia is an archipelagic country, in addition to causing the land area to be smaller than the ocean area. Geographically, Indonesia's territory, especially in this case, Riau Province, is directly adjacent to neighboring countries such as Malaysia and Singapore.

Riau Province has a total area of 87,023.66 km² with a coastline of 3201.95 km, directly opposite the Malacca Strait, including the Bantan District located in

H. Tampubolon (✉)
University of Riau, Riau, Indonesia
e-mail: lilyartha1234@gmail.com

Bengkalis Regency and is one of the outer islands in Riau Province, which is experiencing coastal abrasion problems.

Observation Background Changes in geomorphological processes result from a number of oceanographic parameters that play a role, such as waves, currents, and tides [1]. This abrasion is caused by the impact of ocean waves and the conversion of land which was originally mangroves into oil palm plantations. The waves come from the Andaman Sea, where there is a large fetch whose height is further magnified by narrowing the waters in the Malacca Strait. The study by [2] stated that the average abrasion on Bengkalis Island reached 32.75 m per year. Dynamic nature is an indicator of coastal erosion and accretion [3]. The regional map of Bantan District is shown in Fig. 1.

This threatens the lives of coastal residents and the tourism sector of Riau, as well as the diminishing boundaries of the sovereignty of the Republic of Indonesia, which are caused by the retreat of the coastline. The purpose of this study is to determine the characteristics and problems that exist in the coastal area and the causes of changes in the coastline, both technically and non-technically which have an impact on reducing the boundaries of the sovereignty of the State of Indonesia.



Fig. 1 Regional map of Bantan district. Source The Central Bureau of Statistics

2 Methodology

2.1 Research Sites

Bantan District is one of the districts in Bengkalis Regency, precisely on the island of Bengkalis, with an area of 495 km², where the largest village is Bantan Tua with an area of 39 km² or 7.88% of the total area of Bantan District. Bantan District is flat to wavy, the type of soil in Bantan District is organic soil which is very susceptible to abrasion. As reported by [4], the northern part of Bengkalis Island is directly adjacent to the Malacca Strait, so that the influence of waves and currents that occur there is quite large.

Research data in the form of primary data originating from the observation location and secondary data from the relevant department in Bengkalis Regency as well as interviews with the community at the observation location. In general, the condition of this beach is not so potential because it does not have white sand, and most of the coastline area is only used as an area for coconut plantations and shrubs. Located at an altitude of 2–5 m above sea level, it has a tropical climate with air temperatures ranging from 26 to 30 °C. The state of rainfall every year with an average of 189.1 m²/year. Geographically it is located at 1020.00 East Longitude—102°30'29" East Longitude and 10.15 North Latitude—1°36'43" North Latitude, based on observations at the research location in Bantan district, Bengkalis Regency in 2020 there was cliff damage that had an impact on public facilities, and setbacks. Coastline, whose position is on the outermost island and affects the boundaries of the sovereignty of the Republic of Indonesia. This location is a natural beach area and some (at some points) are used as tourist attractions. The location of an unspoiled beach with a high level of abrasion is in Muntai village. While the beaches used as tourist attractions are Parit 2 beach, Parit 3 beach and Madani beach which is located in Teluk Pambang Village. The location of the coast that experienced a decline in coastline due to abrasion can be seen in Figs. 2 and 3. The picture shows the damage caused by abrasion and also changes in the shoreline from 2015 to 2019.

2.2 Wave Period

The wind causes ocean waves, therefore wind data can be used to estimate the height and direction of waves at the study site. Wind data is needed as input data in wave forecasting so that the design wave height is obtained. Wind data required is hourly wind data along with information about its direction. Analysis of the design wind distribution pattern in the study area was also carried out using various distributions, namely the Log-Normal, Pearson, Log Pearson, and Gumbel distributions. Furthermore, the most suitable distribution will be obtained to be applied to the wind patterns that occur in the study area. Maximum wind speed at the study site is shown in Table 1.



Fig. 2 Villages affected by abrasion (Parit 3, Parit Madani, Parit 2) in Bantan district

To get the design wave, a post-wave forecast is carried out based on long-term wind data. The method applied follows the Method given in the Shore Protection Manual [5] edition which is a standard reference for practitioners of coastal development, protection and preservation works. Long-term wind data, a minimum of 10 years, provide more convincing statistical data for this hindcasting method. To forecast waves in water required input in the form of wind data and bathymetry

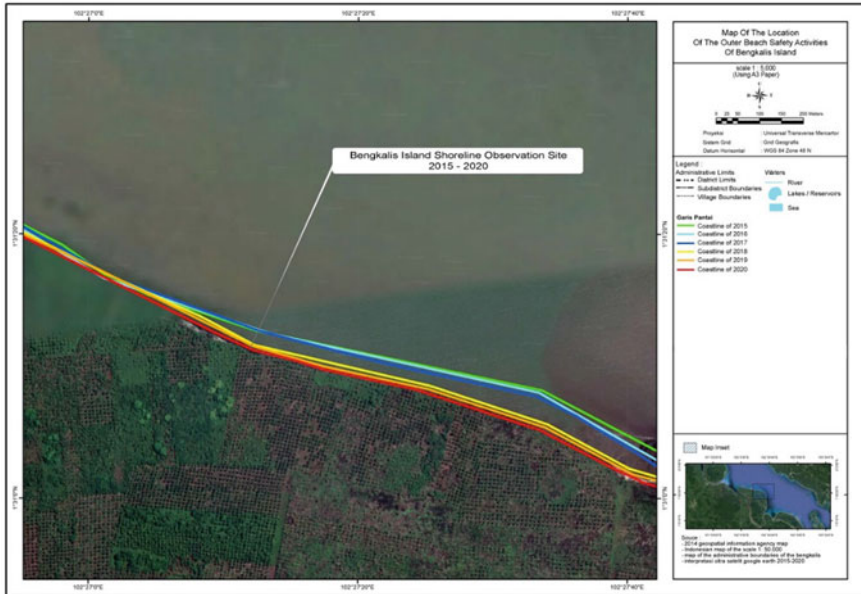


Fig. 3 Shoreline changes from 2015 to 2020

Table 1 Bengkalis Island effective fetch calculation results

No	Direction		Effective fetch (m)
1	N	North	64.77
2	NE	North East	52.792
3	E	East	105.989
4	SE	South East	82.662
5	S	South	—
6	SW	South West	—
7	W	West	—
8	NW	North West	120.058

maps. The interaction between the wind and the surface of the water causes waves (wind-induced waves). A map of the location and surrounding waters is needed to determine the size of the “fetch” or wave formation area, the fetch length is measured from the observation point at 50 intervals.

2.3 Modeling Methodology

Wave forecasting is based on wind data as the main wave generator and wave formation area (fetch). The wind data used is obtained from BMKG Tanjung Balai Karimun wind data from 2010 to 2019.

Wind climate data is presented in the form of monthly windrose or in total. The total windrose is presented in Fig. 4, while the distribution of the number and percentage of wind events is presented in Tables 2 and 3.

2.4 Shoreline Change Modeling

One of the problems in this research is to determine the pattern of sediment movement or the pattern of shoreline changes that have occurred or will occur in a certain period of time. By knowing the pattern that occurs, it will be easy to study the characteristics of the beach.

Sediment transport analysis was carried out to obtain the following parameters:

1. The rate of bottom sediment transport, whether caused by currents alone or a combination of currents and waves.
2. The rate of deposition of floating sediments in harbor ponds and shipping lanes.

According to the Shore Protection Manual 1984 [5], the longshore transport of sedimentary material is called longshore transport. The naming of longshore

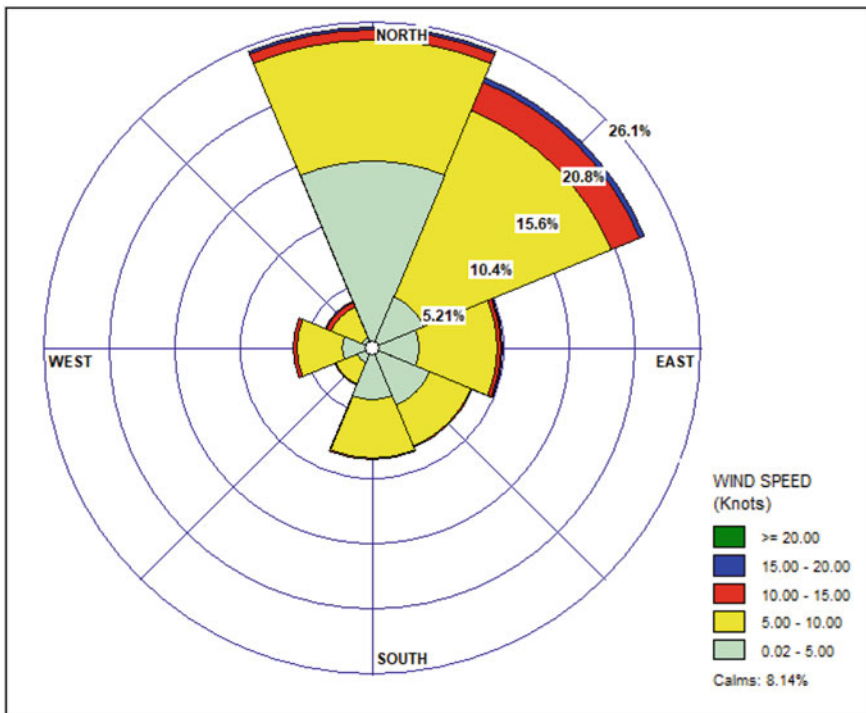


Fig. 4 Total windrose from wind observation station at BMKG Tanjung Balai Karimun

Table 2 Distribution of total wind speed and direction of BMKG Tanjung Balai Karimun (number of hours)

Direction	Number of hours					Total
	<5	5–10	10–15	15–20	>20	
North	13,096	8399	688	168	32	22,383
North East	3888	14,016	2152	360	32	20,448
East	3264	5400	288	64	8	9024
South East	4360	3072	96	48	0	7576
South	3672	4008	152	0	0	7832
South West	1136	1640	40	16	0	2832
West	2096	3160	256	16	8	5536
North West	784	2360	360	24	0	3528
Windy						79,159
Not windy						7128
Not recorded						1313
Total						87,600

Table 3 Distribution of total wind speed and direction of BMKG Tanjung Balai Karimun (percentage)

Direction	Percentage					Total
	<5	5–10	10–15	15–20	>20	
North	14.95	9.59	0.79	0.19	0.04	25.55
North East	4.44	16	2.46	0.41	0.04	23.34
East	3.73	6.16	0.33	0.07	0.01	10.30
South East	4.98	3.51	0.11	0.05	0	8.65
South	4.19	4.58	0.17	0	0	8.94
South West	1.30	1.87	0.05	0.02	0	3.23
West	2.39	3.61	0.29	0.02	0.01	6.32
North West	0.89	2.69	0.41	0.03	0	4.03
Windy						90.36
Not windy						8.14
Not recorded						1.5
Total						100.00

transport has the same meaning as littoral transport or the movement of littoral drift, which is sediment that moves in the littoral zone. The littoral zone in coastal terminology is the area of water from the shoreline to just before the wave area breaks.

In determining the pattern of sediment movement or the pattern of shoreline changes that occur or will occur over a certain period of time, the GENESIS (Generalized Model for Simulating Shoreline Change) simulation program from the US Army Corps of Engineers (ASCE) is used.

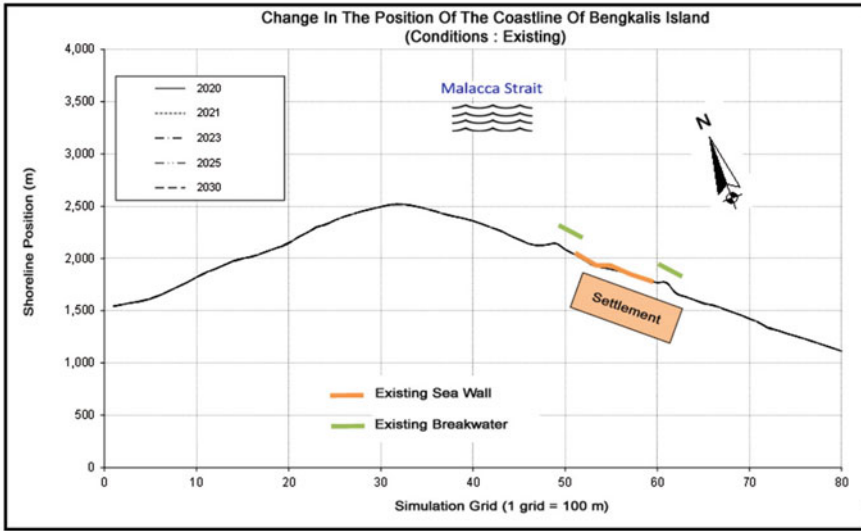


Fig. 5 Layout modeling the shoreline of the existing condition of the Bengkalis Island

Because the movement is parallel to the coast, there are two possible directions of movement, namely towards the right and left relative to an observer standing on the beach facing the sea, as shown in Figs. 5 and 6.

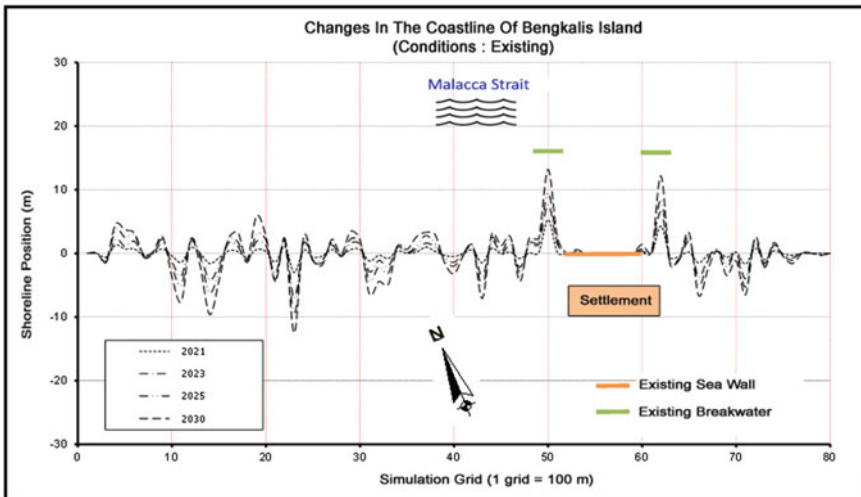


Fig. 6 Changes to the shoreline of the existing condition of Bengkalis Island

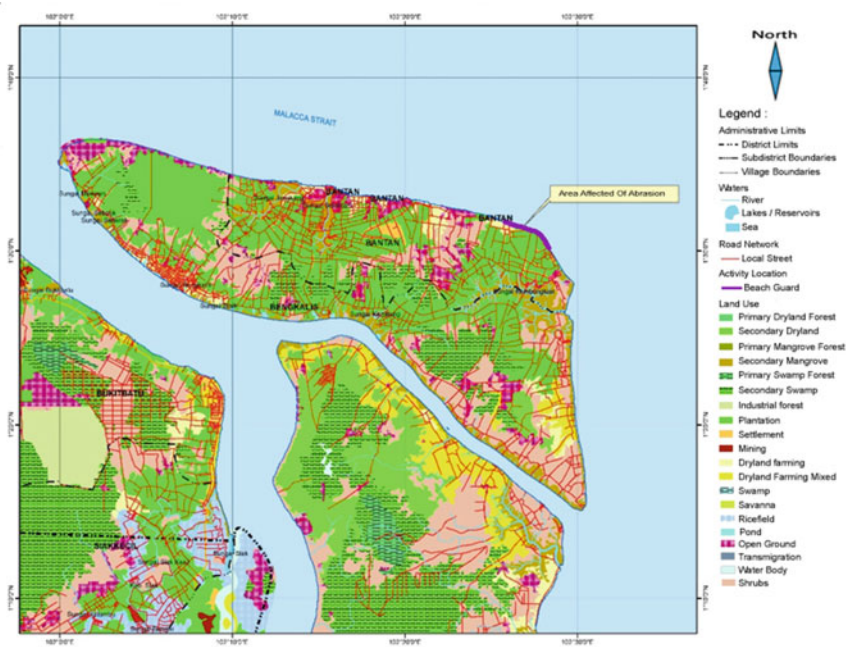


Fig. 7 Measurement and Bathymetry of Bengkalis Island

3 Discussion

3.1 Bathymetry

Bathymetry surveys or often also called sounding, are carried out to measure and observe the depth of the water using a depth measuring instrument so that an overview of the seabed formation, positions of large rocks, or the position of objects that can affect wave and current deformation can be obtained seen in Figs. 7 and 8.

Refraction/diffraction analysis that requires a rather large area of water can be obtained from the Hydro-Oceanography Service of the Indonesian Navy (DISHIDROSAL).

3.2 Tides

The coastal environment of Bengkalis Island that is of concern is the condition of coastal erosion that has occurred every time. This erosion event resulted in the reduction of the shoreline to be more protruding into the sea. Suppose this is allowed to result in land loss around the coast. Likewise, public facilities around the

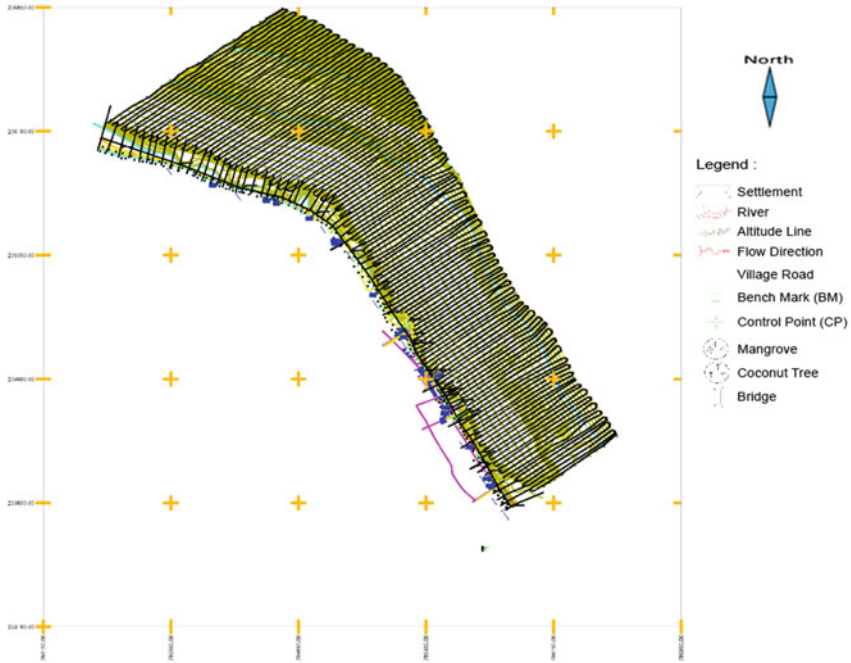


Fig. 8 Topographic map and Bathymetry of Bengkalis Island

coast will be disturbed and even lost due to the brunt of the water, both from waves and from the ebb and flow of seawater.

Tides are the movement of rising and falling sea levels, where the amplitude and phase are directly related to periodic geophysical forces. In this case, sea level elevation (Mean High Water Level, Mean Low Water Level, Mean Sea Level) is determined based on tidal measurements for a minimum of 15 days. Measurements are carried out using a local topographic system at the worksite/project location. With 15 days of observation, one tidal cycle has been covered which includes spring tides and neap tides, as shown in Tables 4 and 5 and Fig. 9 for tidal chart.

3.3 *Beach Sedimentation*

Sediment produced by the erosion process and carried away by the flow of water will be deposited in a place where the speed of the water slows down or stops. This depositional event is known as a sedimentation event or process [6].

A sampling of basic and suspended sediments was carried out at the same time and position as the current measurement. Time of collection is also done at spring

Table 4 Bengkalis Island plan wave 0–12 (waves in the deep sea)

Tidal analysis table (admiralty method)													
									Altitude:		0 0 0 South altitude		
Short series (15 days) in 2020			Location: Bengkalis Island						Longitude:		0 0 0 West longitude		
Date	Time												
	0	1	2	3	4	5	6	7	8	9	10	11	12
24-Jun	230	180	130	100	85	35	40	60	110	150	170	180	155
25-Jun	270	190	110	80	45	19	15	35	70	130	150	170	160
26-Jun	250	220	190	150	120	80	55	55	60	115	150	170	180
27-Jun	240	230	180	160	130	105	80	60	40	75	200	180	170
28-Jun	190	200	180	160	150	140	120	100	50	55	70	90	120
29-Jun	130	160	190	150	120	110	95	95	70	55	55	85	100
30-Jun	95	100	116	125	140	160	140	110	80	60	60	60	70
1-Jul	75	80	105	140	140	145	140	140	110	80	60	45	30
2-Jul	55	60	70	80	120	145	170	155	140	130	100	70	45
3-Jul	80	50	45	75	125	140	160	180	150	130	100	70	50
4-Jul	100	75	60	50	55	110	140	165	180	160	130	90	50
5-Jul	160	100	75	45	85	110	160	180	190	190	170	120	50
6-Jul	180	150	130	125	95	80	75	100	160	190	165	160	130
7-Jul	220	180	160	140	30	50	60	170	185	190	195	200	180
8-Jul	220	160	140	110	60	70	75	80	110	130	150	180	165

tide and neap tide. The results of the sediment samples obtained were then tested in the laboratory to obtain the characteristics of the sediment samples, namely d50 and specific gravity, as shown in Table 6.

3.4 Wave Height

The wave height used as input data for this numerical model is the wave height obtained from the post-wave forecast based on long-term wind data. According to information from the local community and based on observations in the field, the abrasion at this location is very disturbing. The abrasion that has occurred has worried residents because agricultural crops and community land have been lost. So that residents expect from the government of Bengkalis Regency to immediately anticipate the damage caused by this abrasion. This condition is triggered by high waves which are estimated to be as high as 3 m and erode the land. This location is on the edge of the beach facing the Malacca strait, which if not addressed immediately can drift and turn into the ocean.

Table 5 Bengkalis Island plan wave 13–23 (waves in the deep sea)

Tidal analysis table (admiralty methode)												
							Altitude:	0 0 0 South altitude				
Short series (15 days) in 2020							Longitude:	0 0 0 West longitude				
Date	Time											
	13	14	15	16	17	18	19	20	21	22	23	
24-Jun	120	75	35	10	2	23	70	120	150	230	240	
25-Jun	120	105	60	35	15	10	50	110	180	200	230	
26-Jun	160	150	100	70	40	20	23	60	130	180	235	
27-Jun	160	150	130	110	80	50	55	55	140	155	170	
28-Jun	140	130	120	100	90	70	50	45	35	3	50	
29-Jun	140	165	180	175	150	140	100	80	40	35	50	
30-Jun	120	140	160	175	190	170	150	125	90	80	60	
1-Jul	10	130	170	200	220	240	200	170	130	120	100	
2-Jul	55	65	110	150	180	220	240	260	240	170	100	
3-Jul	20	15	100	110	180	230	260	240	220	200	140	
4-Jul	30	20	30	50	60	190	240	270	275	260	170	
5-Jul	40	15	40	80	100	150	230	250	270	260	200	
6-Jul	75	40	25	3	45	110	180	250	260	170	170	
7-Jul	70	60	50	80	85	90	130	210	230	260	240	
8-Jul	150	130	100	70	30	85	140	180	210	220	230	

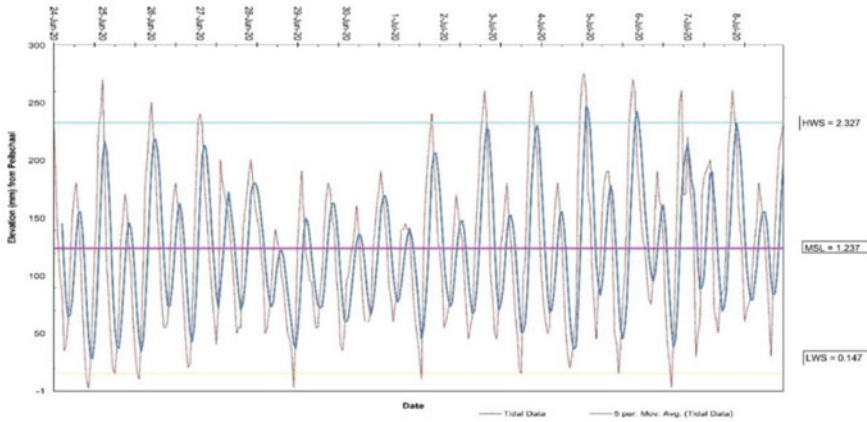


Fig. 9 Tidal chart

Table 6 Description of sediment at the point of retrieval

Sediment 01	00.00–00.10	00.10	Clay, black, medium plastic, medium stiffness, high moisture content
	00.10–00.50	00.40	Clay, brown, medium plastic, moderate stiffness, moderate to high moisture content
Sediment 02	00.00–00.10	00.10	Clay, blackish, medium plastic, moderate stiffness, high moisture content
	00.10–00.50	00.40	Clay, brown, medium plastic, medium stiffness, high moisture content
Sediment 03	00.00–00.15	00.15	Clay, blackish, medium plastic, medium stiffness, high moisture content
	00.15–00.50	00.35	Clay, yellow, medium plastic high, medium stiffness, high moisture content
Sediment 04	00.00–00.40	00.40	Peat, dark brown, medium plastic, low stiffness, moderate to high moisture content

4 Conclusion

1. Beach conditions in the sub-district are still natural with a very high level of abrasions, such as in Parit 3, Parit 2, and Madani
2. Abrasion on the island can cause the shrinkage of Indonesia's maritime boundaries which are internationally measured from the country's outermost coastline. Abrasion resulting in loss of coastline in the outermost island coast of Riau Province which is directly adjacent to Malaysia and Singapore and the Melaka strait as an international shipping lane
3. Coastal erosion occurs due to changes in the balance of the coast, namely the balance of sediment transport by waves and the supply of sediment
4. To protect houses from the threat of waves, the residents have made sea walls, which are generally upright sea walls without foot protectors as wave absorbers
5. The condition of the waters on Bengkalis Island requires a breakwater to protect the coastline/shoreline which has been eroded by sea waves.

With the existence of a protective building for ocean currents and waves, it will be reduced, and this will actually trigger sedimentation around the breakwater.





References

1. Opa ET (2011) Perubahan garis pantai Desa Bentenan Kecamatan Pusomaen, Minahasa Tenggara. *Jurnal Perikanan dan Kelautan Tropis* 7(3):109–114
2. Sutikno S (2014) Analisis laju abrasi pantai Pulau Bengkalis dengan menggunakan data satelit. In: *Pertemuan Ilmiah Tahunan (PIT) HATHI (Himpunan Ahli Teknik Hidraulik Indonesia) XXXI*, Padang

3. Ghosh MK, Kumar L, Roy C (2015) Monitoring the coastline change of Hatiya Island in Bangladesh using remote sensing techniques. *ISPRS J Photogrammetry Remote Sens* 101:137–144. <https://doi.org/10.1016/j.isprsjprs.2014.12.009>
4. Loka Penelitian Sumberdaya dan Kerentana Pesisir (2012) Laporan Akhir: Kajian Kerentanan Pesisir Berdasarkan Karakteristik dan Geodinamika Pantai (Studi kasus Kab. Agam dan Kab. Bengkalis). BPPKP DKP Bengkalis, Riau
5. Coastal Engineering Research Center (1984) Shore protection manual. US Army Corps of Engineers, Washington DC
6. Rantung MM, Binilang A, Wuisan EM, Halim F (2013) Analisis Erosi dan Sedimentasi Lahan di Sub DAS Panasen Kabupaten Minahasa. *Jurnal Sipil Statik* 1(5):309–317

Nonlinear Effect of Fluid–Structure Interaction Modeling in the Rock-Fill Dam Jatiluhur



Albert Sulaiman , Wati A. Pranoto , Tati Zera ,
and Mouli De Rizka Dewantoro 

Abstract Earthquake effects, hydrodynamic forces, and nonlinear effects (structure properties represented by elastic constants) on rock-fill dam vibrations are investigated with a special case in the Jatiluhur dam, Indonesia. The vibration was studied by using the Single Degree of Freedom (SdoF) model with hydrodynamic forces and earthquakes as external forces. The analytical solution is obtained by the Laplace transform. Variations in hydrodynamic forces are obtained from water level measurement data where three scenarios are carried out, namely the lowest water level, middle and highest. The results show that the resulting hydrodynamic force does not have a significant effect on the vibration of the dam. The change in the vibration amplitude corresponds to the earthquake amplitude when the earthquake ends. The effects of the earthquake are still felt for a few seconds. The second model is to study the inhomogeneous-isotropic behavior of the Dam constituent material in a nonlinear elastic coefficient. We express the elastic properties of the material in terms of the Taylor expansion. By using the Taylor expansion for the nonlinear effect up to the fifth-order show that the nonlinear term did not give effect on the vibration amplitude but the vibration shift.

Keywords Fluid-structure · Groundmotion · Jatiluhur · Rock-fill dam

A. Sulaiman (✉)

Research Center for Physics, Indonesian Institute of Science—LIPI, Jakarta, Indonesia

e-mail: albertus.sulaiman@lipi.go.id

A. Sulaiman · W. A. Pranoto

Department of Civil Engineering, Universitas Tarumanagara, Jakarta, Indonesia

e-mail: watip@ft.untar.ac.id

T. Zera

Faculty of Science and Technology, Universitas Islam Negeri Syari Hidayatullah, Tangerang, Indonesia

e-mail: tati_zera@uinjkt.ac.id

M. De Rizka Dewantoro

Jasa Tirta II Public Corporation, Purwakarta, Indonesia

e-mail: derizkadewantoro@jasatirta2.co.id

© The Author(s), under exclusive license to Springer Nature Singapore Pte Ltd. 2022

H. A. Lie et al. (eds.), *Proceedings of the Second International Conference*

of Construction, Infrastructure, and Materials, Lecture Notes in Civil Engineering 216,

https://doi.org/10.1007/978-981-16-7949-0_5

1 Introduction

The Dam is a hydraulic structure that is very important for humans life, so that it has received serious attention, especially in the aspect of structural durability due to environmental influences. An important environmental effect is a force due to water itself which takes place continuously, the abundance of excess rainfall (overtopping), landslides, and earthquakes, especially for earthquake-prone areas. The failure or breaking of a rockfill or gravity dam during an earthquake is extensive cracking and deformation in the zone between the base of the dam and the foundation rock. In the event of an earthquake, the interaction between rigid structures (dams) and water creates additional (hydrodynamics) pressure upstream of the dam. The hydrodynamic force which is manifested in continuous hydrodynamic pressure will give dam elastic deformation. This is called the water-structure interaction and the excitation effect due to earthquakes has become a hot topic that has been studied a lot [1, 2]. Related to the research, many approaches have been developed where one of the most popular is the finite element method. This method is used to determine the acceleration demands of the floor in gravity dam vulnerability due to earthquakes. The studies and simulation are very useful for the evaluation of the safety of the dam structure [3].

Several studies related to the effects of earthquakes on dam structures have been carried out, such as soil-structure interactions where the material damage for both soil and structure occurs as a result of the dissipation of earthquake energy acting on it [4, 5]. Studies related to earthquake wave response (seismic) on concrete gravity dam in near-fault and far-fault ground motion [6]. Several studies related to dam-reservoir interactions have been carried out, especially by looking at the effect of acceleration amplification on the dam crest which is calculated based on the harmonic acceleration load. Estimation of stress and strain on the dam will be underestimated if this effect is neglected [7, 8]. On the other hand, earthquake is studied by taking into account the stochastic effect of vibrations on the dam structure. The results show that the random effect of vibrations after the peak of the earthquake affects the fragility and fatigue of the dam structure [9]. The stochastic effect was also studied by using wavelet transform, which can be used to detect damage from noisy [10]. The physical model approach is also carried out by giving more realistic results but requires a large amount of money and time [11].

In this paper, the fluid-structure interaction of a rock-fill Jatiluhur Dam (see Fig. 1) subjected to horizontal ground motion due to earthquake and hydrostatic pressure is investigated. This Dam started operations in 1967 with gravity construction with a rock embankment structure where the center is filled with clay. This structure has a length of 1.2 km and dams the Citarum river with water storage is about 4500 km². The water capacity is 12.9 billion m³/year and installed six turbine units with the power of 187 MW with an average electricity production of 1000 million kWh per year. In addition, Jatiluhur Dam has the function of providing irrigation water for 242,000 ha of rice fields (twice a year), drinking water, fisheries cultivation, and flood control. In the case of the Jatiluhur dam, we use water level

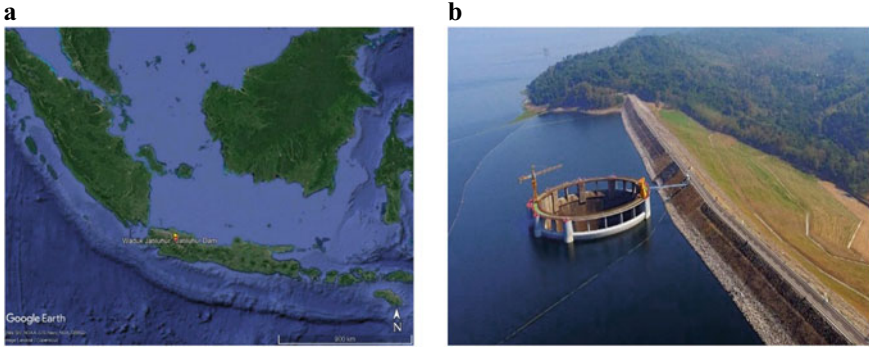


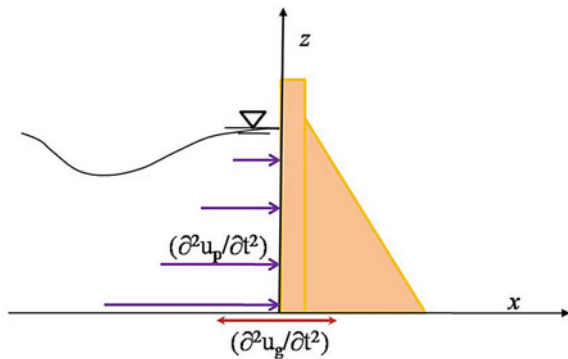
Fig. 1 a Location of Jatiluhur dam in Java Island, Indonesia, b the rock-fill Jatiluhur dam. *Source* Perusahaan Jasa Tirta II

measurement to analyze the hydrodynamics force and seismograph waveform for earthquake effect.

2 The Model

In this paper, we investigate the vibrational behavior of the Dam structure due to the effects of earth echoes and hydrodynamic forces working on it. The geometry of the model is depicted in Fig. 2. First, we use a one-dimensional vibration model with external forces in the form of the hydrodynamic forces and the earthquakes known as the single degree of freedom model. Second, we study the stiffness properties of the Dam structure on vibration due to hydrodynamic and earthquake forces where the effect of the structure is modeled by taking into account the nonlinear terms of the coefficient of elasticity.

Fig. 2 Idealized of the Jatiluhur dam, hydrodynamics forces (purple arrow), ground motion due to earthquake (red arrow)



2.1 Single Degree of Freedom (SdoF)

In general, the interaction of rock-fill Dam with water in a reservoir is formulated in terms of finite elements that describe the interactions solid field elasticity and fluid-based potential expressed in Eq. 1. [3],

$$\begin{bmatrix} m & 0 \\ 0 & -\varepsilon_k \end{bmatrix} \begin{bmatrix} \ddot{u} \\ \dot{\phi} \end{bmatrix} + \begin{bmatrix} c_s & c_{fs} \\ c_{sf} & c_f \end{bmatrix} \begin{bmatrix} \dot{u} \\ \dot{\phi} \end{bmatrix} + \begin{bmatrix} k_s & 0 \\ 0 & k_f \end{bmatrix} \begin{bmatrix} u \\ \phi \end{bmatrix} = [I] \begin{bmatrix} -\ddot{u}_g \\ -\dot{u}_g \end{bmatrix} \quad (1)$$

where u is an element of dam displacement (x -coordinate, m is the mass of an element of structure, k_s is the stiffness, c_s is a damping factor, c_f is viscous damping, c_{sf} is the damping of water-structure interaction, ϕ is the potential velocity of water, ε_k , and k_f are the potential, and kinetic energy of water particle and u_g is displacement due to earthquake. The 'dot' means derivative with respect to the time coordinate.

In this paper, the hydrodynamic force is studied with the water level data at the Jatiluhur Dam so that to simplify the problem. We look at the hydrodynamic force as an input to the vibrational dynamics of the dam structure. Many external forces affect vibration in a Dam, but the most important are hydrodynamic forces and earthquakes [1]. With the height (H_d) of a rock-fill Dam subjected to a horizontal ground acceleration due to earthquake ($\partial^2 u_g / \partial t^2$) and hydrodynamics acceleration ($\partial u_p / \partial t$) with u_p is a particle fluid velocity, then the single degree of freedom of the Dam system is given in Eq. 2 [3],

$$\frac{d^2 u}{dt^2} + \gamma \frac{du}{dt} + \omega^2 u = - \left(\frac{\partial u_p}{\partial t} + \frac{\partial^2 u_g}{\partial t^2} \right) \quad (2)$$

where $\gamma = cs/m$, $\omega = \sqrt{ks}/m$, m is the mass of an element of structure, and $u_p = \partial \phi / \partial z$ is horizontal particle velocity due to hydrodynamics pressure. It is not difficult to show, by using Laplace transform, we have an analytic solution of Eq. 2 as shown in Eq. 3.

$$\begin{aligned} u(t) = & u(0)e^{-\gamma t} \cos\left(\sqrt{\omega^2 - \gamma^2}t\right) + \frac{(u(0) + u'(0))}{\sqrt{\omega^2 - \gamma^2}} e^{-\gamma t} \sin\left(\sqrt{\omega^2 - \gamma^2}t\right) \\ & + \frac{1}{m\sqrt{\omega^2 - \gamma^2}} \int_0^t e^{-\gamma(t-\tau)} \sin\left(\sqrt{\omega^2 - \gamma^2}(t-\tau)\right) \left(\frac{\partial u_p}{\partial \tau} + \frac{\partial^2 u_p}{\partial \tau^2}\right) d\tau \end{aligned} \quad (3)$$

2.2 Nonlinear Model

The elastic coefficient in Eq. 2 is constant so that the material making up the dam is considered to be homogeneous-isotropic. For rock-fill Dam such as Jatiluhur, the material is not homogeneous isotropic so that the elastic coefficient is not constant and the material properties are no longer linear. The relationship between stress and strain is no longer linear. In this paper, we study the inhomogeneous-isotropic behavior of the Dam constituent material in a nonlinear elastic coefficient. We express the elastic properties of the material in terms of the Taylor expansion. This is the simplest method in the theory of nonlinear elasticity. The expression of the Taylor series of the sine function is $\sin(ku) \sim ku - 1/3!k_3u^3 + 1/5!k_5u^5 - \dots$. By maintaining until the second term then Eq. 2 becomes Eq. 4.

$$\frac{d^2u}{dt^2} + \gamma \frac{du}{dt} + \omega^2u - \alpha u^3 + \beta u^5 = -\left(\frac{\partial u_p}{\partial t} + \frac{\partial^2 u_g}{\partial t^2}\right) \tag{4}$$

If we perform the following transformation in Eq. 5, this yields Eq. 6.

$$\frac{du}{dt} = v \tag{5}$$

$$\frac{dv}{dt} = -\gamma v - \omega^2u + \alpha u^3 - \beta u^5 - \left(\frac{\partial u_p}{\partial t} + \frac{\partial^2 u_g}{\partial t^2}\right) \tag{6}$$

This is a system of first-order nonlinear ordinary differential equations with unknown functions u and v . This equation will be solved using the Runge–Kutta method with Matlab software.

3 Result and Discussion

The multipurpose Jatiluhur Dam is located in West Java Province at a position of 7° South and 107° East, 130 km southeast of Jakarta. This dams the Citarum River in the Purwakarta Regency area and has functions for flood control, water supply irrigation, drinking water, and industrial and hydroelectric power plants. With a design capacity of 3.00 billion m³, this dam is capable of ensuring water supply to irrigation areas to the west, north, and east of the River Citarum. In addition to controlling the irrigation area, the Jatiluhur Dam is also a source of hydroelectric power plants with a production of 1.12 billion kWh per year and flood control as well as tourism and freshwater aquaculture. Jatiluhur Dam is designed to hold water with a maximum height of 109 m above sea level. The varying water level is depicted in Fig. 3. The result shows that the time series of water level has the peak of spectrum around 370 days. This indicates that the annual variability is influenced

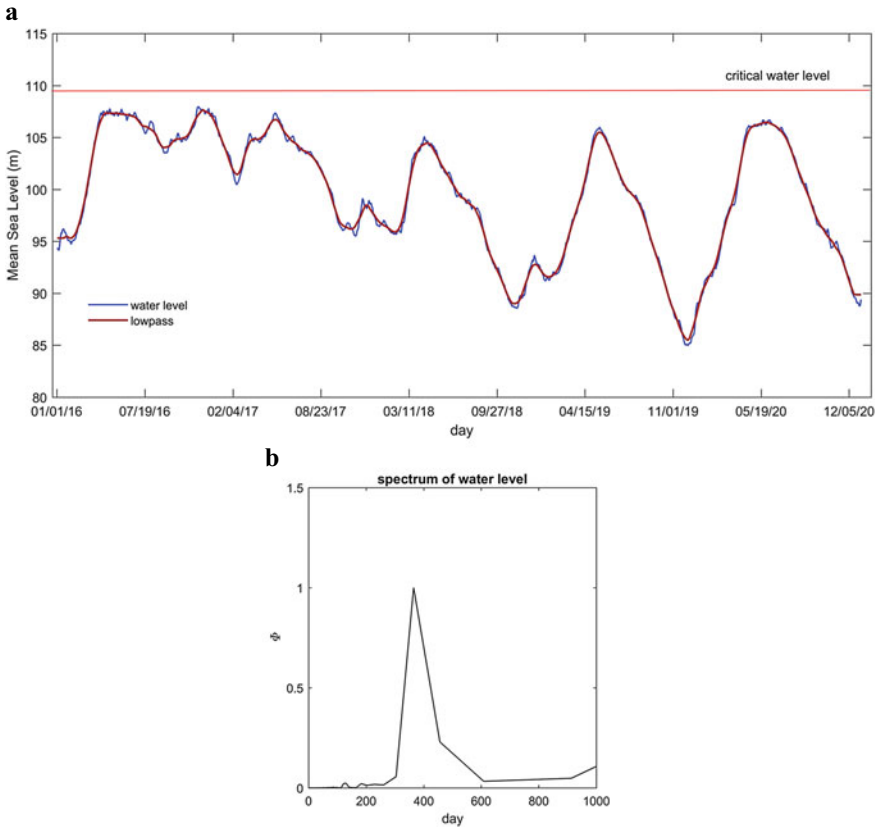


Fig. 3 **a** The time series of water level on the Jatiluhur dam and the lowpass filter with cut-off period 30 days, **b** normalized power spectrum with the maximum energy 370 days

strongly by the monsoon system. The lowpass filter pattern (30 days cutoff period) is significant, indicating that the daily-weekly variability is not dominant. So the quantity of water sources in the Jatiluhur reservoir is stable.

We study the effects of earthquakes and hydrostatic pressure on the upstream face of the dam. The hydrodynamic pressure can be estimated by using Westergaard’s (1933) formula, which uses a parabolic approximation for additional stress due to an earthquake. Westergaard’s hydrodynamics pressure $p = 7/8\rho ax\sqrt{hz}$ where ρ water density, $ax = \partial up/\partial t$ horizontal acceleration, h the depth of dam, and z is the water level. In calculations it is assumed that $\rho = 1000 \text{ kgm}^{-3}$ and $g = 10 \text{ ms}^{-2}$. With the length of the Jatiluhur dam is about 1220 m, the maximum depth is 110 m, then hydrodynamics acceleration is given by $ah = p/(\rho A)$ with A is the area of interest. The Dam vibration due to ground motion and the hydrodynamics forces for the lowest water table is depicted in Fig. 4. In the simulation, we assume the Dam has $m \sim 2 \text{ ton/m}^3$, $k = 0.5 \text{ N/m}$ [5], and the damping coefficient is about 0.0005 Nms^{-1} .

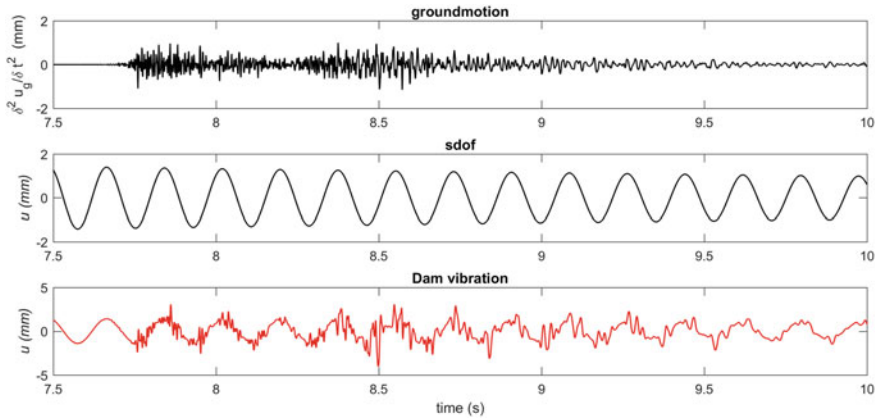


Fig. 4 The ground motion and the dam vibration with normalized of ground motion and SdoF

By using the Westergaard formula and the synthetic ground motion data, we calculate the Dam vibration due to these two forces, as shown in Fig. 4. In general, changes in the vibration amplitude correspond to the earthquake amplitude when the earthquake ends. The effects of the earthquake are still felt for a few seconds. Meanwhile, the change in hydrodynamic force (as seen from the change in water level) is depicted in Fig. 5. In general, a change in depth of about 10–20 m does not give a significant change in the vibration amplitude.

In this study, hydrodynamic data has different time intervals from earthquakes where the water level has daily intervals. In an earthquake interval of milliseconds, the hydrodynamic force is constant. So that, we consider the hydrodynamic forces in the three scenarios above. Next, we calculate the effect of change in hydrodynamic forces due to changes in water level on the vibration response during an earthquake. These results are shown in Fig. 6. The results show that the change in hydrodynamic force due to changes in the water level of about 20 m (green line) has no significant effect on the vibration amplitude.

Furthermore, by expanding the elastic terms in the nonlinear term to the fifth-order (Eq. 4), the simulation results are expressed in Fig. 7. This solution is obtained by converting second-order differential equations into a first-order system of differential equations by transforming through Eq. 5. The solution is solved by the Runge–Kutta method. The simulation shows that the nonlinear effect does not significantly contribute to the amplitude but has a shift effect on the vibrational motion. Previous paper studies have shown that an earthquake acceleration amplitude of 1 m/s^2 can increase the vibration amplitude by about 10 mm [5]. In this paper, we use normalized synthetic data which increases amplitude by about 5 mm. The use of real waveforms will give more qualitative results. This will be done in future research.

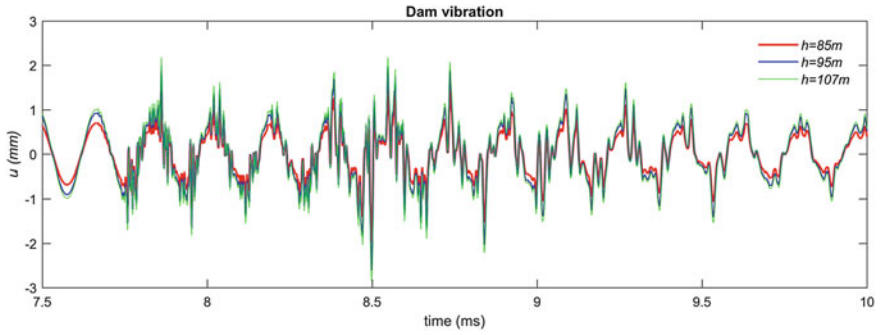


Fig. 5 The dam vibration with the middle and the highest water table

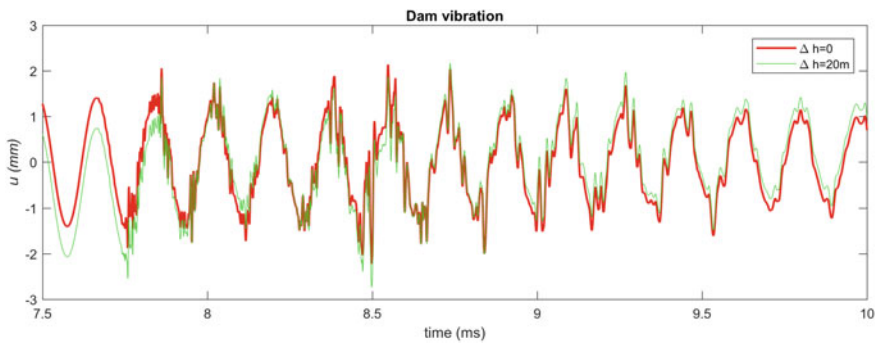


Fig. 6 The dam vibration or conditions without hydrodynamic forces and with hydrodynamic forces due to changes in water level 20 m

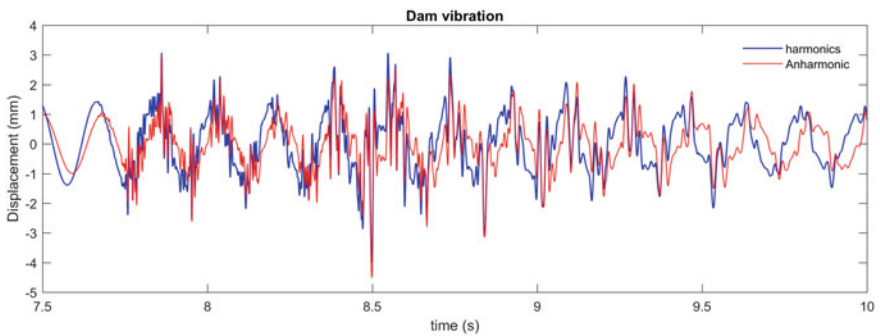


Fig. 7 Nonlinear effect of SdoF related to hydrodynamics and earthquake in dam vibration

4 Conclusion

The behavior of Jatiluhur Dam vibration with the hydrodynamic forces and earthquakes as external forces have been investigated in this paper. The basic model used in the investigation is called the SdoF where the analytical solution has been founded with the Laplace transform methods. The result shows that changes in the vibration amplitude correspond to the earthquake amplitude when the earthquake ends, the effects of the earthquake are still felt for a few seconds. Variations in hydrodynamic forces are obtained from water level measurement data where three scenarios are carried out, namely when the water level is lowest, middle, and highest. The results show that the resulting hydrodynamic force does not have a significant effect on the vibration of the dam. The hydrodynamic forces due to the difference in water level did not have a significant effect on the Dam vibration. In other words, the hydrodynamic forces may only have a long-term effect on the Dam vibration. The second model is to study the stiffness behavior of building materials by looking at the non-linear stiffness coefficients. By using the Taylor expansion for the nonlinear effect up to the fifth-order show that the nonlinear term did not give effect on the vibration amplitude but the vibration shift.

Acknowledgements This research funded by P2FT-LIPI and Magister Teknik Sipil Universitas Tarumanagara for fiscal year 2021. We also to thank the anonymous reviewer who has made a lot of improvements to this manuscript.







References

1. Novák P, Moffat AIB, Nalluri C, Narayanan RAIB (2017) Hydraulic structures. CRC Press, United States
2. Faria R, Oliveira S, Silvestre AL (2019) A fluid-structure interaction model for dam-water systems: analytical study and application to seismic behavior. *Adv Math Phys* 2019. <https://doi.org/10.1155/2019/8083906>
3. Bouaanani N, Renaud S (2014) Effects of fluid–structure interaction modeling assumptions on seismic floor acceleration demands within gravity dams. *Eng Struct* 67:1–18
4. De Falco A, Mori M, Sevieri G (2019) Soil-structure interaction modeling for the dynamic analysis of concrete gravity dams. In: *COMPdyn proceedings*, vol 3. European Community on Computational Methods in Applied Sciences (ECCOMAS), pp 5662–5673
5. Oliveira S, Silvestre A, Espada M, Câmara R (2014) Modeling the dynamic behavior of dam-reservoir-foundation systems considering generalized damping. Development of a 3DFEM state formulation. In: *9th international conference on structural dynamics, EUROdyn*
6. Akköse M, Şimşek E (2010) Non-linear seismic response of concrete gravity dams to near-fault ground motions including dam-water-sediment-foundation interaction. *Appl Math Modell* 34(11):3685–3700
7. Pelecanos L, Kontoe S, Zdravković L (2016) Dam–reservoir interaction effects on the elastic dynamic response of concrete and earth dams. *Soil Dyn Earthq Eng* 82:138–141

8. Pelecanos L, Kontoe S, Zdravković L (2020) The effects of dam–reservoir interaction on the nonlinear seismic response of earth dams. *J Earthq Eng* 24(6):1034–1056. <https://doi.org/10.1080/13632469.2018.1453409>
9. Xu Q, Xu S, Chen J (2020) Li J (2020) Investigation of stochastic seismic response and index correlation of an arch dam using endurance time analysis method. *Adv Civ Eng* 2:1–23. <https://doi.org/10.1155/2020/8862869>
10. Vaez SRH, Arefzade T (2017) Vibration-based damage detection of concrete gravity dam monolith via wavelet transform. *J Vibroengineering* 19(1):204–213
11. Rosca B (2008) Physical model method for seismic study of concrete dam. *Buletinul Institutului Politehnic din Iasi. Sectia Constructii, Arhitectura* 54(3):57

Assessment of Flooding Event in the Upper Sunter Watershed, Jakarta, Indonesia



Anasya Arsita Laksmi , Anthony Harlly Sasono Putro ,
Wisnu Setia Dharma , Pungky Dharma Saputra ,
Nina Purwanti , and Muhammad Hamzah Fansuri 

Abstract Flood is one of Jakarta's tremendous problems, which induces loss and damage to society. Thus, the city needs improvements from many aspects, especially the assimilation between hard and soft solutions to provide an integrated flood risk management system. As one of 13 rivers that flow across Jakarta, Sunter River is threatened by floods every rainy season. The flooding behavior was assessed by analyzing hydrologic modeling. As the flood assessment, the objective of this research focused on developing the hydrologic model to simulate hourly rainfall events in the Sunter River generated using Hydrologic Modelling System (HEC-HMS) software. The condition of the simulation also depends on the environmental situation in this watershed, such as land use and availability of its flood plain. Then, the calibration and validation processes produce the optimized parameter value based on the model efficiencies parameters. These results were used to simulate the storm designs for several return periods. Therefore, the peak of discharge for each return period can be assessed value for flooding behavior. This assessment analysis can be used and improved for early warning system analysis and further design as a soft structure solution. Hence, the strategic plan for flood management can be formulated in the watershed.

Keywords Flood · Hydrologic modelling · Sunter river

A. A. Laksmi (✉) · P. D. Saputra · N. Purwanti · M. H. Fansuri
Department of Civil Engineering, Faculty of Military Engineering, Republic of Indonesia
Defense University, Bogor, Indonesia
e-mail: anasyaarsita@gmail.com

A. H. S. Putro
Directorate General of Water Resources, Ministry of Public Works and Housing, Jakarta,
Indonesia

W. S. Dharma
Engineering Procurement and Construction Division, PT Waskita Karya (Persero) Tbk,
Pekanbaru, Indonesia

1 Introduction

Jakarta, the capital city of Indonesia, has been overwhelmed by tremendous floods in the last decade, with at least three major flood events that happened in 2002, 2007, and 2013. The floods occurred due to some causes, such as climate change, urbanization, and land subsidence. Flooding in Jakarta left unsolved problems for a long time in rescue or rehabilitation of health, environment, employment, and many other issues. It takes billions of rupiah as well as material losses for the people who live along the riverbank. Additionally, the megacity's economic development allows the opportunity of working and accommodation to its citizen [1]. It leads to rapid urbanization that contributes to the worse land use situation and has led to the reduction of water infiltration ability. The data from Indonesian Bureau Statistics shows that the city has a population rate of 0.92% and is predicted to grow in the future [2].

As one of the river basins in Jakarta, Sunter Watershed is prone to flood events. The 56 km long river has a total area of around 181.24 km² and the slope is approximately 25–35% [3]. This river flows along with several inundation areas, such as Pondok Gede, Cipinang, and Kelapa Gading, a dense population and the center of business and housing. Even though the hard-structure solution by constructing the East Flood Canal (KBT) was performed to reduce the discharge downstream, it does not immediately free the watershed from flood risk. Aside from KBT construction, a soft-structure approach is needed to improve the city's integrated flood risk management system.

Thus, this study aims to assess the flooding event in the upper area of Sunter Watershed as one of the most prone areas. A rainfall-runoff simulation model using the Hydrologic Modelling System (HEC-HMS) was performed to assess the area in several storm events. The model also generates the discharge data based on the design storm events for several return-period from 2 to 200 years. In future research, the output of this study is expected to be implemented for society education about flood events as a part of the early warning system in Jakarta.

2 Study Site

The study area of this research is located at the upper of Sunter Watershed, as shown in Fig. 1. The watershed contains two upstream rivers: Sunter River and Cipinang River that merge into one main river downstream. The maximum length of the watershed is approximately 37 km stream, and the river basin of 329.93 km² with an annual average temperature in the area is 26 °C. In addition, the average annual rainfall is around 1883 mm based on Cipinang gauge station data from 2001 to 2007. The Cipinang Gauge is the streamflow observation point located at point 4 of Fig. 1. According to [4], the water usage of the rivers is categorized for agricultural purposes, urban business, and the hydroelectric power industry. Nevertheless, the river function is only for urban purposes nowadays.

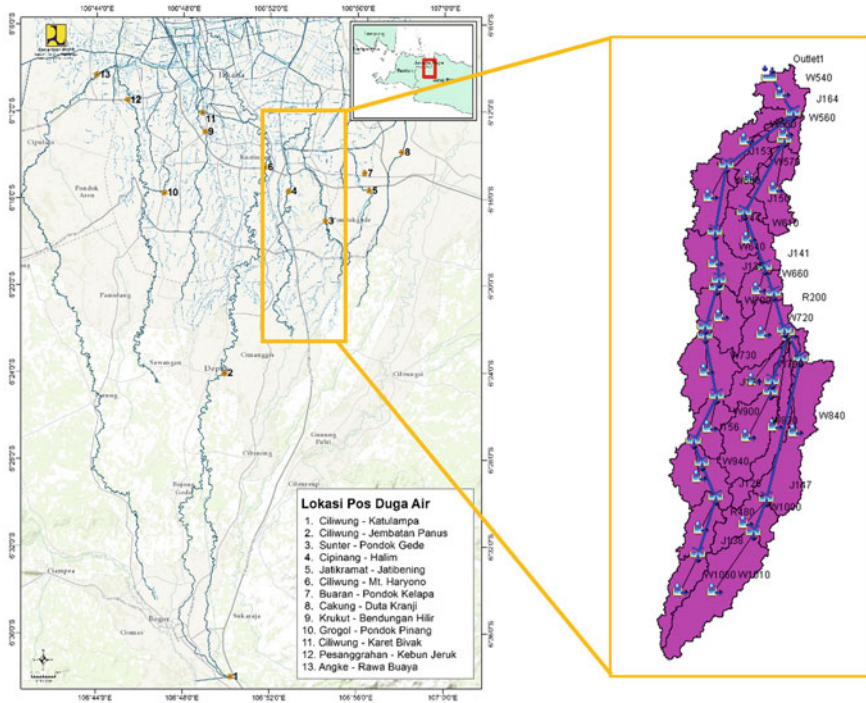


Fig. 1 The study area of Sunter watershed

3 Materials and Methods

3.1 Data

In order to set up the map of the watershed for modeling in HEC-HMS, this study used several diverse datasets (raster data), such as Digital Elevation Model (DEM), land use, and soil. The DEM data was extracted from U.S. Geological Survey (USGS) repository global data with 30 m resolution. The Global Hydrologic Soil Groups (HSGs) NASA provides the soil dataset with a projected resolution of approximately 250 m, and the land use data supplied from WaterBase of United Nations University global repository data with 400 m resolution for Australia/Pacific data. Additionally, the hydrologic model simulation uses the selected rainfall events of the hourly rainfall data from January 2000 to May 2008. These data were obtained from the Meteorological, Climatological, and Geophysical Agency of Indonesia at Station No: Meteorologi 745. Furthermore, the calibration and validation of the hydrologic model were performed using daily discharge data from 2000 to 2008 which was obtained from the Ministry of Public Works and Housing at Cipinang Station. Since the observed precipitation and discharge dataset

is in a different time base, the methodology in this research accommodates several additional steps to obtain an acceptable analysis result.

3.2 Methodology

The first step of this research was developing a model for the watershed basin using ArcGIS and HEC-GeoHMS, consisting of several processes using the input: DEM, land use, and soil map. HEC-GeoHMS is a tool developed by the U.S. Army Corps of Engineers to generate a map in ArcGIS with the output of a basin model that can be imported directly to HEC-HMS. In the process, the watershed system can be delineated into some sub-basins, reaches, and junctions.

After the development of the basin model, HEC-HMS was performed to simulate the selected precipitation model. This software has an important role in producing hydrological simulations based on the hourly and daily data in the dendritic watershed system. The software consists of several methods to conduct the analysis, such as the Loss method (e.g., Initial and Constant, Soil Conservation Service (SCS) Curve Number, Smith Parlange), Transformation method (e.g., Mod Clark, Snyder Unit Hydrograph, SCS Unit Hydrograph), and Routing method (e.g., Kinematic Wave, Muskingum, Muskingum-Cunge) [5]. Furthermore, this study specifies the SCS Curve Number for Loss method, SCS Unit Hydrograph for the Transformation method, and Muskingum for Routing method. In addition, the applied parameters in this study were SCS Curve Number, Initial Abstraction, Impervious (Loss), SCS Unit Hydrograph, Lag Time (transform), Muskingum K, Muskingum X, Number of Subreaches (routing). Those parameters were adjusted to get the nearest value of simulation discharge to the observation data. This study simulated 3 (three) selected rainfall storm events (Event 1: 12–18 March 2007, Event 2: 9–17 December 2004, Event 3: 9–15 February 2005).

The simulation output was calibrated using the observed discharge data to improve the result. However, the observed discharge data were on a daily basis. Thus, the hourly discharge simulation result is processed to get the average daily streamflow. Then, the WHAT program, developed by Purdue University, was performed to separate the baseflow to get the direct runoff output. WHAT program is an internet-based tool to analyze streamflow time series data. In this case, the observation and simulation discharge compared until the model efficiency criteria show an acceptable outcome. After the calibration process, several values for the optimized parameter were obtained and used to validate several rainfall-runoff events. This study used the selected optimized parameter to simulate 2 (two) selected storm events (Event 1: 24 February–03 March 2003 and Event 2: 04–12 February 2006) for validation.

Moreover, the input parameter was also used for the design storm model, which simulated for several return periods from 2 to 200 years. This study also used HEC-HMS to produce hydrographs for each design storm. Furthermore, the methodology of the hydrological simulation in this study can be seen in Fig. 2.

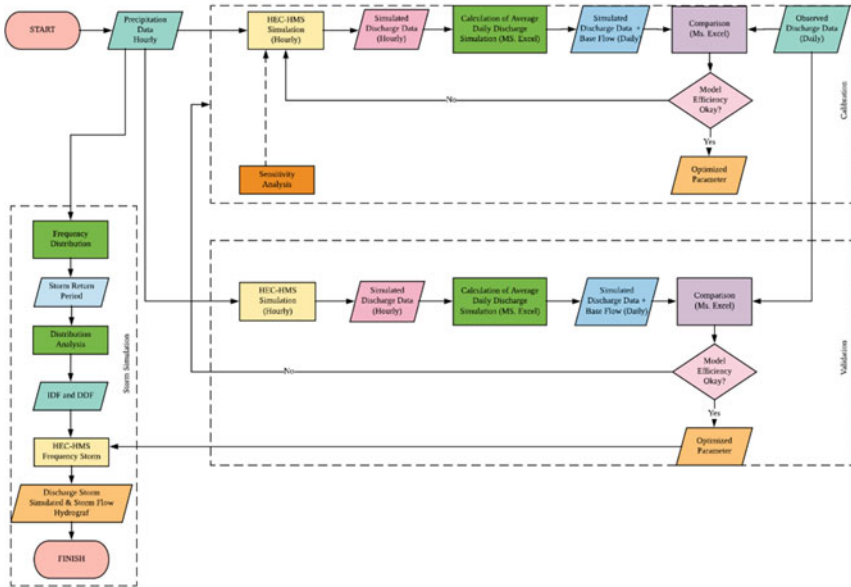


Fig. 2 The methodology used to perform the modeling

3.3 Model Performance Criteria

Several parameters of model efficiency were used to evaluate the accuracy of the calibration and validation model in this research. This study used R-squared (R^2), Nash–Sutcliffe Efficiency (NSE), and Root Mean Square Error (RMSE) to evaluate the accuracy. R^2 is a statistical measure of curve distance to the fitted regression line. It is also known as the coefficient of determination or the coefficient of multiple determination for multiple regression. R^2 ranges from 0 to 1, with higher values indicating less error variance, and typically values greater than 0.5 are considered acceptable. The equation for R^2 is shown in Eq. 1, in which n , Q_0 , and Q_s are the total sample size, observed discharge, and simulated discharge, respectively.

$$R^2 = \left[\frac{(n \sum Q_0 Q_s) - (\sum Q_0)(\sum Q_s)}{\sqrt{((n \sum Q_0^2) - (\sum Q_0)^2)(n \sum Q_s^2) - (\sum Q_s)^2}} \right]^2 \quad (1)$$

The second model efficiency is RMSE or Root Mean Square Error which is commonly used to analyze the error-index statistics. The lower RMSE shows better model performance. According to [6], the equation can be seen in Eq. 2.

$$RMSE = \sqrt{\left(\sum(Q_0 - Q_s)^2\right)} \quad (2)$$

Meanwhile, Nash–Sutcliffe Efficiency (NSE) is used to assess the predictive power of hydrological models. According to [7], the formula is presented in Eq. 3.

$$NSE = 1 - \left[\left(\sum(Q_0 - Q_s)^2\right) / (Q_0 - \bar{Q})^2\right] \quad (3)$$

4 Results and Discussion

The HEC-HMS simulation result for the selected rainfall period was calibrated using daily discharge observed data. Some parameters, such as Muskingum-K, Muskingum-X, and impervious, were adjusted to perform the calibration process. This study used 3 (three) periods of rainfall events for the calibration process to obtain the optimum value for the rainfall model at Sunter River. In order to get the optimum value for each simulation, the model efficiency was tested for each simulation by using several objective values such as Nash–Sutcliffe (N.S.), root mean square error (RMSE), R-squared (R^2). Table 1 shows the optimum parameter for each calibration simulation. The daily and the hourly result of the calibration graph for case 1 (12–18 March 2007) can be seen in Figs. 3, 4, 5 and 6 show the calibration of case 2 (9–17 December 2004), while case 3 (9–15 February 2005) results are shown in Figs. 7 and 8.

Moreover, the model efficiency output for each calibration case can be seen in Table 2. The average acceptable value was indicated from the result of calibration 2. Therefore, the parameter used in calibration 2 was performed in the validation process.

Furthermore, the optimum value for each model was validated with two periods of rainfall events, as shown in Figs. 9 and 10 for the daily hydrograph and the hourly hydrograph of validation case 1 (24 February–03 March 2003), respectively. Figures 11 and 12 show the result for validation 2 (04–12 February 2006). In this case, the optimum value obtained based on the model efficiencies in the validation process can be seen in Table 3.

Table 1 The parameter value for three calibration cases

Parameter	Calibration 1	Calibration 2	Calibration 3
Muskingum-K (h)	6	30	80
Muskingum-X	0.01	0.01	0.01
Impervious (%)	0	0	0

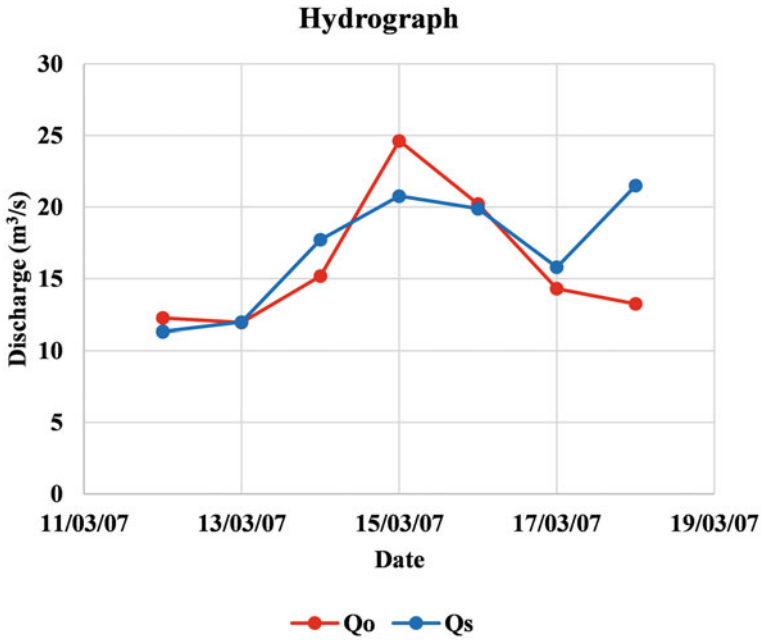


Fig. 3 The daily calibration model result for Calibration 1 (12–18 March 2007) scenario

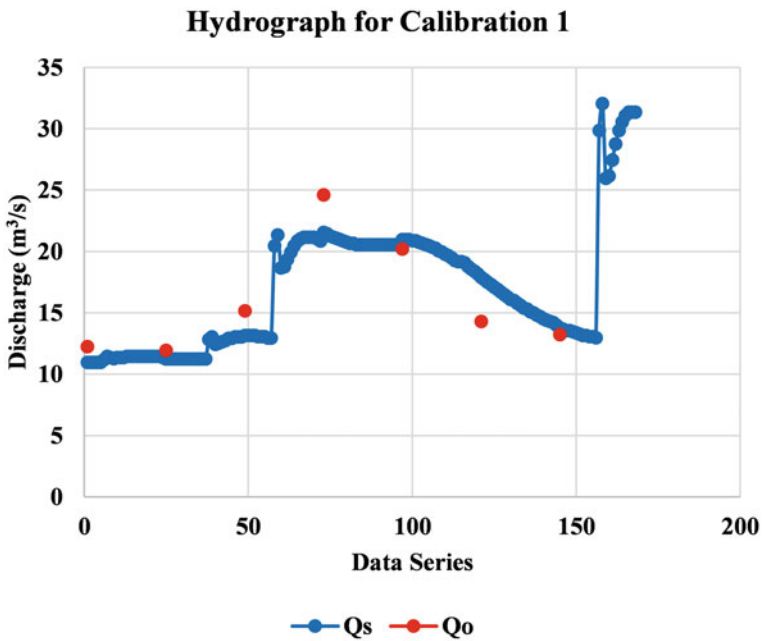


Fig. 4 The hourly calibration model result for Calibration 1 (12–18 March 2007) scenario

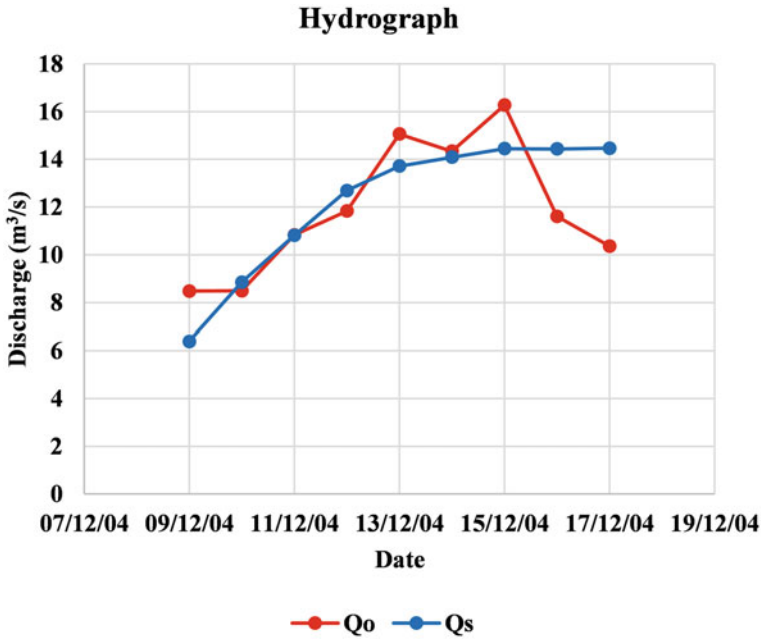


Fig. 5 The daily calibration model result for Calibration 2 (9–17 December 2004) scenario

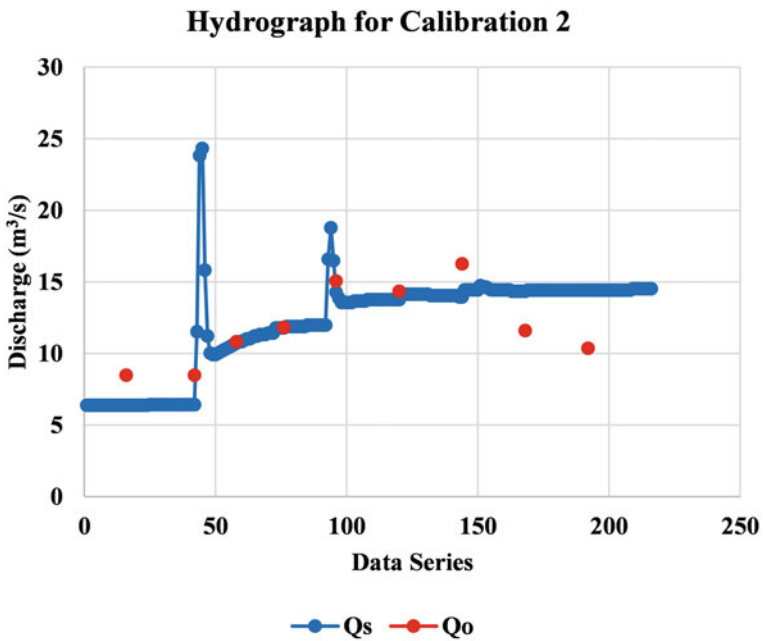


Fig. 6 The hourly calibration model result for Calibration 2 (9–17 December 2004) scenario

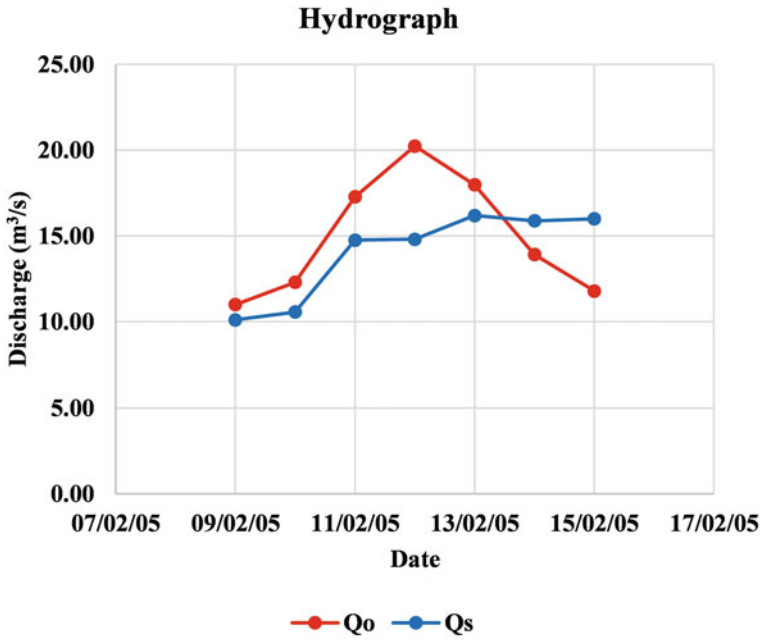


Fig. 7 The daily calibration model result for Calibration 3 (9–15 February 2005) scenario

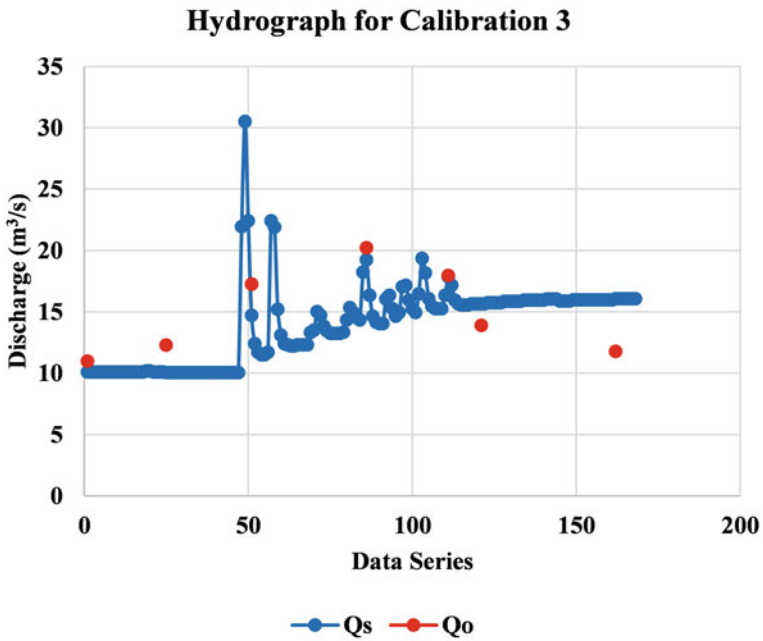


Fig. 8 The hourly calibration model result for Calibration 3 (9–15 February 2005) scenario

Table 2 The model efficiency output for each calibration case

Parameter	RMSE	R ²	NSE
Calibration 1	9.64	0.41	0.31
Calibration 2	5.94	0.54	0.43
Calibration 3	8.03	0.27	0.16

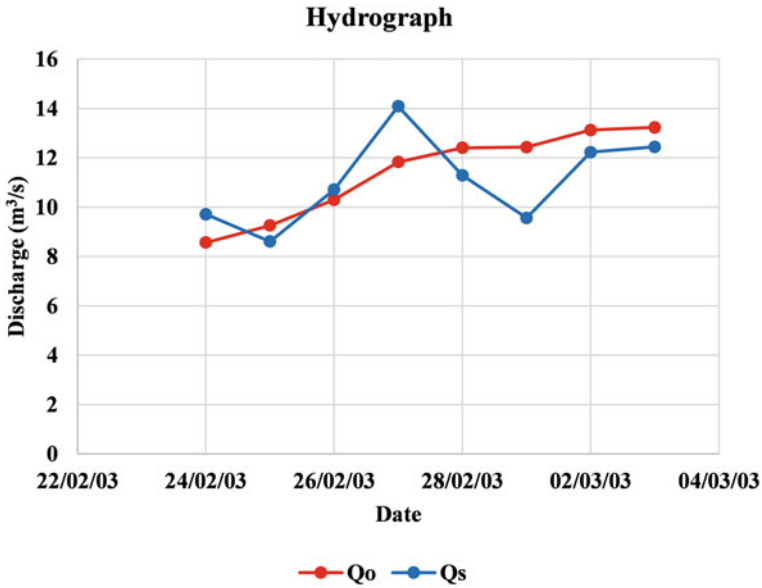


Fig. 9 The daily validation model result for Validation 1 (24 February–03 March 2003) scenario

Moreover, the result shows that the model efficiency output for each validation process has an acceptable value. It indicates that the optimized parameters from calibration 2 can be used for flood modeling in the Sunter Watershed. Furthermore, the selected optimized parameter (Muskingum $K = 30$; Muskingum $x = 0.01$; and impervious = 0) used to simulate design storm for several return periods.

4.1 Design Storm Simulation

After the calibration and validation process, the optimized parameter was used to simulate the design storm. According to [8], several design storm events for Sunter Watershed were calculated by using Fisher Tippet I Distribution methods for several return periods from 2 to 200 years. Table 4 shows the calculation result in the value of 24-h rainfall (mm) for the selected return period. The analysis of storm

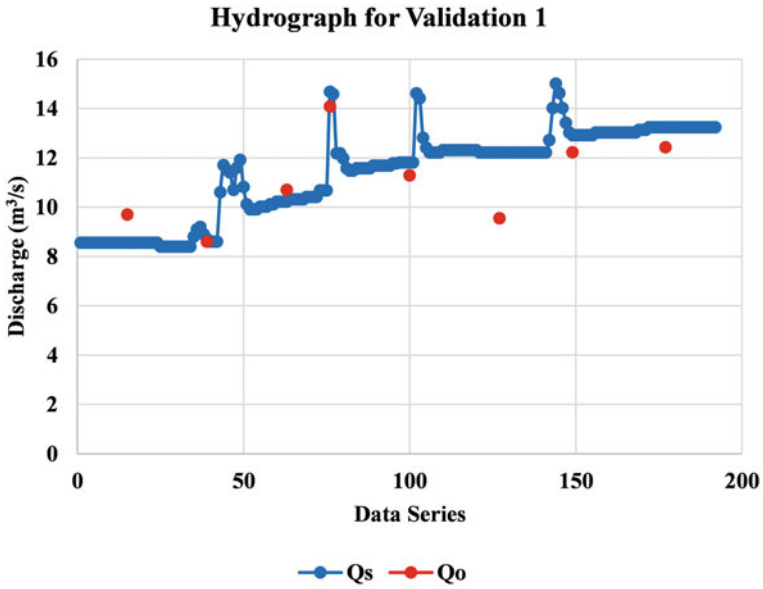


Fig. 10 The hourly validation model result for Validation 1 (24 February–03 March 2003) scenario

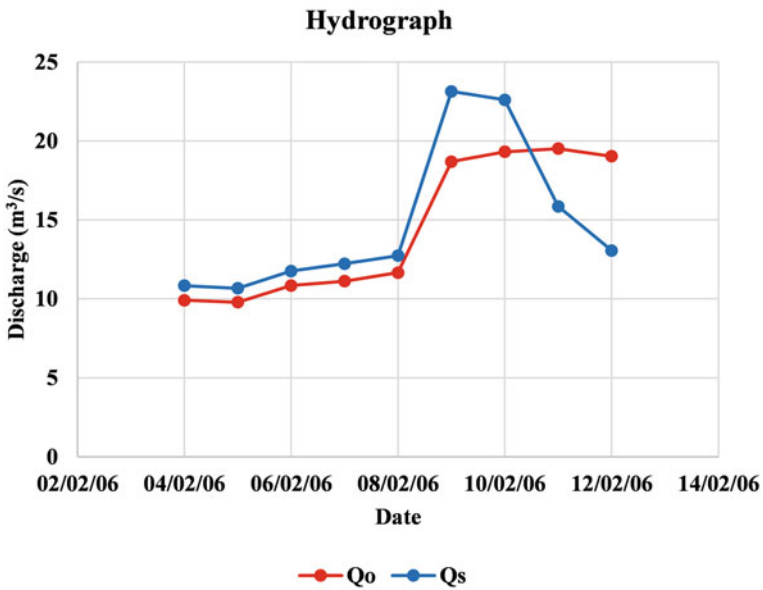


Fig. 11 The daily validation model result for Validation 2 (04–12 February 2006) scenario

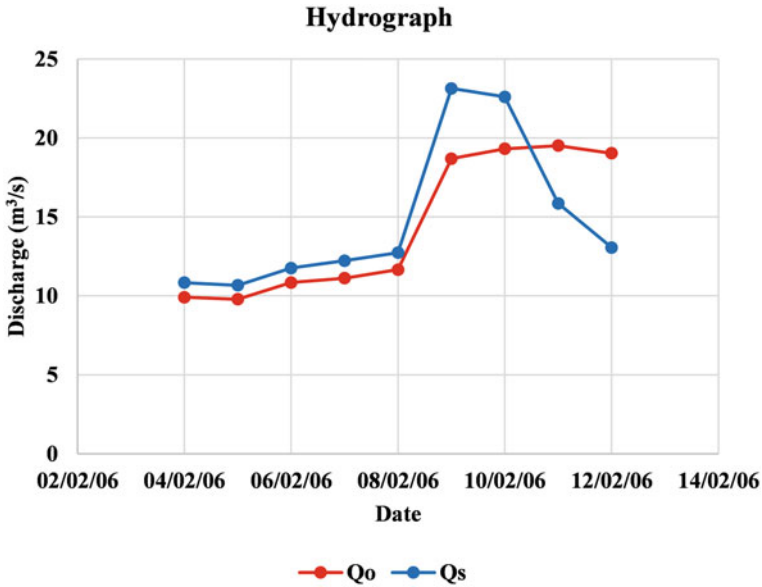


Fig. 12 The hourly validation model result for Validation 2 (04–12 February 2006) scenario

Table 3 Model efficiency for validation case

Simulation	RMSE	R ²	NSE
Validation 1	4.23	0.38	0.21
Validation 2	9.20	0.58	0.55

Table 4 The return period and the value of the 24-h rainfall event

Return period (Tr)	R ₂₄ (mm)
2	135.97
5	189.97
10	225.72
25	270.90
50	304.42
100	337.68
200	370.83

events was performed using the Depth-Duration-Frequency (DDF) curves. In addition, Fig. 13 shows the DDF curves for the selected return period.

The design storms were simulated in the HEC-HMS by using the optimized parameter to generate the hydrograph for 48 h by performing the Frequency Storm module in HEC-HMS, as shown in Figs. 14, 15, 16, 17, 18, 19 and 20. The summary of peak discharge data of each graph is presented in Table 5. The

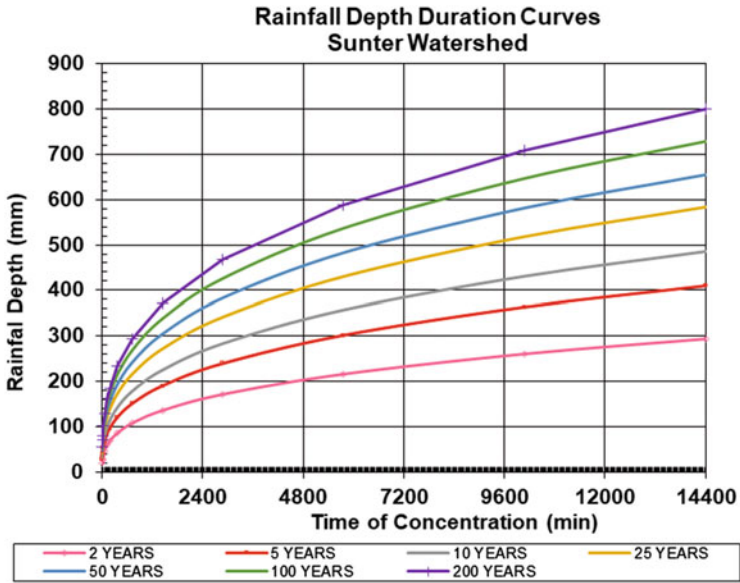


Fig. 13 Rainfall depth duration curves for Sunter watershed

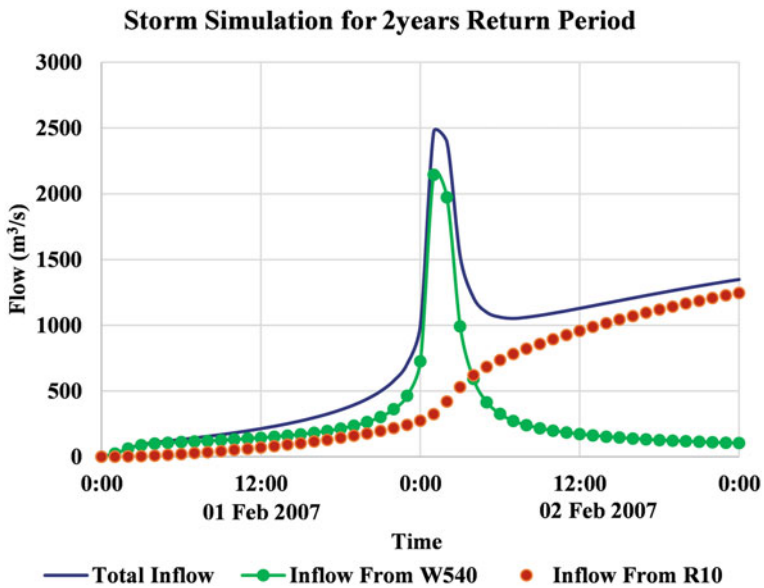


Fig. 14 The simulation of design storm at Sunter watershed using 2 years return period

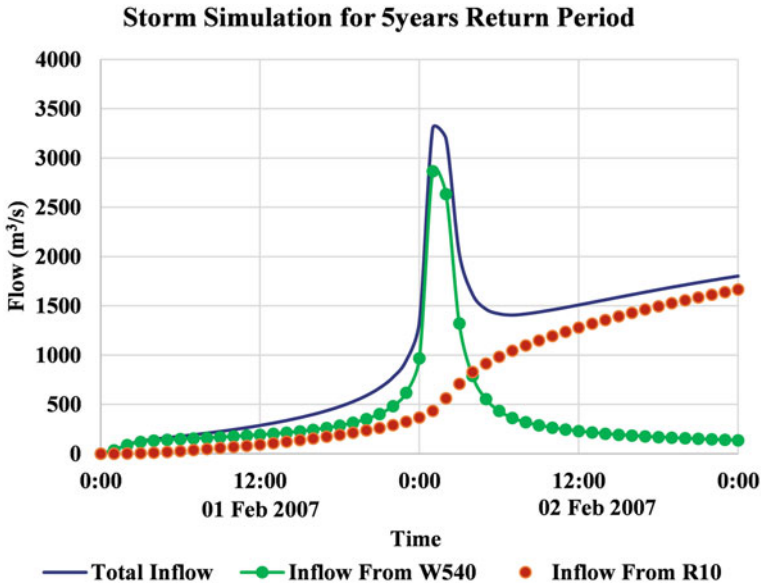


Fig. 15 The simulation of design storm at Sunter watershed using 5 years return period

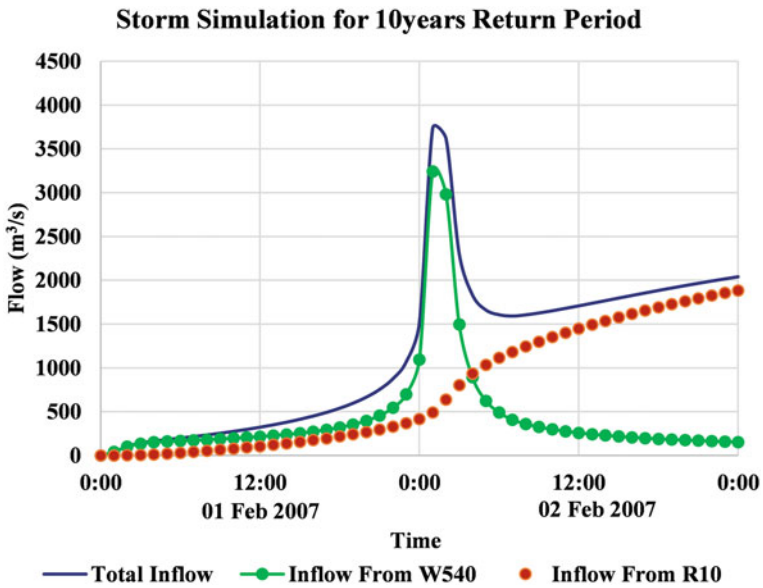


Fig. 16 The simulation of design storm at Sunter watershed using 10 years return period

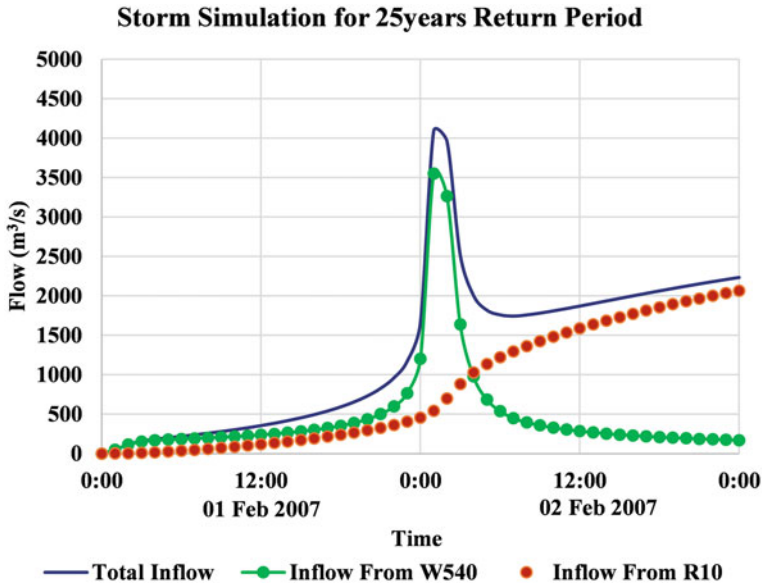


Fig. 17 The simulation of design storm at Sunter watershed using 25 years return period

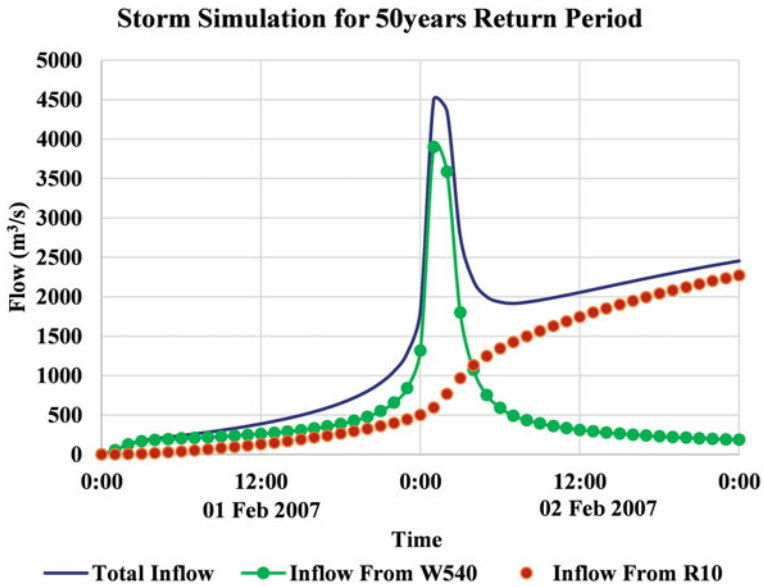


Fig. 18 The simulation of design storm at Sunter watershed using 50 years return period

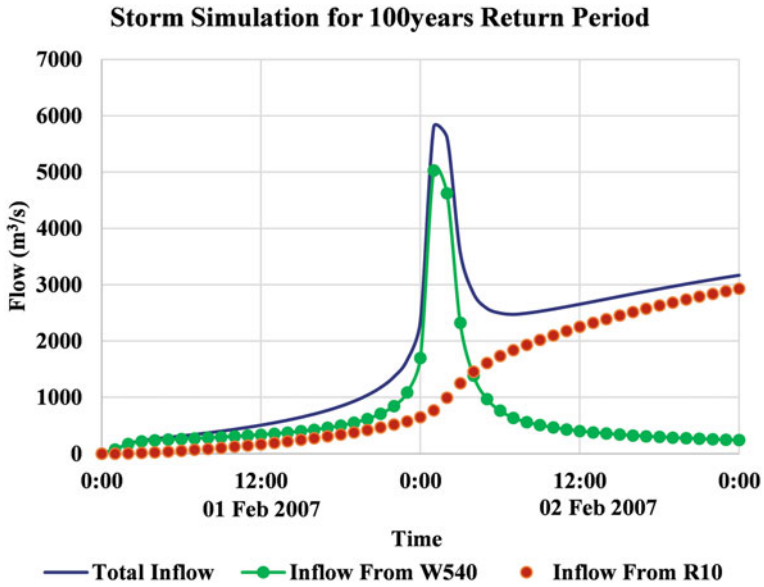


Fig. 19 The simulation of design storm at Sunter watershed using 100 years return period

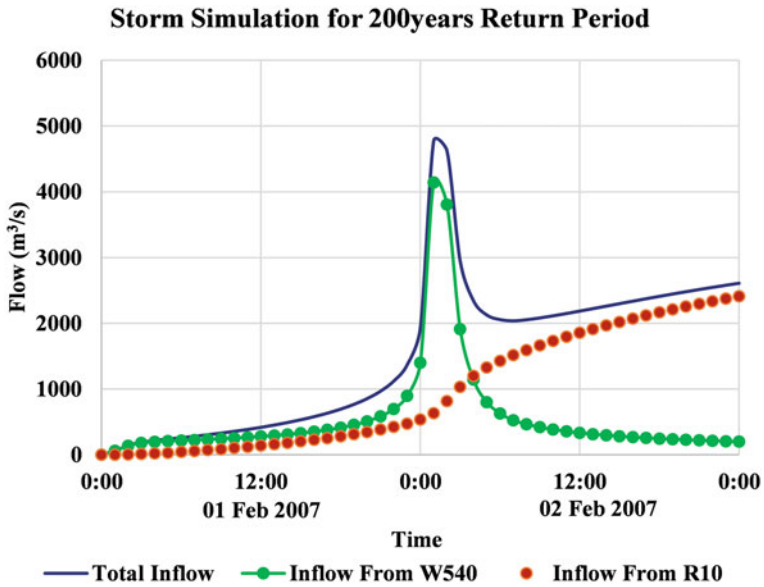


Fig. 20 The simulation of design storm at Sunter watershed using 200 years return period

Table 5 The peak value of the simulated design storm

Return period (T_r)	Discharge (m^3/s)
2	2329.4
5	3257.0
10	3871.1
25	4647.1
50	5222.9
100	5794.3
200	6363.6

frequency storm result shows a very high value of inflow in the watershed. This data could be used for the basis of infrastructure design or hazard prevention in the future. Generally, the design of hydraulic structure use at least 50 years return period. Thus, the estimated discharge of the Sunter Watershed is 5222.9 m^3/s .

5 Conclusions

Sunter Watershed is one of the most flood-prone areas in Jakarta, with some inundation areas, such as Pondok Gede, Cipinang, and Kelapa Gading. This research developed a hydrological model to assess the rainfall events in the upper Sunter Watershed with the simulation input of hourly precipitation data and daily river discharge data. The model performance criteria (R^2 , NSE, and RMSE) are used to optimize the calibration and validation process, in which the simulation demonstrates an accepted result. Moreover, the storm event simulation of Sunter River presents the peak value of 50 until 100 years return periods are 5333.9 m^3/s to 5794.3 m^3/s , respectively. This value can be considered as the design storm result for hydraulic structure design purposes. Additionally, the methodology of the study is expected to be implemented in the analysis of another watershed with a lack of hourly discharge data.

Acknowledgements The author gratefully acknowledges the Ministry of Public Works and Housing of the Republic of Indonesia for providing the data of this research and Dr. Younghyun Cho from K-Water South Korea for the assistance on the data processing.

References

1. Sagala S, Lassa J, Yasaditama H, Hudalah D (2013) The evolution of risk and vulnerability in Greater Jakarta: contesting government policy in dealing with a megacity's exposure to flooding. IRGSC Working Paper No. 2, p 18
2. Central Board of Statistics (2020) Results of population census DKI Jakarta Province (Jakarta: BPS). Badan Pusat Statistik, Jakarta

3. The World Bank (2007) Jakarta Tantangan Perkotaan Seiring Perubahan Iklim 1. The World Bank, Jakarta
4. Governor of DKI Jakarta (1995) Keputusan Gubernur DKI Jakarta Nomor 582 Tahun 1995 Tanggal 12 Juni 1995 tentang Penetapan Peruntukan dan Baku Mutu Air Sungai/Badan Air Serta Baku Mutu Limbah Cair di Wilayah Daerah Khusus Ibukota Jakarta. Peraturan Daerah DKI Jakarta, Jakarta
5. Rafiei Emam A, Mishra BK, Kumar P, Masago Y, Fukushi K (2016) Impact assessment of climate and land-use changes on flooding behavior in the Upper Ciliwung River, Jakarta. Indonesia. *Water* 8(12):559
6. Moriasi DN, Arnold JG, Van Liew MW, Bingner RL, Harmel RD, Veith TL (2007) Model evaluation guidelines for systematic quantification of accuracy in watershed simulations. *Trans ASABE* 50(3):885–900
7. Nash JE, Sutcliffe JV (1970) River flow forecasting through conceptual models part I—a discussion of principles. *J Hydrol* 10(3):282–290
8. Indonesia SN (2016) Tata Cara Perhitungan Debit Banjir. Badan Standardisasi Nasional, Jakarta

Modeling of Flood Propagation in the Lower Citarum River Using a Coupled 1D-2D HEC-RAS Model



Angga Prawirakusuma, Sri Legowo Wignyo Darsono,
and Arno Adi Kuntoro

Abstract Lower Citarum experiences recurring flood that caused by extreme rainfalls. Study of flood models is now needed to anticipate and prepare flood risk management to reduce losses. This study presents the modeling of the Lower Citarum flood flow using 1D-2D flood modeling in HEC-RAS to understand the behavior of floods. A combination of topographic survey and satellite data was used to model the river channel. Fifteen lateral structures were used to couple the 1D and 2D regimes, where the locations of the structure were based on observations. Results showed minor excesses over the lateral structures, which gradually grow into large areas over time. The study identifies locations with a high risk of flooding in the Lower Citarum Zone, which can be used in further studies for academic and practical purposes. The model result has a discrepancy with the observed data. This difference probably occurred due to the different analysis methods between the observed data and flood modeling or the model's accuracy.

Keywords Flood · Coupled 1D-2D · HEC-RAS · Lower Citarum

1 Introduction

Weather changes cause the natural flow of rivers and streams to vary significantly over time. Periods of overflow and valley flooding may occur alternately with low flows or droughts. Therefore, the role of reservoirs is to retain water during periods of high flow, thereby preventing catastrophic flooding and then allowing the gradual release of water during periods of low flow [1]. Simple reservoirs were

A. Prawirakusuma (✉)

Doctoral Program of Civil Engineering, Institut Teknologi Bandung, Jalan Ganesa No. 10, Bandung 40132, Indonesia

e-mail: aprawirakusuma@students.itb.ac.id

S. L. W. Darsono · A. A. Kuntoro

Water Resources Engineering Research Group, Institut Teknologi Bandung, Jalan Ganesa No. 10, Bandung 40132, Indonesia

created early in human history to provide water for drinking and irrigation. From southern Asia and northern Africa, reservoir use spread to Europe and other continents. The history of reservoir construction in Indonesia has also experienced physical and functional development [2].

In West Java, Indonesia, the Citarum River is the longest and biggest river. After Bengawan Solo and Brantas, it is Java Island’s third longest river. It plays a significant role in the lives of the inhabitants of West Java since it provides water, agriculture, fisheries, industry, sewerage, and energy to a population of 25 million people [3]. It is one of the world’s most polluted rivers. All rivers in the Citarum River Basin flow from south to north, with their headwaters at the surrounding area of Bandung City. The river empties into the north coast (Java Sea) in the Muara Gembong area, Java Sea. Citarum zones are divided into upper, middle, and lower Citarum. The Upper Citarum zone starts from the upstream of the river to the inlet of the Saguling Reservoir. The Middle Citarum zone is a series of Saguling-Cirata-Jatiluhur cascade reservoirs, and the Lower Citarum Zone is limited between the outlet of the Jatiluhur Reservoir to its estuary at Muara Gembong. Figure 1 presents the division of Citarum River Zones.



Fig. 1 Citarum zone divisions

The Lower Citarum is experiencing degradation of flood control infrastructure and irrigation network infrastructure. There are even some points that lack flood control infrastructure in the estuary. Besides that, there is also coastal abrasion in the estuary, which exacerbates the situation. Floods are caused by high rainfall that takes place continuously. Simultaneously with the overflowing of the Cikao River in Purwakarta, the Cibee River in Karawang flows into the Citarum River. The Citarum River channel in Karawang could no longer accommodate flood discharges from upstream, resulting in flooding in Karawang and Bekasi Regencies.

Flood modeling is one of the methods which able to assist flood event analysis. Hydraulic model dimensionality could affect the result simulations. 1D hydraulic modeling using HEC-RAS Software is widely used to describe the flood event in the main channel, yet the 2D hydraulic modeling can be used to analyze the floodplain. In order to obtain an optimal approach to a modeling flood event, 1D and 2D hydraulic modeling can be combined and known as coupled 1D-2D model. Some previous studies used coupled 1D-2D model in simulating flood events. The model results provide an accurate estimation of the flood hazard area and show similarities with the observed data [4, 5]. This study presents the modeling of the Lower Citarum flood flow using 1D-2D flooding using HEC-RAS. This research aims to understand the behavior of floods in the Lower Citarum river and its potential solutions. This study can be used to analyze further studies both for academic and practical purposes.

2 Methodology

The study of flood models is now needed to anticipate and prepare flood risk management due to flooding. Simulation or modeling of flood inundation can be done using a 1-dimensional (1D) hydrodynamic model combined with two dimensions (2D), called a 1D-2D coupled model. This hydrodynamic model is used to calculate flood Water Surface Elevation (WSE). 1D and 2D modeling have either advantages and disadvantages, especially regarding accuracy. The advantages of 1D modeling are the accuracy of the flow in the river channel and the fast runtime. The disadvantages are that it is less accurate in overland flow and the tedious model building. The advantages of 2D modeling are high accuracy in overland flow and rapid model building. At the same time, 2D modeling is not accurate enough to model the flow in the river channel and the model time running is longer. Coupled 1D-2D modeling combines the advantages of 1D model accuracy on river flow and 2D model accuracy on overland flow, with the cost of more complex model building and slower run. Flood modeling using HEC-RAS software is one of the hydrodynamic models that has been recognized by the Federal Management Agency (FEMA). HEC-RAS is a software developed by the Hydrologic Engineering Center

(HEC) under the US Army Corps of Engineers (USACE) [6]. HEC-RAS uses the Saint–Venant equation or diffusion wave in the simulation process.

Primary topographic survey data were used to model the river channel, while the overland flow uses MERIT Digital Elevation Model (DEM). Each dataset is required to model the 1D and 2D portions of the model, respectively. The HEC-RAS’s lateral structure feature couples the 1D and 2D hydrodynamic models. The 1D and 2D model is connected by using lateral structures command in HEC-RAS. The type of lateral structure is weir/embankment by coupling 1D and 2D model using this command, when the water spill from the river to the bank, it will flow to the 2D flow area (overland flow). Figure 2 presents the screenshot of the 1D-2D model building process. There are 15 points of lateral structures modeled along the Lower Citarum River (which is shown by red color in Fig. 2). These points were identified from field observations conducted by The Citarum River Basin Authority (BBWS Citarum). There are eight and seven lateral structures on the left and right sides of the river, respectively. The grid size for each 2D Flow Area is 200×200 , while the distance between cross sections is 50 m.

The modeling scenario is unsteady flow using historical discharge data for the release of the Jatiluhur Reservoir and the discharge of the Cibee River on March 18–23, 2010. The modeling period was chosen because there was an extreme flood event in the Lower Citarum Zone since the discharge was relatively high. Those data are used as input at the upstream. Then for boundary condition of the downstream is 0 m above sea level.

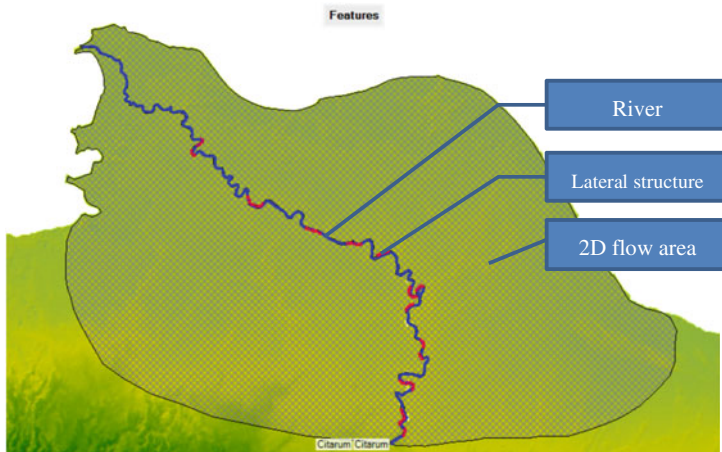


Fig. 2 Screenshot of the 1D-2D domain model building process using HEC-RAS software

3 Results and Discussion

Modeling is carried out along the Citarum Hilir section from the Citarum-Cibeet confluence to Muara Gembong. The discharge scenario used is historical discharge data, as mentioned in the previous section. The modeling is conducted using a coupled 1D-2D model to obtain accuracy in river flow and inundation areas. Merging 1D-2D was carried out at 15 lateral structures, which were identified as points prone to flooding. As shown in the flood modeling results in Fig. 3, the blue area is the inundation area based on the flood depth. The flooded overflow has slowly occurred since March 19, 2010. At this modeling stage, overflow occurred in each lateral structure. The overflow then gradually increased as the day progressed so that the peak was obtained on March 23, 2010. The accumulation of floods that occurred caused the flow to cross laterally to the west and east.

BNPB (The National Agency for Disaster Mitigation), as the national agency that handles and mitigates disasters, including floods, also issued a map of flood events during that period [7]. This flood map was prepared by identifying the field, then marking each sub-district affected by the flood using shading. Because of this, the flood map produced by BNPB uses a sub-district basis. The comparison between the HEC-RAS model result and the BNPB flood event map is shown in Fig. 4. HEC-RAS modeling detects the area's topography from the DEM in the simulations. As for the relationship between the HEC-RAS modeling and comparisons to the BNPB flood event map, the HEC-RAS model can identify locations that experience overflow more accurately, especially at points in the middle section of the Lower Citarum River. Based on Fig. 4, there is a significant difference in the west-east area away from the Citarum River. The difference is probable to occur because HEC-RAS modeling is using a different method from the BNPB observation.

Another thing that can cause differences in the result is the input data. In this model, the input data is limited to only use historical discharge data to release the

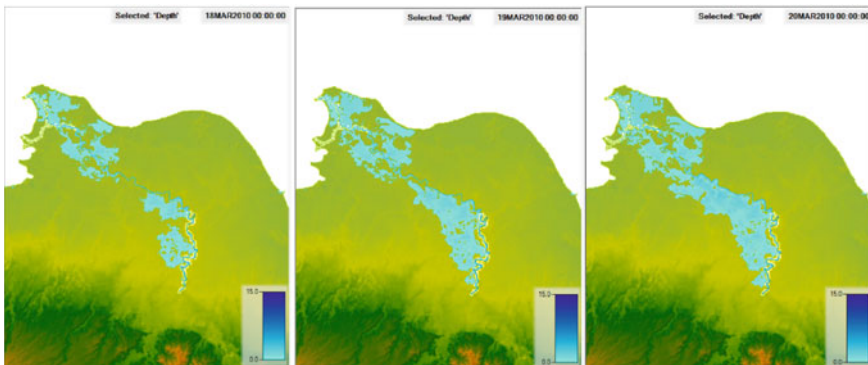


Fig. 3 Flood inundation area process modeled by coupled 1D-2D process using HEC-RAS

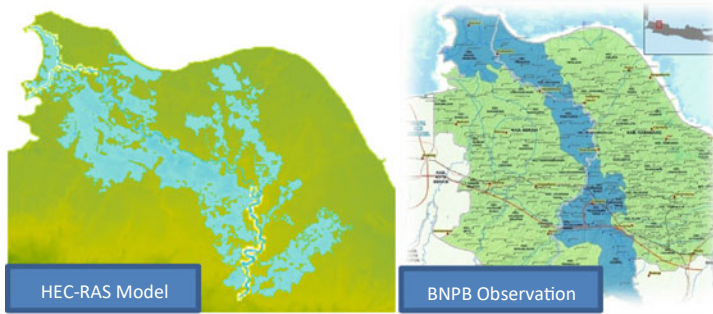


Fig. 4 Comparison between HEC-RAS model and BNPB observation [7]

Jatiluhur Reservoir and the discharge of the Cibeet River. The local discharge, such as from local rainfall in Lower Citarum Zone, has not been included yet. The location of the lateral structure also determines the model result. Thus, for further study, the lateral structure can be more accurate to increase model accuracy towards the observation data. Nevertheless, through this study, a coupled 1D-2D HEC-RAS model can be developed for analyzing flood events.

4 Conclusions

This study presented the modeling of the Lower Citarum flood flow using a 1D-2D coupled model using HEC-RAS. The model's objective is to understand the flood in the modeling period, i.e., 18–23 March 2010, where an extreme flood occurred in the Lower Citarum River. The model used 15 lateral structures to connect the 1D and 2D regimes, while geometrical data is built on topographical and satellite-based elevation surveys. The model presented the flood inundation process, which started with minor overflows in the lateral structures on March 19, 2010. Then the flood gradually grows into larger inundation areas. Comparing with the observation conducted by the BNPB, there were agreements around the area on the inundated regions. However, significant discrepancies were still present in the lateral directions (west–east area away from the Citarum River). This discrepancy could be caused either by BNPB's methodology or the accuracy of the coupled model. The findings presented in this study can be used as an analysis for further studies both for academic and practical purposes.

References

1. Zhao G, Gao H, Naz BS, Kao SC, Voisin N (2016) Integrating a reservoir regulation scheme into a spatially distributed hydrological model. *Adv Water Resour* 98:16–31
2. Schnitter NJ (1994) *A history of dams: the useful pyramids*. Balkema, Rotterdam
3. Fulazzaky MA (2010) Water quality evaluation system to assess the status and the suitability of the Citarum river water to different uses. *Environ Monit Assess* 168(1):669–684
4. Vozinaki AEK, Morianou GG, Alexakis DD, Tsanis IK (2017) Comparing 1D and combined 1D/2D hydraulic simulations using high-resolution topographic data: a case study of the Koiliaris basin. Greece. *Hydrol Sci J* 62(4):642–656
5. Dasallas L, Kim Y, An H (2019) Case study of HEC-RAS 1D–2D coupling simulation: 2002 Baeksan flood event in Korea. *Water* 11(10):2048
6. Brunner GW (2002) Hec-ras (river analysis system). In: *North American water and environment congress & destructive water*, pp 3782–3787. ASCE
7. BNPB Homepage (2021). <https://www.bnpb.go.id/>. Accessed 11 Jun 2021

Review: Effects of Climate on the Geochemical Properties of Volcanic Rocks



Novi Asniar , Yusep Muslih Purwana, Niken Silmi Surjandari, and Bambang Setiawan

Abstract Volcanic rocks are formed from lithification magma that occurs on the surface of the earth. This lithification process can be influenced by climatic conditions in locations where volcanic rocks are formed. Koppen's climate map divides the region in the world into 5 (five) climates, namely: tropical climates, dry climates, temperate/mesothermal climates, continental/microthermal climates, and polar climates. This study was conducted by collecting various literature from the results of research on the geochemical content of volcanic rocks from various locations in the world to classify the types/types of volcanic rocks based on their climate. Grouping types/types of volcanic rocks are using a diagram of Total Alkali versus Silica (TAS diagram). From the results of this review, it was found that volcanic rocks in tropical climates generally are basalt and andesite; volcanic rocks in dry climates generally vary from basaltic trachyte-andesite, trachyte-andesite, andesite, and trachyte; volcanic rocks in the temperate/mesothermal climates generally are dacite and trachydacite; the volcanic rocks of the continental/microthermal climates are generally basaltic andesite, andesite, and dacite.

Keywords Volcanic rock · Climate · Geochemical · TAS diagram

1 Introduction

Climate is a statistical probability for various atmospheric conditions such as temperature, pressure, wind, humidity that occur in an area for a long period of time with an investigation of at least 30 years and covering a large area. Climate is a continuation of the results of recording weather elements from day by day for a long time so that it is referred to as the average of the weather element in general.

N. Asniar (✉)

Civil Engineering Department, Perjuangan University, Tasikmalaya, Indonesia
e-mail: asniarnovi78@gmail.com

Y. M. Purwana · N. S. Surjandari · B. Setiawan

Civil Engineering Department, Sebelas Maret University, Surakarta, Indonesia

Climate affects every aspect of human life. One of them is the process of rock formation on earth. The rock cycle on earth involves three main rocks, namely igneous, sedimentary, and metamorphic rocks. The process of forming these three rocks is influenced by climate, especially the temperature at the location where the process takes place. Temperature is an important factor in the formation, modification, destruction, and re-formation of rocks.

Igneous rock as part of the rock cycle, formed by the cooling process of magma that occurs beneath the surface of the earth (intrusive) and on the surface of the earth (extrusive). Extrusive igneous rocks are often referred to as volcanic rocks. Volcanic rocks are formed when the lava that comes out to the surface of the earth meets the air temperature then cools rapidly. This fast cooling process forms fine-grained rocks, for example, basalt rocks. Besides rock texture, the oxidation process can change silicon as the main material for lava into Silicon dioxide, also known as silica (SiO_2).

The major oxides of the rocks are generally determined by their silica content: rocks with low silica content are rich in magnesium oxide (MgO) and iron oxides (FeO , Fe_2O_3 , and Fe_3O_4) and depleted in soda (Na_2O) and potassium (K_2O); whereas rocks with high silica content have low magnesium and iron oxides but are enriched with soda and potassium. Because of the importance of this silica content, it is common to use these features of igneous rocks as a basis for dividing them into the following groups: silicate or felsic (or acidic), intermediate, mafic, and ultramafic.

Igneous rock classification is generally based on two diagrams: the QAPF diagram of quartz (Q), alkali feldspars (A), plagioclase feldspars (P), and feldspathoids (F) for plutonic rocks and the TAS diagram of Total Alkali versus Silica for volcanic rock. TAS diagrams can be used to classify common types of volcanic rock based on the relationship between combined alkali content and silica content. This chemical composition is useful because the relative proportions of alkali and silica are very important in determining actual mineralogy and normative mineralogy. Volcanic rocks that have been chemically analyzed will be more easily classified with the help of TAS diagrams [1].

This paper aims to analyze the relationship between the classification of volcanic rocks from around the world with the climate conditions of the location. Geochemical analysis data of volcanic rocks from several studies that have been conducted are then analyzed using TAS diagrams to determine the classification of volcanic rocks. Then concluded the relationship between the classification of volcanic rock and the climatic conditions in the location of the volcanic rock is located.

2 Previous Study

A study on the geochemistry of volcanic rocks has been carried out by researchers to identify the characteristics of rocks and their classification. The location of the previous study and the number of samples are shown in Table 1.

Table 1 Location of the previous study and number of samples

Location	Researchers	Number of samples
Rinjani Mountain, Indonesia	Wahidah et al. [1]	30
Galunggung Mountain, Indonesia	Ramadhan et al. [2]	8
Singa Mountain, Hulu Lisung Mountain, Indonesia	Hutabarat [3]	8
the South Kaua`i Swell Volcano, Hawai`i	Ito et al. [4]	111
South Neyshabour, NE Iran	Harsini et al. [5]	20
West and South West of Salafchegan, Qom, Iran	Taheri et al. [6]	29
Ghezelmehkand (NE Ghorveh), Iran	Sheikhzakariaee et al. [7]	11
Jeju Island, South Korea	Tatsumi et al. [8]	42
Dufur West Quadrangle, Oregon	Herinckx et al. [9]	28
Andes, Chile	Lopez-Escobar et al. [10]	32
Gurasada Area, Southern Aouseni MTS, Romania	Constantina et al. [11]	10
Valencia, Spain	Ryan et al. [12]	9
The Crommyonia volcanic rocks, Greece	Soen [13]	35
Andes, Southern Peru	Aramaki et al. [14]	87
Chispa Mountain Quadrangle, Texas	Teal et al. [15]	66
Tampomas, Mountain, Indonesia	Mesker [16]	18

3 Köppen Climate Classification

One of the most widely used climate classification systems is The Köppen Climate Classification. It was the Russian climatologist Wladimir Köppen who first introduced this climate classification in 1884. The Köppen climate classification divides the climate into five main climate groups (Fig. 1). Five climate groups are divided based on seasonal rainfall and temperature patterns, namely Group A (tropical), Group B (dry), Group C (moderate), Group D (continental), and Group E (polar). Each group and subgroup is represented by a letter. The first letter represents the name of the group and the second letter represents the subgroup. All climates have group and subgroup names, except climate E, which has no subgroups.

Group A: Tropical (Mega Thermal) Climates This type of climate has an average temperature of 18 °C (64.4 °F) throughout the year or higher, with a significant rainfall.

Group B: Dry (Arid and Semiarid) Climates This type of climate is characterized by little rainfall and an annual average temperature of 20 °C.

Group C: Temperate (Mesothermal) Climates This type of climate has the coldest month with an average temperature of between 0 °C (32 °F) or 3 °C (27 °F)

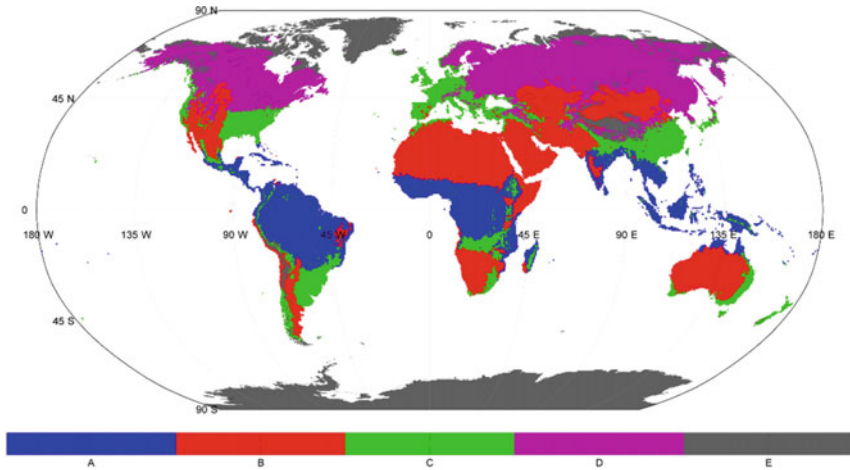


Fig. 1 The Köppen climate classification map [17]

and 18 °C (64.4 °F) and at least one month the average temperature is above 10 °C (50 °F).

Group D: Continental (Microthermal) Climates This type of climate has at least one month with an average temperature below 0 °C (32 °F) or 3 °C (27 °F) and at least one month with an average temperature above 10 °C (50 °F).

Group E: Polar and Alpine (Montane) Climates This type of climate has an average temperature of below 10 °C (50 °F) throughout the year.

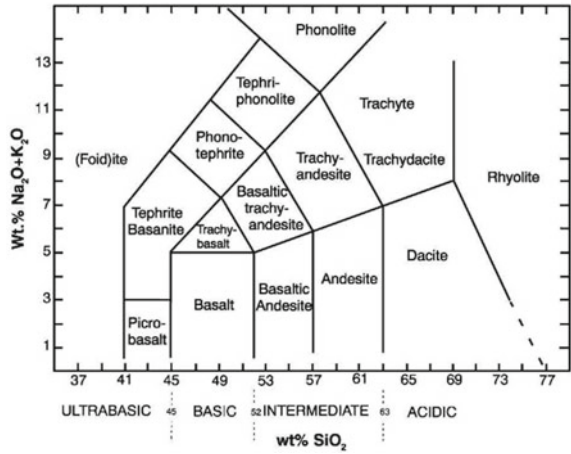
4 Total Alkali Versus Silika (TAS) Diagram

The TAS classification diagram has proven useful for the following reasons: (a) it is based on simple chemical parameters and not on modal content because it is very difficult to determine aphanitic or glassy content; (b) use straight lines to define the classification field; (c) the chemical composition of most natural rocks can be plotted on this diagram [18]. TAS diagram is shown in Fig. 2.

5 Methodology

Geochemical analysis using the XRF method produces percent chemical elements of oxides such as SiO₂, TiO₂, Al₂O₃, Fe₂O₃, MnO₃, CaO, MgO, Na₂O, K₂O, and P₂O₅. The results of this analysis will determine the characteristics of volcanic rocks and are also used as a basis for the classification of volcanic rocks using TAS

Fig. 2 The Total Alkali-Silica (TAS) diagram [18]



diagrams. The Total Alkali-Silica (TAS) diagram used is binary diagram Le Bas et al. [19].

Geochemical analysis of volcanic rocks from various locations in the world is collected, and the classification of volcanic rocks is based on TAS diagrams. The next step is to divide the locations of the research into the Koppen world climate classification map.

6 Data and Analysis

Geochemical data of volcanic rocks from several studies that have been carried out are then set in the Total Alkali versus Silica (TAS) diagram to determine the classification of volcanic rocks. So that the type of volcanic rock that dominates can be known. Then, using the Koppen climate classification map, we can determine the climatic conditions of the location where samples of volcanic rock were taken. The results of this data analysis are shown in Table 2.

In the process of cooling magma where the magma is not all frozen immediately but slowly decreases the temperature even quickly. This decrease in temperature is followed by the start of the formation and deposition of certain minerals according to their temperature. The formation of minerals in magma due to a decrease in temperature was compiled by Bowen [20]. Bowen has made a table of mineral formation for use in interpreting these minerals (Fig. 3).

On the left represents mafic minerals, the first to form at very high temperatures is Olivine. However, if the magma is saturated by SiO_2 , then Pyroxene is formed first. The temperature decreases continuously and the formation of minerals occurs according to the temperature. The last mineral formed is Biotite. It is formed in low temperatures.

Table 2 Climate classification and dominance of volcanic rock types

Location	Climate classification	Volcanic rock types
Rinjani Mt., Indonesia	Tropical	Basalt, Basaltic trachy-andesite, trachy-andesite
Galunggung Mt., Indonesia	Tropical	Basalt, Basaltic andesite, andesite
Singa Mt. and Hulu Lisung Mt., Indonesia	Tropical	Andesite, Dacite
South Kaua'i Swell, Hawai'i	Tropical	Basalt
Tampomas Mt., Indonesia	Tropical	Basaltic andesite, andesite, dacite
South Neyshabour, NE Iran	Dry	Basaltic trachy-andesite, trachy-andesite, trachyte, trachy-dacite
West and South West of Salafchegan, Qom, Iran	Dry	Basaltic andesite, andesite, dacite
Ghezlechekand (NE Ghorveh), Iran	Dry	Tephrite, phonotephrite, basaltic trachy-andesite
Andes, Chile	Dry	Basalt, basaltic andesite
Andes, South Peru	Dry	Andesite, Dacite
Chispa Mountain Quadrangle, Texas	Dry	Basaltic trachy-andesite, trachy-andesite, trachy-dacite
Jeju Island, South Korea	Continental	Trachy-basalt, basaltic trachy-andesite, trachy-andesite
Gurusada Area, Southern Apuseni MTS, Romania	Continental	Basaltic andesite, andesite, dacite
Dufur West Quadrangle, Oregon	Temperate	Andesite, dacite
Valencia, Spain	Temperate	Basaltic andesite, andesite, dacite
The Crommyonia volcanic rocks north of the Saronic Gulf, Greece	Temperate	Dacite, Rhyolite

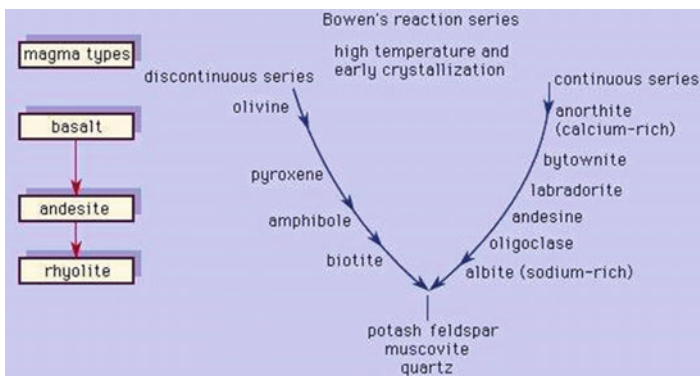


Fig. 3 The Bowen reaction series shows the order in which minerals will form and disappear during the fractional crystallization of Molten Magma. The left shows minerals crystallized in Magma [20]

The mineral on the right is represented by the Plagioclase group mineral because it is the most abundant and widely distributed. Anorthite is a mineral that was first formed at high temperatures and is abundant in alkaline igneous rocks such as Basalt. Andesin forms a medium temperature gap, and there are Andesite igneous rocks. While minerals formed at low temperatures are albites, these minerals are widely spread on acidic rocks such as dacite or rhyolite.

The dry climate has an average temperature above 30 °C and a little rainfall in each year, so the process of decreasing the temperature of magma is slower than the tropical climate which has high humidity and rainfall, so that volcanic rocks in dry climates generally are basalt rocks with the amount of total alkaline are quite high compared to basalt rocks that found in tropical climates. Volcanic rocks in a tropical climate are generally basalt and andesite rocks because the process of decreasing the temperature of the magma is still slow.

In continental and temperate climates, the average temperature is below 18 °C each year, so the magma temperature drops faster. Therefore, volcanic rocks that are formed generally are dacite or rhyolite.

7 Conclusion

The process of forming Igneous rocks, Sedimentary Rocks, and Metamorphic are influenced by climate, especially temperature at the location where the process takes place. Temperature is an important factor in the formation, modification, destruction, and re-formation of rocks.

The Köppen climate classification divides the climate into five main climate groups. Five climate groups are divided based on seasonal rainfall and temperature patterns, namely Group A (tropical), Group B (dry), Group C (moderate), Group D (continental), and Group E (polar).

Volcanic rocks in dry climates generally are basalt and basaltic trachyandesite rocks with the amount of total alkaline are quite high. Volcanic rocks in a tropical climate are generally basalt and andesite rocks because the process of decreasing the temperature of the magma is still slow. In continental and temperate climates, volcanic rocks that are formed generally are dacite or rhyolite.

References

1. Wahidah AN, Rachmat H, Rosana MF, Rinjani G, Aikmel K, Lombok K (2016) Petrogenesis batuan piroklastik Gunung Rinjani. In: Proceeding, Seminar Nasional Kebumian ke-9 Peran Penelitian Ilmu Kebumian Dalam Pemberdayaan Masyarakat 6–7 Oktober 2016; Grha Sabha Pramana
2. Ramadhan ED, Hutabarat J, Mulyo A (1982) Perbedaan karakteristik mineralogi matriks breksi vulkanik pada endapan fasies proksimal atas-bawah Gunung Galunggung. Semin Nas Ke—III Fak Tek Geol Univ Padjadjaran

3. Hutabarat J (2007) Studi geokimia batuan vulkanik primer kompleks Gunung Singa-Gunung Hulu Lisung Bogor-Jawa Barat. *Bull Sci Contrib* 5:141–151
4. Garcia MO, Weis D, Swinnard L, Ito G, Pietruszka AJ (2015) Petrology and geochemistry of volcanic rocks from the South Kauai swell volcano, Hawaii: implications for the lithology and composition of the Hawaiian mantle plume. *J Petrol* 56(6):1173–1197
5. Entezari Harsini A, Mazaheri SA, Saadat S, Santos JF (2017) Geochemistry, petrology, and mineralization in volcanic rocks located in south Neyshabour. NE Iran. *J Min Environ* 8 (2):139–154
6. Taheri M, Ardalan AA, Emami MH, Zakariay SJS (2017) Petrology and tectonic setting of volcanic rocks in west and south west of Salafchegan, Qom, Iran. *Open J Geol* 7(06):745
7. Sheikhzakariaee SJ, Kazemi H, Abedini MV, Emami MH (2015) Petrography and geochemistry of volcanic rocks of GhezalcheKand (NE Ghorveh). Iran. *J Bio Env Sci* 6 (2):423–433
8. Tatsumi Y, Shukuno H, Yoshikawa M, Chang Q, Sato K, Lee MW (2005) The petrology and geochemistry of volcanic rocks on Jeju Island: plume magmatism along the Asian continental margin. *J Petrol* 46(3):523–553
9. Herinckx HH (2015) Geochemistry and petrography of igneous components of the Dalles Formation in the Dufur West quadrangle, Oregon
10. López-Escobar L, Kilian R, Kempton PD, Tagiri M (1993) Petrography and geochemistry of quaternary rocks from the southern volcanic zone of the Andes between 41 30' and 46 00'S. Chile. *Andean Geol* 20(1):33–55
11. Constantina C, Szakacs A, Pecskey Z (2009) Petrography, geochemistry and age of volcanic rocks in the gurasada area, southern apuseni mts. *Carpathian J Earth Environ Sci* 4(1):31–47
12. Ryan WBF, Hsu KJ, Honnorez J (2007) Petrography of the Valencia trough volcanic rocks
13. Soens B, Smet I, Klaver M, Vanhaecke F, Van Ranst E, Claeys P, De Grave J (2016) Petrology and geochemistry of the Crommyonia volcanic rocks north of the Saronic Gulf, Greece. In: *Geologica Belgica Master day*, vol 19, no 3–4, pp 302–303
14. Aramaki S, Onuma N, Portillo F (1984) Petrography and major element chemistry of the volcanic rocks of the Andes, southern Peru. *Geochem J* 18(5):217–232
15. Teal LW, Hoffer JM (1980) New Mexico Geological Society Mountain quadrangle, Culberson and Jeff Davis Counties, Texas. In: *NMGS fall field conference*, pp 241–244
16. Dirk MH (2008) Petrologi-geokimia batuan Gunung Api Tampomas dan sekitarnya. *Indonesian J Geosci* 3(1):23–35
17. Chen D, Chen HW (2013) Using the Köppen classification to quantify climate variation and change: an example for 1901–2010. *Environ Dev* 6:69–79. <https://doi.org/10.1016/j.envdev.2013.03.007>
18. Verma SP, Torres-Alvarado IS, Sotelo-Rodríguez ZT (2002) SINCLAS: standard igneous norm and volcanic rock classification system. *Comput Geosci* 28(5):711–715
19. Bas ML, Maitre RL, Streckeisen A, Zanettin B (1986) IUGS subcommission on the systematics of igneous rocks. A chemical classification of volcanic rocks based on the total alkali-silica diagram. *J Petrol* 27(3):745–750
20. Bowen NL (1928) *The evolution of the igneous rocks*. First. Princeton University Press, London, p 332

Analysis of the Utilization of the Embung Klampeyan, Tlogoadi Village, Mlati District, Sleman Regency, Indonesia



Edy Sriyono 

Abstract Embung Klampeyan which was established in 2009, has an area of approximately $54 \times 329 \text{ m}^2$ with a depth of 4.15 m with a water capacity of $15,000 \text{ m}^3$ and can drain water up to 25 ha. Currently the Embung Klampeyan is still functioning properly. The dam performance will be reviewed using a system-based approach: physical aspects, utilization aspects, as well as operational and maintenance aspects. Descriptive procedure with quantitative approach is used in this research. Descriptive analysis is intended to describe the results of the research to each of the assessed aspect variables. The Likert scale is used to assess/measure the attitudes, opinions and perceptions of a person or group of people towards research variables in the form of events or social symptoms that specifically determined. The results of the analysis show that the Physical Aspects have a value of 4.02 in very good conditions, the Utilization Aspects have a value of 4.13 in very good conditions, and the Operations and Maintenance Aspects have a value of 4.06 in very good conditions as well. Thus it can be concluded that the Klampeyan Embung is in very good condition or can provide very good benefits for the surrounding community.

Keywords Physical · Utilization · Operation and maintenance · Embung Klampeyan

1 Introduction

Embung Klampeyan is a pond or a small reservoir that is used to store water when there is excess water during the rainy season and is used when there is a shortage of water during the dry season, for several purposes, among others drinking water, tourism, irrigation, flood control, and others [1, 2]. In Undang-Undang Republik Indonesia Number 17 of 2019 concerning Water Resources, it is explained that the

E. Sriyono (✉)

Janabadra University, Jalan Tentara Rakyat Mataram 55-57, Yogyakarta 55231, Indonesia
e-mail: edysriyono@janabadra.ac.id

community can play a role when carrying out the operation and maintenance (OM) of water resources, including reservoirs [3]. The operation of the reservoir is an effort made to optimally use the water stored in the effective reservoir. Meanwhile, reservoir maintenance is an effort made to maintain that existing infrastructure facilities can function properly during the life of the reservoir building and during the planned service time [4].

Embung Klampeyan is located in Toragan Hamlet, Tlogoadi Village, Mlati District, Sleman Regency, Yogyakarta Special Region. Embung Klampeyan is one of several artificial lakes that have been built by the Regional Government of Sleman Regency, the implementation of which was carried out in three stages starting from 2007 to 2009 by the Department of Irrigation, Mining and Natural Disaster Management of Sleman Regency. Embung Klampeyan has an area of $54 \times 329 \text{ m}^2$ with a depth of 4.15 m. The water capacity of this reservoir is planned to reach 15,000 m and can drain up to 25 ha of land around the reservoir area. The Embung Klampeyan has the function of storing water when there is more water when it rains to be used when there is a shortage of water during the dry season. In addition, the dam also functions as an interesting tourist attraction. This reservoir is also filled with fish seeds, and because the location of the reservoir is located in the middle of a fairly beautiful rice field area, it can become a separate tourist attraction for the surrounding community.

In addition, in Mozambique, small dams or dams were also built in semi-arid areas or other locations to overcome the problem of water scarcity [5]. Meanwhile, in the Sleman district of the Special Region of Yogyakarta, Indonesia, the reservoir can also function as a source of clean water for the city of Yogyakarta [6].

With this research, it will be known the benefits of the construction of the Embung Klampeyan in the Toragan hamlet, Tlogoadi village, for the community in the Tlogoadi village and its surroundings in terms of: Physical, Utilization, and Operation, and Maintenance.

2 Literature Review

2.1 Embung Klampeyan Component

Embung Klampeyan buildings usually consist of several components, namely: rain-fed areas, storage areas, embankments, spillways, distribution and transmission pipelines, service tanks such as clean water tanks, livestock water tanks, garden water tanks, safety fences (fences around embankments and puddles, as well as gates), and complementary buildings such as peil schaal, benchmarks, and the nameplate of the reservoir [1].

2.2 *Embung Klampeyan Operation and Maintenance*

There are three parts to the operation and maintenance of the reservoir as follows:

1. Embung Klampeyan operation activities

Considering the limited volume of water in the reservoir, a plan for the operation of the reservoir must be made in advance. Based on the calculation of water needs, the amount of water distribution provided to the population can be determined.

2. Monitoring and inspection activities

In order to obtain correct and precise data, regular monitoring is necessary. Monitoring is carried out to organize operational activities and early inspection of the reservoir for the safety of the reservoir itself after the reservoir is operated. The data that must be monitored continuously are data: rainfall, discharge that runs over spillway buildings, raw water supply discharge at the valve house, water level elevation in the upstream section of the dike, and seepage discharge data in the downstream section of the dike. In addition, it is also necessary to check the overall condition of the dike building.

3. Embung Klampeyan maintenance and repair

In order to maintain the sustainability of the function of the reservoir building, it is necessary to carry out routine maintenance of all components and completeness of the reservoir building. Routine maintenance activities, consisting of:

- Dike maintenance

Dike damage is generally in the form of cracks, leaks, and so on. Therefore the planted grass needs to be watered during the dry season and cut to determine possible damage to the dike.

- Storage pool maintenance

Garbage such as tree trunks sometimes enters the reservoir column, so cleaning is necessary.

- Maintenance of spillway

It is also necessary to clean up trash or tree trunks carried by runoff water and prevent perennials from growing along or along the edge of the spillway.

- Maintenance of distribution network and supporting buildings for reservoirs

The importance of maintenance is to prevent damage or leakage, which can result in water loss and uneven water distribution.

2.3 *Aspects Reviewed*

Embung Klampeyan has 3 (three) important aspects that must be reviewed, namely aspects: physical, utilization, and Operation and Maintenance (OM). In each aspect, there are several variables [2, 7].

1. Physical Aspect

- The dike consists of: Areas of seepage through the reservoir body or local landslides on the foundation because the soil is saturated, Areas of seepage along the reservoir body, Transverse cracks in the reservoir body, Longitudinal cracks at the top of the reservoir body. These cracks can be straight or curved, Shrinkage cracks, generally short, shallow, narrow, numerous, and irregular in direction, Erosion of grooves in the reservoir body, and Perennials along the pond body.
 - Spillway, consisting of: Collapse in the spillway, Erosion of grooves in the spillway, and local scour on the spillway.
 - Storage pond, consisting of: silt sediment, garbage/rotten tree branches, fence around the pond, peil schaal, buoy, and water availability.
 - Distribution network pipelines, consisting of: Transmission pipelines, and distribution pipelines.
 - Tub service, consisting of: tanks for humans, tanks for livestock, and tanks for gardens.
2. Aspects of Utilization, consisting of: Water distribution, feeling of comfort in the existence of guaranteed water for the reservoir, and Improving the standard of living/health of the community around the reservoir.
 3. Operation and Maintenance Aspects, consisting of: The implementation of OM implementation, Availability of OM facilities and budget, Subsidies, and Implementation of OM training.

3 Method

3.1 Research Sites

This research was conducted in the Embung Klampeyan location in Toragan Hamlet, Tlogoadi Village, Mlati District, Sleman Regency, Yogyakarta Special Region Province, Indonesia as shown in Figs. 1 and 2.

3.2 Population and Sample

The population in this study consisted of the relevant and the community who used the Embung Klampeyan water along with their education ranging from elementary school to undergraduate. The sample determined in this study used a proportional stratified random sampling system, which is a technique where the population has members with different educational levels. The reason for using the sampling technique mentioned above is because the users of the Embung Klampeyan have

Fig. 1 Research sites



Fig. 2 Top view of the Embung Klampeyan



educational levels that vary from elementary to undergraduate, with a total population of 232 people. Furthermore, data collection was carried out in 2020.

The Taro Yaname and Slovin formulas are used to determine the total number of sample members. This refers to the opinion [8] that the sampling technique can be used if the population is known and consists of more than 100 people. The formula of number of sample members is shown in Eq. 1.

$$n = \frac{N}{N \times d^2 + 1} \tag{1}$$

where n is the number of sample members, N is the number of population, and d^2 is the precision. The precision is set at 10%, then: $n = \frac{N}{N \times d^2 + 1} = \frac{232}{232 \cdot (0.1)^2 + 1} = 70$ respondent.

The number of sample members is calculated by the proportional allocation formula in Eq. 2.

$$n_i = \frac{N_i}{N} \times n \tag{2}$$

where n_i is the number of sample members by strata, n is the total number of sample members, N_i is the number of population members by strata, and N is the total number of population members.

So the number of sample members based on education level is:

Elementary School = 15 people, Junior High School 17 people, High School = 34 people, Diploma = 1 person, and Bachelor = 3 people. The occupations of the people around Embung Klampeyan are all farmers.

3.3 Data Collection

Field observation techniques and questionnaires were used to collect data by using descriptive methods through quantitative approaches and data collection techniques. Quantitative research is research that determines a sample of the population through a questionnaire that serves as the main data collection tool [9]. The observation technique is a field research technique that is useful for collecting data with the researcher become participants in the cultural environment of the research object [10].

Analysis Questionnaire technique is a way of collecting data by giving a series of questions which are generally in the form of written questions to be answered by respondents [11]. In this study used a questionnaire with a Likert scale [11]. With a Likert Scale, attitudes, opinions, and perceptions of a person or group of people towards social phenomena can be measured/assessed. Variables that are measured/assessed on a Likert scale are described as variable indicators. Then this indicator is used as a starting point for compiling instrument items, either statements or questions. The answer to each instrument item with a Likert scale will have a gradation ranging from very positive to negative.

3.4 Data Analysis

All research data were then analyzed using the Likert scale method, namely by giving a certain value to each variable. With a Likert scale, the attitudes, opinions, and perceptions of a particular person or group of people towards a phenomenon can be measured. The phenomenon in question is a research variable that has been specifically determined. The Likert scale has a value of:

- | | |
|---|---|
| 1. Strongly Agree or Always or Very Important | 5 |
| 2. Agree or Important or Often | 4 |
| 3. Doubtful or Fairly Important or Almost Never | 3 |
| 4. Less Agree or Less Important or Almost Never | 2 |
| 5. Disagree or Not Important or Never | 1 |

Every aspect that is reviewed, its performance is measured with the value mentioned above. Each aspect that has the same value indicates that each component of all variables has the same contribution to the management of the Embung Klampeyan. Table 1 is used to assess the performance of each aspect of a reservoir.

Table 1 Embung Klampeyan performance scores for various interpretations [11]

Aspect	Value				
	Very good	Good	Pretty good	Not good	Not very good
Physical	4.01–5.00	3.51–4.00	2.51–3.50	1.51–2.50	1.00–1.50
Utilization	4.01–5.00	3.51–4.00	2.51–3.50	1.51–2.50	1.00–1.50
Operation and maintenance	4.01–5.00	3.51–4.00	2.51–3.50	1.51–2.50	1.00–1.50

The questionnaire has two types of questions or statements using positive sentences or negative sentences, with the aim that respondents can give answers to each question seriously and not mechanistically. The value of answers to questions or statements with positive sentences is:

- 1. Strongly Agree or Very Important or Always 5
- 2. Agree or Important or Often 4
- 3. Doubtful or Quite Important or Sometimes 3
- 4. Less Agree or Less Important or Never 2
- 5. Disagree or Not Important or Never 1

The value of answers to questions or statements with negative sentences is:

- 1. Strongly agree or Very Important or Always 1
- 2. Agree or Important or Often 2
- 3. Doubtful or Quite Important or Sometimes 3
- 4. Less Agree or Less Important or Never 4
- 5. Disagree or Not Important or Never 5

Each variable contains several questions or statements with positive sentences or negative sentences, so the assessment is the number of positive sentence answers and the number of negative sentence answers added and then divided by the number of questions from all these variables. After the value of each variable is obtained, then the sum of the variables is carried out to obtain the average value of each variable. To calculate the average value, use formula in Eq. 3.

$$\bar{x} = \frac{x_1 + x_2 + \dots + x_n}{n} \tag{3}$$

with \bar{x} is mean, x_1, x_2, \dots, x_n , is the value of the nth variable according to the Likert scale, and n is the number of variables or it can be written as in Eq. 4.

$$\bar{x} = \frac{\sum f_i x_i}{\sum f_i} \tag{4}$$

with \bar{x} is mean, f_i is the number of variables, and x_i is the value of the n th variable according to the Likert scale, and n is the number of variables.

Then the conclusion of whether the performance of the reservoir management is optimal according to the plan or not is obtained from the average value of the three aspects of the value of the benefit, namely aspects: physical, utilization, and OM (Operations and Maintenance). Then the final scores of the three aspects mentioned above are averaged. This is the final answer to this research problem. To calculate the average value, use formula in Eq. 5.

$$N_{FINAL} = \frac{N_{AF} + N_{AP} + N_{AOP}}{3} \quad (5)$$

with N_{FINAL} is Final value, N_{AF} is the mean value of the physical aspect, N_{AP} is the mean value of the aspect of utilization and N_{AOP} is the mean value of O&M aspects.

4 Results and Discussion

4.1 Respondent Characteristics

1. Number of respondents from citizen and users of the Embung Klampeyan: 70 people
2. Gender: Male = 58 people and female = 12 people
3. Age: 25–30 years = 1 person, 31–35 years = 6 people, 36–40 years = 4 people, 41–45 years = 8 people, 46–50 years old = 16 people, 51–55 years old = 26 people, and 56–60 years old = 9 people
4. Education: Elementary School = 15 people, Junior High School 17 people, High School = 34 people, Diploma = 1 person, and Bachelor = 3 people.

4.2 Physical Aspect

Table 2 shows that the respondent's observations of the dike are in good condition, the spillway is in good condition, the storage pond is in good condition, the distribution network pipe is in very good condition, and the service tank is in good condition.

Most respondents answered very well on the physical aspect, and it can be concluded that the 5 (five) physical aspects of the Embung Klampeyan, namely embankments, storage ponds, spillways, distribution network pipes, and service tanks are in very good condition, so that the utilization factor of the Embung Klampeyan is already functioning very good.

Table 2 Variable condition value for physical aspect

No	Variable	Value	% of respondents
1	Embankment	4.00	19
2	Spillway	4.00	19
3	Storage pool	4.00	19
4	Distribution network pipeline	5.00	24
5	Service tank	4.00	19
Total		21.00	100
Mean value		4.02	

4.3 Utilization Aspect

Table 3 shows that most of the respondents answered very well on the condition value of each variable in the utilization aspect. Respondents stated that the water distribution is in very good condition, there was no conflict in the struggle for the distribution of water in the Embung Klampeyan, the respondents felt comfortable with the existence of water guarantees in the long dry season because the reservoir water is never dry, and there was an increase in the quality of life with the existence of tourist attractions so that it can improve the welfare of the residents of Tlogoadi village and its surroundings.

4.4 Operation and Maintenance Aspect

Table 4 shows that the majority of respondents responded very well to aspects of surgery and maintenance. This shows that respondents consider operational and maintenance training activities very good, the availability of facilities and funds for maintenance surgery is very good, subsidies are considered good, and compliance with surgery and maintenance is also good. considered very good.

Table 3 Variable condition value for utilization aspect

No	Variable	Value	% of respondents
1	Water distribution	4.11	32
2	Comfort with water guarantee	4.12	33
3	Improving the quality of life of a tourist attraction	4.15	35
Total		12.38	100
Mean value		4.13	

Table 4 Variable condition value for operation and maintenance aspect

No	Variable	Value	% of respondents
1	Obedience to carry out operation and maintenance	4.05	25
2	Availability of operation and maintenance funds	4.08	25
3	Subsidy	4.01	24
4	Operation and maintenance training activities	4.10	26
Total		16.24	100
Mean value		4.06	

4.5 Utilization Analysis

Based on the results of information analysis and reviews of research results on aspects of: physical, utilization, and surgery and maintenance, it can be seen that the overall value of the benefit analysis of the Embung Klampeyan is: NAF = 4.02, NAP = 4.13, and NAOP = 4, Utilization analysis of the Embung Klampeyan = $\frac{NAF + NAP + NAOP}{3} = \frac{4.02 + 4.13 + 4.06}{3} = 4.07$.

Based on the results of the analysis, it can be seen that the overall Embung Klampeyan is in very good condition. This condition is certainly due to the influence of aspects: physical, utilization, and Operation and Maintenance. The achievements of each variable can be seen in Fig. 3.

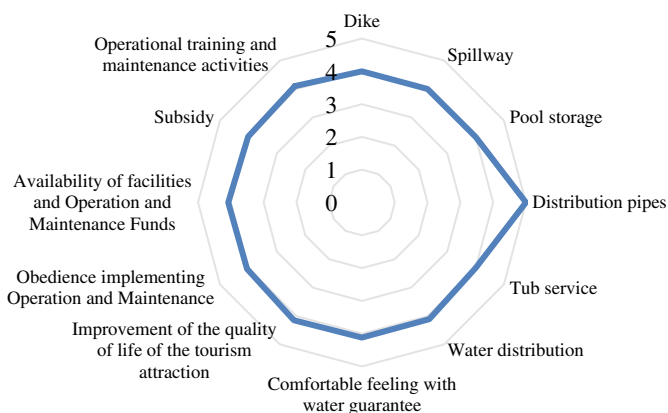


Fig. 3 Research variable radar diagram graph

5 Conclusions and Recommendations

5.1 Conclusions

Based on the results of the utilization analysis of the Embung Klampeyan, the following conclusions are obtained:

1. Based on the physical aspect, the reservoir has a value of 4.02. This indicates that the overall parts of the reservoir are in very good condition, be it embankments, spillways, storage ponds, pipelines, and service tanks.
2. Based on the aspect of the use of the reservoir, it has a value of 4.13. This indicates that the reservoir has been used very well by the community.
3. Based on the operational and maintenance aspects, the reservoir has a value of 4.06. This indicates that the O&M reservoir is in very good condition.

Based on the results of the total analysis, the use of the Embung Klampeyan is in very good condition. This means that Embung Klampeyan can provide very good benefits for the surrounding community, both based on aspects: physical, utilization, as well as based on operation and maintenance.

5.2 Recommendations

Based on conclusions such as those described above, some suggestions can be made as follows:

1. There is a need for increased compliance in carrying out the operation and maintenance (O&M) of Embung Klampeyan.
2. It is necessary to add an operational standard (SOP) in carrying out the O&M of the Klampeyan Embung so that the entire user community can better understand the importance of the operation and maintenance system and know what actions to take if problems occur in the Klampeyan Embung.
3. It is necessary to make a Regent's Decree (SK) regarding village regulations governing the distribution of reservoir water.
4. There needs to be an independent maintenance fee from the village that does not depend on the government to pay for the maintenance of the reservoir.
5. It is necessary to pay attention to physical aspects such as embankments, overflow buildings, water storage ponds, network pipes, and service tanks in order to keep the dams functioning properly.

References

1. Direktorat Bina Rehabilitasi dan Pengembangan Lahan (1998) Petunjuk Teknis Pembuatan Embung. Direktorat Bina Rehabilitasi dan Pengembangan Lahan, Jakarta
2. Kasiro I, Wanny-Rusli BSN, Sunario CL (1994) Pedoman kriteria desain embung kecil untuk daerah semi kering di Indonesia. Direktorat Jenderal Pengairan Departemen Pekerjaan Umum, Jakarta
3. Pemerintah Republik Indonesia (2019) Undang-undang Republik Indonesia Nomor 17 Tahun 2019 Tentang Sumber Daya Air. Pemerintah Republik Indonesia, Jakarta
4. Suripin (2002) Pelestarian sumber daya tanah dan air. Penerbit Andi, Yogyakarta
5. dos Anjos LA, Cabral P (2021) Small dams/reservoirs site location analysis in a semi-arid region of Mozambique. *Int Soil Water Conserv Res* 9(3):381–393
6. Sriyono E, Purwanto A, Sardi NCK, Bhakty TE, Biddinika MK (2020) Assessing the Potential of Tambakboyo Retention Basin for Raw Water Supply in the City of Yogyakarta Indonesia. In: *Proceedings of the 2nd ICASESS 2019*, pp 96–100
7. Sardi FHL, Sriyono E, Kresnanto NC, Bhakty TE, Biddinika MK (2020) Analysis of Embung Abimanyu Utilization in Temanggung, Central Java, Indonesia. In: *Proceedings of the 2nd ICASESS 2019*, pp 143–148
8. Reduwan E (2007) Teknik Pengambilan Sample Taro Yamane atau Solvin. Alfabeta, Bandung
9. Masri S, Effendi S (1989) Metode Penelitian Survei. LP3ES, Jakarta
10. Mantju (1994) Teknik Perekaman Data. Lemlit IKIP, Malang
11. Sugiyono (2011) Statika dan Penelitian. Cetakan ke-18. Alfabeta, Bandung

Analysis of Shift Pile Foundation on Mall and Hotel Projects in Bontang, East Kalimantan



Nicholas Joshua and Alfred Jonathan Susilo

Abstract Indonesia has many areas dominated by clay soils. Including in Bontang city, East Kalimantan. This research focuses on malls and hotel projects located at that location. Regarding the construction in this project, there is a case of foundation pile shifting due to several factors, including the soil embankment factor. It causes additional loads outside the design of the foundation pile and the clay soil type factor with high moisture content and plasticity, as well as the impact load factor caused by the driving machine foundation pile. So, an analysis of the foundation piles before and after the addition of the load was carried out using the p-y curve method to find the maximum lateral load. It focuses on the Mall and Hotel project in Bontang, which is shifting pile due to additional loads such as soil embankment and driving machine pile. The two analyses will be compared and searched for the two piles' lateral bearing capacity and can later improve the case or prevent similar cases in other projects. The main result is maximum lateral load (3.436 Ton), additional lateral loads (8.157 Ton), so the conclusion is the pile cannot hold the lateral loads.

Keywords Shift pile · Lateral load · Clay soil · Additional lateral load · Bontang

1 Introduction

The discussion of this research focuses on the case of the shift of the foundation piles in the Mall and Hotel project in Bontang to a distance of approximately 1.5 m due to the addition of unplanned loads when designing the foundation piles. The load in question is the 5-m high project land embankment due to the excavated soil that is not removed or moved because the soil condition is too plastic, so that it is

N. Joshua (✉) · A. J. Susilo
Universitas Tarumanagara, Letjen S. Parman Street No.1, Jakarta, Indonesia
e-mail: nicholas.325170123@stu.untar.ac.id

A. J. Susilo
e-mail: alfred@ft.untar.ac.id

difficult to dispose or transfer the excavated soil. Then there is also an additional load in the form of an impact load from the heavy pile driving equipment, namely the 120 Ton Hydraulic Static Pile Driver (HSPD). If the project is continued without any repairs, then the building above it will not be able to withstand the load because the foundation piles are tilted due to the shift of the piles [1]. For this reason, it is necessary to calculate the maximum lateral load that the foundation piles on the project can receive. This study uses the p-y curve method for calculating the maximum lateral load. There is also a calculation of the addition lateral loads to the pile due to soil embankment at the project site, and also the addition lateral loads due to the movement of the piling machine (HSPD) by finding the magnitude of the impact load using the method discovered by Boussinesq [2].

1.1 p-y Curve Method

In 2010, Georgiadis proposed a p-y curve construction approach compared to the Finite Element approach. Georgiadis modified an equation that has often been adopted to interpret the pile test results [3]. This curve has an initial slope of K_i and is described by the hyperbolic equation in Eq. 1.

$$p = \frac{y}{\frac{1}{k_i} + \frac{y}{p_u}} \quad (1)$$

Determining the value of P_u (ultimate load) based on the depth of the point is considered necessary in constructing the p-y curve. Based on the results of research by Georgiadis [3], P_u can be calculated by Eq. 2.

$$p_u = N_p \cdot C_u \cdot D \quad (2)$$

where N_p is the bearing capacity factor which can be calculated by Eq. 3.

$$p = N_p u - (N_p u - N_p o \cos \theta) e^{-\lambda \left(\frac{z}{D}\right) / (1 + \tan \theta)} \quad (3)$$

where $N_p u$ is the ultimate lateral bearing capacity factor that can be calculated by Eq. 4, $N_p o$ is the surface bearing capacity factor for horizontal soils, λ is a dimensionless factor, z is the depth point under consideration, and D is D the pile diameter. $N_p o$ and λ are derived from the finite element method analysis conducted by Georgiadis [3] and depend on the pile-soil adhesion factor (α).

$$N_p u = \pi + 2\Delta + 2\cos\Delta + 4 \left(\cos \frac{\Delta}{2} + \sin \frac{\Delta}{2} \right) \quad (4)$$

which $\Delta = \sin - 1\alpha$.

The N_{po} value can be calculated by Eq. 5.

$$N_{po} = 2 + 1.5\alpha \tag{5}$$

And the value λ of can be calculated by Eq. 6.

$$\lambda = 0.55 - 0.15\alpha \tag{6}$$

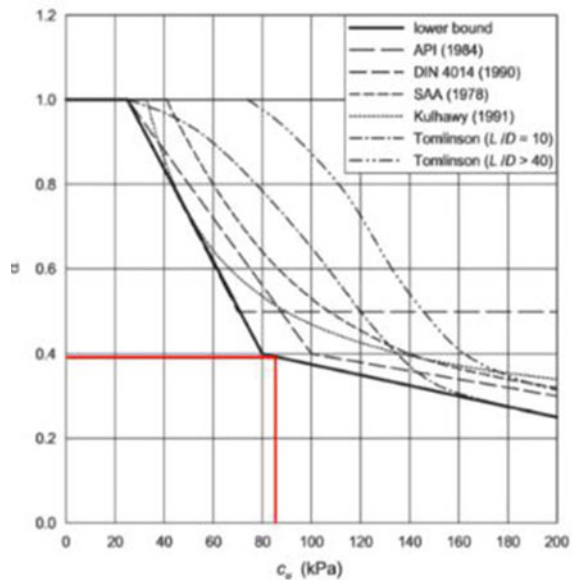
The pile-soil adhesion factor (α) can be determined from the c_u (undrained shear strength) and z/D parameters where z is the depth of the pile under consideration and D is the diameter of the pile with the graph shown in Fig. 1.

In 1961 Vesic proposed the correlation relation of the subgrade reaction k_s for beams in elastic half-space to the elastic properties of the beam and soil [4]. Rajashree and Sitharam proposed that the initial stiffness k_i of the p-y curve is twice the value of k_s determined based on the proposed Vesic correlation as shown in Eq. 7 [5].

$$k_i = \frac{1.3E_i}{1 - \mu^2} \cdot \left(\frac{E_i D^4}{E_p I_p} \right)^{\frac{1}{2}} \tag{7}$$

where E_i is the initial modulus of elasticity, μ is the Poisson ratio of the soil, E_p is the modulus of elasticity of the pile, I_p is the moment of inertia of the pile section and D is the pile diameter [4].

Fig. 1 Graph of relationship between α and c_u (kPa) [3]



1.2 Vertical Stress Due to Point Load (Boussinesq Method)

In 1883 Boussinesq solved the magnitude of the stress produced at each point, which is homogeneous and isotropic due to the point load applied to the soil surface. Figure 2 shows how point load causes vertical stress [6].

The equations to calculate vertical stress are shown in Eqs. 8–10.

$$\Delta\sigma_z = \frac{3Pz^3}{2\pi L^5} = \frac{3P}{2\pi} \frac{z^3}{(r^2 + z^2)^{5/3}} \quad (8)$$

$$r = \sqrt{x^2 + y^2} \quad (9)$$

$$L = \sqrt{x^2 + y^2 + z^2} = \sqrt{r^2 + z^2} \quad (10)$$

Description:

$\Delta\sigma_z$: Vertical Stress (kN/m²)

P: Large Applied Load $\times 2$ (kN).

2 Research Methods

In general, the procedures carried out in this study are as follows:

1. The initial stage is to determine the land data to be used.
2. The next step is to check the soil types and their properties through the results of soil correlation.

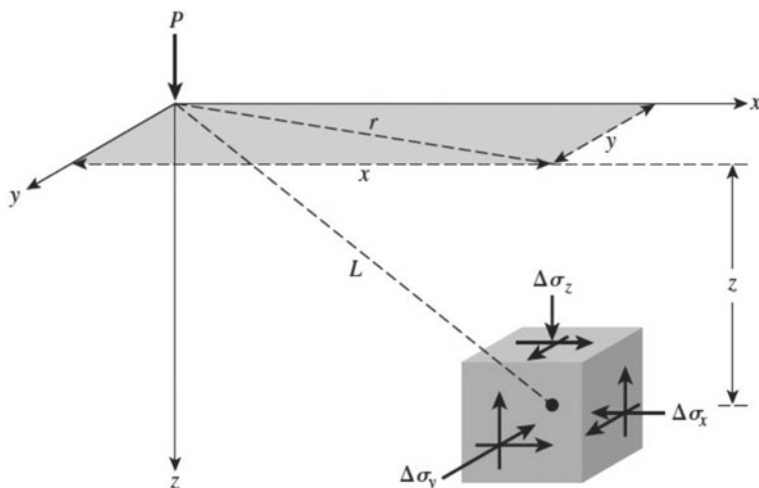


Fig. 2 Vertical stress due to point load [6]

3. Then carried out a literature study on the shift of the foundation pile and the lateral bearing capacity of the pile.
4. The next stage is to design the foundation piles before and after adding the load.
5. The next step is to analyze the lateral bearing capacity of the pile using the p-y curve method.
6. Then analyze the lateral bearing capacity compared to the lateral load.
7. Next, check the pile foundation that has been added to the load and before it is added.
8. The next stage is to check the applicable terms and conditions. If it does not meet the requirements, then there is a need for additional reinforcement considerations or options and will be rechecked whether it meets the requirements or not.
9. The last stage is to formulate conclusions that can be useful for future planners.

Pile Foundation Design Data Fig. 3 shows the building layout of the research subject location, explaining the pile number and explaining that only axle J and I need to be concerned. Tables 1 and 2 illustrate that all piles on both axles can withstand the total lateral load before the additional load, so there is no need to add piles on both axles.

Fig. 3 Building layout

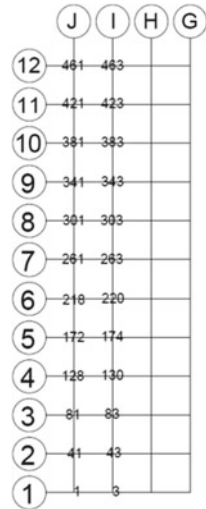


Table 1 Efficiency pile group on Axle J

Joint	Force (kN)	n Pile	Efficiency	Force/Pile (kN)	Force of 1 pile	Need to add pile
1	31.77	2	0.83	15.89	28.52	No
41	58.41	3	0.88	19.47	30.47	No
81	58.18	3	0.88	19.39	30.47	No
128	58.21	3	0.88	19.40	30.47	No
172	58.23	3	0.88	19.41	30.47	No
218	58.23	3	0.88	19.41	30.47	No
261	58.23	3	0.88	19.41	30.47	No
301	58.21	3	0.88	19.40	30.47	No
341	58.17	3	0.88	19.39	30.47	No
381	58.13	3	0.88	19.37	30.47	No
421	58.35	3	0.88	19.45	30.47	No
461	31.70	2	0.83	15.85	28.52	No

Table 2 Efficiency pile group on Axle I

Joint	Force (kN)	n Pile	Efficiency	Force/Pile (kN)	Force of 1 pile	Need to add pile
3	0.95	4	0.77	0.239	28.52	No
43	0.87	5	0.90	0.174	30.47	No
83	0.67	5	0.90	0.134	30.47	No
130	0.72	5	0.90	0.144	30.47	No
174	0.73	5	0.90	0.147	30.47	No
220	0.75	5	0.90	0.15	30.47	No
263	0.78	5	0.90	0.157	30.47	No
303	0.79	5	0.90	0.158	30.47	No
343	0.79	5	0.90	0.159	30.47	No
383	0.74	5	0.90	0.148	30.47	No
423	0.88	5	0.90	0.176	30.47	No
463	0.92	4	0.77	0.231	28.52	No

3 Result

3.1 Recap of Maximum Lateral Load Calculation Using the p-y Curve Method

This method requires the following data that are useful in calculations:

C_u (undrained shear strength) = 84 kPa

S'_{vo} (effective overburden stress at depth z) = 87 kPa

Table 3 Results of calculations using the p-y curve method

y (mm)	p (kN/m)
0	0
1	55.70
2	70.18
3	80.33
4	88.42
5	95.25
6	101.21
7	106.55

- J (soil coefficient) = 0.5
- e50 (soil coefficient) = 0.02
- K (soil coefficient) = 8140 kPa/m
- Nc (bearing capacity factor) = 9
- Pu (ultimate load) = 302.4 kN/m
- Depth z = 30 m
- B (pile size) = 0.4 m
- k'h (slope at 0.5 pu) = 7560 kN/m²
- k'hi (initial slope) = 244,200 kN/m²
- yc (plot slope on curve) = 20 mm
- 8 yc (plot slope on curve 8 times yc) = 160 mm

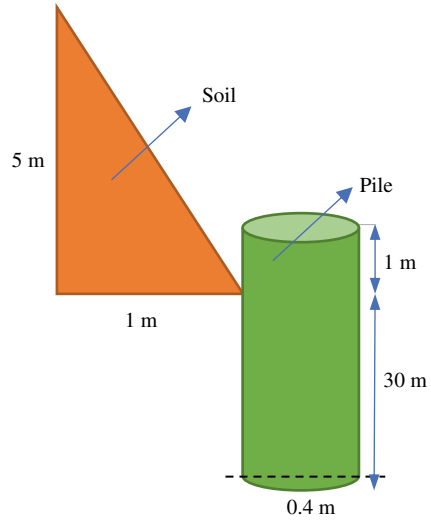
From the data above, the calculation process, the results, and graphs of the p-y curve are as shown in Table 3.

From Table 3, the allowable deflection is 6.35 mm with force (P) of 10.3089 tons and divided by a safety factor of 3, so the maximum lateral force of 3.436 tons is used.

3.2 Summary of Calculation of Added Load Due to Land Embankment

After the project took place and the pile shift occurred, several speculations about the cause of the pile shift had previously been designed and calculated that the pile was strong enough to withstand lateral loads. The addition of lateral loads includes soil embankment at the project site with a height of about 5 m, as shown in Fig. 4. So in this study, the addition of lateral loads caused by soil embankment was calculated.

Fig. 4 Illustration of calculation of added load due to landfill



Assuming the width of the land is 1 m.

$$\text{Volume} = 0.5 \times 5 \times 1 \times 1$$

$$= 2.5 \text{ m}^3$$

$$\lambda = 1.8 \text{ Ton/m}^3$$

$$P = 1.8 \times 2.5$$

$$= 4.5 \text{ Ton}$$

$$\text{Momen} = \frac{4.5 \times 2}{3}$$

$$= 3 \text{ Ton m}$$

$$P \text{ Lateral} = 3 \text{ Ton (Left direction)}$$

So the addition of lateral load due to soil embankment is 3 Tons to the left.

3.3 *Summary of Additional Load Due to Impact Load with Boussinesq Method*

The addition of lateral loads occurs due to soil movement due to the movement of piling machines such as HSPD and others. This study focuses on the impact of the HSPD Jacking Pile machine with a total machine weight of 54 Tons.

The calculation refers to the Boussinesq method, which can solve the problem of the stress magnitude at each point on the ground surface, following the calculation [6]:

Due to Impact Load (HSPD Machine):

$$r_1 = \sqrt{x^2 + y^2} = \sqrt{0^2 + 0^2} = 0$$

$$L_1 = \sqrt{r^2 + z^2} = \sqrt{0^2 + 2^2} = 2$$

$$\Delta\sigma_z(1) = \frac{3Pz^3}{2\pi L^5} = \frac{3 \times 529.74 \times 2^3}{2\pi \times 2^5} = 63.233 \text{ kN/m}^2$$

Based on the conditions at this project location, the depth used is 2 m because the most extreme pile shift occurs at this depth, and refers to Boussinesq's theory that the pressure generated by the impact load is getting smaller and smaller. Furthermore, it is necessary to find the addition of lateral loads due to the impact load utilizing stress multiplied by area.

Additional Lateral Load:

$$\begin{aligned} P &= \Delta\sigma_z(1) \times 0.4 \times 2 \\ &= 63.233 \times 0.4 \times 2 \\ &= 50.586 \text{ kN} = 5.157 \text{ Ton (left direction)} \end{aligned}$$

So the total additional load due to soil embankment and impact load is 8.157 Tons to the left.

3.4 Summary of Lateral Efficiency Results of Axle J and Axle I After Adding Load

After calculating the additional lateral loads to the piles, these loads are included in the lateral piles' efficiency calculation and compared with the results of the p-y curve calculations that have been obtained. Then it will be checked whether the foundation pile can withstand the total lateral load that occurs or the reinforcement or pile foundation needs to be added.

Table 4 explains that all piles cannot withstand the total lateral load after the additional load, so adding piles on axle J is needed. For example, in Joint 1, the total lateral load is 55.89 kN, but the maximum force of the pile is only 28.52 kN. The conclusion is the pile cannot withstand the lateral load.

Table 5 explains that after the additional load, only two piles cannot withstand the total lateral load, which is pile on joint 3 and joint 463, so adding piles on this both joint are needed. For example, in Joint 1, the total lateral load is 31.60 kN, but the maximum force of the pile is only 28.52 kN. The conclusion is the pile cannot withstand the lateral load.

Table 4 Efficiency pile group on axle J after adding load

Joint	Force (kN)	n Pile	Efficiency	Force/Pile (kN)	Force of 1 pile	Need to add pile
1	111.79	2	0.83	55.89	28.52	Yes
41	138.43	3	0.88	46.14	30.47	Yes
81	138.20	3	0.88	46.06	30.47	Yes
128	138.23	3	0.88	46.07	30.47	Yes
172	138.25	3	0.88	46.08	30.47	Yes
218	138.25	3	0.88	46.08	30.47	Yes
261	138.25	3	0.88	46.08	30.47	Yes
301	138.23	3	0.88	46.07	30.47	Yes
341	138.19	3	0.88	46.06	30.47	Yes
381	138.15	3	0.88	46.05	30.47	Yes
421	138.37	3	0.88	46.12	30.47	Yes
461	111.72	2	0.83	55.86	28.52	Yes

Table 5 Efficiency pile group on axle I after adding load

Joint	Force (kN)	n Pile	Efficiency	Force/Pile (kN)	Force of 1 pile	Need to add pile
3	126.40	4	0.77	31.60	28.52	Yes
43	106.32	5	0.9	21.26	30.47	No
83	106.12	5	0.9	21.22	30.47	No
130	106.17	5	0.9	21.23	30.47	No
174	106.18	5	0.9	21.23	30.47	No
220	106.20	5	0.9	21.24	30.47	No
263	106.24	5	0.9	21.24	30.47	No
303	106.24	5	0.9	21.24	30.47	No
343	106.24	5	0.9	21.24	30.47	No
383	106.19	5	0.9	21.23	30.47	No
423	106.33	5	0.9	21.26	30.47	No
463	124.37	4	0.77	31.09	28.52	Yes

4 Conclusions and Suggestions

4.1 Conclusions

Based on the results of the analysis that has been carried out, the following conclusions are obtained:

1. Based on the soil data obtained, the soil type is clay with high plasticity and small bearing capacity.

2. Based on calculations using the p-y curve method, the maximum lateral bearing capacity for foundation piles with a diameter of 0.4 m and a depth of 30 m is 3.436 tons.
3. Based on the building data obtained, the calculation results for the maximum lateral pile capacity are sufficient to withstand the load.
4. After the analysis, the results showed that the pile shift occurred due to the addition of an unplanned load, namely the load of the soil embankment and also the impact load of the HSPD piling machine.
5. Based on the additional lateral load calculation from the soil embankment is 3 Tons to the left.
6. Based on the Boussinesq method calculation, the additional lateral load from the impact load is 5.157 tons to the left.
7. The total additional load outside the plan is 8.157 tons.
8. After adding a load of 8.157 Tons in an Axle J group pile efficiency calculation, all piles cannot withstand the total lateral load. In Axle I, two piles are unable to withstand the total lateral load, causing a pile shift in these two axles to occur.

4.2 Suggestions

Based on the results of research and analysis conducted, the following are suggestions to complete this study:

1. The soil test results must be reviewed to be able to determine with certainty the types of soil and how the properties of the soil. In this project, the type of clay soil with high plasticity properties. So it should be repaired first.
2. The recommended soil improvement is jet grouting by adding cement material into the soil to become denser and harder. This method also does not cause vibration or noise.
3. If the project is already running without any improvement, it should be strengthened by adding drill piles into the existing pile group foundation.
4. Do not stockpile too much soil at the project site and soil filling should be carried out gradually and removed gradually as well.
5. In the field conditions of this project and based on the type and nature of the soil, a drilled pile foundation should be used so as not to cause an impact load that can cause additional lateral loads.

References

1. Meyerhof GG, Mathur SK, Valsangkar AJ (1981) Lateral resistance and deflection of rigid walls and piles in layered soils. *Can Geotech J* 18(2):159–170
2. Hakim AR, Akbar A (2018) Analisis Produktivitas Hydraulic Static Pile Driver Pada Pembangunan Apartemen Victoria Square Tower B Tangerang Banten. *Jurnal Teknik Sipil ITB* 25(2):103–112

3. Georgiadis M, Georgiadis K (2010) Undrained lateral pile response in sloping ground. *J Geotech Geoenviron Eng* 136(11):1489–1500
4. Vesic AB (1961) Bending of beams resting on isotropic elastic solid. *J Eng Mech Div* 87 (2):35–53
5. Rajashree SS, Sitharam TG (2001) Nonlinear finite-element modeling of batter piles under lateral load. *J Geotech Geoenviron Eng* 127(7):604–612
6. Das BM, Sobhan K (2014) *Principles of geotechnical engineering*. Cengage Learning, Connecticut

Analysis of Diaphragm Wall Stability with Dewatering and Ground Freezing Treatment



Eduard Teja and Aniek Prihatiningsih

Abstract In underground construction, we really need to consider the presence of groundwater. Groundwater can interfere and even endanger the construction and excavation process. Usually, in the tunnel construction process, groundwater needs to be eliminated. So that the tunnel construction process can be carried out as safely as possible. Sometimes the construction of a tunnel in the middle of a city also needs some soil reinforcement to not disturb the surrounding buildings. One method that can be used to eliminate and strengthen excavated walls is ground freezing. Also, we know the dewatering process to eliminate the effects of groundwater by lowering the groundwater level. In this research, the effect of the dewatering and ground freezing processes will be calculated by stabilizing the diaphragm wall. Ground freezing will cause the bonding of soil particles to become stronger. Then the stability of the soil will be much better than dewatering. The result shows that ground freezing has the smallest deflection and moment. So, the stability of the ground freezing excavation has the best value. However, in terms of the price of ground freezing, it is still too high, so studies are needed to minimize the price.

Keywords Ground freezing · Dewatering · Diaphragm wall

1 Introduction

Indonesia is one of the largest countries in Southeast Asia in terms of regional area and population. It is very important for Indonesia to continue to improve its infrastructure development. One of the infrastructures that are being built rapidly is transportation. As we know in Jakarta has just had MRT (Mass Rapid Transit) and LRT (Light Rail Transit). In the construction of MRT and LRT must have high

E. Teja (✉) · A. Prihatiningsih
Universitas Tarumanagara, Letjen S. Parman Street No. 1, Jakarta, Indonesia
e-mail: eduard.325170114@stu.untar.ac.id

A. Prihatiningsih
e-mail: aniekp@ft.untar.ac.id

work safety. The most crucial thing is the excavation for the tunnels, this is crucial because the excavation of the tunnels is below groundwater level, at a depth of 17–36 m below ground level [1].

In excavation that are under groundwater, the thing that must be prevented is swelling. Swelling of the soil occurs due to the pressure of water trying to get out of the ground. This pressure will later become a disturbance in the installation of the tunnel shield/tunnel wall and can cause failure in excavation stability. If this problem is not addressed, it will be very dangerous and can even cause fatalities, so for this reason, this problem must be prevented. Various precautions can be taken to prevent swelling. The thing that is often applied is dewatering.

Dewatering (Fig. 1) is done by lowering the groundwater level to an adjustable depth. By lowering the groundwater level to minimize swelling. In addition to dewatering abroad, there is also a ground freezing method. The ground freezing method itself is done by freezing the groundwater around the excavation so that a waterproof layer is formed around the excavation. This waterproof layer is useful for protecting excavations. Before determining the dewatering method to be used, the nature of the soil must be considered. Because if we use the wrong dewatering method, it will not only hamper the project but also increase the costs incurred [2].

Ground freezing (Fig. 2) has been carried out since 1862 where this method is used to build mining tunnels [4]. Ground freezing was first time used in North Wales. With the development of the era, this method can be used for tunnel



Fig. 1 Wellpoint system [3]

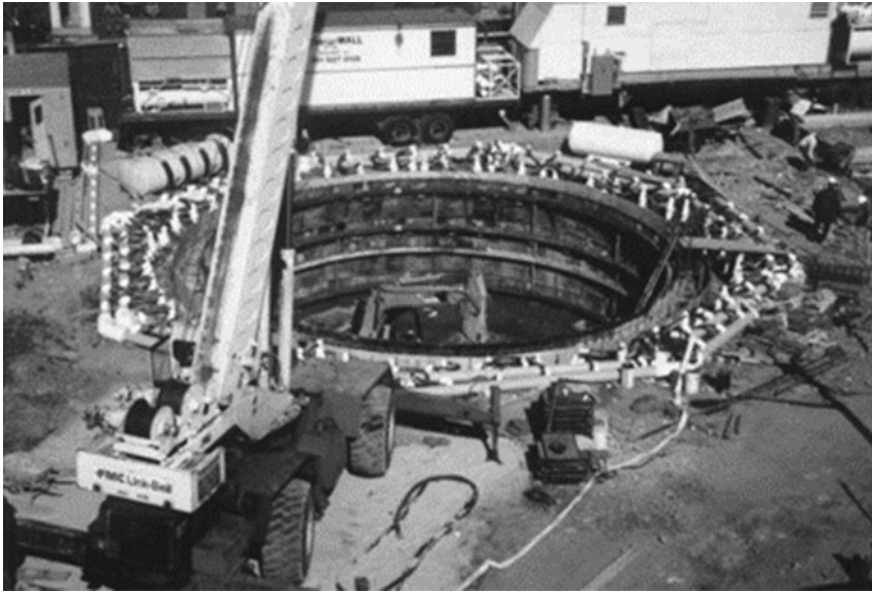


Fig. 2 Ground freezing [5]

construction. Ground freezing is done by inserting a pipe around the excavation. This pipe installation also needs to be considered because pipes with different sizes and different temperatures can affect the area of land that can be frozen. The ground freezing method has not been used in Indonesia, but in Singapore, it was used during the construction of the Thomson East-Coast Line Marina Bay Station.

1.1 Diaphragm Wall

The diaphragm wall or bulkhead wall is an artificial membrane with a certain thickness (according to the thickness of the digging tool called a grabber) and a certain depth [6]. A diaphragm wall is a retaining wall that is installed as a system for further development of the secant pile and contiguous pile system. In calculating the stability of the diaphragm wall, it will be done by calculating the active and passive earth stresses that appear in Eqs. 1–4 [7].

$$P_a = \gamma h k_a \quad (1)$$

$$k_a = \tan^2 \left(45 - \frac{\phi}{2} \right) \quad (2)$$

$$P_p = \gamma h k_p \quad (3)$$

$$k_p = \tan^2\left(45 + \frac{\phi}{2}\right) \tag{4}$$

The formulas above are used because the soil is considered unable to hold itself (worst condition). For condition 4, a formula will be used where the ability of the soil to hold itself is considered. Because when ground freezing, the water around the soil freezes so that the soil bonds become stronger. In theory, this freezing will increase the compressive strength of the soil to be stronger. As a result, the shear strength of the soil also increases (Fig. 3).

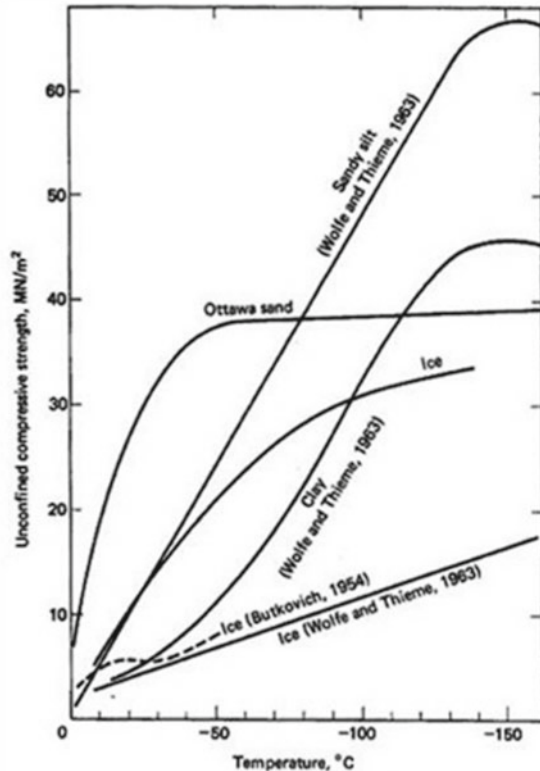
So, to calculate the ability of the soil to hold itself underground freezing conditions, the following formula is shown in Eqs. 5 and 6.

$$P_a = \gamma h k_a - 2c\sqrt{k_a} \tag{5}$$

$$P_p = \gamma h k_p + 2c\sqrt{k_p} \tag{6}$$

for k_a and k_p , use the same formula as before.

Fig. 3 Relationship between temperature and unconfined compressive strength [8]



2 Research Methods

The research will be carried out in 4 soil conditions with excavations held in place with a diaphragm wall. Excavation with a depth of 20 m and a diaphragm wall with a depth of 40 m. The size of the diaphragm wall used is 1 m with a calculation of every 1 m, so a cross-section of 1×1 m is used. The first condition is in-situ soil, where the unit weight of soil used is obtained from correlation and laboratory data. In condition 2, the soil is saturated, then the unit weight of soil is used to use the saturated specific gravity obtained from the correlation. Condition 3 occurs in soil with dewatering treatment where it is considered that in the lower soil (soil under excavation), there is still water flow due to dewatering. So that at a depth of 20–40 m, the unit weight of soil used is the saturation density, and for a depth of 0–20 m, the in-situ unit weight of soil is used. Then for condition 4, namely the ground freezing condition, the in-situ unit weight of soil will be used. The difference with the in-situ condition is the use of soil properties.

2.1 Soil Properties

Unit weight of soil was obtained from correlation and laboratory data. Unit weight is divided into 2, namely the state of the original soil (in-situ) and the state of wet soil. For wet soil conditions, the density with the largest number will be taken in the correlation table. In the original soil condition, the density of laboratory results and correlations will be used. Then soil density will be obtained and tabulated as Table 1.

Cohesion is obtained from laboratory results and correlations which will then be taken the average value of correlations and laboratory data. Then it will be tabulated as Table 2.

The value of undrained shear strength is obtained from the correlation and tabulated in Table 3.

Table 1 Unit weight of soil

Soil layer		Soil classification	γ_{sat} (kN/m ³)	γ (kN/m ³)
Top elev. (m)	Bottom elev. (m)			
0	7	Fine grained	22	15
7	11	Fine grained	22	16
11	20	Coarse grained	20	20
20	23	Fine grained	22	15
23	26	Coarse grained	20	19
26	35	Fine grained	22	19
35	40	Fine grained	22	19

Table 2 Cohesion

Soil layer		Soil classification	Consistency	C' (kPa)
Top elev. (m)	Bottom elev. (m)			
0	7	Fine grained	Very soft	8
7	11	Fine grained	Stiff	24
11	20	Coarse grained	Dense	–
20	23	Fine grained	Soft	20
23	26	Coarse grained	Dense	–
26	35	Fine grained	Very stiff	30
35	40	Fine grained	Hard	60

Table 3 Shear strength

Soil layer		Soil classification	Consistency	Su (kPa)
Top elev. (m)	Bottom elev. (m)			
0	7	Fine grained	Very soft	9.6
7	11	Fine grained	Stiff	81.439
11	20	Coarse grained	Dense	90
20	23	Fine grained	Soft	28.8
23	26	Coarse grained	Dense	90
26	35	Fine grained	Very stiff	109.867
35	40	Fine grained	Hard	194.133

The value of the internal shear angle is obtained from the correlation and tabulated in Table 4.

The correlation results and lab data will then be processed to obtain the earth stress acting on the wall. Then the deflection will be searched, and the results will be compared. In the calculation of the earth lateral pressure, the following results are obtained. For Fig. 4 shows the earth's stress in in-situ conditions. Figure 5 for earth stress at saturation condition. Figure 6 is an image of the earth's stress for the dewatering condition. The ground freezing conditions are depicted in Fig. 7.

Table 4 Shear angle

Soil layer		Soil classification	Consistency	Φ' (°)
Top elev. (m)	Bottom elev. (m)			
0	7	Fine grained	Very soft	10
7	11	Fine grained	Stiff	17
11	20	Coarse grained	Dense	35
20	23	Fine grained	Soft	14
23	26	Coarse grained	Dense	35
26	35	Fine grained	Very stiff	17
35	40	Fine grained	Hard	26

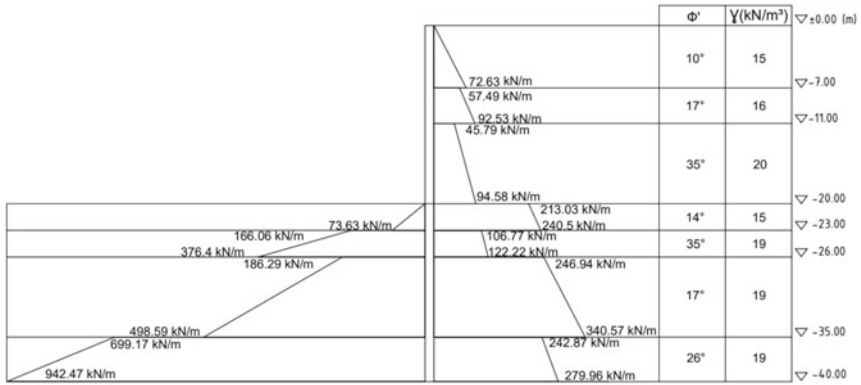


Fig. 4 Earth lateral pressure in-situ conditions

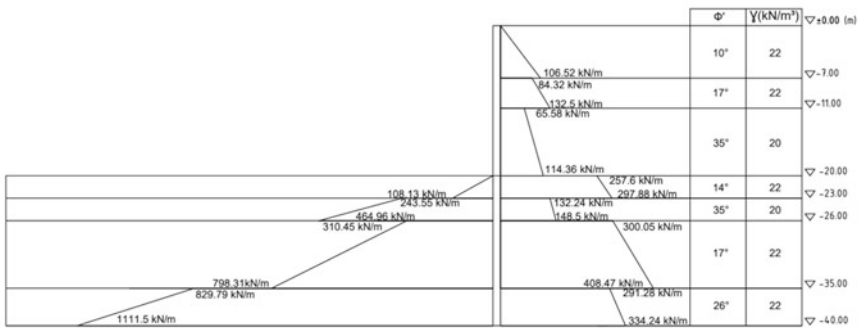


Fig. 5 Earth lateral pressure saturated conditions

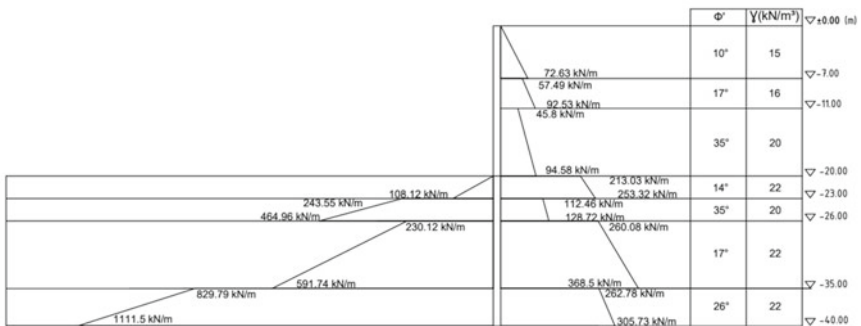


Fig. 6 Earth lateral pressure dewatering conditions

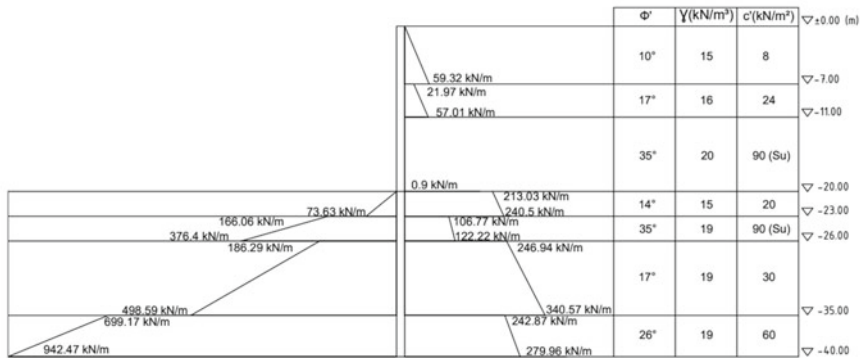


Fig. 7 Earth lateral pressure ground freezing conditions

3 Result

3.1 Deflection and Moment

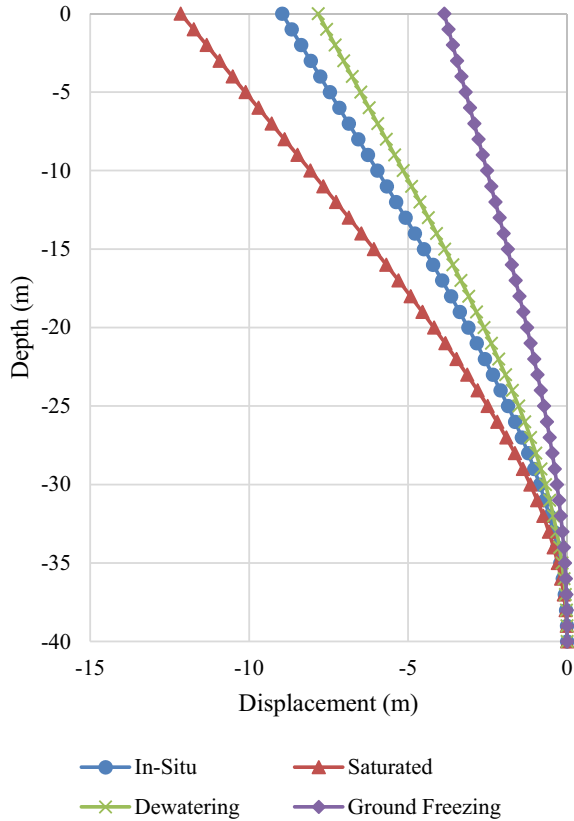
The results are as shown in Figs. 8 and 9. For in-situ conditions, the maximum deflection is 8.964 m, the saturation condition is maximum deflection 12.154 m, and for dewatering conditions, the maximum deflection is 7.831 m. For ground freezing conditions, if we look at the graph, the maximum is 3.865 m.

4 Conclusions and Suggestions

4.1 Conclusions

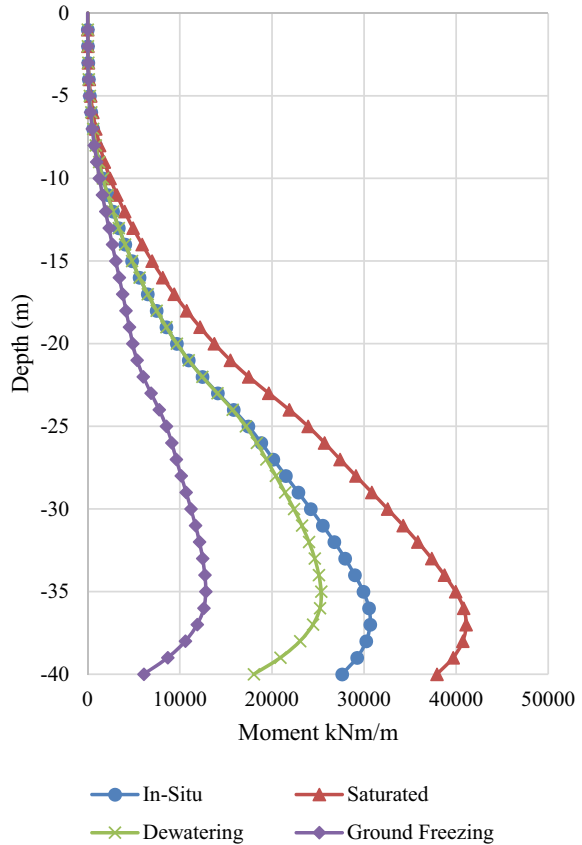
1. The greatest deflection occurs when the soil is saturated, which is 12.154 m. Then the second largest deflection is 8.964 m in in-situ conditions. The third-largest deflection is the dewatering condition, which is 7.831 m. The smallest deflection during ground freezing is 3.865 m.
2. From the results of the deflection comparison, it can be concluded that when ground freezing produces the best soil stability.
3. The deflection that occurs in 4 conditions is still more than the permitted limit, namely $L/360$ or 111 mm.
4. The biggest moment that the wall must hold is during saturation conditions with a moment magnitude of 41,082 kNm/m and the smallest moment is during ground freezing conditions, which is 17,818 kNm/m.
5. Each condition requires reinforcement in the excavation.

Fig. 8 Deflection results



4.2 Suggestions

1. Even though ground freezing is the best method, it is expensive in terms of price. Therefore, it is necessary to conduct further studies or research to reduce and develop this method in Indonesia.
2. The disadvantage of in-situ conditions is that the deflection is too large so that it cannot rely solely on the ability of the retaining wall, and therefore it is necessary to do much more reinforcement compared to dewatering or ground freezing.
3. In the use of ground freezing, because it is only up to a depth of 20 m (equivalent to excavation) and the calculation using the worst cohesion and shear strength (in-situ soil properties), results are obtained that still require reinforcement. If ground freezing is done at different depths and a cooler temperature is used. Then the possibility of ground freezing does not require reinforcement at all so that an open excavation can be done.

Fig. 9 Moment results

- The use of ground freezing also has additional benefits, one of which is that it does not cause additional settlement due to underground water flow during dewatering which carries fine particles and erodes the soil. Ground freezing should be considered in the future.

References

- Jakarta MRT (2020) Profil MRT Jakarta Fase 2A. <https://jakartamrt.co.id/id/info-terkini/profil-mrt-jakarta-fase-2a>. Accessed 15 Feb 2021
- Federal Highway Administration (1982) Groundwater control in tunneling. Department of Transportation, Massachusetts
- Cashman PM, Preene M (2020) Groundwater lowering in construction: a practical guide to dewatering. CRC Press, Florida
- Vakulenko I (2018) Feasibility of ground freezing as potential stabilizing measure for tunnelling through soil filled depression at Bergåsen road tunnel. Master's thesis, NTNU

5. Powers JP, Corwin AB, Schmall PC, Kaeck WE (2007) Construction dewatering and groundwater control: new methods and applications. Wiley, New Jersey
6. Mistra H (2012) Struktur dan konstruksi bangunan tinggi sistem top and down. Griya Kreasi, Jakarta
7. Bowles JE (1997) Foundation analysis and design. McGraw-Hill, Illinois
8. Sayles FH (1966) Low temperature soil mechanics. Technical Note, Cold Regions Research and Engineering Laboratory, Hanover, NH

Analysis of Hollow Concrete Column with CFRP Wrapping Using Finite Element Method



William Supardjo and Sunarjo Leman

Abstract The use of concrete in construction is very common even though there are several problems such as massive structure self-weight and it causes the increment of the seismic load carried by structure. Therefore, engineers usually prefer the use of hollow cross-sections in reinforced concrete since it gives higher structural efficiency. This research was done to analyze Hollow Concrete Column (HCC) using the finite element method with the help of MIDAS FEA application to obtain an efficient and effective model ratio between the hollow-core variation which use CFRP (Carbon Fiber Reinforced Polymer) as wrapping. The analysis result shows that for the solid cross-section sample, the use of CFRP correlates to the needs of force resistance because the effectivity curve shows that the line intersects with one another at some variety of eccentricity. It also shows even though the effectivity increases with the increment of the hollow ratio, there is a capacity reduction of $\mp 5.5\%$ for each 5% increment. From the analysis, it shows that the effectivity of the sample with CFRP wrapping exceeds the solid conventional sample, where the best ratio is 30%.

Keywords Carbon fiber reinforced polymer · Hollow concrete column · Finite element method

1 Introduction

Part of vertical structure which function is to support axial load either with or without a moment is called a column [1]. The use of concrete in construction is very common even though there is some problem especially the massive self-weight that

W. Supardjo (✉) · S. Leman

Department of Civil Engineering, Tarumangara University, Jl. Letjen S. Parman No. 1, Jakarta, Indonesia

e-mail: williamsupardjo@gmail.com

will affect the seismic load carried by structure. It can be illustrated with basic physics theory ($F = m.a$), which shows that forces will increase along with the increment of masses [1].

Since such a problem has arisen, the use of hollow cross-section has become more preferable in construction because it will give a better structural efficiency from the power or stiffness to masses ratio point of view [2]. Hollow Concrete Columns (HCCs) is one of the main choices in civil construction, including bridge pile with expectation in reducing the overall weight and the cost since there will be less use of concrete in the column and pile construction [3]. Although the benefit of using HCC has been explained, it has not been used extensively in seismic design practice because there is still not enough understanding about the confinement behavior and design guide [4].

This research was initiated to analyze the HCC using the finite element method to obtain an effective and efficient ratio among variations of hollow-core with CFRP (Carbon Fiber Reinforced Polymer) as a wrapping and hopefully by using CFRP wrapping on the outside can give better performance even though there is a hollow-core. Hence, the observed force in this paper will strictly be axial and moment only. The main purpose was to achieve maximum volume reduction with a minimum capacity decrease to produce higher sample effectivity than a conventional column. The effectivity mentioned in this paper will be about the ratio between the column, whether moment or axial compared to the volume. The greater the ratio, the better effectivity it will have since it will have less concrete but the same capacity. The result hopefully also could be additional literature in HCC practice application.

To predict and validate the result from MIDAS FEA, there will be a manual calculation to make a column interaction diagram as a method of approach for the tested samples, which was based on the guidance in ACI 318-14 [5] and ACI 440 2R-17. For validation purposes (see Fig. 1), only three conditions in the manual interaction diagram that corresponded with the compression-controlled failure will be used [6].

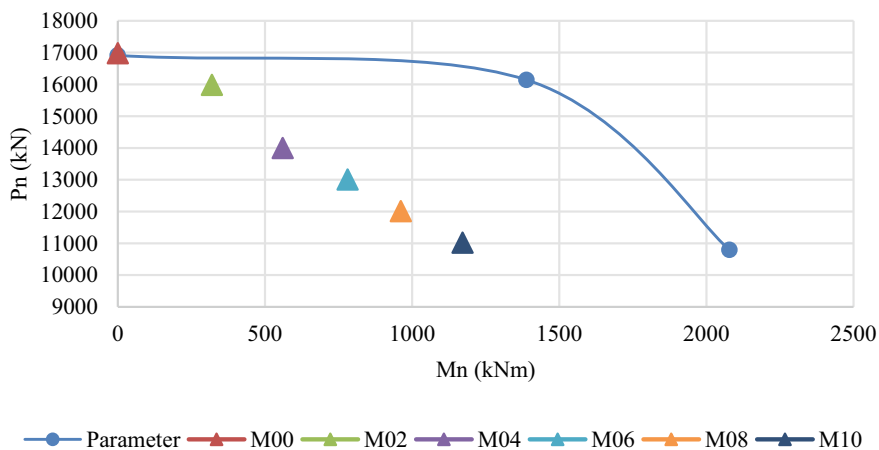


Fig. 1 Manual versus MIDAS strength analysis result comparison example

1.1 FRP (Fiber Reinforced Polymer)

Fiber Reinforced Polymer (FRP) is a composite-based material that was made with polymer matrix and strengthened by using fiber. Generally, fiber can be glass, carbon, or aramid, even though another fiber is sometimes being used, such as paper, wood, or even asbestos. The commonly used polymer is epoxy, vinyl ester, or polyester thermosetting plastic, and phenol–formaldehyde resins. FRP applications are common in several industries such as aerospace, automotive, marine, and construction industries [7].

The reason this material is very popular as a construction retrofitting option is a significantly higher addition in strength, especially in tension. Because as we all know, concrete is very vulnerable to tension. The tension strength possessed by this material is very high, around 20–100% higher or even more depends on the material properties. Table 1 shows that FRP has a relatively higher tensile strength depends on the fiber content in the FRP and Table 2 shows that carbon has better strength than others.

2 Research Methodology

2.1 Specimen ID

There is a total of seven specimen that will be tested and each one of them will have a unique ID to differentiate them from one another (see Fig. 2). The first sample

Table 1 Composite and steel tension strength comparison [8]

No.	Properties	Fiber glass	Tensile strength	
	Unit		%	10 ³ psi
	Test method	D790	D638	
A.	Fiber reinforced thermoset			
1	Polyester (pultrusion)	22	30	206.85
2	Polyester (woven roving)	50	37	255.115
3	Epoxy (filament winding)	80	80	551.6
B.	Fiber reinforced thermoplas			
1	Polypropylene	20	6.5	44.8175
2	Nylon 6	30	23	158.585
3	Polycarbonate	10	12	82.74
C.	Metal			
1	ASTM A-606 HSLA cold rolled steel	–	65	448.175
2	AISI 304 stainless steel	–	80	551.6
3	2036-T4 wrought aluminium	–	49	337.855

Table 2 Basic material strength comparison [9]

	Glass profile	Carbon profile	Steel	Aluminium	PVC	Wood
Density (kg/m ³)	2100	1650	7900	2700	1380	520
Flexural strength (MPa)	1000–1400	1400–2500	400–1200	180	44	150
Flexural modulus (GPa)	45–56	120–300	196	70	2.4	10
Tensile strength (MPa)	1000–1400	1400	400–1200	180	70	100
Tensile modulus (GPa)	45	140	196	70	2.4	9
Thermal conductivity (w/m k)	0.5	1.4	47	209	0.24	0.47
Coefficient of linear thermal expansion (1/k)	10 ⁻⁵	-0.2 × 10 ⁻⁶	10 ⁻⁵	2.3 × 10 ⁻⁵	10	10
Specific heat capacity (J/kg K)	1880	950	461	921	1100	1700

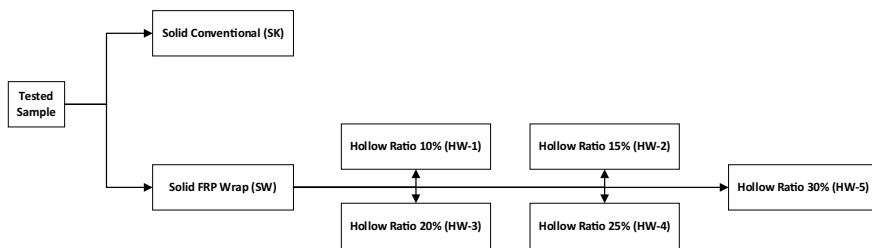


Fig. 2 Specimen ID diagram

will be SK which stands for Solid Conventional Column with Steel Rebar. The rest of the sample will be a variation of Column with CFRP Wrapping. So, there will be six variations which will be labeled by number such as SW (Solid Column with CFRP Wrapping), HW-1, HW-2, HW-3, HW-4, and HW-5. The number will represent the increment of 5% hollow-core ratio from a solid cross-section.

2.2 Properties Specification

The sample was modeled with 35 MPa of concrete compressive strength specification, 850 mm of outside diameter, and 4200 mm length. Conventional concrete with a solid cross-section and steel rebar (SK) is used as the control sample. It was modeled using a rebar with 400 MPa yield strength and 550 MPa ultimate strength.

As for the sample with CFRP wrapping (SW and HW), it was modeled with a 966 MPa tensile strength and 66,190 MPa modulus of elasticity specification.

2.3 MIDAS FEA Modelling

Structural Geometry Modelling Column modeling used the solid element for the concrete, 3D line element to make the rebar, and shell element in modeling the CFRP Wrapping.

Material Modelling and Its Function Every structural geometry that was made will have different material and function. For rebar and CFRP Wrapping, a hardening function was used and the parameter will be manually inputted, such as material yield and ultimate strength according to the factory specification. For concrete, the total strain crack function will be used. For the compressive behavior (as shown in Fig. 3a), the Thorenfeldt function was used (as shown in Fig. 3b). As for the tensile behavior, the brittle function was used (as shown in Fig. 3c).

Model Meshing After all the structural and material modeling was done, then meshing needed to be done in order to merge the modeled geometry and material into one element (see Fig. 4a, b).

Interface Modelling The interface was needed in modeling the CFRP wrapping because the bonding between the wrapping and concrete must be made so that the condition can represent the real-time condition in which the wrapping will give an effect to the structure and became one unity with the concrete. The interface was modeled using rigid parameter because it was assumed to have a perfect bonding between the CFRP and concrete.

Constraint and Load Modelling Constraint and load were modeled using the help of rigid link option where it will make only one joint that is needed to be put load and constraint since it will represent the whole surface is loaded and can support the load evenly (see Fig. 5a, b).

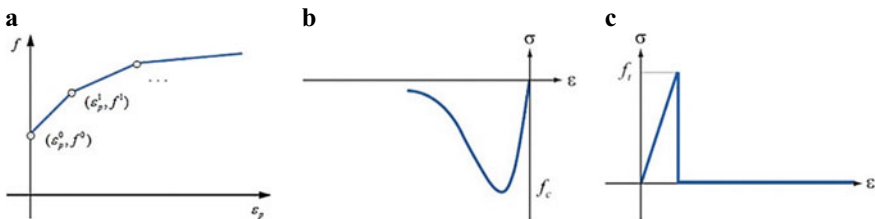


Fig. 3 Material function. **a** Rebar hardening, **b** concrete compression (Thorenfeldt), **c** concrete tension (Brittle)

Fig. 4 MIDAS FEA meshing view for **a** concrete and rebar, **b** CFRP wrapping

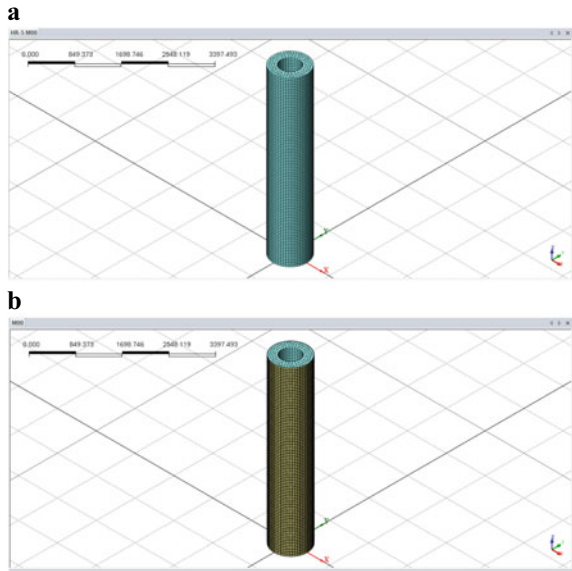
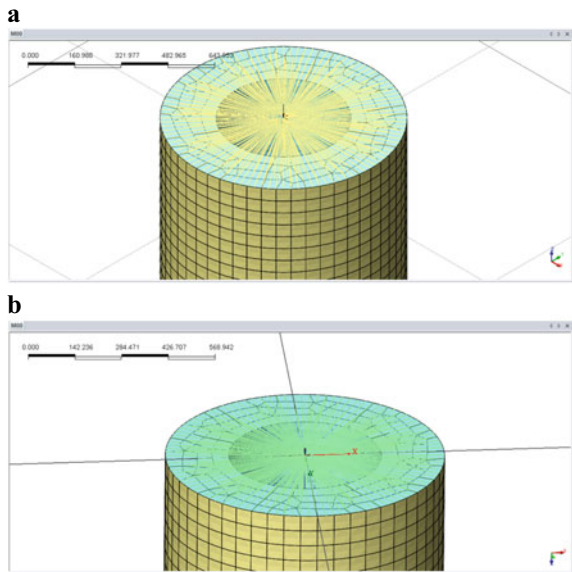


Fig. 5 MIDAS FEA load view **a** and constraint view **b** with rigid link



Determining the Analysis Case Analysis case needed to be set so the app will analyze the sample with nonlinear analysis. In the analysis case, we also need to choose the iteration model and in this case, the Newton–Raphson iteration was used. The number of load steps and iteration can also be adjusted to obtain the best result.

Solving the Model After all the structural modeling and analysis control was done, then everything is set to be analyzed using the solving option in MIDAS FEA. After the option was run, the app will analyze the sample using the finite element method and produce the needed output.

2.4 Data Compilation

Data were obtained using the MIDAS FEA application that calculates the crack and displacement pattern of nonlinear analysis with the finite element method. The load step and eccentricity which caused a reasonable crack pattern will be taken as the axial and moment value for analysis. Then the value will be divided with the sample volume so the ratio of axial to force and moment to force will be obtained. From the ratio comparison, it will show which sample gives the best ratio effectivity.

3 Analysis and Discussion

3.1 Solid Cross Section Column

Based on the result comparison between all three of the solid cross-section sample (see Fig. 6a), it shows that the sample that has a good decreasing consistency in strength is SW and excels in several conditions as the moment increases but shows that it underperformed in strength especially when the sample was applied with the biggest moment. The sample which has the biggest strength when tested with the biggest eccentricity was SK.

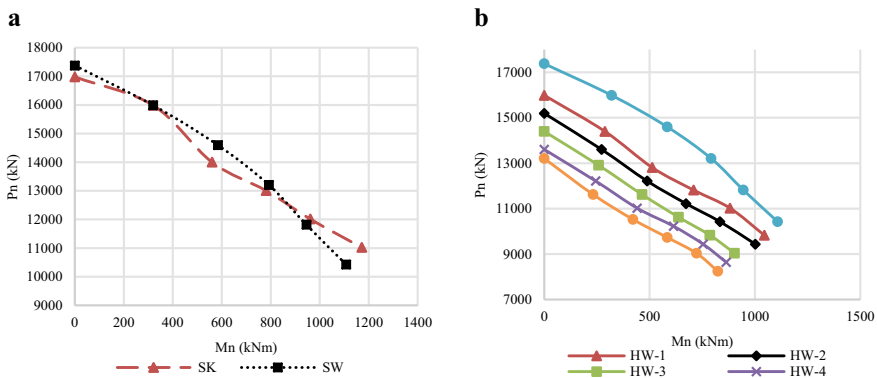


Fig. 6 Strength comparison of a SK versus SW, b hollow cross-section with CFRP wrapping sample

From this result, it shows that sample selection to be used in construction practice depends on the force that needs to be carried by the element because SK will be the best choice if the carried moment and axial compression was above 900 kNm and under 12,000 kN. But besides these two conditions, SW will be the best choice available.

3.2 Hollow Cross Section Column with CFRP Wrapping

The result shows that there are decreases in strength along with the increment of the hollow-core ratio (see Fig. 6b). The decrease in strength has already been anticipated since the net cross-section area will decrease along with the increment of the hollow-core ratio. This statement is given based on the P-M Curve calculation theory.

The decrease in strength is not that big of a problem since what needs to be checked further is the strength to volume ratio (Effectivity Ratio). The checking was done to know whether a certain hollow-core sample effectivity can give a result that differs from a downward trend referring to the P-M Curve theory.

3.3 Sample Effectivity

The sample effectivity was obtained that HW gives a similar effectivity ratio with the SK from the 10–15% hollow-core ratio (see Figs. 7 and 8). When it was 20–25%, the effectivity slowly surpassing the SK effectivity and finally, at the 30% hollow-core ratio, it shows that the HR effectivity surpasses the SK effectivity by +7%.

4 Conclusion

Based on the modeling and analysis done with the MIDAS FEA application, the conclusion was:

1. It shows that there is a decrease in strength as big as +5.5% for every 5% hollow ratio increment.
2. From the analysis result, it shows that the best hollow core ratio is 30%. It is because even though the sample experiencing a decrease in strength along with the hollow ratio increment, the sample effectivity increases both in axial and moment capacity.

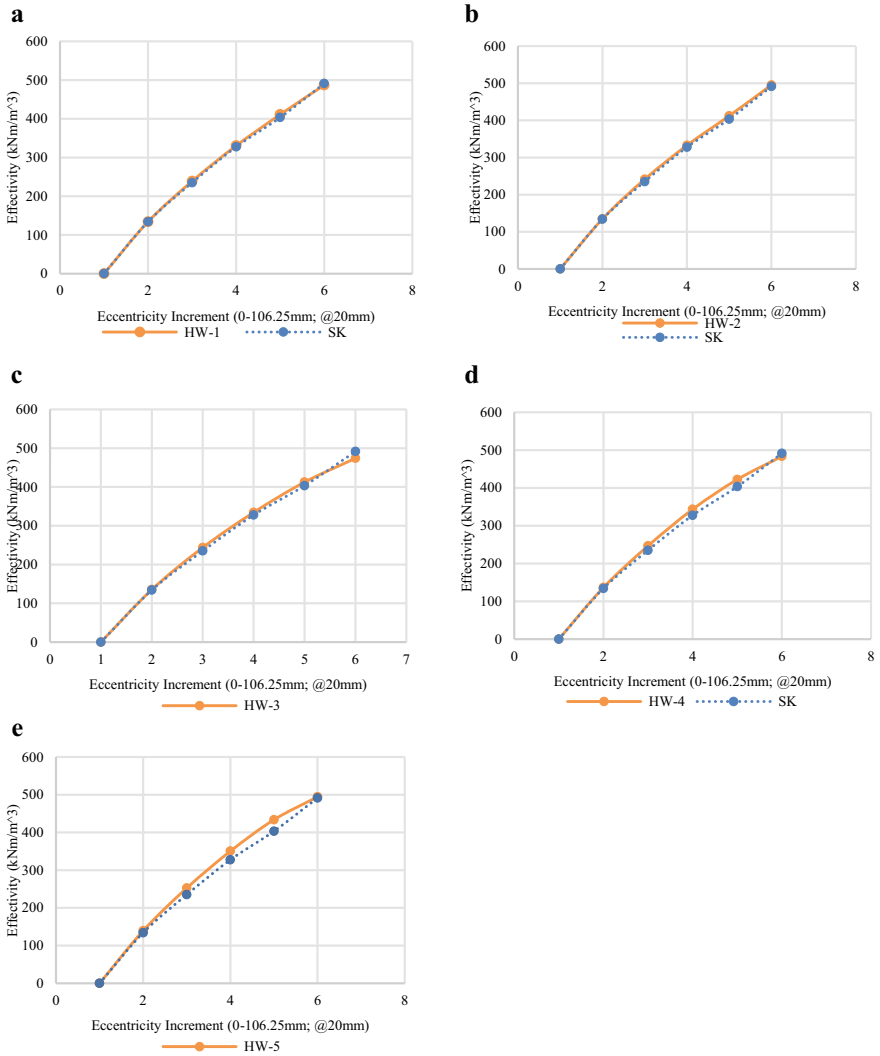


Fig. 7 Moment capacity to volume effectivity ratio comparison of **a** HW-1 versus SK, **b** HW-2 versus SK, **c** HW-3 versus SK, **d** HW-4 versus SK, **e** HW-5 versus SK

3. The analysis result shows that none of the hollow samples with CFRP wrapping can give a higher strength compare to SK (Solid Conventional Sample with Steel Rebar).
4. From an effectivity point of view, it shows that there is some variation of HW, which has an effectivity that exceeds SK.
5. MIDAS FEA application able to simulates crack pattern step by step from initial loading until it reaches collapse state (see Fig. 9).

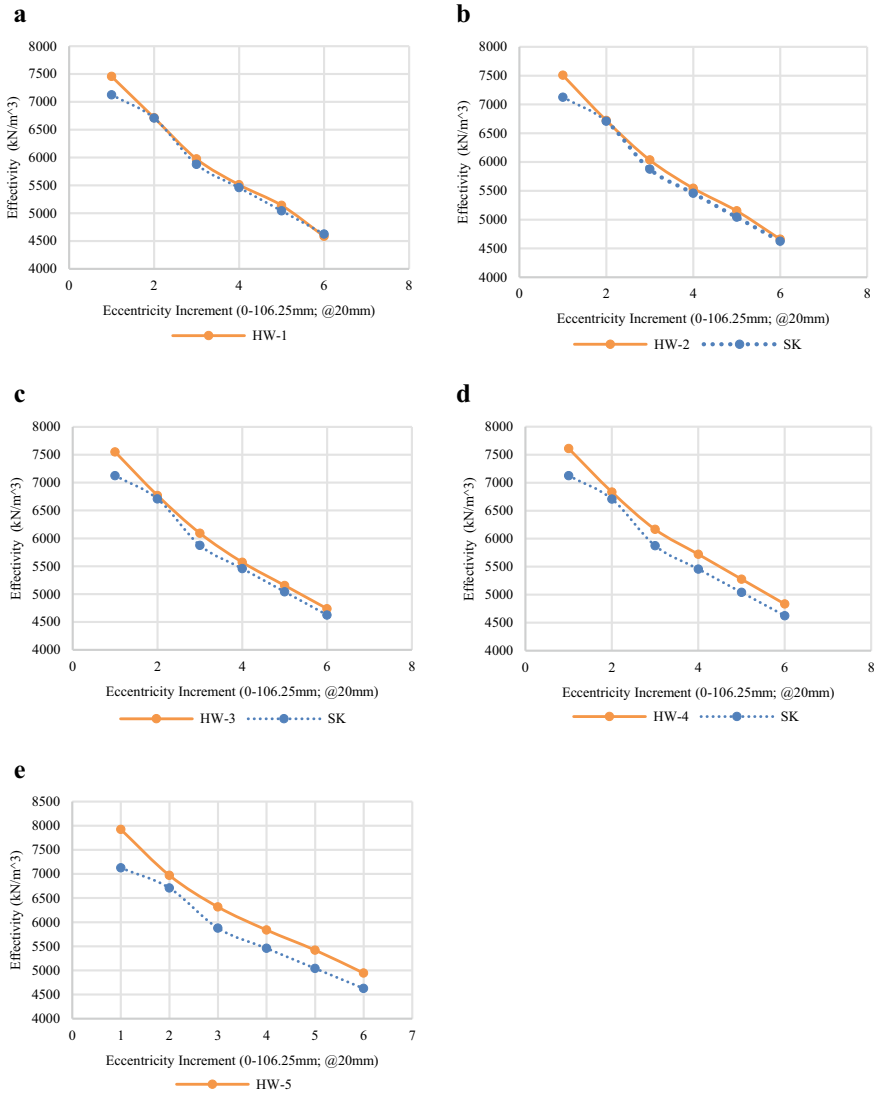


Fig. 8 Axial capacity to volume effectivity ratio comparison of **a** HW-1 versus SK, **b** HW-2 versus SK, **c** HW-3 versus SK, **d** HW-4 versus SK, **e** HW-5 versus SK

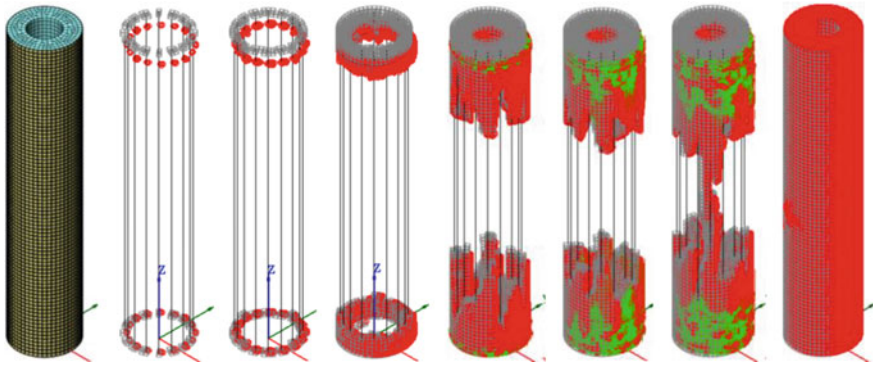


Fig. 9 Step by step cracking pattern output in MIDAS FEA

References

1. Wight JK, Richart FE (2016) Reinforced concrete mechanics and design, 7th edn. Pearson Education, New Jersey
2. Mo Y, Wong D, Maekawa K (2003) Seismic performance of Hollow bridge column. *ACI Struct J* 100(3):337–348
3. AlAjarmeh OS, Manalo AC, Benmokrane B (2020) Effect of spiral spacing and concrete strength on behavior of GFRP-reinforced hollow concrete columns. *J Compos Constr* 24 (1):04019054
4. Liang X, Sritharan S (2019) Effects of confinement in square hollow concrete column sections. *Eng Struct* 191:526–535
5. ACI Committee 318 (2014) Building code requirements for structural concrete (ACI 318–14). American Concrete Institute, Farmington Hills
6. ACI Committee 440 (2017) ACI 440.2R-17: guide for the design and construction of externally bonded FRP systems for strengthening concrete structures. American Concrete Institute, Farmington Hills
7. Masuelli MA (2013) Introduction of fibre-reinforced polymers—polymers and composites: concepts, properties and processes. Fiber reinforced polymers—the technology applied for concrete repair. IntechOpen. <https://doi.org/10.5772/54629>
8. Molded Fiber Glass Companies (2003) Designing with fiber reinforced plastics/composites. Molded Fiber Glass Companies, Ohio
9. Unicomposite (n.d.) Carbon Fiber/Roller. <https://www.unicomposite.com/product/carbon-fiber-roller/>. Accessed 15 Sep 2020

The Use of Fly Ash in Pervious Concrete Containing Plastic Waste Aggregate for Sustainable Green Infrastructure



Steve W. M. Supit  and Priyono

Abstract The aim of this research is to experimentally investigate the use of fly ash in pervious concrete containing plastic waste aggregate for solving environmental problems. The effects of fly ash are investigated based on the weight of volume concrete, compressive strength, and void ratio of pervious concrete samples. The percentages of 5, 10, and 15% plastic were used to replace the natural aggregate content. The amount of 15% fly ash is selected based on the optimum compressive strength of cement mortar tested seven days after water curing. This percentage was then used in pervious concrete containing 5% of plastic waste aggregate that achieved the highest compressive strength in comparison to other mixtures. The results show that pervious concrete incorporated with 15% fly ash and 5% plastic waste aggregate reduced the weight of the volume of pervious concrete compared to control concrete without plastic aggregate addition. In terms of compressive strength and void ratio, the use of fly ash shows comparable results with the control specimens. Furthermore, combining 15% fly ash and 5% plastic waste in making pervious concrete can be considered as one of the environmentally construction materials for sustainable green infrastructure.

Keywords Fly ash · Pervious concrete · Plastic waste · Compressive strength · Void ratio

1 Introduction

Pervious concrete can be defined as a special type of concrete consists of cement, coarse aggregate, a little to no fine aggregates, additives, and water that is normally used for improving the ecological environment of soil and water quality, protecting

S. W. M. Supit (✉)

Civil Engineering Department, Manado State Polytechnic, Manado, Indonesia
e-mail: stevewmsupit@gmail.com

Priyono

Mechanical Engineering, Manado State Polytechnic, Manado, Indonesia

groundwater resources, and managing storm-water runoff [1, 2]. When compared to normal or typical concrete, pervious concrete is more permeable with a porous structure (15–30% per volume) that allows the water to penetrate through the concrete matrix and offers sustainable drainage solutions. Some major factors that generally influence the performances of pervious concrete are the water/cement ratio, the aggregate sizes, aggregate: cement ratio, void volume. Upon the benefits of pervious concrete, some disadvantages have been discussed in relation to the characteristics of typical pervious concrete, such as limited bond strength between the aggregates, risk of clogging by organic and inorganic material, and low durability resistance [3]. These issues have brought more experimental works in order to enhance the properties of pervious concrete, for example by partially replacing cement with a variety of supplementary cementitious materials like natural pozzolans and by-product materials. One of the by-product materials that has been widely used to substitute cement content in the proportion of normal concrete is fly ash.

Fly ash has been known as a fuel combustion product (ASTM C618-17a, 2017) [4] composed of glassy particles that can act as a pozzolanic material with the presence of silicate and aluminate to contribute to the strength and durability properties of concrete [5–7]. The pozzolanic products of Calcium Silicate Hydrate (CSH) and Calcium Aluminate Hydrate (CAH) formed by the reaction of fly ash with calcium hydroxide can be very effective in making a denser matrix leading to the increase of mechanical strength and durability resistance [8, 9].

Based on the discussions above, the effect of fly ash in pervious concrete containing plastic waste aggregate is interesting to be evaluated. The efforts of maximizing the plastic waste to substitute aggregate in concrete have been investigated recently in order to overcome the environmental problem due to the increase in the quantity of plastic-based waste. Reference [10] reported that concrete containing 15% replacement of stone aggregate by recycled plastic improved the compressive strength of concrete up to 18.34 MPa, making it applicable for structural application. On the other study conducted by Rahmani et al. [11], it was reported that concrete containing plastic aggregate type Polyethylene Terephthalate (PET) as fine aggregate increased the compressive strength of concrete with the maximum replacement of fine aggregate was 5%. This study also found that the ductility behavior can be obtained in concrete with 10% PET waste particles with no negative effect on its compressive strength. Among the results from previous studies, very few reports are available on the use of plastic waste as a natural aggregate replacement in pervious concrete. The report on the effect of fly ash in pervious concrete is also still limited. Therefore, the reinforcement of fly ash in pervious concrete containing plastic waste aggregate is interesting to be evaluated. The outcome results on the inclusion of fly ash in pervious concrete with plastic waste aggregate can be an alternative sustainable construction material for a structural and non-structural application.

2 Materials

Materials used in this experiment are cement type Portland Composite Cement (PCC), fly ash type C from Steam Power Plant (PLTU) 2 Amurang, natural coarse aggregate with a maximum size of 20 mm, water and superplasticizer type F as chemical admixture. Table 1 presents the chemical composition of PCC and fly ash used in this experiment.

Moreover, the plastic waste sourced from the plastic bottle type Polyethylene Terephthalate (PET) was prepared following the procedure are presented in Fig. 1. The plastic bottle was cut into small pieces then melted under a temperature of

Table 1 Chemical composition of PCC and fly ash (%)

Chemical analysis	PCC	Fly ash
SiO ₂	8.43	18.77
Al ₂ O ₃	1.65	6.89
Fe ₂ O ₃	4.81	21.8
CaO	73.12	28.13
MgO	–	4.65
K ₂ O	–	1.38
Na ₂ O	–	7.41
SO ₃	2.71	6.65



Fig. 1 Procedure on obtaining plastic waste aggregate

150 °C. The melted plastic was poured into the mold and pressed to form a hardened paving block. The plastic paving block was then crushed manually with a hammer to obtain a plastic aggregate with a maximum size that is similar to the natural coarse aggregate.

3 Experimental Method

The experimental works are divided into three parts. The first part investigated the optimum percentage of fly ash when replacing PCC in the mortar with the dosage of 10, 15, 20, and 25% by weight of cement. The evaluation was taken based on the compressive strength of mortar tested 7 days after curing in water. The mixture proportions of mortar with fly ash can be seen in Table 2. In this part, cement and fly ash were dried mixed before mixing it with water using the mortar mixer. After completing the mixes for around 10 min, the mixtures were then placed into the molds with a size of 50 mm × 50 mm × 50 mm. After 24 h, the samples were then demolded for curing until the day of testing. The second part investigated the effect of plastic waste aggregate in pervious concrete with the variation of replacement, i.e., 5, 10, and 15% by weight of total natural aggregate. The mixture proportions of different types of pervious concrete are presented in Table 3. In this

Table 2 Mixture proportions of mortars containing fly ash

Type of mortar	Cement (g)	Fly ash (g)	Fine aggregate (g)	Water (ml)
CM	500	0	1200	120
FA-10%	450	50	1140	120
FA-15%	425	75	1080	120
FA-20%	400	100	1020	120
FA-25%	375	125	1140	120

CM control mortar, FA-10% 10% fly ash in mortar, FA-15% 15% fly ash in mortar, FA-20% 20% fly ash in mortar, FA 25% 25% fly ash in mortar

Table 3 Mixture proportions of different type of pervious concrete (kg/m³)

Type of concrete	Cement	Fly ash	Natural coarse aggregate	Plastic coarse aggregate	Water	Superplasticizer
PC	400	0	1200	0	120	2
PW-5%	400	0	1140	60	120	2
PW-10%	400	0	1080	120	120	2
PW-15%	400	0	1020	180	120	2
PC-PW5%-FA15%	340	60	1140	60	120	2

PC porous concrete, PC-5% 5% plastic in concrete, PC-10% 10% plastic in concrete, PC-15% 15% plastic in concrete, PC-PW5%-FA15% 5% plastic in concrete with 15% fly ash

part, the natural aggregate was mixed with the plastic aggregate and then poured into the concrete mixer containing cement paste with a water binder ratio of 0.3 and aggregate: cement ratio = 1:3. The dosage of 0.5% superplasticizer by weight of cement was selected to be used in this mixture. The pervious concrete mixtures were then cast in 100 mm/200 mm size of cylinder specimens for compressive strength and voids ratio testing after curing underwater at 7 and 28 days. The third part evaluates the characteristics of pervious concrete when mixed with fly ash and plastic waste aggregate with the percentage used is based on the results gained from the first and second parts.

3.1 Compressive Strength Fly Ash Mortar and Pervious Concrete

The compressive strength of mortar is conducted based on ASTM C109 (ASTM) [12] using the 50 mm × 50 mm × 50 mm cube size specimens while the ASTM C39/C39M-18 [13] standard is used for conducting the compressive strength test of pervious concrete. The concrete cylinder with the size of 100/200 mm was used. The mortar and concrete sample was placed on the compression machine and the load was applied until fracture. The ultimate load of each sample was then recorded, and the average of three samples on each mixture was used as the final result.

3.2 Weight Volume of Pervious Concrete

The weight of the volume of pervious concrete was calculated after the samples were cured at 7 and 28 days and weighed in air. The weight (kg) of each sample was then divided by the volume (cm³) to determine the effect of using fly ash and plastic waste in the pervious concrete mixture.

3.3 Void Ratio of Pervious Concrete

This test was proposed by Japan Concrete Institute (JCI) [14] and conducted in order to calculate the total void ratio that is defined as the percentage of the total volume of voids to the total volume of the specimen. In this test, the concrete cylinder specimens with the size of 100 × 200 mm were prepared after curing at 7 and 28 days. The volume of specimens was measured as V_1 . After water curing, the mass of samples in water was recorded (W_1). The samples were then left for 24 h at room temperature and then weighted as W_2 . On the next day, the measurement in

water was taken again (W_3) to calculate the total void ratio (A_t) based on the formula in Eq. 1.

$$A_t (\%) = 1 - \frac{(W_2 - W_1)/\rho_w}{V_1} \times 100 \quad (1)$$

Additionally, the continuous void ratio (A_c) can be also calculated using the formula in Eq. 2.

$$A_c (\%) = A_t - \frac{(W_1 - W_3)/\rho_w}{V_1} \times 100 \quad (2)$$

4 Results and Discussions

4.1 Compressive Strength of Mortars Containing Fly Ash

Figure 2 presents the compressive strength results of typical mortars containing different percentages of fly ash tested after water curing at 7 days. The results were calculated as the average of three pervious concrete samples on each mixture. The error bars are also presented to represent the standard deviation. This part was conducted in order to evaluate the maximum percentage replacement of fly ash that contributed to the higher compressive strength. The figure shows that maximum compressive strength is achieved by mortar with 15% fly ash by weight of cement. Increasing the fly ash content up to 20 and 25% reduces the compression load resistance. By comparing the strength of CM and FA-15% samples, CM sample has

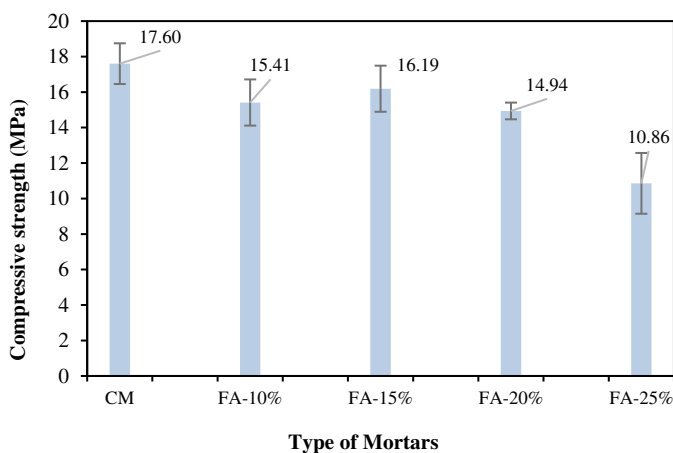


Fig. 2 Compressive strength of mortar containing fly ash at 7 days

higher compressive strength than FA-15% mortar with the difference is about 8%. Another study conducted by Ref. [15] also reported a similar trend when using the same source of fly ash. In this study, it was found that mortar with the proportion of 1 cement: 3 sand and 15% fly ash by wt. of cement achieved 27.71 MPa of compressive strength on the 28th day. However, increasing the sand content up to five times of cement resulted in reducing the compressive strength results but still acceptable to be used as a pavement mixture. Furthermore, according to the preliminary results on mortar, 15% of fly ash was selected to replace cement in the pervious concrete mixture.

4.2 Compressive Strength of Pervious Concrete Containing Plastic Waste and Fly Ash

The compressive strength results of pervious concrete containing plastic waste and fly ash can be seen in Fig. 3. It can be clearly seen the effect of replacing partially natural aggregate with plastic waste aggregate. In this case, the pervious concrete with 5% plastic waste that replaces the natural coarse exhibited higher compressive strength at 7 days when compared to the strength of normal concrete. On the 28th day, the strength on compression load was found comparable with the value of 19 MPa. Increasing the plastic waste content reduced the compressive strength development of pervious concrete after all curing periods. The significant effect of using plastic waste in pervious concrete can be found on the 7th day since all of percentages replacement of natural coarse aggregate with the plastic waste aggregate performed higher strength than the normal concrete (PC).

The influence of PET particles was also commented on by the study from Rahmani [11]. In this study, the presence of PET particles was found to act as a

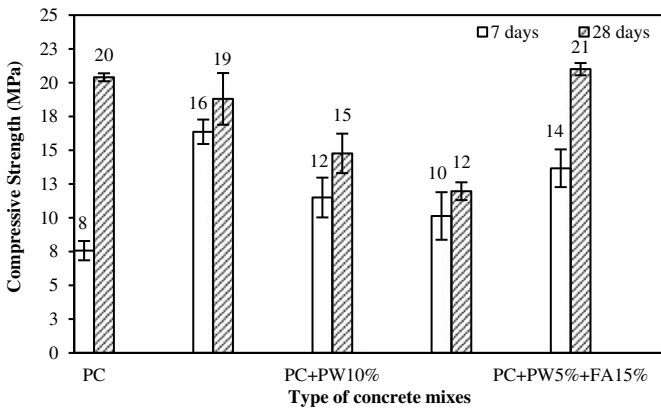


Fig. 3 Compressive strength of pervious concrete at 7 and 28 days

barrier that prevented the transition zone between cement paste and aggregates. However, the presence of plastic particles is beneficial when ductility is concerned.

When the pervious concrete with 5% plastic aggregate is combined with 15% fly ash as a cement replacement, the compressive strength results show that the replacement of cement using fly ash was less effective in improving the compressive strength on the 7th day. However, there is an increase of strength is found at the 28th day on pervious concrete containing 15% fly ash. The addition of fly ash affects the cement paste thickness leading to an increase in the bonding between aggregates, thus influences the compression load resistance of pervious concrete. Torres et al. [16] also reported that a thicker cement coating could give a positive effect on the mechanical strength improvement. However, the use of mineral admixtures on pervious concrete as a cement replacement should be properly proportioned in order to achieve the desired strength without defeating the purpose of pervious concrete. Overall, all of the compressive strength of pervious concrete results fall within the range of 2.8–20 MPa, as reported in ACI 522R-10 [17].

Considering the compressive strength of the combined plastic waste aggregate and fly ash in pervious concrete that reached 21 MPa on the 28th day, the applications of this pervious concrete mixture are potential for parking lots, lightweight wall structure when thermal insulation is considered, base course for roads, sea-walls, embankments, etc. [18]. Since the research in Ref. [19] reported the improvement of splitting and flexural strength of pervious concrete due to the presence of fly ash as supplementary cementitious materials, further research on other mechanical properties such as splitting and flexural strength test should be taken into account for the pervious concrete containing fly ash and plastic waste.

4.3 Weight Volume of Porous Concrete

The weight volume of porous concrete containing fly ash and different percentage of plastic waste is presented in Fig. 4. The weight of volume was determined after the samples were cured in water at 7 and 28 days. As seen, there is no significant change in the weight volume of pervious concrete due to a longer curing period. The interesting point that can be observed is the effect of replacing the natural aggregate with some percentage of plastic waste, which are 5, 10, and 15%. The increase of plastic waste content up to 15% significantly reduces the weight volume of porous concrete that can be due to the smaller specific gravity of plastic aggregate compared to the natural aggregate that leads to form lightweight pervious concrete. According to the research reported in Ref. [20], the specific gravity of crushed plastic aggregates with sizes 4.75 to 20 mm is 0.93 with a density of 0.84 g/cc. This is an indication that including plastic waste aggregate has a potential application in forming lightweight construction materials. By adding 15% fly ash into the 5% plastic waste concrete, the weight volume is increased but still lighter than the control pervious concrete. This trend can be found in the case of 7 and 28 days after water curing.

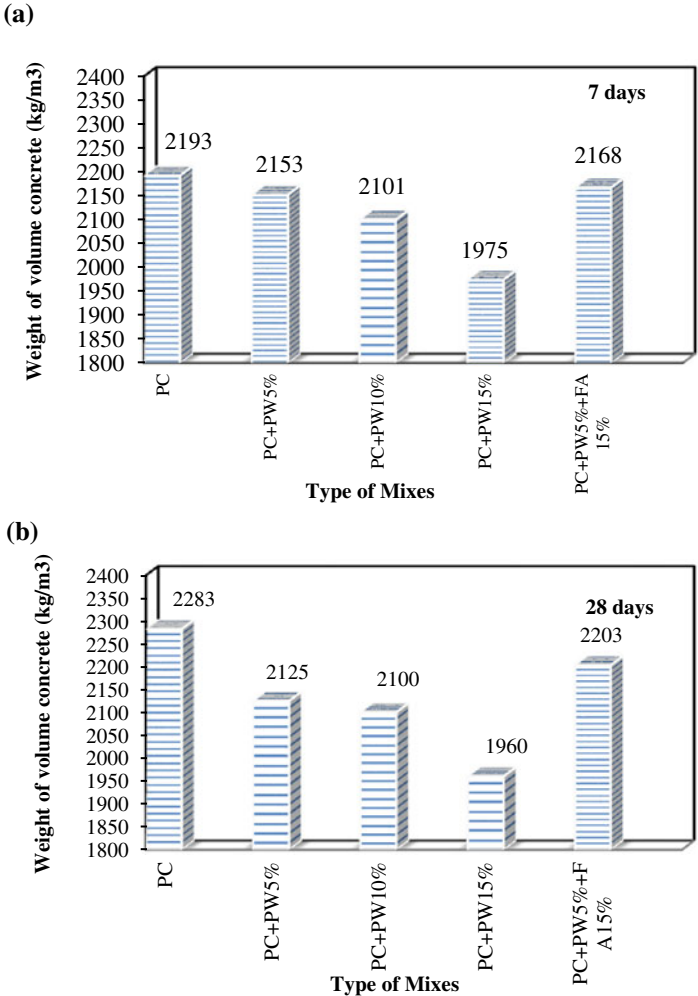


Fig. 4 Weight of volume of different types of pervious concrete at a 7 d days, b 28 days

4.4 Void Ratio of Pervious Concrete

The results of the void ratio of pervious concrete containing plastic waste with and without the addition of fly ash are presented in Table 4. In these results, the percentage of continuous voids represents the bonding performance between the aggregate and the cement paste. It can be clearly seen that the total voids of PC-5% are 18.4% at 7 days and around 17.5% at 28 days. The results are higher than the total voids of pervious concrete without plastic waste aggregate. It means that the pervious concrete when combined with plastic waste aggregate obtains a higher

Table 4 Percentage of voids in different types of concrete

Type of mixes	7 days			28 days		
	Total voids— A_t (%)	Continuous voids— A_c (%)	Discontinuous voids— A_d (%)	Total voids— A_t (%)	Continuous voids— A_c (%)	Discontinuous voids— A_d (%)
NC	10.5	10.0	0.5	11.0	8.8	2.2
PC-PW5%	18.4	17.7	0.7	17.5	17.1	0.4
PC-PW5%-FA	11.8	11.2	0.6	10.4	9.6	0.8

percentage of total voids in comparison to the normal concrete sample. However, the continuous voids of pervious concrete with 5% plastic waste addition (PC-5%) is observed higher than the NC sample indicating the presence of 5% plastic waste as a natural coarse aggregate replacement increases the bonding of the coated thin layer among the coarse aggregate due to its sharp edges and corner shape that also leads to the improvement of compressive strength. On the other hand, the addition of 15% fly ash as cement could lower the total voids content, lower than the total voids of PC-5% concrete, and comparable with NC concrete sample. This can be suggested due to the micro-filler effect of fly ash that increases the paste thickness of pervious concrete, thereby reducing the total voids content from 17.7 to 10.4%.

The reduction of total voids due to fly ash involvement is also reported in the study of Ref. [21]. It was reported that the reduction of the total voids could be due to the micro-filler effect of fly ash and the plasticizer used that caused a cohesive action. The beneficial effects of fly ash in terms of technical, economic, and environmental were also reported in this study.

5 Conclusions

According to the results presented in this experiment, some valuable conclusions could be drawn for further research as follows:

1. The results from the compressive strength test show that the pervious concrete containing 5% plastic waste aggregate is 16 and 19 MPa at 7 and 28 days, respectively, higher when compared to the compressive strength of normal pervious concrete. From the void ratio results, this specimen also increases the continuous voids indicating that the presence of 5% plastic waste as a natural coarse aggregate replacement could increase the bonding of the coated thin layer among the coarse aggregate.
2. Combining fly ash with a dosage of 15% by weight of cement effectively increases the compressive strength due to the thicker paste layer formed that also reduced the void ratio leading to the strength improvement. However, there is no significant difference found when the results are compared with the pervious concrete containing 5% of the plastic waste aggregate.

3. By adding 15% fly ash into the 5% plastic waste concrete, the weight volume is increased but still lighter than the control pervious concrete. On the other hand, the increase of plastic waste content up to 15% significantly reduces the weight volume of porous concrete leading to form lightweight pervious concrete.
4. Combining fly ash with plastic waste aggregate to make pervious concrete is very promising for maximizing the utilization of waste, including by-products materials for application in the construction field. Based on the compressive strength results, the mixture can be used in the pavement for a light load, such as for pedestrian walks or parking lots.

Acknowledgements The authors would like to thank Direktorat Sumber Daya, Direktorat Jenderal Pendidikan Tinggi Kementerian Pendidikan, Kebudayaan, Riset, dan Teknologi Republik Indonesia for the research funding under scheme Penelitian Dasar Unggulan Perguruan Tinggi Year 2021 No. 095/E4.1/AK.04.PT/2021—12 Juli 2021.

References

1. Uma Magesvari M, Sundararajan T (2017) Influence of fly ash and fine aggregates on the characteristics of pervious concrete. *Int J Appl Eng Res* 12(8):1598–1609
2. Zhong R, Wille K (2015) Material design and characterization of high performance pervious concrete. *Constr Build Mater* 98:51–60. <https://doi.org/10.1016/j.conbuildmat.2015.08.027>
3. ASTM C618–17a (2017) Standard specification for coal fly ash and raw or calcined natural pozzolan for use in concrete. ASTM International, Pennsylvania
4. Saraswathy V, Song HW (2006) Corrosion performance of fly ash blended cement concrete: a state-of-art review. *Corros Rev*. <https://doi.org/10.1515/CORRREV.2006.24.1-2.87>
5. Malvar LJ, Lenke LR (2006) Efficiency of fly ash in mitigating alkali silica based on chemical composition. *ACI Mater J* 103(5):319–326
6. Xu GQ, Liu JH, Qiao L, Sun YM (2010) Experimental study on carbonation and steel corrosion of high volume fly ash concrete. In: *Asia-Pacific Power and Energy Engineering Conference (APPEEC)*, 28 Mar 2010. <https://doi.org/10.1109/APPEEC.2010.5448649>
7. Bendapudi SC, Saha P (2011) Contribution of fly ash to the properties of mortar and concrete. *Int J Earth Sci Eng* 4(6):1017–1023
8. Chindapasirt P, Kanchanda P, Sathonsaowaphak A, Cao HT (2007) Sulfate resistance of blended cements containing fly ash and rice husk ash. *Constr Build Mater*. <https://doi.org/10.1016/j.conbuildmat.2005.10.005>
9. Malvar LJ, Lenke LR (2005) Minimum fly ash cement replacement to mitigate alkali silica reaction. In: *World of coal ash (WOCA) conference*, Lexington
10. Habib M, Alom M, Hoque M (2017) Concrete production using recycled waste plastic as aggregate. *J Civ Eng* 45(1):11–17
11. Rahmani E, Dehestani M, Beygi MHA, Allahyari H, Nikbin IM (2013) On the mechanical properties of concrete containing waste PET particles. *Constr Build Mater* 47:1302–1308. <https://doi.org/10.1016/j.conbuildmat.2013.06.041>
12. ASTM C109 (2000) Standard test method for compressive strength of hydraulic cement mortars. ASTM International, West Conshohocken. <https://doi.org/10.1520/C0109>
13. ASTM C39–12 (2012) Standard specification for compressive strength of cylindrical concrete specimens. ASTM International, West Conshohocken

14. Tamai M, Mizuguchi H, Hatanaka S (2004) Design, construction and recent application of porous concrete in Japan. In: Proceedings of the JCI symposium on design, construction and recent applications of porous concrete. Japan Concrete Institute, Tokyo, pp 1–10
15. Wenno R, Wallah S, Pandaleke R (2014) Kuat tekan mortar dengan menggunakan abu terbang (fly ash) asal PLTU Amurang sebagai substitusi parsial semen. *Jurnal Sipil Statik* 2 (5):252–259
16. Torres A, Hu J, Ramos A (2015) The effect of the cementitious paste thickness on the performance of pervious concrete. *Constr Build Mater* 95:850–859
17. ACI Committee 522R-10 (2010) Report on pervious concrete. American Concrete Institute, Michigan
18. Ahmed T, Hoque S (2020) Study on pervious concrete pavement mix designs. In: 2nd international conference on civil & environmental engineering, Kedah, November 2019, vol 476. iop conference series earth environmental science, p 012062 (IOPscience). <https://doi.org/10.1088/1755-1315/476/1/012062>
19. Arifi E, Cahya EN (2020) Evaluation of fly ash as supplementaru cementitious material to the mechanical properties of recycled aggregate pervious concrete. *Int J GEOMATE* 18(66):44–49
20. Dhanani G, Bhimani P (2016) Effect of use plastic aggregates as partial replacement of natural aggregates in concrete with plastic fibres. *Int Res J Eng Technol (IRJET)* 3(4):2569–2573
21. Muthaiyan UM, Thirumalai S, Hussain RR (2017) Studies on the properties of pervious fly ash-cement concrete as a pavement material. *Cogent Eng* 4(1):1318802. <https://doi.org/10.1080/23311916.2017.1318802>

Artificial Aggregate Made from Expanded Polystyrene Beads Coated with Cement Kiln Dust—An Experimental Trial



A. P. Wibowo , M. Saidani, and M. Khorami

Abstract The use of waste materials from industrial products to support green building and environmentally friendly construction needs more attention and becomes a common thought. The use of waste materials such as Cement Kiln Dust (CKD) or often referred to as Bypass Dust (BPD), as a concrete substitution material, has been done a lot and not a few have given positive results. However, it is necessary to have other alternatives regarding using this waste material, one of which is to try to use it as a coating material for lightweight materials such as Expanded Polystyrene (EPS) to manufacture artificial aggregate. This coating technique uses a solvent/adhesive in the form of liquid (acetone–water and polyvinyl acetate–water). The resulting weights of coated EPS with BPD are 154–175 g/l. Artificial lightweight aggregate made from EPS grains coated with CKD powder with an adhesive solution of a mixture of Polyvinyl Acetate (PVA)–water gave more promising results than an acetone–water binder. The process of creating coated EPS shows the potential as artificial aggregates for a lightweight concrete. The coated EPS gives a better result in strength than pure EPS beads when replacing the coarse aggregate.

Keywords Expanded polystyrene (EPS) beads · Coating · Cement Kiln dust (CKD) · Acetone · Polyvinyl acetate

1 Introduction

Cement Kiln Dust (CKD) or often called Bypass Dust (BPD) [1], is the residual/waste material from the cement manufacturing process. The amount of CKD waste generated from the rotary kiln during the calcination process can reach 8–20% of

A. P. Wibowo (✉)

Department of Architecture, Universitas Atma Jaya Yogyakarta, Sleman, Indonesia
e-mail: andi.prasetyo@uajy.ac.id

A. P. Wibowo · M. Saidani · M. Khorami

Institute for Future Transport and Cities, Coventry University, Coventry, United Kingdom

the total cement production [2, 3]. Therefore, the large amount of waste generated needs to be adequately managed and handled in the name of the environment. The use of waste materials from industrial products to support green building and environmentally friendly construction needs more attention and becomes a common thought.

In concrete technology, the use of CKD is mainly used as a substitute for cement. Replacing cement with up to 60% CKD [4] can produce concrete with compressive strength and durability performance comparable to normal concrete and capable of producing high-quality concrete. However, it still has to be combined with other materials such as Nano Silica [5]. In another study, CKD had been used as material to create an environmentally friendly lightweight brick [6], which was then tried to be developed by Saleh et al., which combines other waste materials such as polystyrene waste [7].

The use of Expanded Polystyrene (EPS) in lightweight concrete has been studied and has been widely used for decades. However, the weight of EPS beads and their smooth surface make this material segregate in the concrete matrix, impacting the weak bond and strength of the concrete. Modifications are needed to anticipate and reduce these weaknesses. Based on previous research, CKD can positively affect increasing flow ability and reduce segregation in a Controlled Low-Strength Material (CLSM), which is also cement-based [8]. There have also been many attempts to create artificial aggregates from concrete waste products by utilizing waste concrete powder obtained from crushed waste concrete [9] and the building's debris of post-earthquake [10]. These studies produced aggregates that can substitute natural aggregates even though the concrete strength is still below whilst using natural aggregates. Some of the research listed above then become an insight for further study to use cement/concrete-based waste materials by incorporating different materials to create types of artificial aggregates in the manufacture of concrete.

This research will focus on creating lightweight aggregates using CKD as a coating material for EPS beads. Besides utilizing waste materials, combining these two materials might be considered as a development for an alternative of lightweight aggregates to create lightweight concrete.

2 Material and Method

This study is a laboratory-based experimental activity. The study was conducted at the Concrete and Materials Laboratory, Faculty of Engineering, Environment and Computing, Coventry University, United Kingdom. In addition, the literature study method was also used to be the basis of theories as a literature study and to support the analysis and discussion. This experiment focuses on creating an artificial aggregate and reporting the result as a part of an ongoing and enhancements process for further research.

2.1 Materials

The material used in this study consists of three parts. First, EPS grain is the main part of the artificial aggregate creation. Second, the material/powder that will be used as a coating, and third, the solution that functions as an adhesive or binder. The EPS beads used in this study have a range of diameter between 3 and 6 mm, with the weight of 8–9.5 g per 1000 ml. The coating material utilizes the residual waste material from cement production, namely Cement Kiln Dust (CKD) or Bypass Dust (BPD). The CKD material cement material obtained from Rugby Cement Plant of CEMEX company that also used by previous research [11]. There were two types of binder that is used in this research. The first type is a mixture of acetone and water, and the second type by using a mixture of PVA (Polyvinyl Acetate) and water (as shown in Table 1). The composition for EPS beads: binder: CKD is 5:0.1:1 by volume for acetone binder, and 1:4:40 by weight for PVA binder (Figs. 1, 2, and 3 and Table 2). The proportion of acetone solution/binder is 1:3 (acetone: water) by volume, while the PVA binder is created from the proportion by weight 1:1.5 (PVA: water).

2.2 Mixing and Coating Process

The mixing process was carried out in a mechanical mixer. For the type of acetone–water binder, the EPS beads were placed in the mixer container (Fig. 4). The mixer was turned on at low speed, then CKD/BPD powder was put into the mixer container. The solution mixture was sprayed into the mixer container. For the type of PVA-water binder, firstly PVA mixed with water to create a solution like glue (Fig. 5). The mixing process then carries on in the mixer.

Table 1 Composition for coated EPS beads as an artificial aggregate

Type of binder	Materials	Proportion by volume	Proportion by weight
Aceton: water 1:2	EPS beads	5	–
	Cement Kiln Dust (CKD)	1	–
	Binder/solution	0.1	–
PVA: water 1:1.5	EPS beads	–	1
	Cement Kiln Dust (CKD)	–	40
	Binder/solution	–	4



Fig. 1 EPS beads (diameter 3–6 mm)

2.3 Replacing the Coarse Aggregate with Coated Expanded Polystyrene

To determine the effect on the resulting concrete, the use of coated EPS beads in concrete will be compared as a substitute for coarse aggregate. In addition to comparing with normal concrete, the use of EPS beads without coating will also be compared. Calculation of the concrete composition (mix design) is presented in Table 3.

3 Result and Discussion

A mechanical mixer tends to produce homogeneous mixing. The composition of the solution made of acetone and water ratio of 1:2 only tends to wet it, without drastically changing the shape of the EPS beads (The physical form of EPS beads was still in granular shape). This is likely affected by the ratio of acetone and water ratio. The optimum water acetone ratio as the binder was expected to make the bond better. Acetone makes it possible to make the EPS surface melted and slightly rough (Fig. 6). It can be considered to increase the ratio of the amount of acetone in the composition to the ratio of the adhesive solution components to create better bonding. On the other hand, mixing with PVA-water binder tends to give a better result (Fig. 7).

From the visual observation of the results of the mixing/stirring with acetone-water binder, there were still some EPS beads that have not been completely coated

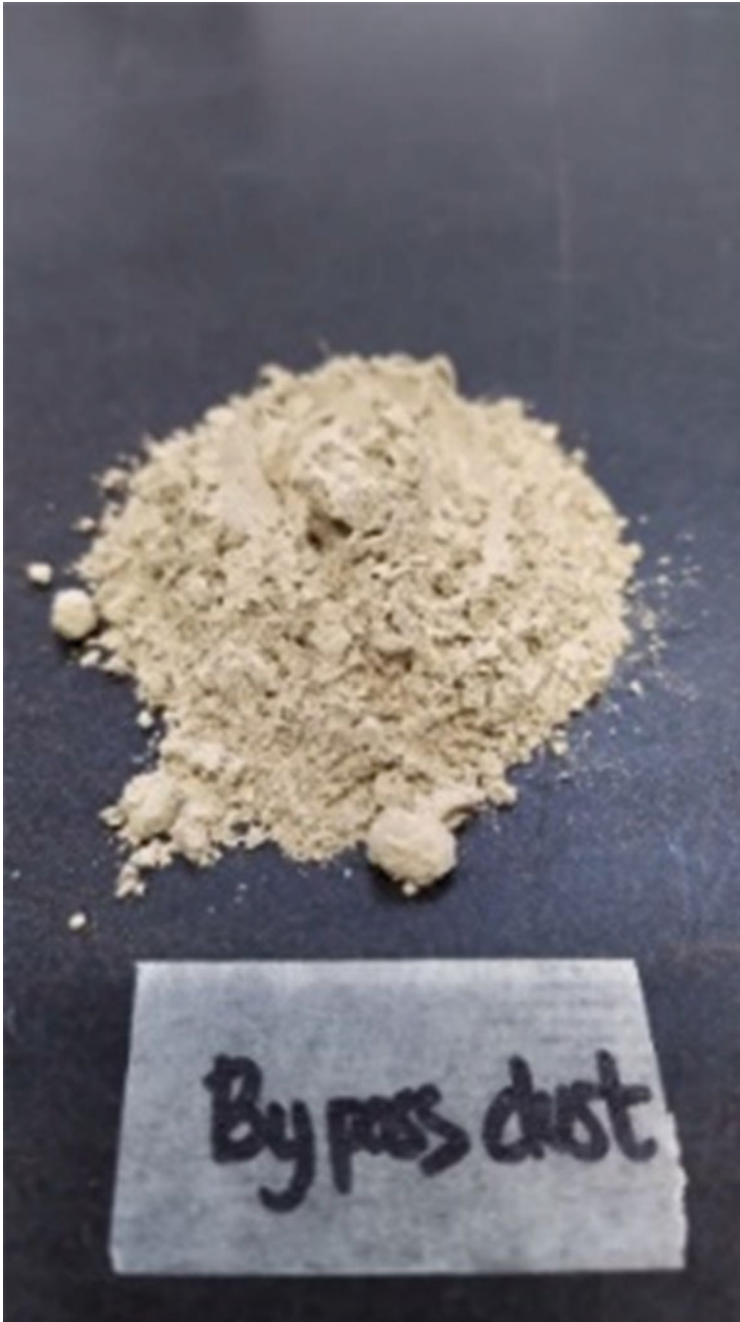


Fig. 2 Bypass dust or cement kiln dust



Fig. 3 PVA and acetone as a binder

Table 2 Chemical composition of CKD [11]

Chemical composition	wt%
SiO ₂	12.45
Al ₂ O ₃	3.68
Fe ₂ O ₃	2.14
MgO	0.93
CaO	36.96
Na ₂ O	1.22
K ₂ O	6.15
SO ₃	9.06
Cl	7.43
LOI	5.87

(white appearance). This could be possible due to the insufficient amount of CKD powder to coat the entire surface of the EPS. Some sections also show clumps of CKD paste combining 2–3 EPS grains. There is a possibility that because the most significant element of CKD is lime (CaO), so that when it reacts with water, it produces a kind of clay form which, if not adequately distributed, tends to clump. Determining the right amount of coating powder is expected to provide a more even coating without causing many paste clumps. The result of the mixing/stirring with PVA-water binder gives a more promising result since almost all the EPS beads are coated with the CKD powder.

After the stirring process, the weight of the EPS indicated a significant increase, from the original 8–9.5 g per 1000 ml to 154–175 g per liter. Thus, this weight was



Fig. 4 Mixing/coating process with acetone–water binder



Fig. 5 Preparation before mixing/coating process with PVA/water binder

Table 3 Concrete mix design (per m³)

Type of concrete	Cement (kg)	w/c	Fine aggregate (sand) (kg)	Coarse aggregate (gravel) (kg)	EPS beads (kg)
NC	445	0.54	848	882	–
EPS-C	445	0.6	848	–	5.4
CEPS-C	445	0.6	848	–	106

NC normal concrete, EPS-C concrete with pure EPS, CEPS-C concrete with coated EPS

much lighter than the modification using cement paste carried out by previous studies, resulting in a weight of coated EPS weighing 517 kg/m³ [12]. This result shows the potential for the use of CKD powder and coating techniques with the help of binder (acetone–water and PVA–water) to be continued in the effort to create artificial lightweight aggregates.

The use of EPS as a substitute for coarse aggregate is very influential on the weight of the concrete and also on its strength. The data is expected to be able to provide an overview of the trend comparison between three types of concrete with different types of coarse aggregate. The coating treatment on EPS beads gave better results compared to the use of EPS without coating. The results of the comparison of density and compressive strength of concrete can be seen in Table 4. The density and compressive strength test for NC (normal concrete) based on 100 × 100 × 100 mm cube specimens, while the EPS-C and CEPS-C used 50 × 50 × 50 mm cube specimens.



Fig. 6 Coated EPS beads with acetone–water binder

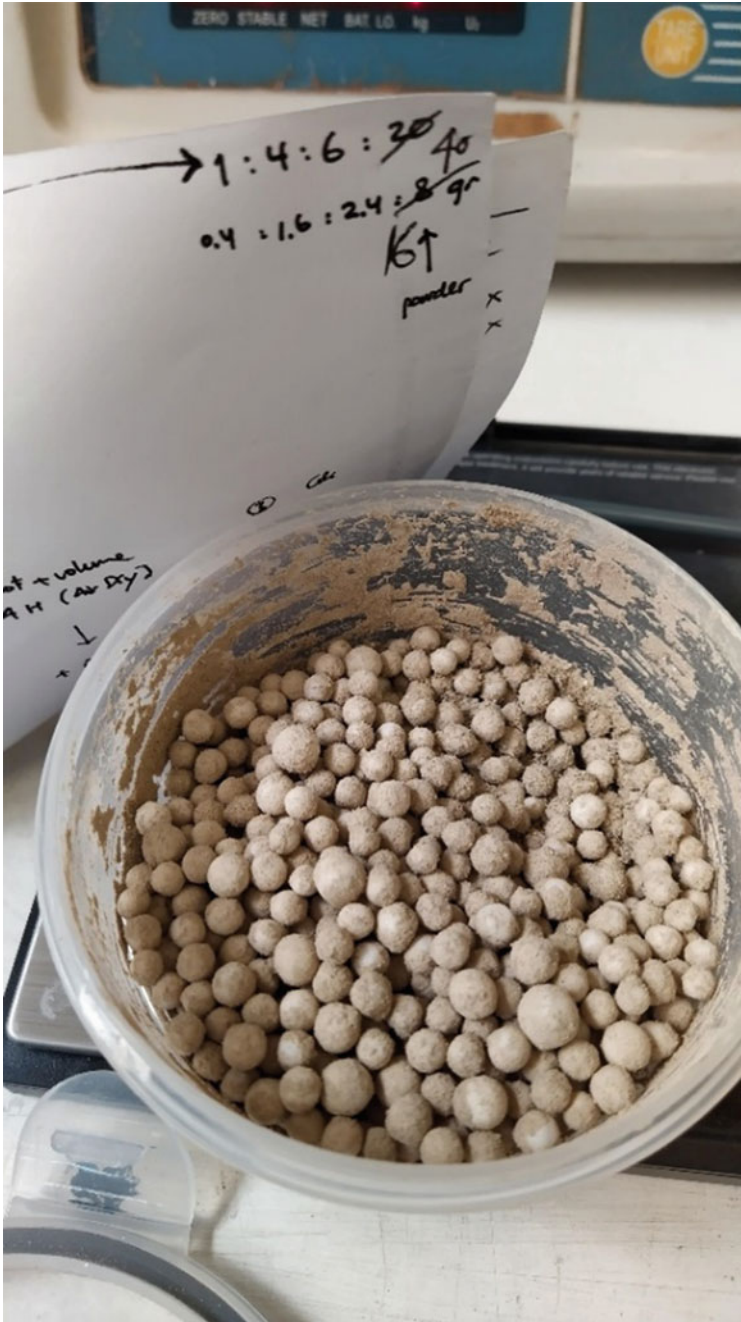


Fig. 7 Coated EPS beads with PVA-water binder

Table 4 Density and compressive strength

Type of concrete	Density (kg/m ³)	7 days strength (MPa)	14 days strength (MPa)	28 days strength (MPa)
NC	2300	35.04	44.39	45.07
EPS-C	1420	4.32	4.96	5.10
CEPS-C	1600	4.44	6.12	7.84

4 Conclusions

Artificial lightweight aggregate made from EPS grains coated with CKD powder with an adhesive solution of a mixture of PVA-water gave more promising results than acetone-water binder. The process of creating coated EPS shows the potential as artificial aggregates for a lightweight concrete. The coated EPS gives a better result in strength than pure EPS beads when replacing the coarse aggregate. However, there are still many trials and errors to perfecting this technique in terms of better coating rates, better adhesion, and finding the best proportion of mix design.

The creation of artificial aggregates is expected to provide positive support to reduce the exploitation of natural materials in the construction process, especially in the manufacture of concrete. Techniques for making lightweight aggregates from lightweight materials reinforced with coating techniques provide opportunities to continue to be developed. There is still a need for further research by expanding the variety of mixtures and types of coating materials, and not to be forgotten the advanced testing techniques to obtain more comprehensive data. Inventing the artificial aggregate itself does not stop at the stage of creation itself. It is a wide possibility for further research to study its effect on concrete.

Acknowledgements The first author expresses his appreciation to the Directorate General of Higher Education, Ministry of Education and Culture, the Republic of Indonesia for the financial support for his Ph.D. scholarship [BPPLN DIKTI 2019].

References

1. Barnat-Hunek D, Góra J, Suchorab Z, Łagód G (2018) Cement kiln dust. Waste and supplementary cementitious materials in concrete: characterisation, properties and applications, pp 149–180
2. Peethamparan S, Olek J, Lovell J (2008) Influence of chemical and physical characteristics of cement kiln dusts (CKDs) on their hydration behavior and potential suitability for soil stabilization. *Cem Concr Res* 38(6):803–815
3. Kaliyavaradhan SK, Ling TC, Mo KH (2020) Valorization of waste powders from cement-concrete life cycle: a pathway to circular future. *J Cleaner Prod* 268:122358

4. Shubbar AA, Jafer H, Abdulredha M, Al-Khafaji ZS, Nasr MS, Al Masoodi Z, Sadique M (2020) Properties of cement mortar incorporated high volume fraction of GGBFS and CKD from 1 day to 550 days. *J Build Eng* 30:101327
5. AlKhatib A, Maslehuddin M, Al-Dulaijan SU (2020) Development of high performance concrete using industrial waste materials and nano-silica. *J Mater Res Technol* 9(3):6696–6711
6. Ali MAM, Yang HS (2011) Utilization of cement kiln dust in industry cement bricks. *Geosystem Eng* 14(1):29–34
7. Saleh HM, Salman AA, Faheim AA, El-Sayed AM (2020) Sustainable composite of improved lightweight concrete from cement kiln dust with grated poly(styrene). *J Clean Prod* 277:123491
8. Lachemi M, Şahmaran M, Hossain KMA, Lotfy A, Shehata M (2010) Properties of controlled low-strength materials incorporating cement kiln dust and slag. *Cem Concr Compos* 32(8):623–629
9. Jiang Y, Ling TC, Shi M (2020) Strength enhancement of artificial aggregate prepared with waste concrete powder and its impact on concrete properties. *J Clean Prod* 257:120515
10. Wibowo AP (2018) Efficiency of house-walls construction using building ruins. *IOP Conf Ser Mater Sci Eng* 401:012017 (IOPScience)
11. Kamara KBB, Bure K (2020) Making road base and foundation from secondary waste minerals and recycled aggregates. Coventry University
12. Enda D (2016) Kajian eksperimental kekuatan agregat kasar styrofoam dengan lapisan coating pada pembuatan beton ringan. *Inovtek* 6(2):103–111

Load Transfer Shear Wall to Pile Cap Modelling Partially for Group Precast Pile



Daud Rahmat Wiyono, Roi Milyardi, Yosafat Aji Pranata, Asriwiyanti Desiani, Ginardi Husada, and Maria Christine Sutandi

Abstract Pile cap has the function to transfer the load from the upper structure to group of piles. Purpose of this research is comparing the support reaction of pile cap which loads from support reaction and loads from internal forces with pile cap modelling partially in elevator shaft. Building 14th story with shear wall frame has two model pile cap that are pile cap 1 (5 element pier with 44 piles) and pile cap 2 (11 element pier with 108 piles). The conclusion are the difference between support reaction as loads and support reaction correction are 49.10% in pile cap 1 and 56.11% in pile cap 2, and the difference between support reaction correction as loads and internal forces shear wall in 1st floor as loads are 3.86% in pile cap 1, and 3.19% in pile cap 2. With modelling pile cap partially with stiffness of piles are considered, the support reaction from support reaction correction comparing with support reaction pile cap are 3.68% in pile cap 1 and 2.51% in pile cap 2, and the support reaction from internal forces as loads comparing with support reaction pile cap are 50.11% in pile cap 1 and 69.93% in pile cap 2.

Keywords Load transfer · Shear wall · Pile cap · Stiffness

1 Introduction

In the upper structure, the location of loads from the upper structure to pile cap is important because it can give a different value of support reaction from piles modeling as support in pile cap. Loads of element shear wall are in the center of gravity of the element, and the loads from support reaction of upper structure are in the location of support in the shear wall if do not mesh in the shear wall, so the restraint is at the end of element pier [1]. Some shear walls are connected together as elevator shaft given duplicated support reaction in the joint which connected with

D. R. Wiyono (✉) · R. Milyardi · Y. A. Pranata · A. Desiani · G. Husada · M. C. Sutandi
Department of Civil Engineering, Faculty of Engineering, Universitas Kristen Maranatha,
Bandung, West Java, Indonesia
e-mail: hwiesiong@gmail.com

© The Author(s), under exclusive license to Springer Nature Singapore Pte Ltd. 2022
H. A. Lie et al. (eds.), *Proceedings of the Second International Conference of Construction, Infrastructure, and Materials*, Lecture Notes in Civil Engineering 216,
https://doi.org/10.1007/978-981-16-7949-0_15

another shear wall. In modeling a partially pile cap, the support reaction depends on the position of group piles as support. SAP 2000 can provide modeling as one pile cap as block foundation to received loads from several shear walls [2]. This software can give the support reaction in piles near the actual condition by input stiffness of piles [3].

The purpose of this research is to give the difference between without modeling pile caps partially and with modeling pile caps partially as one block foundation. The variation of loads are loads from support reaction with a correction from the duplicate node at the joint between other shear walls and loads from internal forces of the shear wall at 1st story. The variation of support is by using the stiffness of piles and by restraint as usual. Focusing on supporting reaction given from modeling pile cap partially as one block foundation. To modeling, the pile cap is used a thick shell element. The difference stress from internal forces as loads and support reaction correction as loads are obtained too.

2 Literature Study

Two methods are commonly used in pile cap design. There are beam theory and truss analogy/method of strut and tie. The pile cap is designed as a beam for internal forces, which are bending and shear. Types of pile caps use in this paper are shown in the following Fig. 1.

Figure 1 has shown the position of several shear walls connected to each other. The reaction from the upper structure is not the same as the reaction from a group of

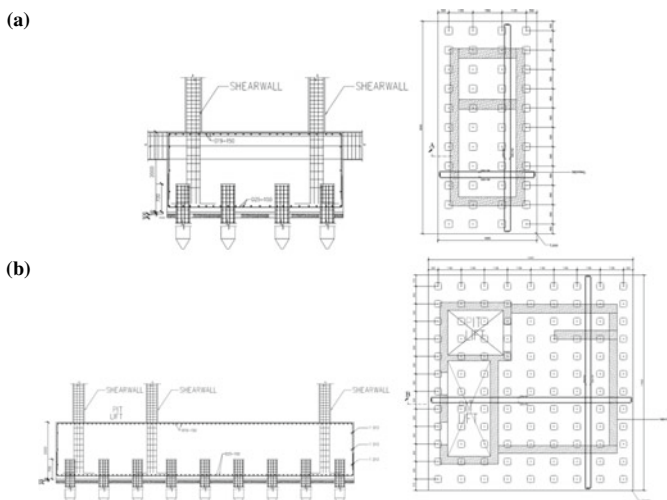


Fig. 1 Type of pile cap model **a** pile cap with 5 element pier 44 piles, **b** pile cap with 11 element piers with 108 piles

piles. That is why it can be modeling pile cap partially to obtain the reaction of group piles. Stiffness has been determined by soil investigations on the soil profile and characteristics. Pile caps design must satisfy to resist the punching shear of each pile [3]. The bearing force in the pile cap and the piles do not exceed the capacity of the element [4]. The pile cap reinforcement depends on the loading on the pile cap, the spacing of the piles, and the depth of the pile cap. To design pile foundations is done using finite element software, which is SAP2000 nonlinear, to calculate the reaction of piles. Shell thick element is used to model the pile cap element. The pile cap is assumed to be rigid, and at the top and at the bottom of the pile are pinned. The pile receives vertical load and receives force in terms proportional to the displacement [3].

3 Numerical Model

The 14th floor reinforced concrete shear wall frames building is modeling with SAP 2000 given in Fig. 2a. There are two elevator shafts on the left side and right side of the building. The elevator shaft on the left side is pile cap 1, and the elevator shaft on the right side is pile cap 2. The loads from internal forces and from support reaction are displayed in Fig. 2b–e. In Fig. 3a–d are displayed the loads from bending moment of the pile cap [4–10].

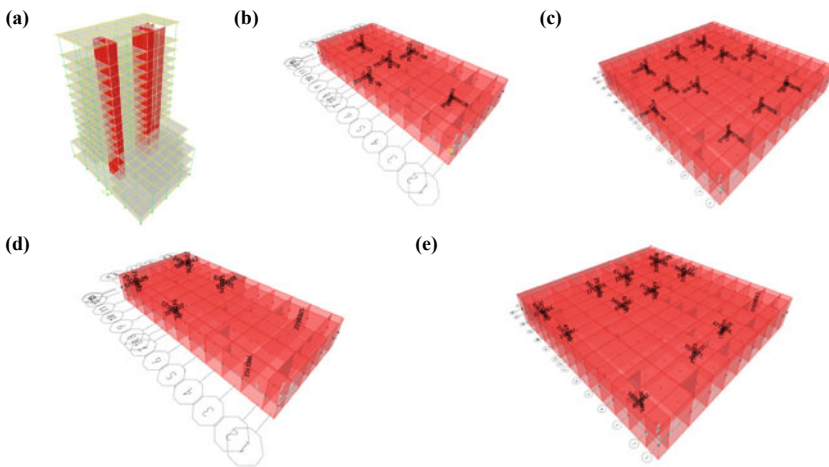


Fig. 2 Building model and loads from internal forces and loads from support reaction **a** 3D building model, **b** pile cap 1 (internal forces), **c** pile cap 2 (internal forces), **d** pile cap 1 (support reaction), **e** pile cap 2 (support reaction)

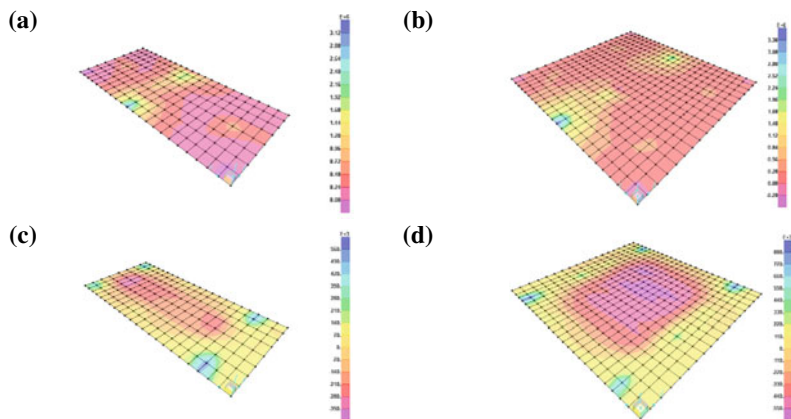


Fig. 3 Bending moment of loads from internal forces and loads from support reaction **a** pile cap 1 (internal forces), **b** pile cap 2 (internal forces), **c** pile cap 1 (support reaction), **d** pile cap 2 (support reaction)

4 Result and Discussion

Pile cap modeling as one because there are two groups of shear wall naming by pile cap with five-element pier 44 piles and pile cap with 11 element piers with 108 piles. Pile cap 1 (44 piles) without pile cap modeling partially in Tables 1, 2, and 3, and support reaction as a loads comparison, the value of support reaction correction as loads is 49.1% lower, the value of internal forces as loads is 49.1% lower, when support reaction correction as loads, the value of internal forces as loads is 3.86% higher, when support reaction as loads, the value is 57.91% lower, when support reaction correction as loads, the value of at support reaction 14.13% lower. When pile cap modeling partially and the stiffness of piles are considered in Tables 4

Table 1 Comparison loads of pile cap 1 (44 piles) without pile cap modeling partially (support reaction vs. support reaction correction)

Story name	Pier ID	P load ETABS support reaction (kN)	P load ETABS support reaction correction (kN)	Difference with support reaction (%)
Story1	P1	50,285	50,285	0.00
Story1	P2	50,569	50,569	0.00
Story1	P3	44,423	44,423	0.00
Story1	P4	45,517	45,517	0.00
Story1	P14	10,914	10,914	0.00
Total		201,708	201,708	-49.10
Story1	Other correction	0	102,854	-49.10
Total		201,708	98,854	-49.10

Table 2 Comparison loads of pile cap 1 (44 piles) without pile cap modeling partially (internal forces at internal forces location)

Story name	Pier ID	P load ETABS at internal forces Story 1 (kN)	Difference with support reaction (%)	Difference with support reaction correction (%)
Story1	P1	27,695	-44.92	
Story1	P2	25,393	-49.79	
Story1	P3	20,412	-54.05	
Story1	P4	19,090	-58.06	
Story1	P14	10,079	-7.65	
Total		102,669	-49.10	
Story1	Other correction	0	0.00	
Total		102,669	-49.10	3.86

Table 3 Comparison loads of pile cap 1 (44 piles) without pile cap modeling partially (support reaction at support reaction location)

Story name	Pier ID	P load ETABS at support reaction (kN)	Difference with support reaction (%)	Difference at support reaction correction (%)
Story1	P1	25,290	-49.71	
Story1	P2	26,857	-46.89	
Story1	P3	16,057	-63.85	
Story1	P4	9811	-78.45	
Story1	P14	6875	-37.01	
Total		84,890	-57.91	
Story1	Other correction	0		
Total		84,890	-57.91	-14.13

Table 4 Comparison support reaction of pile cap 1 (44 piles) with pile cap modeling with the stiffness of piles considered (with stiffness support reaction at support reaction location)

Story name	Pier ID	P load ETABS support reaction correction (kN)	P reaction ETABS support reaction from support reaction axial + moment stiffness = 169,600 (kN)	Difference with support reaction correction (%)
Story1	P1	50,285	25,290	
Story1	P2	50,569	26,857	
Story1	P3	44,423	16,057	
Story1	P4	45,517	6875	
Story1	P14	10,914	10,914	
Total		201,708	84,890	
Story1	Other correction	102,854	17,606	
Total		98,854	102,495	3.68

Table 5 Comparison support reaction of pile cap 1 (44 piles) with pile cap modeling with the stiffness of piles considered (with stiffness internal forces at internal forces location)

Story name	Pier ID	P load ETABS internal forces Story 1 axial + moment stiffness = 169,600 (kN)	P reaction ETABS support reaction from internal forces axial + moment stiffness = 169,600 (kN)	Difference with internal forces (%)
Story1	P1	27,695	12,811	-53.74
Story1	P2	25,393	6574	-74.11
Story1	P3	20,412	5722	-71.97
Story1	P4	19,090	4589	-75.96
Story1	P14	10,079	4205	-58.28
Total		102,669	33,901	-66.98
Story1	Other correction		17,322	16.87
Total		102,669	51,223	-50.11

and 5 and support reaction correction as a loads comparison, the value of support reaction from support reaction as loads is 57.91% lower, and when internal forces as loads comparison the value of support reaction from internal forces as loads is 66.98% lower. When the support as a restraint in Tables 6 and 7 and support reaction correction as loads comparison, the value of support reaction from support reaction as loads is 0.86% lower, and when internal forces as loads comparison the value of support reaction from internal forces as loads is 75.87% lower. For pile cap 2 (108 piles) without pile cap modeling partially in Tables 8, 9 and 10, and support reaction as loads comparison, the value of support reaction correction as loads is 56.11% lower, the value of internal forces as loads is 56.11% lower, when support reaction correction as loads, the value of internal forces as loads is 3.19% lower, when support reaction as loads, the value is 72.89% lower, when support reaction

Table 6 Comparison support reaction of pile cap 1 (44 piles) with pile cap modeling with restraint at support (with restraint support reaction at support reaction location)

Story name	Pier ID	P load ETABS support reaction correction (kN)	P reaction ETABS support reaction from support reaction axial and moment restraint (kN)	Difference with support reaction correction (%)
Story1	P1	50,285	49,652	
Story1	P2	50,569	51,935	
Story1	P3	44,423	42,863	
Story1	P4	45,517	45,662	
Story1	P14	10,914	11,098	
Total		201,708	201,209	
Story1	Other correction	102,854	-98,714	
Total		98,854	102,495	3.68

Table 7 Comparison support reaction of pile cap 1 (44 piles) with pile cap modeling with restraint at support (with restraint internal forces at internal forces location)

Story name	Pier ID	P load ETABS internal forces Story 1 axial and moment restraint (kN)	P reaction ETABS support reaction from internal forces axial + moment restraint (kN)	Difference % with internal forces (%)
Story1	P1	27,695	386	-98.61
Story1	P2	25,393	-3836	-115.11
Story1	P3	20,412	11,702	-42.67
Story1	P4	19,090	11,069	-42.01
Story1	P14	10,079	5449	-45.94
Total		102,669	24,771	-75.87
Story1	Other correction		17,322	16.87
Total		102,669	51,223	-50.11

Table 8 Comparison loads of pile cap 2 (108 piles) without pile cap modeling partially (support reaction vs. support reaction correction)

Story name	Pier ID	P load ETABS support reaction (kN)	P load ETABS support reaction correction (kN)	Difference with support reaction (%)
Story1	P5	66,543	66,543	
Story1	P6	55,937	55,937	0.00
Story1	P7	57,512	57,512	0.00
Story1	P8	51,382	51,382	0.00
Story1	P10	68,268	68,268	0.00
Story1	P11	45,831	45,831	0.00
Story1	P12	44,958	44,958	0.00
Story1	P13	13,586	13,586	0.00
Story1	P15	11,580	11,580	0.00
Story1	P16	39,215	39,215	0.00
Story1	P18	41,115	41,115	0.00
Total		495,930	495,930	-56.11
Story1	Other correction	0	271,080	-56.11
Total		495,930	224,851	-56.11

correction as loads, the value of at support reaction 40.20% lower. When pile cap modeling partially and the stiffness of piles considered in Tables 11 and 12 and support reaction correction as loads comparison, the value of support reaction from support reaction as loads is 2.51% higher, and when internal forces as loads comparison the value of support reaction from internal forces as loads is 69.93% lower. When the support as a restraint in Tables 13 and 14 and support reaction

Table 9 Comparison loads of pile cap 2 (108 piles) without pile cap modeling partially (internal forces at internal forces location)

Story name	Pier ID	P load ETABS at internal forces Story 1 (kN)	Difference with support reaction (%)	Difference with support reaction correction (%)
Story1	P5	41,105	-38.23	
Story1	P6	14,598	-73.90	
Story1	P7	18,594	-67.67	
Story1	P8	17,830	-65.30	
Story1	P10	42,577	-37.63	
Story1	P11	18,874	-58.82	
Story1	P12	16,186	-64.00	
Story1	P13	13,328	-1.90	
Story1	P15	11,407	-1.49	
Story1	P16	10,972	-72.02	
Story1	P18	12,205	-70.31	
Total		217,675	-56.11	
Story1	Other correction	0	0	
Total		217,675	-56.11	-3.19

Table 10 Comparison loads of pile cap 2 (108 piles) without pile cap modeling partially (support reaction at support reaction location)

Story name	Pier ID	P load ETABS at support reaction (kN)	Difference with support reaction (%)	Difference at support reaction correction (%)
Story1	P5	23,948	-64.01	
Story1	P6	19,113	-65.83	
Story1	P7	11,131	-80.65	
Story1	P8	8847	-82.78	
Story1	P10	23,073	-66.20	
Story1	P11	10,255	-77.63	
Story1	P12	8969	-80.05	
Story1	P13	8170	-39.87	
Story1	P15	7707	-33.45	
Story1	P16	6007	-84.68	
Story1	P18	7229	-82.42	
Total		134,450	-72.89	
Story1	Other correction	0		
Total		134,450	-72.89	-40.20

Table 11 Comparison support reaction of pile cap 2 (108 piles) with pile cap modeling with the stiffness of piles considered (with stiffness support reaction at support reaction location)

Story name	Pier ID	P load ETABS support reaction correction (kN)	P reaction ETABS support reaction from support reaction axial + moment stiffness = 169,600 (kN)	Difference with support reaction correction (%)
Story1	P5	66,543	23,948	
Story1	P6	55,937	19,113	
Story1	P7	57,512	11,131	
Story1	P8	51,382	8847	
Story1	P10	68,268	23,073	
Story1	P11	45,831	10,255	
Story1	P12	44,958	8969	
Story1	P13	13,586	8170	
Story1	P15	11,580	7707	
Story1	P16	39,215	6007	
Story1	P18	41,115	7229	
Total		495,930	134,450	
Story1	Other correction	271,080	96,055	
Total		224,851	230,505	2.51

Table 12 Comparison support reaction of pile cap 2 (108 piles) with pile cap modeling with the stiffness of piles considered (with stiffness internal forces at internal forces location)

Story name	Pier ID	P load ETABS internal forces Story 1 axial + moment stiffness = 169,600 (kN)	P reaction ETABS support reaction from internal forces axial + moment stiffness = 169,600 (kN)	Difference with internal forces (%)
Story1	P5	41,105	3936	-90.42
Story1	P6	14,598	5659	-61.23
Story1	P7	18,594	2533	-86.38
Story1	P8	17,830	1111	-93.77
Story1	P10	42,577	7255	-82.96
Story1	P11	18,874	2910	-84.58
Story1	P12	16,186	1898	-88.27
Story1	P13	13,328	2298	-82.76
Story1	P15	11,407	2303	-79.81
Story1	P16	10,972	1463	-86.66
Story1	P18	12,205	2481	-79.68
Total		217,675	33,848	-84.45
Story1	Other correction		31,602	14.49
Total		217,675	65,449	-69.93

Table 13 Comparison support reaction of pile cap 2 (108 piles) with pile cap modeling with restraint at support (with restraint support reaction at support reaction location)

Story name	Pier ID	P load ETABS support reaction correction (kN)	P reaction ETABS support reaction from support reaction axial and moment restraint (kN)	Difference with support reaction correction (%)
Story1	P5	66,543	66,375	
Story1	P6	55,937	56,524	
Story1	P7	57,512	57,689	
Story1	P8	51,382	51,436	
Story1	P10	68,268	69,847	
Story1	P11	45,831	46,179	
Story1	P12	44,958	45,193	
Story1	P13	13,586	13,792	
Story1	P15	11,580	11,867	
Story1	P16	39,215	39,341	
Story1	P18	41,115	41,334	
Total		495,930	499,577	
Story1	Other correction	271,080	269,072	
Total		224,851	230,505	2.51

Table 14 Comparison support reaction of pile cap 2 (108 piles) with pile cap modeling with restraint at support (with restraint internal forces at internal forces location)

Story name	Pier ID	P load ETABS internal forces Story 1 axial and moment restraint (kN)	P reaction ETABS support reaction from internal forces axial + moment restraint (kN)	Difference % with internal forces (%)
Story1	P5	41,105	2538	-93.83
Story1	P6	14,598	594	-95.93
Story1	P7	18,594	277	-98.51
Story1	P8	17,830	223	-98.75
Story1	P10	42,577	-1172	-102.75
Story1	P11	18,874	46,179	0.88
Story1	P12	16,186	16,354	1.04
Story1	P13	13,328	13,612	2.14
Story1	P15	11,407	11,588	1.58
Story1	P16	10,972	690	-93.71
Story1	P18	12,205	842	-93.10
Total		217,675	64,586	-70.33
Story1	Other correction		863	0.40
Total		217,675	65,449	-69.93

correction as loads comparison, the value of support reaction from support reaction as loads is 2.51% higher, the value of support reaction from internal forces as loads is 69.93% lower. The location of the higher bending moment shown in the picture is near the position of the loads.

5 Conclusion

The conclusions are:

1. Without modeling pile cap partially, the difference between support reaction as loads and support reaction correction as loads are 49.10% in pile cap 1 and 56.11% in pile cap 2, and the difference between support reaction correction as loads and internal forces shear wall in 1st floor as loads are 3.86% in pile cap 1 and 3.19% in pile cap 2.
2. With modeling pile cap partially in condition stiffness of piles is considered, the support reaction from support reaction correction compare with support reaction pile cap are 3.68% in pile cap 1 and 2.51% in pile cap 2, and the support reaction from internal forces as loads compare with support reaction pile cap are 50.11% in pile cap 1 and 69.93% in pile cap 2, 3. With modeling pile cap partially in condition restraint, the support reaction from support reaction correction compare with support reaction pile cap are 3.68% in pile cap 1 and 2.51% in pile cap 2, and the support reaction from internal forces as loads compare with support reaction pile cap are 50.11% in pile cap 1 and 69.93% in pile cap 2.

References

1. MacLeod IA (1970) Shear wall-frame interaction: a design aid. Portland Cement Association, Illinois
2. Mays TW (2015) Design guide for pile caps. Concrete Reinforcing Steel Institute, Illinois, p 156
3. Van De Graaf AV (2006) Structural design of reinforced concrete pile caps: the strut-and-tie method extended with the stringer-panel method. Graduation Report, TUDelft
4. Magade SB, Ingle RK (2020) Comparison of moments for pile-cap design. *Soil Mech Found Eng* 56(6):414–419. <https://doi.org/10.1007/s11204-020-09624-9>
5. Nageh M (2007) How to model and design high rise building using ETABS program. Scientific Book House for Publishing and Distributing, Cairo, Cairo
6. Atkins Structural Department (2007) Manual for analysis & design using ETABS. Atkins Dubai, Dubai
7. Computers and Structures Inc (2000) CSI ETABS: concrete shearwall design manual. Computers and Structures Inc., California

8. Wight JK, MacGregor JG (2012) Reinforced concrete: mechanics and design, 6th edn. Pearson Education Inc., New Jersey
9. American Concrete Institute (2011) Building code requirements for reinforced concrete (ACI 318-11). American Concrete Institute, Michigan
10. Badan Standarisasi Nasional (2012) Tata cara perencanaan ketahanan gempa untuk struktur bangunan gedung dan non gedung (SNI 1726:2012). Badan Standarisasi Nasional, Jakarta

Effect of Cement–Water Ratio on the Mechanical Properties of Reactive Powder Concrete with Marble Powder as Constituent Materials



Widodo Kushartomo, Henny Wiyanto, and Daniel Christianto

Abstract The main principle of developing reactive powder concrete is to improve the microstructure by compacting density and increasing toughness. To achieve this principle very high-grade cement is used together with pozzolanic materials. The research was conducted to study the effect of the water-cement ratio on the mechanical properties of reactive powder concrete with marble powder as constituent materials. Trial mixes were prepared using cement, sand, silica fume, marble powder, and super-plasticizer. A mix ratio of 1.0:1.1:0.2:0.1:0.03 was adopted with water-cement ratio of 0.18, 0.20, and 0.22. Concrete cylinder of size $\varnothing 10 \text{ cm} \times 20 \text{ cm}$ and the concrete beam of size $10 \text{ cm} \times 10 \text{ cm} \times 35 \text{ cm}$ were cast and cured in steam curing at $95 \text{ }^\circ\text{C}$ for 4 h and tested to study the compressive strength, modulus elasticity, splitting strength, and flexural strength in relation to the water-cement ratio. The results indicate that reduced water-cement ratio from 0.22 to 0.18 increases the compressive strength, modulus elasticity, splitting strength, and flexural strength. Using a lower water-cement ratio for the mixing process is difficult to handle, so this research recommended a 0.20 water-cement ratio to produce reactive powder concrete with optimum mechanical properties.

Keywords Concrete · Water-cement ratio · Mechanical properties · Strength · Marble powder

1 Introduction

The low water-cement ratio (w/c ratio) impacts concrete's high strength and durability, as shown in Fig. 1 [1], but a lower water-cement ratio resulted in difficulties in mixing and placing. Workability can be resolve by using admixture such as super-plasticizer.

W. Kushartomo (✉) · H. Wiyanto · D. Christianto
Department of Civil Engineering, Faculty of Engineering, Universitas Tarumanagara, Jakarta 11440, Indonesia
e-mail: widodo@untar.ac.id

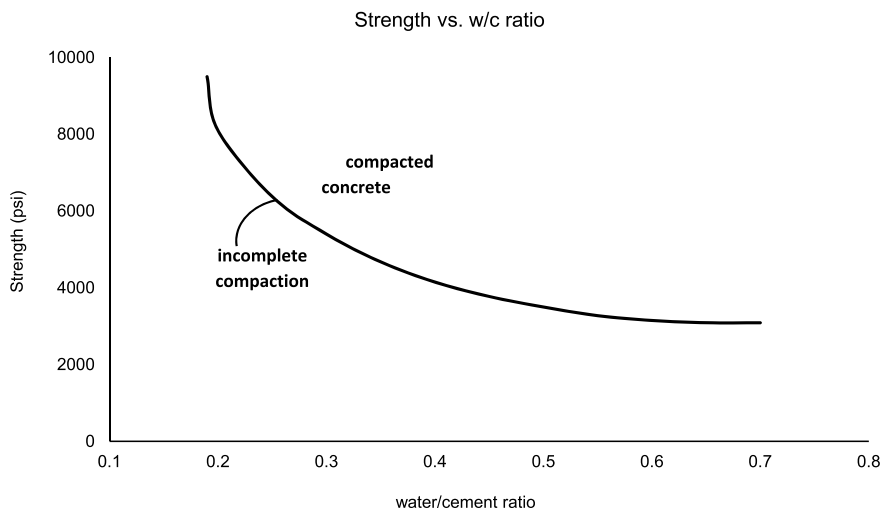


Fig. 1 Correlation water-cement ratio with compressive strength for normal concrete [1]

However, a mixture with a water-cement ratio between 0.18 and 0.22 will not mix well and is not plastic enough to be poured into the formwork. The presence of water is technically required for the hydration reaction to occur in cement. Water-cement ratios between 0.45 and 0.60 are more often used in regular concrete. For high-strength concrete, use a low water-cement ratio plus a plasticizer to increase workability. Excess water in a mixture causes segregation of the coarse aggregate to the cement paste. Water that is not used in the hydration reaction, when the concrete hardens, will leave a trail in the form of pores, whether the pores are open or closed. The pores that are formed will reduce the strength of concrete. A concrete mix with too much water can also cause shrinkage as the concrete dries and cracks concrete corners. The shrinkage in the end also reduces the strength of the concrete [1].

Reactive powder concrete (RPC) is categorized as ultra-high-performance concrete (UHPC). The term reactive powder means that all powder components in RPC can react chemically. However, the word concrete is preferred over mortar to describe UHPC by including steel fiber as one of its compositions. The use of steel fiber aims to increase its ductility. However, the RPC development does not include steel fiber as one of the development objects. The microstructural modification method is chosen as an effort to develop RPC with very high compressive strength, very high durability, and very high toughness. The principles of RPC development are as follows:

- Develop microstructure and eliminate coarse aggregate
- Enhance particle packing
- Increase toughness.

RPC's performance is associated with a low water-cement ratio, admixture, fineness of quartz sand, super-plasticizer, and small-sized steel fiber. Due to its excellent mechanical properties, RPC is exhibited in various applications in the construction field, such as bridge structures, high rise buildings, nuclear waste structures, marine structures, precast applications, and as an effective repair material [2].

To achieve the perfect density and homogeneity of the matrix to form pores as minimal as possible, the RPC must be related to the aggregate gradation between 150 and 600 μm . It is not recommended to use fine aggregate with a grain size below 150 μm to produce an optimum granular packing [2].

The function of marble powder is as a paste-aggregate interface filler, which significantly reduces the void of RPC, which will cause the pores to break and result in very low permeability, no cracks, and thus increase the strength. An improvement of the RPC microstructure can be made by increasing the curing temperature, which causes the C-S-H (Calcium Silicate Hydrate) chain to be longer due to the high hydration of the cement. The high curing temperature also causes an increasing pozzolanic activity from marble powder to reactive silica, thus encouraging the pozzolanic reaction and producing more CSH gel [1, 2].

The addition of marble powder to the RPC can increase the compressive strength by up to 20%. The amount of marble powder used in the manufacture of RPC should be 10–30% of the amount of cement.

RPC quality can be achieved if the ratio of the amount of water-cement ranges from 0.18 to 0.22. The low water-cement ratio will reduce porosity on RPC and increase the compact density. Increasing compact density has a positive impact on decreasing porosity in the mortar.

The primary purpose of the RPC mix design development process is to get the best mechanical properties. There are two basic parameters in achieving the best mechanical properties:

- Appropriate selection of RPC constituent materials
- Water-cement ratio.

Packing density for RPC can be achieved by adjusting all grain sizes used, such as fine aggregate, silica fume, and quartz powder. Temperature and maintenance pressure also significantly affect the mechanical properties of RPC. Steam maintenance at high temperature and pressure can accelerate the hydration reaction and force a chemical reaction to occur in all RPC ingredients.

This study aims to develop the mechanical properties of RPC with the water-cement ratio as an influencing component.

2 Methodology

The materials used in this investigation are cement, sand, silica fume, marble powder, and super-plasticizer, and water. Experimental Test Procedures Mix proportions of 1.0:1.1:0.25:0.1:0.03 were adopted with a water-cement ratio of 0.22, 0.20, and 0.18 was determined using cement, fine aggregates, silica fume, marble powder, and super-plasticizer, respectively as shown in Table 1. The cylinder $\varnothing 10 \text{ cm} \times 20 \text{ cm}$ and the beam of size $10 \text{ cm} \times 10 \text{ cm} \times 35 \text{ cm}$ molds of concrete were oiled to ease the de-molding process late. After 24 h of sitting time, the samples were de-molded and placed in a curing water tank for 7. After that, the samples were cast and cured in steam curing at $95 \text{ }^\circ\text{C}$ for 4 h. All samples were tested to study the compressive strength, splitting strength, and flexural strength in relation to the water-cement ratio at 28 age.

3 Result and Discussion

The mechanical properties of reactive powder concrete (RPC) as w/c ratio functions results are presented in Fig. 2. The strength value of mechanical properties RPC will be increased if the w/c ratio reduces. The highest value of mechanical properties reached the lowest w/c ratio, which corresponds to an improvement of microstructure, particle packing, and cementitious constituents.

3.1 Improvement of Microstructure

RPC's mechanical properties and durability are influenced by the bond between the cement paste and aggregate, known as the Interfacial Transition Zone (ITZ). Observing the microstructure in the ITZ area shows the pattern of micro cracks and

Table 1 Materials composition

Materials	ρ (kg/m ³)	w/c = 0.22		w/c = 0.20		w/c = 0.18	
		Ratio	Wight (kg)	Ratio	Wight (kg)	Ratio	Wight (kg)
Cement	3150.0	1.00	880.00	1.00	896.00	1.00	912.00
Water	1000.0	0.22	193.60	0.20	179.20	0.18	164.16
Micro silica	2200.0	0.25	220.00	0.25	224.00	0.25	228.00
Sand	2617.8	1.10	968.00	1.10	985.60	1.10	1003.20
Marble powder	2563.0	0.10	88.00	0.10	89.60	0.10	91.20
Superplasticizer	1150.0	0.03	26.40	0.03	26.88	0.03	27.36

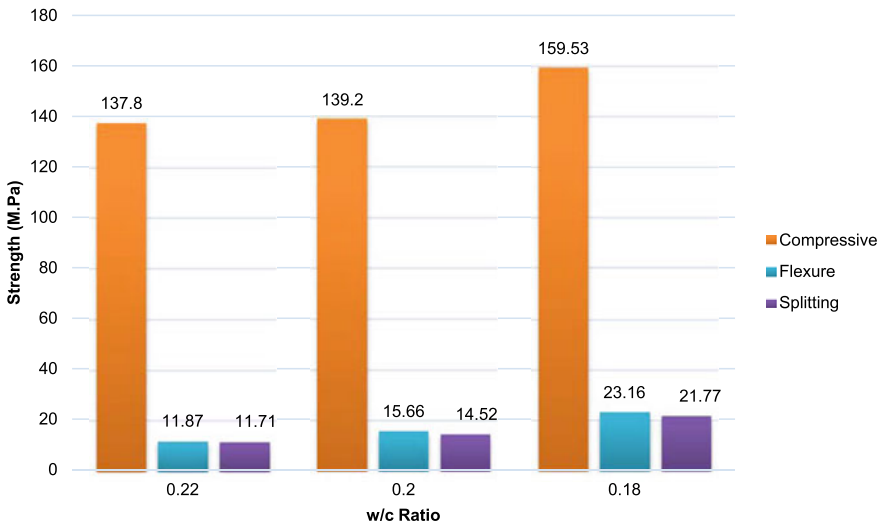


Fig. 2 Mechanical properties of RPC as w/c ratio functions

the occurrence of crack propagation. The stress–strain graph for aggregate, concrete, and cement paste is shown in Fig. 3 [2].

Figure 3 shows the elastic and brittle behavior of cement paste and aggregate, while concrete shows ductile behavior. This is related to the development of the rift in the ITZ area. RPC is designed by developing microstructures, such as compact density using pozzolanic materials and admixtures that increase its homogeneity. The addition of fine particles such as marble powder can increase the packing density, increasing the density in the ITZ region without noticeable pores, as shown in Fig. 4. The low water-cement ratio significantly impacts the decrease in porosity, as shown in Fig. 4.

As shown in Fig. 4, ettringite is formed between the material that is not entirely hydrated and the C-S-H gel. The main hydration products (C-S-H gel) were homogeneous, $\text{Ca}(\text{OH})_2$ was not found, and ettringite was formed [1, 2].

The microstructure of RPC depends on the conditions of heat treatment behavior. This is because the treatment temperature can change the microstructure of ITZ and the activity of pozzolanic materials.

The real improvement in improving the microstructure of RPC as well as distinguishing RPC from other classic high-performance concrete HPC is the removal of coarse aggregate and replacing it with quartz sand to increase bond strength within the matrix, increase homogeneity, reduce the effect of heterogeneity of microstructure which minimizes internal defects of the material such as voids and microcrack [2].

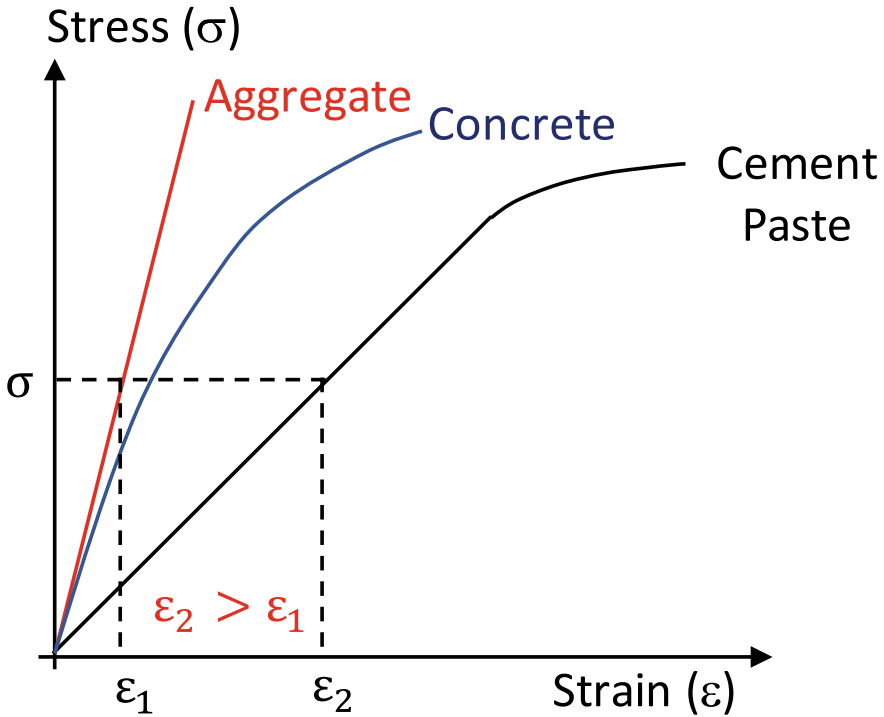


Fig. 3 Comparative stress–strain curves for aggregate, paste, and concrete [2]

3.2 Particle Packing

The primary purpose of applying the packing density model is to obtain high mechanical strength. This can be achieved by combining the appropriate size and proportion of small particles to reduce the voids formed. In this case, the performance of RPC is influenced by the size and percentage of pores formed, which affects the type and a density level of the constituent components. The finer particles fill the voids found between the cement and the aggregate particles. This causes efficient compaction of the voids between cement grains so that the overall performance of the concrete mix increases significantly [2–4].

The performance of RPC is enhanced by incorporating powder into the mix, which is the opposite of ordinary concrete which is highly affected by these fine materials. This powder creates a large surface area which requires high amounts of C-S-H gel. The high cement content in the RPC anticipates the formation of large C-S-H gels and increases the powder's surface area, thereby increasing the packing density [1, 2].

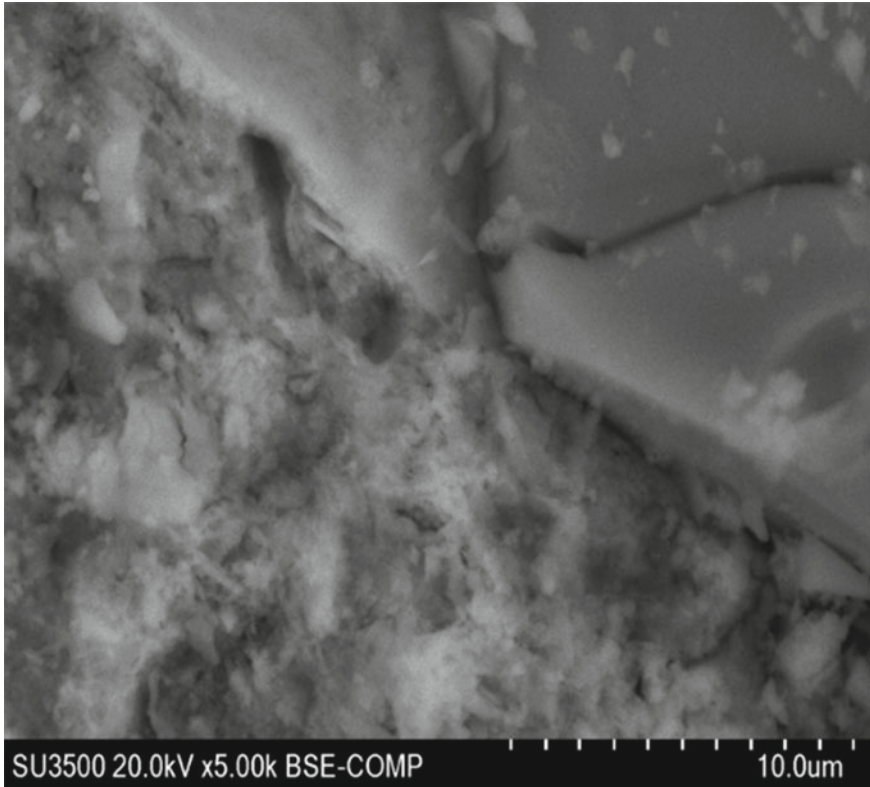


Fig. 4 Scanning electron microscope (SEM) of RPC, compacting interfacial transition zone with low w/c ratio

Ideally, the gradation curve and filling properties of powder materials such as cement, silica fume, quartz sand, and marble powder are the main concepts of the packing density approach, as shown in Fig. 5.

Some of the cement grains remain hydrated in the RPC mixture due to the low moisture content. Cement granules play a crucial role in the packing density of RPC because the grain size is between the sizes of silica fume and marble powder, thus helping in the process of filling pores [2, 4, 5].

The distance between the particles is filled with finer grains so that the density becomes better, as shown in Fig. 4. Using the principle of granular packing of cementations materials in RPC, capillary porosity in RPC is significantly reduced.

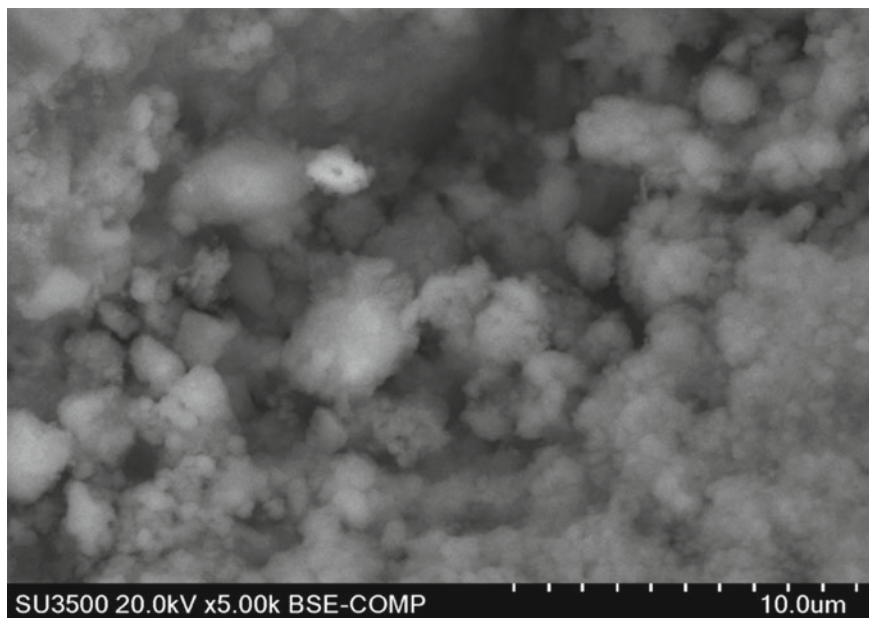


Fig. 5 Scanning electron microscope (SEM) of RPC, particle packing

3.3 *Cementitious Constituents*

The binder in RPC is divided into two materials, namely cement and pozzolan. The most used pozzolanic material is silica fume.

The cement and pozzolan used in the manufacture of RPC can be anything because there are no special requirements for the type of cement and pozzolan. The cement that is often used is cement with a low heat of hydration, considering that the quantity used is very high, namely type II cement. In the selection of cement, the cement grain size is also a consideration. Using cement with a high level of fineness will consume large amounts of water. The low water-cement ratio and the fine grain size of cement in RPC impact the mortar's performance factor, so caution is needed to use cement dosage. The dosage of cement commonly used in RPC ranges from about 700–1000 kg/m³ to achieve ultra-high strength with very low moisture content. High cement content is vital to increase the formation of C-S-H gel to cause the compaction of particles in fine grains. Incomplete hydration of cement in RPC causes a lot of free cement granules. These grains play an essential role in the granular packing in RPC [1, 2, 6].

The use of enormous amounts of cement in RPC has many disadvantages to the environment, cost, and concrete behavior when it hardens. A high temperature of hydration, shrinkage, and dimensional stability are problems that often arise in using a lot of cement. Mineral admixtures such as silica fume can be an excellent alternative to reduce the adverse effects of using high cement content in RPC.

Improvement of concrete performance through the packing density effect activates a pozzolanic reaction. It accelerates the cement hydration process, which increases the formation of calcium silicate hydrate (C–S–H) and its derivatives. In terms of mechanics and durability, the advantages obtained from combining steel fiber and pozzolanic materials in RPC are high tensile strength, high flexural strength, high compressive strength, low permeability, high resistance to chemical attack (acid, nitric, chloride, and sulfate), high abrasion resistance, toughness, excellent durability [1, 2, 4].

4 Conclusions

1. The mechanical properties of RPC are determined mainly by the water-cement ratio and the components used. The smaller the value of the water-cement ratio, the greater the value of the mechanical strength of the RPC. Likewise, the finer the grain of the components used, the higher the value of the RPC mechanical strength.
2. Improvement of microstructure, removing coarse aggregate, adjusting grain size are the basic principles in the manufacture of RPC to improve its mechanical properties.
3. RPC requires high cement content, and pozzolanic materials must be used to obtain the required reactivity.
4. The enhancement in compressive strength can reach when using marble powder.

References

1. Mindess S, Young JF (2002) Concrete. Prentice Hall, New Jersey
2. Mayhoub OA, Nasr ESAR, Ali YA, Kohail M (2021) The influence of ingredients on the properties of reactive powder concrete: a review. *Ain Shams Eng J* 12(1):145–158. <https://doi.org/10.1016/J.ASEJ.2020.07.016>
3. Kim YY, Lee KM, Bang JW, Kwon SJ (2014) Effect of W/C ratio on durability and porosity in cement mortar with constant cement amount. *Adv Mater Sci Eng* 2014. <https://doi.org/10.1155/2014/273460>
4. Apebo NS, Shiwua AJ (2013) Effect of water-cement ratio on the compressive strength of gravel—crushed over burnt bricks concrete. *Civ Environ Res* 3:74–81
5. Hiremath PN, Yaragal SC (2017) Effect of different curing regimes and durations on early strength development of reactive powder concrete. *Constr Build Mater* 154:72–87. <https://doi.org/10.1016/J.CONBUILDMAT.2017.07.181>
6. Al-Tikrite A, Hadi MNS (2017) Mechanical properties of reactive powder concrete containing industrial and waste steel fibres at different ratios under compression. *Constr Build Mater* 154:1024–1034. <https://doi.org/10.1016/J.CONBUILDMAT.2017.08.024>

Structural Analysis Using Matched Acceleration Time Histories



Windu Partono

Abstract The seismic design of buildings in Indonesia is usually calculated using response spectral acceleration (RSA) design. This seismic force model can be obtained based on the Indonesian seismic code. Another seismic force model that can be used for structural analysis can be developed using acceleration time histories (TH). The TH used for structural analysis should be matched with the RSA design. This paper describes the structural analysis of buildings using two different seismic force models, response spectra acceleration and acceleration time histories. The analysis was carried out at a sample building in Semarang. Two different soil investigations were carried out at the building area: soil boring and array microtremor. The purpose of the array microtremor investigation is to predict the bedrock position and soil profile from bedrock elevation up to the earth's surface. However, the purpose of the soil boring investigation is to obtain the site soil class. In terms of horizontal floor displacement and internal drift ratio, the performance of RSA design and matched TH (matched to RSA design) earthquake force models were almost equal, and no significant output differences were obtained using these two seismic force models.

Keywords Acceleration time histories • Bedrock • Microtremor • Response spectra design

1 Introduction

The structural analysis of buildings under seismic forces is usually performed using Response Spectral Acceleration (RSA) design, the seismic force model that was developed based on the Indonesian seismic code [1, 2]. Another seismic force model that can be used for structural analysis is acceleration time histories

W. Partono (✉)

Civil Engineering Department, Engineering Faculty, Diponegoro University, Semarang 50275, Indonesia

e-mail: windupartono@lecturer.undip.ac.id

(TH) [3–5]. This seismic force model can be obtained using TH data recorded from specific earthquake events or earthquake databases. For building design purposes, the TH collected from seismic events or earthquake databases cannot be directly used for building design. The TH should be matched with the RSA design calculated based on the Indonesian seismic code.

This paper describes the dynamic structural analysis of a building using two different seismic force models, response spectral acceleration and acceleration time histories. The building is located in Semarang, Indonesia. The TH used in this structural analysis was collected from a Shallow Crustal Fault (Semarang Fault) earthquake scenario located close to the building position. According to the 2017 Indonesian seismic map, the Semarang Fault is a reverse mechanism earthquake source and part of the Baribis-Kendeng seismic fault trace. Figure 1a shows the building position, site class distribution map developed by [6], and Semarang fault trace. Figure 1b shows the predicted bedrock elevation of Semarang, developed by [7] using a single station microtremor. The earthquake magnitude and epicenter distance used in this study were 6.5 Mw and ± 5 km, respectively. The earthquake source and magnitude used in this study were obtained from the 2017 Indonesian seismic map [8]. Due to the existing condition of the Semarang fault seismic source, no earthquake event had a magnitude 6.5 Mw and ± 5 km epicenter distance, so the TH used in the analysis was obtained from the Pacific Earthquake Engineering Research (PEER) ground motion database.

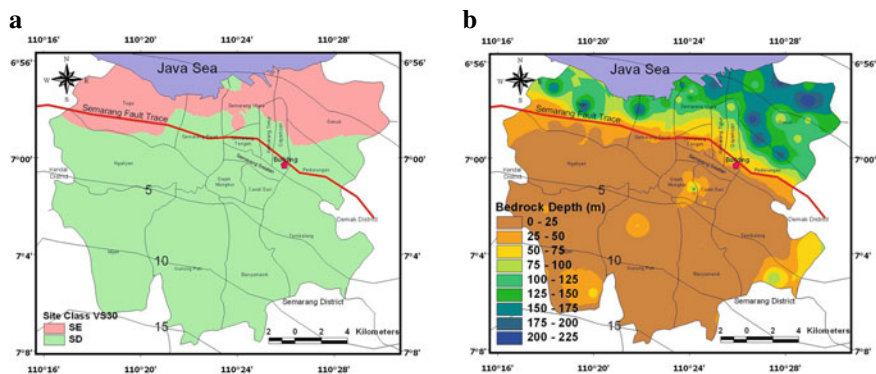


Fig. 1 a Building position, Semarang fault trace and predicted distance to Semarang fault, b predicted bedrock elevation

2 Methodology

Structural analysis of the building was carried out based on soil boring and array microtremor investigations, site-specific analysis, matching analysis, and dynamic structural analysis. The purpose of soil boring observation was to find the soil profile figure, in terms of N-SPT (Standard Penetration Test) and the site soil class. Three boring investigations were carried out in the study area. Figure 2a shows the N-SPT profile developed, based on the boring-log records. The second soil investigation carried out in the study area related to the bedrock elevation and soil profile, in terms of shear wave velocity profile (Vs) and predicted soil density (from bedrock up to the soil surface). Figure 2b shows the predicted soil profile, in terms of Vs values developed by a one array microtremor investigation. Figures 3a, b show the predicted shear wave velocity and soil density contours, obtained from one array microtremor investigation position. Based on the soil boring and array microtremor investigations, the study area is located in a medium soil class (SD). The soil profile model for site analysis was developed based on three soil boring and array microtremor investigations. Figure 3c shows the soil profile model used for site analysis. Figure 4 shows the structural analysis flowchart conducted in this study. The soil properties, such as soil density and shear wave velocity (Fig. 3c), were adjusted based on soil boring and microtremor investigation data. The shear wave of each soil layer in the top 30 m was calculated based on the average of three empirical correlations, proposed by [9–11]. The shear modulus (G) for each soil layer located in the top 30 m was developed based on the N-SPT and G empirical correlation [9, 10, 12].

Based on the soil boring and microtremor investigations, site analysis was conducted at the study area. The purpose of the site analysis is to calculate surface TH by conducting seismic wave or TH propagation analysis from bedrock up to surface elevation. The TH used for site analysis was first evaluated and adjusted

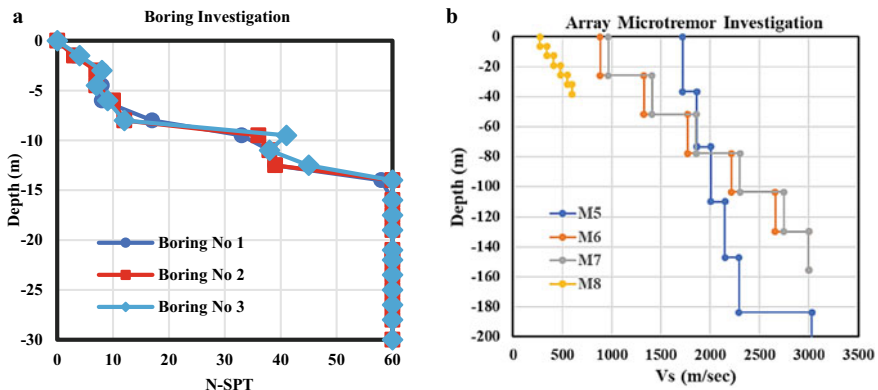


Fig. 2 a N-SPT profile, b Vs profile investigation results at the study area

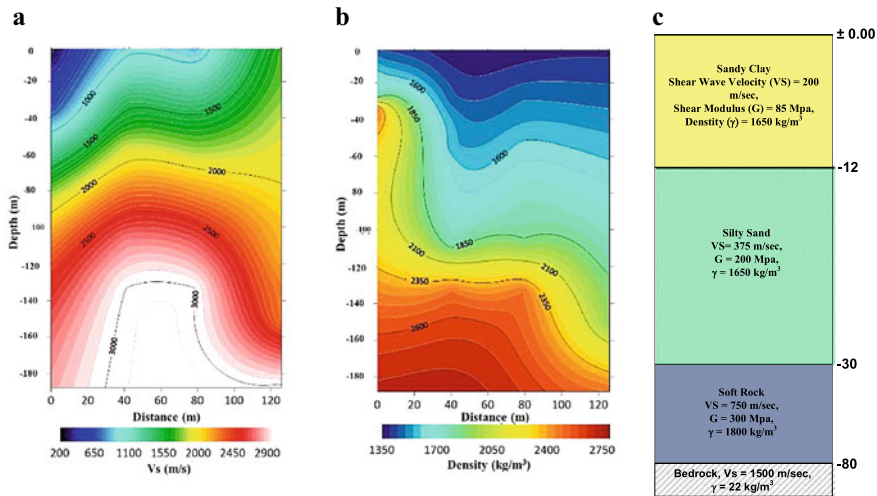


Fig. 3 a Shear wave velocity (V_s), b density contour at the study area, c soil profile model for site analysis

using spectral matching analysis. To perform spectral matching analysis at bedrock elevation, a scenario spectral target was calculated using deterministic seismic hazard analysis (DSHA) of a 6.5 Mw earthquake model, having an epicenter distance of ± 5 km. The spectral matching analysis was carried out because no real TH data can be used or investigated from the Semarang Fault earthquake event. The TH was collected from the San Simeon earthquake event (6.52 Mw and with an epicenter distance of 6.59 km) and applied as PEER time histories. Figure 5 shows the response spectral matching analysis results from two directions, NS (North–South) and EW (East–West) TH of the San Simeon TH.

The site analysis was carried out based on one-dimensional direction propagation analysis of matched (Original) TH at bedrock position. Figure 6 shows the two different results of site analyses conducted in two matched TH directions. These two TH are also popular as surface TH.

Two directions surface TH, obtained from site analysis, were then re-calculated using response spectral matching by conducting RSA design SNI 1726:2019 as a target spectral acceleration. The spectral acceleration design used for spectral matching was developed up to a maximum period of 5 s. The maximum period of RSA design was developed based on the natural period of the building. A comparative study in developing spectral matching analysis was conducted using bedrock (original) TH. No site analysis was carried out for the second model of TH. Figure 7 shows the RSA design developed, based on SNI 1726:2019, the modified/matched two RS4 (developed using surface time histories) and modified two RS2 (developed directly from bedrock/original TH). All modified RS2 and RS4 were calculated using response spectral matching. According to Fig. 7c, no significant

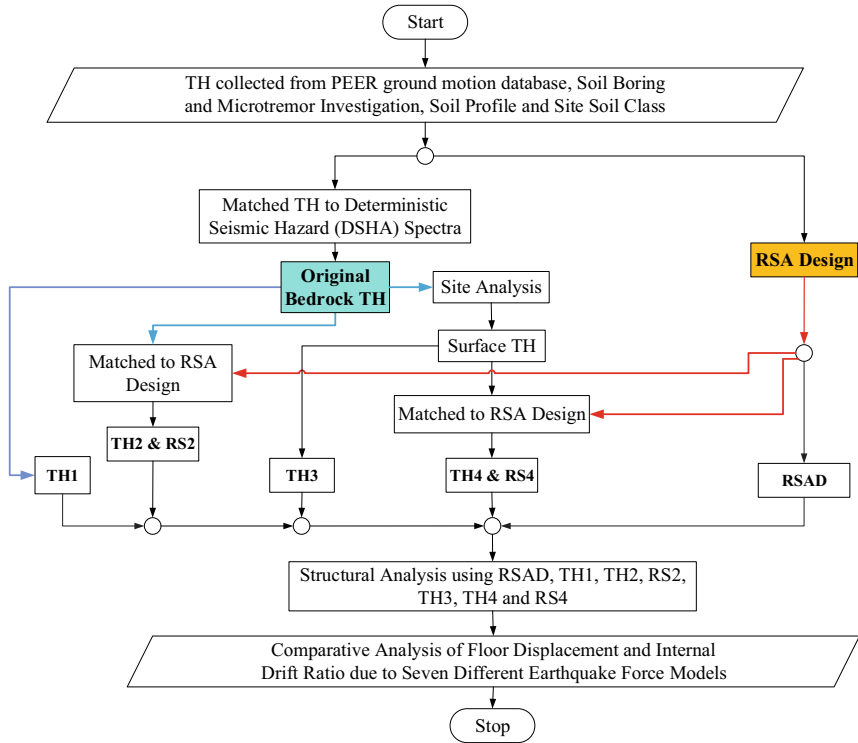


Fig. 4 Structural analysis flowchart

difference of matched response spectral acceleration was developed directly using surface TH and bedrock (original) TH.

Figures 8a, b show two TH developed using response spectral matching analysis of two direction surface TH (NS and EW) (TH4). These two surface TH (NS and EW) were obtained from site analysis. Figures 9a, b show two matched TH, developed using response spectral matching analysis of the bedrock (original) TH (TH2).

The dynamic structural analysis conducted in this study, related to the calculation of horizontal floor displacement and internal drift ratio. The results of structural analysis are not all described in this paper. The purpose of this analysis was to evaluate the performance of TH used for dynamic structural analysis. Seven different seismic force models were applied to the structure (see Fig. 4), such as RSA design (RSAD), bedrock/original TH (TH1), surface TH (TH3), matched spectral acceleration obtained from surface TH (RS4), matched spectra acceleration obtained from bedrock (original) TH (RS2), matched surface TH (TH4) and matched bedrock TH (TH2). All horizontal floor displacement and internal drift ratio results, calculated using these models of seismic forces, were then re-evaluated to

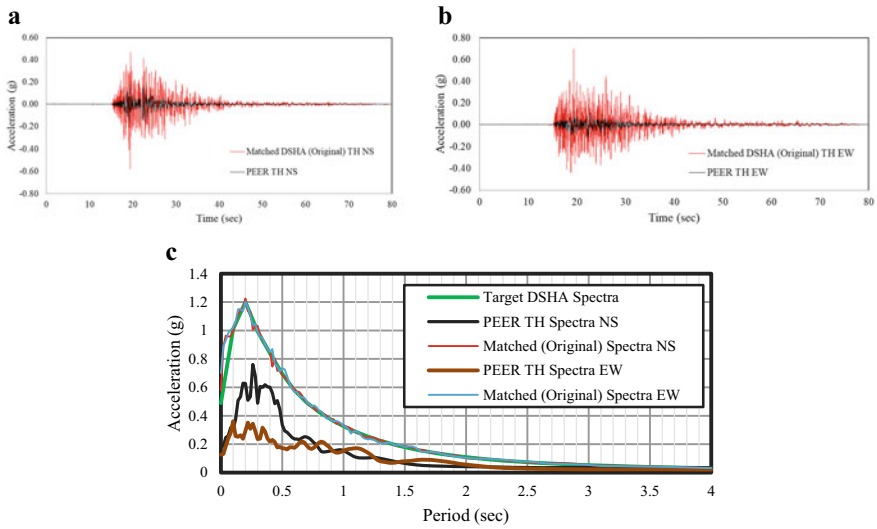


Fig. 5 **a** Response spectral matching of PEER for North–South TH direction, **b** East–West TH direction at bedrock elevation, **c** All response spectral matching analysis results

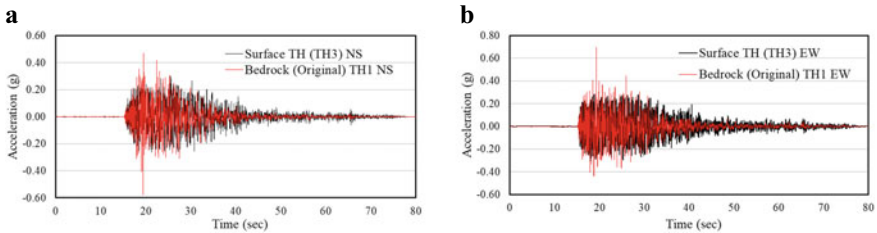


Fig. 6 Matched bedrock/original TH (TH1) and surface TH (TH3), **a** NS, **b** EW directions results developed from site analysis

observe the performance of matched response spectra and matched TH. A comparative analysis, in terms of horizontal floor displacement and internal drift ratio, between the RSAD, surface, and bedrock (original) TH was also carried out in this study. The purpose of the comparative study was to evaluate the performance of bedrock/original and surface time histories for dynamic structural analysis. Figure 10 shows the 3D and 2D structural model: 13 stories, $23.36 \times 34.75 \text{ m}^2$ plan, and 45.8 m height.

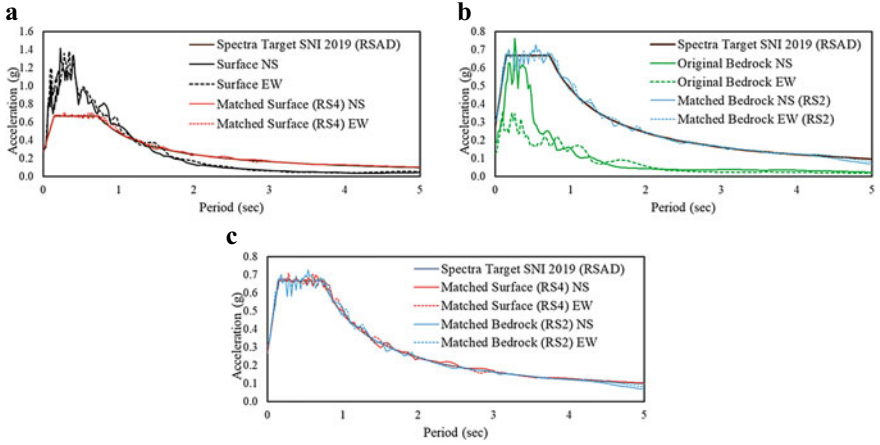


Fig. 7 **a** Response spectral accelerations developed from spectral matching to RSAD spectra target using surface TH (RS4), **b** matched bedrock/original TH (RS2), and **c** all matched response spectral acceleration

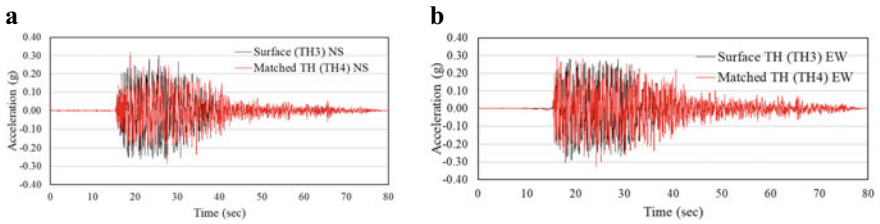


Fig. 8 Surface TH (TH3) and matched TH (TH4), **a** NS, and **b** EW directions

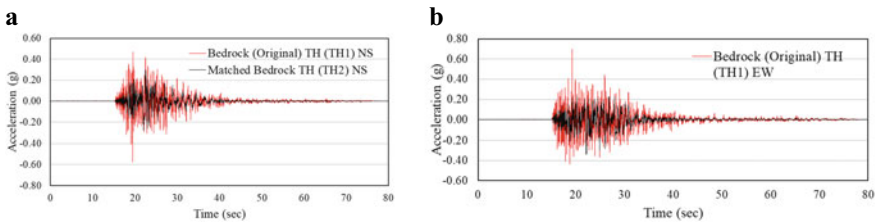


Fig. 9 Original TH (TH1) and matched TH (TH2), **a** NS, and **b** EW directions

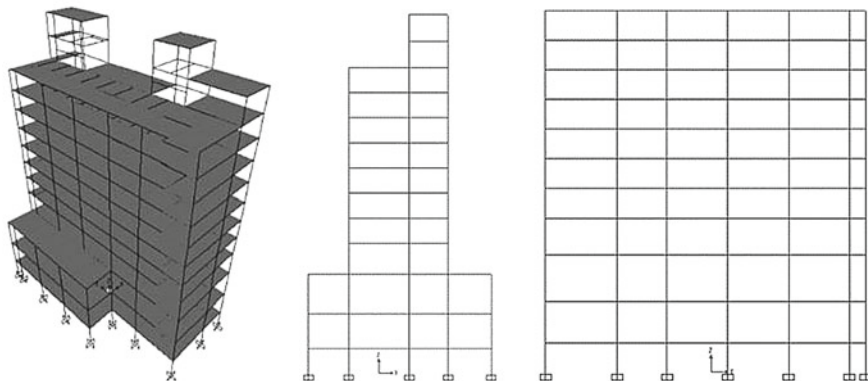


Fig. 10 Reinforced concrete structural model

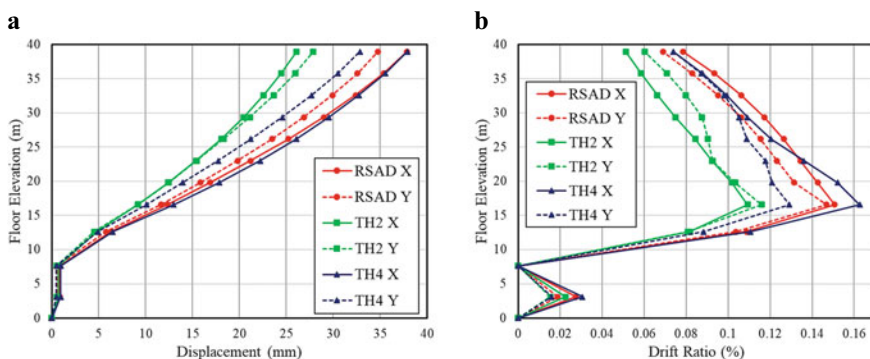


Fig. 11 a Horizontal floor displacement and b internal drift ratio due to RSAD, TH2, and TH4

3 Result and Discussions

The first structural analysis was carried out by conducting RSAD, TH2, and TH4. The structural analysis was carried out following the Indonesian Codes SNI 1726:2019 [1], SNI 2847:2019 [13], and SNI 1727:2013 [14]. Figure 11 shows the floor displacement and internal drift ratio performance of the structural model. Table 1 shows the absolute difference of floor displacement and drift ratio of RSDA compared to TH2 and TH4, respectively. The smaller the difference of displacement and drift ratio compared to the RSDA model, the better the performance of the model. As can be seen in Fig. 11 and Table 1, the performance of structural analysis, using matched surface TH (TH4), is better compared to the same analysis using matched bedrock (original) TH (TH2).

Figure 12 shows horizontal floor displacement, and internal drift ratio results performance due to RSAD, RS2, and RS4 earthquake force models. According to

Table 1 Maximum displacement and internal drift ratio due to RSAD, TH2, and TH4

	RSAD X	RSAD Y	TH2 X	TH2 Y	Absolute difference	TH4 X	TH4 Y	Absolute difference
Disp. (mm)	37.9	34.8	26.1	27.9	6.9–11.8	37.9	32.9	0–1.9
Drift ratio (%)	15.1	14.7	10.9	11.6	3.1–4.2	16.3	12.9	1.2–1.8

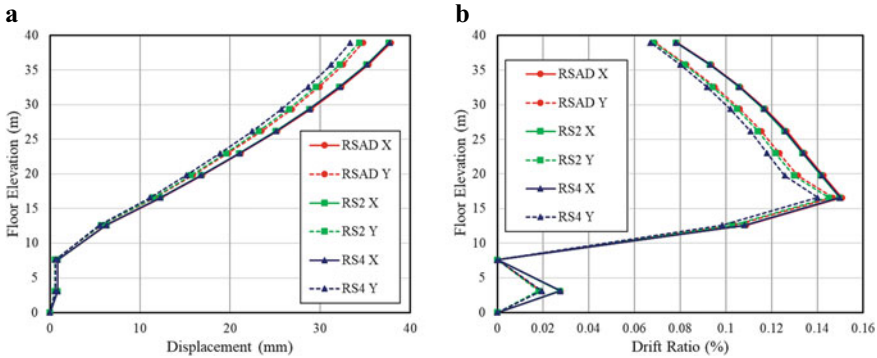


Fig. 12 a Horizontal floor displacement and b internal drift ratio due to RSAD, RS2, and RS4

Table 2 Maximum displacement and internal drift ratio due to RSAD, RS2, and RS4

	RSAD X	RSAD Y	RS2 X	RS2 Y	Absolute difference	RS4 X	RS4 Y	Absolute difference
Disp. (mm)	37.9	34.8	37.6	34.4	0.3–0.4	37.7	33.4	0.2–1.4
Drift ratio (%)	15.1	14.7	15.0	14.5	0.1–0.2	15.0	14.0	0.1–0.7

this figure, no significant differences in horizontal floor displacement and internal drift ratio were observed, using three different response spectral acceleration models. Table 2 shows the maximum absolute difference of floor displacement and drift ratio calculated using RSAD, RS2, and RS4 earthquake force models. Compared to the previous horizontal floor displacement and internal drift ratio calculation using TH2 and TH4, the performance of RS2 and RS4 earthquake models for structural analysis are better.

Figure 13 and Table 3 show the horizontal floor displacement and internal drift ratio results calculated using RSAD, bedrock (original) TH (TH1), and surface TH (TH3). According to Fig. 13 and Table 3, it seems that the differences of TH1 and TH3 to RSAD model are greater than TH2 and TH4. The surface and bedrock TH cannot be directly used for dynamic structural analysis.

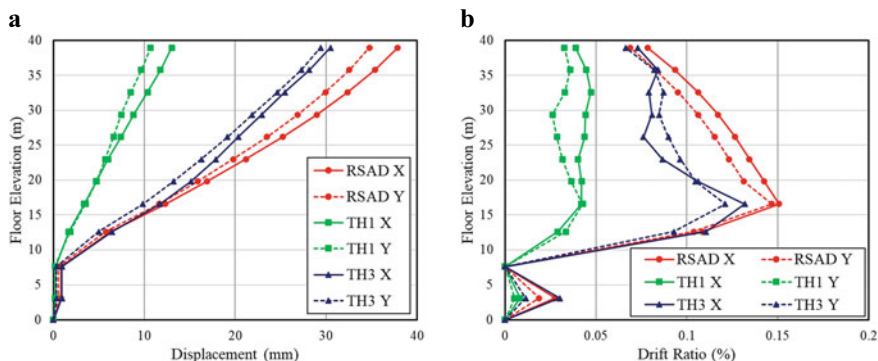


Fig. 13 a Horizontal floor displacement and b internal drift ratio due to RSAD, TH1, and TH3

Table 3 Maximum displacement and internal drift ratio due to RSAD, TH1, and TH3

	RSAD X	RSAD Y	TH1 X	TH1 Y	Absolute difference	TH3 X	TH3 Y	Absolute difference
Disp. (mm)	37.9	34.8	13.0	10.7	24.1–24.9	30.5	29.4	5.4–7.4
Drift ratio (%)	15.1	14.7	4.2	4.3	10.4–10.9	13.2	12.1	1.9–2.6

Based on the analysis conducted for the building model developed in this study, a better performance of TH used for dynamic structural analysis can be obtained for TH, developed using site analysis. The best performance of TH used for structural analysis was observed when the TH was developed using matched surface TH (TH4).

4 Conclusions

Dynamic structural analysis of buildings is usually performed using RSA design, the earthquake model calculated based on the Indonesian seismic code. The acceleration time histories (TH) collected from specific earthquake events or national/international ground motion databases can also be used as an alternative earthquake force model. For building design purposes, when TH is used as a model of earthquake force, the TH used in the structural analysis should be matched with the RSA design used at the building position.

The acceleration time histories used for building design can be obtained directly from matched bedrock (original) TH or matched surface TH, two different matched time histories developed using RSA design as a spectral acceleration target. The matched surface TH can be obtained using site analysis of bedrock (original) TH at the building location. In terms of horizontal floor displacement and internal drift

ratio calculation, the performance of matched surface TH is better, compared to matched bedrock TH.

Modified response spectral acceleration can also be developed using spectral matching analysis of bedrock (original) and surface time histories and conducting RSA design as a spectral acceleration target. In terms of horizontal floor displacement and internal drift ratio, no significant difference was obtained in the results when the dynamic structural analysis was calculated using RSA design and matched response spectral acceleration, as a model of seismic force.

The bedrock/original time histories (obtained from national/international ground motion databases or from specific earthquake events) or surface time histories developed from site analysis cannot be directly used for dynamic structural analysis design. Matched analysis to RSA design as a spectral acceleration target should be performed to get a better performance of structural analysis results.

Acknowledgements This paper was financially supported by the Faculty of Engineering, Diponegoro University, Semarang, Indonesia, through the Strategic Research Grant 2021.

References

1. National Standardisation Agency of Indonesia (2019) SNI 1726:2019, seismic resistance design codes for building and other structures. National Standardisation Agency of Indonesia, Jakarta
2. American Society of Civil Engineers (2017) ASCE/SEI 7–16. American Society of Civil Engineers, Virginia, Minimum design loads and associated criteria for buildings and other structures
3. Wong KKF, Harris JL (2010) Nonlinear modal analysis and superposition. In: The 9th U.S. national and 10th Canadian conference on earthquake engineering, Toronto, Ontario, Canada, 25–29 July 2010
4. Peng X, Teng Y, Lin C, Zhou Y (2015) Dynamic time-history analysis of steel frame composite steel plate shear wall structures. In: 4th international conference on sensors, measurement and intelligent materials (ICSMIM), 2015
5. Partono W, Irsyam M, Asrurifak M, Sari UC, Sumarsono (2020) Improvement of structural analysis by modification of site response analysis and earthquake force direction. *Int J GEOMATE* 75:115–121
6. Partono W, Asrurifak M, Tonnizam E, Kistiani F, Sari UC, Putra KCA (2021) Site soil classification interpretation based on standard penetration test and shear wave velocity data. *J Eng Technol Sci* 53(2):76–89
7. Partono W, Wardani SPR, Irsyam M, Maarif S (2016) Seismic microzonation of Semarang, Indonesia based on site response analysis using 30 m soil deposit model. *Jurnal Teknologi* 78 (8–5):31–38
8. Ministry of Public Works and Human Settlements (2017) National Center for earthquake studies, Indonesian seismic sources and seismic hazard maps. Centre for Research and Development of Housing and Resettlement, pp 1–377. ISBN 978-602-5489-01-3
9. Ohsaki Y, Iwasaki R (1973) On dynamics shear moduli and Poisson's ratio of soil deposits, soil and foundations. *JSSMFE* 13:59–73
10. Imai T, Tonouchi K (1982) Correlation of N-value with S-wave velocity and shear modulus. In: Second European symposium on penetration testing, Amsterdam, The Netherlands, pp 67–72

11. Ohta Y, Goto N (1928) Empirical shear wave velocity equations in terms of characteristic soil indexes. *Earthq Eng Struct Dyn* 6:167–187
12. Seed HB, Idriss IM, Arango I (1983) Evaluation of liquefaction potential using fields performance data. *J Geotechnic Eng Div ASCE* 109(3):458–482
13. National Standardization Agency of Indonesia (2019) Concrete design requirement for building structure, SNI 2847:2019. National Standardization Agency of Indonesia, Jakarta
14. National Standardization Agency of Indonesia (2013) Minimum design loads for building and other structures design, SNI 1727:2013. National Standardization Agency of Indonesia, Jakarta

Non-linear Analysis of Steel Shear Key at Epoxy Joint



Khairunnisa Masturoh, Nuraziz Handika, and Heru Purnomo

Abstract As a crucial part of a precast concrete segmental bridge system, connection joints should ensure shear force propagation due to the loading application from the bridge's deck to the section below. In this study, double L-shaped concrete blocks connected by a steel shear key with epoxy are numerically simulated using Midas FEA to represent the precast concrete segmental bridge connections. The L-shaped concrete blocks are loaded in two directions, vertical load, which represents the deck load, while horizontal load acts as a prestressed load. By applying horizontal load separately on the segmental precast, epoxy shear stress is increased by 4–8%, as well as 6–13% for concrete shear stress. The highest horizontal load application is 14.7 kN at K1P6E-NL specimen on 2-stage modeling. Overall from 3 specimens, the maximum force difference between numerical results and previous experiments is from 1 to 28%, while the maximum displacement reaches a difference of up to 40%. The experimental results show a continuous constant trend after the failure of the epoxy. This means that the upper L-shaped block has already touched the lower one. The numerical simulation results proved that the epoxy joint provides brittle failure.

Keywords Epoxy · Shear stress · Steel shear key · Shear key C capacity

K. Masturoh (✉) · N. Handika · H. Purnomo
Departement of Civil Engineering, Faculty of Engineering, Universitas Indonesia,
Kampus UI Depok, Depok 16424, Indonesia
e-mail: khairunnisa.masturoh@ui.ac.id

N. Handika
e-mail: nuraziz.handika@ui.ac.id

H. Purnomo
e-mail: heru.purnomo@ui.ac.id

1 Introduction

The precast concrete segmental bridge is one type of bridge that is commonly used in long-span (or medium-span) bridge structures. However, the connection between precast concrete segments needs to be considered. This connection is very important in transferring the forces from the bridge decks to the girder segments, which are then passed on by the column to the foundation. Each segment is joined by a shear key, which is either made of the concrete segment itself (with serrated form) or steel material. Shear capacity is the main parameter to be increased in the joint connection. Moreover, steel as a shear key material is considered promising as it has advantages in terms of strength, stiffness, and ductility, making it very suitable for use in structures that withstand certain loads.

Based on the characteristics of the joints, shear keys can be categorized into two types of joints. The first type is called dry joint, where the adjacent precast segments are not coated with any substance. The second type is called epoxy joints, where the two adjacent precast segments are coated by adhesive material, epoxy, with a thickness of 1 mm up to 3 mm [1]. Based on the results of experiments conducted by Buyukozturk, 1 mm thickness of epoxy gives the best results compared to 2 and 3 mm thickness of epoxy [2]. The dry joints are highly dependent on the friction force possessed by the joints between the two segments themselves. The transfer of shear is due to the operation of the shear forces in the potential crack area, which can be resisted by the frictional force from the normal compressive force along with the joint [3].

The failure that occurs in epoxy joints is in the form of brittle failure, where the load will suddenly drop after the load has increased constantly [2]. On the other hand, in epoxy joints, the epoxy played several important roles [4]:

- During assembly before hardening:
 - To lubricate the mating surface while final positioning took place.
 - To compensate for minor imperfections in the match-cast surface.
- In the finished structure after hardening:
 - To ensure the water-tightness of joints, especially in the top slab.
 - To participate in the structural resistance by transmitting compression and shear force.

In this study, a numerical analysis is carried out using the Midas FEA program to study the stress behavior of steel shear keys. To do so, numerical modeling is performed on a precast concrete segment which is described as two L-shaped concrete blocks. These two concrete blocks are joined by a steel shear key. One layer of epoxy is used at the joint interface of the concrete blocks, with pinned and roller boundaries as its boundary condition on the bottom and side of the concrete blocks. The loading applications (in the form of imposed displacement) are applied in the vertical direction. The constitutive law used for concrete is the Total Strain Crack Model (T-S Model) [5], and the Von Mises yield criterion [6] for steel shear key material.

2 Methodology

The non-linear analysis is carried out by creating a numerical model using Midas FEA (PKID: 09AQPQZGB7QLN8EP). The modeling results are then compared with the results of experiments of previous works [7]. Numerical modeling is done following the geometry of two L-shaped concrete blocks with a pair of shear key (male–female) connections and one layer of 1 mm epoxy adhesive on the two concrete blocks surfaces, forming an area of 150×150 mm. Detail of the shear key and the concrete blocks can be seen in Fig. 1.

As boundary condition, pinned support is set at the bottom side of the concrete block, and roller support is on the right side of the concrete block, as shown in Fig. 2. Vertical loading is set as incrementally imposed displacement whilst the horizontal load is given as a constant rate during the analysis, which represents the prestress load. Three horizontal load variations are given (see Table 1) at the point of horizontal load, as can be seen in Fig. 2.

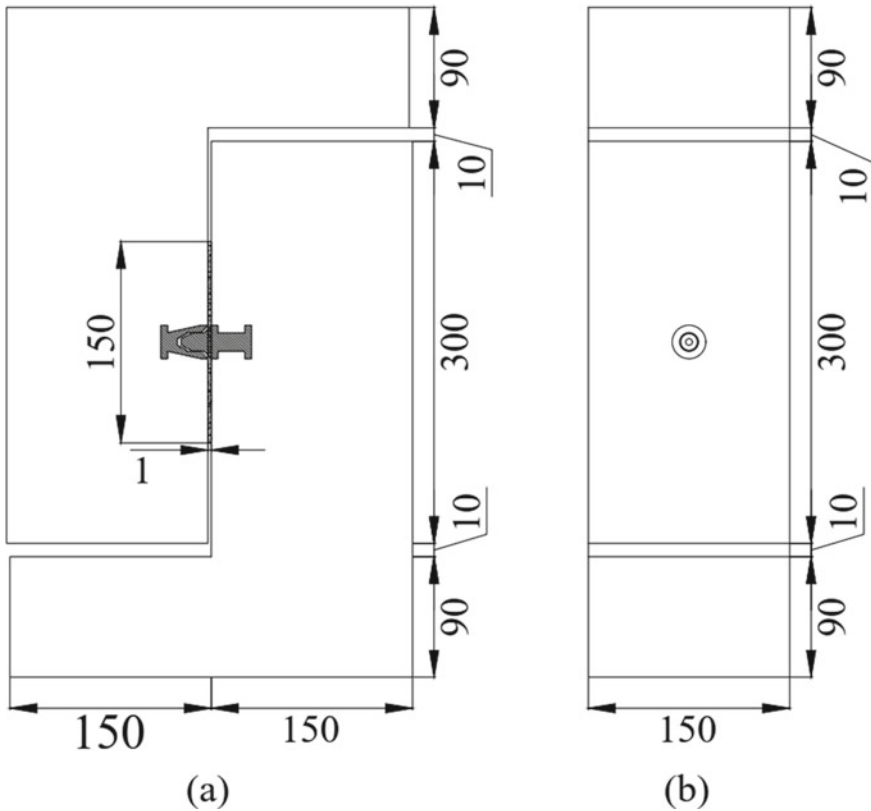
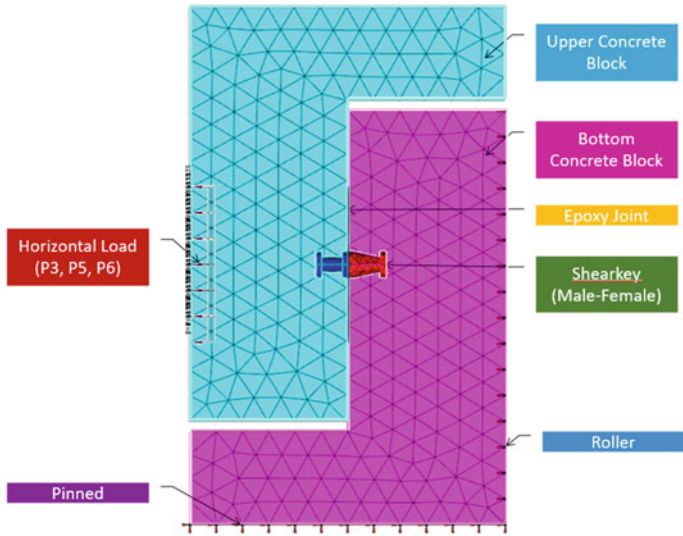


Fig. 1 Shear key geometry (unit: mm) **a** lateral-section of concrete blocks, **b** cross-section of concrete block

(a) **Model-1**



(b) **Model-2**

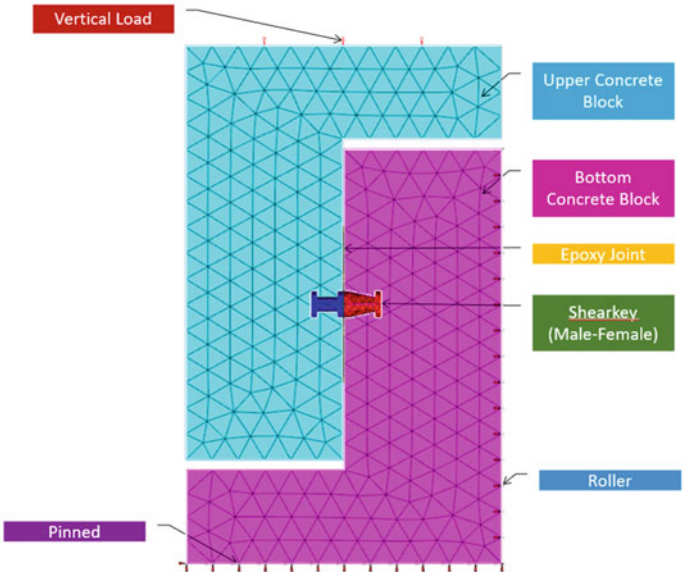


Fig. 2 Modeling in Midas FEA **a** Model-1, **b** Model-2

Table 1 Horizontal load application variation

Shearkey geometry	Code	Horizontal load (Kn)
K1	K1P3E-NL*	7.358
	K1P5E-NL*	11.036
	K1P6E-NL*	14.715

*Code E refers to model with epoxy joint; and NL refers to non-linear analysis

The geometry of the shear key and concrete block is modeled with a scale of 50% from its prototype [8] (see Fig. 1). The data of material used in this modeling is defined from the result of previous experiments [7] (see Table 2, Fig. 3), whilst the geometry of the L-shaped blocks and shear key in Midas FEA are as presented in Fig. 2.

The constitutive law of concrete used in this modeling is the Total Strain Crack Model (T-S Model) following [5]. T-S Model refers to the model from The Modified Compression Field, which was first proposed by Vecchio and Collins. This model is able to predict the load–displacement response in the plane as well as the shear stress [5]. Some advantages of the total strain crack model are that the crack distribution is easy to display and the crack unit does not separate at the crack position, the direction of the crack changes with the direction of the principal strain, and only the normal stress is generated on the surface of the crack, so the calculation process is simpler [8].

Furthermore, the constitutive law used for steel shear key material is the Von Mises yield criterion following [6]. This criterion, which is mostly used for ductile materials such as metals, defines a threshold where the yielding process begins. It is defined as the strain-energy density distortion at a certain point that is the same as the strain-energy density distortion when yielding at uniaxial tension, or uniaxial compression occurs [6]. The Von Mises yield criterion characterizes the condition that is equal to or greater than the threshold of yield limit as the yielded condition.

Table 2 Material properties [7]

Propeties	Units	Materials		
		Concrete	Epoxy	Steel
Tensile strength	MPa	3.3	9.53	–
Compressive strength	MPa	41.2	34.56	–
Elastic modulus	MPa	27,526.11	4476.807	129,259.26
Weight density	N/mm ³	2.353E–05	–	7.698E–05
Poisson’s ration	–	0.2	–	0.3
Shear strength	MPa	–	17.6	–
Shear modulus	MPa	–	2819.75	–
Yield stress	MPa	–	–	410
Tensile stress	MPa	–	–	645
Elongation	%	–	–	26.64

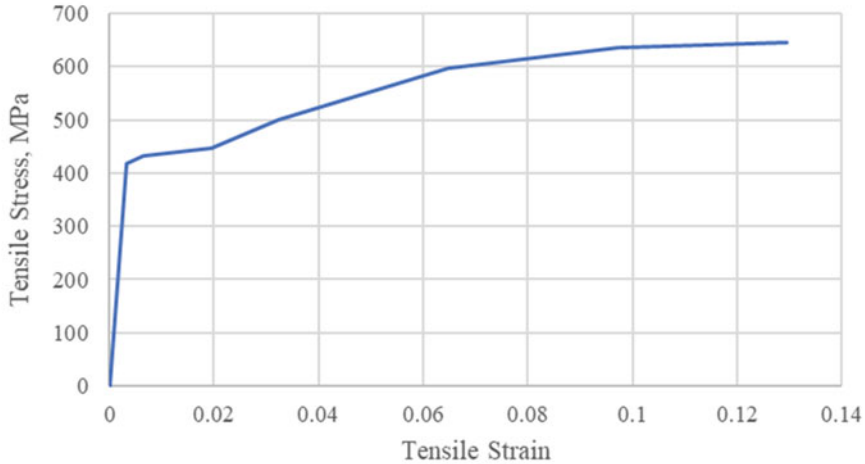


Fig. 3 Tensile stress–tensile strain curve for steel [7]

During the numerical simulation, Midas FEA has not been able to distinguish the two loading stages for the two directions of loading at the same time. Instead of being loaded constantly, the horizontal loading is given incrementally at the same moment as the vertical imposed-displacement load. The vertical load is intentionally given incrementally. Therefore, as an approximation regarding this condition, the numerical modeling is performed with two steps simultaneously; the two models are called Model-1 and Model-2 for the first and the second step, respectively.

In the first step, Model-1, linear static analysis is carried out by only providing horizontal loads and recording the stress changes that occur in the model. Then, these changes are applied and added to the calculated average stress that occurs to the shear stress-shear strain curve of the epoxy and to the concrete property material data. Thus, the modification of shear stress-shear strain is now obtained and can be used as input data for Model-2. In the second step, Model-2 with additional shear stress capacity from Model-1 as obtained previously is loaded in vertical imposed displacement. The results of the analysis of Model-2 are then compared with the experimental results [7].

3 Result and Discussion

3.1 Model-1

From the model-1 simulation results, the three horizontal load variations provide different average shear stress values in concrete and epoxy. Figure 4 shows the superimposed shear stress–strain stress curves. The black dash line in Fig. 4a, b

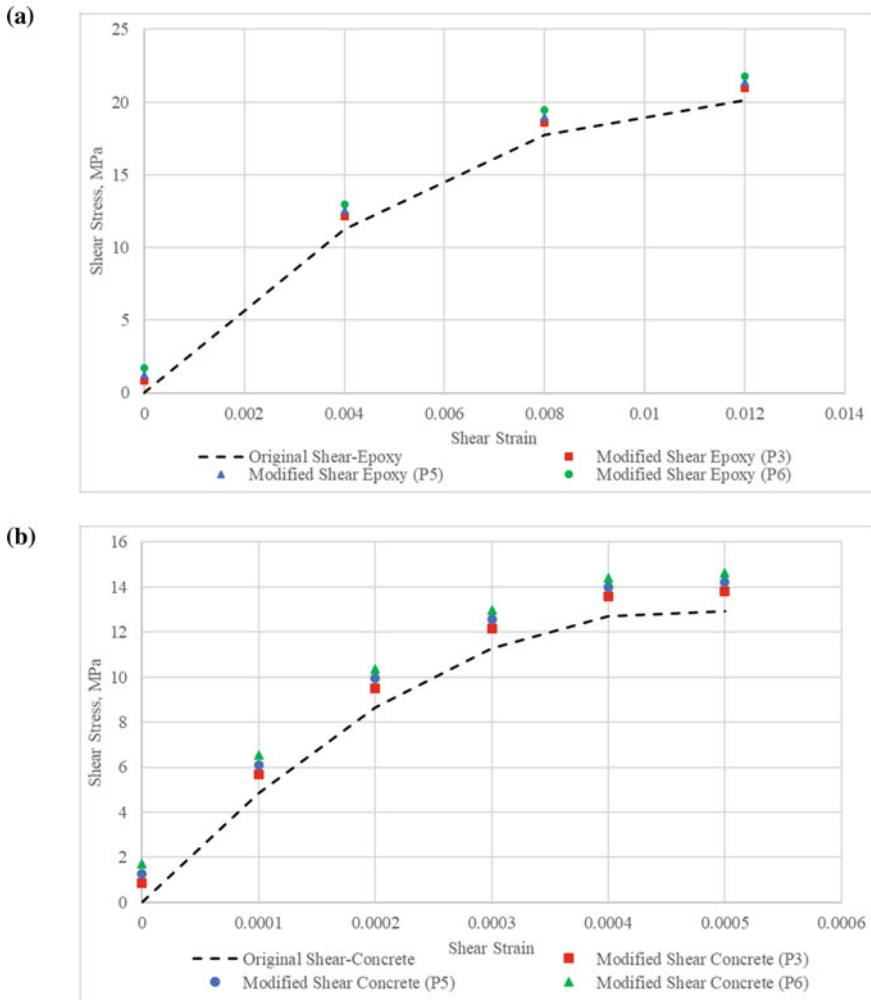


Fig. 4 a Shear stress–shear strain curve for epoxy, **b** shear stress–shear strain curve for concrete

shows the original condition. The dotted points represent the modified conditions, with red, blue, and green representing 7.358, 11.036, and 14.715 kN. There is a slight increase in the average shear stress resulting from the addition of horizontal loads. The increase of average shear stress values for horizontal loads P3, P5, and P6 respectively are 0.86 MPa, 1.28 MPa, and 1.70 MPa (both epoxy and concrete), with a difference of 4–8% for epoxy and 6–13% for concrete (see Fig. 4 and Table 3). It can be seen that the higher the prestress (horizontal) force exerted on the precast concrete segment, the higher the increase of the shear capacity of the epoxy joints shear key.

Table 3 Comparison of experiment versus numerical analysis results (Model-2)

Code	Max displacement (mm)		Percentage (%)	Max. force (kN)		Percentage (%)
	Experiment	Numeric		Experiment	Numeric	
K1P3E-NL	0.63	0.70	12	96.63	114.69	19
K1P5E-NL	0.34	0.48	40	77.01	98.30	28
K1P6E-NL	1.01	0.90	11	130.18	131.07	1

3.2 Model-2

For the numerical modeling of Model-2, using the additional shear capacity obtained from Model-1 and the same configuration of concrete L-shaped blocks and steel shear key, a vertical load is incrementally applied until the shear key joint collapses. Figure 5 shows the numerical modeling results (vertical load displacement) compared to the experimental results for the 3 cases of horizontal prestress forces.

Epoxy Steel Shear Key with Horizontal Load 7.358 kN The maximum vertical load obtained from the numerical modeling for the K1P3E-NL is 114.69 kN (see Fig. 5), with a 19% difference in the maximum load value between the numerical and experimental results. The displacement values that occur when the maximum load is reached are 0.70 mm (numerical analysis) and 0.63 mm (experimental),

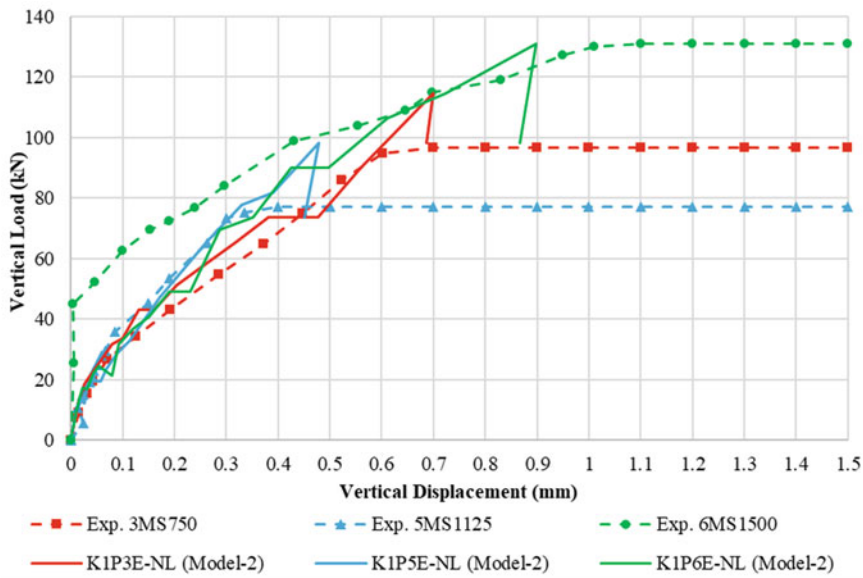


Fig. 5 Force–displacement curve, numerical modeling result using Midas FEA and experimental result [7]

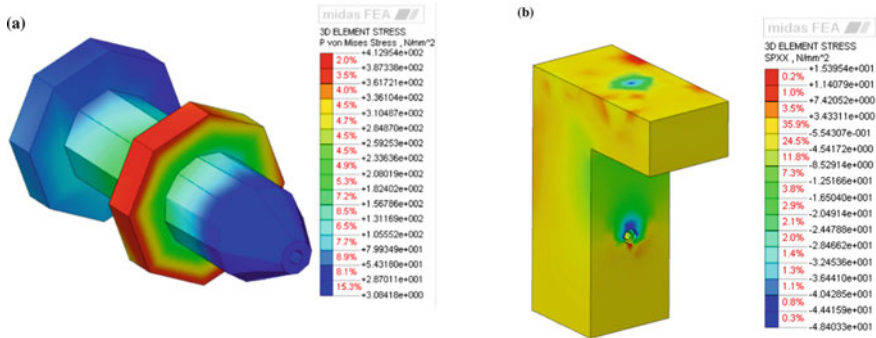


Fig. 6 3D Element stress for K1P3E-NL: male-shear key and concrete block **a** Von Mises stress on male-shear key, **b** SPXX on upper concrete block

with a difference of 12% (see Table 3). Experiment results are shown to continuously be constant after the failure of the epoxy [7]. It means that the upper L-shaped block already touched the lower one. In Fig. 6, Von Mises stress on the shear key (P Von Mises, in unit N/mm²), and primary stress in x-direction force (SPXX, in unit N/mm²) on the L-shaped concrete blocks are shown. Furthermore, Fig. 7 shows crack status. The cracking status indicates whether a tension cutoff limit has been exceeded at an integration point [9]. The types of crack status that appear in the output indicating the branch on the tension softening diagram (tensioning softening is not taken into the calculation).

The maximum Von Mises stress on the shear key is 412.9 MPa, while the compressive stress on the concrete block is 48.4 MPa. Figure 6 shows the stress on the concrete block, which is centered around the shear key. Meanwhile, on the shear key, the stress is centered on the outer radial of the shear key. When the load reaches 18.4 kN, the epoxy begins to crack (at shear stress occurs 0.846 MPa), until finally, the epoxy fails (at shear stress occurs 8.012 MPa) when the load reaches

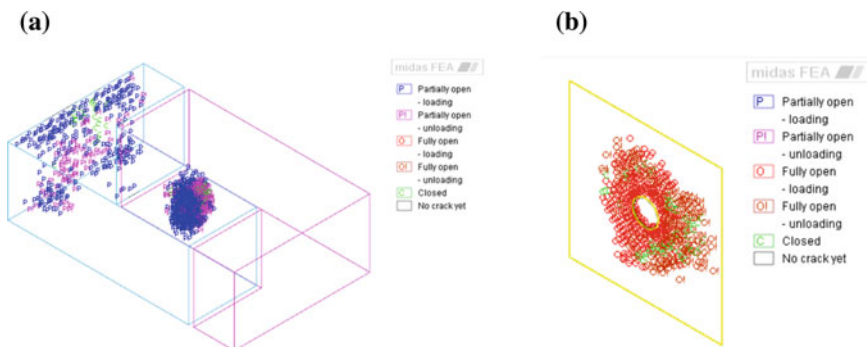


Fig. 7 Crack status for K1P3E-NL: concrete block and epoxy **a** status crack on concrete block at maximum load, **b** Status crack on epoxy at load 65.5 kN

65.5 kN. In that condition, the joint is only held by the shear key until it fails when the load reaches 114.69 kN. Based on Fig. 7, cracks occur on the shear key area and at the location of vertical load application.

Epoxy Steel Shear Key with Horizontal Load 11.036 kN The maximum vertical load obtained from numerical modeling for the K1P5E-NL is 98.30 kN (see Fig. 5), with a 28% difference in the maximum load value between the numerical and experimental results. The displacement values that occur when reaching the maximum load are 0.48 mm (numerical analysis) and 0.34 mm (experimental), with a difference of 40% (see Table 3).

The maximum Von Mises stress on the shear key is 406 MPa, while the compressive stress on the concrete block is 47.8 MPa. Figure 8 shows that stress on the concrete block is centered around the shear key. Meanwhile, on the shear key, stress is centered on the outer radial of the shear key. When the load reaches 14.08 kN, the epoxy begins to crack (at shear stress occurs 0.537 MPa), until finally, the epoxy fails (at shear stress occurs 9.21 MPa) when the load reaches 81.9 kN. In that condition, the joint is only held by the shear key until it fails when the load reaches 98.3 kN. Based on Fig. 9, cracks occur on the shear key area and at the location of vertical load application.

Epoxy Steel Shear Key with Horizontal Load 14.715 kN The maximum vertical load obtained from numerical modeling for the K1P6E-NL is 131.07 kN (see Fig. 5), with a 1% difference in the maximum load values between the numerical and experimental results. The displacement values that occur when reaching the maximum load are 0.9 mm (numerical analysis) and 1.01 mm (experimental), with a difference of 11% (see Table 3).

The maximum Von Mises stress on the shear key is 412.95 MPa, while the compressive stress on the concrete block is 45.3 MPa. Figure 10 shows that stress on the concrete block is centered around the shear key. Meanwhile, on the shear key, stress is centered on the outer radial of the shear key. When the load reaches

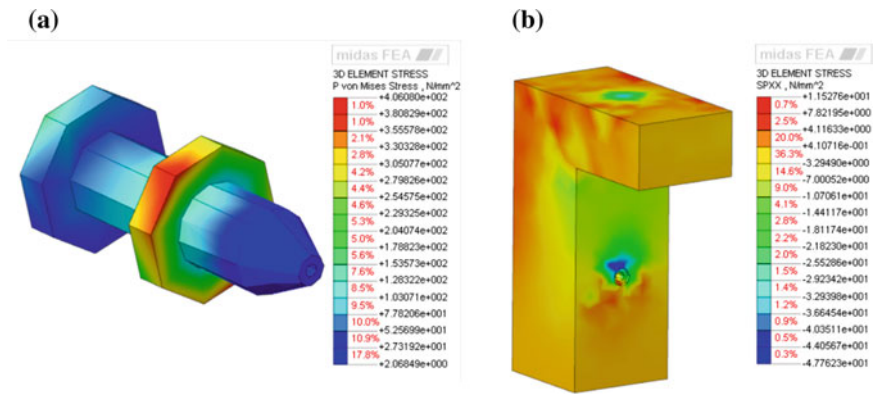


Fig. 8 3D Element stress for K1P5E-NL: male-shear key and concrete block **a** Von Mises stress on male-shear key, **b** SPXX on upper concrete block

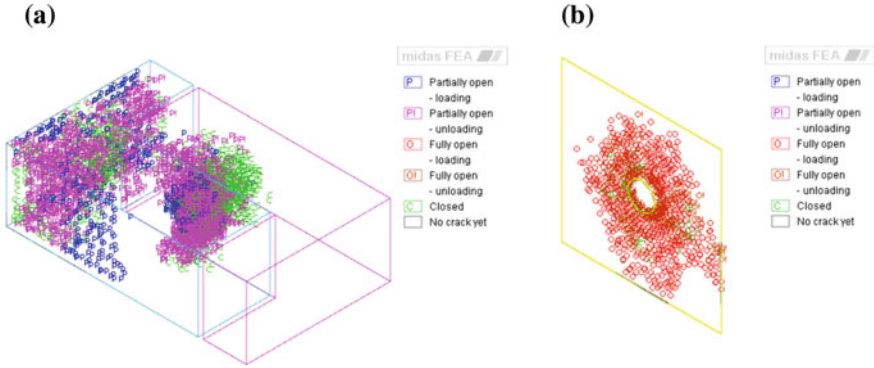


Fig. 9 Crack status for KIP5E-NL: concrete and epoxy **a** status crack on concrete block at maximum load, **b** status crack on epoxy at load 81.9 kN

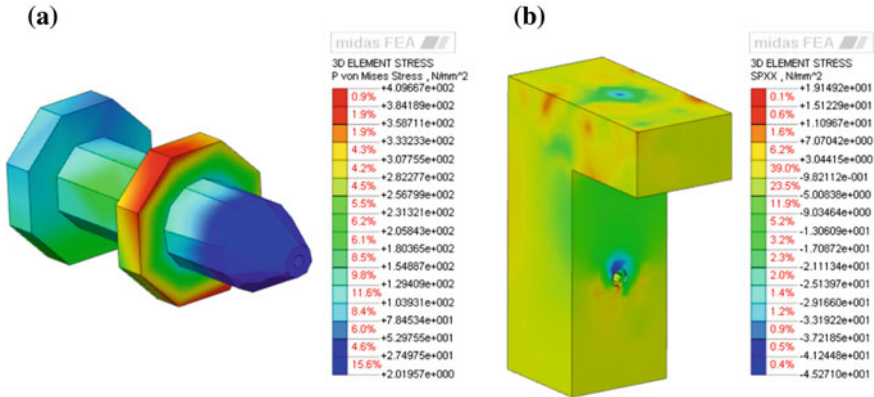


Fig. 10 3D element stress for KIP6E-NL: male-shear key and concrete block **a** Von Mises stress on male-shear key, **b** SPXX on upper concrete block

17.41 kN, the epoxy begins to crack (at shear stress occurs 0.766 MPa), until finally, the epoxy fails (at shear stress occurs 13.267 MPa) when the load reaches 90.1 kN. In that condition, the joint is only held by the shear key until it fails when the load reaches 131.07 kN. Based on Fig. 11, cracks occur on the shear key area and at the location of vertical load application.

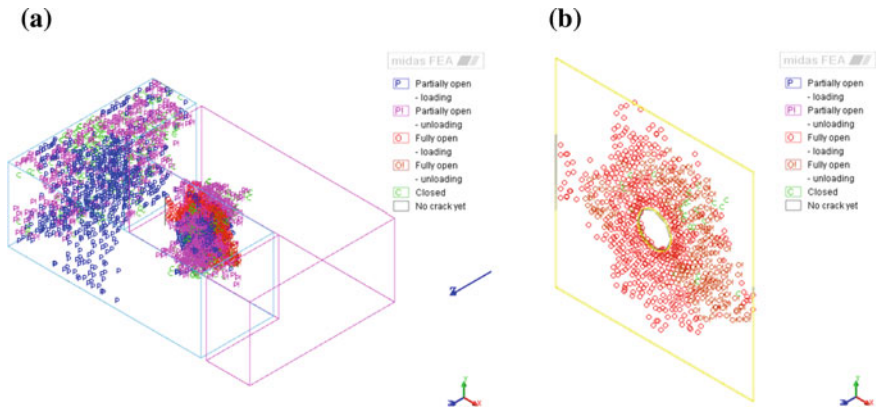


Fig. 11 Crack status for K1P6E-NL: concrete and epoxy **a** status crack on concrete block at maximum load, **b** status crack on epoxy at load 90.1 kN

4 Conclusion

Numerical modeling using Midas FEA with two loading directions can be performed separately and consecutively. The use of two separate models is an approximative approach. At stage 1 (Model-1), each horizontal load variation gives 4–8% epoxy shear stress escalation, as well as 6–13% escalation for concrete shear stress. The numerical results provide a significant difference with experimental results, with a difference of up to 28% (K1P3E-NL). In the K1P6E-NL model, the maximum force that can be held is 131.07 kN, which is 33 and 14% greater than the ones from K1P3E-NL and K1P4E-NL, respectively. This value is very similar to the experimental results of 130.18 kN, with a difference of only 1%. This shows that K1P6E-NL is the most optimum load to give the best results compared to the two other horizontal load cases on 2-stage modeling. Numerical simulation results proved that the epoxy joint provides brittle failure, where the load is held by the epoxy in the beginning, but once the epoxy has collapsed, the load will be held by the shear key, which will then experience a sudden drop in load and the connection will fail.

References

1. Cruzado HJ (1998) Assesment of a precast prestressed segmental concrete rail transit guideway design. Dissertation, Massachusetts Institute of Technology
2. Buyukozturk O, Bakhoum MM, Michael BS (1990) Shear behavior of joints in precast concrete segmental bridges. *J Struct Eng* 116(12):3380–3401

3. Koseki K, Breen JE (1983) Exploratory study of shear strength of joints for precast segmental bridges No. FHWA-TX-84-32+ 248-1 Intrm Rpt. The National Academies of Sciences, Engineering, and Medicine, Washington DC
4. Podolny W Jr, Muller JM (1982) Construction and design of prestressed concrete segmental bridges. A Wiley-Interscience Publication, USA
5. Vecchio FJ, Collins MP (1986) The modified compression field theory for reinforced concrete elements subjected to shear ACI J 83(22):219-231
6. Boresi AP, Schmidt RJ (2003) Advanced mechanics of materials, 6th edn. Wiley, USA
7. Tjiknang F (2017) Study of mild steel shear key behaviour with 50% reduction scale on segmental precast bridge subjected to vertical load. Universitas Indonesia
8. Purnomo H, Nursani R, Mentari S, Rahim SA, Tjahjono E (2017) Numerical evaluation of the shear behavior of a metal shear key used in joining precast concrete segmental bridge girders without epoxy. Int J Technol 8(6):1050-1059
9. Midas (n.d) Midas IT analysis and algorithm. <https://globalsupport.midasuser.com/helpdesk>. Accessed 16 April 2021

On-Field Testing of the Monolith Joint of the Full Slab on a Slab-on-Pile Bridge



Ahmad Zaki Risadi, Josia Irwan Rastandi,
Bastian Okto Bangkit Sentosa, and Nuraziz Handika

Abstract Indonesia's acceleration of infrastructure development brings about issues regarding land availability, suboptimal soil conditions, and the need for faster constructions, which are resolved by using slab-on-pile bridges for bridge constructions. However, the lack of beam elements in slab-on-pile bridges makes the monitoring of slab joint deflections more significant. Static and dynamic load tests are necessary to make sure the joint performs as well as designed. The tests were conducted using weighted trucks to induce the static and forced vibration. The data is compared to numerical analysis results. The results show that the occurring deflections are significantly smaller than the numerical results. The natural frequencies of the structure (16.05–18.75 Hz) is higher than the numerical analysis natural frequency (11.84 Hz). The maximum tensile strains of the structure (241.329 and 19.058 microstrains) are lower than the numerical analysis tensile strain (329.9 microstrains). This is due to the numerical analysis not factoring the extra stiffness due to prestressing, causing the structure to perform better than designed. The deflections of adjacent slab elements are almost identical, suggesting that the joint performs well and allows the slabs to behave as one unity. The dynamic amplification factor is calculated to be 1.325–1.563.

Keywords Slab-on-pile bridge · Static loading test · Dynamic loading test · Forced vibration

A. Z. Risadi (✉) · J. I. Rastandi · B. O. B. Sentosa · N. Handika
Department of Civil and Environmental Engineering, Faculty of Engineering, Universitas
Indonesia, Depok 16424, Indonesia
e-mail: ahmad.zaki91@ui.ac.id

J. I. Rastandi
e-mail: jrastandi@eng.ui.ac.id

B. O. B. Sentosa
e-mail: bastian.sentosa@ui.ac.id

N. Handika
e-mail: nhandika@ui.ac.id

1 Introduction

In recent years, Indonesia has implemented policies to accelerate the development of infrastructures. Due to this condition, several issues revolving around bridge constructions have emerged, namely lack of land availability, suboptimal soil conditions, and the need for faster constructions. Slab-on-pile bridges serve as an alternative for resolving the previously mentioned issues [1].

A slab-on-pile bridge structure is a bridge that does not require a beam element. Slab-on-pile bridges, also known as slab bridges, consist of a plate element that is placed on pile caps, which are held up by singular piles, not pile groups. A Slab-on-pile bridge is an attractive alternative due to its simplicity in construction as well as requiring lower cost to construct [2].

However, due to the nature of the slab-on-pile bridge structure that does not have a beam element, there is no structural element that provides support to reduce the deflection of the slabs. Therefore, the deflection on the slabs needs to be specially monitored so that it does not exceed the code limits. Section 9.2.1 of Indonesia Nasional Standard RSNI T-12-2004 [3] states that the serviceability limit state for midspan deflection is $L/800$.

To make up for the absence of beam elements, the slabs on slab-on-pile bridges are given prestressing tendons to provide more stiffness and vertical support. However, since the prestressing provide support to deflections only in the x-direction, the connection of the slabs in the y-direction becomes more significant. Therefore, the connections must perform as well as they are designed.

This study aims to evaluate the performance of a joint on a full slab element of a slab-on-pile bridge structure. Static and dynamic load tests were conducted using weighted trucks to induce the static and forced vibration loading on the structure. A static load test was conducted to measure the structure's deflections and strains, while a dynamic loading test was conducted to determine the natural frequency of the structure. The data is then compared to numerical analysis results, which are obtained through numerical modeling.

2 Structural Data

The structure that is to be modeled is a slab-on-pile bridge with six spans, each of which is 7.5 m in length. The width of the bridge is 32.4 m long, supported by eight piles with a distance of 4.3 m from one another. The cross-sectional view of the bridge can be seen in Fig. 1. The data of the materials used in the structure are as described in Table 1.

The slabs are connected with a 42 MPa non-shrink concrete. The non-shrink concrete ties the slabs with an anchor. The non-shrink concrete has a width of 1000 mm and is placed on a pile cap.

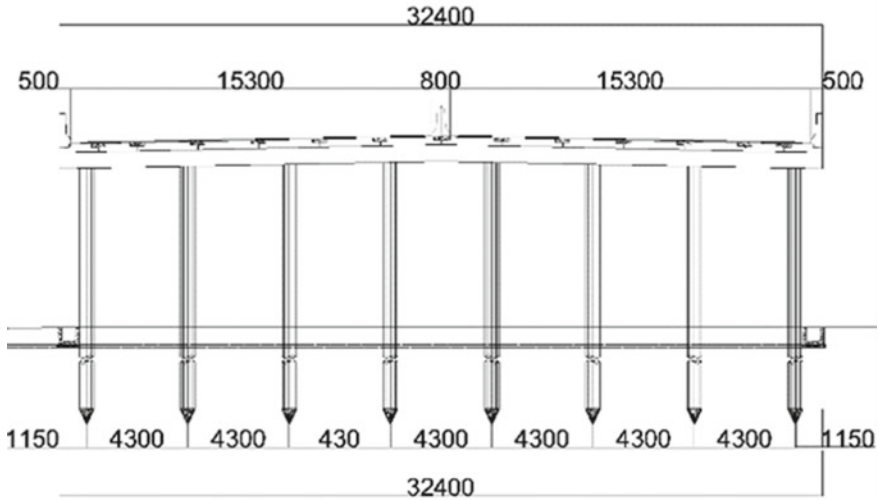


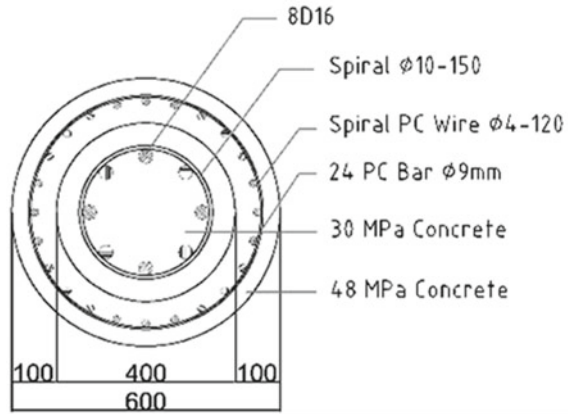
Fig. 1 A sectional view of the bridge structure

Table 1 Material data, as tested by the consultant prior to the conduct of the field tests

	Value	Unit
Full slab concrete grade (f_c')	42	MPa
Pile cap concrete grade (f_c')	30	MPa
Steel rebar grade (f_y)	400	MPa
Full slab prestress strand size	12.7	mm
Full slab prestress standard	JIS-3536 or ASTM A-416	
F_{ci} (at strand release)	30	MPa
Jacking force	77.5%	UTS
Spun pile prestressed concrete grade (f_c')	48	MPa
Spun pile prestressed concrete bars standard	JIS G 3137-2008 Grade 1 Class 1 SBPD 1275/1420	
Spun pile M_{crack}	25	T.m
Spun pile M_{ult}	45	T.m
Spun pile $P_{allowable}$	120	Ton

The foundation of the structure is a spun pile foundation with a diameter of 600 mm and a wall thickness of 100 mm. The hollow pipe is supported with 24 prestressed concrete (PC) bars of 9 mm diameter. The PC bars are tied with a spiral PC wire of 4 mm diameter with 120 mm spacing. The inner part of the spun pile foundation is filled with 30 MPa concrete and supported with a longitudinal reinforcement of 8D16, tied with \varnothing 10-150 spiral ties. The cross-sectional view of the spun pile foundation is as illustrated in Fig. 2.

Fig. 2 Cross-sectional view of the foundation



Pile caps are placed on top of the piles to support the slabs. There are two pile caps: inner pile caps (continuous pile caps) and outer pile caps (expansion joint pile caps). The expansion joint pile cap is placed where two sections of the bridge meet. One side of the pile cap is made fixed while the other is made rolling. The expansion joint pile cap has a size of 1100 × 700 mm. The continuous pile cap is placed where slabs of the same section of the bridge meet. This pile cap has a size of 1400 × 600 mm.

3 Static Loading Test

Table 2 shows the amount of equipment used for the static loading test. Vibrating wire strain gauges (VWSG) from Geokon were used. This device measures the strain that occurs during loading. The VWSG Datalogger records the data from the VWSG devices. Dial gauges were also used. The dial gauges measured the displacement that occurs on the expansion joints. Lastly, OU Displacement Transducers were used, which is a mixture of a circular plate and a strain gauge. The device was placed below the structure. When loading is applied, the plate deforms, which is measured by the gauge and recorded on the datalogger.

Table 2 The number of the equipment for the static loading test

Equipment	Amount	Unit
Displacement transducer	4	set
Vibrating wire strain gauge	7	set
VWSG datalogger	2	set
Displacement transducer datalogger	1	set
Dial gauge	4	set

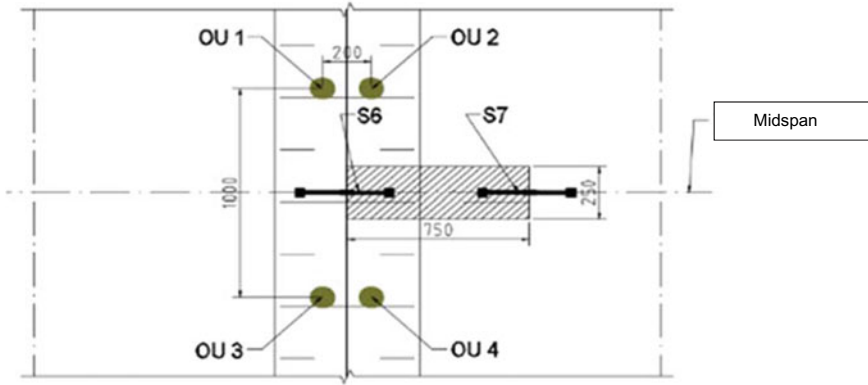


Fig. 3 Detailed top view of the placement of the instruments under the slab

The instruments were placed on the joint between two slabs at the middle of the span of the bridge. The location of the instruments in the testing area is described in Fig. 3. More detailed illustrations of the placement of the instruments are shown in Figs. 4 and 5. The strain gauges S1–S5 were placed on the rebars of the full slab joint. The joint was then poured into a non-shrink grout material.

The load for the static loading test used a weighted dump truck with a total load of 42,480 kg and a hind wheel load of 32,400 kg [4–6]. The dimension of the truck is illustrated in Fig. 6. The static loading test was conducted in 5 stages, where the weighted truck was placed in different locations on the slab. The details for the configuration of the five stages of the test are shown in Fig. 7.

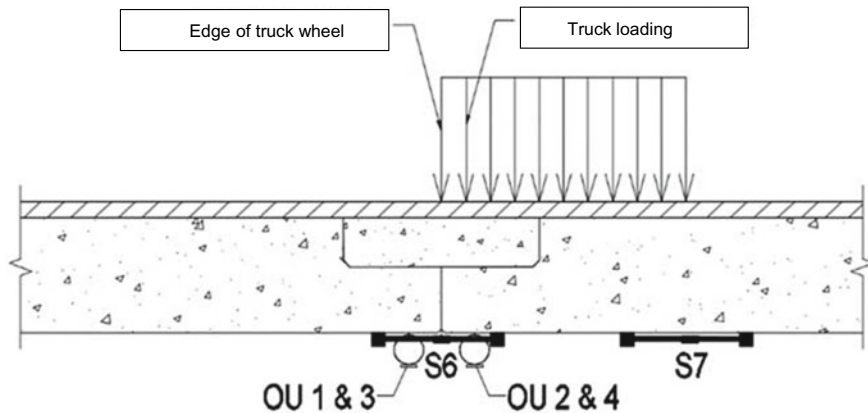


Fig. 4 Side view of the placement of the instruments under the slab

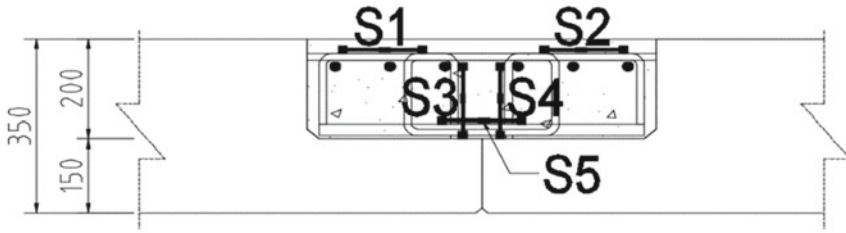


Fig. 5 Detail of the strain gauges located in the full slab joint

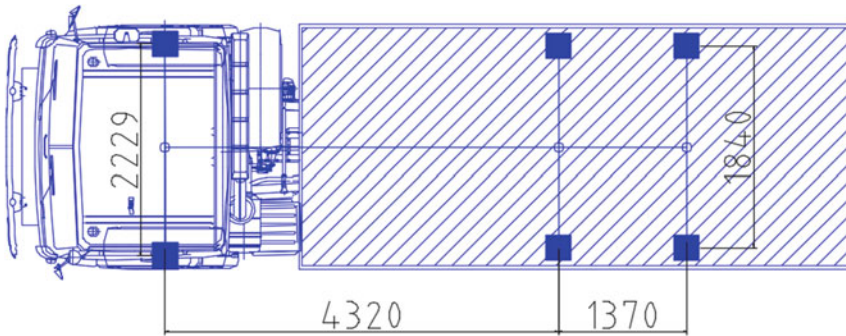


Fig. 6 Truck dimensions in mm

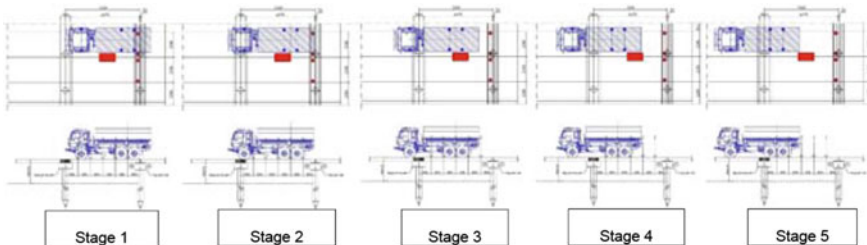
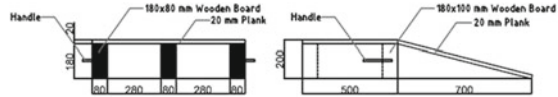


Fig. 7 Stage 1–5 of the static loading test

4 Dynamic Loading Test

For the dynamic loading test, type 8396A accelerometers from Kistler were used to measure the acceleration response. The accelerometers were located at the midspan, adjacent to the ends of the SG6 strain gauge. A data logger from Kistler was used to record the data. To induce the forced vibration on the structure, a jumper was used.

Fig. 8 Side and front view of the jumper



This jumper allows the weighted truck to gain elevation and fall onto the slab at the height of 200 mm. The front and side view of the jumper are shown in Fig. 8.

The procedure of the dynamic loading test began with the front wheels of the truck being placed on the jumper, then turning off the machine to eliminate the external source of vibrations, and then letting the truck fall onto the slabs and immediately pressing the brakes afterward.

The results of the dynamic loading test will be compared with the result from the numerical analysis. The relative damage factor $D_{relative}$ [7] will then be calculated in the following Eq. 1, where f_{theory} and f_{actual} refers to the natural frequency obtained from analysis and from testing, respectively. The structure’s critical damping (h) will also be calculated, following Eq. 2, where A_0 and A_n refers to the 1st and the n th amplitude, respectively, and n being the number of amplitudes. The method used in Eq. 2 is called the logarithmic decrement method [8].

$$D_{relative} = \frac{(f_{theory} - f_{actual})}{f_{theory}} \tag{1}$$

$$h = \frac{\delta}{2\pi} = \frac{1}{n} \frac{1}{2\pi} \ln\left(\frac{A_0}{A_n}\right) \times 100 \tag{2}$$

5 Numerical Analysis

A numerical model has been made on Midas Civil [9]. The model is analyzed replicating the static loading test conditions, and the results of the theoretical deformations are shown in Table 3.

The maximum tensile strain of the lowest part of the full slab is calculated using Eqs. 3 and 4. Equation 3 uses the modulus of rupture (f_r) definition as stated in Section 19.2.3 of SNI 2847:2019 [10], while E is the elastic modulus. The strain distribution in the section is depicted in Fig. 9. The maximum tensile strain at the lowest part of the full slab (ϵ_{s2}) is obtained to be 329.79 microstrains.

$$\epsilon_s = \frac{i}{E} = \frac{0,62\sqrt{42}}{4700\sqrt{42}} = 131,91\mu\epsilon \tag{3}$$

$$\epsilon_{s2} = 131,91\mu\epsilon \times \frac{250}{100} = 329,79\mu\epsilon \tag{4}$$

Table 3 Theoretical deformation due to static loading test simulation

	Deformation			
	OU1-m	OU2-m	OU3-m	OU4-m
Stage 1	-1.626	-1.556	-1.674	-1.597
Stage 2	-1.941	-1.840	-1.990	-1.880
Stage 3	-2.178	-2.058	-2.168	-2.050
Stage 4	-2.028	-1.916	-1.956	-1.856
Stage 5	-1.547	-1.467	-1.457	-1.389

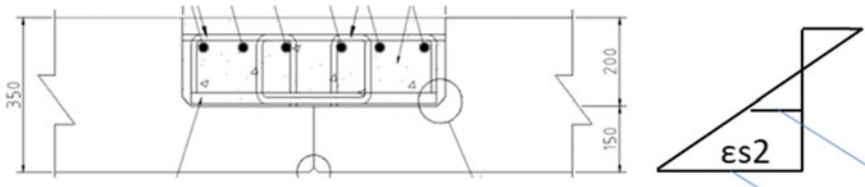


Fig. 9 Strain distribution of the full slab

Modal analysis is also conducted on the model. The mass participation factor of the model can be seen in Table 4. From Table 4, the vertical natural frequencies of the model can be obtained. The vertical natural frequencies of the slab element are taken from mode no. 2 (11.84 Hz) and mode no. 6 (16.98 Hz). The vertical mode shapes are shown in Figs. 10 and 11.

6 Static Load Test Results and Discussion

The readings of OU1–OU4 are presented in Fig. 12. The data are summarized in Table 5. The data is then presented in Fig. 13, where it is compared to the theoretical deformation. The expansion joint support of the slabs is given dial gauges to measure the deflection. The recorded data are summarized in Table 6. The summarized data is then presented in Fig. 14.

The readings on the strain gauges are also recorded. The data for the strain gauges placed on the rebars inside the joint, namely SG1–SG5, is shown below in Fig. 15. The data for the strain gauges placed under the full slab element, namely SG6 & SG7, are shown in Fig. 16. The strain data are then presented in graphs, as shown in Figs. 17 and 18 for SG1–SG5 and SG6 and SG7.

The data presented above in Table 7 shows that all OU readings have displacements lower than the numerical analysis results. This suggests that the actual full slab joint performs better than designed. This is due to the fact that the numerical analysis model does not accommodate the extra stiffness provided by the prestressing in the slabs. This prestressing in the slabs allow the slab to be stiffer, thus having smaller deformation than accounted in the model.

Table 4 Mass participation factor

Mode No.	Frequency (Hz)	Translation-X		Translation-Y		Translation-Z		Rotation-X		Rotation-Y		Rotation-Z	
		Mass (%)	Sum (%)	Mass (%)	Sum (%)	Mass (%)	Sum (%)	Mass (%)	Sum (%)	Mass (%)	Sum (%)	Mass (%)	Sum (%)
1	11.453	5.1	5.1	0	0	0	0	0	0	32.8	32.8	0	0
2	11.848	0	5.1	0	0	12.02	12.02	0	0	0	32.8	0	0
3	13.493	0	5.1	0	0	0	12.02	0	0	0	32.8	0.72	0.72
4	13.507	0	5.1	0.01	0.01	0	12.02	7.17	7.17	0	32.8	0	0.72
5	16.967	3.14	8.24	0	0.01	0	12.02	0	7.17	0.06	32.86	0	0.72
6	16.982	0	8.24	0	0.01	0.01	12.02	0	7.17	0	32.86	0	0.72
7	16.984	0	8.24	0	0.01	0	12.02	0	7.17	0	32.86	87.32	88.04
8	17.321	69.54	77.77	0	0.01	0	12.02	0	7.17	0.35	33.21	0	88.04
9	19.261	0	77.77	76.15	76.16	0	12.02	5.94	13.11	0	33.21	0	88.04
10	19.275	0.46	78.24	0	76.16	0	12.02	0	13.11	2.73	35.94	0	88.04
11	21.676	0	78.24	0	76.16	2.98	15	0	13.11	0	35.94	0	88.04
12	24.668	0	78.24	0	76.16	0	15	0	13.11	0	35.94	0.02	88.06
13	24.669	0	78.24	0.01	76.17	0	15	0	13.11	0	35.94	0	88.06
14	24.695	2.38	80.62	0	76.17	0	15	0	13.11	6.83	42.77	0	88.06
15	26.022	0	80.62	9.55	85.72	0	15	0.16	13.26	0	42.77	0	88.06
16	26.084	0	80.62	0	85.72	0	15	0	13.26	0	42.77	0.04	88.1
17	26.916	0	80.62	0	85.72	1.18	16.18	0	13.26	0	42.77	0	88.1

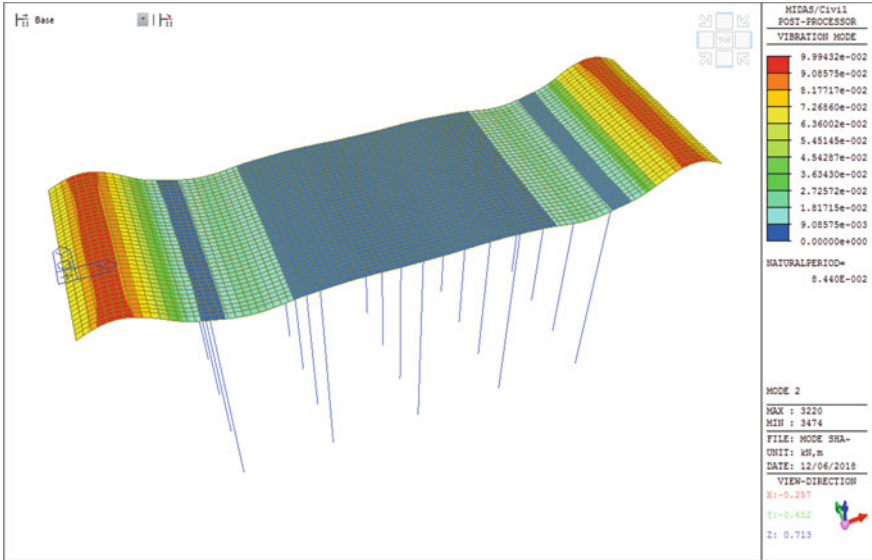


Fig. 10 Mode no. 2

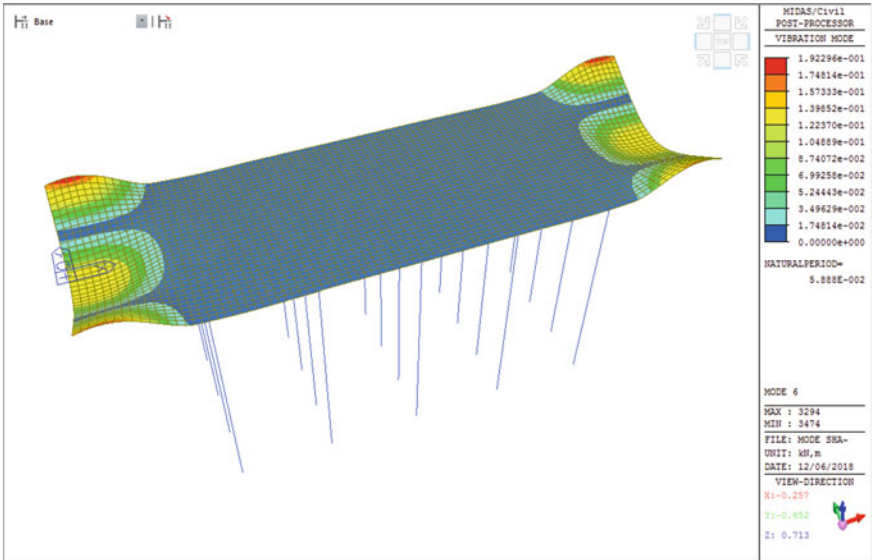


Fig. 11 Mode no. 6

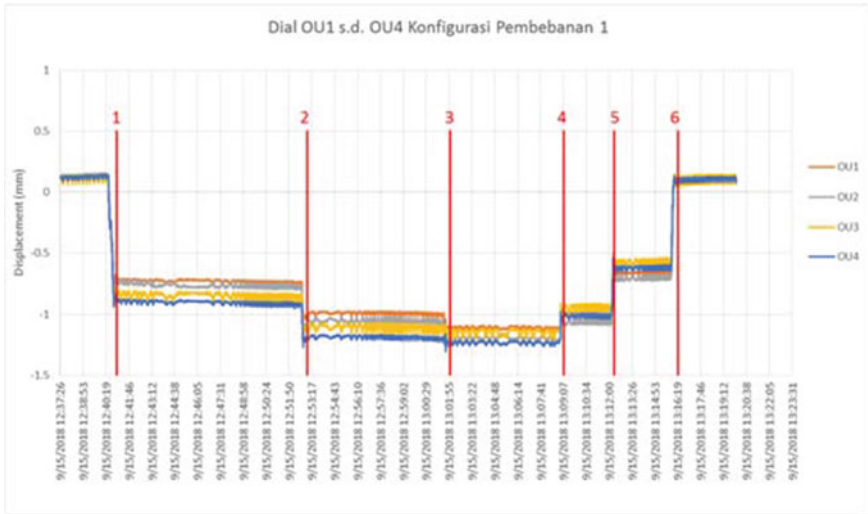


Fig. 12 Deformation on OU1–OU4 displacement transducers

Table 5 Maximum deformation on the OU displacement transducers

Dial	Maximum deformation					
	Step 1	Step 2	Step 3	Step 4	Step 5	Step 6
OU1-e	-0.934	-1.188	-1.302	-1.186	-0.875	-0.052
OU2-e	-0.992	-1.276	-1.409	-1.288	-0.922	-0.071
OU3-e	-1.123	-1.369	-1.407	-1.199	-0.849	-0.058
OU4-e	-1.148	-1.420	-1.461	-1.238	-0.868	-0.066

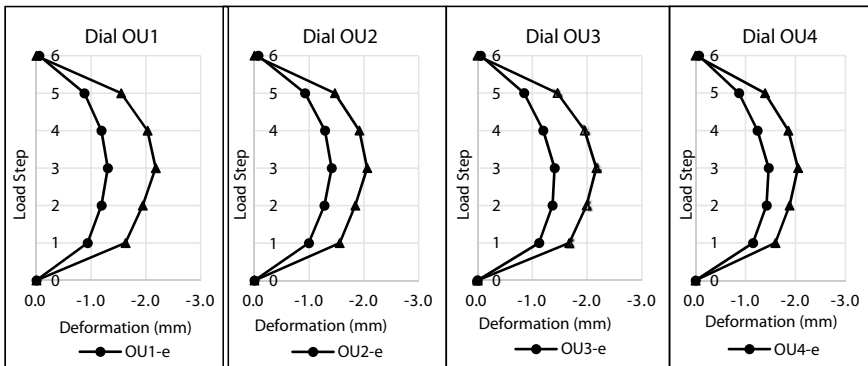


Fig. 13 Deformation versus loading steps of OU1–OU4

Table 6 Deformation on the expansion joint

Stage	Deformation (mm)			
	D1	D2	D3	D4
0	0	0	0	0
1	0.04	0.29	0.38	0.40
2	0.07	0.33	0.41	0.44
3	0.07	0.31	0.37	0.41
4	0.06	0.24	0.29	0.34
5	0.05	0.15	0.19	0.23
6	-0.01	0	0.03	0.04

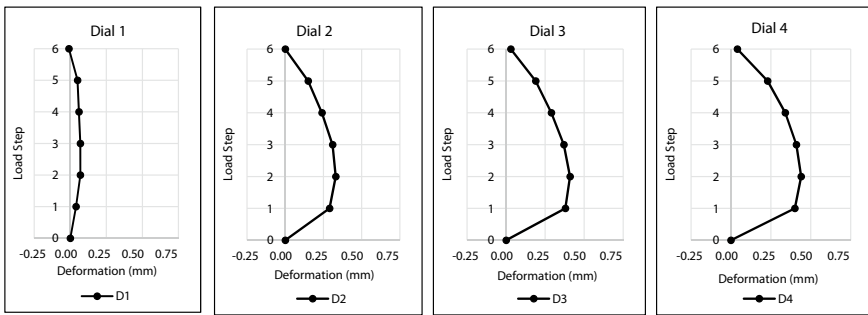


Fig. 14 Deformation versus loading steps at the expansion joint supports

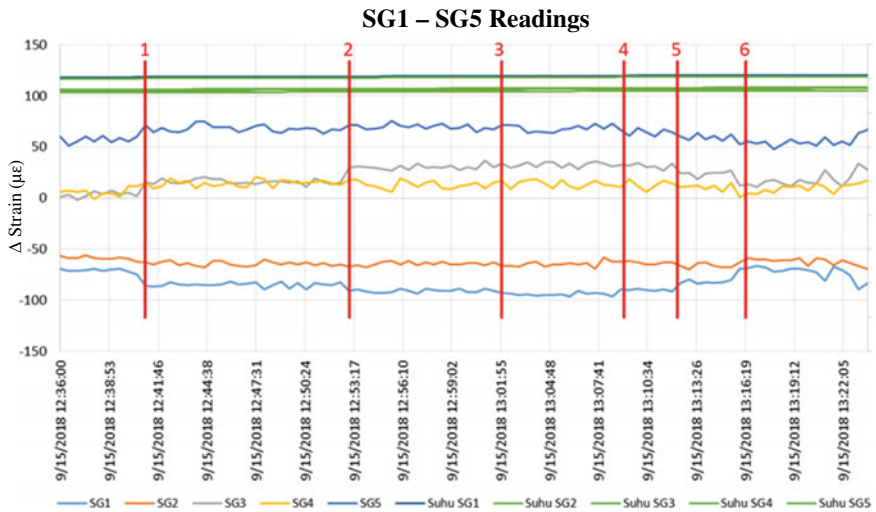


Fig. 15 Strain readings for SG1–SG5

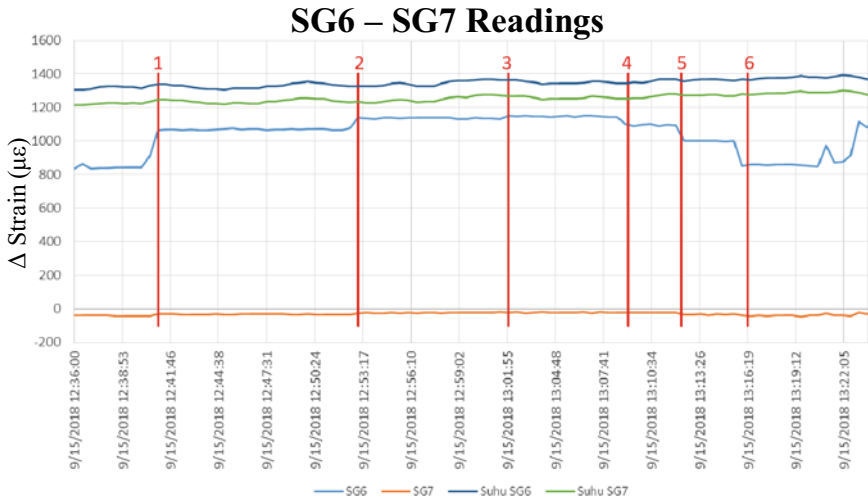


Fig. 16 Strain readings for SG6 and SG7

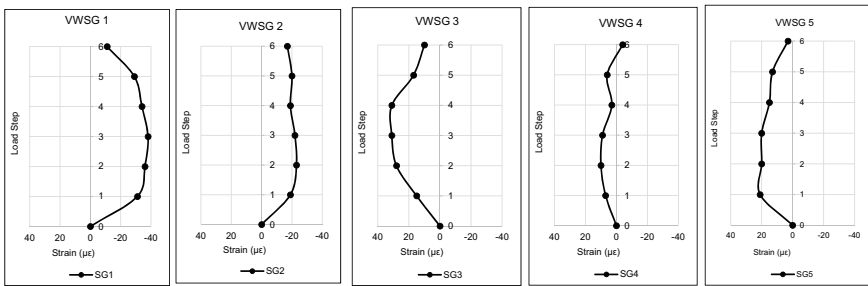


Fig. 17 Strain readings graph for SG1–SG5 during the static loading test

The deformation ratio between OU1:OU2 and OU3:OU4, which are placed across one another as shown in Figs. 3 and 4, are 0.924 and 0.963, respectively. This ratio is very close to 1, which suggests that the 200 × 600 mm connection allows the full slab to perform well and behave as one unity.

The strain readings of SG6 and SG7, as shown in Fig. 18, show maximum tensile strains of 241.329 and 19.058 microstrains, respectively. These values are lower than the theoretical tensile strain obtained from the numerical analysis, defined in Eq. (2) to be 329.9 microstrains. This further proves that the joint performs better than the analysis results since the theoretical model does not accommodate the extra stiffness provided by the prestressing tendons in the slabs.

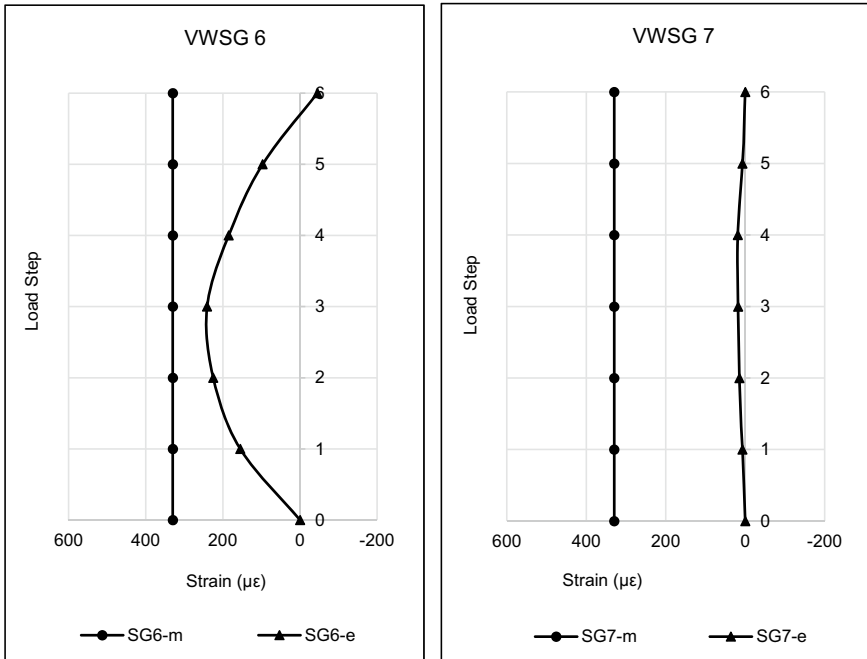


Fig. 18 Strain readings graph for SG6 and SG7 during the static loading test

Table 7 Deformation on the expansion joint due to the static loading test

	Step 3 deformation (mm)			
	OU1	OU2	OU3	OU4
OU displacement transducer reading	-1.302	-1.409	-1.407	-1.461
Numerical analysis result	-2.178	-2.058	-2.168	-2.050

7 Dynamic Load Test Results and Discussion

The forced vibration is induced three times. The reading from the accelerometers have been recorded, such as in Fig. 19, and transformed using the fast Fourier transform method as shown in Fig. 20. The peak natural frequencies from the readings have been obtained. The summary of the accelerometer data is shown in Table 8.

The data in Table 8 shows that all actual natural frequencies are higher than the frequency of the model. This is due to the same phenomenon as discussed previously, where the prestressing in the slabs provide extra stiffness to the structure. The model does not take this into account, thus allowing for the actual structure to perform better.

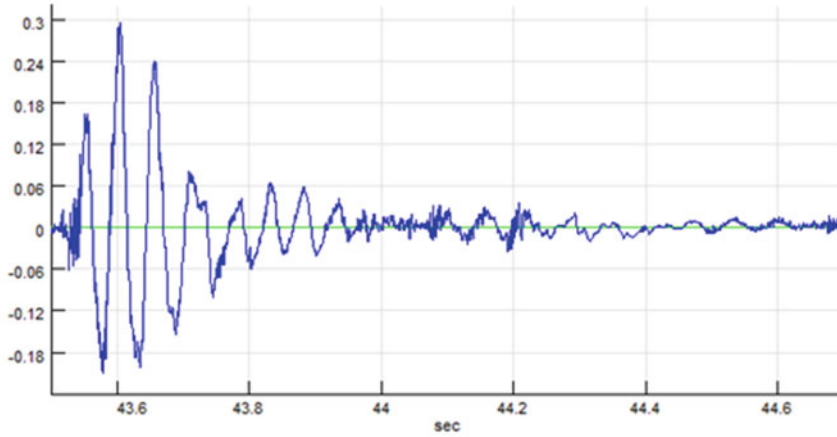


Fig. 19 Time-domain for the 1st vibration reading at point 1

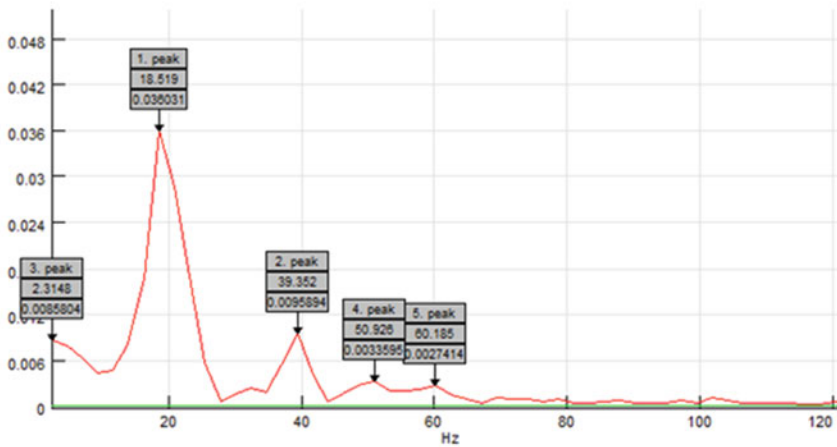


Fig. 20 Frequency domain for the 1st vibration reading at point 1

Readings on the displacement transducers during the vibration testing are recorded. The data, as shown above in Fig. 19 for the reading on OU1 for the 1st vibration, shows an initial displacement U_0 and static displacement U_{st} as marked in Fig. 21. 4 points are observed during three vibration periods. The data are summarized in Table 9.

Table 8 Summary of readings from the accelerometers

	Point 1			Point 2		
	1st vibration	2nd vibration	3rd vibration	1st vibration	2nd vibration	3rd vibration
f_{actual} (Hz)	18.517	18.750	16.050	18.229	18.880	16.670
f_{theory} (Hz)	11.840	11.840	11.840	11.840	11.840	11.840
D_{relative} (%)	-56	-58	-36	-54	-59	-41



Fig. 21 OU1 reading for 1st vibration—time domain

The readings from the transducers cannot be performed for FFT because the data frequency is only 50/s. This is not accurate enough for the calculation of the full slab’s natural frequency.

The critical damping ratio at point 1 is also calculated. Using the formulation in Eq. (2), the critical damping ratio obtained is 10.862%. Using the half-power bandwidth method, the critical damping ratio obtained is 11.25%.

Table 9 Dynamic amplification factor

	1st vibration				2nd vibration				3rd vibration			
	Point 1	Point 2	Point 3	Point 4	Point 1	Point 2	Point 3	Point 4	Point 1	Point 2	Point 3	Point 4
U_0	0.98	1.05	1.00	1.06	1.00	1.06	1.00	1.07	1.09	1.06	1.16	1.14
U_{st}	0.70	0.74	0.64	0.69	0.74	0.78	0.72	0.77	0.80	0.80	0.80	0.84
U_0/U_{st}	1.400	1.419	1.563	1.536	1.351	1.359	1.389	1.390	1.363	1.325	1.450	1.357

8 Conclusion

The measured maximum displacement is smaller than that of the numerical analysis. This is due to the prestressing in the slabs providing extra stiffness, which the numerical analysis does not take into account. The phenomenon also contributes to the actual natural frequency of the structure. The actual natural frequency of the structure is 16.05–18.75 Hz, while the theoretical natural frequency is 11.84 Hz. The strain readings of SG6 and SG7, which are placed under the slabs, show maximum tensile strains of 241.329 and 19.058 microstrains, respectively. These values are lower than the theoretical tensile strain obtained from the numerical analysis, which is 329.9 microstrains. This further proves that the joint performs better than the analysis results.

The vertical displacements of the adjacent displacement transducers are almost identical to one another. This shows that the connection allows the slab elements to perform well and behave as one unity.

The dynamic amplification factor obtained ranges between 1.325 and 1.563.

References

1. Munir M, Yakin YA (2018) Evaluasi Deformasi dan Stabilitas Struktur Tiang Pelat (Pile Slab) di Atas Tanah Gambut (Studi Kasus: Ruas Jalan Tol Pematang Panggang—Kayu Agung, Provinsi Sumatera Selatan). *RekaRacana: Jurnal Teknil Sipil* 4(3):105–116
2. Lin W, Yoda T (2017) *Bridge engineering: classifications, design loading, and analysis methods*. Butterworth-Heinemann, Oxford
3. Badan Standardisasi Nasional (2004) RSNI T-12–2004 Perencanaan struktur beton untuk jembatan. Badan Standardisasi Nasional, Jakarta
4. Badan Standardisasi Nasional (2016) SNI 1725:2016 Pembebanan untuk jembatan. Badan Standardisasi Nasional, Jakarta
5. Direktorat Jenderal Bina Marga (2012) *Manual Konstruksi dan Bangunan: Pelaksanaan Pengujian Jembatan 004/BM/2012*. Direktorat Jenderal Bina Marga, Jakarta
6. Direktorat Jenderal Bina Marga (1992) *Bridge Management System Jilid 1 Peraturan Perencanaan Teknik Jembatan*. Direktorat Jenderal Bina Marga, Jakarta
7. Departemen Permukiman dan Prasarana Wilayah (2002) *Pedoman Konstruksi dan Bangunan: Penilaian Kondisi Jembatan Untuk Bangunan Atas Dengan Cara Uji Getar Pt T-05–2002*. Departemen Permukiman dan Prasarana Wilayah, Jakarta
8. Chopra AK (2011) *Dynamics of structures*, 4th edn. Pearson Education Inc., New Jersey
9. Midas Civil [Computer Software] (2021) <https://www.midasoftware.com/>. Accessed 17 Feb 2021
10. Badan Standardisasi Nasional (2019) SNI 2847:2019 Persyaratan beton struktural untuk bangunan gedung dan penjelasan. Badan Standardisasi Nasional, Jakarta

Seismic Design Load Comparison of Reinforced Concrete Special Moment Frame and Dual Systems Based on SNI 1726:2019



Suradjin Sutjipto  and Indrawati Sumeru 

Abstract The response modification coefficient (R) and the fundamental period of the structure (T) are the two main keys in determining the seismic design load of a building according to the current Indonesian Seismic Code, SNI 1726:2019. The code prescriptively requires that the values of R and T must be established based on the type of structural system. By developing a chart showing the relationships of the various structural systems, the number of stories, the height of the structure, and the approximate fundamental periods of the structure, a structural engineer can easily see which structural system is the most efficient to be applied in the design of buildings in earthquake-prone areas. This paper will demonstrate that the use of a special moment frame system can be much more economical than the dual system, which is more commonly used in practice. For a 32-story reinforced concrete office building, the seismic design load of the special moment frame system can be approximately 30% less than that of the dual system.

Keywords SNI 1726:2019 · Response modification coefficient · Fundamental period · Special moment frame system · Dual system

1 Introduction

In designing high-rise buildings, many structural engineers tend to use a dual system for the lateral force resisting system of the building due to the presence of the elevator core wall. This makes the structural system stiffer but less ductile. Even though low ductility is not suitable for buildings located in areas with high seismicity, this is what is commonly encountered in practice.

S. Sutjipto (✉) · I. Sumeru (✉)
Civil Engineering Department, Universitas Trisakti, Jakarta, Indonesia
e-mail: suradjin@trisakti.ac.id

I. Sumeru
e-mail: indrawati@trisakti.ac.id

Meanwhile, seismic loads stipulated by the newer seismic code are likely to increase, corresponding to the discovery of new earthquake sources that have not been previously revealed. The seismic design requirements for structural systems have also become more stringent in accordance with the recommendations of the latest research results. Therefore, the selection of the type of building seismic force resisting structural system is especially important.

According to the current Indonesian seismic design code SNI 1726:2019 [1], which adopted the ASCE 7–16 [2] with some modifications to suit local Indonesian conditions, the special moment frame system has higher ductility than the dual system. Therefore, the response modification coefficient value (R) is set higher, resulting in a lower design seismic base shear. Furthermore, since the special moment frame system is more flexible, the code gives a bigger allowable limit of the fundamental period (T) compared to the dual system, causing significantly lower design seismic base shear.

Actually, the ductility concept and the determination of the design seismic loads, which depends on the fundamental period of the building structure, have been applied in the Indonesian seismic code since the 1980s [3]. Although several developments and modifications have been implemented, the basic concepts are retained up to now.

For further discussion in this paper, the terminology of special moment frame system refers to the special reinforced concrete moment frames; and the dual system refers to special reinforced concrete shear walls combined with special reinforced concrete moment frames that are capable of resisting at least 25% of prescribed seismic forces, as listed in Table 12 of SNI 1726:2019.

In order to give a clear illustration, this paper will present a comparison of the design seismic base shear of the special moment frame system and the dual system used as a seismic force-resisting system of a high-rise building, following standard design procedures [4].

2 Case Study Building

A 32-story reinforced concrete office building located in Jakarta is considered for a case study. The building has a typical story height of 3.5 m and consists of 15 of 8 by 8 m modules with a total floor area of 960 m². A special moment frame system and a dual system are proposed to be used as structural system alternatives. Their typical floor plans are shown in Fig. 1.

The city of Jakarta was selected because it is located in a moderate seismicity area without design response spectra anomaly, where the design response spectra of site class $SC < SD < SE$ [5, 6].

The design response spectrum parameters are obtained by using the Desain Spektra Indonesia web application (<http://rsa.ciptakarya.pu.go.id/2021/>). For

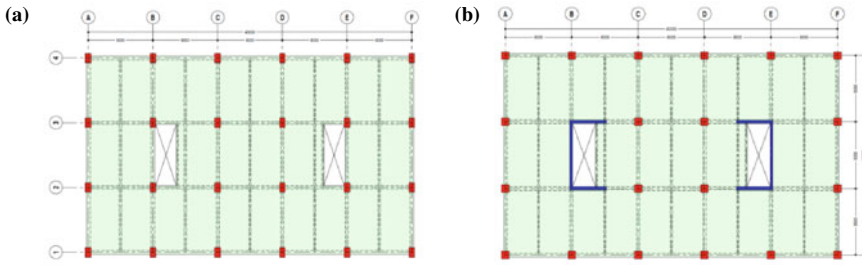


Fig. 1 Floor plans of two structural system alternatives, **a** special moment frame system and **b** dual system

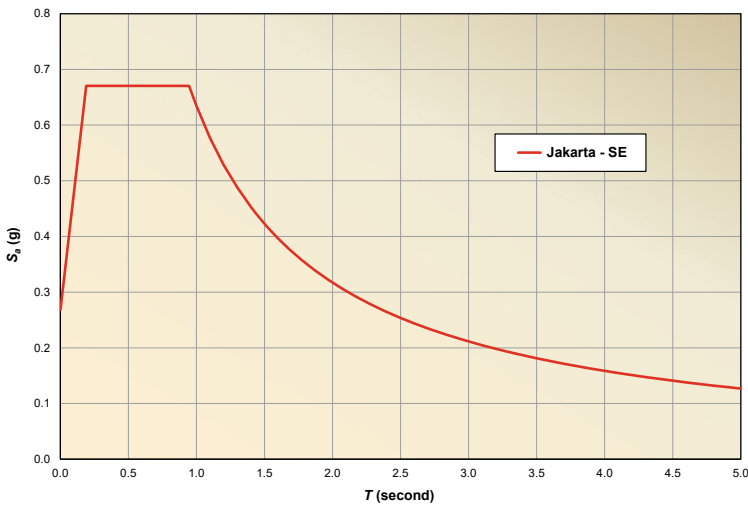


Fig. 2 The design response spectrum of Jakarta with site class category SE

Jakarta with site coordinates of -6.191° (latitude) and 106.786° (longitude), and site class category SE (soft soil), the design spectral response acceleration parameters are $S_{DS} = 0.670$ and $S_{D1} = 0.634$, thus $T_S = 0.946$ s. Based on these values, the design response spectrum curve is plotted and shown in Fig. 2.

With the design spectral response acceleration parameters $S_{DS} = 0.670$ and $S_{D1} = 0.634$, and the risk category II (office building), referring to Tables 8 and 9 in Section 6.5 of SNI 1726:2019, the Seismic Design Category (SDC) of the building is D.

3 Response Modification Coefficient

Section 7.2 of SNI 1726:2019 stipulates the selection of seismic force-resisting systems. Table 12 of Section 7.2 SNI 1726:2019 provides eight groups of structural systems [1]. Each group consists of several structural system types with limitations of use based on SDC and structural height.

According to Table 12 of Section 7.2 SNI 1726:2019, the special reinforced concrete moment frame system and the dual system can be used in SDC D with no height limit (NL).

Furthermore, Table 12 of Section 7.2 SNI 1726:2019 specifies also three design parameters for each structural system: the response modification coefficient (R), the overstrength system factor (Ω_0), and the deflection amplification factor (C_d). In particular, the response modification coefficient, R , is especially important because it is within the seismic response coefficient (C_s), and it is inversely proportional to the seismic design base shear (V). Therefore, the higher the value of R , the lower the seismic design base shear V .

Referring to Table 12 of Section 7.2 SNI 1726:2019, the R -value of the special reinforced concrete moment frame system is 8, and that of the dual system is 7. Accordingly, the base shear of the special reinforced concrete moment frame system is 12.5% lower than that of the dual system. See the comparison of the red and blue curves of C_s in Fig. 4.

4 Fundamental Period

The fundamental period of the building structure (T) is another important value in determining the design seismic load. Similar to the response modification coefficient (R), T is also within the seismic response coefficient (C_s), and it is inversely proportional to the seismic design base shear (V). Hence, the longer the T , the lower the seismic design base shear V .

The SNI 1726:2019 strictly requires that the fundamental period of the building structure (T) is not allowed to be more than the code specified value, $C_u T_a$. This is basically to take into account the additional structural stiffness contributed from structural elements that are not included in the structural analysis model, such as partition walls, façades, and other nonstructural components.

C_u is the upper limit coefficient set in Table 17 of SNI 1726:2019, which its value depends on the design spectral response acceleration parameter at 1 s (S_{DI}). Hence, for the case study building with $S_{DI} = 0.634$, $C_u = 1.4$.

T_a is the approximate fundamental period of the building structure. It is commonly used in the preliminary design stage when the structural member sizes have not been obtained, so that the fundamental period of the building structure cannot be calculated yet. There are three empirical methods provided in Section 7.8.2.1 of SNI 1726:2019 for calculating the approximate fundamental period: Eqs. 36–38.

Table 1 Approximate fundamental period (T_a)

Structural system		T_a
Moment frames	Steel	$0.0724 h_n^{0.8}$
	Reinforced concrete	$0.0466 h_n^{0.9}$
Steel EBF and BRBF		$0.0731 h_n^{0.75}$
All other structural systems		$0.0488 h_n^{0.75}$

Essentially, these equations give the lower limit of the fundamental period of the building structure, which then gives the upper limit of the seismic design base shear V .

Equation 36 of Section 7.8.2.1 SNI 1726:2019 can be used for all types of structures, and it is generally used in the design. Equation 37 of Section 7.8.2.1 SNI 1726:2019 is restricted to reinforced concrete or steel moment frame structures, with a maximum number of stories 12 and a minimum average story height of 3 m. While Eq. 38 of Section 7.8.2.1 SNI 1726:2019 is specified for masonry or concrete shear wall structures.

The approximate fundamental period (T_a) based on Eq. 36 of Section 7.8.2.1 SNI 1726:2019 and Table 18 of SNI 1726:2019 is rewritten in a simpler form in Table 1. Figure 3 presents the plot of the approximate period (T_a) of all structural systems based on the corresponding equations listed in Table 1 for varying numbers of stories and heights of structures. The height of each story is set at a typical 3.5 m. The number of stories is on the left Y-axis and the height of the structure is on the right Y-axis, while T_a is on the X-axis.

Observing the blue and red curved lines in Fig. 3, it appears that up to 40 stories, they are almost straight, and the approximate fundamental period of the reinforced concrete moment frame system is $T_a \approx 0.1 N$, while that of the dual system is $T_a \approx$

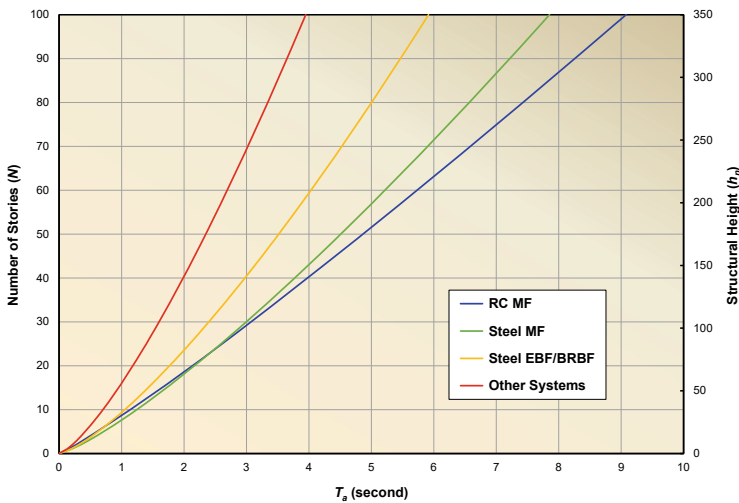


Fig. 3 Approximate period versus the number of stories and structural height

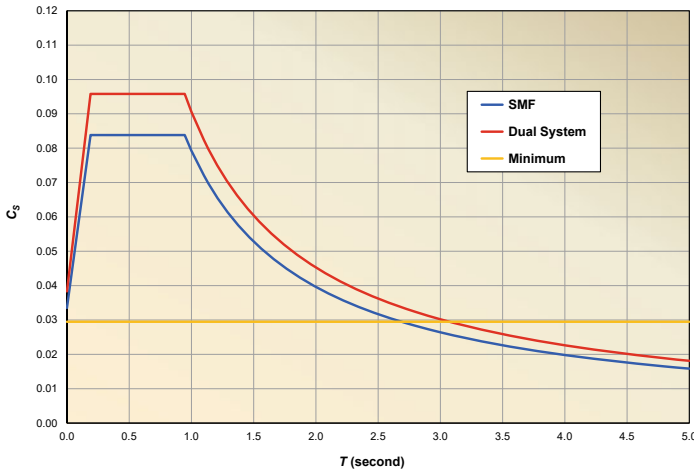


Fig. 4 Seismic response coefficient (C_s) of special moment frame system and dual system

0.05 N , where N = number of stories. It concludes that the fundamental period of the dual system is approximately twice that of the reinforced concrete moment frame system. Therefore, the seismic design base shear (V) of the reinforced concrete moment frame system is half that of the dual system.

5 Seismic Design Load

The seismic design load applied to a building structure is commonly represented by the seismic design base shear (V). In SNI 1726:2019, it is determined by Eq. 30 in Section 7.8.1: $V = C_s W$. C_s is the seismic response coefficient, and W is the effective seismic weight of the building.

According to Section 7.8.1.1 of SNI 1726:2019, the seismic response coefficient is divided into three parts:

$$\text{for } 0 \leq T \leq T_S: C_s = \frac{S_{DS}}{\left(\frac{R}{I_e}\right)} \tag{1}$$

$$\text{for } T_S < T < T_L: C_s = \frac{S_{D1}}{T \left(\frac{R}{I_e}\right)} \tag{2}$$

$$\text{for } T > T_L: C_s = \frac{S_{D1} T_L}{T^2 \left(\frac{R}{I_e}\right)} \tag{3}$$

Table 2 Seismic design base shear comparison

Parameters	Special moment frame system	Dual system
h_n (m)	112	112
T_a (s)	3.256	1.680
C_u	1.4	1.4
$T = C_u T_a$ (s)	4.558	2.352
I_e	1	1
R	8	7
C_s	0.0174	0.0385
S_{DS}	0.670	0.670
$C_{s\ Min}$	0.0295	0.0295
V (kN)	0.0295 W	0.0385 W

Equations 1–3 are basically Eqs. 31–33 in Section 7.8.1.1 of SNI 1726:2019. The code also provides Eq. 34 of Section 7.8.1.1 SNI 1726:2019 which specifies a minimum value of $C_s = 0.044 S_{DS} I_e \geq 0.01$. This lower bound limit usually governs especially for flexible building structural systems with long fundamental periods, including moment frame systems.

The long-period transition period (T_L) for Jakarta is 20 s, which falls within the domain of mega-tall buildings and is beyond the scope of this paper. It also means nothing when the minimum value of C_s applies.

Figure 4 shows the plots of the seismic response coefficients for the special moment frame system and the dual system based on the corresponding R values for each system.

The comparison of the seismic design base shear of the special moment frame system and the dual system based on the previously discussed parameters is presented in Table 2. The ratio is $0.0385/0.0295 = 1.31$, which means that the seismic design load of the dual system is 31% higher than that of the special moment frame system.

If the $C_{s\ Min}$ requirement is neglected, the ratio becomes $0.0385/0.0174 = 2.21$. This means that the seismic design load of the dual system is more than double that of the special moment frame system.

6 Conclusion

The conclusions that can be drawn from the discussion in this paper are:

1. The selection of a structural system is an important decision in the structural design of a building. Something that is commonly done in practice might not be the best choice. Structural system selection should be studied thoroughly to get the best one.

2. The seismic design load of the special moment frame system can be approximately 30% lower than that of the dual system commonly used. Therefore, the special moment frame system is a much more economical structural system that structural engineers should choose for building structures located in earthquake-prone areas.

References

1. Badan Standardisasi Nasional (2019) SNI 1726:2019 Tata cara perencanaan ketahanan gempa untuk struktur bangunan gedung dan non gedung. Badan Standardisasi Nasional, Jakarta
2. American Society of Civil Engineers (2017) ASCE/SEI 7–16 minimum design loads and associated criteria for buildings and other structures. American Society of Civil Engineers, Virginia
3. Sutjipto S (1994) Indonesia international handbook of earthquake engineering—code, programs and examples (Paz m (ed)). Chapman and Hall, New York, pp 277–295
4. Fanella DA (2018) Structural load determination—2018 IBC and ASCE/SEI 7–16. International Code Council, Washington DC
5. Sutjipto S, Sumeru I (2019) Comparison of the RSNI 1726:2018 and the SNI 1726:2012 design response spectra of 17 major cities in Indonesia. In: Proceedings of 1st international conference of construction, infrastructure, and materials, Jakarta. IOP conference series: MSE 650: 012032
6. Sutjipto S, Sumeru I (2021) Anomaly Phenomena on the New Indonesian seismic code SNI 1726:2019 design response spectra. In: Mohammed BS et al (ed) Proceedings of 6th international conference on civil, offshore and environmental engineering 2020, vol 132, LNCE. Springer, Singapore, pp 375–384

Analysis of Asphalt Damping Ratio on Shear Test



Sunarjo Leman, Maria Kevinia Sutanto, Elizabeth Ivana Harsono, Vryscilia Marcella, Anugerah Tiffanyputri, and Yuskar Lase

Abstract Seismic resistance structure on high-rise buildings is considered vital to be applied in present days to reduce structural damage caused by the earthquake. Therefore, it requires technology to control the dynamic response of the structure due to lateral forces, including earthquake force. Passive structure control system altering mass or stiffness and incorporating damping material is one representative technology in which could be applied. This study focuses on damping material-Pertamina asphalt with 60/70 penetration as the additional substance for the damper. Asphalt addition in seismic force damping system is to increase damping ratio on building structure and therefore lateral force from earthquake influencing it, is reduced and diverted to damping system. The behavior of asphalt on the shear test conducted on contact fields 9.3333, 23.0667, and 34.7 cm² become the main objective of this research. The law of Hooke and force equilibrium dynamic equation is applied to analyze the damping ratio. Verdict on the investigation of this study has shown results to be supercritical ($\zeta > 1$).

Keywords Asphalt · Damping · Stiffness

1 Introduction

The gravitational and lateral force is a fundamental contributing factor in the design of structural systems due to the importance of earthquake force. Lateral force on high-rise buildings is considered to be more destructive, in particular, due to

S. Leman · M. K. Sutanto (✉) · V. Marcella · A. Tiffanyputri
Civil Engineering Undergraduate Study Programme Universitas Tarumanagara, Jakarta, Indonesia
e-mail: keviniamaria@gmail.com

E. I. Harsono
Department of Civil Engineering, Dordt University, Sioux Center, USA

Y. Lase
Department of Civil Engineering, Universitas Indonesia, Depok, Indonesia

seismic force. Therefore, the application of earthquake resistance structure is necessary to be carried out on the design of high-rise buildings.

A structure may be designed for earthquake resistance by making it strong and ductile, or by designing it so that plastic beam-column joint may occur in which results in energy reduction and damped structure [1]. In order to decrease the damage to building structures from the earthquake, an alternative design is being established. The reduction of seismic force is able to be practiced by incorporating a damping system on structural components where the primary force from the earthquake working on the building is absorbed.

Increasing the damping ratio on building structure damping systems is another possible method to be applied. Additional damping is expected to carry out more energy absorption due to the occurrence of seismic force so that only a small portion of earthquake force working on the building which reduces possible damage from happening. The method of designing this earthquake resistance structure is known as the passive control system [2].

Damping system using passive control system existing in the time being requires a further upgrade to overcome few issues such as the addition of building mass which results in P-delta effect, influence on structure stiffness and deflection [3, 4]. Due to these objectives, more advanced damping equipment needs to be established. Asphalt could be implemented as an alternative material to increase damping effectivity on the damping apparatus due to the large damping value it has, which results in the absorption of primary force from seismic activity working on building [5].

On a previous study conducted on the analysis of the influence of viscosity on asphalt damping ratio as earthquake force damper with a penetration test method had shown result that asphalt is able to be applied as damping material [6, 7]. The high viscosity of asphalt is able to provide a larger coefficient of damping.

2 Materials and Method

An Analog model is applied to this study to mimic an asphalt damping system focusing on asphalt behavior on conducted shear tests [8]. The area of contact tested on this study vary between 9.3333, 23.0667, and 34.7 cm². An illustration of the model is displayed in Fig. 1.

General equation of motion from the system is stated in Eq. 1:

$$M\ddot{U}(t) + C\dot{U} + KU = 0 \quad (1)$$

where

\ddot{U} acceleration (m/s²)

\dot{U} velocity (m/s)

U displacement (m)

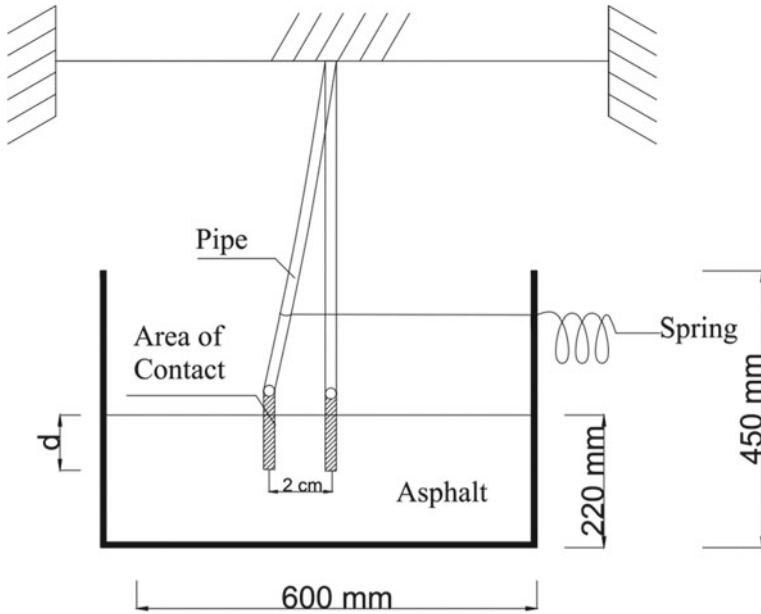


Fig. 1 Asphalt shear test

- M mass (kg)
- C damping (Ns/m)
- k stiffness (N/m)

which also can be written as displayed in Eq. 2:

$$U = e^{-\zeta \cdot \omega_n \cdot t} (A \cos \omega_d \cdot t + B \sin \omega_d \cdot t) \tag{2}$$

With A and B presented in Eqs. 3–4:

$$A = U_0 \tag{3}$$

$$B = \frac{\dot{U}_0 + \zeta \cdot \omega_n \cdot U_0}{\omega_d} \tag{4}$$

where

- U displacement (m)
- ζ damping ratio
- ω_n natural frequency of undamped vibration (rad/s)
- ω_d natural frequency of damped vibration (rad/s)
- t time variable (s)
- U_0 initial displacement (m)
- \dot{U}_0 initial velocity (m/s)

There are three following conditions on viscously damped free vibration [1]:

1. Underdamped system oscillates about its equilibrium position with a progressively decreasing amplitude, where $c < c_{cr}$ and $\zeta < 1$
2. Critically damped system returns to its equilibrium position without oscillating, where $c = c_{cr}$ dan $\zeta = 1$
3. The overdamped system does not oscillate and returns to its equilibrium position as in the critically damped system but at a slower rate, where $c > c_{cr}$, $\zeta > 1$.

Figure 2 shows a plot of the motion $U(t)$ due to initial displacement $U(0)$ for three values of ξ .

By assuming damping is supercritical, the general solution from Eq. 2 are obtained as Eq. 5:

$$U(t) = A.e^{(P_1.t)} + B.e^{(P_2.t)} \tag{5}$$

With A and B values to be calculated as Eqs. 6-7:

$$A = \frac{\dot{U} - U_0.P_2}{P_1 - P_2} \tag{6}$$

$$B = \frac{U_0.P_1 - \dot{U}}{P_1 - P_2} \tag{7}$$

And P_1 and P_2 to be written as Eqs. 8-9:

$$P_1 = -\zeta.\omega + \omega_d \tag{8}$$

$$P_2 = -\zeta.\omega - \omega_d \tag{9}$$

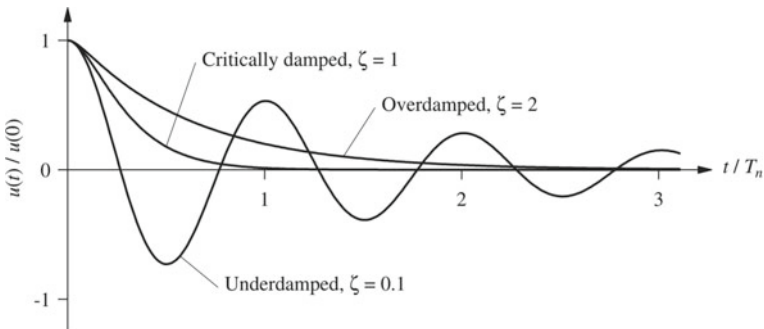


Fig. 2 Free vibration of underdamped, critically damped, and overdamped systems [1]

where

- \dot{U} velocity (m/s)
- U_0 initial displacement (m)
- ζ damping ratio
- ω forcing frequency (rad/s)
- ω_d natural frequency of damped vibration (rad/s)

Through entering boundary condition of the experiment where damped vibration time variable (t_d) and initial velocity (\dot{U}_0) equal to zero onto Eqs. 6 and 7. Therefore a new formula is calculated as displayed on Eq. 10.

$$2\omega_d.U(t) = U_0.\zeta.\omega^{-\zeta.\omega_t}.e^{\omega_d.t} + U_0.\omega_d.e^{-\zeta.\omega_t}.e^{\omega_d.t} - U_0.\zeta.\omega.e^{-\zeta.\omega_t}.e^{-\omega_d.t} + U_0.\omega_d.e^{-\zeta.\omega_t}.e^{-d.t} \tag{10}$$

where

- ω_d natural frequency of damped vibration (rad/s)
- $U(t)$ displacement at certain time variable (m)
- U_0 initial displacement (m)
- ζ damping ratio
- ω forcing frequency (rad/s)
- t time variable (s)

Equation 10 is used on Matlab to analyze the damping ratio of asphalt. The procedure of this study is presented in Fig. 3.

3 Results and Discussion

There are few test objectives conducted in this study which include investigation on asphalt physical properties, stiffness of pipe and spring, and the influence of contact area variation. Test results on asphalt physical characteristics are displayed in Table 1.

The different areas of contact will result in variation of damping coefficient value. This study runs testing on three different areas of contact, where each size of areas is assessed five times. The area of contact tested on this study vary between 9.3333, 23.0667 and 34.7 cm².

Results of damping ratio analysis using Matlab and Eq. 10 are presented in Table 2.

The relation of damping ratio and area of contact is shown in a graphical form in Fig. 4.

From Fig. 4, it can be seen that the asphalt damping ratio for 9.3333 cm² large area is calculated as 1.152, for area size of 23.0667 cm² is 1.184 and for the area of contact 34.7 cm², the analysis of asphalt damping ratio results in the value of 1.091. In contrast, the damping ratio without asphalt incorporation is approximately 0.0018.

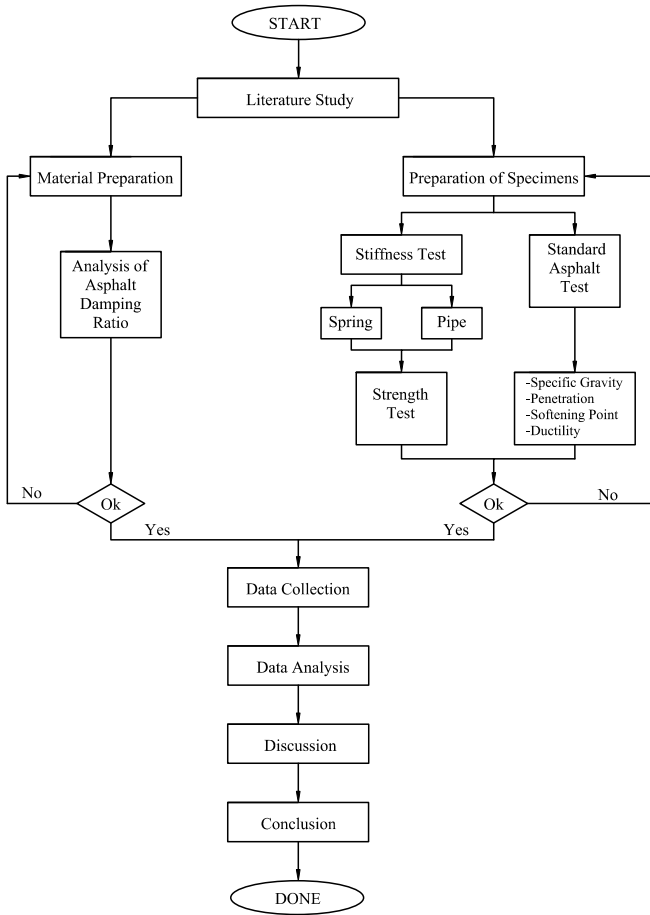


Fig. 3 Research flow chart

Table 1 Results of asphalt physical test

Asphalt test	First experiment	Second experiment	Testing standards
Penetration (%)	59.5	73	[9]
Specific gravity (g/cm ³)	1.04	0.95	[10]
Softening point (°C)	45	45	[11]
Ductility (cm)	>100	>100	[12]

Table 2 Result of damping ratio analysis

Trial	ζ		
	9.3333 cm ²	23.0667 cm ²	34.7 cm ²
1	1.168	1.166	1.060
2	1.151	1.211	1.099
3	1.171	1.148	1.106
4	1.153	1.204	1.093
5	1.116	1.190	1.095

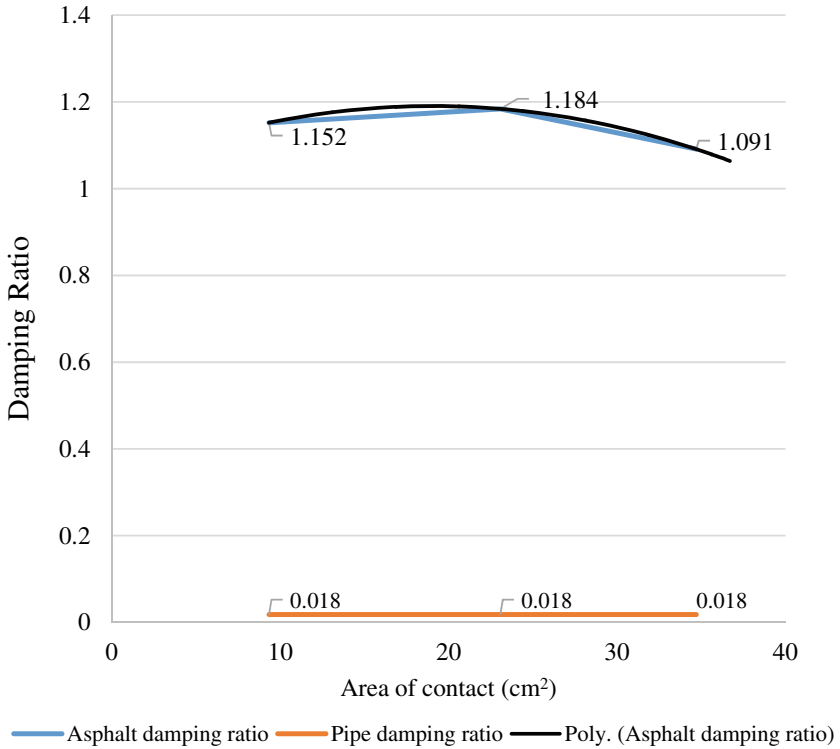


Fig. 4 Damping ratio value

4 Conclusion

Analysis conducted for the objective of this study has shown results that the asphalt damping ratio is larger than one ($\zeta > 1$). This occurrence proves that asphalt damping is found to be supercritical. The damping ratio of asphalt varies between 1.08 and 1.18. On the contrary, the damping ratio of a damping system without asphalt is only 0.018, which proves the compatibility of asphalt as a damping material. Correlation between the area of contact and damping ratio value is presented through $y = 0.0004 x^2 + 0.0155 x + 1.0426$, where y is the damping ratio value and x is the size of the contact area.

The supercritical result of the asphalt damping ratio test makes it a feasible, innovative material to be applied on seismic force damping systems, where it could be studied further in future research.

References

1. Chopra AK (2012) Dynamics of structures: theory and applications to earthquake engineering, 4/E. Pearson, California
2. Symans MD, Constantinou MC (1999) Semi-active control systems for seismic protection of structures: a state-of-the-art review. *Eng Struct* 21(6):469–487
3. Lily S (2000) Structural control systems for earthquake resistant structural design. *Jurnal Teknik Sipil* 6(1):55–66
4. Setio HD, Setio S (2005) Kontrol Vibrasi Struktur Bangunan dengan Menggunakan Peredam Massa Aktif. *Jurnal Infrastruktur dan Lingkungan Binaan* 2:30–39
5. Ashadi (2002) Pengukuran Rasio Redaman pada Material Aspal sebagai Bahan Redaman pada Struktur. Thesis, Universitas Indonesia
6. Gunawan J (2011) Analisis Pengaruh Viskositas Terhadap Koefisien Redaman Aspal Sebagai Alat peredam Gempa. Universitas Tarumanagara. Thesis
7. Christianto D, Surachmat D, Leonardy E, Lim WH, Theodora M (2018) Analysis of damping ratio in passive control devices with graded sand as fillers in the shaft section. In: Tarumanagara international conference on the applications of technology and engineering, Jakarta, 22–23 November 2018. IOP conference series: materials science and engineering, vol 508. IOP Publishing Ltd, Bristol, p 012007
8. Supriyadi Y (2002) Pengukuran Redaman Material Aspal dengan Penambahan Tekanan Lateral. Universitas Indonesia, Thesis
9. Badan Standardisasi Nasional (1991) SNI 06–2456–1991 Bahan aspal, Metode pengujian penetrasi. Badan Standardisasi Nasional, Jakarta
10. Badan Standardisasi Nasional (1991) SNI 06–2441–1991 Metode Pengujian Berat Jenis Aspal Padat. Badan Standardisasi Nasional, Jakarta
11. Badan Standardisasi Nasional (1991) SNI 06–2434–1991 Metode Pengujian Titik Lembek Aspal dan Ter. Badan Standardisasi Nasional, Jakarta
12. Badan Standardisasi Nasional (1991) SNI 06–2432–1991 Metode Pengujian Daktilitas Bahan-bahan Aspal. Badan Standardisasi Nasional, Jakarta

Analysis of the Sand Grains Influence on Damping Ratio Using Shear Test



Daniel Christianto, Vryscilia Marcella, Channy Saka,
Alvira Nathania Tanika, and Yuskar Lase

Abstract The earthquake-resistant structural building design is a necessity nowadays. Therefore, the development of earthquake damping device is indispensable. This research focuses on the usage of sand as an additional damping material on a silencer attached to the building structure. The selection of sand as an additional damper is based on the shape of the grain, which could provide additional internal friction between each grain to cause damping. This research is conducted on various types of grains size retained on the sieve analysis with uniform composition within the container and thin plate as oscillating contact area in the sand. The thin plate is connected to a perfectly fixed acrylic-free end tube. The sensor used is a device to gather oscillation data to be processed for the value of damping ratio to be known. The experimental result shows the disproportionate damping ratio (ξ) increment to the increase of contact area (A) and the sand shear angle.

Keywords Sand · Damping · Stiffness

1 Introduction

In seismic resistant structure design, there is a particular technique to transfer earthquake force from the main structure to a specially designed earthquake damping device to absorb the force from the substructure [1]. To reduce the damage that occurred to the structure even further, the earthquake damping device could be set right to the main structure. Passive structure control system by mass and stiffness modifying or by the addition of damping material to control the lateral

D. Christianto (✉) · V. Marcella · C. Saka · A. N. Tanika
Civil Engineering Undergraduate Study Programme, Universitas Tarumanagara, Jakarta
11440, Indonesia
e-mail: danielc@ft.untar.ac.id

Y. Lase
Department of Civil Engineering, Universitas Indonesia, Depok, West Java 16424, Indonesia

dynamic structure control, including earthquake force [1–3]. The ability of the earthquake damping device to reduce the seismic force is heavily entwined to the making material [3]. In this research, an experiment against sand for additional earthquake damping device material was conducted due to the sand’s ability to dampen the seismic force.

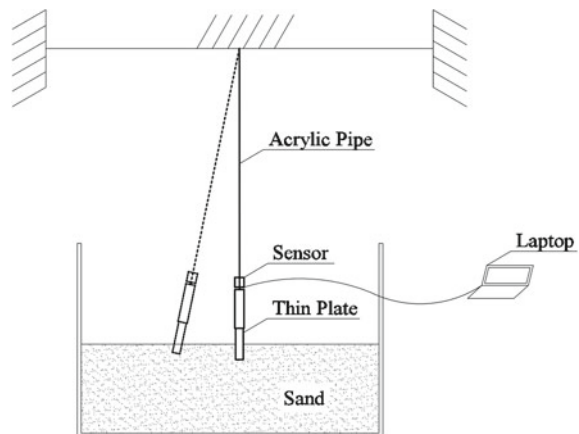
The purpose of this study is to determine the effect of sand materials due to friction between the uniform sand grains and to determine the damping ratio (ξ) of the sand constituent itself. This study rather focused on establishing the outcome on the usage of sand grain size to damping that occurred between sand grains and distinguishes the affiliation between piston’s contact area to damping ratio.

From the analysis carried out, it is expected that the uniform shape of the sand grains will cause friction between the sand itself, causing damping [4]. The shear angle in the sand that of 45° will produce a large coefficient of friction ($\mu = \tan \alpha = 1$). A large coefficient of friction will contribute greatly to damping [5, 6]. Several analyses to the various scope of the problem will take place, in which the sand grains used are the ones with uniform grain size composition that are retained on the sieve no. 4, 10, 20, 40, and 60. The was only carried out to determine the damping ratio of the sand grain material. The data obtained in this study are experimental data.

2 Research Methods

Figure 1 shows the research scheme to find the damping value in sand grains. The value of deviation and vibration time produced in Fig. 2 will be obtained upon oscillating the rod, as seen in Fig. 3 [7].

Fig. 1 Damping experiment schematics



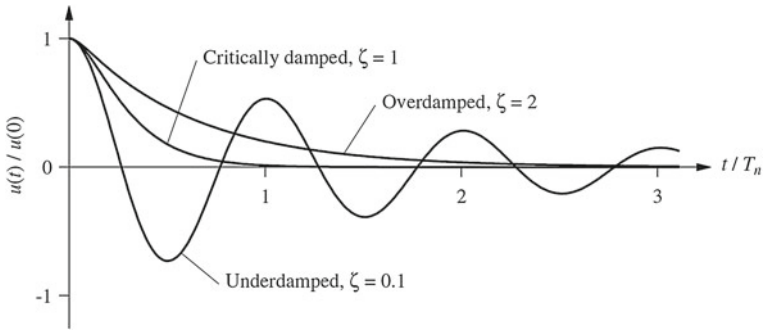
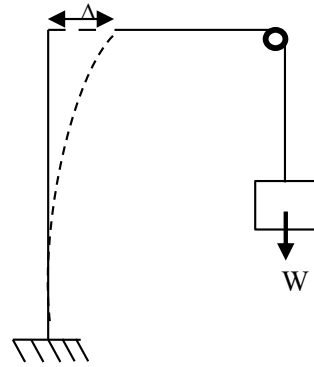


Fig. 2 Critical and supercritical chart [8]

Fig. 3 Rod used to determine rod stiffness



The equations of the chart in Fig. 2 can be seen in Eqs. 1–9.

- Critical condition [8, 9]:

$$U = e^{-\omega t} \left\{ \overset{\circ}{U}_0 + (U_0 + \omega U_0)t \right\} \tag{1}$$

$$\xi = 1 \rightarrow C = C_{cr} \tag{2}$$

$$C_{cr} = 2M\omega = 2\sqrt{KM} \tag{3}$$

- Supercritical condition:

$$U = A \times e^{P_1 \times t} + B \times e^{P_2 \times t} \quad (4)$$

$$A = \frac{\dot{U} - U_0 P_2}{P_1 P_2} \quad (5)$$

$$B = \frac{U_0 P_1 - \dot{U}}{P_1 P_2} \quad (6)$$

$$P_1 = -\xi \omega + \omega_D \quad (7)$$

$$P_2 = -\xi \omega - \omega_D \quad (8)$$

$$\omega_D = \omega \sqrt{\xi^2 - 1} \quad (9)$$

where

\dot{U} velocity (m/s)

U displacement (m)

M mass (kg)

C damping (Ns/m)

k stiffness (N/m)

ξ damping ratio

ω_n natural frequency of undamped vibration (rad/s)

ω_d natural frequency of damped vibration (rad/s)

t time variable (s)

U_0 initial displacement (m)

\dot{U}_0 initial velocity (m/s)

Figure 4 presents the steps of the research methodology as a form of flowchart.

The variable used for the sand grains diameter used for the damping experiment of (0.850, 0.425, 0.250 mm), the contact area of (4.5, 6, 7.2, 8.4, 9.35 cm²), done five times.

As identified in Fig. 5, the damping experiment with the container without sand was conducted five times, and for the sand grains diameter 0.850, 0.425, 0.250 mm done five times with each contact area of 4.5, 6, 7.2, 8.4, 9.35 cm². The whole damping experiment was totaled to 80 times.

The damping ratio is obtained after carrying out damping experiments in the laboratory, as seen in Eq. 10 [8, 9].

$$\xi = \frac{1}{2\pi j} \ln \left(\frac{u_i}{u_{i+j}} \right) \quad (10)$$

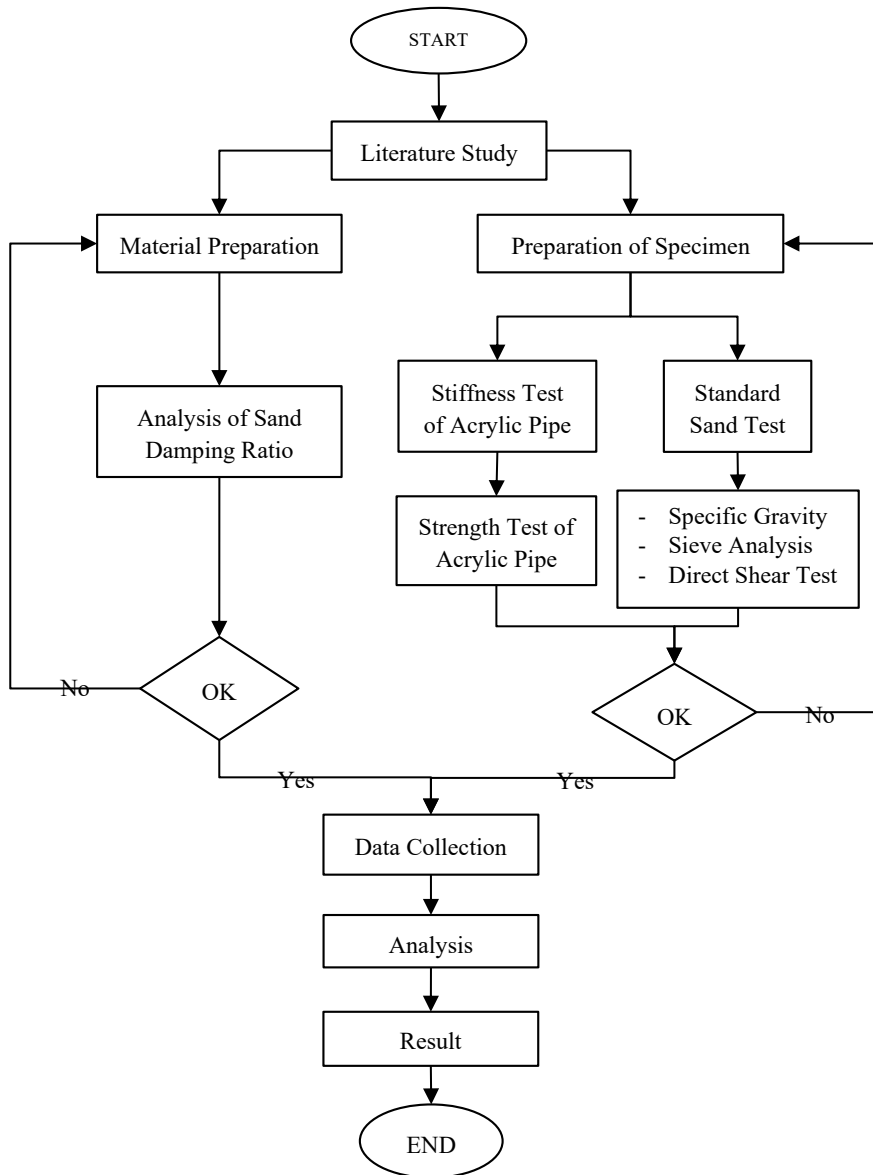


Fig. 4 Research flow chart

3 Results

The relation between the damping and contact area that is directly related to the sand grains can be seen in Fig. 6.

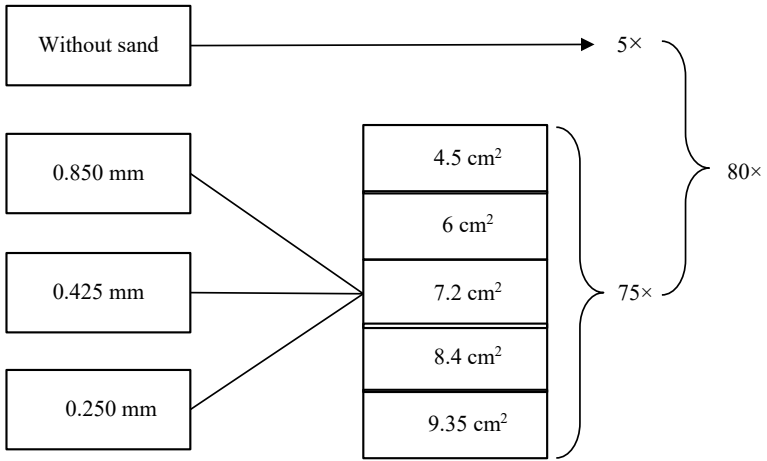


Fig. 5 Variables in damping experiments

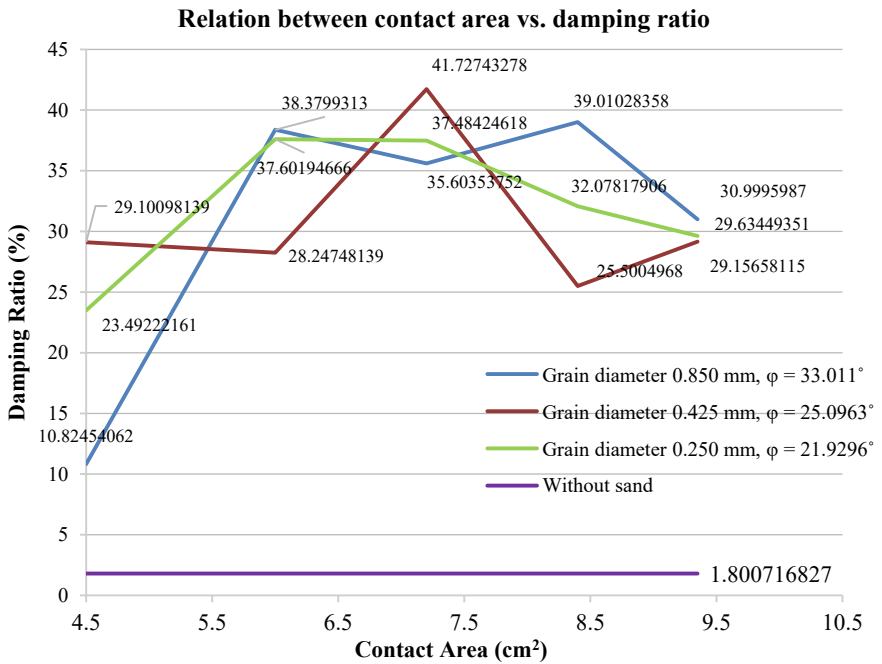


Fig. 6 Relation between contact area versus damping ratio

As seen in Fig. 6, the increment of damping ratio (ξ) is not proportional to the increment of contact area (A) and the sand grains diameter. The maximum damping ratio (ξ) value to each sand grains diameter did not happen on the same contact area (A). According to the provided analysis, the conclusion that contact area and sand grains diameter do not affect sand damping ratio (ξ) could be reached. It has been determined that this research's damping ratio is classified as subcritical (under-damped) on the grounds that obtained damping ratio falls behind 100%.

4 Conclusion

Based on the test results, several conclusions can be drawn, namely the increase in the damping ratio (ξ) is not proportional to the increase of contact area (A) and sand grains diameters. The increase in the damping ratio (ξ) is not proportional to the increase of contact area (A) and sand shear angle. Each of the sand grains diameters has a maximum damping ratio (ξ) in a certain contact area (A). The value of the damping ratio is influenced by the value of the coefficient of friction (μ) between the thin plate with sand. The damping ratio (ξ) in the sand with a diameter of 0.850 mm ranges from 10.8245 to 39.0103%. The damping ratio (ξ) in the sand with a diameter of 0.425 mm ranges from 25.5005 to 41.7274%. The damping ratio (ξ) in the sand with a diameter of 0.250 mm ranges from 23.4922 to 37.6019%.

References

1. Cheng FY, Jiang H, Lou K (2008) Smart structures: innovative systems for seismic response control. CRC Press, Florida
2. Klink BSA, Connor JJ (1996) Motion-based design methodology for buildings. Computational Mechanics Publication, Southampton
3. Takewaki I (2009) Building control with passive dampers: optimal performance-based design for earthquakes. Wiley, Singapore
4. Christianto D, Surachmat D, Leonardy E, Lim WH, Theodora M (2018) Analysis of damping ratio in passive control devices with graded sand as fillers in the shaft section. In: Tarumanagara international conference on the applications of technology and engineering, Jakarta, 22–23 November 2018. IOP conference series: materials science and engineering, vol 508. IOP Publishing Ltd., Bristol, p 012007
5. Pujiyanto A (2009) Pengaruh Lapisan Pasir di Bawah Fondasi terhadap Redaman dan Frekuensi Natural. J Ilm Semesta Tek 12:28–43
6. Yimer G (2010) Shear modulus and damping ratio of dry koka sand using cyclic simple shear test. Addis Ababa University, Addis Ababa
7. Marcella (2014) Analisis Rasio Redaman pada Benda Uji Karet dengan Butiran Pasir Bergradasi Sebagai Pengisi pada Bagian Poros. Universitas Tarumanagara, Thesis
8. Chopra AK (1997) Dynamics of structures: theory and applications to earthquake engineering. Prentice Hall, New Jersey
9. Paz M, Kim YH (1987) Structural dynamics. Van Nostrand Reinhold Company, New York

Parametric Study on Neutral Axis Growth of Concrete Beams Reinforced with Fiber-Reinforced Polymer and Steel Bars



Ahmad Zaki  and Rendy Thamrin 

Abstract This paper presents a parametric study on neutral axis growth of simply supported reinforced concrete (RC) beams. Fifteen reinforced concrete beams have been analyzed. Carbon fiber-reinforced polymer (CFRP), glass fiber-reinforced polymer (GFRP), and steel bars have been used as tensile reinforcements. Two symmetrical concentrated loads were applied to each RC beam specimen. The results show that the RC beams with under-reinforced FRP had experienced the tension failure, while over-reinforced FRP had experienced the compression failure, and all of the beams with steel reinforcement had experienced the tension failure indicated by yielding of tensile reinforcement. The results of the parametric study show that the growth of the neutral axis has been classified into three following zone: the first is the zone before crack, the second is the zone after crack, and the third is the zone after yielding of the tensile reinforcement (in case of steel reinforcement only).

Keywords Neutral axis depth · RC · CFRP · GFRP · Steel reinforcement

1 Introduction

Composites made of fiber-reinforced polymer (FRP) are currently used as cost-effective options for reinforcing, rehabilitating, and strengthening concrete structures [1–4] because of their high stiffness-weight, strength-weight ratio, and durability against reinforcement corrosion. They are highly controllable and frequently utilized to reinforce and strengthen the reinforced concrete (RC) structures

A. Zaki (✉)

Department of Civil Engineering, Faculty of Engineering, Universitas Muhammadiyah Yogyakarta, Bantul, 55183 Daerah Istimewa Yogyakarta, Indonesia
e-mail: ahmad.zaki@umy.ac.id

R. Thamrin

Department of Civil Engineering, Faculty of Engineering, Universitas Andalas, Padang 25163, West Sumatera, Indonesia

[5–7]. Since FRP has several advantages over conventional steel reinforcing bars (rebars) in concrete constructions, research on fiber-reinforced polymer (FRP) has grown more popular than ever. It has been touted as a possible concrete structure reinforcement alternative [8–10].

RC structures possibly not be the best application field for FRP composites because of their mechanical characteristics (i.e., high strength, elastic behavior, and low elastic modulus) which are best utilized when pre- or post-tensioned reinforcement is used [11, 12]. Some applications of FRP composites, such as concrete slabs, bridge decks, retaining walls, and concrete beams. Increasing the durability of FRP rebars by using FRP reinforcement instead of steel rebars is appropriate. The additional benefit of FRP reinforcement is that it can be applied in 2D and 3D fabric networks. By using FRP in these applications, there will be additional benefits as compared to non-prestressed applications [1, 5].

FRP rebars have quite different mechanical characteristics than steel rebars. In addition, several elements of the FRP rebars have exhibited significant differences, such as failure modes, bond mechanisms, ductility, and cracking [1, 5]. The moment against curvature curves of RC beams with steel rebars reinforcing bars have been shown in three separate stages; each was defined by three conditions: cracking of the concrete, yielding of steel rebars, and crushing of concrete [13, 14]. As a result, it is crucial to investigate the growth of the neutral axis until failure load [15–17]. The parameter x/d in failure and its relationship to ductility are also important [17, 18]. This paper aims to investigate the behavior of the neutral axis growth in first cracking, yielding of the reinforcement, and failure of the CFRP, GFRP, and steel-reinforced concrete beams, as well as the possibilities of in-elastic behavior of steel under-reinforced beams, FRP over-reinforced beams, and FRP under-reinforced beams.

2 Materials and Methods

2.1 Concrete Specimens

Fifteen simply longitudinal supported beams reinforced by tensile reinforcement with CFRP, GFRP, and steel rebars have been simulated and analyzed. The data of the concrete beams were obtained from Thamrin [19]. The beams were divided into seven groups: GF1, GF2, G0, G1, G2, G3, and G4 of beam specimens. There were several different parameters of the beam specimens, i.e., type of the reinforcement, the concrete properties, beam length (L), and shear length (L_s). The beam specimens have different dimensions and properties, as shown in Fig. 1 and Table 1.

The types of beam reinforcement are shown in Fig. 2. The beam specimens were divided into two types, i.e., type I (under-reinforced beams) and type II (over-reinforced beams). The width (b), height (h), and length (l) of the beam specimens were 130 mm, 230 mm, and 1300 mm, respectively. Two-point loads with shear spans of 530 mm and 450 mm were applied to the beam specimens.

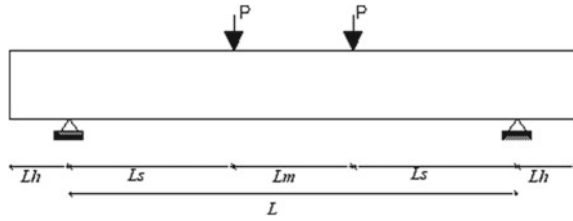


Fig. 1 Dimensions of the beams

Fukui Fibertech, Co. Ltd., Toyohashi (Japan) supplied the CFRP rebars used in this study, which had a nominal diameter of 10.6 mm, as displayed in Fig. 3. The CFRP rebars were pultruded and made of carbon fiber (60%) and epoxy resin (40%). To improve bond characteristics, polyester strands are wrapped around the rebars with a rib width of 6.0 mm and a height of 0.5 mm [20].

2.2 Data Analysis Using RCCSA

The RCCSA program is a FORTRAN language-based computer program to perform flexural analysis of reinforced concrete beams or columns. The method used in the program is the section discretization method of concrete [21, 22]. In the direction of the cross-sectional height, the reinforcement is divided into several layers of small elements [23]. The front page and data input of the RCCSA program can be seen in Fig. 4a, b.

3 Results and Discussion

3.1 Analysis of Load Against Deflection

As depicted in Fig. 5, the load and deflection of the first crack are insignificantly different between the FRP and steel-reinforced concrete beams. However, the load and deflection of failure between FRP and steel-reinforced beams are different due to the relationship of load–deflection. The FRP-reinforced concrete beams (CFRP and GFRP) explain that the load–deflection relationship is linear. After the first visible crack, the FRP reinforcement breaks at the ultimate failure, as displayed in Fig. 5b. Failure loads for GFRP and CFRP reinforced concrete beams are in the 80 kN–100 kN and 20 kN–40 kN ranges, respectively. While for steel reinforcement, the load–deflection relationship is bilinear. The bilinear relationship explains the high ductility of the steel reinforcement. After the reinforcing steel yields, the

Fig. 2 The profile type of the reinforced beams

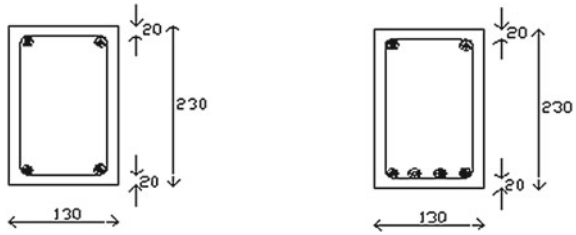
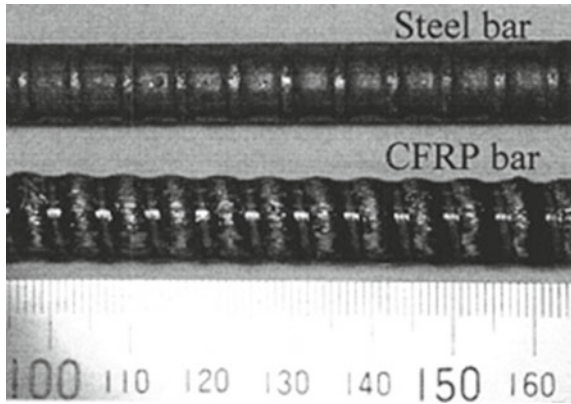


Fig. 3 Steel and CFRP rebars



deflection increases significantly until the reinforcing steel reaches its maximum stress, as demonstrated in Fig. 5c.

Based on the load and deflection graph, there are two different areas for the FRP reinforced beams, i.e., the uncracked beam section and the section after the first crack until the FRP reinforced beam failure, as demonstrated in Fig. 5b. While for the steel-reinforced beams, there are three different areas, i.e., first, before the beam section is cracked, second, after the first crack until reinforcement had reached yield point, and finally, after steel reinforcement had reached yield point until failure of the concrete beam, as depicted in Fig. 5c.

3.2 Analysis of Neutral Axis Growth

Figure 6 exhibits the existence of three distinct areas of the growth of the neutral axis. First, the growth of the neutral axis of the beam specimens at a value of $h/2$. Because of the influence of the compression and tension reinforcement, the neutral axis was located near the section’s midweight in the uncracked state. Second, after the first crack of the beam specimen, the growth of the neutral axis has decreased until the reinforcement reaches the failure point for the CFRP and GFRP reinforcement and reaches the yield point for the steel reinforcement ($f_s = f_y$). The capacity of the beam section during cracking was smaller than the capacity of the

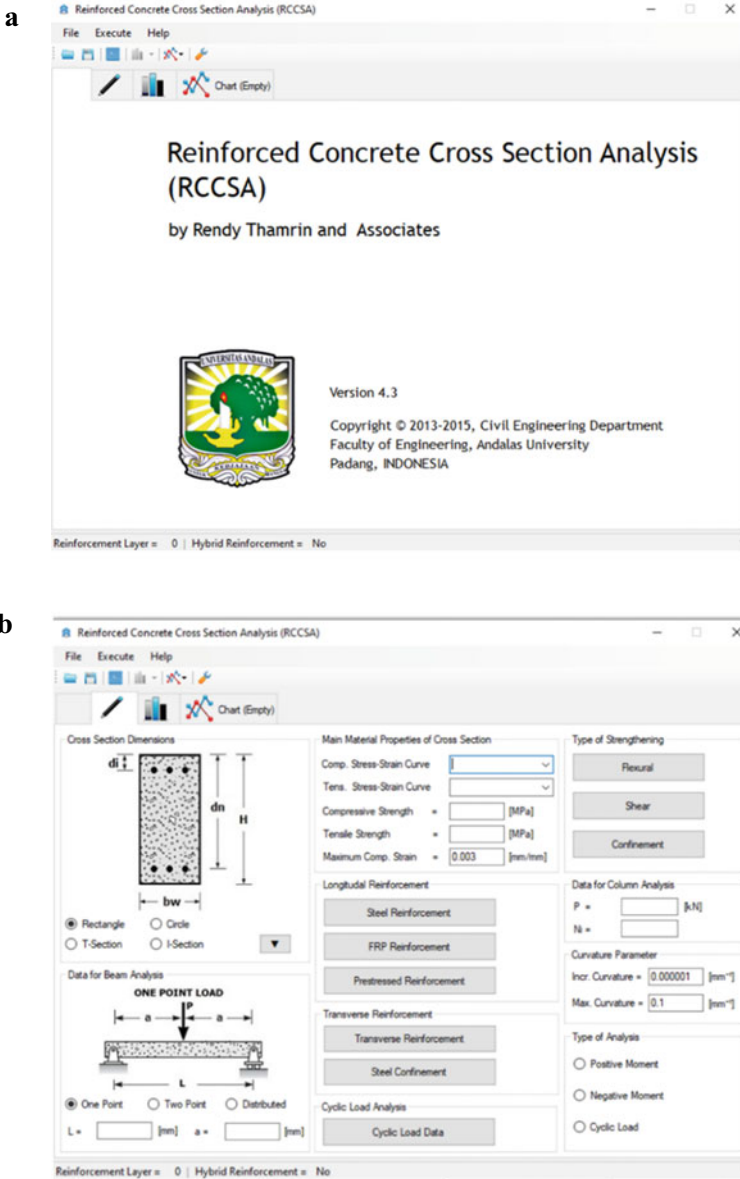
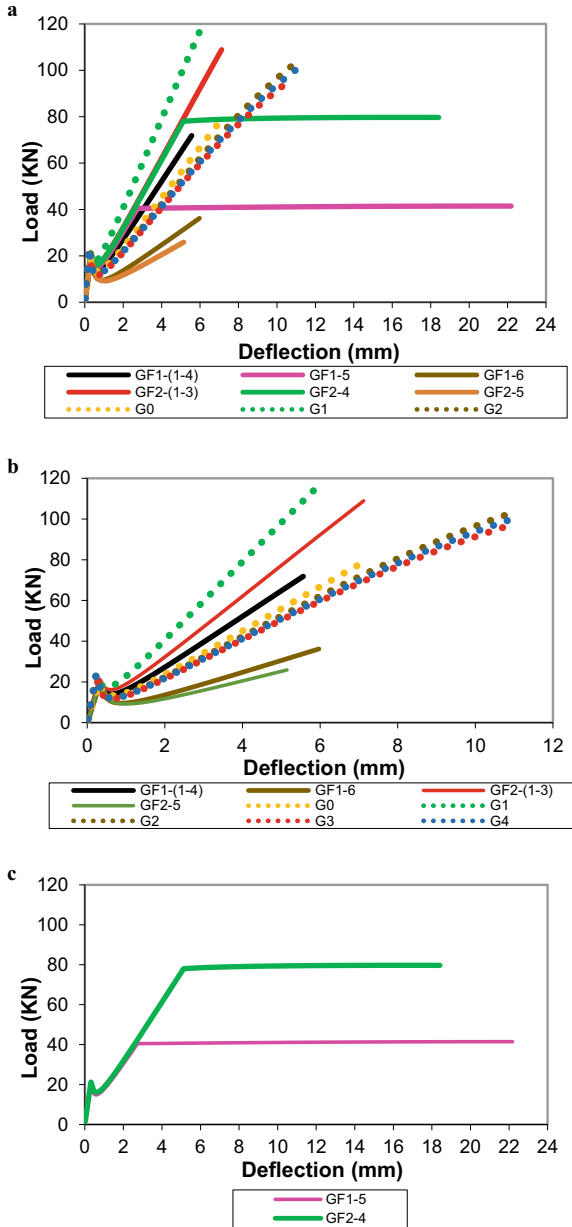


Fig. 4 RCCSA a front page, b data input

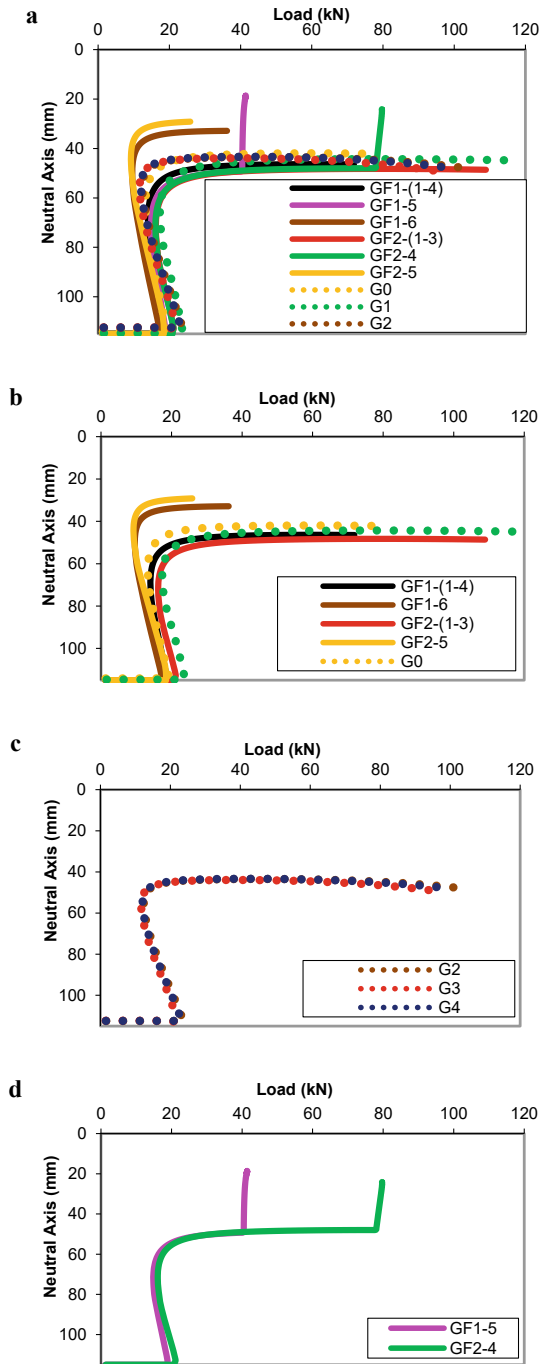
beam section before cracking, causing an uncontrolled crack until the cracking moment. It happened after the first crack until the yield or failure of the reinforcement. Finally, for steel reinforcement, the growth of the neutral axis decreases while the reinforcement reaches the yield point until failure or reaching the

Fig. 5 Graphic load (y) and deflection (x) of the reinforced concrete beams **a** FRP and steel reinforcement, **b** The CFRP and GFRP reinforcement, **c** The steel reinforcement



maximum stress of the concrete beam ($\epsilon_{cm} = 0.003$). Two behaviors of the neutral axis depth of CFRP and GFRP reinforcement are presented in Fig. 6b, c. As a result, the neutral axis growth for steel reinforcement has three behaviors, as presented in Fig. 6d.

Fig. 6 Graphic load (x)—neutral axis depth (y) of the reinforced concrete beams **a** GF1-G4, **b** under-reinforced CFRP and GFRP rebars, **c** over-reinforced CFRP rebars, **d** under-reinforced steel rebars



4 Conclusions

There were three behaviors in the neutral axis growth areas. First, the area indicating the depth of the neutral axis growth was around the center of the beam cross-section ($h/2$). Second, the area showing the neutral axis decreased significantly to a certain depth and, after reaching that, the neutral axis was around that depth. Third, the area depicting the depth of the neutral axis decreased toward the compression reinforcement. For FRP-reinforced concrete beams with under reinforcement, the type of failure was tension—the yielding of the reinforcement before concrete beam failure. Meanwhile, steel-reinforced concrete beams experienced a tension failure, the concrete failure immediately after the reinforcement has yielded. Regarding FRP reinforced concrete beams with over-reinforced reinforcement, the failure was compression—a concrete failure before yielding the reinforcement.

References

1. Sen R (2015) Developments in the durability of FRP-concrete bond. *Constr Build Mater* 78:112–125
2. D'Antino T, Triantafillou TC (2016) Accuracy of design-oriented formulations for evaluating the flexural and shear capacities of FRP-strengthened RC beams. *Struct Concr* 17(3):425–442
3. Deng J, Eisenhauer Tanner J, Mukai D, Hamilton H, Dolan C (2015) Durability performance of carbon fiber-reinforced polymer in repair/strengthening of concrete beams. *ACI Mater J* 11(2):247–257
4. Pellegrino C, Maiorana E, Modena C (2009) FRP strengthening of steel and steel-concrete composite structures: an analytical approach. *Mater Struct* 42(3):353–363
5. Wang JU, Gangarao H, Liang R, Liu W (2016) Durability and prediction models of fiber-reinforced polymer composites under various environmental conditions: a critical review. *J Reinf Plast Compos* 35(3):179–211
6. Singh SB (2015) Analysis and design of FRP reinforced concrete structures. McGraw-Hill Education, New York
7. Zhuang N, Zhou Y, Ma Y, Liao Y, Chen D (2017) Corrosion activity on CFRP-strengthened RC piles of high-pile wharf in a simulated marine environment. *Adv Mater Sci Eng* 2017:7185452. <https://doi.org/10.1155/2017/7185452>
8. Al-Khafaji AF, Myers JJ, Wang W (2021) Bond assessment of two types of SRP strengthening systems subjected to severe conditions. *Constr Build Mater* 273:121968
9. Nanni A (2001) Guides and specifications for the use of composites in concrete and masonry construction in North America. In: International workshop on composites in construction, Capri, 20–21 July 2001
10. Nanni A, De Luca A, Jawaheri Zadeh H (2019) Reinforced concrete with FRP bars: mechanics and design. CRC Press, New York
11. Hui D, Dutta PK (1998) Use of composites in infrastructure. In: Haddad YM (ed) *Advanced multilayered and fibre-reinforced composites*. NATO ASI Series (3. High Technology), vol 43. Springer, Dordrecht. https://doi.org/10.1007/978-94-007-0868-6_1
12. Lee H, Jung WT, Chung W (2019) Post-tension near-surface mounted strengthening system for reinforced concrete beams with changes in concrete condition. *Compos Part B Eng* 161:514–529

13. He T, Wen H, Qin Y (2007) Penetration and perforation of FRP laminates struck transversely by conical-nosed projectiles. *Compos Struct* 81(2):243–252
14. Mustafa SA, Hassan HA (2018) Behavior of concrete beams reinforced with hybrid steel and FRP composites. *HBRC J* 14(3):300–308
15. Lou T, Lopes SM, Lopes AV (2015) Neutral axis depth and moment redistribution in FRP and steel-reinforced concrete continuous beams. *Compos Part B Eng* 70:44–52
16. Nanni A (1993) Flexural behavior and design of RC members using FRP reinforcement. *J Struct Eng* 119(11):3344–3359
17. Lou T, Peng C, Karavasilis TL, Min D, Sun W (2020) Moment redistribution versus neutral axis depth in continuous PSC beams with external CFRP tendons. *Eng Struct* 209:109927
18. Bernardo L, Lopes S (2004) Neutral axis depth versus flexural ductility in high-strength concrete beams. *J Struct Eng* 130(3):452–459
19. Thamrin R (2006) Flexural and bond behavior of reinforced concrete beams with FRP bars. Dissertation, Toyohashi University of Technology
20. Thamrin R, Kaku T (2007) Bond behavior of CFRP bars in simply supported reinforced concrete beam with hanging region. *J Compos Constr* 11(2):129–137
21. Thamrin R (2014) Parametric study of neutral axis movement in reinforced concrete beams with RCCSA program. In: 1st Andalas civil engineering national conference 2014
22. Thamrin R (2015) Stress distribution in reinforced concrete column with variation of reinforcement ratio and concrete quality In: 2nd Andalas civil engineering (ACE) conference 2015
23. Park R, Paulay T (1975) Reinforced concrete structures. Wiley, Toronto

Dr. Saharjo Road Condition Audit Using IRAP Method to Achieve 3 Star Rating



Ni Luh Putu Shinta Eka Setyarini and Garry Edison

Abstract Traffic accidents are not just individual tragedies, but they also hinder economic growth, especially in developing countries. Traffic accidents continue to increase every year. One of the reasons is that there are still many roads that haven't applied the principle of safe roads to their design. The increase in traffic accidents shouldn't be underestimated because traffic accidents are predictable and prevented. To reduce the risk of accidents, it is necessary to carry out a strategy to improve road safety using existing methods. One of the methods is International Road Assessment Programme (IRAP) which was used in this study on Dr. Saharjo Road to achieving star ratings 3. From the observation, it was found the existing road conditions were very good for the vehicle occupant it had reached 4 stars, and it was functional for motorcycles and bicycles it had reached 3 stars, but for pedestrians on the road is still lacking in facilities because it only reaches 2 stars. So, it is necessary to do countermeasures through the existing treatment options to increase the star rating to 3 stars in all road users.

Keywords Accident · Road safety · IRAP · Dr. Saharjo road

1 Introduction

Based on the data received from the police and published by the Ministry of Transportation stated that across 2016 happened as many as 105,374 accident cases caused losses which are estimated to reach 2.9–3.1% of Indonesia's total Gross Domestic Product (GDP) [1]. There is a hypothetical statement that stated a positive relationship between GDP and the traffic accident number that caused death or injury [2]. Along with the increment of traffic accidents in Indonesia, it's harder to achieve good economic growth and development. Therefore, a country from both

N. L. P. S. E. Setyarini (✉) · G. Edison

Department of Civil Engineering Study Program, Tarumanagara University, Jl. Letjen S.

Parman No. 1, Jakarta, Indonesia

e-mail: niluhs@ft.untar.ac.id

government and society's point of view, especially in Indonesia, needs to pay more attention and become more responsive in doing preventive and treatment measures to the occurring accident [3].

Indonesia has also done a traffic accident preventive measure by assembling Presidential Instruction Number 4 of 2013 about a safety action program decade, and by forming Government Regulation Number 37 of 2017 about traffic and road transport safety. The inaction of Section 206 Government Regulation Number 37 of 2017, traffic and road transport safety can be done by using road safety improvement strategies approach with some conditions.

A road segment that has a high number of accidents and fatality rate should receive special attention to decrease both the road accident and fatality rate [4] because basically, road accidents are predictable and preventable [5]. To improve road safety, finding and fixing the existing problem is very important to prevent reoccurring accidents in the same spot [6].

To be able to do a preventive and treatment measure also to improve the road safety optimally, road condition assessment is needed for the existing and operational road [7]. It can be done by using the International Road Assessment Programme (IRAP) method to evaluate the accident-prone area in Dr. Saharjo Road, Menteng Atas Village, Setiabudi District, as shown in Fig. 1. IRAP method can give a measurement to the road safety performance from the road infrastructure point of view. IRAP method can also give the needed treatment recommendation based on the generated performance measurement [8].

Based on this description, this research is to conduct a study of road safety evaluation that has been carried out on the main road of Jakarta, namely Jenderal Sudirman Road, using the IRAP method to achieve Star Rating 4 by examining the existing along with road Star Rating. The examined roads and provide input on improving problematic roads. This research has the following objectives:

1. To find out the Safer Road Investment Plan (SRIP) and calculate the existing star rating of Dr. Saharjo Road using the IRAP method.
2. To find out how to reach Star Rating 3 for Dr. Saharjo Road using the IRAP method.
3. To determine the advantages of the IRAP method through the handling and calculation of the Benefit Cost Ratio (BCR).

The benefit of this research is to provide an evaluation of the IRAP method that was implemented in Indonesia, as well as to provide recommendations for how to repair Dr. Saharjo Road Jakarta that was carried out.

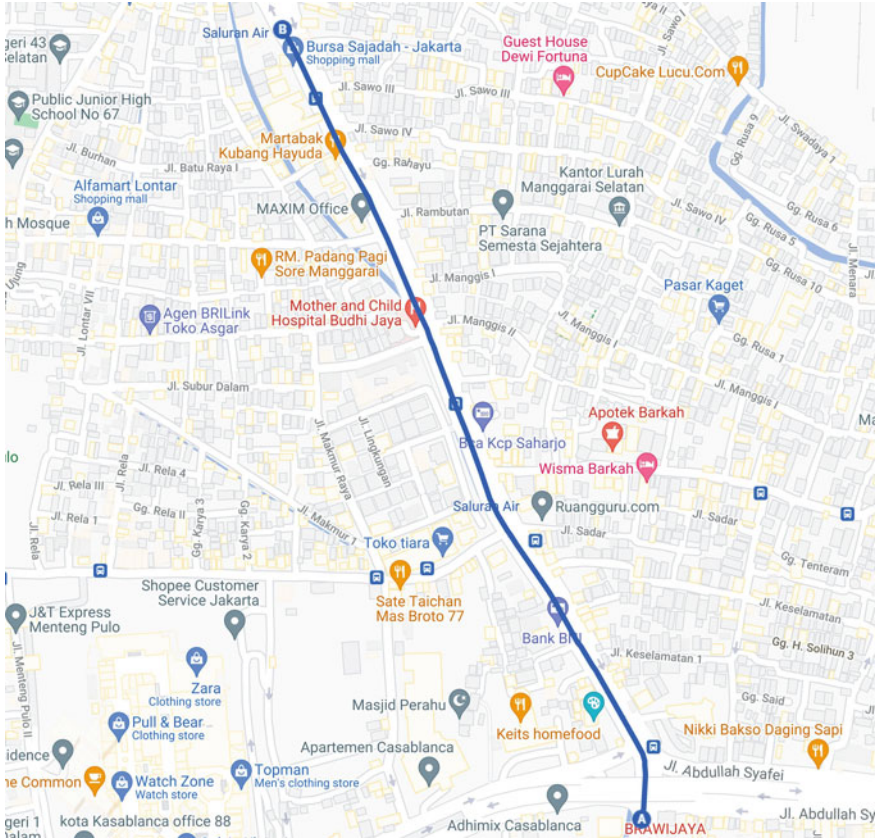


Fig. 1 Dr. Saharjo road section. Source Google Maps

2 Literature Review

Traffic safety is a form of effort/method to prevent accidents in the form of security, comfort, and economy in moving cargo (people or goods/animals) by using certain means of transportation through certain media or routes from the location/place of origin to the location/place of destination, travel [9].

Traffic accidents are a negative event of road infrastructure and accidents also pose a risk to the safety of road users which also results in damage to vehicles and goods so that they become material losses [10].

The International Road Assessment Program (IRAP) is a road assessment program developed by an international organization in the field of road safety that has succeeded in developing ways of assessing road safety for road users through determining the value or risk score that may occur due to road infrastructure elements [11]. There are four protocols in IRAP:

1. Risk mappings, which is road risk mapping using detailed accident data to describe the actual number of deaths and injuries on a road segment.
2. Star Rating, which is the performance shown by a road segment to be classified. In a road segment, there are four modes that were assessed for its star rating, namely passenger vehicles, motorbikes, bicycles, and pedestrians. Increase the star rating on a road segment,
3. A safer road investment plan, which is the preparation of a star rating plan for a road segment. To increase the star rating on a road segment, eligible costs (affordable, eligible) were needed so that one alternative it's was chosen from the best planning.
4. Performance tracking, tracking of a road segment which is repeated continuously and re-evaluated.

Road Attribute is an element in a road segment such as markings, signs, geometric, road sections, complementary road buildings, road equipment.

Star Ratings are based on road inspection data and provide simple and objective measures of road elements installed for passenger vehicles, motorcyclists, cyclists, and pedestrians. Roads with a five-star rating are the safest, while roads with a one-star rating are the least secure. Coding the path attribute is at the heart of the IRAP method. The purpose of coding road attributes is to use images from the geometric reference of the road collected during the survey and record the road attributes of each 100 m segment. Risk factors or Crash Modification Factors (CMF) are used in the IRAP method to relate road attributes and accident rates. CMF is a multiplier factor to estimate the number of accidents after a countermeasure is applied to a certain place. A total of 94 precautions/countermeasures can be used in the IRAP method.

IRAP is a method for measuring the road safety rate based on the infrastructure condition and situation also plans a treatment measure to increase the road safety quality that is developed by a Non-Profit Organization. The purpose of having a partnership with a government and non-government organization was to:

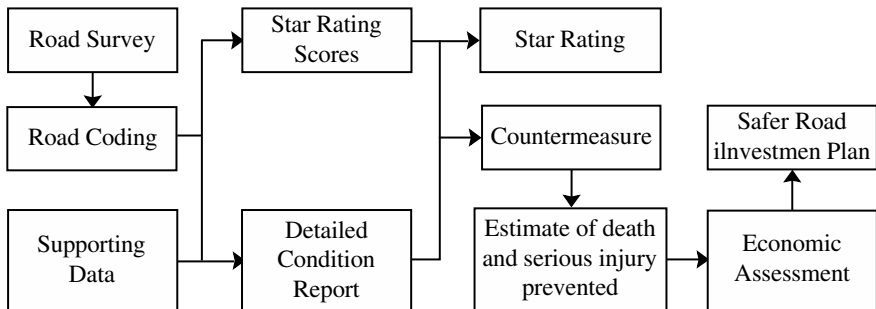


Fig. 2 IRAP road inspection, star rating, and SRIP

1. Assessing the road with high risk and developing a star rating along with a safer road investment plan as shown in Fig. 2.
2. Giving training, technology, and support that can be built and maintain the national, regional, and local ability.
3. Tracking the road safety performance to ensure the investor can assess potential profit from their investment.
4. Has been implemented in many countries, e.g., Brazil, China, Malaysia, Australia, New Zealand, South Africa, India with a real achievement, including in Indonesia.
5. IRAP could evaluate the countermeasure result by calculating the BCR for it to be compared quantitatively (With currency value).
6. Could calculate the recommended implementation result by taking account of the quantitative decrease in the accident rate.

3 Research Methodology

The survey method is direct observation at the location to be reviewed. This method is the primary method of this research which covers many aspects, including geometric, road sections, road markings and signs, road complementary buildings, and road equipment, namely on Jenderal Sudirman Road. Researchers used Google Street View and Google Earth to get the results of the observations and analyze them by the IRAP method. The IRAP method was used to determine and analyze the star rating of the existing roads. In the initial stage, coding is carried out every 100 m road segment according to the Road Attribute form. The attributes reviewed were 78 elements, 66 technical and 12 non-technical. The crash type scores formula can be seen in Eq. 1.

$$\text{Crash Type Scores} = \text{Likelihood} \times \text{Severity} \times \text{Operating speed} \times \text{External flow influence} \times \text{Median traversability} \quad (1)$$

Likelihood refers to the risk factors for the road attribute, which take into account the possibility of accidents occurring. Severity refers to the road attribute risk factors that explain the severity of the accident. Operating Speed refers to the factors that describe the extent to which risk changes with speed. External flow influence factors explain the extent to which a person's risk is involved in an accident which is a function of road use. Median traversability factors take into account the potential for a wrong vehicle to cross the median (only applies to collisions of one vehicle and direct collisions of passenger vehicles and motorcyclists).

The SRS represents the relative risk of death and serious injury for individual road users and the value expressed in Eq. 2.

$$SRS = \sum Crash\ Type\ Scores \tag{2}$$

The SRS value was compared with the Star Rating Band table to obtain the Star Rating results, describe in Table 1

Each color represents a star rating as follows: black in sections represents Star Rating 1, red in sections represents Star Rating 2, orange in sections represents Star Rating 3, yellow in sections represents Star Rating 4, and green in sections represents Star Rating 5. Calibration of accident victims is carried out to relate the amount of traffic flow to the types of accidents that may occur on these roads within one year.

Used the formula of CF VO RO-D = calibration factor for vehicles with a single passenger accident (driver’s side), n = number of segments per 100 m, SRS VO = Star Rating Score for passenger vehicles, a = AADT multiplier = 1, AADT = average daily traffic average, b = AADT power = 1, Fatality growth = 1. The CF VO RO-D = calibration factor for vehicles with a single passenger accident (driver’s side) seen in Eq. 3.

$$CF\ VO-ROD = \frac{\text{the real number of victims dying in a single accident on a road segment}}{\sum_{i=1}^n (SRS_{vo} \times a(AADT)^b \times AADT\ without\ MC \times Fatality\ growth)} \tag{3}$$

With Severity Index we can refers and accounted to the road attribute risk factors that explain the severity of the accident seen in Eq. 4.

$$SI = F \times \frac{\text{the real number of victims who injured in the network/area}}{\text{the real number of victims who died in the network/area}} \tag{4}$$

The next step is calculate FSI total = total number of deaths and serious injuries and calculation of BCR to see the treatment is feasible (BCR value > 1 = feasible), the formula of benefit of the countermeasure can be pictured in Eq. 5.

$$Benefit = FSI\ Saved \times GDP\ per\ capita \tag{5}$$

Table 1 Star rating band [12]

Star rating	Star rating score		
	Vehicle occupants and motorcyclists	Bicyclists	Pedestrians
5	0 to <2.5	0 to <5	0 to <5
4	2.5 to <5	5 to <10	5 to <15
3	5 to <12.5	10 to <30	15 to <40
2	12.5 to <22.5	30 to <60	40 to <90
1	22.5+	60+	90+

With FSI Saved = the number of victims who died and serious injuries were spared after treatment; GDP per capita = gross domestic product per capita.

4 Analysis and Discussion

4.1 Coding of Dr. Saharjo Existing Road Condition Survey Result

The data that was obtained from the survey through Google Street View and Google Maps was used for coding to obtain Dr. Saharjo’s existing road element risk factor. The coding process was done for every 100 m road segment. Table 2 is the coding example for five road attributes and risk factors from the first segment of the existing road.

4.2 Initial Score Rating

To obtain the initial score rating on each road segment, the SRS equation was used. The SRS calculation was done to each road segment, or every 100 m was done based on each road user which is the car, motorcycle, bicycle, and pedestrian. SRS value was adjusted with the risk level, and if the SRS value is high, then the risk level was high, which caused the road to have a low star rating. SRS calculation for vehicle occupant on run-off accident on the Dr. Saharjo Road for every 1 km segment was described in Table 3.

The rating score from the SRS equation used to calculate vehicle occupant, motorcyclist, cyclist, and pedestrian was converted into the star rating range for each road user. The result compilation for all segments is described in Table 4. In segments 1–7 and segment 10, the star rating of the existing road for vehicle occupant, motorcyclist, cyclist, and pedestrian are 4, 3, 3, and 2. That means Dr. Saharjo’s existing road safety condition for the vehicle occupant is high, for motorcyclists and cyclist is worthy of usage, and for the pedestrian, it is very bad.

Table 2 Coding attribute example to obtain the vehicle occupant risk factor

No.	Attributes	Category	Vehicle Occupant	
1	Lane width	Narrow (≥ 0 to 2.75 m)	1.1	1.1
2	Curvature	Straight or gently curving	1	1
3	Quality of curve	Adequate	1	1
4	Delineation	Poor	1.2	
5	Shoulder rumble strips	Not present	1.2	

Table 3 Example of the SRS equation for vehicle occupant on run-off accident (driver side)

Type of risk factor	Category	Risk factor	Score
<i>Road attribute (likelihood)</i>			
Lane width	Narrow (≥ 0 to 2.75 m)	1.1	
Curvature	Straight or gently curving	1	
Quality of curve	Adequate	1	
Delineation	Poor	1.2	
Road condition	Medium	1.2	
Grade	0 to <7.5%	1	
Skid resistance/grip	Sealed—medium	1.4	
Product of road attribute (likelihood) risk factors			2.66112
<i>Road attribute (severity)</i>			
Median type	Physical median width ≥ 1.0 m to <5.0 m	80	
External flow influence	4221 vehicles/day		0.5
Operating speed	50 km/h		0.02
Head-on (loss-of-control) star rating score			2.128896

Table 4 Dr. Saharjo road star rating compilation

Star rating										Road user
Seg. 1	Seg. 2	Seg. 3	Seg. 4	Seg. 5	Seg. 6	Seg. 7	Seg. 8	Seg. 9	Seg. 10	
4	4	4	4	4	4	5	5	5	4	Vehicle occupant
3	3	3	3	3	3	3	3	3	3	Motorcyclist
3	3	3	3	3	3	3	3	3	3	Bicyclist
2	2	2	2	2	2	3	3	3	2	Pedestrian

4.3 Countermeasure

Countermeasure to improve the star rating to 3 through the existing treatment option. The treatments that were chosen are fences in the median, fences on sidewalks, and speed limit signs. Table 5 is the accident data for vehicle occupant that has been calibrated with star rating score, and Table 6 is the example for treatment on vehicle occupant that shows fatal and injury saved if the treatment was done.

Table 5 Vehicle occupant FSI crash type

Crash type	Fatality	Serious injury
Run-off driver side	0.0208	0.2076
Run-off passenger side	0.0726	0.7265
Head-on lost of control	0.2767	2.7675
Head-on overtaking	0.0000	0.0000
Intersection	0.0737	0.7371
Property accident	0.0000	0.0000

Table 6 Countermeasure for vehicle occupant

Vehicle occupant	Risk factor		Accident type	Effectivity (%)	FSI saved
	Before	After			
Median type	Median \geq 0 m to < 1.0 m	Safety barrier— metal			
	90	0	Head-on lost of control	100	3.0442
Road fence	Building	Road fence			
	60	12	Run-off passenger side	80	0.6392
Speed limitation signs	None	Exist			
	1.25	1	Intersection	20	0.1621

4.4 Economic Assessment

The economic assessment was started with the alternative cost calculation for the road element changes that were done in Table 7.

The treatment cost also needs to be optimized with the budget constrain. BCR calculation was used to find out whether the cost for the treatment has already been optimized. Treatment benefits that can be obtained from the calculation are the reduction in FSI which has been calculated. Treatment cost is calculated based was obtained from data by the Center for National Road Implementation VI.

BCR calculation for treatment measures shows that all of the treatment that was done benefits in the next 20 years as the IRAP recommended. Table 8 shows the countermeasure needs a budget of IDR 8,840,597,002 for a 20-year period that generates a profit from the decrease of road accident rate that has been calculated at IDR 6,058,918,001 for the fence addition in the median along 700 m in the

Table 7 Draft budget and treatment cost for 20-year period

Needed treatment		Unit price (IDR)	Total (IDR)	Cost (IDR)
Fence installation on sidewalks	1000 m	2,500,000	2,500,000,000	5,180,240,001
Fence installation in median	700 m	2,500,000	1,750,000,000	3,626,168,001
40 km/h speed limitation signs	4 unit	2,750,000	11,000,000	22,793,000
40 km/h end of speed limitation signs	2 unit	2,750,000	5,500,000	11,396,001

Table 8 Benefit of accident treatment on pedestrian for 20 years period

Countermeasure	Cost (IDR)	Benefit (IDR)	BCR
Median type	3,626,168,001	66,058,918,001	18.22
Road fence	5,180,240,001	63,892,866,001	12.33
Speed limitation signs	34,189,001	3,945,474,002	115.40
Total	8,840,597,002	133,897,258,004	15.15

20 years, then a profit of IDR 63,892,866,001 for the fence addition on the sidewalk, and a profit of IDR 3,945,474,002. BCR result of 15.15 was obtained for all treatments. With the benefit/cost result is above 1, then the treatment is considered worthy.

4.5 Final Score Rating

After the SRS value for each road user on each 100 m road segment was obtain, the SRS value was allocated to the star rating value to determine the star rating for each road segment. Data compilation of initial star rating is shown in Table 9. It can be seen that the road condition which has been countermeasure on each road segment has a star rating increment for the vehicle occupant and pedestrian. It happened because the road elements treatment measure has been rated based on the worthiness standard of the BCR method. With the addition of sidewalks fence, speed limit signs, and fence in road median gives a result which is the achieved star rating for all of the road users are 3 or more, and it made this road became a forgiving road.

Table 9 Dr. Saharjo road final star rating compilation

Star rating										Road user
Seg. 1	Seg. 2	Seg. 3	Seg. 4	Seg. 5	Seg. 6	Seg. 7	Seg. 8	Seg. 9	Seg. 10	
5	5	5	5	5	5	5	5	5	5	Vehicle occupant
3	3	3	3	3	3	3	3	3	3	Motorcyclist
3	3	3	3	3	3	3	3	3	3	Bicyclist
4	4	4	4	4	4	4	4	4	4	Pedestrian

5 Conclusion

Based on the data analysis done by using the IRAP method, the conclusion was:

1. From segment 1–6 and 10 in Dr. Saharjo Road Jakarta, star rating 4, 3, 3, and 2 was obtained for the car, motorcycle, bicycle, and pedestrian on the existing and also because of the fence in the median for segment 7–9, star rating for each road user was 5, 3, and 2.
2. Road existing condition for the car has already had a high safety condition, for the motorcycle and bicycle are categorized as worthy of usage, and for the pedestrian still very bad, which is proved by the star rating of 2.
3. For the pedestrian, crossing the road is being reevaluated for its possibility and severeness since it is the most troublesome one. Reevaluation was done in order to increase the star rating to 3 and 4 stars through the existing treatment measure. The pedestrian fence was chosen as the treatment measure because by adding the fence in the median and sidewalk. Hopefully, it decreases the accident possibility for pedestrians.
4. The final star rating in Dr. Saharjo Road after countermeasure was done to the car, motorcycle, bicycle, and the pedestrian is 5, 3, 3, and 4. It means that by the increment of star rating on this road, the accident possibility and fatality decrease.
5. The advantage of using the IRAP method is that issuing recommendations was done by a certain computerized algorithm based on the international applied empiric rules and faster analysis procedure. Also, besides give a treatment recommendation, it also gives a road attribute rating and the benefits after implementation.

References

1. Prakoso JP (2018) Kerugian Negara Akibat Kecelakaan 2.9%-3.1% dari PDB. In: *Bisnis.com*. <https://ekonomi.bisnis.com/read/>. Accessed 24 Sep 2020
2. Sakhapov R, Nikolaeva R (2018) Traffic safety system management. In: *Proceedings of the thirteenth international conference on organization and traffic safety management in large cities*. Elsevier Procedia, St. Petersburg, Russia
3. Kurniawan R (2016) Kinerja Kepolisian Dalam Penanganan. *E-journal Ilmu Pemerintahan* 4:1879–1892
4. Tobing R (2018) Evaluasi Hasil Star Rating Irup Terhadap Kinerja Keselamatan Infrastruktur Jalan (Studi Kasus: Ruas Jalan Nasional Mantingan Batas Provinsi Jawa Tengah—Batas Kota Ngawi). Thesis, Bandung Institute of Technology
5. Setyarini NLPSE, Lukito BI (2020) Audit Keselamatan Jalan Tol Jagorawi. *Jurnal Muara Sains, Teknologi, Kedokteran, dan Ilmu Kesehatan* 4:403–412
6. Sianturi LFN, Setyarini NLPSE (2020) Audit Keselamatan Jalan Tol Kunciran-Serpong. *Jurnal Mitra Teknik Sipil* 3:639–650
7. Yuniar A (2015) Evaluasi Penerapan IRAP dan Inspeksi Keselamatan Jalan pada Ruas Jalan Nasional (Studi Kasus: Jalan Alamsyah R. Prawiranegara - Jalan Mayjen Yusuf Singadekane, Sumatra Selatan). In: *Proceedings of the 18th FSTPT international symposium*. Lampung University, Lampung, Indonesia
8. Idris M (2015) Pengenalan Konsep Penilaian Jalan Dalam Mengukur Kinerja Keselamatan Jalan Ruas-Ruas Jalan Nasional. In: *Kolokium Jalan dan Jembatan*. Pusat Penelitian dan Pengembangan Jalan dan Jembatan, pp 1–21
9. Ruktiningsih R (2017) Analisis Tingkat Keselamatan Lalu Lintas Kota Semarang. *Jurnal Teknik Sipil Unika Soegijapranata* 1:1–9
10. Zauardi A, Suprayitno H (2018) Analisa Karakteristik Kecelakaan Lalu Lintas Di Jalan Ahmad Yani Surabaya Melalui Pendekatan Knowledge Discovery in Database. *Jurnal Manajemen Aset Infrastruktur & Fasilitas* 2:45–55
11. IRAP (2015) IRAP Pilot technical report. World Bank, Washington DC, United States of America
12. IRAP. iRAP methodology fact sheets. In: IRAP. <https://www.irap.org/methodology>. Accessed 20 Sep 2020

Analyzing Zones and Accessibility of Public Senior High School in Makassar City



Ardiansyah, Syafruddin Rauf, and Sumarni Hamid Aly

Abstract This research analyses the accessibility of public transportation to senior high school locations. There are 12 public transportation routes with 5 sample public senior high schools (SMA Negeri) and 474 students in research of accessibility base on total time and total distance. We use two data in this research, walking to school from public transportation and walking to public transportation from school. SMA Negeri 4 Makassar has high accessibility of public transportation, and it's very good, SMA Negeri 5 Makassar has high accessibility and low accessibility of public transportation and then it is good, SMA Negeri 8 Makassar has very low accessibility public transportation and then it is so bad and must add another public transportation routes around it, SMA Negeri 16 Makassar has low accessibility of public transportation and very low accessibility of public transportation and then a closer public transportation route must add, and SMA Negeri 21 Makassar has medium accessibility of public transportation and then the accessibility of public transportation good enough for school. So, we hope that an additional length of public transportation routes to the school location is expected. In order to be a solution for government relate to public transportation.

Keywords Accessibility · Public transportation · Geographic information system (GIS)

Ardiansyah (✉) · S. Rauf (✉) · S. H. Aly (✉)
Department of Civil Engineering, Hasanuddin University, Gowa, South Celebes, Indonesia
e-mail: ardiday.day@gmail.com

S. Rauf
e-mail: syafrauf@yahoo.co.id

S. H. Aly
e-mail: marni_hamidaly@yahoo.com

1 Introduction

The admission zoning system priority closer distance of student residences to school in addition to increasing students' comfort level psychologically also increases students' and societies' sense of ownership of the school followed by parents and surrounding community [1].

Our proposed competitive accessibility measure combines information about the place of residence of students, the spatial distribution of public schools, and public transport accessibility into a single measure. Travel-to-school times by public transport are based on actual commuting times obtained through use of routing algorithms provided through an online service [2].

Student's journey from home to school is related to transportation. Starting from transportation facilities to infrastructure that connects all trips. Where the student's houses are connecting to the school with transportation infrastructure, road. The influence of traffic flow in students crossing areas makes the problem of density unavoidable. As the students' houses are further away from the school, the accessibility will be lower, which makes the trip even farther, which is directly proportional to the density of traffic flow. If the trip gets farther, the density point will pass by students too [3].

The improvement of public transportation facilities is carrying out in order to attract the public's interest to choosing these facilities on their movements for reducing traffic load on road network due to using private vehicles. The lack of public interest in using public transportation is due to the low accessibility of the transportation network system [4].

Makassar City has a high population density according to Badan Pusat Statistik 2019 data. High population density is relating to the condition of dense transportation flow [5]. The location of the school is one location of congestion due to the large number of public transport waiting for passengers or dropping passengers [6].

This research aims to analyze the accessibility of public transportation to the location of Senior High School.

2 Research Method

Figure 1 shows there are four steps in the research framework. First, the introduction starts from searching literature that relates to the research theme and developing the hypothesis. Second, preparation for survey. Third, collecting data is in two ways with primary data and secondary data. Fourth, analysis and modeling with descriptive and spatial analysis.

2.1 Research Location, Time and Research Tools

This research was conducted from August 2020 to December 2020, during which time the survey was conducting at the research location. Selection of research

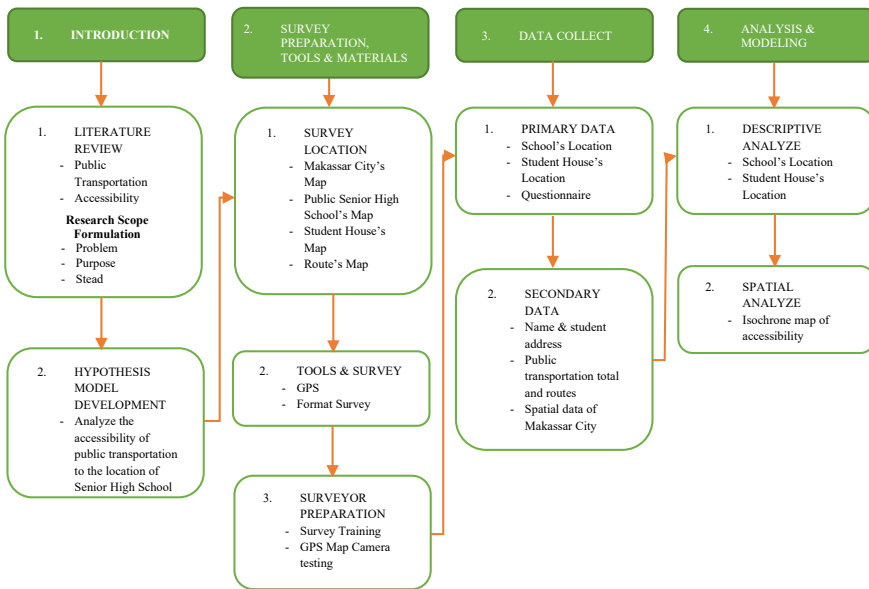


Fig. 1 Research framework

location based on preliminary study observation. The regional scope in this research is Makassar City. There are 22 public senior high schools for this research [7]. Equipment in this research is a GPS application. Where this application we use to sending the location of the school and student’s home. And a camera to take the front of the school.

2.2 Data Collect

In this study, we are using 2 data, primary data and secondary data. Primary data, conducting a direct survey to all locations of public high schools in Makassar City. By using the GPS application in determining the location of the school. Likewise, with the home location of students in the research sample, where the surveyors come to student’s houses and then took the coordinate of students’ houses. After visiting 22 schools, we take five school samples or 22.5% of public senior high schools in five zones in Makassar City (North of Makassar, East of Makassar, South of Makassar, West of Makassar, and Centre of Makassar) as research material because public transportation routes are not equal to all zone. And immediately to get accessibility of five zones in Makassar City. Then distribute questionnaires online and offline to school students. Secondary data, taken from each sample school administration, the form names and addresses of these students.

2.3 Data Analysis

Public transport route data is obtained from Dinas Perhubungan Makassar city which is useful to analyze the accessibility of public transportation to school. The data is entered into the QGIS application. To find out the support of public transportation for schools, data on students walking down from public transportation to school, and data on students walking out of school to public transportation. That data we get from the ORS plugin in the QGIS application. The accessibility of public transportation analyses based on total time and total distance against schools classify as high, medium, low, and very low. This classification is obtained from the results of analysis using SPSS application with percentile statistical method. Then by using the excel application, the accessibility and percentage of public transport accessibility determine to get a conclusion.

3 Research Finding and Discussion

3.1 Makassar City Transport Routes

Figure 2 shows the whole of public transport fleets operating in Makassar City which are 4113 units. And there are 12 city transportation service routes that go along the corner of Makassar City. In Fig. 2, there are 22.72% of public senior high

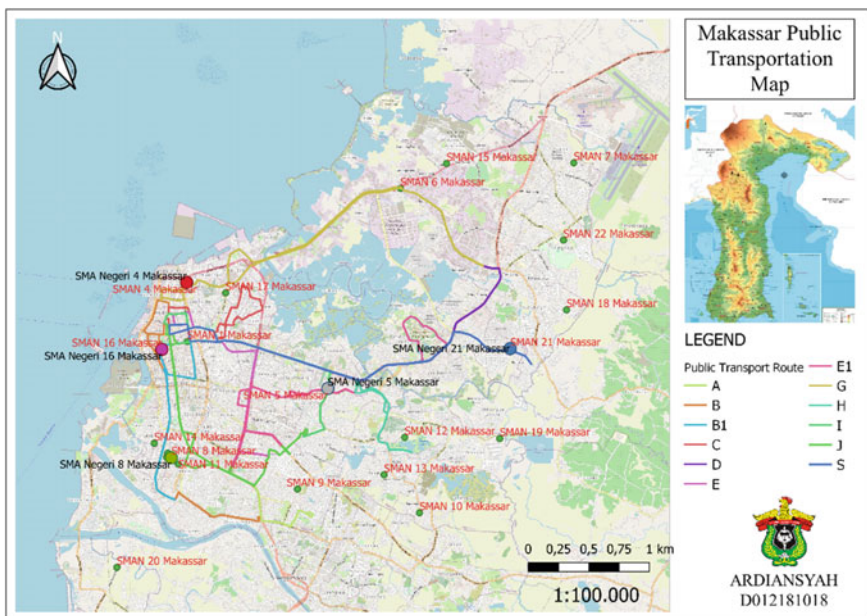


Fig. 2 Makassar public transportation routes map

Table 1 Makassar city public transport route

Code	Street Name	Length
A	Jl. Jend. Sudirman—Jl. DR. Ratulngi—Jl. S. Alauddin	24.252
B	Jl. Sulawesi—Jl. Ahmad Yani—Jl. Botolempangan—Jl. Arief Rate—Jl. Cendrawasih—Jl. Daeng Tata	22.449
B1	Jl. Kampus Unhas—Jl. P. Kemerdekaan—Jl. Urip Sumoharjo—Jl. Bawakaraeng—Jl. Botolempangan—Jl. Arif Rate—Jl. Cendrawasih	35.509
C	Jl. Cokroaminoto—Jl. Bandang—Jl. Mesjid Raya—Jl. Bawakaraeng—Jl. Sunu—Jl. Pongtiku—Jl. A. R. Hakim—Jl. Gatot Subroto—Jl. Juanda	11.322
D	Jl. Kapasa Raya—Jl. P. Kemerdekaan—Jl. Urip Sumoharjo—Jl. Andalas—Jl. K. H. Ramli—Jl. Cokroaminoto—Jl. Mesjid Raya	28.068
E	Jl. Toddopuli Raya—Jl. Tamalate—Jl. Mapala—Jl. A. P. Pettarani—Jl. Urip Sumoharjo—Jl. Andalas—Jl. P. Diponegoro—Jl. Bandang—Jl. Mesjid Raya	20.770
E1	Jl. Kampus Unhas—Jl. P. Kemerdekaan—Jl. Dr. J. Leimena—Jl. Abd. Dg. Sirua—Jl. A. P. Pettarani—Jl. Hertasning—Jl. Toddopuli Raya	30.650
G	Jl. Kalimantan—Jl. Tentara Pelajar—Jl. Yos Sudarso—Jl. Pannampu—Jl. Galangan Kapal—Jl. Teuku Umar—Jl. Prof. Ir. Sutami—Jl. Kapasa Raya	28.690
H	Jl. Dr. J. Leimena—Jl. Urip Sumoharjo—Jl. Jend. Sudirman—Jl. Cokroaminoto—Jl. Dr. W. Sudirohusodo—Jl. P. Diponegoro—Jl. Andalas—Jl. Mesjid Raya	23.313
I	Jl. Toddopuli Raya Timur—Jl. Batua Raya—Jl. Urip Sumoharjo—Jl. Jend. Sudirman—Jl. Cokroaminoto—Jl. Dr. W. Sudirohusodo—Jl. P. Diponegoro—Jl. Andalas—Jl. Mesjid Raya	18.689
J	Jl. Toddopuli Raya—Jl. Tamalate—Jl. S. Alauddin—Jl. Dr. Sam Ratulangi—Jl. Jend. Sudirman—Jl. Cokroaminoto—Jl. Nusa Kambangan	22.025
S	Jl. Tamalanrea Raya—Jl. P. Kemerdekaan—Jl. Urip Sumoharjo—Jl. G. Latimojong—Jl. Andalas—Jl. K. H. Ramli—Jl. Cokroaminoto—Jl. G. Bulusaraung—Jl. Mesjid Raya	27.384

schools that traverse by public transport routes. This will not make public transportation being the main choice.

Table 1 shows the total distance route of public transport and street name of traverse and average distance route of public transportation length in Makassar City is 24.42 km, with the longest distance is code B1 with 35.50 km and the shortest distance is code C with 11.32 km.

3.2 Time and Distance on Foot from Public Transportation to School

There are 474 student samples from 5 schools in Fig. 3 showing time and Fig. 4 showing distance to walk down from public transportation to the school location. At SMA Negeri 4 Makassar, there is one point where students get off from public transportation, which is right in front of the school at a distance of 2 m with a time

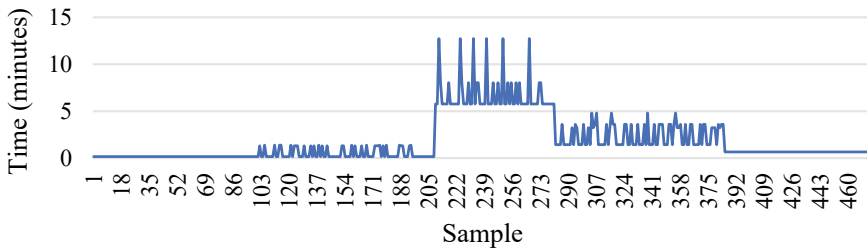


Fig. 3 Time on foot from public transportation to school

in 10 s. At SMA Negeri 5 Makassar, there are three points where students drop off from public transportation, right in front of SMA Negeri 5 Makassar with a distance of 2 m in 10 s, a distance of 112 m with a time in 1 min 19.2 s, and a distance of 116 m in 1 min 22.8 s. At SMA Negeri 8 Makassar, there are three points where students drop off from public transportation, a distance of 479 m in 5 min 45.6 s, a distance of 671 m in 8 min 2.4 s, and a distance of 1 km 59 m in 12 min 43.2 s. At SMA Negeri 16 Makassar, there are three points where students drop off from public transportation, 118 m in 1 min 26.4 s, a distance of 271 m in 3 min 14.4 s, and a distance of 399 m in 4 min 48 s. At SMA Negeri 21 Makassar, there is one point where students drop off from public transportation, a distance of 54 m in 39.6 s.

3.3 Time and Distance on Foot from School to Public Transportation

There are 474 student samples from 5 schools in Fig. 5 showing time and Fig. 6 showing distance on foot out of school to public transportation. At SMA Negeri 4 Makassar, there is one point location to take public transportation, which is right in front of the school at a distance of 2 m in 10 s. At SMA Negeri 5 Makassar, there are three-point locations for public transportation, in front of SMA Negeri 5 Makassar with a distance of 2 m in 10 s, a distance of 112 m in 1 min 19.2 s, and a distance of 116 m in 1 min 22.8 s. At SMA Negeri 8 Makassar, there are three-point locations for public transportation, distance 479 m in 5 min 45.6 s, distance 671 m in 8 min 2.4 s, and distance 1 km 59 m in 12 min 43.2 s. At SMA Negeri 16 Makassar, there are three points to take public transportation, distance 118 m in 1 min 26.4 s, distance 271 m in 3 min 14.4 s, and distance 399 m in 4 min 48 s. At SMA Negeri 21 Makassar, there is one point location for public transportation, the distance of 54 m in 39.6 s.

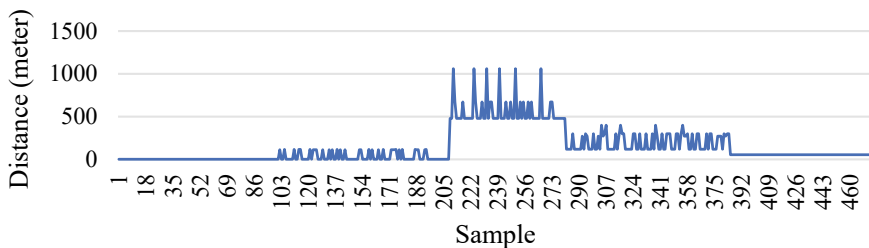


Fig. 4 Distance on foot from public transportation to school

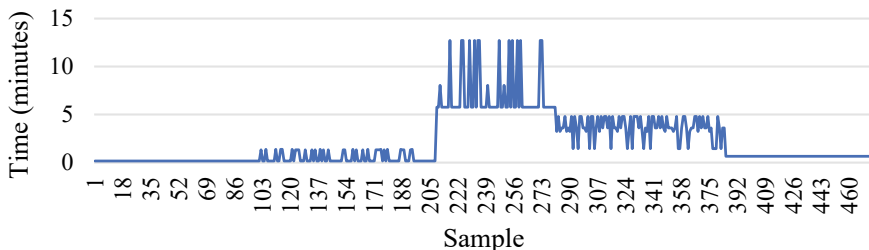


Fig. 5 Time on foot from school to public transportation

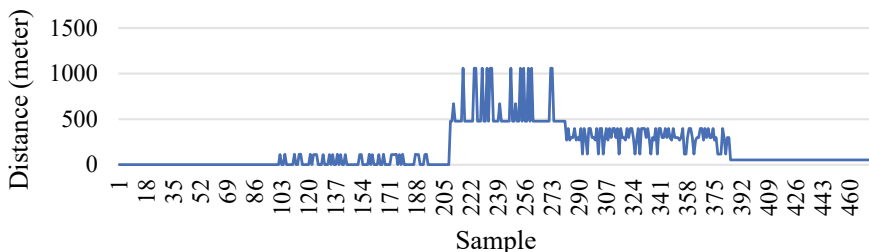


Fig. 6 Distance on foot from school to public transportation

3.4 Accessibility Based on Distance

Accessibility based on distance can be determined from total distance on foot student to public transportation around schools to see the role of public transportation for school. There are 2 data add in this study, distance walking to school and distance walking to public transportation.

Table 2 shows the classification of level accessibility base on total distance is dividing into four parts, starting from high, medium, low, and very low level. This classification is obtaining from results of analysis using SPSS application with percentile statistical method.

Table 2 Accessibility classification based on total distance

Classification	
High accessibility	Distance ≤ 4 m
Medium accessibility	4 m < Distance ≤ 108 m
Low accessibility	108 m < Distance ≤ 517 m
Very low accessibility	Distance >517 m

Figure 7 shows the Isochrone map of the QGIS application. We make this starting from input classification accessibility based on distance nominal to Isochrone Map plugin and the area in every level automatically showing. The white zone is showed high accessibility, the pink zone is showed medium accessibility, the red zone is showed low accessibility, and the dark red is showed very low accessibility.

Table 3 shows the result percentage of public transport accessibility base on the distance of the school sample. SMA Negeri 4 Makassar has high accessibility base on total distance with a value of 100%, SMA Negeri 5 Makassar has high public transportation accessibility with a value of 70.09%, and accessibility of public transportation is low with a value of 29.91% base on total distance, SMA Negeri 8 Makassar has very low public transportation accessibility with a value of 100% base on total distance, SMA Negeri 16 Makassar has low public transportation accessibility with a value of 68.93% and very low public transportation accessibility

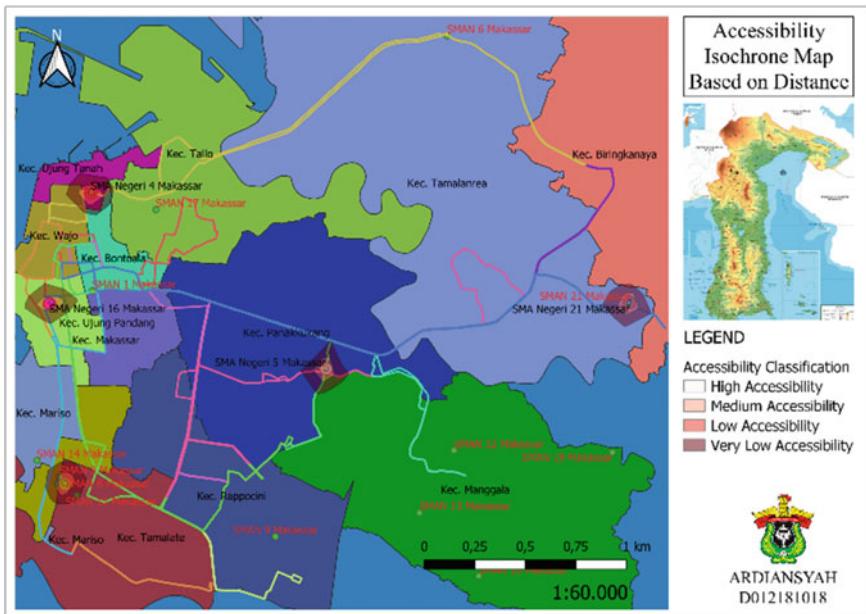


Fig. 7 Isochrone map of accessibility classification based on distance

Table 3 Accessibility percentage based on total distance

Accessibility	Schools				
	SMA Negeri 4 Makassar	SMA Negeri 5 Makassar	SMA Negeri 8 Makassar	SMA Negeri 16 Makassar	SMA Negeri 21 Makassar
High	100%	70.09%	0%	0%	0%
Medium	0%	0%	0%	0%	100%
Low	0%	29.91%	0%	68.93%	0%
Very low	0%	0%	100%	31.07%	0%

with a value of 31.07% base on total distance. And SMA Negeri 21 Makassar has medium public transportation accessibility with a value of 100% base on total distances.

3.5 Accessibility Based on Time

Accessibility based on time can be determined from the total foot time of students on public transportation around the school to see the role of public transportation for schools. There are 2 data adding in this study, time walking to school and time walking to public transportation.

Table 4 shows the classification of level accessibility based on total time is dividing into four parts, starting from high, medium, low, and very low level. This classification is obtaining from results analysis using SPSS application with percentile statistical method.

Figure 8 shows the Isochrone map of the QGIS application. We make this starting from input classification accessibility based on time nominal to Isochrone Map plugin and the area in every level automatically showing. The white zone is showed high accessibility, the pink zone is showed medium accessibility, the red zone is showed low accessibility, and the dark red is showed very low accessibility.

Table 5 shows the results percentage of public transport accessibility base on time in sample schools. SMA Negeri 4 Makassar has high accessibility base on total time with a value of 100%, SMA Negeri 5 Makassar has high public transportation accessibility with a value of 70.09%, and accessibility of public transportation is

Table 4 Accessibility classification based on total time

Classification	
High accessibility	Time \leq 20 s
Medium accessibility	20 s < Time \leq 1 m 19.2 s
Low accessibility	1 m 19.2 s < Time \leq 6 m 14.4 s
Very low accessibility	Time > 6 m 14.4 s

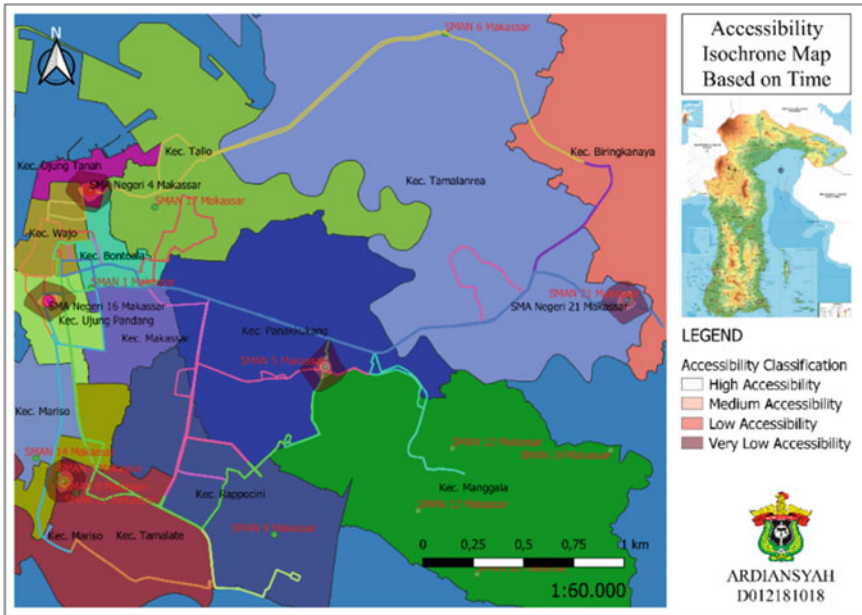


Fig. 8 Isochrone map of accessibility classification based on time

low with a value of 29.91% based on the total time, SMA Negeri 8 Makassar has very low public transportation accessibility with a value of 100% base on the total time, SMA Negeri 16 Makassar has low public transportation accessibility with a value of 68.93% and very low public transportation accessibility with a value of 31.07% base on the total time, and SMA Negeri 21 Makassar has medium public transportation accessibility with a value of 100% base on total time.

Table 5 Accessibility percentage based on total time

Accessibility	School				
	SMA Negeri 4 Makassar	SMA Negeri 5 Makassar	SMA Negeri 8 Makassar	SMA Negeri 16 Makassar	SMA Negeri 21 Makassar
High	100%	70.09%	0%	0%	0%
Medium	0%	0%	0%	0%	100%
Low	0%	29.91%	0%	68.93%	0%
Very low	0%	0%	100%	31.07%	0%

4 Conclusion

The accessibility of public transportation to the location of Senior High School is seeing from the total distance and total time that students on foot to public transportation around schools to see the role of public transportation for schools. There are two data adding in this research, total time and total distance walking to school and total time and total distance walking to public transportation. So that the data obtains to showing that the accessibility of public transportation is still very low to Senior High School location. From our research, SMA Negeri 4 Makassar has high accessibility base on total time and total distance with a value of 100% then the accessibility of public transportation is very good, SMA Negeri 5 Makassar has high public transportation accessibility with a value of 70.09% and low public transportation accessibility with a value of 29.91% base on total time and total distances and then the accessibility of public transportation is good, SMA Negeri 8 Makassar has very low public transport accessibility with a value of 100% base on total time and total distances and then it makes public transportation accessibility to SMA Negeri 8 Makassar very bad and must add public transportation routes around it, SMA Negeri 16 Makassar has low public transportation accessibility with a value of 68.93% and public transportation accessibility is very low with a value of 31.07% and then the accessibility of public transportation is poor to serve schools which must be add public transport route closer, and SMA Negeri 21 Makassar has medium public transport accessibility with a value of 100% and then the accessibility of public transportation is good enough for schools. An evaluation must make for good accessibility of public transportation and as soon as possible to add other public transportation routes to school locations and the surrounding locations.

Acknowledgements We would like to thank all those who support this research: our parents who always provide moral and material support, our supervisors Mr. Syafruddin Rauf and Mrs. Sumarni Hamid who give their time in preparation of this research, to school principals and staff who supported us in sampling the research, to leader and staff of BPS Makassar City, and to leader and staff of Dinas Perhubungan Makassar City who gives us access to data collection.

References

1. Bakar AK, Supriyati Y, Hanafi I (2019) Evaluation of admission student policy based on zoning system for acceleration education quality in Indonesia. *Journal of Management Info* 6:19–24
2. Moreno-Monroy IA, Ramos FR, Lovelace R (2018) Public transport and school location impacts on educational inequalities: insights from São Paulo. *J Transp Geogr* 67:110–118
3. Rauf S, Aboe F, Samang L (2013) Rute Pemetaan Dan Permintaan Angkutan Umum Kampus Universitas Hasanuddin Makassar Berbasis Quantum Gis Open Source, 1–10
4. Suthanaya PA (2009) Analisis Aksesibilitas Penumpang Angkutan Umum Menuju Pusat Kota Denpasar di Provinsi Bali. *GaneC, Swara Edisi Khusus* 3:87–93
5. Tamin O (2000) *Perencanaan & Pemodelan Transportasi*. Bandung Institute of Technology, Bandung, Indonesia

6. Perdana N (2019) Implementasi PPDB zonasi dalam upaya pemerataan akses dan mutu Pendidikan. *Jurnal Pendidikan Glasser* 3:1–15
7. Kementerian Pendidikan dan Kebudayaan Republik Indonesia (2019) Peraturan Menteri Pendidikan dan Kebudayaan Republik Indonesia Nomor 44 Tahun 2019 tentang Penerimaan Peserta Didik Baru pada Taman Kanak-kanak, Sekolah Dasar, Sekolah Menengah Pertama, Sekolah Menengah Atas, dan Sekolah Menengah Kejuruan, Jakarta, Indonesia

Evaluation Readiness of Contractor and Government in Implementing the Road Preservation Program: Case Study National Road in Indonesia



Maharani Pasha Umar, Ayomi Dita Rarasati,
and R. Jachrizal Sumabrata

Abstract The implementation of the road preservation program in Indonesia has been regulated by the Ministry of Public Works and Public Housing to ensure that road infrastructure can carry out its role properly to improve Indonesia's social and economic mobility. The implementation of the road preservation program is very dependent on the stakeholders who carry it out. The performance indicators of contractors and government are the main things in achieving the quality of the output from implementing the road preservation program. The contractor's performance and government's performance were obtained from the distribution of questionnaires filled out with a total of 62 respondents. The results show that the readiness of the contractor to support the government is 80.65%, the attitude of the contractor is 93.55%, the understanding of the contractor is 90.32%, the financial aspect is 93.54%, and the accuracy of the schedule is 80.65% of the implementation performance—road preservation program. Meanwhile, the government's readiness for the application of technology was 35.48%, and the government's attitude was 45.16% on the performance of the road preservation program implementation and all the hypotheses are accepted.

Keywords Contractor readiness · Government readiness · Road preservation program

1 Introduction

Based on data from the Ministry of Public Works and Public Housing, the length of the national road in Indonesia reaches 47,017.39 km (under the authority of the central government). Based on road conditions, 50% of national roads are in moderate, damaged, and severely damaged condition which is 23,293.05 km.

M. P. Umar (✉) · A. D. Rarasati · R. J. Sumabrata
Department of Civil Engineering, Faculty of Engineering, Universitas Indonesia, Depok,
Indonesia
e-mail: maharanipashaumar@gmail.com

Meanwhile, 50% of national roads are in good condition which is 23,724.34 km [1]. According to the United States National Park Service, road conditions will start to deteriorate due to solar radiation, waterlogging, and traffic loads that are not as planned [2].

Preventive maintenance is maintenance that is carried out before component failure in a predetermined period before or by specified criteria and is provided to reduce the failure rate or deterioration of the function of an object [3]. Meanwhile, based on the Regulation of the Minister of Public Works Number 13/PRT/M/2011, road maintenance is divided into 4, namely: (1) routine maintenance, (2) periodic maintenance, (3) rehabilitation, (4) reconstruction [4]. Suppose the road preservation program in Indonesia has been running optimally. In that case, good road conditions in Indonesia should dominate over damaged road conditions, so it is necessary to evaluate the performance of contractors and the government in implementing the road preservation program. Meanwhile, based on the surface, 326,629 km (60.7%) of roads in Indonesia are in the form of asphalt, 179,457 km (33.37%) are gravel and soil, and the surface in other forms reaches 31,752 km (5.9%).

The indicators that influence the optimal implementation of the road preservation program carried out by the government are: (1) the application of technology, (2) government attitude. Apart from the government, indicators that affect the optimal implementation of the road preservation program carried out by contractors must also be evaluated, namely: (1) support for the government, (2) contractor attitude, (3) contractor's understanding, (4) financial aspects, (5) schedule accuracy.

This research aims to evaluate the performance of contractors and the government in implementing the road preservation program from indicators related to the questionnaire method.

2 Method

The framework used to conduct research using the method of distributing questionnaires to respondents. Respondents for contractor readiness are government employees. Meanwhile, respondents for government readiness are contractor employees with the following criteria for respondents: (1) minimum education 3-year Diploma, (2) minimum three years experience in the road preservation program.

Respondents will provide an assessment of the implementation of the road preservation program implemented by the contractor or government to determine the performance or readiness of the contractor and the government; the assessment is carried out using a Likert scale from a scale of 1 (strongly disagrees) and 6 (strongly agrees). From 31 people who filled out the questionnaire, 29% had work experience for 3–5 years, 3% for 11–15 years, while 68% had 16–20 years. And, 45% have educational qualifications as a bachelor's degree and 55% as an

undergraduate degree. While filling out the questionnaire related to the readiness to government consisted of 31 respondents with work experience qualifications of 90% for 3–5 years and 10% for 6–10 years. And, 19% have educational qualifications as an associate’s degree, 78% as a bachelor degree, and 3% as an undergraduate degree.

The operational research model consists of: (1) literature studies are used to determine the problem by collecting data from various sources related to the topic raised, (2) problem identification is used to determine the problem which will be discussed in research, (3) variable determination is used to specify indicators that determine the readiness of contractor and government, (4) questionnaire deployment for the readiness of the contractor is deployed to government employees whilst questionnaire deployment for the readiness of government is deployed to contractor employees, (5) data collection is done online which spreads the questionnaire to the respondents who meet the criteria, (6) validity and reliability test for the instrument in the questionnaire, from determining indicators the readiness of contractor and government are divided into 3 categories which are high, medium, and low, (7) linear regression analysis is done to know if the indicators which affect the contractor and government readiness to be accepted or not.

3 Data Analysis

3.1 Contractor Readiness

Research to determine the performance of contractors in implementing road preservation programs using primary data, namely answers from respondents. The construct variables used in this study consist of 6 indicators with 42 instruments [5–11], the indicators that affect the readiness of the contractor and indicator the readiness of the contractor can be seen in Tables 1, 2, 3, 4, 5, and 6.

These are five indicators that determine the contractor’s readiness to implement the road preservation program, with readiness divided into three categories: high, medium, and low. The contractor readiness and indicators that affect can be seen in Tables 7, 8, 9, 10, and 11.

Table 1 Support for the government indicator that affects the readiness of contractor

Variable	Reliability	Validity
The contractor responds to the government quickly	0.8020654	Valid
The contractor has the same thought as the government		Valid

Table 2 Contractor attitude indicator that affects the readiness of contractor

Variable	Reliability	Validity
The contractor always coordinates with the government on any problems	0.87357496	Valid
The contractor takes corrective action for the needs of the project		Valid
The contractor selects equipment effectively and as needed		Valid
The contractor provides additional resources to meet targets		Valid
The contractor conducts the survey on an ongoing basis		Valid
The contractor inputs data online and in real-time		Valid
The contractor carries out a preservation program in accordance with the work plan		Valid
The contractor evaluates after every repair		Valid
The contractor carries out heavy equipment maintenance		Valid
The contractor conducts a daily inspection of pavement conditions, cut and fill, drainage, and all structures		Valid
The contractor follows the inspection results for maintenance work planning		Valid
The contractor carries out emergency maintenance in the event of an accident or disaster		Valid
The contractor has technical specifications for road maintenance based on on-site surveys, natural conditions surveys, social and environmental surveys		Valid
If a scope change occurs, the contractor quickly notifies every stakeholder		Valid

Table 3 Contractor’s understanding indicator that affects the readiness of contractor

Variable	Reliability	Validity
The contractor more concerns with project quality	0.8226	Valid
The contractor knows the age of the pavement under review		Valid
The contractor knows the cause of the damage		Valid
The contractor determines the extent of the damage		Valid
The contractor determines the priority of the roads that receive corrective action		Valid
The contractor uses work methods that comply with quality standards		Valid
The contractor uses a work method in accordance with the characteristics of the material		Valid
The contractor uses a work method in accordance with the environment		Valid
The contractor has a form to document field data		Valid

Table 4 Financial aspect indicator that affects the readiness of contractor

Variable	Reliability	Validity
The contractor has a clear payment system in the internal system	0.6855	Valid
The contractor and the government have a payment agreement that is in accordance with the agreement		Valid
The contractor always coordinates with the government on any problems		Valid
The contractor prepares for construction material price fluctuations		Valid

Table 5 Schedule accuracy indicator that affects the readiness of contractor

Variable	Reliability	Validity
The contractor always works according to the planned schedule	0.9227	Valid
The contractor prioritizes the project objectives so that there is no overscheduling		Valid

Table 6 Indicators of the readiness of contractor

Variable	Reliability	Validity
The project did not exceed the budget due to negligence of the contractor	0.8389	Valid
The project head has good managerial skills		Valid
The contractor distributes the workforce as needed		Valid
The contractor has the ability to solve a problem quickly and precisely		Valid
The contractor has experience working on similar projects in the past		Valid
Contractors working on projects meet technical specifications		Valid
The contractor evaluates the performance of the supplier/ subcontractor		Valid
The contractor has a skilled workforce in implementing road preservation programs		Valid
The contractor applies reward and punishment to workers		Valid
The contractor meets safety standards in implementing the road preservation program		Valid

Table 7 Contractor's readiness for support to the government

Category	Interval	F	%
High	10–12	25	80.65
Medium	6–9	6	19.35
Low	2–5	0	0.00
Total		31	100.00

Table 8 Contractor’s readiness for support to contractor’s attitude

Category	Interval	F	%
High	61–84	29	93.55
Medium	38–60	2	6.45
Low	14–37	0	0.00
Total		31	100.00

Table 9 Contractor’s readiness for support to contractor’s understanding

Category	Interval	F	%
High	44–60	28	90.32
Medium	28–43	3	9.68
Low	10–27	0	0.00
Total		31	100.00

Table 10 Contractor’s readiness for support to financial aspects

Category	Interval	F	%
High	18–24	29	93.5483871
Medium	11–17	2	6.451612903
Low	4–10	0	0
Total		31	100.00

Table 11 Contractor’s readiness for support to schedule accuracy

Category	Interval	F	%
High	10–12	25	80.65
Medium	6–9	6	19.35
Low	2–5	0	0.00
Total		31	100.00

3.2 Government Readiness

Research to determine government performance in implementing road preservation programs uses primary data, namely answers from respondents. The construct variables used in this study consist of 3 indicators with 36 instruments [7, 9–13], the indicators that affect the readiness of government and indicators of the readiness of contractor can be seen in Tables 12, 13, and 14.

There are two indicators determining the government’s readiness to implement the road preservation program, with readiness divided into three categories: high, medium, and low. The government readiness and indicators that affect can be seen in Tables 15 and 16.

Table 12 Technology indicators that affect the readiness of government

Variable	Reliability	Validity
The government chooses to use the latest technology in the implementation of the road preservation program	0.6761	Valid
The government has a development strategy related to road preservation programs		Valid

Table 13 Government attitude indicators that affect the readiness of government

Variable	Reliability	Validity
The government collects project-related information	0.8527	Valid
The government gathers stakeholders		Valid
At the planning stage, the government conducts negotiations with stakeholders		Valid
The government regularly updates the scheduling		Valid
The government manages risks that occur during the implementation period		Valid
The government carefully manages every procurement		Valid
At the closing stage, the government closes any work with stakeholders administratively		Valid
The government conducts an environmental and social impact assessment		Valid
The government conducts an evaluation after road repair		Valid
The government controls the contractors		Valid
The government controls the supervisory consultant		Valid
The government controls implementations costs		Valid
The government controls the quality of construction		Valid
The government carries out routine monitoring		Valid
The government maintains a relationship with the community so that the community always provides input on road conditions	Valid	

3.3 Linear Regression Analysis

Linear regression analysis is done by comparing t-table and t-test. To get t-test, the instrument is processed using software SPSS whilst the t-table is got by calculating $(a/2; n - 1)$. The hypothesis used in this research is:

- H0 = Contractor and government readiness do not affect the implementation of the road preservation program.
- H1 = Contractor and government readiness affect the implementation of the road preservation program.

Table 14 Indicators of the readiness of government

Variable	Reliability	Validity
The government has the ability and empowerment to implement road preservation programs	0.9504	Valid
The government has workers with educational qualifications and skills in accordance with the needs of the person in charge of implementing the road preservation program		Valid
The government has workers who obey the rules that have been set		Valid
The government has a budget related to the implementation of the road preservation program		Valid
The government has the engineered funding so that maintenance funds are always available		Valid
The government has managerial experience in the road preservation program		Valid
The government is able to control contract administration		Valid
The government has a list of road ownership		Valid
The government has a road management list		Valid
The government has road identification data under review		Valid
The government has documents of the road damage conditions		Valid
The government conducts a road structural assessment (IRI score) twice a year		Valid
The government has Average Daily Traffic (ADT) data		Valid
The government know the weather conditions		Valid
The government has a track record of implementation		Valid
The government has Term of Reference (TOR)		Valid
The government knows the conditions in the field		Valid
The government has the policy to prevent traffic accidents	Valid	

Table 15 Government readiness to technology application

Category	Interval	F	%
High	10–12	11	35.48
Medium	6–9	19	61.29
Low	2–5	1	3.23
Total		31	100

Table 16 Government readiness to government attitude

Category	Interval	F	%
High	69–96	14	45.16
Medium	43–68	17	54.84
Low	16–42	0	0.00
Total		31	100

The following is the result of the linear regression analysis:

1. Support for the government, from data processing using SPSS software can be seen in Table 17.

Based on data analysis using SPSS, the result of the regression equation are shown in Eq. 1.

$$Y = 25.088 + 2.642 \tag{1}$$

With the following conclusions:

- The constant value of the regression equation of the relationship between the independent variable and dependent variable is 25.088, meaning that if there is no change in the variable (Support to the Government), then the contractor’s readiness to implement the preservation is 25.088 units
 - The t-test value was 4.496, while the t-table value = 2.04227. so that the t-test value is bigger than the t-table (4.496 > 2.04227), then h0 is rejected, and h1 is accepted, so the hypothesis which reads that support for the government affects the implementation of the road preservation program is accepted.
2. Contractor attitude, from data processing using SPSS software can be seen in Table 18.

Based on data analysis using SPSS, the results of the regression equation are shown in Eq. 2.

$$Y = 8.876 + 0.618 \tag{2}$$

With the following conclusions:

- The constant of the regression equation of the relationship between the independent variable and the dependent variable is 8.876, meaning that if there is no change in a variable (Contractor’s Attitude), then the contractor’s readiness for the implementation of the preservation program is 8.876 units.
- The t-test value was 7.515, while the t-table value = 2.04227. So that the t-test value is bigger than the t-table (7.515 > 2.04227), then h0 is rejected, and h1 is

Table 17 Regression test results in support for the government

Coefficients ^a						
Model		Unstandardized coefficients		Standardized coefficients	t	Sig
		B	Std. Error	Beta		
1	(Constant)	25.088	6.509		3.854	0.001
	Support to the Government	2.642	0.588	0.641	4.496	0.000

^aDependent variable: contractor readiness

Table 18 Regression test results contractor attitude

Coefficients ^a						
Model		Unstandardized coefficients		Standardized coefficients	t	Sig
		B	Std. Error	Beta		
1	(Constant)	8.876	6.053		1.466	0.153
	Contractor attitude	0.618	0.082	0.813	7.515	0.000

^aDependent variable: contractor readiness

Table 19 Regression test results contractor’s understanding

Coefficients ^a						
Model		Unstandardized coefficients		Standardized coefficients	t	Sig
		B	Std. Error	Beta		
1	(Constant)	20.179	9.041		2.232	0.034
	Contractor’s understanding	0.663	0.176	0.574	3.770	0.001

^aDependent variable: contractor readiness

accepted, so the hypothesis that says contractor attitude affects the implementation of the road preservation program is accepted.

3. The contractor’s understanding of data processing using SPSS software can be seen in Table 19.

Based on data analysis using SPSS, the results of the regression equation are shown in Eq. 3.

$$Y = 20.179 + 0.663 \tag{3}$$

With the following conclusions:

- The constant value of the regression equation of the relationship between the independent variable and the dependent variable is 20.179, meaning that if there is no change in a variable (Contractor’s Understanding), then the contractor’s readiness for the implementation of the preservation program is 20.179 units
 - The t-test value was 3.770, while the t-table value = 2.04227. So that the t-test value is bigger than the t-table (3.770 > 2.04227), then h0 is rejected, and h1 is accepted, so the hypothesis which reads that contractor understanding affects the implementation of the road preservation program is accepted.
4. The financial aspect, from data processing using SPSS software can be seen in Table 20.

Table 20 Regression test results financial aspect

Coefficients ^a						
Model		Unstandardized coefficients		Standardized coefficients	t	Sig
		B	Std. Error	Beta		
1	(Constant)	13.751	5.817		2.364	0.025
	Financial aspect	1.938	0.277	0.792	6.986	0.000

^aDependent variable: contractor readiness

Based on data analysis using SPSS, the results of the regression equation are shown in Eq. 4.

$$Y = 13.751 + 1.938 \tag{4}$$

With the following conclusions:

- The constant value of the regression equation of the relationship between the independent variable and the dependent variable is 13.751, meaning that if there is no change in a variable (Financial Aspect), the contractor’s readiness for the implementation of the preservation program is 13.751 units
- The t-test value was 6.986 while the t-table value = 2.04227. So that the t-test value is bigger than the t-table (6.986 > 2.04227), then h0 is rejected, and h1 is accepted, so that the hypothesis that the financial aspect affects the implementation of the road preservation program is accepted.

5. Schedule accuracy from data processing using SPSS software can be seen in Table 21.

Based on data analysis using SPSS, the results of the regression equation are shown in Eq. 5.

$$Y = 20.338 + 3.066 \tag{5}$$

Table 21 Regression test results schedule accuracy

Coefficients ^a						
Model		Unstandardized coefficients		Standardized coefficients	t	Sig
		B	Std. Error	Beta		
1	(Constant)	20.338	3.351		6.070	0.000
	Schedule accuracy	3.066	0.300	0.884	10.206	0.000

^aDependent variable: contractor readiness

With the following conclusions:

- The constant value of the regression equation of the relationship between the independent variable and the dependent variable is 20.338, meaning that if there is no change in the variable (Schedule Accuracy), the contractor’s readiness for the preservation program is 20.338 units
 - The t-test value was 10.206 while the t-table value = 2.04227. So that the t-test value is bigger than the t-table (10.206 > 2.04227), then h0 is rejected, and h1 is accepted, so that the hypothesis that reads schedule accuracy affects the implementation of the road preservation program is accepted.
6. Technology, from data processing using SPSS software can be seen in Table 22.

Based on data analysis using SPSS, the results of the regression equation are shown in Eq. 6.

$$Y = 32.170 + 5.673 \tag{6}$$

With the following conclusions:

- The constant value of the regression equation of the relationship between the independent variable and the dependent variable is 32.170, meaning that if there is no change in the variable (Technology Application), then the government’s readiness to implement the preservation program is 32.170 units
 - The t-test value was 5.885 while the t-table value = 2.04227. So that the t-test value is bigger than the t-table (5.885 > 2.04227), then h0 is rejected, and h1 is accepted, so the hypothesis which reads that technology affects the implementation of the road preservation program is accepted.
7. Government attitude, from data processing using SPSS software can be seen in Table 23.

Based on data analysis using SPSS, the results of the regression equation are shown in Eq. 7.

$$Y = 4.343 + 1.124 \tag{7}$$

Table 22 Regression test results technology

Coefficients ^a						
Model		Unstandardized coefficients		Standardized coefficients	t	Sig
		B	Std. Error	Beta		
1	(Constant)	32.170	8.498		3.785	0.001
	Technology	5.673	0.964	0.738	5.885	0.000

^aDependent variable: Government readiness

Table 23 Regression test results government attitude

Coefficients ^a						
Model		Unstandardized coefficients		Standardized coefficients	T	Sig
		B	Std. Error	Beta		
1	(Constant)	4.343	9.759		0.445	0.660
	Government attitude	1.124	0.141	0.828	7.953	0.000

^aDependent variable: Government readiness

With the following conclusions:

- The constant value of the regression equation of the relationship between the independent variable and the dependent variable is 4.343, meaning that if there is no change in the variable (Government Attitude), then the government’s readiness to implement the preservation program is 4.343 units.
- The t-test value was 7.953 while the t-table value = 2.04227. So that the t-test value is bigger than the t-table ($7.953 > 2.04227$), then h_0 is rejected, and h_1 is accepted, so the hypothesis which reads that government attitude affects the implementation of the road preservation program is accepted.

4 Conclusion

The contractor’s readiness to support the government was 80.65%, the contractor’s attitude was 93.55%, the contractor’s understanding was 90.32%, the financial aspect was 93.54%, and the accuracy of the schedule was 80.65% on the performance of the implementation of the road preservation program.

Meanwhile, the government’s readiness for the application of technology was 35.48%, and the government’s attitude was 45.16% on the performance of the road preservation program implementation, which was obtained from 31 respondents as government employees and 31 respondents for contractor employees. All the results from linear regression analysis show all the hypotheses are accepted.

5 Result and Discussion

It can be seen from the results that the readiness of contractors from all indicators is greater than 80% with input from government employees, namely that it must improve the quality of human resources, while the readiness of the government of all indicators is not more than 50%. With input from contractor employees,

improving standard operating procedures for road preservation programs and conducting detailed evaluations every time they perform maintenance. The application of technology is unavoidable at this time; the use of an integrated system is something that can facilitate road maintenance decisions in the implementation of road preservation programs so that a breakthrough is needed that connects the information system and the implementation of road preservation program.

References

1. Direktorat Pengembangan Jaringan Jalan (2019) Laporan Kondisi Jalan Nasional. Direktorat Jenderal Bina Marga, Jakarta, Indonesia
2. National Park Service U.S. Department of Interior (2018) National park service active transportation guidebook. National Park Service U.S. Department of Interior, Washington DC, United States of America
3. Tsang AHC (1995) Condition-based maintenance: tools and decision making. *J Qual Maint Eng* 1:3–17
4. Peraturan Menteri Pekerjaan Umum dan Perumahan Rakyat (2011) Peraturan Menteri Pekerjaan Umum dan Perumahan Rakyat tentang Tata Cara Pemeliharaan dan Penilikan Jalan. Kementerian Pekerjaan Umum dan Perumahan Rakyat, Jakarta, Indonesia
5. Bryde DJ, Robinson L (2005) Client versus contractor perspectives on project success criteria. *Int J Project Manage* 23:622–629. <https://doi.org/10.1016/j.ijproman.2005.05.003>
6. Selatan DIS (2017) Kesiapan Kontraktor Terhadap Kebijakan Preservasi Jalan Nasional Di Sumatera Selatan. *Jurnal HPJI* 2:133–142
7. JICA (2015) Chapter 14 Proposed road operation and maintenance plan. In: Proposed road operation and maintenance plan. JICA, Tokyo, Japan, pp 1–112
8. Ramadhan A, Latief Y, Sagita L (2019) Development of risk-based standardized work breakdown structure for quality planning of airport construction project. *J Phys: Conf Ser* 1360:2593–2602. <https://doi.org/10.1088/1742-6596/1360/1/012005>
9. Kiranasari RW, Aryani RA, Suparyitno H (2020) Penentuan Faktor bagi Analisis Faktor Keberhasilan Proyek Preservasi Jalan Skema Long segment factors determination for success factor analysis of long segment. *Jurnal Manajemen Aset Infrastruktur Dan Fasilitas* 4:77–90
10. Hakim MLA (2015) Studi Evaluasi Pelaksanaan Kebijakan Pemeliharaan Jalan Kota di Kota Surabaya. *Kebijakan Dan Manajemen Publik* 3:1–11
11. Nugraha YA (2010) Pada Program Preservasi Jalan. Direktorat Preservasi Jalan, Jakarta, Indonesia
12. Davis FD (1989) Perceived usefulness, perceived ease of use, and user acceptance of information technology. *MIS Q: Manage Inf Syst* 13:319–339. <https://doi.org/10.2307/249008>
13. Andersen ES (2012) Illuminating the role of the project owner. *Int J Manag Proj Bus* 5:1–15. <https://doi.org/10.1108/17538371211192900>

Analysis of Travel Behavior Under Flooding Condition Based on Probe Data in Ubon Ratchathani City, Thailand



Noriyasu Tsumita, Kohga Miyamura, Sittha Jaensirisak, and Atsushi Fukuda

Abstract Recently, urban floods have frequently occurred and severely affected urban activities in developing cities. To minimize the impacts of transport from urban flooding, it is essential to implement adaptation measures in the transport field. Firstly, it is crucial to understand the impacts of travel behaviors and traffic states from urban flooding. Therefore, this study focused on the relationship between travel speed and inundation depth and evaluating adaptation measures in the transport field. The relationship between travel speed and inundation depth was analyzed based on the probe data. A traffic assignment model was developed to evaluate the raising arterial road measure as an adaptation measure in the transport field while reflecting the analysis results of relationships between travel speed and inundation depth. This found that the implementation in raising arterial road measure for the western bypass could be an effective adaptation measure by reducing Vehicle Kilometer Traveled (VKT) by 65% while decreasing the number of detoured by 5000 vehicles compared to the flooding situation without taking any adaptation measures.

Keywords Travel behavior · Urban flooding · Probe data · Adaptation measure

N. Tsumita (✉) · K. Miyamura

Program of Transportation Systems Engineering, Nihon University College of Science and Technology, Narashinodai Funabashi-shi 2748501, Japan
e-mail: csno20001@g.nihon-u.ac.jp

S. Jaensirisak

Department of Civil Engineering, Faculty of Engineering, Ubon Ratchathani University, Ubon Ratchathani 34190, Thailand

A. Fukuda

Department of Transportation Systems Engineering, Nihon University College of Science and Technology, Narashinodai Funabashi-shi 2748501, Japan

1 Introduction

Nowadays, the impacts of extreme weather events such as downpours and storms could no longer be neglected in the cities of Southeast Asia. 30% of the total floods occurred in the Asia region [1, 2]. Urban flooding has caused severe damages to the residents. Not only does it cause buildings and housings to collapse, but it also hinders urban activities due to disruptions of road sections and bridges. With the growing concerns of global warming, the negative impact on transportation tends to become more severe due to extreme weather events caused by climate change. Ensuring a resilient urban transport system is necessary to minimize the effects of urban life on residents and social or economic costs [3, 4].

To counter the effects of urban floods on urban activities, including transportation, it is essential to implement adaptation measures by focusing on the transport field. Therefore, some of the national and local governments have established climate change adaptation plans and strategies during the last decade [5]. For example, the Thai government has begun developing a draft of the National Adaptation Plan (NAP) [6]. Mainly, in developing countries, it is essential to take mitigation policies to minimize greenhouse gas emissions and adaptation measures to prevent the increase in damages caused by natural disasters, including urban floods. This means that urban transportation should be both low carbon and resilient as much as possible. Until now, mitigation policies in the transport field are actively discussed not only in developed countries but also in developing countries. However, it is insufficient to implement and evaluate adaptation measures in the transport field. To minimize the impacts of extreme weather events damages and to take effective adaptation measures, it is necessary to appropriately understand the impacts of transport and analyze adaptation measures in the transport field, including the actual travel behavior data and traffic state data.

Thus, this study aims to analyze the travel behaviors under the flooding condition and evaluate the adaptation measures in Ubon Ratchathani City, Thailand. Specifically, the impacts of traffic states were analyzed using probe data under the flooding conditions. The relationships with the inundation depth for five travel speed range under the usual condition and flooding condition were estimated. Furthermore, the raising arterial road measure was evaluated based on the results of traffic assignment reflecting the analysis of probe data, which shows the relationship between travel speed and inundation depth. By reflecting on these data, it is possible to analyze and evaluate the adaptation measures under the actual impacts of urban floods on transport systems.

This study proceeded according to the following procedure. In Sect. 2, some literature about the analysis of traffic states based on the various data and the evaluation of adaptation measures in the transport field was reviewed. The analysis framework details, analysis of traffic states by the probe data, and the methodology for evaluating adaptation measures in the transport field are explained in Sect. 3. The results and discussions of the impacts on traffic state under flooding conditions

and simulated traffic assignment for evaluation of adaptation measures, including the analysis of probe data, are presented in Sect. 4. Finally, Sect. 5 concludes the main idea of the paper.

2 Literature Review

Recently, utilizing mobile data has become effective for the method of grasping changes in traffic conditions on the road. The most common is research that estimates traffic states based on big data extracted from probe data. There are many studies using this approach to analyze the impact of urban floods on urban activity [7–9]. These studies have clarified the traffic states, such as travel time and route choice behavior under usual and flooding conditions. Adaptation measures to avoid and reduce the flooding impacts on travel behaviors have been considered and evaluated [10–12]. To ensure mobility in the network, many studies were done to identify effective adaptation measures prioritizing resilient transport systems by selecting vulnerable road sections, and critical points should be identified. Also, various studies on road transportation have identified transport system vulnerabilities, especially road transportation, through network analysis (e.g., Multicriteria analysis, Accessibility, Serviceability) based on graph theory [13, 14]. Moreover, to analyze the impacts of traffic status under the flooding condition, some studies focused on the relationship between travel speed and inundation depth or volume of rainfall based on the literature reviews and experimental data [15–18]. These studies clarified that the inundation caused by the flood has a significant influence on the traffic condition.

However, many existing studies have insufficiently considered the evaluation of adaptation measures in the transport field, including actual travel behaviors or traffic status based on past travel behavior data under the flooding condition. In this study, the relationship between travel speed and inundation depth based on the analysis of probe data was clarified. After that, the adaptation measures on the transport field by traffic assignment reflecting based on that relationship was evaluated as a case study of Ubon Ratchathani City, Thailand.

3 Methodology

In order to understand the flooding impacts on road transportation, the difference in travel speed under the usual and flooding conditions was analyzed based on the probe data as a case study of Ubon Ratchathani City, Thailand. Specifically, travel speed was calculated and compared under both conditions for understanding the relationship between expected inundation depth data and decrease in travel speed. When analyzing the decrease in travel speed, even at the same inundation depth, the volume of decrease in travel speed could differ depending on the travel speed until a

certain inundation depth. Therefore, this study classified the travel speed under the usual condition and analyzed the decrease in travel speed in each travel speed range based on the inundation depth. After that, the raising arterial road measure as an adaptation measure in the transport field was evaluated to reduce urban flood damages, reflecting this relationship by using calculation of traffic assignment.

3.1 Study Area

In this study, we selected Ubon Ratchathani City in Northeastern Thailand as the case study area, as shown in Table 1. Citizens in Ubon Ratchathani City have suffered severe damages caused by urban floods during the rainy seasons (May–October). This city was divided into north and south areas by the Mun River, which could get over this river by four road sections (No. 1: Western Bypass, No. 2 and 3: Center Bridge, and No. 4: Eastern Bypass), as shown in Fig. 1.

In this city, the most severe floods occurred in 1938, 1950, 1978, and 1998–2002 due to a significant runoff in the upstream water. In 2002, many buildings and road sections, including four bridges crossing the river, were inundated and disrupted, caused by an urban flood. The total losses were estimated at more than 1 billion THB (31.4 THB \approx 1 US\$). However, flood countermeasures such as the development of floodwalls and dams could not wholly avoid the impacts of urban floods. Therefore, the mobility or accessibility for residents has a substantial reduction. To ensure mobility under flooding conditions, the local government has elevated the western and eastern bypasses by approximately 50–150 cm after urban floods occurred in 2002 [19]. Elevation of bypasses was expected to prevent the interruption of all the Mun River crossings and maintained accessibility during floods for reducing the adverse effects in the residents' routines and urban activities.

Later in September 2019, the harshest urban floods in the past 17 years occurred in Ubon Ratchathani City (shown in Fig. 2 [20]). Fortunately, the eastern and western bypasses were not disrupted because the level of the bypasses was raised

Table 1 Adaptation measures on the transport field

Classification	Adaptation measures
Soft	Improvement of climatic prediction
	Provision of condition and extreme weather
	Regulation of information on condition/extreme weather
	Development of emergency plans among transportation
	The usage of hazard maps
Hard	Elevation of roads
	The setting of emergency roads
	Improvement of drainage systems
	The usage of drainage asphalt

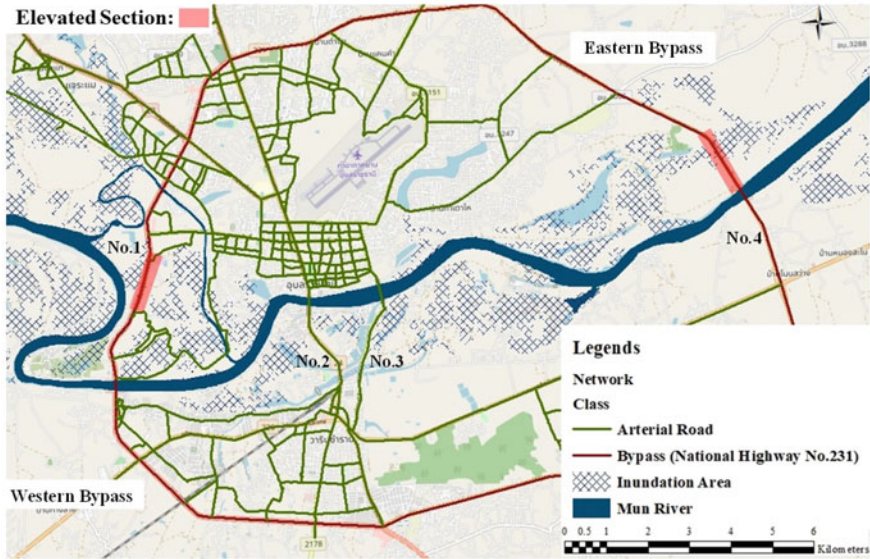


Fig. 1 Map of Ubon Ratchathani City, Thailand

after flooding in 2002. Thus, these bypasses were used as alternative routes (red lines in Fig. 1). On the other hand, some of the western bypasses were flooded if the inundation depth is significantly high, making it difficult to pass through (with relatively slow speed). However, the western bypass was also sometimes used as an alternative route for residents because of the shorter distance (compared to the western side). The level of the routes in the middle (No. 2 and 3) were very low, so they were flooded with a high depth of water.



Fig. 2 Actual flooding condition in September 2019 [20]

3.2 Analysis of Relationship Between Travel Speed and Inundation Depth

To understand the effects of the urban flood on travel behaviors, this study compared travel speed under the usual and flooding conditions, based on the taxi probe data during September and October 2019, which were released by the Thai Intelligent Traffic Information Center Foundation (iTIC) [21]. This data consists of Vehicle ID, GPS location collected every minute, Timestamp, and Travel speed. In this study, national highway No. 231 (Bypass) was chosen and analyzed. The national highway No. 231 is the main road section in Ubon Ratchathani City, which is used by many residents on a daily basis. As shown in Fig. 1, The Bypass was divided into eight sections.

One day was divided into four periods (Midnight—6 a.m., 6 a.m.—12 Noon, 12 Noon—6 p.m., 6 p.m. —Midnight), and the travel speeds under the usual and flooding conditions were calculated and compared. The presence or absence of floods was set by referring to the published flooding data from the Thai Flood Monitoring System [22]. The results of previous studies have clarified that higher inundation depth and precipitation affect the decrease of travel speed. However, these existing studies have not considered the variations of travel speed under the usual condition. Therefore, the usual travel speed in each road section was firstly calculated and then classified into five travel speed ranges. Afterward, the relationship between the decrease in travel speed and inundation depth was analyzed for each of the five usual travel speed ranges. The reason is that even if the same inundation level depth occurs in the different road sections, the proportion of decrease in travel speed differs depending on the travel speed under the usual condition for low levels of inundation depth. However, if the inundation depth is critically high, it is reasonable to maintain a constant travel speed. In other words, the more inundation depth, the less travel speed variation. From these detailed decreases in travel speed results, by classifying each travel speed, a more realistic impact of inundation for road transportation could be expressed. The inundation depth was estimated based on the questionnaire survey results from a past study [23].

3.3 Analysis of Relationship Between Travel Speed and Inundation Depth

This study evaluated the adaptation measure in the transport field to reduce the impacts of road transport under flood conditions. Reflecting for analysis results of the relationship between travel speed and inundation depth, traffic assignment was applied to estimate the impacts of some assumed scenarios. In Table 1, adaptation measures from existing studies or reports have been shown. These measures were classified into “Soft” and “Hard” categories, which were reviewed and summarized. In this study, the raising arterial road measure was selected and evaluated (Road section No. 1).

To evaluate the raising arterial road measure, the traffic assignment model was carried out based on OD table data and road network data using macroscopic multi-modal traffic flow simulation software PTV VISUM. Concerning OD table data, it was made from Person Trip Survey data in 2015, which was conducted by the Office of Transport and Traffic Policy and Planning (OTP [24]). Regarding the network data, when an urban flood occurs, the road sections located in flooded areas express the impacts of urban floods as decreasing travel speed or cutting off depending on inundation depth. Based on the analysis of the relationship between travel speed and inundation depth, the impacts of urban floods for road network was represented.

Moreover, in evaluating the raising arterial road measure, the effects of this measure could be represented by comparing the allocated hourly traffic volume, Vehicle Kilometer Traveled (VKT). It was assumed that the evaluated road sections were available for passenger cars and motorcycles by introducing this measure. In order to estimate the effect of introducing the raising arterial road measure, scenarios were created by combining the case where the traffic demand fluctuated in which the road section would be improved to increase the effect. The details of the assumed scenarios are shown below. As shown in Table 2, six scenarios were assumed that combine fluctuations in traffic demand and implementation in raising arterial road measure for the western bypass (Road section No. 1). Specifically, the traffic demand assumed three cases as “No change”, “Increment 10%”, and “Increment 20%”. Raising the arterial road measure for Road section No. 1, against when doing nothing during flooding, were compared. There are two reasons for the assumption of an increase in travel demand in this study. Firstly, the travel pattern under the flooding condition could not be clarified, and there was the possibility to vary the trip rate. Secondly, some people need to conduct evacuation behaviors for the avoidance of urban flood damages. Thus, three traffic volume cases were assumed. These cases were combined and made a total of six scenarios.

Table 2 Scenario setting

		Adaptation measure	
		Nothing	Road section No. 1
Demand	No change	Scenario 1	Scenario 4
	+10%	Scenario 2	Scenario 5
	+20%	Scenario 3	Scenario 6

4 Results

4.1 Analysis of Relationship Between Travel Speed and Inundation Depth

In this study, the probe data was analyzed, and the travel speed under the usual and flooding conditions was calculated. The travel speed and vehicle trajectory data under the flooding conditions were represented in Fig. 3. Under the flooding condition, there were no data that could be collected from the probe data on the center of two bridges. From this data, it shows that people could not pass through these road sections under the flooding condition. The travel speed under the flooding condition of all bypasses was estimated to be 20–40 km/h. The travel speed under the usual condition was also estimated based on the probe data. The comparison results with the difference in 85 percentile value of travel speed under the usual and flooding conditions for each road section were shown in Fig. 4. This Figure shows the comparison of the decrease in 85 percentile value of travel speed under the flooding condition with the travel speed under the usual condition and overlaying of expected inundation depth based on the questionnaire survey result in the past study [23]. From this result, particularly on section No.6 in Fig. 4, 85 percentile value of travel speed under the flooding condition was decreased by

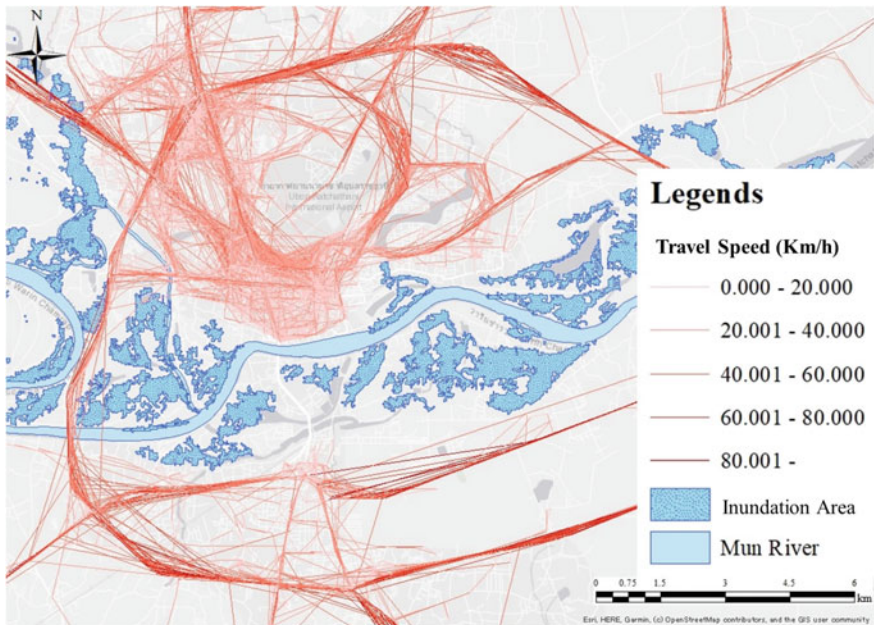


Fig. 3 Travel speed under flooding condition

approximately 38.9 km/h, and 85 percentile value of travel speed of the whole road sections was decreased by approximately 12.9 km/h.

Moreover, the relationship between the decrease in travel speed from the usual condition and inundation depth was shown in Fig. 5. This Figure shows the relationship between the decrease in travel speed based on the five usual travel speed ranges (21–30, 31–40, 41–50, 51–60, 61–70 km/h) and four inundation categories (0.01–0.10, 0.11–0.30, 0.31–0.50, 0.51–1.00 m). It shows that the decrease in travel speed due to the inundation depth differs greatly depending on the travel speed under the usual condition. When the travel speed was 41–50 km/h, the travel speed under flooding conditions was estimated at 40 km/h, and it decreased by 5 km/h at an inundation depth of 0.01–0.10 m. Moreover, for inundation depth of 0.51–1.00 m, travel speed was reduced by approximately 20 km/h. On the other hand, when the usual travel speed was 31–40 km/h, the travel speed was estimated at 30 km/h and decreased by 5 km/h when inundation depth was 0.01–0.10 m. From these results, even at the same inundation depth, the rate of decrease in speed differs depending on the usual travel speed. If the inundation depth is relatively high, such as over 0.70 m, the travel speed under the flooding condition could be reliably estimated at a constant of 20 km/h. However, if it is lower than 0.70 m, it was shown that travel speed reduction would differ depending on the usual travel speed. The variations of travel speed may be because of different types of vehicles. At the same inundation depth, small and low vehicles tend to drive slower than bigger and higher vehicles, particularly at the high depth.

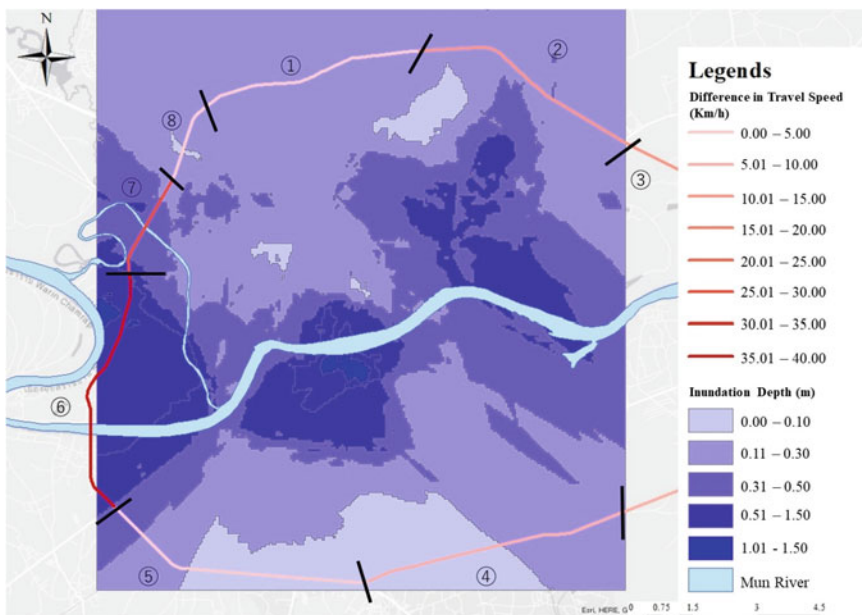


Fig. 4 The difference in travel speed under both conditions (usual-flooding)

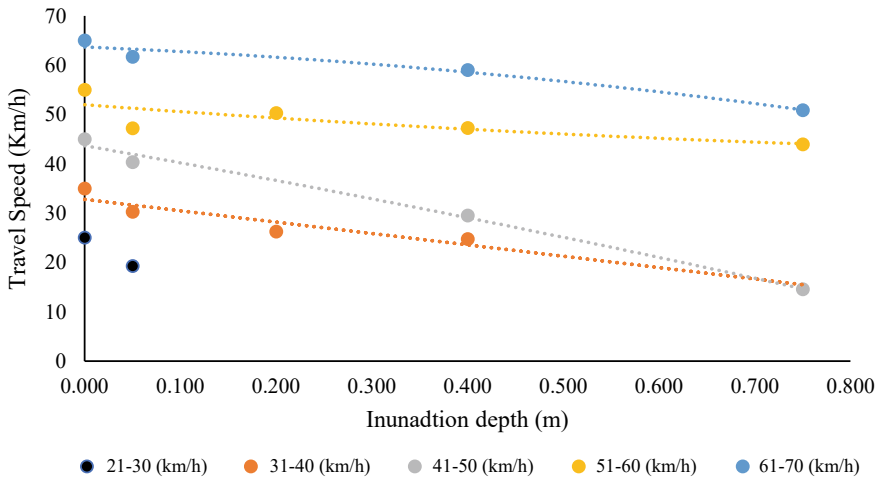


Fig. 5 Relationship between travel speed and inundation depth

4.2 Evaluation of Adaptation Measure Impacts

The traffic assignment result under flooding conditions without and with raising arterial road measure has shown in Figs. 6 and 7. Under the flooding condition, residents are necessary to detour the eastern bypass because of the inability to pass through the western bypass (Road section No. 1) and center two bridges (Road section No. 2 and 3). On the eastern bypass, the number of hourly traffic was assigned approximately 7000 vehicles under flood conditions without raising arterial road measures to implement in the western bypass during one hour of peak time. By elevating the western and passing through under the flooding condition, the number of the hourly detoured vehicle was decreased by 5000 vehicles.

In order to evaluate the elevated arterial road measure, including fluctuation of traffic volume, this study simulated six scenarios to apply to the traffic assignment in PTV VISUM and calculated the VKT, which was a multiplication of the travel distance and the number of vehicles. The results of hourly VKT during the peak time of each scenario are shown in Fig. 8. Scenario 1 shows that the analysis results in a situation where the traffic demand does not fluctuate and no implementation of raising any road sections under flood conditions. Approximately 37,000 km are estimated to be traveled during 1-h of peak time. When the traffic demand increases 10% and 20% during one hour of peak-time, VKT increased by about 4000 km and 8000 km, respectively.

On the other hand, when the western bypass (Road section No. 1) is raised, vehicles could pass through (Scenario 4–6) under flood conditions. It is possible to decrease the VKT value by approximately 65% of each situation by comparing it with the case without any measures such as raising the arterial road (Scenario 1–3). This is because the residents who detoured the eastern bypass could pass through

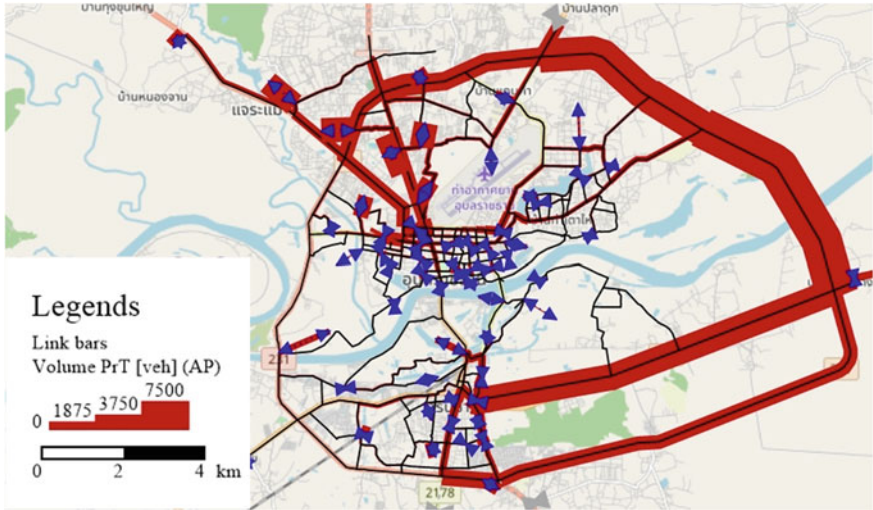


Fig. 6 Traffic assignment result under flooding condition without taking any measure case (result of Scenario 1)

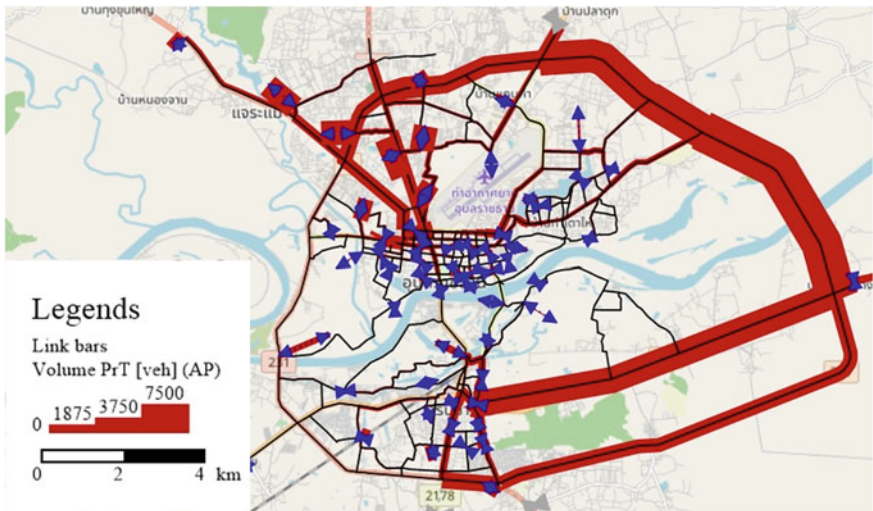


Fig. 7 Traffic assignment result under flooding condition with raising arterial road measure case (result of Scenario 2)

the western bypass and decrease the trip length compared to no elevated road section case. To clarify the impacts of implementation in raising arterial road measure, VKT under usual conditions and raising arterial road measure case were compared. Even if the arterial road was raised as a measure for the western bypass,

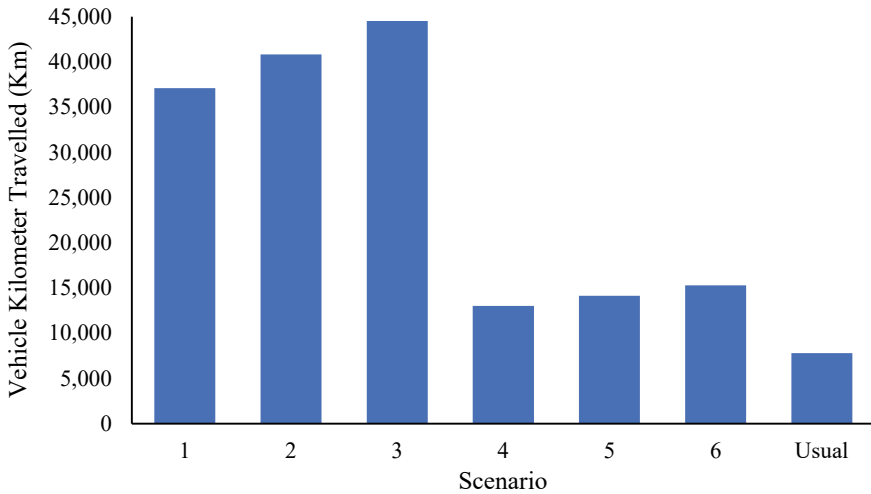


Fig. 8 Vehicle kilometer traveled (VKT) each scenario

it was shown that the VKT was estimated to increase by 1.5–2.0 times than VKT under usual conditions (8000 km). This is because Bridges 2 and 3 could not allow vehicles to pass through due to inundation, and some vehicles were still assigned for the eastern bypass, approximately 2000 vehicles during one hour of peak time.

5 Discussion and Conclusion

In this study, to analyze the impacts on traffic states caused by urban floods, the probe data was used and estimated the travel speed under usual and flooding conditions. Furthermore, these analysis results were reflected to evaluate the raising arterial road measure as an adaptation measure in the transport field for urban floods in Ubon Ratchathani City, Thailand. Firstly, the relationship between the decrease in travel speed and inundation depth was examined by comparing the travel speed under usual and flooding conditions using probe data during September and October 2019. This specific analysis of probe data confirmed that the travel speed under flooding conditions was decreased by a maximum of 38.9 km/h during peak time. This analysis was also clarified that the decrease in travel speed due to flooding was significantly different depending on the travel speed under the usual condition. As a result, it was found that urban floods had a significant impact on road transportation by decreasing travel speed.

Additionally, the relationship between the travel speed and inundation depth was assessed by applying traffic assignment. The result was clarified that the raising arterial road measure could decrease VKT by approximately 65% and decrease the taking traffic detour by 5000 vehicles compared to the urban flooding condition

without implementation in any other adaptation measures. These results showed that raising as a measure for the western bypass could be an effective adaptation.

However, this study only evaluated raising arterial road measure as a “Hard” aspect adaptation measure on the transport field and could not express the change in travel behaviors caused by the variance of service level of the road network for trip rate or modal choice, etc. Therefore, in a further study, other adaptation measures in the transport field including, “Soft” aspect measures, such as traffic regulation for deep inundation area and optimization of signalization, will need to be evaluated. Nevertheless, it is necessary to consider adaptation measures carefully. This is because of the possibility to affect conversely increasing vulnerability and damages by adaptation measures. Moreover, based on the analysis of the probe data, the traffic states were seen to be dramatically different under the flood conditions compared with the usual conditions. Thus, this analysis might not ultimately be able to reflect the effect of the different traffic states. Therefore, it could consider only individual activities, while a more detailed activity-based travel demand model could be applied in the future. By focusing on the individual person’s activities and trips, it is possible to adequately represent the change in travel behaviors for not only travel patterns but also destination choice and modal choice caused by urban flooding.

Acknowledgements The authors would like to express our appreciation to Mr. Joseph Falout for his helpful editing of the paper.

References

1. Dutta D, Hearath S (2004) Trend of floods in Asia and flood risk management with integrated river basin approach. In: Proceedings of the 2nd international conference of Asia-Pacific hydrology and water resources association, pp 55–63
2. OECD. OECD financial management of flood-risk. <https://www.oecd.org/daf/fin/insurance/OECD-Financial-Management-of-Flood-Risk.pdf>. Accessed 15 Sep 2020
3. Zhou Y, Wang J, Yang H (2018) Resilience of transportation systems: concepts and comprehensive review. *IEEE Trans Intell Transp Syst* 99:1–15
4. Eichhorst U, Bongardt D, Miramontes M (2011) Climate-proof urban transport planning: opportunities and challenges in developing cities. In: Otto-Zimmermann K (ed) *Resilient cities. Local sustainability*. pp 91–105
5. UNFCCC The Paris Agreement United Nations Framework Convention on Climate Change. In: UNFCCC. http://unfccc.int/paris_agreement/items/9485.php. Accessed 10 May 2021
6. UNFCCC intended nationally determined contribution and relevant information. In: The Office of Natural Resources and Environmental Policy and Planning (ONEP) 2015 Submission by Thailand. https://www4.unfccc.int/sites/ndcstaging/PublishedDocuments/Thailand%20First/Thailand_INDC.pdf. Accessed 5 May 2021
7. Takano T, Morita H, Nakamura S et al (2020) Impact of rainfall on urban traffic flow based on probe vehicle data in Bangkok. *J Intell Inf Smart Technol* 4:72–76
8. Khan MH, Fujita M, Wisetjindawat W (2016) Analysis on car commuters’ behavior during a massive downpour based on probe data and questionnaire survey. *J Japan Soc Civil Eng, Ser F3 (Civil Engineering Informatics)* 72:1–13. https://doi.org/10.2208/jscejcei.72.i_1

9. Umeda S, Kawasaki Y, Kuwahara M (2019) Analysis of traffic state during a heavy rain disaster using probe data. *J Disaster Res* 14:466–477
10. Stamos I, Mistakis E, Grau J (2015) Roadmaps for adaptation measures of transportation to climate change
11. Aparicio A (2017) Transport adaptation policies in Europe from incremental actions to long-term visions. *Transp Res Procedia* 25:3541–3553
12. Chen X, Lu Q, Peng Z, Ash JE (2015) Analysis of transportation network vulnerability under flooding disasters. *J Transp Res Record* 2532:37–44
13. Sohn J (2015) Evaluating the significance of highway network links under the damage: flooding an accessibility approach. *Transp Res Part A* 40:491–506
14. Taylor MAP, Sekhar SVC, D'Este GM (2006) Application of accessibility based methods for vulnerability analysis of strategic road networks. *Netw Spat Econ* 6:267–291
15. Li J Lam WHK, Li X (2016) Modeling the effects of rainfall intensity on the heteroscedastic traffic speed dispersion on urban roads. *J Transp Eng* 142(6):1–9
16. Pregnolato M, Ford A, Wilkinson M, Dawson R (2017) The impacts of flooding on road transport: a depth-disruption function. *Transp Res Part D* 55:67–81
17. Choo SK, Kang HD, Kim SB (2020) Impact assessment of urban flood on traffic disruption using rainfall-depth-vehicle speed relationship. *Water* 12:1–21
18. Hilly G, Vojinovic Z, Weesakul S et al (2018) Methodological framework for analyzing cascading effects from flood events: the case of Sukhumvit area, Bangkok, Thailand. *Water* 10:1–26
19. Bhokha S, Sangtian N, Kuntiyawichai K (2006) Future paradigm and approaches for sustainable planning, design and, management of bridge in flood plain a case study: bridge in Ubon Ratchathani, Thailand. In: *Proceeding the tenth East Asia-Pacific conference on structural engineering and construction (EASC-7)*
20. Chutchai information systems for monitoring, surveillance, warning, rescue and, evasion flood disaster in Ubon Ratchathani province in 2019. In: Chutchai. <http://chutchai.cs.ubru.ac.th/>. Accessed 6 May 2021
21. iTIC foundation historical raw vehicle and mobile probes data in 2019. In: iTIC foundation. <https://www.iticfoundation.org/>. Accessed 6 May 2021
22. Sentinel Asia Thailand floods in Sept. 2019. In: Sentinel Asia. <https://sentinel-asia.org/EO/article20190920TH.html>. Accessed 20 Sep 2020
23. Tsumita N, Jaensirisak S, Kikuchi H, Fukuda A (2020) Analysis of travel behaviors during floods in Ubon Ratchathani City, Thailand. In: *IOP conference series: earth and environmental science*, Yogyakarta, Indonesia, pp 1–12
24. The Office of Transport and Traffic Policy and Planning (2015) The study of the master plan development of the public transportation system in cities, regions of the country, Thailand, pp 37

Modeling Movement of Rice Commodities Between Provinces in Indonesia



Dwi Novi Wulansari, Saskia Kanisaa Puspanikan,
and Zafir Istawa Pramoedy

Abstract The performance of the national logistics system will affect the economy in Indonesia. One of the important movements of logistics goods in Indonesia is the movement of the rice commodity. The rice commodity is a product of paddy cultivation and is a staple food product for the majority of the world's population, especially in Indonesia. To support the performance of the logistics system in Indonesia that is effective and efficient, several studies are needed that can provide an overview of the transportation of goods in Indonesia, including modeling the current and future movements of rice commodities. This study aims to model the movement of rice commodities between provinces in Indonesia. The research method uses descriptive quantitative methods. The data used in this study were data on the movement of rice commodities in Indonesia in 2016. The analytical approach used is a zone-based correlation-analysis model, and statistical tests are carried out on the regression equation function to test the significant level of the model. The modeling results show that rice production will affect the generation and attraction of rice commodity movements linearly and positively.

Keywords Movement modeling · Rice commodities · Logistics · Transportation

1 Introduction

The logistics system performance affects the economy in a country, including in Indonesia. According to the Blueprint for the Development of the National Logistics System [1], logistics costs in Indonesia reach 27% of Gross Domestic Product and the inadequate quality of service is indicated by: (a) low levels of infrastructure provision, both quantity and quality, (b) there are still levies unofficial and transaction costs that cause a high cost economy, (c) still high export–import

D. N. Wulansari (✉) · S. K. Puspanikan · Z. I. Pramoedy
Logistics Engineering Study Program, Universitas Pendidikan Indonesia, 229 Dr. Setiabudi
Street, Bandung, Indonesia
e-mail: dwinovi@upi.edu

service times and the existence of service operational barriers at ports, (d) limited capacity and service network of national logistics service providers, (e) still scarcity of stock and fluctuations in the price of people's staple goods, especially on national and religious holidays, and (e) high price disparities in the border, remote and outermost areas.

The poor performance of the logistics system also affects the supply chain for superior commodities in Indonesia, including commodities in the agricultural sector. The main product of commodity production in agriculture is the paddy. Paddy is one of the cultivated plants that produces rice and is a staple food product for the majority of the world's population, especially in Indonesia. Rice is also used as a staple in the manufacture of food industries such as pastries or the rice flour industry. According to the Indonesian Central Statistics Agency, the total production of milled dry unhulled rice (GKG) in Indonesia reached 54,649,202.24 tons in 2020 [2], if the production of milled dry unhulled rice is converted to rice based on the GKG conversion rate of 64.02% [3], the total rice production in Indonesia reached 34,986,419.27 tons in 2020.

Support from various sectors is needed to accelerate the pace of the economy and the movement of goods in the logistics system in Indonesia. The transportation sector is one of the sectors that can support economic activity. Currently, goods transportation in Indonesia is served by land transportation, sea transportation, and air transportation. To support the performance of the logistics system in Indonesia that is effective and efficient, several studies are needed that can provide an overview of the transportation of goods in Indonesia, including modeling the current and future movements of rice commodities. The movement of the rice commodity must be regulated, in the sense that there is a balance between supply and demand by taking into account the factors that influence the movement.

2 Literature Review

To represent reality in a simpler, inexpensive, fast, precise, and easy way is through modeling. In the modeling process, a simplification process is carried out. It is necessary to have a process of disposing of unnecessary information that can be justified statistically. Movement is a journey from the origin zone to the destination zone. Movement can be separated between generation movement and attraction movement. In modeling the movement of generation and attraction, it is necessary to pay attention to the movement of people and the movement of goods. The movement of goods can be estimated based on the number of vehicles (vehicle-based model) or the number (unit value of tons) of the commodity (commodity-based model) [4]. Commodity movements are usually represented by an origin–destination matrix containing the type and quality of goods being moved, while vehicle movements are represented by traffic flows in different types of vehicles [5]. Most models developed in recent years are categorized into the commodity-based group [6]. One of the approaches used in calculating the

movement of goods is the four-step commodity model. The four-step approach to freight modeling is an adaptation of the traditional urban passenger travel demand modeling system [7]. The main steps in the four-step modeling are movement generation, distribution, mode choice, and route assignment. The commodity generation models estimate the total number of tons produced and attracted by each of the individual zones comprising the study area. The movement of goods is influenced by the number of jobs, the number of marketplaces, the industrial roof area, and the total area [8].

3 Methodology and Data

3.1 Zone-Based Correlation Analysis Model

In this study, the modeling of the movement of rice commodities in Indonesia uses a zone-based correlation-analysis model. This model aims to obtain a linear relationship between the amount of movement generated or attracted by the zone and the average socio-economic characteristics of the household in each zone. There are three methods of analysis that can be used in this model, namely:

- Step-by-step analysis method type 1;
- Step-by-step analysis method type 2;
- The Trial Method.

This model also uses the assumption that the generation and attraction of movement can be expressed as a function of several zone-based socio-economic attributes so that the relationship in numerical form and the variables are related to each other. The function is described in Eqs. 1 and 2.

$$P = f(X_1, X_2, \dots, X_N) \quad (1)$$

$$A = f(X_1, X_2, \dots, X_N) \quad (2)$$

where P: trip generation, A: trip attraction, X: zone-based socio-economic attributes.

The movement modeling approach can use linear regression analysis. Regression analysis was conducted to measure the relationship between the dependent variable (y) and the independent variable (x) in the form of an equation function. Linear regression analysis can be expressed in Eq. 3.

$$y = a + bx \quad (3)$$

where y = dependent variable, x = independent variable, a = constant of the regression line intercept on the y-axis, b = regression line coefficient.

To determine the degree of the relationship between the two variables, it is necessary to do a correlation test, where the independent variables cannot have a relationship, while the independent variables and the dependent variables must have a relationship. The correlation technique used is the product moment (Pearson) correlation test proposed by Karl Pearson in 1990 [9] with Eq. 4.

$$r_{xy} = \frac{n(\sum xy) - (\sum x)(\sum y)}{\sqrt{\{n \sum x^2 - (\sum x)^2\} \{n \sum y^2 - (\sum y)^2\}}} \quad (4)$$

where r_{xy} : Correlation coefficient, n : Amount of data, $\sum xy$: The sum of the product of the value of the independent and dependent variables, $\sum x$: Total value of the independent variable, $\sum y$: Total value of dependent variables, $\sum x^2$: The sum of the squares of the independent variable values, $\sum y^2$: The sum of the squares of the dependent variable value.

Statistical tests are used to determine the important characteristics that are the basis for understanding and predicting behavior, namely the concept of the significance test (t-test and F-test). The t-test is intended to test the effect of each independent variable one by one on the dependent variable. ANOVA test (F-test) aims to reflect the effect of independent variables simultaneously on dependent variables. The level of significance used for the t-test and ANOVA test was 0.05.

3.2 Rice Commodity Movement Pattern

The movement patterns (vehicles, passengers, and goods) moving from the origin zone to the destination zone within the study area and over a certain period of time can be described by the origin–destination matrix and desire line graphs. In this study, the movement of the rice commodity is described by the desire line, which contains information about the orientation of the movement of rice between zones viewed through the thickness of the desire line. The data of the generation and attraction movement of the rice commodity were obtained from the results of the 2016 ATTN Goods survey by the Ministry of Transportation of the Republic of Indonesia [10]. From these data, a desire line model with two constraints can be generated, namely a model with a generation-limitation and a model with an attraction-limitation.

Figure 1 shows the orientation of the movement of rice commodities as illustrated by the thickness of the line on a scale of 396,114 tons/month, 792,228 tons/month, and 1,584,456 tons/month. Meanwhile, the movement of fewer than 396,114 tons/month is not shown in Fig. 1. Based on the desire line, it can be seen that the largest movement of rice commodities occurred between West Java Province, East Java Province, Central Java Province, South Sumatra Province, South Sulawesi Province, Lampung Province, and Banten Province.

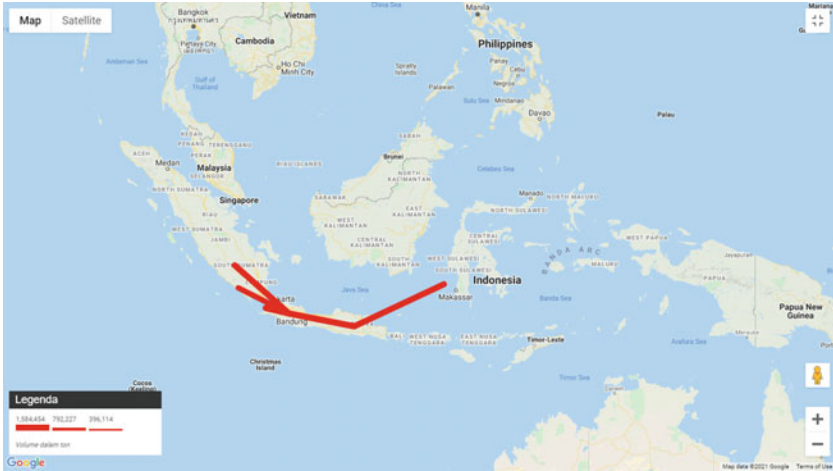


Fig. 1 Desire line for the movement of rice commodities

3.3 Rice Commodity Movement Data

Movement analysis uses a zone-based correlation-analysis method using generation and attraction data for the movement of rice commodities in 2016 as independent variables. Meanwhile, the dependent variable was rice production in 2016 in each zone under review, namely 34 provinces in Indonesia. Generation and attraction data for the movement of rice commodities and rice production are shown in Table 1.

4 The Result and Discussion

4.1 Movement Generation Model

The results of linear regression analysis for modeling the generation of rice commodity movements in brief can be seen in Table 2.

Based on the results of linear regression analysis in Table 2, Eq. 5. functions for the generation of rice commodity movements are produced.

$$Y = -36,934.47 + 0.57X \tag{5}$$

from Eq. 5, it can be concluded that:

Table 1 Data of movement generation and attraction of rice commodities and rice production

No.	Zone	Movement generation (tons/month)	Movement attraction (tons/month)	Rice production (tons/year)
1	Aceh	1,137,799	556,498	2,205,056
2	Bali	536,541	644,739	845,559
3	Banten	1,282,067	2,095,175	2,358,202
4	Bengkulu	371,170	247,034	641,881
5	DI Yogyakarta	171,725	759,825	882,702
6	DKI Jakarta	4,731	1,886,939	5,342
7	Gorontalo	166,744	102,840	344,869
8	Jambi	415,839	433,013	752,811
9	West Java	7,297,648	9,343,320	12,540,550
10	Central Java	6,044,281	7,378,885	11,473,161
11	East Java	8,388,837	8,437,350	13,633,701
12	West Borneo	856,465	518,863	1,364,524
13	South Borneo	1,304,481	632,105	2,313,574
14	Central Borneo	521,822	310,313	774,466
15	East Borneo	228,429	308,280	305,337
16	North Borneo	71,461	32,770	81,854
17	Bangka Belitung Islands	14,687	166,076	35,388
18	Riau islands	874	187,684	627
19	Lampung	2,078,976	1,345,623	4,020,420
20	Maluku	62,688	88,235	99,088
21	North Maluku	44,129	71,051	82,213
22	West Nusa Tenggara	1,321,133	750,006	2,095,117
23	East Nusa Tenggara	513,367	455,507	924,403
24	Papua	116,846	63,591	233,599
25	West Papua	–	–	27,840
26	Riau	241,100	736,248	373,536
27	West Sulawesi	277,024	191,655	548,536
28	South Sulawesi	3,192,760	1,623,315	5,727,081
29	Central Sulawesi	625,977	321,335	1,101,994
30	Southeast Sulawesi	401,171	305,181	695,329
31	North Sulawesi	362,906	220,829	678,151
32	West Sumatra	1,576,022	766,235	2,503,452
33	South Sumatra	2,297,150	1,233,932	5,074,613
34	North Sumatra	2,272,026	1,984,424	4,609,791

Table 2 Results of movement generation regression analysis

Regression statistics				
Multiple R	1.00			
R square	0.99			
Adjusted R square	0.99			
Standard error	204,324.02			
Observations	34			
	Coefficients	Standard error	t Stat	P-value
Intercept	-36,934.47	42,053.99	-0.88	0.39
Rice production (tonnes/year)	0.57	0.01	57.50	7.16E-34

- A constant value of -36,934.47 provides information that if the amount of rice production does not change, the generation of rice commodity movements will decrease by 36,934.47. The high constant value indicates that there are other independent variables that affect the movement of rice commodities.
- The independent variable which is rice production has a coefficient value of 0.57 indicating that if there is a change in rice production by 1 unit, the generation of rice commodity movement will experience a change of 0.57.
- In Table 2, it is known that the sign of the coefficient of the free variable equation is positive (+). It can be concluded that the greater the rice production, the generation of movement of rice commodities will be generated.
- The value of r2 in the results of the analysis above is 0.99 or 99%, which means that rice production is able to explain changes in the generation of rice commodity movements and the rest is explained by variables not found in the model by 1%.

4.2 Movement Attraction Model

The results of linear regression analysis for modeling the attraction movement of the rice commodity in brief can be seen in Table 3.

Based on the results of the linear regression analysis in Table 3, the function of the attraction equation for the movement of the following rice commodity is produced.

$$Y = -138,683.64 + 0.62X \tag{6}$$

from Eq. 6, it can be concluded that:

Table 3 Results of movement attraction regression analysis

Regression statistics				
Multiple R	0.95			
R square	0.90			
Adjusted R square	0.89			
Standard error	754,073.36			
Observations	34			
	Coefficients	Standard error	t Stat	P-value
Intercept	-138,683.64	155,203.46	-0.89	0.38
Rice production (tonnes/year)	0.62	0.04	16.77	2.09E-17

- A constant value of -138,683.64 provides information that if the amount of rice production does not change, then the movement of rice commodities will decrease by 138,683.64. The high constant value indicates that there are other independent variables that affect the movement of rice commodities.
- The independent variable which is rice production has a coefficient value of 0.62 indicating that if there is a change in rice production by 1 unit, the movement of rice commodity will change by 0.62.
- In Table 3, it is known that the sign of the coefficient of the free variable equation is positive (+). It can be concluded that the greater the rice production, the more attractive the movement of rice commodities will be.
- The value of r² in the results of the above analysis is 0.90 or 90%, which means that rice production is able to explain changes in the movement of rice commodities and the rest is explained by variables not found in the model by 10%.

4.3 Correlation Test

Correlation is used to measure the strength of the relationship between the two variables and also to be able to determine the form of the relationship between the two variables which is quantitative in nature. The strength of the relationship between the two variables referred to here is whether the relationship is close, weak, or not close. While the form of the relationship is whether the form of correlation is the linear positive or linear negative. A good correlation between the variables X and Y is indicated by the value of the relationship between 0.5 and 1.0. The results of the correlation test that have been carried out are shown in Table 4.

Table 4 Correlation analysis results

	Generation movement	Attraction movement	Rice production
Generation movement	1		
Attraction movement	0.953	1	
Rice production	0.995	0.948	1

From Table 4, it can be seen that the correlation value between independent variables and dependent variables is as follows:

- The correlation value between the generation of rice commodity movements and rice production is $0.953 \geq 0.5$, so it can be seen that the generation of rice commodity movements and rice production has a strong/close relationship. In addition, the correlation value is positive (+), which means that the form of the relationship between the two variables is positive linear.
- The correlation value between the attraction of rice commodity movements and rice production is $0.995 \geq 0.5$, so it can be seen that the rise of the movement of rice commodities and rice production has a strong/close relationship. In addition, the correlation value is positive (+), which means that the form of the relationship between the two variables is positive linear.

4.4 *Statistic Test*

T-test The t-test or partial test is intended to test the effect of each independent variable one by one on the dependent variable. Based on the results of linear regression analysis of the movement generation model (Table 2) and the movement attraction (Table 3), it can be concluded that:

- Rice production (x) has a t-count of 57.50 which is greater than the t-table of 1.69, and the probability is $7.16E-34 < 0.05$, so it can be said that rice production has a positive and significant effect on the generation of movement of rice commodities.
- Rice production (x) has a t-count of 16.77, greater than the t-table of 1.69, and a probability of $2.09E-17 < 0.05$. It can be said that rice production has a positive and significant effect on the attraction of the movement of rice commodities.

ANOVA Test ANOVA test (F-test) or simultaneous test aims to reflect the effect of the independent variables together on the generation and attraction of the movement of rice commodities. The results of the calculation are briefly shown in Table 5.

Table 5 The results of the analysis of the movement generation ANOVA test

	df	SS	MS	F	Significance F
Regression	1	1.38E+14	1.38E+14	3306	7.16E-34
Residual	32	1.34E+12	4.17E+10		
Total	33	1.39E+14			

Table 6 The results of the analysis of the movement attraction ANOVA test

	df	SS	MS	F	Significance F
Regression	1	1.60E+14	1.60E+14	281	2.09E-17
Residual	32	1.82E+13	5.69E+11		
Total	33	1.78E+14			

From Table 5, it is known that the F-count value is $3306 > 4.17$ (F-table) and a significant value of $7.16E-34 < 0.05$ which indicates that overall rice production has an effect on the generation of movement of rice commodities.

From Table 6, it is known that the F-count value is $281 > 4.17$ (F-table) and a significant value is $2.09E-17 < 0.05$, which indicates that overall rice production has an effect on the attraction of movement of rice commodities.

5 Conclusion

Based on the modeling of the movement of rice commodities in Indonesia, it is known that rice production will affect the generation and attraction of rice commodity movements linearly and positively. However, the model has a high constant value indicating that there are other independent variables that affect the movement of rice commodities. Commodity-based modeling has the potential to capture the mechanisms driving transport demand but cannot adequately model empty trips. This situation suggests that integrating commodity-based and vehicle-based modeling will provide a better understanding of the movement of goods [11].

References

1. Presidential Regulation (2012) Presidential regulation no. 26/2012 concerning blueprint for the Development of the National Logistics System. Republic of Indonesia, Jakarta, Indonesia
2. Ministry of agriculture of the Republic of Indonesia rice production by province 2014–2018. In: Pertanian.go.id. <https://www.pertanian.go.id/home/?show=page&act=view&id=61>. Accessed 14 Mar 2021
3. Central Bureau of Statistics of the Republic of Indonesia (2018) Conversion of grain to rice in 2018. Central Bureau of Statistics, Jakarta, Indonesia
4. Kulpa T (2014) Freight truck trip generation modelling at regional level. Proc Soc Behav Sci 111:197–202

5. Jin TG, Saito M, Schultz GG (2012) Development of a statewide commodity flow distribution model using composite friction factors. *Proc Soc Behav Sci* 43:406–417
6. Wisetjindawat W, Yamamoto K, Marchal F (2012) A commodity distribution model for a multi-agent freight system. *Proc Soc Behav Sci* 39:534–542
7. Cambridge Systematics, Inc (1997) A guidebook for forecasting freight transportation demand. NCHRP Report 388. Transportation Research Board, National Academy Press, Washington DC, United States of America
8. Tamin OZ (2008) *Perencanaan, Pemodelan dan Rekayasa Transportasi*. Insitut Teknologi Bandung, Bandung, Indonesia
9. Irianto A (2014) *Statistik Konsep Dasar, Aplikasi dan Pengembangannya*. Kencana Prenadamedia Group, Jakarta, Indonesia
10. Ministry of transportation of the republic of indonesia portal of origin destination for goods transportation. In: Portal ATTN. <https://attn-barang.dephub.go.id/data/site/front/?page=pergerakan>. Accessed 14 Mar 2021
11. Holguín-Veras J, Thorson E (2000) Trip length distributions in commodity-based and trip-based freight demand modeling: investigation of relationships. *Transp Res Rec* 1707: 37–48

Single Tariff System to Provide Incentive for Longer Distance Users and to Keep Efficient Toll Gates Operations



Apta Sampoerna and Leksmono Suryo Putranto 

Abstract Due to limited investment funds, the toll road construction usually should be in stages in several segments. The toll tariff of segments that were operated in the earlier stages may only be determined by the length of the segment in km multiplied by toll tariff per km. After all segments have been operated, we also need to consider additional factors, e.g., an incentive to longer distance users, efficient toll gate operations, and smooth toll gate services. Integrated toll road payment system usually implements open toll payment system with uniform tariff. Logistic vehicles which usually traveled longer distances will be subsidized by vehicles traveling shorter distances. The open toll payment system is usually implemented by payment in the upstream barrier toll gates. It will keep efficient toll gate operations by concentrating all payment equipment and officers in the upstream barrier toll gates. This paper will discuss the single tariff determination of Jakarta Outer Ring Road (JORR) 2 Area 1 connecting Jagorawi-Cinere-Serpong-Kunciran-Cengkareng. There were several factors considered, i.e., road user ability/willingness to pay, breakeven point based on predicted average annual daily traffic, and related regulations. The resulted single tariff was Rp. 20,000.-.

Keywords Single tariff · Incentive · Efficient introduction

1 Background

Building additional road segments might be considered as a non-sustainable transport supply program as it might encourage massive development along the road and at the end will create a congested car-dependent corridor. However, we cannot rely on a transport system on public transport provision only. The system is for passenger service. For goods transport (logistics) and for certain passenger

A. Sampoerna · L. S. Putranto (✉)
Universitas Tarumanagara, Jakarta 11440, Indonesia
e-mail: leksmonop@ft.untar.ac.id
URL: <http://leksmono.com>

© The Author(s), under exclusive license to Springer Nature Singapore Pte Ltd. 2022
H. A. Lie et al. (eds.), *Proceedings of the Second International Conference of Construction, Infrastructure, and Materials*, Lecture Notes in Civil Engineering 216, https://doi.org/10.1007/978-981-16-7949-0_29

329

movements (e.g., last-mile and first-mile transport) road transport is essential. Therefore, in a long-term plan of a city transport system, road network completeness, to avoid missing links and bottlenecks (including in toll road sub-systems) is a must.

Infrastructure (including toll road) development should be given priority in developing countries. However, the national budget is usually limited and/or should be distributed proportionally to other sub-sectors. Private-sector funding would be an alternatives source fund but might need time to be invested. Therefore, the toll road construction usually should be in stages in several segments.

The toll tariff of segments that were operated in the earlier stages may only be determined by the length of the segment in km multiplied by toll tariff per km. After all segments have been operated, we also need to consider additional factors, such as an incentive to longer distance users, efficient toll gate operations, and smooth toll gate services.

Integrated toll road payment system usually implements open toll payment system with uniform tariff regardless of the distance. Logistic vehicles which usually traveled longer distances should be provided with an incentive to support national welfare. They will be subsidized by vehicles traveling a shorter distance [1]. An open toll payment system is usually implemented by payment in the upstream barrier toll gates. It will keep efficient toll gate operations by concentrating all payment equipment and officers in the upstream barrier toll gates instead of distributing payment equipment in remote downstream tollgates. However, this may create a long queue in upstream barrier toll gates if no attention was not given to this matter. Nevertheless, the smoothness of toll gate services will not be covered by this paper. This paper will discuss the single tariff determination of Jakarta Outer Ring Road (JORR) 2 Area 1. Total observed length 50.43 km (Fig. 1). The reason to conduct this research was to balance benefits received by road users and toll investors. There were several factors considered, i.e., road user Ability to Pay (ATP), Willingness to Pay (WTP), breakeven point based on predicted Average Annual Daily Traffic (AADT), and related regulations.

1.1 Scopes

To include ATP and WTP analysis, the only group I vehicles (passenger car, jeep, pick-up, small truck, and bus) were observed (comprise of 80–90% of toll road users). ATP and WTP questionnaire items are not relevant to company vehicles which predominantly comprise heavy logistic vehicles (from group II to V). Hypothetically this will not significantly affect the resulted single tariff determination. Moreover, the variability of travel length of private light vehicle users is usually the highest among other toll road users and, therefore, more relevant in the determination of a single tariff.



Fig. 1 JORR 2 Area 1 (circled with green line)

2 Literature Review

2.1 Types of Toll Transaction System

There are three types of toll transaction systems [2], i.e.:

- Open transaction system (single tariff) and the payment conducted in off-ramp (downstream). Please refer to Fig. 2.
- Open transaction system (single tariff) and the payment conducted in on-ramp (upstream). Please refer to Fig. 3.
- Closed transaction system (based on distance) and therefore the vehicle should be identified in the on-ramp (upstream) and payment conducted in off-ramp (downstream) based on identified distance. Please refer to Fig. 4

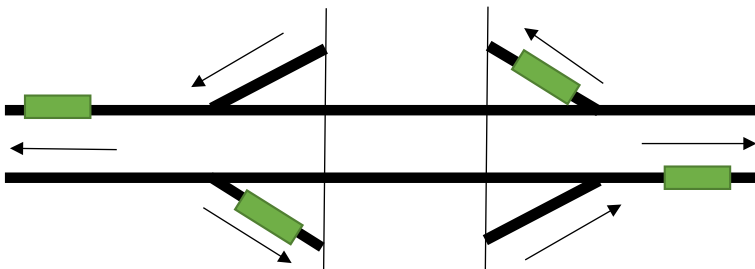


Fig. 2 Open transaction system (off-ramp payment)

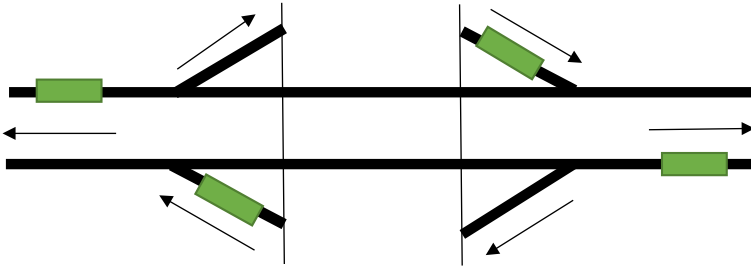


Fig. 3 Open transaction system (on-ramp payment)

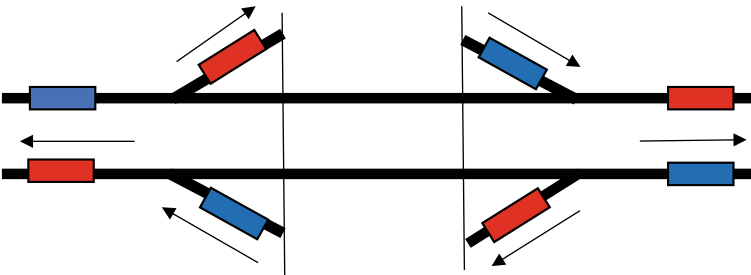


Fig. 4 Closed transaction system

2.2 ATP and WTP

ATP is the ability of someone to pay for the received services based on his/her wealth level. The approach used in ATP analysis is based on transport cost analysis from routine income earned. In other words, ATP is the ability of the public to pay his/her travel costs as stated by Tamin et al. [3]. According to Yulianto et al. [4], there were several factors affecting ATP, i.e., the amount of the income, transport demand, total transport cost, and percentage of income disbursed for transport cost.

WTP is the willingness of service users to pay for the received services. According to Hotmaida [5] and Nugroho et al. [6], several factors were affecting WTP, i.e., offered product, service quality, user utility of the transport services, and transport user behavior.

3 Method of Data Collection and Analysis

3.1 Method of Data Collection

There were two groups of data used in this paper, i.e., secondary data and primary data. The main secondary data was predicted AADT and regulations regarding toll road financing to calculate tariff based on breakeven point. Primary data was collected from group I vehicle users, consist of:

- General data (name, age, gender, educational attainment, and occupation).
- ATP data (monthly travel frequency, average travel time, travel period, monthly income, monthly toll road expenses, and travel purpose)
- WTP data (choice between 10, 20 and 30 min time saving for choice of tariff between twenty thousand rupiahs and thirty thousand rupiahs)

3.2 Method of Data Analysis

Figures 5, 6, and 7 describe the steps taken for determining the single tariff:

4 Profile of Respondents

There were 126 respondents (40 females and 86 males). However, only 122 responded to ATP-related questions and therefore, the ATP/ km data was only calculated from those 122 respondents. Their mean age was about 37 years old

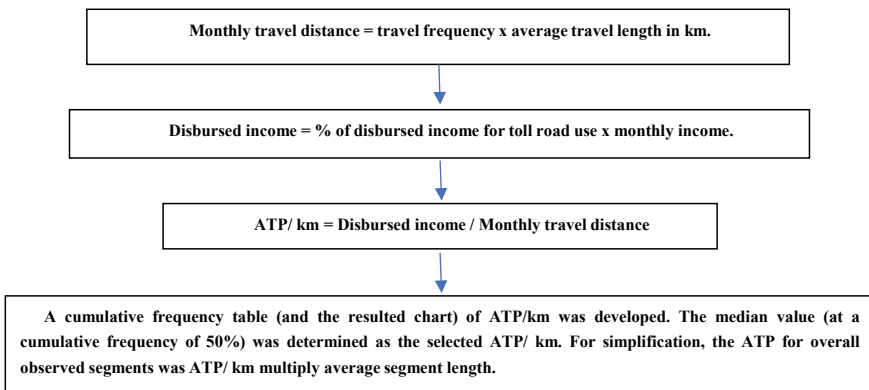


Fig. 5 Determination of ATP

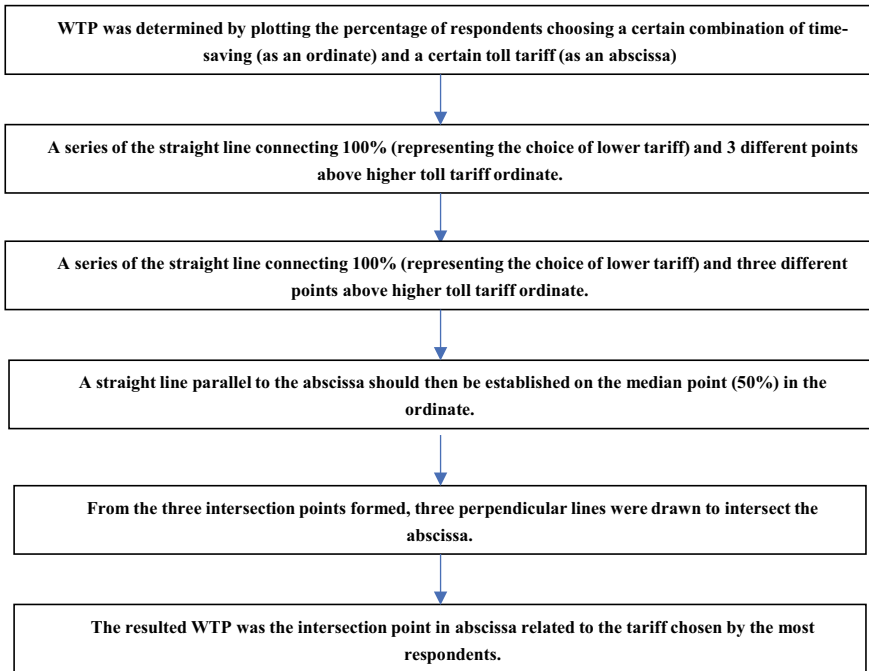


Fig. 6 Determination of WTP

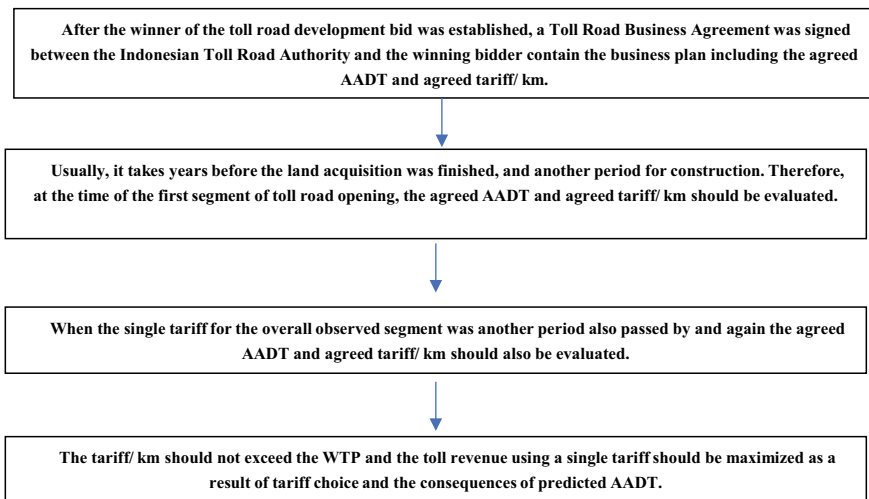


Fig. 7 Adjustment of selected single tariff

(standard deviation of 12) and ranged between 19 and 64 years old. Most of them (about 55%) earned less than 10 million rupiahs (USD 696 as 22 May 2021 exchange rate) monthly, about 33% earned above 10 million rupiahs up to 20 million rupiahs (USD 1392) monthly, about 8% earned above 20 million rupiahs up to 30 million rupiahs (USD 2088) monthly, and less than 5% earned above 30 million rupiahs monthly. About 31% of them spend less than 1 million rupiahs (USD 70) on toll roads monthly, about 27% spend more than 1 million rupiahs up to 3 million rupiahs (USD 209) monthly and most of them (about 42%) spend more than 3 million rupiahs monthly. The monthly travel frequency of most of them (54%) was more than seven times while the rest travel less. Travel time on the toll of most of them (about 63%) spends 30 to 60 min while the rest travel with a less or longer period. Most of the respondents travel on toll roads during morning and afternoon peak hours. Most of them (66%) travel on the toll road for work/ business purposes and the rest for various non-work purposes.

5 Results

5.1 ATP Analysis

Figure 8 shows that the 50-percentile of ATP was Rp. 2,800.-/ km. Therefore the ATP of each segment was Rp. 39,732.- (Jagorawi-Cinere), Rp. 28,392.- (Cinere-Serpong), Rp. 31,920.- (Serpong-Kunciran) and Rp. 39,732.- (Kunciran-Cengkareng) respectively. To simplify the overall ATP determination, an average of ATP of overall JORR 2 Area 1 weighted by each segment length was established as representative ATP, i.e., Rp. 36,102.-

5.2 WTP Analysis

Table 1 shows the number and percentage of respondents choosing each pair of time-saving and toll tariff. The lowest choice tariff (Rp. 20,000.-) was assumed to be chosen by 100% of the respondent while the percentage higher choice of tariff (Rp. 30,000.-) was calculated by dividing the number of respondents choosing it divided by the total respondent choosing the particular time-saving.

Figure 9 shows the WTP for all segments in the observed JORR 2 Area 1.

The determination of WTP at three different time-savings was by selecting the value chosen by most respondents. In this case, it was Rp. 29,000.- for a time-saving of 30 min.

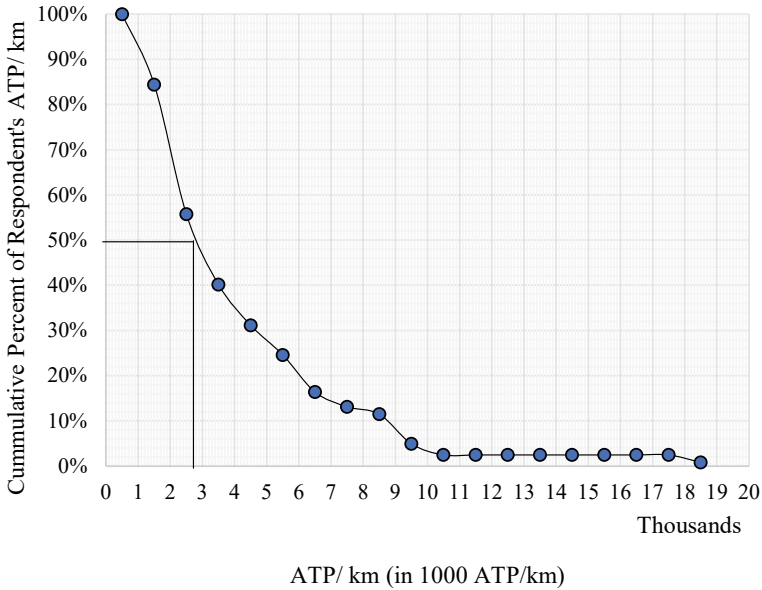


Fig. 8 50-percentile of ATP, i.e. Rp. 2,800.-/ km

Table 1 Number and percentage of respondents choosing certain pair of time-saving and toll-tariff

Ruas	Percentage of respondent (%)			Number of respondents			
	10 min	20 min	30 min	10 min	20 min	30 min	
<i>JORR 2 Area 1 (50.43 km)</i>							
Tariff	20,000	100.0	100.0	100.0	93	140	162
Tariff	30,000	34.4	39.3	44.4	32	55	72

5.3 Single Tariff Adjustment

After the Toll Road Business Agreement was signed between the Indonesian Toll Road Authority and the winning bidder, a business plan containing an agreed AADT and an agreed toll tariff was established. Table 2 shows the agreed figures in this stage, let's call it stage 1.

Stage 2 was adjusted business plan after the opening of the first segment, as shown in Table 3.

At stage 3, the adjustment was conducted using a trial and error process to maximize re-venue whilst keeping the tariff below the WTP as can be seen in Tables 4, 5, 6, and 7. The AADT in Tables 5, 6, and 7 was adjusted inversely to the

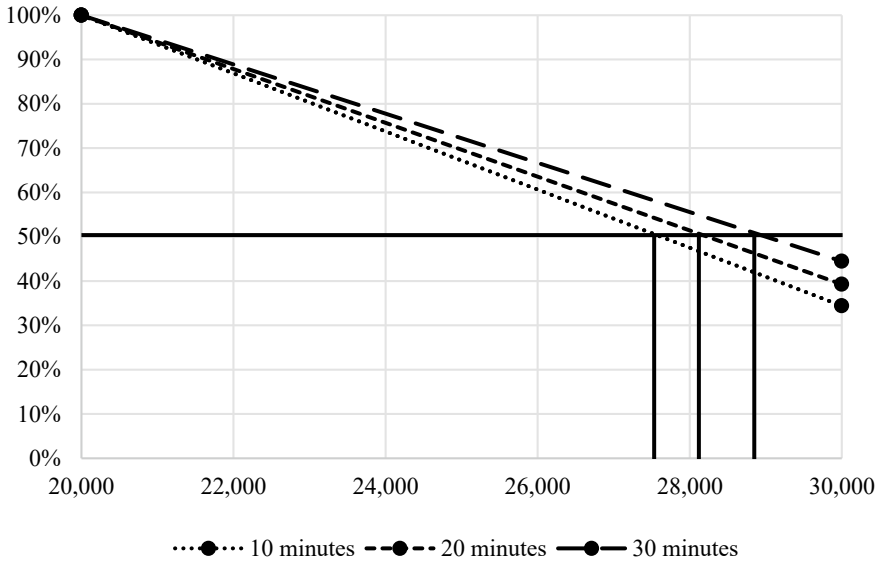


Fig. 9 WTP for all segments in the observed JORR 2 Area 1

Table 2 Toll road business plan at stage 1

AADT	Toll tariff in Rupiah	Toll revenue in Rupiah
42,084	22,000	333,305,280,000
52,911	17,500	333,339,300,000
62,843	17,500	395,390,910,000
44,314	19,500	311,084,280,000
Total revenue in Rupiah		1,373,639,760,000

Table 3 Toll road business plan at stage 2

AADT	Toll tariff in Rupiah	Toll revenue in Rupiah
26,697	22,000	211,440,240,000
31,977	17,500	201,455,100,000
24,732	17,500	155,811,600,000
41,313	19,500	290,017,260,000
Total revenue in Rupiah		858,724,200,000

toll tariff on trial. The trial in this stage stop at Table 7 as the total revenue has reached its maximum value in Table 6. Therefore, the resulting single tariff was Rp. 20,000.-. The value was acceptable as it was still under the WTP (Rp. 29,000.-).

Table 4 Toll road business plan at stage 3-trial 1

AADT	Toll tariff in Rupiah	Toll revenue in Rupiah
29,540	15,000	159,516,000,000
35,383	15,000	191,068,200,000
27,366	15,000	147,776,400,000
45,713	15,000	246,850,200,000
Total revenue in Rupiah		745,210,800,000

Table 5 Toll road business plan at stage 3-trial 2

AADT	Toll tariff in Rupiah	Toll revenue in Rupiah
25,490	17,500	160,587,000,000
30,531	17,500	192,345,300,000
23,614	17,500	148,768,200,000
39,445	17,500	248,503,500,000
Total revenue in Rupiah		750,204,000,000

Table 6 Toll road business plan at stage 3-trial 3

AADT	Toll tariff in Rupiah	Toll revenue in Rupiah
22,379	20,000	161,128,800,000
26,805	20,000	192,996,000,000
20,731	20,000	149,263,200,000
34,631	20,000	249,343,200,000
Total revenue in Rupiah		752,731,200,000

Table 7 Toll road business plan at stage 3-trial 4

AADT	Toll tariff in Rupiah	Toll revenue in Rupiah
19,715	22,500	159,691,500,000
23,615	22,500	191,281,500,000
18,265	22,500	147,946,500,000
30,510	22,500	247,131,000,000
Total revenue in Rupiah		746,050,500,000

6 Conclusions and Recommendations

Based on the analysis in this paper, several conclusions can be made as follow:

1. The ATP/ km for JORR 2 Area 1 was Rp. 2,800.-/ km.
2. The overall ATP for JORR 2 Area 1 was Rp. 36,102.-.
3. The WTP for JORR 2 Area 1 was Rp. 29,000.-.
4. After conducting three stages of tariff adjustment, the resulting single tariff was Rp. 20,000.- which was still less than WTP and therefore can be applied.

The recommended toll transaction system is an open transaction system with on-ramp payment to avoid the provision of transaction equipment in remote gates from the upstream barrier gate. Therefore, the toll gate operation will be more efficient.

References

1. Panou K (2020) An empirical model for setting and adjusting road-toll rates based on optimized equity and affordability strategies. *Case Stud Transport Policy* 8:1256–1269. <https://doi.org/10.1016/j.cstp.2020.08.006>
2. Indonesian Highway Cooperation (2007). Operation and management division: Manajemen pengumpulan tol, sistem transaksi, pentarifan & peramalan volume lalu-lintas. Indonesian Highway Cooperation, Jakarta
3. Tamin OZ, Rahman H, Kusumawati A, Munandar AS, Setiadji BH (1999) Evaluasi tarif angkutan umum dan analisis ability to Pay (ATP) dan willingness to pay (WTP) di DKI Jakarta. *Jurnal Transportasi Forum Studi Transportasi antar Perguruan Tinggi (FSTPT)* 1:121–139
4. Yulianto B, Legowo SJ, Atmojo MS (2017) Analisis potensi demand pada sekolah serta ability to pay (ATP) dan willingness to pay (WTP) pada Batik Solo Trans (BST) Koridor Empat di Surakarta. *Matriks Teknik Sipil* 5:1094–1101
5. Hotmaida B (1999) Analisis Ability To Pay dan Willingness To Pay Tarif Angkutan Umum Kota (Studi Kasus: Kotamadya Medan). Thesis, Master Thesis in Transportation Engineering, Civil Engineering, Postgraduate Program, Institut Teknologi Bandung
6. Nugroho IW, Kusuma RA, Setijowarno D, Ruktiningsih R (2007) Konferensi Teknik Sipil I. Analisis ability to pay (ATP) dan willingness to pay (WTP) Jalan Tol Semarang-Solo. Universitas Atma Jaya Yogyakarta, Yogyakarta, Indonesia, pp 461–474

Analysis of Transportation Accessibility in Shopping Areas in Makassar City



Jefryanto Londongsalu, Syafruddin Rauf, and Sumarni Hamid Aly

Abstract Accessibility has an important role for road users, both for users of private vehicles and public transportation. The ease of traveling by public transport will affect the use of this mode of transportation. This study was conducted to analyze the accessibility of public transportation to the shopping area (Mall). There are two data added in this study, namely walking distance and travel time from the point of public transportation to the shopping area (Mall) or vice versa. There are 3 shopping areas (malls) that are sampled in this study. The classification of accessibility levels based on distance and travel time is obtained from the results of the analysis using the percentile statistical method which is divided into four parts, namely high, medium, low and very low. The results showed that Makassar Town Square Mall has a high accessibility of public transportation that is 90.43%, Trans Mall has a low accessibility that is 61.62%. And Panakkukang Mall has moderate accessibility, which is 68%. To improve accessibility in this shopping area (Mall), it is recommended to add new public transportation routes to the Mall and provide scheduled services.

Keywords Accessibility · Public transportation · Geographic information system (GIS) · Statistical package for the social science (SPSS)

1 Introduction

Economic development and societal progress generate new expectations with regard to mobility, environmental protection, and quality of life [1]. A more sustainable urban development is one of the greatest challenges of modern times. The

J. Londongsalu (✉) · S. Rauf (✉) · S. H. Aly (✉)
Department of Civil Engineering, Hasanuddin University, Gowa, South Sulawesi, Indonesia
e-mail: jefryantohelo@gmail.com

S. Rauf
e-mail: syafraus@yahoo.co.id

S. H. Aly
e-mail: marni_hamidaly@yahoo.com

transport system has a great impact on regional development patterns, economic viability, environment, and promotion of socially acceptable quality of life levels [2]. Transportation, in general, is connected to all aspects of urban life: Leisure, education, business, and industry [3]. Increasing population growth from day to day has implications for the increasing need for supporting facilities and infrastructure in transportation. In addition, population growth has implications for higher population mobilization [4]. Makassar City is one of the largest cities in Eastern Indonesia and is the center of community activities in various sectors, namely trade, industry, and even education in South Sulawesi Province. Along with the development of the population in Makassar City which continues to grow from year to year with an area of 175.77 km², as well as community activities that continue to increase, so that the need for transportation facilities and infrastructure is increasingly urgent. As one of the largest trading cities in eastern Indonesia, Makassar City is never deserted from traffic activities, especially the travel route to the shopping areas (Mall). This is indicated by frequent traffic jams on the roads leading to the shopping area. In terms of efficiency, the congestion factor that increases travel time contributes significantly to the process of traffic transportation on the route to shopping areas (Malls), especially public transportation. Public transport has a very important role to play in the sustainability of urban settings. Mass mobility and quality of life in the city can be enhanced by developing public transport networks, with stops accessible to pedestrians at a reasonable walking distance. Accessibility of public transport is determined by how easily people get to the stops [5, 6]. For that, we need to analyze the accessibility of public transport passenger travel in order to determine the effectiveness and ease of reaching the location of the shopping area (Mall). On the way to the shopping center, there are many travel routes that have different accessibility values due to quite influential factors. These factors include time, distance, and speed in accessing the destination (Mall). The purpose of this study was to analyze the accessibility of public transportation to the location of Shopping Areas (malls). In a previous study, Syamsuri Nurman (2013) *Performance Analysis of Public Transportation in Makassar City Based On Open Source GIS (Case Study of Non-Campus Travel)*. The service of public transportation can be seen from the effectiveness and efficiency of public transportation operation. The effectiveness can be seen through several indicators such as accessibility, capacity, average celerity, and frequency headway. On the other hand, efficiency can be seen through some indicators such as achievability, expediency, utility, operational level, load factor, and the age of transportation. Based on its effectiveness and efficiency, the performance of public transportation in Makassar can be analyzed. From the analysis, it is known that 25.13% of passengers state that the public transportation (pete-pete) services are good while from the analysis of public transportation celerity meet the world standard, i.e., 10–12 km/hour for high density and 25 km/hour for low density [7].

2 Research Method

In this study, the stages of research implementation consist of four stages as shown in Fig. 1: the preliminary studies stage, In stage preparation tools and materials, the stage of collection or survey and data compilation and analysis or modeling stage.

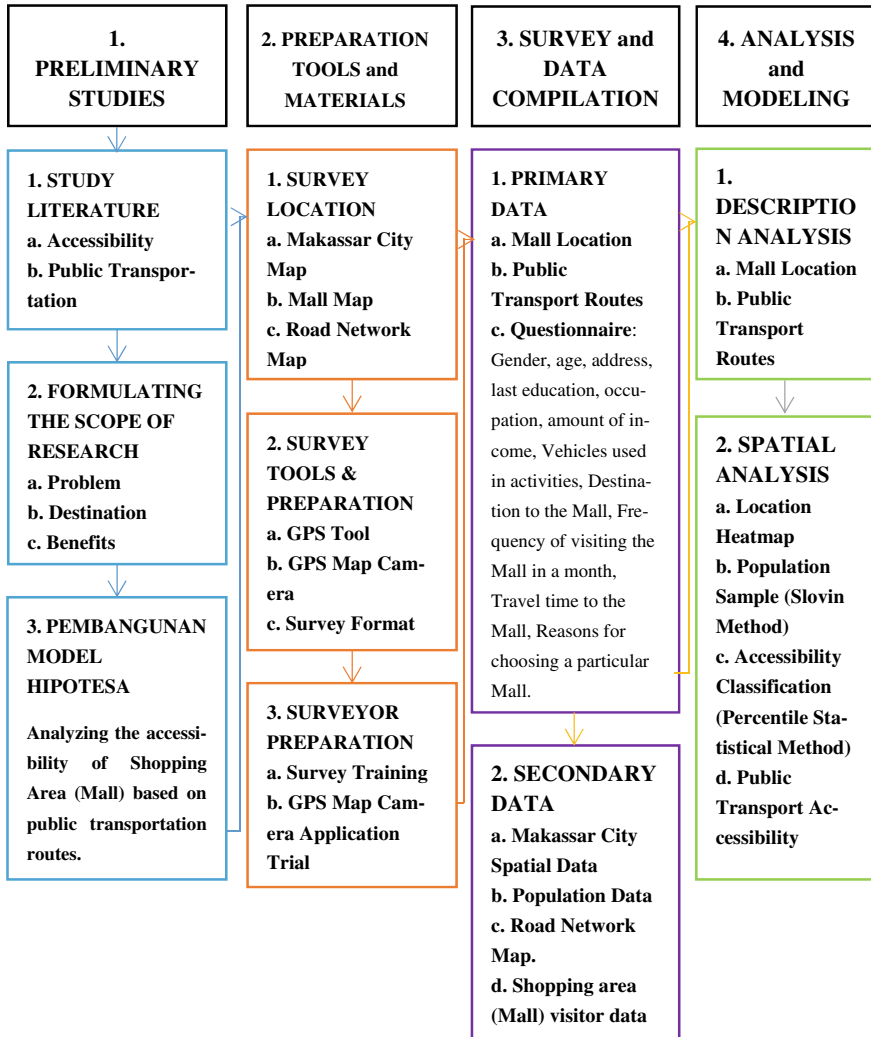


Fig. 1 Research flow scheme

2.1 Research Location, Time and Research Tools

This research was carried out in November 2020–January 2021, during which time a survey was conducted at the research location. The choice of research location was based on preliminary study observations. The territorial scope of this research is Makassar City. There are ten shopping areas in Makassar City, but three shopping areas are the research locations. The equipment used in this study is a GPS application. We use this application to send the location of the shopping area and public transport routes. And a camera to take a front view of the research site.

2.2 Data Collect

In this study, there are 2 data used, namely primary data and secondary data. Primary data, conducted by a direct survey to 3 shopping locations (Mall) in Makassar City. Then distribute online and offline questionnaires to mall visitors. Secondary data are Makassar City spatial data, population data, road network maps obtained from Makassar City BPS and Makassar City Transportation Service and shopping area visitor data (Mall) obtained from Mall management.

2.3 Data Analysis

Data on public transportation routes are obtained from the Makassar City Transportation Service which is useful for analyzing the accessibility of public transportation to shopping areas (Mall). The data is entered into the QGIS application. To find out the support of public transportation to the Mall, the data used is the data of respondents departing from the point of public transportation to the shopping area (Mall) or the data of respondents leaving the shopping area (Mall) to the point of public transportation. The results of the respondents' distance and travel time data were obtained from the ORS plugin in the QGIS application. Furthermore, the accessibility of public transport will be analyzed based on the percentile statistical method obtained from the SPSS application so that it can classify accessibility into four groups, namely high, medium, low, and very low. Using the Excel application will determine the level of accessibility and the percentage of accessibility of public transportation to the shopping area (Mall) so as to produce a conclusion.

3 Research Finding and Discussion

3.1 Makassar City Transport Routes

Based on Fig. 2, there are 13 public transportation routes operating in Makassar City. The length of the public transport routes in Makassar City is obtained from the results of the analysis on the QGIS application, with the longest route being the F1 public transport route with a distance of 38,850 km and the shortest public transport route code C with a distance of 11,322 km. The entire public transportation fleet operating in Makassar City is 5069 units.

The number of city transportation fleets operating in Makassar City is 5069 units. And there are 13 city transportation service routes that follow to the corners of Makassar City. Table 1 shows a list of public transportation service routes in the city of Makassar.

3.2 Sample Population

The method that the researcher uses to determine the number of samples is the Slovin formula. The Slovin formula is a mathematical system that is used to calculate the number of a population of certain objects whose characteristics are not known with certainty. Equation 1 shows the Slovin formula is commonly used for a study on a particular object in a large population, so it is used to examine a sample of a large population of objects.

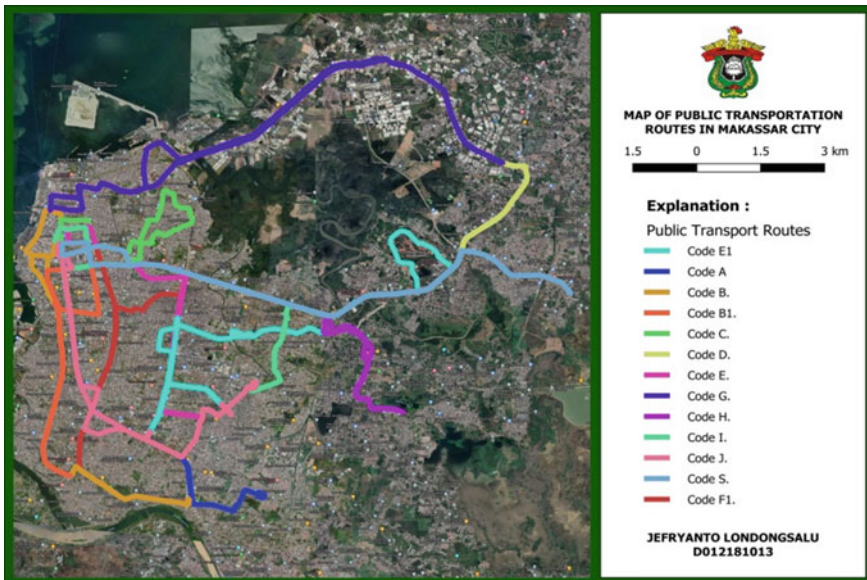


Fig. 2 Makassar public transportation routes map

Table 1 Makassar City public transport routes

Code	Route	Length (km)
A	BTN Minasa Upa—Jl. Syech Yusuf—Jl. Sultan Alauddin—Jl. Andi Tonro—Jl. Kumala—Jl. Ratulangi—Jl. Jendral Sudirman (Karebosi Timur)—Jl. HOS Cokroaminoto (Sentral)—KH. Wahid Hasyim—Jl. Wahidin Sudirohusodo—Jl. Pasar Butung	24.252
B	Jl. Terminal Tamalate—Jl. Malengkeri—Jl. Daeng Tata—Jl. Abdul Kadir—Jl. Dangko—Jl. Cendrawasih—Jl. Arief Rate—Jl. Sultan Hasanuddin—Jl. Patimura—Ujungpandang—Jl. Riburane—Jl. Jendral Achmad Yani (Balaikota)—Jl. Pasar Butung	22.45
B1	Jl. Cendrawasih—Jl. Arif Rate—Jl. Sultan Hasanudin—Jl. Sawerigading—Jl. Botolempangan—Jl. Karunrung—Jl. Sungai Saddang—Jl. G. Latimojong—Jl. Masjid Raya—Jl. Urip Sumoharjo—Jl. Perintis Kemerdekaan—Kampus Unhas	35.51
C	Jl. KH.Wahid.Hasyim—Jl. DR. Wahidin Sudirohusodo - Jl. Buru—Jl. Bandang—Jl. Masjid Raya—Jl. Cumi-Cumi—Jl. Pongtiku—Jl. Ujung Pandang Baru—Jl. Gatot Subroto—Jl. Juanda—Jl. Regge—Jl. Rappokalling	11.322
D	Terminal Daya—Jl. Perintis Kemerdekaan—Jl. Urip Sumoharjo—Jl. AP. Pettarani—Jl. Bawakaraeng—Jl. G.Latimojong—Jl. Andalas—Jl. Laiya—Selatan Makassar Mall	28.068
E	Terminal Panakkukang—Jl. Toddopuli—Jl. Tamalate—Jl. Emmy Saelan—Jl. Mapala—Jl. AP. Pettarani—Jl. Maccini Raya—Jl. Urip Sumoharjo—Jl. Bawakaraeng—Jl. G. Latimojong—Jl. Andalas—Jl. Laiya—Jl. KH. Agus Salim—Timur Makassar Mall	20.77
E1	Terminal Panakkukang—Jl. Toddopuli Raya—Jl. Perumnas—Jl. Hertasing—Jl. AP. Pettarani—Jl. Kampus IKIP—Jl. Gunung Sari—Jl. AP. Pettarani—Jl. Pelita Raya—Jl. AP. Pettarani—Jl. Abdullah Daeng Sirua—PLTU—Jl. Urip Sumoharjo—Jl. Perintis Kemerdekaan—Kampus Unhas	30.651
F1	Terminal Tamalate—Jl. Mallengkeri—Jl. Daeng Tata—Jl. M. Tahir—Jl. Kumala—Jl. Veteran—Jl. Masjid Raya—Jl. Urip Sumoharjo—Jl. Perintis Kemerdekaan—Kampus Unhas	38.85
G	Terminal Daya—Jl. Kima—TOL (Ir. Sutami)—Jl. Tinumbu—Jl. Cakalang—Jl. Yos Sudarso—Jl. Tentara Pelajar—Jl. Kalimantan—Pasar Butung	28.69
H	Perumnas Antang—Jl. Antang Raya—Jl. Urip Sumiharjo—Jl. Bawakaraeng—Jl. Jenderal Sudirman—Jl. DR. Wahidin Sudirohusodo—Jl. P. Diponegoro	23.314
I	Terminal Panakkukang—Toddopuli Raya—Borong—Batua Raya—Jl. Taman Makam Pahlawan - Jl. Urip Sumihorjo Jl. Bawakaraeng—Jl. Jenderal Sudirman—Jl. DR. Wahidin Sudirohusodo—Jl. P. Diponegoro - Jl. Andalas - Jl. Masjid Raya	18.69
J	Terminal Panakkukang—Jl. Toddopuli Raya—Jl. Tamalate—Jl. Emmy Saelan—Jl. Sultan Alauddin—Jl. Andi Tonro—Jl. Kumala—Jl. Ratulangi—Jl. Jenderal Sudirman—Jl. HOS Cokroaminoto—Jl. Nusakambangan	22.026
S	BTP Tamalanrea—Jl. Perintis Kemerdekaan—Jl. Urip Sumoharjo—Jl. AP. Pettarani—Jl. Bawakaraeng—Jl. Latimojong—Jl. Andalas—Jl. Laiya—Selatan Makassar Mall	27.384

Table 2 Total of respondents in each shopping area (mall)

	Makassar Town Square Mall	Trans Mall	Panakkukang Mall
Total	94	99	50
Percentage (%)	38.68	40.74	20.58

$$n = N(1 + Ne^2) \tag{1}$$

n = Number of Samples
 N = Total Population
 e = Error Tolerance (set 10% or 0.1)
 90% confidence level.

Table 2 shows a number of respondents sample based on the location of the shopping area (Mall).

3.3 *Distance and Time on Foot from Public Transportation to Shopping Area (Mall) or Distance and Time on Foot from Shopping Are (Mall) to Public Transportation*

A sample of 243 respondents from three Shopping Areas (Mall) in Fig. 3 shows the distance, and Fig. 4 shows the walking time from public transportation to the location of the Shopping Areas (mall). The average walking time from the Makassar Town Square Mall location to the public transportation point or vice versa is 0.018 h or 18 min and a distance of 0.09 km or 90 m. Most of the respondent's walking time is quite short because the public transportation line is right in front of the mall and is the only point for respondents to use public transportation. However, there are some respondents who have to walk a bit far to get to the public transportation point in the direction of their house.

In the Trans Mall based on the purpose of each respondent, there are two public transportation codes which are the main transportation of respondents, namely Transport Codes B1 and J because only these transportation codes have the closest distance to Trans Mall even though the distance between Trans Mall and public transportation points is quite far. The distance between the Trans Mall and the B1 public transportation point is 3275 km with a travel time of 0.655 h, and the J code public transportation is 3,584 km with a travel time of 0.717 h, so it greatly affects the travel time as well. However, there were two respondents who did not reach the point of public transportation because their area of residence was in Barombong and Galesong.

At Panakkukang Mall, based on the purpose of each respondent, there are two different public transportation points which are the respondents' main transportation, namely Transportation Code E1 as far as 0.805 km with a time of 0.161 h and Transport Codes J and I as far as 1079 km with a time of 0.216 h because only transportation codes This one has the closest distance to Panakkukang Mall. However, there are two respondents who do not use public transportation because the location of their residence is close to the Panakkukang Mall location.

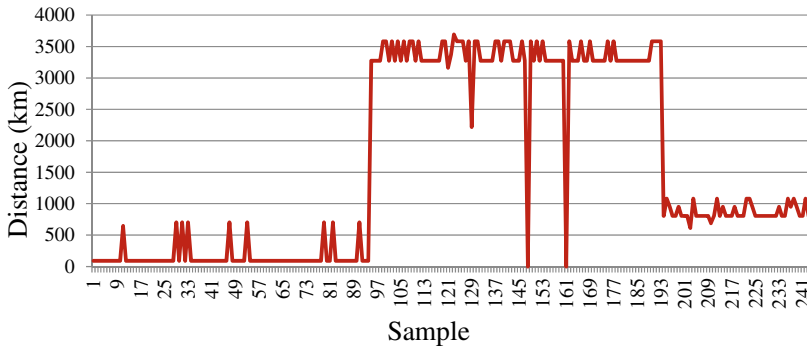


Fig. 3 Distance on foot from public transportation to shopping area (mall) or distance on foot from shopping area (mall) to public transportation

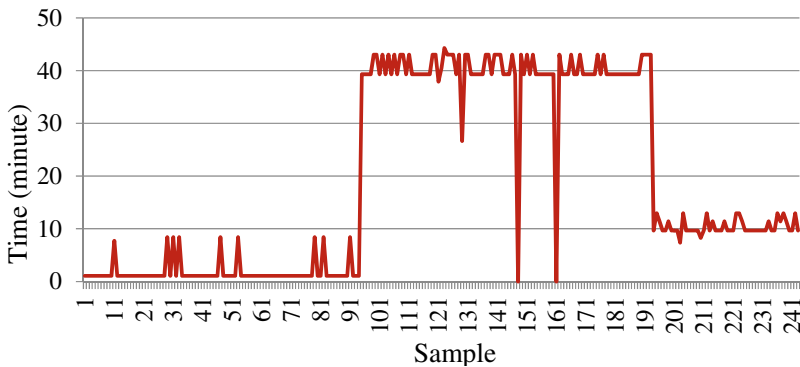


Fig. 4 Time on foot from public transportation to shopping area (mall) or time on foot from shopping area (mall) to public transportation

3.4 Accessibility Based on Distance

Accessibility based on distance can be determined based on the respondent's travel distance from the shopping area (Mall) to public transportation points around the mall to see the role of public transportation to the mall. Table 3 shows the classification of the level of accessibility is divided into four parts, starting from high,

Table 3 Accessibility classification based on distance

Classification	
High accessibility	Distance \leq 90 m
Medium accessibility	90 m < Distance \leq 805 m
Low accessibility	805 m < Distance \leq 3275 m
Very low accessibility	Distance > 3275 m

Table 4 Accessibility percentage based on distance

No.	Accessibility	Accessibility percentage (%)		
		Makassar Town Square Mall	Trans Mall	Panakkukang Mall
1	High	90.43	0.00	0.00
2	Medium	9.57	0.00	68.00
3	Low	0.00	61.62	32.00
4	Very low	0.00	38.38	0.00

medium, low, and very low levels. This classification is obtained from the results of the analysis using the SPSS application with percentile statistical method.

Table 4 shows that the accessibility of Makassar Town Square Mall to public transportation points based on distance has a high value, which is around 90.43%, because the public transportation point is right in front of the Mall location, making it easier for visitors to use public transportation in accordance with the direction of their destination. Compared to the Trans Mall, which has low accessibility, namely 61.62%, even very low, namely 38.38% due to the absence of access or public transportation routes that are close to the Mall. Visitors have to travel a long distance to get to the point of public transportation. Meanwhile, at Panakkukang Mall, the accessibility is moderate, which is around 68.00%.

3.5 Accessibility Based on Time

Accessibility based on time can be determined based on the respondent’s travel time from the shopping area (Mall) to public transportation points around the mall to see the role of public transportation to the mall. Table 5 shows the classification of the level of accessibility is divided into four parts, starting from high, medium, low, and very low levels. This classification is obtained from the results of the analysis using the SPSS application with percentile statistical method.

Table 6 shows that the accessibility of Makassar Town Square Mall to public transportation points based on travel time has a high value, which is around 90.43%, because the public transportation point is right in front of the Mall location, making it easier for visitors to use public transportation in accordance with the direction of their destination. Compared to the Trans Mall, which has low

Table 5 Accessibility classification based on travel time

Classification	
High accessibility	Time ≤ 1.08 m
Medium accessibility	1.08 m < Time ≤ 9.66 m
Low accessibility	9.66 m < Time ≤ 39.30 m
Very low accessibility	Time > 39.30 m

Table 6 Accessibility percentage based on travel time

No.	Accessibility	Accessibility percentage (%)		
		Makassar Town Square Mall	Trans Mall	Panakkukang Mall
1	High	90.43	0.00	0.00
2	Medium	9.57	0.00	68.00
3	Low	0.00	61.62	32.00
4	Very low	0.00	38.38	0.00

accessibility, namely 61.62%, even very low, namely 38.38% due to the absence of access or public transportation routes that are close to the Mall. Visitors have to travel a long distance to get to the point of public transportation. Meanwhile, at Panakkukang Mall, the accessibility is moderate, which is around 68.00%.

4 Conclusion

The accessibility of shopping areas (Mall) to public transportation routes is seen from the distance and travel time of respondents (mall visitors) from public transportation points to shopping areas (Mall). To see the role of public transportation on the location of the mall, there are data obtained, namely the walking distance from the public transportation point to the mall and the walking distance from the mall to the public transportation point. So that the data obtained that the accessibility of public transportation to the 3 locations of the shopping center (Mall) studied is still very low. As is the case with the Trans Mall, which is very low at around 61.62% because it is not accessible by public transportation routes. The distance between the Trans Mall and public transportation points is very far. At Panakkukang Mall, the value of public transportation accessibility to mall locations is included in the medium category, which is around 68%. Unlike the Makassar Town Square Mall which has a high accessibility value of 90.43% because the location of the mall can be reached by all public transportation routes and is right in front of the mall so that respondents (mall visitors) easily get access to their homes. However, there are some respondents who have to connect and change public transportation codes because the location of their homes cannot be reached by only one public transportation code.

Acknowledgements Thanks to God Almighty for His inclusion so that we can complete this research. We also thank all those who have supported this research: our parents who have always provided moral and material support, our supervisors Mr. Syafruddin Rauf and Mrs. Sumarni Hamid Aly who have taken the time to prepare this research, to the leadership and staff of BPS Makassar City, as well as to the leadership and staff of the Makassar City Transportation Service who have provided us with access to data collection. And to the managers of Makassar Town Square Mall, Trans Mall, and Panakkukang Mall.

References

1. Kittelson & Associates Inc (2003) Transit capacity and quality of service manual (2nd ed.), TCRP Project 100. TRB National Research Council, Washington DC, United States of America
2. Murray AT, Davis R, Stimson RJ, Ferreira L (1998) Public transportation access. *Transp Res D Transp Environ* 3:319–328
3. Olawole MO (2012) CODATU XV conference, the role of urban mobility in (re)shaping cities. In: *Accessibility to Lagos bus rapid transit (BRT LITE) bus stops: an empirical study*. Codatu, Lyon, France, pp 1–15
4. Hasanuddin (2014) Analisis Aksesibilitas Angkutan Pribadi Menuju Kampus Universitas Hasanuddin. Dissertation, Universitas Hasanuddin
5. Wachs M, Kumagai TG (1973) Physical accessibility as a social indicator socio-econ plan. *Science* 7:437–456
6. Bok J, Kwon Y (2016) Comparable measures of accessibility to public transport using the general transit feed specification. *Sustainability* 8:224
7. Syamsuri N (2013) Analisa Kinerja Angkutan Umum Di Kota Makassar Berbasis GIS Open Source (Studi Kasus Trayek Non Kampus). *Jurnal Penelitian Jurusan Sipil Fakultas Teknik Universitas Hasanuddin*

Priority of Sustainable Transport Policy Implementation in Expert Perspective



Nindyo Cahyo Kresnanto , Ricko Nasrianda Sinaga, Risdiyanto ,
and Wika Harisa Putri 

Abstract Implementing sustainable transportation policies is a fundamental problem for all countries, especially in choosing which policies are priorities to be implemented. A method is needed to prioritize the implementation of the policy. This study will develop priorities for implementing sustainable transportation policies with an analytical hierarchy process (AHP) and involve nineteen experts as respondents. The respondents consisted of two transportation experts from academia, eight people from the general public, three policymakers in the provincial police, three people from the Provincial Development Planning Agency, and two public transport operators. The results of the AHP analysis show that the K1 policy (the application of technology to improve vehicle fuel efficiency or the use of environmentally friendly fuels) is the most recommended policy by experts in addition to the K3 (improved mobility and land use management) and K2 (mode shift and travel behavior change) policies. The three most recommended policy alternatives to be implemented in support of sustainable transportation are A2 (providing incentives for purchasing eco-friendly vehicles for vehicle renewal), A1 (building an environmentally friendly vehicle industry), and A5 (promoting better transportation infrastructure).

Keywords AHP · Policy · Priority · Sustainable transport

N. C. Kresnanto (✉) · R. N. Sinaga · Risdiyanto
Department of Civil Engineering, Janabadra University, Yogyakarta, Indonesia
e-mail: nindyo_ck@janabadra.ac.id

W. H. Putri
Janabadra University, Yogyakarta, Indonesia
e-mail: wikaharisa@janabadra.ac.id

1 Introduction

The whole world is currently faced with transportation problems, such as high vehicle ownership [1–3], increasing pollution [4, 5], and high fuel consumption for transportation [6]. The high level of motorized vehicle ownership continues to increase throughout the year, especially in Organisation for Economic Co-operation and Development (OECD) countries. By 2030 it is predicted that 56% of world vehicle ownership will be in OECD countries, which is a substantial increase from 24% in 2004 [7]. In Indonesia in 2019, the growth of motorized vehicles was 14.55% per year, car ownership reached 324 vehicles per 1000 population [8]. This rapid growth of vehicles will of course, also impact the growth of fuel demand. This problem certainly has a terrible impact on the community's environmental, social and economic conditions.

Various efforts to overcome this have been implemented, especially by implementing policies that support sustainable transportation. Policies related to this are of course, very diverse and mutually supportive of each other. There are at least three main policies to support sustainable transportation, namely: (1) technology application, (2) pricing and financing, and (3) transportation integration with land use. [9]. Of the three main policies, experts then go into detail at the implementation level [10, 11], and the implementation can vary greatly depending on each region [12]. To determine what policies will be prioritized, a lot is also done by making policy priorities.

One of the tools to prioritize policy implementation is Multiple-Criteria-Decision-Making (MCDM). One method of MCDM is the analytical hierarchy process (AHP). In this research, AHP will apply to prioritize the implementation of sustainable transportation policies from expert perceptions.

2 Literature Review

Sustainable transportation define as the ability to support community mobility without causing negative impacts on the environment, social, and economic [13, 14]. Sustainable transportation policy should be directed towards the goal at least [15]:

1. involving best practices on the cost–benefit analysis and environmental assessment in the decision-making process;
2. efficient and coherent pricing and financing of infrastructure;
3. reducing CO₂ emissions from road transport;
4. promoting the utilization of low emission trucks;
5. improving the competitiveness of street options—rail and inland transportation—and eliminating hindrances to the worldwide improvement of their business sectors;

6. improving street security;
7. resolving struggles among transport and sustainable development in downtown environments.

This study uses the Analytic Hierarchy Process (AHP) to make policy priorities about sustainable transportation as a tool for decision-making. Thomas L. Saaty developed AHP in the 70s. This method will extenuate complex multi-criteria issues into a hierarchy. Hierarchy is characterized as a portrayal of an intricate issue in a layered structure. The primary level is the objective, trailed by the degree of elements, rules, sub-standards, and the last, degree of choices [16, 17].

AHP is part of the MCDM or Multiple-Criteria-Decision-Analysis (MCDA) family. MCDM that is popularly used today are: AHP, Scoring Model, Utility Model, Analytic Network Process (ANP), Out Ranking Method, Technique for Others Reference by Similarity to Ideal Solution (TOPSIS), and others. [18]. MCDM is a sub-order of tasks research that expressly assesses a few clashing measures in decision making. MCDM is communicated as a decision-making technique to decide the best option from a few options dependent on specific criteria [19]. The advantage of this method is that it can consider both financial and non-financial impacts (measured and immeasurable) [20].

3 Methodology

They were gathering information for the contribution of this strategy utilizing a survey intended for AHP investigation. Respondents were approached to contrast the models and pairwise correlations. Pairwise correlations survey the overall significance of standards/sub measures on a scale of 1, 3, 5, 7, and 9 [17]. Respondents are experts in the field of transportation from several government agencies, lecturers, and business actors. The respondents consisted of two transportation experts from academia, eight people from the general public, three policymakers in the provincial police, three people from the Provincial Development Planning Agency, and two public transport operators. The MCDA interaction with AHP for surveying the components that most impact the travel ridership will be done utilizing the accompanying advances.

Step 1. Characterize the issue and decide the ideal arrangement. The problem to be researched is determining what policies can be done to support sustainable transportation based on previous studies. This study will analyze three factors at the criteria level (K) and seven factors at the sub-criteria level (A) based on the previous data review (Fig. 1).

Step 2. Make a hierarchical structure that beginnings with an overall objective, trailed by sub-targets, standards, and possible alternatives at the lowest level of criteria (Fig. 1).

Step 3. Make a pairwise comparison matrix that represents each element's relative contribution or impact on every one of the objectives or standards above it.

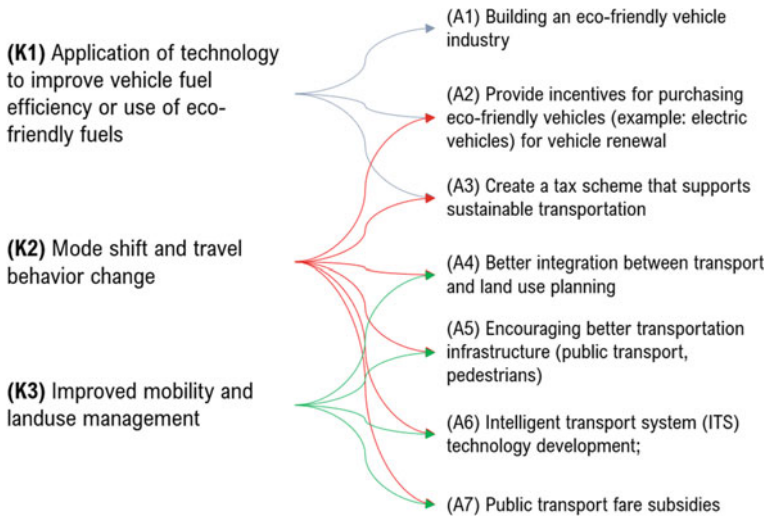


Fig. 1 General hierarchy structure in prioritizing sustainable transportation action

Comparison is settled on the decision-making judgment by evaluating the significance of a component contrasted with different components.

In the significance of weighting or pairwise comparison evaluation, the reciprocal axiom applies. Implying that component A_n is viewed as more significant (5) than component B. B is more significant 1/5 contrasted with component A. On the off chance that component A_n is pretty much as significant as B, each worth = 1. Doing a pairwise comparison with the goal that general judgment is gotten $n[(n - 1)/2]$ pieces, where n is the quantity of standards thought about, for this situation, the all-out judgment in level models is $n [(n - 1)/2] = 3[(3 - 1)/2] = 3$ cells. With the same calculation, at the K1 sub-criteria level, there are three judgments. At the K2 sub-criteria level, there are 15 judgments, and at the K3 sub-criteria level, there are six judgments.

The original judgment matrix, A_s , in subsegment s of each respondent was initially normalized to matrix B_s . The elements in each column of the matrix (α_{ij}) were divided by the sum of the elements of the same column (s_j) to get the normalized elements, as shown in Eq. 1.

$$A_s = \begin{bmatrix} \alpha_{11} & \dots & \alpha_{17} \\ \vdots & \ddots & \vdots \\ \alpha_{71} & \dots & \alpha_{77} \end{bmatrix}; B_s = \begin{bmatrix} \alpha_{11}/s_1 & \dots & \alpha_{17}/s_7 \\ \vdots & \ddots & \vdots \\ \alpha_{71}/s_1 & \dots & \alpha_{77}/s_7 \end{bmatrix} = \begin{bmatrix} \beta_{11} & \dots & \beta_{17} \\ \vdots & \ddots & \vdots \\ \beta_{71} & \dots & \beta_{77} \end{bmatrix} \tag{1}$$

where β_{ij} is a normalized element in the matrix, B_s . The priority vector V_s was then determined by getting the average of each row, as shown in Eq. 2.

Table 1 Random index value

Ordo matrix	1	2	3	4	5	6	7	8	9	10
RI	0	0	0.58	0.9	1.12	1.24	1.32	1.41	1.45	1.49

$$V_s = \begin{bmatrix} (\beta_{11} + \beta_{12} + \dots + \beta_{17})/7 \\ \vdots \\ (\beta_{71} + \beta_{72} + \dots + \beta_{77})/7 \end{bmatrix}_s = \begin{bmatrix} v_1 \\ \vdots \\ v_7 \end{bmatrix}_s \tag{2}$$

Step 4. Compute eigenvalues and test the consistency of every respondent. If it is not consistent, information recovery is rehashed, or conflicting information is disposed of. The fundamental guideline in this consistency test is that if A is a higher priority than B, B is a higher priority than C, so it is absolutely impossible that C is a higher priority than A. The benchmark utilized is CI (Consistency Index) versus RI (Ratio Index) or CR (Consistency Ratio), CR and CI can calculated by using Eq. 3, C_s counted by using Eq. 4, and RI is determined based on prior research (Table 1) [21]

$$CR_s = \frac{CI_s}{RI}; CI_s = \frac{(\lambda_s - n)}{(n - 1)}; \lambda_s = C_s/n \tag{3}$$

$$C_s = A_s V_s = \begin{bmatrix} \alpha_{11} & \dots & \alpha_{17} \\ \vdots & \ddots & \vdots \\ \alpha_{71} & \dots & \alpha_{77} \end{bmatrix} \begin{bmatrix} v_1 \\ \vdots \\ v_7 \end{bmatrix} = \begin{bmatrix} c_1/v_1 \\ \vdots \\ c_7/v_7 \end{bmatrix} \tag{4}$$

Step 5. Check the CR. On the off chance that the worth is in excess of 10%, the judgment information should be improved—the generation of a new judgment matrix. In view of the consequences of the past advance, a new judgment matrix developed. Judgment matrices were consistently retained, while those otherwise were revised. Since the quantity of respondents is more than one individual, it is important to join the respondents’ sentiments by utilizing the average geometry equation before the AHP computation is performed. The assessment of respondents utilized is the assessment of respondents who have tried their consistency through an interaction of consistency testing with $CR \leq 0.10$.

4 Discussion

The results of the AHP analysis at the criterion level obtained eigenvalues and priority rankings for implementing sustainable transportation policies, as shown in Table 2. According to experts, the K1 policy (application of technology to improve vehicle fuel efficiency on the use of environmentally friendly fuels) is the most

Table 2 Eigenvalue and priority at the criteria level

	K1	K2	K3	Eigenvalue	Ranking priority
K1	0.545	0.500	0.571	0.539	1
K2	0.182	0.167	0.143	0.164	3
K3	0.273	0.333	0.286	0.297	2

prioritized policy. The next ranking is a policy of increasing mobility and land use (K3) and a policy of changing modes and changing travel behavior (K2). With the results of the calculation of the value of $CR = 0.00964 < 0.100$, it means that the respondent's preference is consistent or valid.

Furthermore, at the sub-criteria level of the K1 criteria, the expert judgment results are obtained, as shown in Table 3. Sub-criteria A2 is the alternative with the highest eigenvalue (0.490), meaning it is the most prioritized to run if it only considers the K1 criteria. With the results of the calculation of the value of $CR = 0.05234 < 0.100$, it means that the respondent's preference is consistent or valid.

At the sub-criteria level in the K2 criteria, the CR value is obtained = $0.0997 < 0.100$, which means that the respondent's preferences are consistent. Based on Table 4, it can be concluded that in implementing the K2 criteria, alternative A5 (encouraging better transportation infrastructure) is the most priority alternative to be implemented. It is evidenced by the weight value obtained is 0.277. While in second place, there is alternative A7 (subsidy for public transport fares) with a weight of 0.179. Third, there are alternative A4 (better integration between transportation planning and land use) with a weight of 0.172. Fourth, alternative A3 (making a tax scheme that supports eco-friendly transportation) with a weight of 0.153. Fifth, there is alternative A2 with a weight of 0.110. While in the last place, there is an alternative A6 (development of intelligent transport system technology) with a weight of 0.109.

Based on Table 5, it can be concluded that in implementing the K3 criteria, the most priority alternative to be applied is alternative A5. It is evidenced by the weight value obtained is in the first position with a weight value of 0.387 or 38.7%. In second place is alternative A4, with a weight of 0.275 or 27.5%. The third position is the alternative A6 with a weight of 0.198 or 19.8%. In the last position, there is an alternative A7 with a weight of 0.140 or 14.0%. With the value of $CR = 0.0501 < 0.1$.

Table 3 Eigenvalue and priority at sub-criteria level K1

	A1	A2	A3	Sum	Eigenvalue	Rank
A1	0.286	0.250	0.400	0.936	0.312	2
A2	0.571	0.500	0.400	1.471	0.490	1
A3	0.143	0.250	0.200	0.593	0.198	3

Table 4 Eigenvalue and priority at sub-criteria level K2

	A2	A3	A4	A5	A6	A7	Sum	Eigenvalue	Rank
A2	0.105	0.063	0.077	0.150	0.190	0.077	0.662	0.110	5
A3	0.211	0.125	0.077	0.150	0.048	0.308	0.918	0.153	4
A4	0.211	0.250	0.154	0.150	0.190	0.077	1.032	0.172	3
A5	0.211	0.250	0.308	0.300	0.286	0.308	1.662	0.277	1
A6	0.053	0.250	0.077	0.100	0.095	0.077	0.652	0.109	6
A7	0.211	0.063	0.308	0.150	0.190	0.154	1.075	0.179	2

Table 5 Eigenvalue and priority at sub-criteria level K3

	A4	A5	A6	A7	Eigenvalue	Rank
A4	0.250	0.200	0.364	0.286	0.275	2
A5	0.500	0.400	0.364	0.286	0.387	1
A6	0.125	0.200	0.182	0.286	0.198	3
A7	0.125	0.200	0.091	0.143	0.140	4

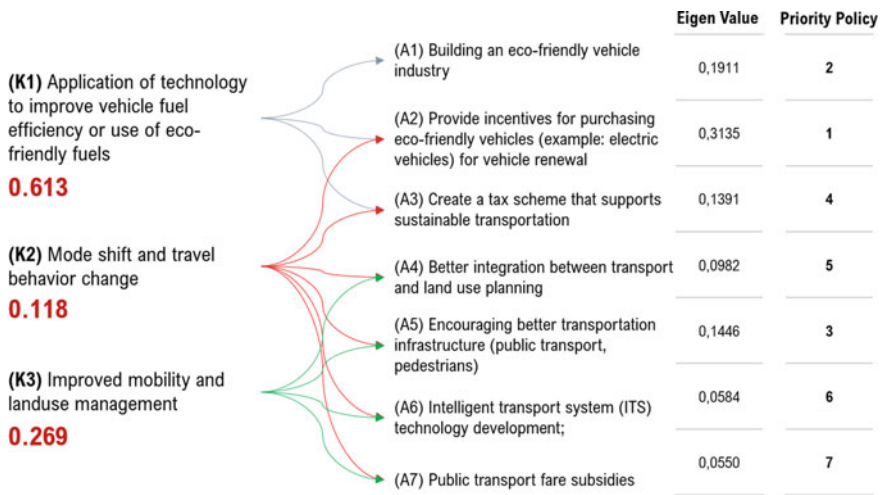


Fig. 2 Eigenvalue and priority policy

Based on the normalized pairwise comparison matrix results, it can also be seen that the ranking of all alternatives (Fig. 2). This ranking can be used as one of the suggestions in developing alternative implementations. As for getting the ranking results on the alternatives offered, it will be multiplied by the evaluation factor (eigenvector) of each alternative by the criteria evaluation factor.

5 Conclusions

The results showed that the K1 policy (the application of technology to improve vehicle fuel efficiency or the use of environmentally friendly fuels) was the most recommended policy by experts in addition to the K3 and K2 policies. The three most recommended policy alternatives to be implemented in support of sustainable transportation are A2 (providing incentives to purchase eco-friendly vehicles for vehicle renewal), A1 (building an environmentally friendly vehicle industry), and A5 (encouraging better transportation infrastructure).


References

1. Kresnanto NC, Wicaksono BK (2021) The impact of growth in vehicle ownership on commuter travel time. https://doi.org/10.1007/978-981-33-6311-3_85
2. Harriet T, Poku K, Kwabena AE (2013) An assessment of traffic congestion and its effect on productivity in urban Ghana. *Int J Bus Soc Sci* 4:1–10
3. Dargay J, Gately D, Sommer M (2007) Vehicle ownership and income growth world wide: 1960–2030. *Energy J* 28:1–32
4. Anggarani D, Rahardjo M, Nurjazuli N (2016) Hubungan Kepadatan Lalu Lintas Dengan Konsentrasi C0hb Pada Masyarakat Berisiko Tinggi Di Sepanjang Jalan Nasional Kota Semarang. *J Kesehatan Masy* 4:139–148
5. Akgüngör AP, Demirel A (2008) Investigating urban traffic based noise pollution in the city of Kirikkale, Turkey. *Transport* 23:273–278. <https://doi.org/10.3846/1648-4142.2008.23.273-278>
6. Gallagher KS, Muehlegger E (2011) Giving green to get green? Incentives and consumer adoption of hybrid vehicle technology. *J Environ Econ Manage* 61:1–15. <https://doi.org/10.1016/j.jeem.2010.05.004>
7. Dargay J, Gately D, Sommer M (2007) Vehicle ownership and income growth, worldwide: 1960–2030. *Energy J* 28:143–170. <https://doi.org/10.5547/ISSN0195-6574-EJ-Vol28-No4-7>
8. Kresnanto NC (2019) Model of relationship between car ownership growth and economic growth in Java. *IOP Conf Ser Mater Sci Eng* 650:8. <https://doi.org/10.1088/1757-899X/650/1/012047>
9. Greene DL (1997) Sustainable transport. *J Transp Geogr* 5:177–190. <https://doi.org/10.1016/C2013-0-17820-8>
10. Ogryzek M, Adamska-Kmieć D, Klimach A (2020) Sustainable transport an efficient transportation network—case study. *Sustainability* 1–14
11. Pujiati A, Nihayah DM, Adzim F, Nikensari SI (2020) Implementation of sustainable transportation using gap analysis: case study of semarang city. *J Crit Rev* 7:47–54. <https://doi.org/10.31838/jcr.07.07.09>
12. Pettersson F, Stjernborg V, Curtis C (2021) Critical challenges in implementing sustainable transport policy in Stockholm and Gothenburg. *Cities* 113:103153. <https://doi.org/10.1016/j.cities.2021.103153>
13. Rodrigue J-P. Transportation, sustainability and decarbonization. In: *The geography of transport systems*. <https://transportgeography.org/contents/chapter4/transportation-sustainability-decarbonization/>. Accessed 9 Jul 2021
14. Cruzado I (2005) Sustainable transportation system. *WIT Trans Built Environ* 77:343–349. <https://doi.org/10.35940/ijtee.b1229.1292s219>

15. ECOM (European Conference of Ministers of Transport) (2000). Sustainable transport policies
16. Saaty TL (2008) Decision making with the analytic hierarchy process. *Int J Serv Sci* 1:83. <https://doi.org/10.1504/ijssci.2008.017590>
17. Saaty TL (1990) How to make a decision: the analytic hierarchy process. *Eur J Oper Res* 48:9–26. [https://doi.org/10.1016/0377-2217\(90\)90057-i](https://doi.org/10.1016/0377-2217(90)90057-i)
18. Kornysheva E, Salinesi C (2007) MCDM techniques selection approaches: state of the art. *IEEE Symp Comput Intell Multi-criteria Decis Making* 2007:22–29. <https://doi.org/10.1109/mcdm.2007.369412>
19. Kusumadewi S, Hartati S, Harjoko A (2006) Fuzzy multi attribute decision making (Fuzzy MADM). *Graha Ilmu*, Yogyakarta, Indonesia
20. Kahraman C (2008) Fuzzy multi-criteria decision making. *Springer Optim Its Appl*. <https://doi.org/10.1007/978-0-387-76813-7>
21. Podvezko V, Sivilevicius H, Podvezko A (2014) Scientific applications of the AHP method in transport problems. *Arch Transp* 29:47–54. <https://doi.org/10.5604/08669546.1146966>

Prioritizing District Road Maintenance Using AHP Method



Nindyo Cahyo Kresnanto 

Abstract Efforts to extend the useful life of roads are carried out by routine, periodic maintenance, or reconstruction. In Indonesia, maintenance of district roads is carried out based on the Technical Guidelines for District Road Planning and Programming (SK No. 77 of the Directorate General of Highways, 1990). Road maintenance regarding these instructions prioritizes roads that are maintained by 5 criteria and 17 sub-criteria conditions that must be considered. Of course, it is not easy to prioritize with so many criteria and sub-criteria. This study will prioritize road maintenance based on the criteria/sub-criteria used by the Analytic Hierarchy Process (AHP) method. The research was conducted by interviewing respondents who are road maintenance experts. Furthermore, the results of respondents' assumptions as measured by a Likert scale were analyzed using the AHP method, which resulted in the weight of the influence of the criteria/sub-criteria on the priority of road maintenance. The results showed that the most important order of priority for road maintenance is the traffic volume factor, the road condition factor, the policy factor, the economic factor, and the last factor is land use.

Keywords Analytic hierarchy process (AHP) · Priority · Rehabilitation

1 Introduction

With age, the road will experience a decrease in the level of service. In addition to traffic loads, other factors that can damage roads are temperature, weather, air content, and road quality. To extend the life of the road, it is necessary to carry out routine or periodic maintenance so that the road is always in a state of high service level. The relationship between the level of road service, rehabilitation, and duration of road use can be seen in Fig. 1 [1].

N. C. Kresnanto (✉)
Civil Engineering, Janabadra University, Yogyakarta, Indonesia
e-mail: nindyo_ck@janabadra.ac.id

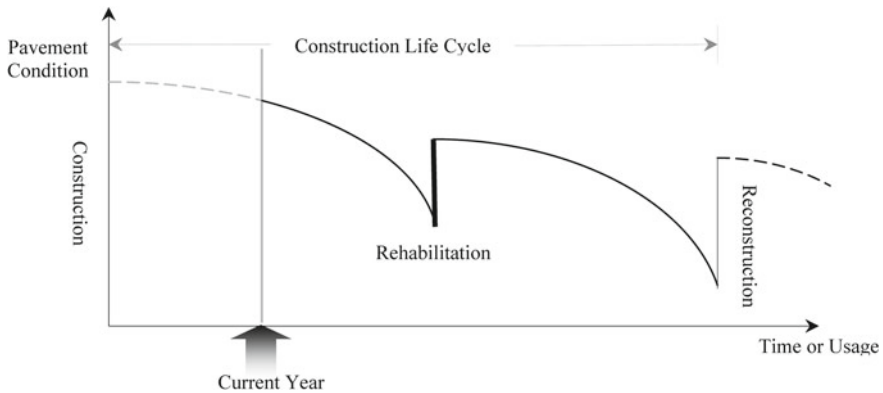


Fig. 1 Rehabilitation and construction life-cycles for new and existing pavements [1]

The maintenance/rehabilitation process must be carried out with priority by assessing road conditions based on specific criteria [2–4]. It was done because, especially for roads with the status of district roads, the amount of maintenance funds was not proportional to the number/length of roads that had to be handled [5, 6]. However, its condition was never reported. Thus, stakeholders who are authorized to carry out maintenance activities must assess the condition of roads and prioritize which roads should be rehabilitated. Prioritization is carried out by referring to Decree No. 77 of the Directorate General of Highways (1990). There are at least five criteria and 17 sub-criteria in this decree that must be considered in setting priorities.

In this condition, it is necessary to calculate the weight of the influence of each criterion/sub-criteria on the priority priorities. One of the tools used for this weighting is the Analytical Hierarchy Process (AHP) [7, 8]. AHP is a decision-making method developed by Thomas L Saaty in 1970 [9]. This method is part of the Multi Criteria Decision Making (MCDM) [10]. So, in terms of prioritizing which roads will be maintained, the question that must be resolved is the priority order of road handling at the maintenance stage using the AHP method. The explanation of these questions is the purpose of this study, namely determining the order of priority for road handling based on the AHP method.

2 Literature Review

2.1 Priority Scale Based on Decree No. 77 Director General of Highways 1990

The procedure for SK No. 77/KPTS/Db/1990 from the Director General of Highways is a district road planning guide issued by the Director General of

Highways as a reference in determining the priority order of district road handling. However, the procedure does not provide how much weight value the influence of the criteria on priority determination. In general, the priority criteria for road handling according to the procedure are as follows:

1. The primary criterion for priority selection is to prioritize the project with the highest Net Present Value (NPV)/Km.
2. A project evaluation code is also provided for projects marked with an NPV/Km range to guide their selection, with the following selection instructions.
3. Give priority to the project group that has the highest feasibility.
4. Give the lowest priority to the project group with the most insufficient feasibility.
5. Prioritizing rollout projects, especially the completion of projects whose implementation is divided or in stages.
6. Completion of the project according to the initial plan or according to the initial design will provide full benefits for the investment.
7. Avoid very long projects (generally projects longer than 15 km) should be avoided at the project determination stage.
8. Prioritizing the strategic road network sections that have been determined.
9. Give priority to projects that meet district development objectives.

2.2 Analytical Hierarchy Process (AHP)

Analytical Hierarchy Process (AHP) is a complex decision-making technique with a pairwise comparison approach between criteria and results in an assessment of the weight of the influence of the criteria on the decision-making objectives. This method was first developed by Thomas L Saaty in 1970. The use of the AHP method for decision-making in the transportation sector has been widely used, among others: to evaluate the performance of public transportation [8, 11–13], for decision making on road safety [14], including to prioritize road maintenance [15–17]. Several researchers have also prioritized roads with certain statuses, such as: prioritizing the handling of district roads with four criteria (road conditions, traffic, land use, and economy) [18], and priority one level with five criteria in district road (road condition, traffic volume, accessibility, policy, and land use) [19, 20]. Some researchers have also done something similar with case studies on roads with national road status [21, 22].

3 Methodology

The processes carried out in the AHP method are as follows:

1. Step 1. Define the issue and decide on the best remedy. In this study, the problem to be solved is determining the priority of road maintenance based on various criteria.
2. Step 2. Create a hierarchical structure starting with a general goal followed by criteria and possible alternatives at the lowest criteria level. A hierarchy is formed with five criteria and 17 sub-criteria to prioritize road maintenance. In this study, the hierarchical level arrangement used in the Analytical Hierarchy Process (AHP) method is as follows:
 - Level I (Goal) is the purpose of determining the priority of road maintenance.
 - Level II (Criteria) consists of criteria in determining road priorities, namely: Road Conditions (A), Road Hierarchy (B), Social Aspects (C), Economic Aspects (D), Land Use Aspects (E)
 - Level III (Sub Criteria), Sub Criteria for Road Condition Aspects, Road Class, Economic Aspects, Road Hierarchy Aspects, Social Aspects, and Land Use Aspects. The hierarchy chart from level I to level III can be seen in Fig. 2.
3. Step 3. Create a pairwise comparison matrix that describes the contribution or influence of each element on the criteria specified in it.

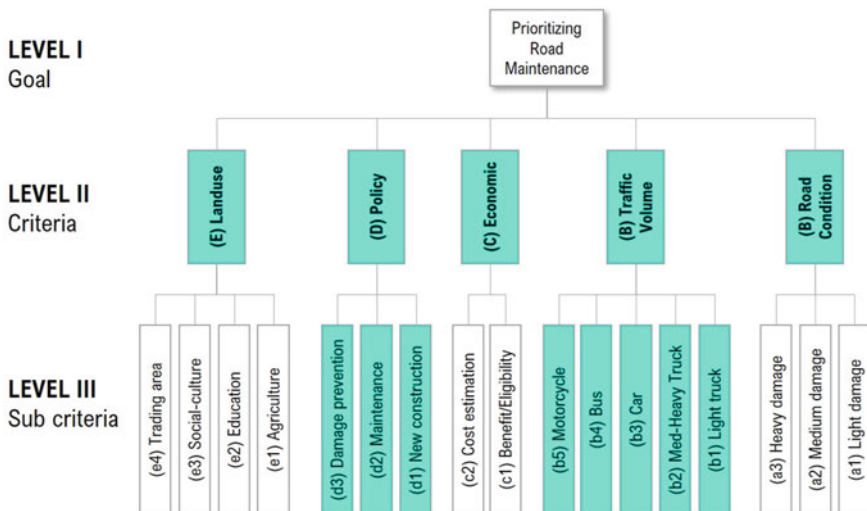


Fig. 2 AHP hierarchy to prioritize road maintenance

Table 1 Pairwise comparison matrix scale [23]

Intensity of importance	Definition
1	Elements that are equally significant to others
3	One factor is slightly more significant than the others
5	The importance of one over the other is moderate
7	Very strong important
9	Extreme importance of one over another
2, 4, 6, 8	Intermediate value between two adjacent value

Table 2 Random index value

Ordo matrix	1	2	3	4	5	6	7	8	9	10
RI	0	0	0.58	0.9	1.12	1.24	1.32	1.41	1.45	1.49

4. Step 4. Perform pairwise comparisons so that $n[(n - 1)/2]$ scores are obtained, where n is the number of elements being compared, with five criteria elements, $5 [(5 - 1)/2] = 10$ pairwise comparisons at the criterion level. At the sub-criteria level, there will be a total of $17[(17 - 1)/2] = 136$. Pairwise comparisons are graded using a scale, as shown in Table 1.
5. Step 5. Calculate eigenvalues and assess each respondent’s consistency. Data retrieval is repeated if it is not consistent, or inconsistent data is discarded. The basic principle in this consistency test is that if A is more important than B, B is more important than C, so there is no way C is more important than A. The benchmark used is CI (Consistency Index) versus RI (Ratio Index) or CR (Consistency Ratio). RI is determined based on previous studies [24], as shown in Table 2.
6. Step 6. Repeat steps 3, 4, and 5 for each hierarchy.
7. Step 7. Determine each pairwise comparison matrix’s eigenvector.
8. Step 8. Verify the hierarchy’s consistency. The judgment data assessment must be modified if the value is greater than 10%.

4 Discussion and Result

Respondents in this study were experts in the field of road maintenance/rehabilitation. The number of respondents was 29 people, consisting of eight people from the Public Works Department's Binamarga Expert Staff, six people from Sleman Regency, five people from Kulon Progo Regency, seven people from Bantul Regency, and three people from Gunung Kidul Regency.

Initial assessment of pairwise comparisons between criteria A (Road Conditions), B (Traffic Volume), C (Policy), D (Economic) and E (Land Use), W_i values, eigenvector values (E), and λ_{max} can be seen in Table 3.

The consistency value as a measure of the control model is calculated using the consistency ratio (CR) by first calculating the consistency index (CI) = $(\lambda_{max} - n) / (n - 1) = (5.100 - 5) / (5 - 1) = 0.025$ (where n denotes the matrix's size 5×5 . CR = CI/RI, the value of RI is taken from Table 2, so CR = $0.025 / 1.12 = 0.02223 < 0.1$ (meaning that the answers from respondents can be accounted for because they are consistent).

After analyzing the calculations using the AHP for each criterion and sub-criteria according to the calculation flow as above, the influence weight of each criterion and sub-criteria is obtained as shown in Table 4.

Table 3 Average original judgment matrix, W_i , E, and λ_{max}

	A	B	C	D	E	$\sum A_i$	$W_i = \sqrt[n]{\sum A_i}$	Eigen vector $E = W_i / \sum W_i$	$\lambda_{max} = E_i / \sum A_j$
A	1.000	0.949	1.138	1.805	2.457	4.790	1.368	0.257	0.999
B	1.054	1.000	2.375	1.754	2.149	9.433	1.567	0.294	1.000
C	0.879	0.421	1.000	1.485	1.724	0.947	0.989	0.185	1.070
D	0.554	0.570	0.673	1.000	2.235	0.475	0.862	0.162	1.049
E	0.407	0.465	0.580	0.447	1.000	0.049	0.547	0.103	0.982
$\sum A_j$	3.893	3.406	5.766	6.491	9.565	15.695	5.333	1.000	
								λ_{max}	5.100

Table 4 Aggregated priority weights and rankings of criteria

Criteria		Subcriteria	
Factor	Weight against criteria (%)	Factor	Weight against sub-criteria (%)
(A) Road condition	25.70	Light damage	33.90
		Medium damage	44.70
		Heavy damage	21.40
(B) Traffic volume	29.40	Light truck	26.80
		Medium-heavy truck	35.80
		Car	12.80
		Bus	17.80
		Motorcycle	6.86
(C) Economic	16.20	Benefits/Eligibility	66.30
		Construction cost estimation	33.70
(D) Policy	18.50	New road construction	13.90
		Maintenance	55.60
		Damage prevention	30.50
(E) Landuse	10.30	Agriculture	26.40
		Education	34.01
		Socio-cultural	14.85
		Trading area	24.74

5 Conclusions

From the research results that have been described in the discussion, conclusions can be drawn, as follows:

1. The application of the AHP method can help provide alternative decision-making in road maintenance, according to several aspects of the criteria that are considered to affect road maintenance.
2. The results of the priority order of road handling criteria (level I) indicate that the Traffic Volume factor is preferred, with a weight of 0.294 (29.4%), then followed by the Road Condition factor of 0.257 (25.7%), the policy factor is 0.185 (18.5%), economic factors 0.162 (16.2%) and finally land-use factors 0.103 (10.3%).

References

1. Lamptey G, Ahmad M, Labi S, Sinha K (2005) Life cycle cost analysis for INDOT pavement design procedures. *Fed Highw Adm* 53:1689–1699
2. Jordaan G (2015) The art of road pavement rehabilitation design. In: 11th Conference on asphalt pavements for Southern Africa (CAPSA), North West, South Africa, pp 1–15
3. Direktorat Jenderal Bina Marga (1990) Petunjuk Teknik Perencanaan dan Penyusunan Program Jalan Kabupaten
4. National Cooperative Highway Research Program (NCHRP) (2014) NCHRP Report 758: trip generation rates for transportation impact analyses of infill developments. Transportation Research Board (TRB), Massachusetts, United States of America
5. Trissiyana (2017) Penentuan Prioritas Pemeliharaan Jalan Kabupaten Trissiyana. *Media Ilm Tek Lingkung* 2:13–19
6. Anugrah D (2011) Mnalisis biaya rehabilitasi dan pemeliharaan jalan akibat muatan lebih (Ruas Jalan Puding Besar—Kota Waringin Kabupaten Bangka). Thesis, UNS-Pascasarjana Prodi Teknik Sipil
7. Fitriastuti F, Kresnanto NC (2021) Measurement of user interest in public transport performance variables using AHP. https://doi.org/10.1007/978-981-33-6311-3_86
8. Risdiyanto R, Kresnanto NC (2019) Angkutan Umum Perkotaan Menggunakan Metode Analytic Hierarchy Process (AHP). In: Simposium Forum Studi Transportasi antar Perguruan Tinggi ke-22. Universitas Halu Oleo, Kendari, Indonesia
9. Wikipedia (2018) Analytic hierarchy process. In: Wikipedia. https://en.wikipedia.org/wiki/Analytic_hierarchy_process. Accessed 7 Jul 2021
10. Wikipedia (2007) Multiple-criteria decision analysis. In: Wikipedia. https://en.wikipedia.org/wiki/Multiple-criteria_decision_analysis#MCDM_methods. Accessed 18 Jan 2020
11. Moslem S, Duleba S (2017) Analytic hierarchy process evaluation of public transport system in Budapest, Hungary. pp 660–665
12. Kumar R, Madhu E, Dahiya A, Sinha S (2015) Analytical hierarchy process for assessing sustainability. *World J Sci Technol Sustain Dev* 12:281–293. <https://doi.org/10.1108/wjstsd-05-2015-0027>
13. Nosal K, Solecka K (2014) Application of AHP method for multi-criteria evaluation of variants of the integration of Urban public transport. *Transp Res Procedia* 3:269–278. <https://doi.org/10.1016/j.trpro.2014.10.006>
14. Podvezko V, Sivilevicius H, Podvezko A (2014) Scientific applications of the AHP method in transport problems. *Arch Transp* 29:47–54. <https://doi.org/10.5604/08669546.1146966>
15. Ramadhan RH, Al-Abdul HIW, Duffuaa SO (1999) The use of an analytical hierarchy process in pavement maintenance priority ranking. *J Qual Maint Eng* 5:25–39. <https://doi.org/10.1108/13552519910257041>
16. Farhan J, Fwa TF (2011) Use of analytic hierarchy process to prioritize network-level maintenance of pavement segments with multiple distresses. *Transp Res Rec* 11–20. <https://doi.org/10.3141/2225-02>
17. Ahmed S, Vedagiri P, Krishna Rao KV (2017) Prioritization of pavement maintenance sections using objective based analytic hierarchy process. *Int J Pavement Res Technol* 10:158–170. <https://doi.org/10.1016/j.ijprt.2017.01.001>
18. Siswanto H, Supriyanto B, Pranoto, et al (2019) District road maintenance priority using analytical hierarchy process. *AIP Conf Proc*. <https://doi.org/10.1063/1.5112490>
19. Hargi B, Foralisa M, Susanti B (2018) Prioritization of road management in district Ogan Komering Ulu Selatan based on analytical hierarchy process method. *Int J Sci Technol Res* 7:237–241
20. Kurniawan H, Ratnaningsih A, Hasanuddin A (2020) Priority determination of road maintenance in Lumajang regency using the AHP method. *Int J Sci Basic Appl Res* 52:149–160

21. Barić D, Pilko H, Strujić J (2016) An analytic hierarchy process model to evaluate road section design. *Transport* 31:312–321. <https://doi.org/10.3846/16484142.2016.1157830>
22. Benardus Munthe R, Hario Setiadji B, Darsono S (2016) Menentukan Prioritas Penanganan Ruas Jalan Nasional di Pulau Bangka. *Media Komun Tek Sipil* 21:57. <https://doi.org/10.14710/mkts.v21i1.11231>
23. Saaty TL (1980) *The analytic hierarchy process*. McGraw-Hill, New York, United States of America
24. Saaty TL (1990) How to make a decision: the analytic hierarchy process. *Eur J Oper Res* 48:9–26. [https://doi.org/10.1016/0377-2217\(90\)90057-i](https://doi.org/10.1016/0377-2217(90)90057-i)

Overview of Side Friction Factors for Evaluation of Capacity Calculation at Indonesian Highway Capacity Manual



Najid and Tamara Marlianny

Abstract The Indonesian Highway Capacity Manual (IHCM) as a reference in determining road capacity in Indonesia was made in 1997 by the Directorate General of Highways, Ministry of Public Works and Public Housing. Currently, the composition of traffic on roads and the number of residents is very significantly different from the year 1997. Road capacity based on a current calculation based on IHCM shows very pessimistically compared with the traffic volume data. Those very significant differences indicate the need to evaluate the method of determining road capacity based on the IHCM. To evaluate and revise the IHCM, research was conducted on several roads grouped by road type. This research was conducted at road type 4/2 D (four lanes two ways with separator) on the H.R. Rasuna Said Jakarta. The survey results obtained traffic volume, speed, side friction in the morning, midday, and afternoon. Results analysis side friction values obtained are not accommodated with those in the IHCM, so revisions are needed for other parameters that have a greater influence, namely basic capacity.

Keywords Road capacity · Side friction · IHCM 1997

1 Introduction

1.1 Background

The IHCM (Indonesian Highway Capacity Manual), which was made in 1997, requires evaluation and revision considering that the manual is already 24 years old and the value of the road capacity calculated based on the IHCM looks no longer in accordance with current traffic conditions, especially with the actual road capacity conditions. The road has several types, namely 6/2 D (six lanes two ways with

Najid (✉) · T. Marlianny
Department of Civil Engineering, Engineering Faculty, Universitas Tarumanagara, Jakarta, Indonesia
e-mail: najid@ft.untar.ac.id

separator), 4/2 D (four lanes two ways with separator), 2/2 UD (two lanes two ways without separator), 4/2 UD (four lanes two ways without separator). Thus, evaluation and revision plans are based on the type of road [1].

From the survey results, the traffic volume is often much higher than the road capacity value based on the IHCM, so the traffic volume value that much higher than the road capacity value can be assumed as the estimated road capacity value. The value of side friction has influenced the value of traffic volume as a result of the survey. The estimated side friction can be determined from the estimated road capacity.

In IHCM 1997, the road capacity is calculated based on five parameters, namely the basic capacity parameter, correction factor for road lane width, the correction factor for the proportion of way traffic flow, the correction factor for side friction, and the correction factor for city size. The side friction factor is an influencing parameter that is easier to observe for evaluation. The side friction factor is determined by the accumulation of weighted summation of type side friction and pedestrian facility-wide. Type of side friction consisting of stop vehicle, the vehicle from access of roadside, pedestrian, and nonmotorized vehicle at along of the roadside.

This study needs to analyze the magnitude of the side drag adjustment factor based on the capacity estimation results and compare it with the side friction factor in the IHCM. To estimate the order of influence, each side friction type to road capacity was analyzed based on respondent perception data.

1.2 Problem Identification

1. The results of the traffic volume survey are greater than the value of the Road Capacity based on IHCM, 1997.
2. Road users' perceptions of traffic conditions due to the influence of side friction.
3. Revision of road capacity analysis based on IHCM 1997 by analyzing roadside friction factor.
4. The side friction factor on the H.R Rasuna Said road is more determined by stop vehicles and vehicles access from the side of the road.

1.3 Problem Limitation

1. The location of this study was carried out on Jalan H.R Rasuna Said, Jakarta, with the type of road is 4/2 D.
2. Data was obtained through observation (Survey Data) and questionnaire survey with Google Form.

1.4 Problem Formulation

1. How is the analysis of the effect of side friction on road capacity on Jalan H.R Rasuna Said based on IHCM 1997?
2. How is the road capacity revision based on IHCM1997 by utilizing the roadside friction factor?
3. How is the estimated side friction factor according to the estimated road capacity?

1.5 Objectives

1. To analyze the effect of side friction on the road capacity of H.R Rasuna Said based on the IHCM 1997.
2. To analyze the estimation of side drag factors based on the estimated road capacity on the H.R Rasuna Said road.
3. To evaluate the calculation of road capacity according to IHCM 1997.

2 Literature Review

2.1 Capacity

Road Capacity is the maximum number of vehicles crossing a point on the road path at a certain time under certain road conditions or is the maximum flow that can be passed on a road path expressed in units of vehicles per hour or units of passenger cars per hour (pcu/h). The method for calculating road capacity based on the 1997 Indonesian Road Capacity Manual is shown on Eq. 1 [1].

$$C = C_o \times FC_w \times FC_{sp} \times FC_{sf} \times FC_{cs} \quad (1)$$

where

- C Capacity (pcu/h)
- C_o Basic Capacity (pcu/h)
- FC_w Lane Width Adjustment Factor
- FC_{sp} Split Proportion Adjustment Factor
- FC_{sf} Side Friction Adjustment Factor
- FC_{cs} City Size Adjustment Factor.

2.2 Basic Capacity

Basic capacity can be defined as the maximum number of vehicles that can cross a certain road cross-section for one hour under ideal road and traffic conditions. The conditions for basic capacity per lane based on road type are shown in Table 1.

2.3 Lane Width Adjustment Factor (FCw)

The determination of the capacity adjustment factor for the traffic lane width (FCw) based on the traffic lane width can be obtained from Table 2.

2.4 Split Proportion Adjustment Factor (FCsp)

This factor is an adjustment factor due to the separation of ways of traffic flow and is specially used for the road without road separator such as road type 4/2 UD and type 2/2 UD. The split proportion adjustment factor for road type 4/2 D or 6/2 D can be used value is one.

Table 1 Basic capacity (Co) [1]

Road type	Basic capacity (pcu/h)	Note
4/2 D	1650	Per lane
4/2 UD	1500	Per lane
2/2 UD	2900	Total two lanes

Table 2 FCw based on effective lane width [1]

Road type	Effective lane width (Wc)	FCw
	Per lane (m)	
4/2 D	3.00	0.92
	3.25	0.96
	3.50	1.00
	3.75	1.04
	4.00	1.08

2.5 Side Friction Adjustment Factor (FCsf)

Side friction adjustment factor value obtained from pedestrian facility width and side friction class can be seen in Table 3.

Side Friction Class is determined by the number of events of each side friction type and their weight, shown in Tables 4 and 5.

Table 3 FCsf road with kerbs [1]

Road type	Side friction class	FCsf			
		Distance Kerbs to Obstacle (Ws)			
		≤ 0.5	1.0	1.5	≥ 2
4/2 D	VL (Very low)	1.00	1.01	1.01	1.02
	L (Low)	0.97	0.98	0.99	1.00
	M (Medium)	0.93	0.95	0.97	0.99
	H (High)	0.87	0.90	0.93	0.96
	VH (Very high)	0.81	0.85	0.88	0.92

Table 4 Weight of side friction [1]

Side friction type	Weight
Pedestrian	0.50
Public transport and vehicle stop	1.00
Access vehicle	0.70
Unmotorized vehicle	0.40

Table 5 Side friction class [2]

Side friction class (SFC)	Code	Weighted number of events per 200 m/h	Typical condition
Very low	VL	<100	Residential area, road with frontage road
Low	L	100–299	Residential area, some public transport etc.
Medium	M	300–499	Industrial area with roadside shops
High	H	500–899	Commercial area, high roadside activity
Very high	VH	>900	Commercial area with roadside market activities

2.6 City Size Factor

Capacity adjustment factors for city size (FCcs) are assessed based on the population. Table 6 is a table of capacity adjustment factors for city roads based on the IHCM 1997.

3 Methodology

Based on Previous Research and the actual problem which traffic flow or traffic volume have a value more than IHCM's Capacity, it needs evaluation of the IHCM, especially the calculation of road capacity. To evaluate the IHCM's capacity, the observation of traffic flow condition at the certain segment road when at the same the side friction occurred.

The position of side friction type based on influence weight is needed to evaluate based on car user experience that has to survey by questionnaire and analysis the result of the survey then will be compared with IHCM. To see the process of research can be seen in Fig. 1.

Method Approach of the Research for Data Collection:

1. Observation survey method on the road by counting the number of passing vehicles within a period of fifteen minutes in the morning period (07.00–09.00), the afternoon period (12.00–14.00), and the afternoon period (16.00–18.00).
2. Perception survey method using Questionnaire distributed using Google Form with 100 respondents, with questions grouped into questions about respondent characteristics, travel characteristics, and respondents' perceptions of the disturbances of each type of side friction.

Method Approach of the Research for Data Analysis:

1. Using linear equation analysis to get the side resistance factor and compare it with IHCM [2].
2. Analysis of the data from the questionnaire which is the respondent's perception of how far the influence of each type of side friction on the flow or smoothness of traffic.

Table 6 FCcs based on population number in the city [1]

City size (million population)	City size factor
<0.1	0.86
0.1–0.5	0.90
0.5–1.0	0.94
1.0–3.0	1.00
>3.0	1.04

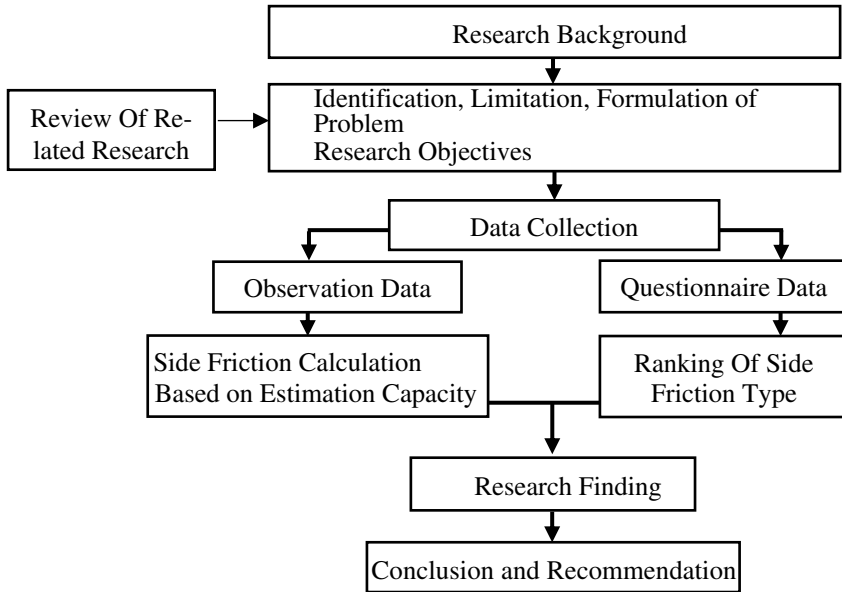


Fig. 1 Research process

4 Data Collection

Observation data that collected last year from Edmund and Najid [2]. Characteristic of the location shown in Table 7 [3].

Side Friction Data consist of the type of vehicle stopped and access from the side of the road for motorcycle (MC), light vehicles (LV), and heavy vehicles shown in Table 8.

Observation data of traffic volume by time slice for every 15 min at H. R. Rasuna Said road for ways Gatot Subroto to Menteng as shown in Table 9.

Table 7 Location characteristics (observation survey)

No.	Description	Measurement
1	Lane width	3.5 m
2	Lane number	Two lanes per way
3	Road type	4/2 D
4	Pedestrian facility width	1.5 m
5	City size	>3 million population
6	Road side activity	Commercial and office

Table 8 Side friction data

Time	Vehicle stop			Access vehicle at road side		
	MC	LV	HV	MC	LV	HV
16.30–17.30	96	45	2	115	56	8
16.45–17.45	27	23	7	81	32	15
17.00–18.00	15	14	3	45	18	4

Table 9 Traffic Volume Data

Time slice	Vehicle group						Passenger car unit (PCU)
	Car/Light vehicle	Medium bus/Truck	Big truck/Bus (2 axle)	Big bus/Truck (3 axle)	Big bus/Truck (>3 axle)	Motor cycle	
16.00–16.15	1116	48	40	32	3	2037	1772.9
16.15–16.30	1215	32	42	46	9	3528	2251.8
16.30–16.45	1161	24	39	33	10	3072	2056.2
16.45–17.00	1170	28	51	38	7	3432	2176.8
17.00–17.15	1314	36	42	25	14	3273	2272.7
17.15–17.30	1134	36	44	14	4	4635	2410.4
17.30–17.45	1104	32	31	20	9	4332	2297.4
17.45–18.00	1206	32	48	37	12	5061	2626.1

Table 10 Respondent perception about how influence each type side friction

No.	Type side friction	Congestion condition				Not congestion condition			
		1	2	3	4	1	2	3	4
		1	Stop vehicle	63	32	9	0	56	34
2	Access vehicle from road side	43	38	18	1	44	38	16	2
3	Pedestrian	45	30	17	8	41	30	16	13
4	Unmotorized vehicle	37	37	12	14	39	31	18	12

where 1: Very influence, 2: Influence, 3: Influence, 4: Not Influence

To mention how much is the influence of interference from each type of side friction is carried out by a questionnaire survey. The respondent was asked to rank each type of side friction their influence on traffic flow based on the respondent’s perception.

From Table 10, the ranking results for each type of side restriction are obtained are the most affecting road capacity on traffic jam and on smooth road conditions. Analyses of the observation data to get the side friction factor and capacity are shown in Tables 11, 12, 13, and 14. Analysis of those data in Table 10 based on respondent’s perception is shown in Table 15.

5 Data Analysis

5.1 Observation Data Analysis

Side Friction Analysis

Result of side friction analysis in Table 11 shown that the level of side friction is appropriate with side friction level based on the land use condition in survey location (see Table 5 and Table 7).

Ratio Volume and Capacity Analysis Based On IHCM

Capacity 16.30–17.45 (fcsf L) = $2 \times 1650 \times 1 \times 1 \times 1 \times 1.04 = 3432$ pcu/h

Capacity 17.00–18.00 (fcsf VL) = $2 \times 1650 \times 1 \times 1 \times 1.01 \times 1.04 = 3466$ pcu/h

From Table 12 shown traffic volume ratio at times 16.30–17.30, 16.45–17.45, and 17.00–18.00 have a higher value than others. The V/C ratio then used to analysis capacity estimate in Table 13.

Table 11 Data analysis of side friction

Time	Vehicle stop	Access vehicle	Total side friction	Class
16.30–17.30	143	179	268.3	L
16.45–17.45	57	128	146.6	L
17.00–18.00	32	67	78.9	VL

Table 12 Peak hour traffic volume and V/C

No.	Time	Traffic volume	V/C
1	16.00–17.00	8257.7	2.41
2	16.15–17.15	8757.5	2.55
3	16.30–17.30	8916.0	2.60
4	16.45–17.45	9157.2	2.67
5	17.00–18.00	9606.5	2.77

Table 13 Estimate capacity

No.	W time	Estimate capacity	Side friction data	
			Vehicle stop	Access vehicle
1	16.30–17.30	8916.0	143	179
2	16.45–17.45	9157.2	57	128
3	17.00–18.00	9606.5	32	67

Table 14 Estimate FCsf

No.	Time	Co+	Estimate capacity	Estimate FCsf	Remark
1	16.30–17.30	3432	8916.0	2.6	(Not available at table C-4.1 IHCM)
2	16.45–17.45	3432	9157.2	2.7	(Not available at table C-4.1 IHCM)
3	17.00–18.00	3432	9606.5	2.8	(Not available at table C-4.1 IHCM)

Estimate Capacity and Estimate Side Friction Factor

Estimate capacity is shown in Table 13 and estimate side friction (Fcsf) is shown in Table 14.

$$Co+ = 2 \times (Co \times Fcw \times FCsp \times FCcs) = 2 (1650 \times 1 \times 1 \times 1.04) = 3432 \text{ pcu/h}$$

This value of Co+ use for calculate the estimate side friction factor based on value of estimate capacity that calculate from traffic volume at peak hour, the result of analysis is shown in Table 14.

Example Calculation Estimate FCsf at time (16.30–17.30):

$$Est.C = Co+ \times FCsf$$

$$8916 = 3432 \times FCsf$$

$$FCsf = 2.6 \text{ (not available at table C-4.1 IHCM).}$$

The previous revision of IHCM is PKJI, but the revision version of PKJI only majority is about the name of variable or parameter [4, 5].

5.2 Perception Data Analysis

The weighted total of respondent’s perceptions of the questionnaire survey is shown in Table 15.

Table 15 Ranking of type of side friction

No.	Side friction type	Congestion condition	Ranking	Not congestion condition	Ranking
1	Vehicle stop	152	1	155	1
2	Access vehicle	177	2	172	2
3	Pedestrian	188	3	201	3
4	Unmotorized vehicle	203	4	203	4

6 Conclusions and Recommendations

6.1 Conclusions

1. There is frontage road and Public Transport at Kuningan road, so side friction class as a result of the survey is appropriate with IHCM, namely Very Low and Low.
2. Ratio traffic volume and Road Capacity is highest during the afternoon peak hour.
3. Traffic volume at afternoon peak hours can be used to estimate capacity.
4. Estimate side friction factor using estimate capacity and side friction data produce estimate side friction factor unaccommodated in IHCM.
5. Other parameters need to be corrected, such as basic capacity, which has the greatest influence to determine the capacity.
6. From analysis from perception survey, get the ranking result appropriate with IHCM.

6.2 Recommendation

The same survey and analysis need to be carried out on roads of the same type, namely four lanes two ways with separator.

References

1. IHCM (1997) Indonesian road capacity manual (IHCM). Directorate General of Highways Ministry of Public Works, Jakarta, Indonesia
2. Jaya ES, Najid (2021) Analisis Kapasitas dan Kinerja Lalu Lintas di Jalan H.R. Rasuna Said Jakarta. *Jurnal Mitra Teknik Sipil* 4:383–396
3. Najid (2019) Evaluation of side friction in IHCM for highway two lanes two ways. In: Proceedings of the 2nd international symposium on transportation studies in developing countries (ISTSDC 2019), Atlantis Press, pp 116–119
4. Kristiawan D, Najid (2019) Analisis Pengaruh Hambatan Samping Akibat Aktivitas Tata Guna Lahan di Jalan MH. Thamrin Tangerang dan Jalan Raya Serpong. *Jurnal Mitra Teknik Sipil* 2:31–38
5. Lowenta L, Najid (2019) Penentuan Kapasitas Jalan Dua Lajur Dua Arah Tidak Terbagi Dengan Metode MKJI, Konsep PKJI, dan Survei. *Jurnal Mitra Teknik Sipil* 2:27–34

Thickness Pavement Design Based on Heavy Vehicle Loads



Anita Rahmawati, Emil Adly, and Wahyu Widodo

Abstract Some roads in central Bengkulu often experiences pavement deterioration caused by the high number of heavy vehicles carrying load containing natural products. One of the roads being reviewed is Karang Tinggi Penanding road with quite severe damage. This study aimed at knowing if the current pavement thickness could accommodate loads of vehicles passing through the road or it needed to redesign the pavement thickness to accommodate the current traffic. The method used for determining the pavement thickness was the Manual Design 2017 from Bina Marga while knowing a load of heavy vehicles passing through the road was done by using a 2-pad portable weighbridge. The analysis of pavement layer thickness due to the standard load and overloading by using the method of Binamarga 2017, it can be obtained the pavement layer thickness with a standard and overload for surface layer are 30 mm for Hot Rolled Sheet Wearing Course (HRS WC) and 35 mm for Hot Rolled Sheet Base Course (HRS BC), the base course layer is 250 mm and the subbase course layer is 125 mm. The thickness of the pavement obtained is the same because the Cumulative Equivalent Single Axle (CESA) 5 burden obtained is still relatively low.

Keywords Manual design 2017 · Overloading · Pavement thickness

1 Introduction

The high intensity of road traffic overloading the required standard leads to quick road pavement deterioration and a reduction in service design life. Flexible pavement has viscoelastic property, whereby when it carries overloading, the pavement will lose its material stiffness. Let alone, if road maintenance is not performed, the road will have a declining service life. In general, the factors causing declining

A. Rahmawati (✉) · E. Adly · W. Widodo

Department of Civil Engineering, Faculty of Engineering, Universitas Muhammadiyah Yogyakarta, Jl. Brawijaya, Bantul, Daerah Istimewa Yogyakarta 55183, Indonesia
e-mail: anita.rahmawati@umy.ac.id

service life or road deterioration are the traffic design life exceeding the initial planning, puddles on the road surface caused by poor drainage sanitation, the error in road planning and construction, poor pavement quality, overloaded vehicles (overloading) that will make the road service life shorter than the design life that has been established during the planning. The causes of overloaded vehicles (overloading) strongly result in declining road service. The Karang Tinggi–Penanding road in central Bengkulu often experiences road pavement damage caused by many vehicles carrying natural products, such as oil palm, wood and coal, overloading the required standard load. Therefore, this study aimed at knowing the pavement thickness that could accommodate the load of heavy vehicles passing through The Karang Tinggi–Penanding road in Central Bengkulu Tengah according to the design life. This study used the Manual Design 2017 by Bina Marga for identifying the required pavement thickness based on the standardized maximum load and the data of weighbridge testing in the field.

Vehicles passing on roads, which bring load exceed the maximum specified load, cause excessive loading on the pavement and affect the design life on the road [1]. Based on some previous studies, it can be concluded that overloading can decrease the design life. The study which using AASHTO 1993 and the calculation of cumulative ESAL (Equivalent Standard Axle Load) values, then the remaining pavement life was obtained. This section contains the research background, purpose, contribution (the research benefit from theoretical and practical), research result and implication (Practical advice based on research result). The research result and implication in the introduction section are only suggestions (not mandatory) [2]. Based on the design life of the 20-year plan, the cumulative ESAL value is 64,533,642 SAL, so there is a decrease in the service life of eight years. The remaining life of the pavement plan is only 54.75% and a pavement service life is reduced by 25.94%. Similar research on the effect of overloading was also not much different from previous research [3, 4].

The research regarding the effect of overloading with slightly different methods showed that there was a reduction in service life from the design life and caused various road damage problems [5–14]. This study discussed the effect of overloading on design life and pavement thickness. Furthermore, this study used the method of Binamarga 2017 to analyze the effect of overloading on pavement thickness [15].

2 Literature Review

Rahmawati et al. [16] conducted a study on Solo–Yogyakarta highway KM 9–15; this study found that several vehicles violated the use of maximum load causing road deterioration and declining road service life than it should be. One of the road deteriorations due to the high number of vehicles violating the maximum load is overloading. Based on the previous study, there was a reduction in the road service life of 8 years from the total service life of 20 years. The solution conducted in the

previous study for the overloading problem was redesigning the pavement thickness to accommodate the overloading condition. Meanwhile, the study conducted in this paper used an application known as Circlly 6.0 for analyzing the deflection that occurred on Solo–Yogyakarta Highway KM 9–15 to examine the flexible pavement that had been constructed in the previous study. Re-designing was calculated using the Bina Marga method in 2002 and then, the collected pavement thickness would be analyzed using the Circlly 6.0 program for analyzing the deflection and the force that occurred on the pavement of Solo–Yogyakarta Highway KM 9–15. Hence, it can be identified if the pavement that had been designed was eligible or not to be used.

A study on overloading was conducted on Lago–Sorek road KM 77–78 for rigid pavement. The method used for analyzing the pavement structure was AASHTO 1993. After observing, it was found that there was an overloading of 17.98%. The result obtained in the study was the declining service life due to overloading of 25.94% [2]. Sari [1] was conducted on the provincial border of Jambi–Peninggalan on overloading. Many vehicles violated the standard load by overloading on the road even though Integrated Checkpoints (PPT) existed for weighing the vehicle load. After analyzing using the ESAL with a design life of 10 years, it was found that normal load for vehicles had a remaining road service life of 99.955%, while the remaining road service life with overloading conditions was 48.393%.

A study by Wandī et al. [10] was conducted on the national road of Banda Aceh–Meulaboh. This study aimed at knowing the vehicle damage factor caused by overloading. From the data, it collected an average of 45.57% for the vehicles that violated out of the total truck passing through the road. The result based on the CESA analysis showed that there was a decline in the road service life of 9 years, while, according to the effective formula, the road service life declined by 10.77 years from the design life of 20 years. Suriyatno et al. [4] was an analysis of flexible pavement thickness and the design life caused by overloaded vehicles. The case study was conducted on four different roads, namely, Tanah Badantung–Kiliran Jao road, Border of Padang–Painan cities, provincial border of Riau–Payakumbuh and Sicincin–Lubuk Alung road. The result showed that the actual traffic load was higher than the standard load resulting in a higher overlay than it should be. The big difference of load was on Tanah Badantung–Kiliran Jao, whereby the overlay thickness for the actual traffic load was higher, or around 56.4%, than the standard load. The overload traffic load led to a declining road service life by 56.8% from the five years of road service life or equal to two years and ten months.

Atiya [7] conducted a study on an analysis of weighbridge performance against the pavement performance and the design life on Jembatan Timbang Salam, Magelang. The background of the study was the high number of heavy vehicles passing through Keprekan road–the border of Yogyakarta that is sometimes overloading. On the road, there was Jembatan Timbang Salam. The method used for calculating the CESA recapitulation on the remaining design life was by dividing it into several conditions. First, condition A (the actual condition where the overloaded vehicles are only fined or receive a traffic ticket and they were allowed to

continue their travel. Condition B is where the maximum overload tolerance is 125% from weight allowed). Condition C is that the maximum overload tolerance is 115% and condition D is that the maximum overload tolerance is 105%). The conclusion that can be drawn is as follows: for Condition A. In the actual condition, the road pavement design life is declining from 10 years to 9.48 years in the first analysis and the design life for Condition A in the second analysis is 9.53 years. Syafriana et al. [8] was evaluating the road service life by calculating the overloading condition on the East Cross Road of Aceh Province, Bireuen road, the border of Lhokseumawe city. The method used in this study was the guideline planning of overlay thickness of flexible pavement using the deflection method. Based on the analysis that had been conducted, the result showed that the Vehicle Damage Factor (VDF) value for the overloading condition was 696%, higher than the VDF value in a normal load condition. Meanwhile, the result of the Cumulative Equivalent Standard Axle (CESA) analysis showed that there was a declining road service life on that road to 4.3 years from the design life of 10 years.

3 Research Method

3.1 The Step of Research

In this step, the arrangement of planning and observing on the preliminary stage will be carried out in order to obtain a general description of the problems in the field. The preparation stage carried out in this study is shown in Fig. 1.

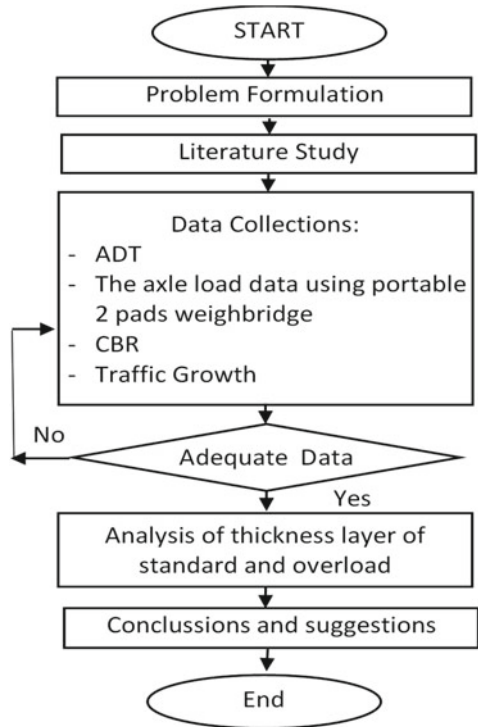
3.2 Research Location

This research was conducted on The Karang Tinggi–Penanding roads, Bengkulu Tengah district (Fig. 2).

3.3 Data Collection Technique

The primary data came from the field observation and the secondary data was obtained from related agencies. The technique of data collection in this study was by finding the primary and secondary information that will be used as data processing material. The primary data were obtained directly in the research location both through observation or survey. The observation and survey were done through taking pictures of heavy vehicles and conducting a survey on road surface conditions on Pasar The Karang Tinggi–Penanding road, average daily traffic (ADT), the

Fig. 1 Chart of research flow



results of weighing heavy vehicles. The data were obtained from indirect research at related agencies such as the National Road Planning and Supervision Service of the Special Province of Bengkulu. The secondary data were CBR data and the percentage growth of traffic per year on The Karang Tinggi–Penanding Road.

4 Result and Discussion

4.1 Traffic Counting Data

Traffic Counting is the traffic volume calculation that is based on the vehicle types and the period. Traffic counting that was conducted aimed to know the vehicle movement and the road capacity on the road. The data collection for the traffic volume was done using a manual method or a direct calculation in the field with an interval of one hour and the survey was conducted for 16 h from 07:00 to 23:00. The recording was classified based on time, location and movement direction. The result of the ADT can be seen in Table 1.



Fig. 2 Research location

Table 1 ADT of The Karang Tinggi–Penanding road

Class of vehicle	Types	ADT
1	Motorcycle, Scooter, and three-wheeled vehicles	4224
2	Sedans, Jeeps, and station wagons	144
4	Pick Up, Micro truck, and delivery cars	96
6	Truck 2 Axle	240

4.2 Data for Heavy Vehicles

The data for heavy vehicles were collected from the testing using the 2-pad portable weighbridge conducted on Karang Tinggi–Penanding road. The following is the result of a heavy vehicle survey on two roads being reviewed. It consists of the method and instruments for a 2-pad survey for identifying the heavy vehicle load on the two roads. The total of overloaded vehicles on the roads being reviewed can be seen in Table 1 and Fig. 3.



Fig. 3 Documentation of collecting heavy vehicle load data on The Karang Tinggi–Penanding road

Table 2 Axis load testing on The Karang Tinggi–Penanding road

No. Police	Type of load	Number of axis		Load (kg) Standard	Load (kg)		Total load (kg)	Notes
		Front	Rear		Front	Rear		
BD 8329 CK	Sand truck	1	1	8200	1600	5320	6920	OK
BD 8028 AS	Sand truck	1	1	8200	3535	5200	8735	Overload
BD 8162 G	Sand truck	1	1	8200	2620	3620	6240	OK
BD 8159 AH	Sand truck	1	1	8200	3410	3270	6680	OK
BD 8920 AG	Sand truck	1	1	8250	5090	5010	10,100	Overload
BD 8097 Y	Sand truck	1	1	8250	5320	5150	10,470	Overload
BD 8105 AD	Sand truck	1	1	8250	2970	3390	6360	OK
BD 8096 Y	Sand truck	1	1	8250	5745	5485	11,230	Overload
BD 8101 AI	Sand truck	1	1	8250	6155	5825	11,980	Overload
BD 8170 YL	Sand truck	1	1	8250	4015	3920	7935	OK
BD 8275 IU	Sand truck	1	1	8250	4895	4350	9245	Overload
BD 8227 Y	Sand truck	1	1	8250	3655	3725	7380	OK
BD 8202 Y	Sand truck	1	1	8250	4815	5680	10,495	Overload
BD 8057 Y	Sand truck	1	1	8250	3485	5075	8560	Overload

The number of vehicles that are overloaded on the roads under review can be seen in Table 2.

Based on Table 2, the number of overloading violations of the Karang Tinggi–Penanding section can be seen that trucks that violate the permissible load (overload) are higher than trucks that do not violate. The total number of trucks that violated the weighbridge was eight vehicles. Percentage of violations that occurred 57.2%.

4.3 Pavement Thickness Analysis

From the daily traffic load on those roads, the VDF value and the traffic load that can be accommodated by the existing road pavement would be calculated.

Vehicle Damage Factor (VDF). VDF is a number expressing the comparison between the distress severities against the road pavement due to the single axle load vehicles by the standard axle load for a single axle of 8.16 tons by the Ministry of Public Works (2002). The data from the field obtained the condition of pavement structure for The Karang Tinggi–Penanding road with 1.72 km length with damage road condition around the 0.52 km. By the 2-lane and 2-way road, the vehicle distribution was 0.5 if it was in a standard load condition with the current average traffic load and the growth rate was 10% (the secondary data from the IRMS technical planning of Central Bengkulu District). An equivalent number can be calculated using Eq. 1.

$$VDF_4 = \left[\frac{\text{the load of each axle}}{8,160} \right]^4 \quad (1)$$

- Class of Vehicle 2 (Sedans, Jeeps and Station Wagons)

Total load = 2000 kg, load distribution (50% front and 50% rear)

$$\begin{aligned} VDF_4 &= \left[\frac{50\% \times 2000}{8160} \right]^4 + \left[\frac{50\% \times 2000}{8160} \right]^4 \\ &= 0.0023 + 0.0023 = 0.0046 \end{aligned}$$

- Class of Vehicle 4 (Pick Up, Micro Truck and Delivery Cars)

Total load = 5000 kg, load distribution (50% front and 50% rear)

$$\begin{aligned} VDF_4 &= \left[\frac{50\% \times 5000}{8160} \right]^4 + \left[\frac{50\% \times 5000}{8160} \right]^4 \\ &= 0.0088 + 0.0088 = 0.0176 \end{aligned}$$

- Class of Vehicle 6 (Truck 2 Axle) (Standard Load)

Total load = 8250 kg, load distribution (50% front and 50% rear)

$$\begin{aligned}
 VDF_4 &= \left[\frac{50\% \times 8250}{8160} \right]^4 + \left[\frac{50\% \times 8250}{8160} \right]^4 \\
 &= 0.065305 + 0.065305 = 0.13061
 \end{aligned}$$

- Class of Vehicle 6 (Truck 2 Axle) (Overload)

Total average overload = 10,102 kg, load ditribution (50% front and 50% rear)

$$\begin{aligned}
 VDF_4 &= \left[\frac{50\% \times 10,102}{8160} \right]^4 + \left[\frac{50\% \times 10,102}{8160} \right]^4 \\
 &= 0.146808 + 0.146808 = 0.293616
 \end{aligned}$$

Correlation Factor Between Traffic Growth and Design Life (R). Based on secondary data from the IRMS technical planning of Central Bengkulu District, traffic growth was obtained by 10%. In planning, the design life of 20 years is used so that the R value can be seen in Eq. 2.

$$R = \frac{(1 + 0.01i)^{UR} - 1}{0.01i} \tag{2}$$

$$R = \frac{(1 + 0.01i)^{UR} - 1}{0.01i} = \frac{(1 + (0.01 \times 0.1))^{20} - 1}{0.01 \times 0.1} = 57.275$$

Commutative Equivalent Single Axle (CESA). The load caused by traffic can be calculated based on the equivalent method toward a load of standard axle and overloading. To determine the accumulation of traffic axle load during the design life, the CESA₄ (Cumulative Equivalent Standard Axle) formula can be used in Eq. 3. The result of the calculation of CESA₄ for the standard load can be seen in Table 3.

$$CESA_4 = ADT \times DD \times DL \times R \times VDF_4 \times 365 \tag{3}$$

From Table 3, it can be seen that the CESA₄ was obtained for a standard load of 345,899. The TM value used to calculate CESA₅ is 2, so the CESA₅ value is 691,798. The result of the calculation of CESA₄ for overload can be seen in Table 4.

From Table 4, it can be seen that the CESA₄ was obtained for an overload of 579,253. The TM value used to calculate CESA₅ is 2, so the CESA₅ value is 1,158,506.

Pavement Layer Thickness for Standard Load and Overload. The analysis of the effect of the load against pavement thickness performance aims to know the

Table 3 CESA₄ value of Karang Tinggi–Penanding road for standard load

Class of vehicle	Types	ADT	DD	DL	R	VDF ₄	365	CESA ₄
1	Motorcycle, Scooter, and three-wheeled vehicles	4224	0.5	1	57.257	0	365	0
2	Sedans, Jeeps, and station wagons	144	0.5	1	57.257	0.00046	365	692
4	Pick Up, Micro truck, and delivery cars	96	0.5	1	57.257	0.01760	365	17,655
6	Truck 2 axle	240	0.5	1	57.257	0.13061	365	327,551
CESA ₄ Total								345,899

Table 4 CESA₄ Value of Karang Tinggi–Penanding road for overload

Class of vehicle	Types	ADT	DD	DL	R	VDF ₄	365	CESA ₄
1	Motorcycle, Scooter, and three-wheeled vehicles	4224	0.5	1	57.257	0	365	0
2	Sedans, Jeeps, and station wagons	144	0.5	1	57.257	0.00046	365	692
4	Pick Up, Micro truck, and delivery cars	96	0.5	1	57.257	0.01760	365	17,655
6	Truck 2 axle	103	0.5	1	57.257	0.130610	365	140,574
		137				0.29362		420,331
CESA ₄ Total								579,253

pavement thickness performance that was caused by the standard load and overload. Table 5 is used to determine which number of pavement designs are appropriate.

Table 5 is used to determine which number of pavement designs are appropriate. The type of pavement design is 3A because the value of total CESA₅ on standard and overload ranges between 0.1–4 millions. Pavement thickness is determined by plotting the CESA₅ value in Table 6 for standard load and overloading.

The analysis of pavement layer thickness due to the standard load and overloading by using the method of Binamarga 2017, it can be obtained the pavement layer thickness with a standard and overload for the surface layer are 30 mm for

Table 5 Type of pavement structure [15]

Pavement structures	Design chart	ESA4 (million) within 20 years				
		0–0.5	0.1–4	>4–10	>10–30	>30–200
Rigid pavement with heavy traffic (CBR ≥ 2.5%)	4	–	–	2	2	2
Rigid pavement with low traffic (CBR ≥ 2.5%)	4A	–	1.2	–	–	–
Modified AC-WC and modified SMA with CTB (ESA5)	3	–	–	–	2	2
AC with CTB (ESA5)	3	–	–	–	2	2
AC ≥ 100 mm thick with a graded foundation layer (ESA5)	3B	–	–	1.2	2	2
AC or thin HRS on a graded foundation layer	3A	–	1.2	–	–	–
Chip Seal or Double Chip Seal Class A Subbase	5	3	3	–	–	–
Soil cement foundation layer	6	1	1	–	–	–
Unpaved layer	7	1	–	–	–	–

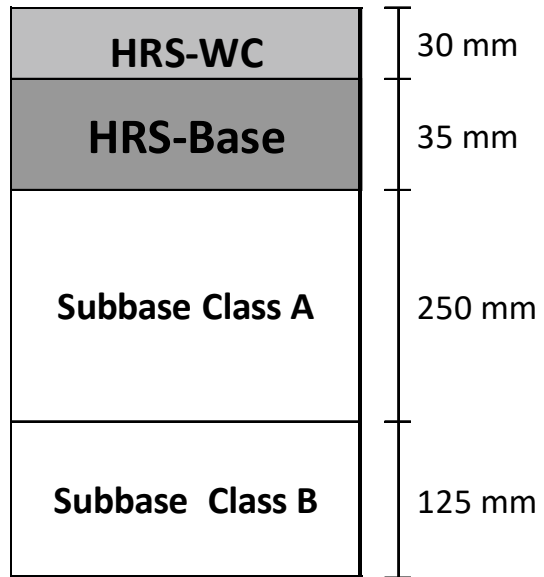
Table 6 Design chart 3A

CESA ₅ for 20 year on the design lane (10 ⁶)	FF1 CESA ₅ < 0.5	FF2 0.5 ≤ CESA ₅ ≤ 4
Surface types	HRS or Macadam	HRS
HRS WC	50	30
HRS Base	–	35
Class A Subbase	150	250
Class A Subbase/Class B Subbase/Stabilization with CBR > 10%	150	125

Flexible pavement design with HRS [15]

HRS WC and 35 mm for HRS Base, the class A subbase course layer is 250 mm and the class B subbase course layer is 125 mm. From chart 3A, it can be seen that with a standard load of 691,798 and an overload of 1,158,506, the thickness of the pavement obtained is the same. This is because the CESA₅ burden obtained is still relatively low, less than 4 million. The composition of pavement thickness can be seen in Fig. 4.

Fig. 4 Pavement thickness based on the standard load and overloading condition on The Karang Tinggi–Penanding road



5 Conclusion

Based on the analysis of the survey on The Karang Tinggi–Penanding road, it can conclude that the road condition experiences moderate damage due to overloaded vehicles because the result from the survey shows that the number of vehicles overloading the standard axle is less. Consequently, the following conclusions can be drawn:

1. The damage that occurred was caused by an excess load of heavy vehicle that passed through the road by approximately 57.2%.
2. The analysis of pavement layer thickness due to the standard load and overloading by using the method of Binamarga 2017, it can be obtained the pavement layer thickness with a standard and overload for the surface layer are 30 mm for HRS WC and 35 mm for HRS Base, the class A subbase course layer is 250 mm and the class B subbase course layer is 125 mm. From chart 3A, it can be seen that with a standard load of 691,798 and an overload of 1,158,506, the thickness of the pavement obtained is the same. This is because the CESA 5 burden obtained is still relatively low.

References

1. Sari DN (2014) Analisa Beban Kendaraan Terhadap Derajat Kerusakan Jalan dan Umur Sisa. *Jurnal Teknik Sipil dan Lingkungan* 2(4):615–620
2. Sentosa L, Roza AA (2012) Analisis Dampak Beban Overloading Kendaraan pada Struktur Rigid Pavemenet Terhadap Umur Rencana Perkerasan. *Jurnal Teknik Sipil* 19(2):61–168
3. Morisca M (2014) Evaluasi Beban Kendaraan Terhadap Derajat Kerusakan dan Umur Jalan. *Jurnal Teknik Sipil dan Lingkungan* 2(4):692–699
4. Suriyatno P, Putri EE (2015) Analisis Tebal lapis Tambah dan Umur Sisa Perkerasan Akibat Beban Berlebih Kendaraan. In: *Proceedings annual civil engineering seminar 2015*, Pekanbaru, 4 Nov 2015, p 164–176
5. Simanjuntak GI, Pramusetyo A, Riyanto B, dan Supriyanto (2014) Analisis Pengaruh Muatan Lebih (Overloading) Terhadap Kinerja Jalan dan Umur Rencana Perkerasan Lentur. *Jurnal Karya Teknik Sipil* 3(3):539–551
6. Situmorang RA, Wartadinata PW, Setiadji BH, Supriyono (2013) Analisis Kinerja dan Perkerasan Lentur akibat Pengaruh Muatan Lebih (Overloading). *Jurnal Karya Teknik Sipil* 2(2):359–370
7. Atiya AF, Sari OD, Purwanto D, dan Setiadji BH, (2014) Analisis Pengaruh Kinerja Jembatan Timbang Terhadap Kinerja Perkerasan dan Umur Rencana Jalan. *Jurnal Karya Teknik Sipil* 3(3):662–673
8. Syafriana SSF, Anggraini R (2015) Evaluasi Umur Layan Jalan dengan Memperhitungkan Beban Berlebih di Ruas Jalan Lintas Timur Provinsi Aceh. *Jurnal Transportasi* 15(2):115–124
9. Pandey SV (2013) Kerusakan Jalan Daerah Akibat beban Overloading. *Jurnal Tekno Sipil* 11(58):1–8
10. Wandu A, Saleh SM, Isya M (2016) Analisis Kerusakan Jalan Akibat Beban Berlebih. *Jurnal Teknik Sipil* 5(3):317–328
11. Saleh SM, Sjafruddin A, Tamin OZ, Frazila RB (2009) Pengaruh Muatan Truk Berlebih Terhadap Biaya pemeliharaan Jalan. *Jurnal Transportasi* 9(1):79–89
12. Cahyono SD (2012) Pengaruh Beban Lalu Lintas Terhadap Kerusakan pada Jalan Raya Ngawi- Caruban. *Jurnal Teknik Sipil* 13(1):66–73
13. Syaifullah WIPA, Herijanto W (2013) Analisis Pengaruh Beban Berlebih Kendaraan Terhadap Pembebanan Biaya Pemeliharaan Jalan. *Jurnal Teknik Sipil* 2:1–8
14. Martina R, Saleh SM, Isya M (2018) Kajian Beban Aktual Kendaraan pada Konstruksi Jalan Menggunakan Weight In Motion (WIM). *Jurnal Teknik Sipil* 1(3):701–714
15. Departemen Pekerjaan Umum (2017) Pedoman Perencanaan Tebal Perkerasan Lentur. Direktorat Jendral Bina Marga, Jakarta
16. Rahmawati A, Emil A, Lutfiyanto I, Syifa A (2019) The overloading effect on the design life of road and thickness of pavement layer. In: *First international conference of construction, infrastructure, and materials*, Jakarta, 16–17 July 2019. IOP Material Science and Engineering, vol 650. IOP Publishing Ltd, Bristol, p 012051

Performance of Polymer Modified Asphalt Mixture Using Gypsum Filler



Rindu Twidi Bethary , Dwi Esti Intari , and Siti Asyiah 

Abstract Road infrastructure is a means of transportation that is quite important in developing the economy in a region, so it is necessary to increase the quality and quantity of materials used and to add or modify the material used in the asphalt mixture by using gypsum powder waste and polymer asphalt. This study was aimed to determine the performance of the polymer-modified asphalt mixture using gypsum powder filler on the Asphalt Concrete Wearing Course (AC-WC) layer. The method used in this study was a laboratory experiment with Marshall testing with variations in the content of gypsum powder fillers, namely 0, 1, 2 and 3%. The results showed that the addition of gypsum powder filler could increase the value of the void in the mixture and the void in mineral aggregates, but it can reduce the value void filled with asphalt, stability and flow values. This affected the specific gravity and reduced durability of the asphalt mixture, but it provided the benefit of being able to accelerate the stiffening of the asphalt and make the asphalt mixture more, resulting in resistance to deformation damage.

Keywords Polymer asphalt · Gypsum · Filler · AC-WC

1 Introduction

Road infrastructure plays a very important role in the development of activities in a region in supporting economic, social and cultural growth [1, 2]. This activity will develop if it has good transportation infrastructure and facilities. Therefore, it is necessary to increase the quality and quantity of road infrastructure to meet the needs of the community. Flexible stiffening, one of the road constructions used in various countries, consists of four main materials, namely coarse aggregate, fine aggregate, filler and bitumen [3]. The use of fillers has an effective role in deter-

R. T. Bethary (✉) · D. E. Intari · S. Asyiah
Department of Civil Engineering, Sultan Ageng Tirtayasa University, Cilegon, Banten,
Indonesia
e-mail: rindutwidibethary@gmail.com

mining the properties and behavior of asphalt mixtures [4, 5], rock ash and Portland Cement (PC). They are usually used as fillers that are the result of limited production quantities and are quite expensive, so that alternative materials are needed.

The use of waste in the construction industry is important because the high amount of waste produced has a significant impact on the environment [6, 7], several waste materials used as fillers in asphalt mixtures have been developed, including lime recycled waste [8], coal fly ash [9], slag [10], gypsum powder [11] and other non-plastic mineral materials. In this study, a filler of gypsum powder containing a mineral with calcium sulfate ($\text{CaSO}_4 \cdot 2\text{H}_2\text{O}$) was used, which is often used as an adhesive, flame retardant and easy to repair. This makes gypsum waste good for use as a filler. Besides being able to bind asphalt better, it also does not cause environmental pollution [11, 12].

One type of asphalt pavement is concrete asphalt layer where the pavement structure that is directly in contact with air and vehicle loads is the AC-WC (Asphalt Concrete-Wearing Course) surface layer and the watertight layer so that in addition to the selection of aggregates, it is also influenced by the quality and the quantity of the asphalt binder [13, 14]. Asphalt material can be developed and modified to improve its performance. This is because asphalt is a viscoelastic material so that when the stiffness is high, cracks occur and if it is too flexible, deformation will occur, so that appropriate modification to performance is required. Polymer is one of the modifications of asphalt which is used as an effective modifier to improve the performance of the mixture and increase the strength so that the design life is longer [15]. Besides that, polymer modifier can also overcome various damages that occur on the pavement such as permanent deformation, temperature changes, cracking and raveling [16, 17]. This can be achieved if it is by the characteristics of the location, traffic loading and the environment.

Increased material requirements, decreased road performance and environmental problems can be overcome by the use of appropriate materials, where filler and asphalt have an important role in the mixture, so based on this it is necessary to carry out further studies to determine the performance of polymer modified asphalt mixtures using powder fillers gypsum.

2 Materials and Methods

2.1 Aggregate

The aggregate material used was from Bojonegaro, Serang Regency, Banten Province. There are 2 types of aggregate sizes used, namely coarse aggregate split 1–2 and screening, then fine aggregate (rock ash). The test results for coarse and fine aggregates can be seen in Table 1, where the characteristics showed that the aggregate meets the general specifications of Bina Marga in 2018 division 6 [18].

Table 1 Characteristics of coarse aggregates

No.	Testing	Result	Test specification	
			Minimum	Maximum
<i>Coarse aggregates</i>				
1	Bulk specific gravity	2.72	2.5	–
2	Apparent specific gravity	2.82	2.5	–
3	SSD specific gravity	2.76	2.5	–
4	Absorption (%)	1.21	–	3
<i>Fine aggregates</i>				
1	Bulk specific gravity	2.61	2.5	–
2	Apparent specific gravity	2.76	2.5	–
3	SSD specific gravity	2.67	2.5	–
4	Absorption (%)	2.04	–	3

Table 2 Characteristics of asphalt

No.	Testing	Result	Test specification	
			Minimum	Maximum
1	Penetration 25 °C; 100 g, 5 s, 0.1 mm	56.3	40	–
2	Lost weight (%)	0.06	–	0.8
3	Specific gravity	1.042	1.0	–

2.2 Asphalt

The asphalt used in this study was asphalt modified polymer type elastomer (E-55) equal to the value of PG-76 (Performance Grade) and entered into type II modified asphalt, which was then tested for physical properties which can be seen in Table 2. Based on the test results, it was obtained that the asphalt met the General Specifications of Bina Marga 2018 division 6.

2.3 Gypsum

The minerals contained in gypsum are sulfates, which are sedimentary rocks with the composition of calcium sulfate dihydrate ($\text{CaSO}_4 \cdot 2\text{H}_2\text{O}$). Gypsum has physical properties in the form of crystals that have gradations of white, gray, yellow, orange or black, with water content in the structure with the content of approximately 23.3% for lime (Ca) and sulfur (S) of 18.5%. The following is in Table 3 the chemical composition contained in gypsum [19].

There are various types of gypsum, the most commonly found is calcium sulfate hydrate with the formula $\text{CaSO}_4 \cdot 2\text{H}_2\text{O}$ (Calcium Sulfate Dihydrate). Evaporated

Table 3 Gypsum powder chemical composition

No.	Material	Content
1	Calcium (Ca)	23.82
2	Hydrogen (H)	2.34
3	Calcium Oxide (CaO)	32.57
4	Water (H ₂ O)	20.93
5	Sulphur (S)	18.62

minerals such as carbonate, borate, nitrate and sulfate can form gypsum by depositing these 25 minerals in oceans, lakes, caves and salt layers [11].

2.4 Method

The study on the performance of asphalt mixtures using modified elastomeric polymer asphalt and gypsum filler used laboratory experimental methods, where the study stages consisted of preliminary literature studies, material characteristics testing, making asphalt mix designs, testing Marshall mixes with the Marshall method and determining the optimum asphalt content in each mixture.

The mixing method used was asphalt mixed first with gypsum powder and then mixed with aggregate. There were 4 variations of the mixture which are differentiated based on the gypsum filler content, namely 0, 1, 2 and 3% % with the proportion of weight calculation to the total filler. The following in Fig. 1 describes the methodology in this study.

3 Analysis

3.1 AC-WC Layer Mixed Design

In the mixed design, the first stage was the determination of the proportion of the aggregate in the mixture by testing the sieve analysis to get the percentage passing of each fraction used in the mixture. Based on the gradation calculation, the mix

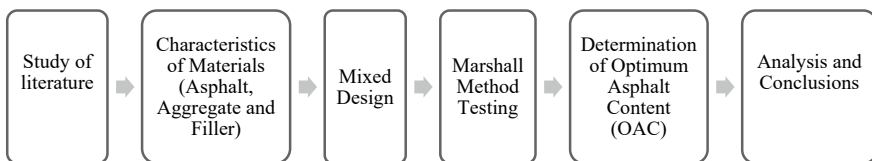


Fig. 1 The methodology of study

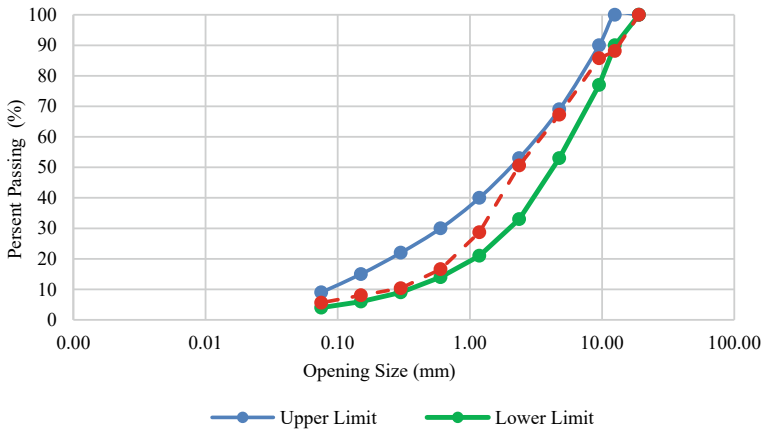


Fig. 2 Gradation design

design value with the composition used for split aggregates 1–2 is 15%, fraction 24% and 61% screening for rock ash aggregate. The mixed grade used was by Fig. 2, where the design can be said to be a good proportion because the mixed aggregate was graded close to the middle gradation of General Bina Marga 2018 specification range division 6 with the layer type (AC-WC).

3.2 Characteristic of Mix Asphalt

The use of the gypsum grade variation determined the volumetric parameters in the mixture, where the variation is one of the factors that influence the properties of the asphalt mixture. Analysis of the volumetric characteristics and the Marshall test are as follows.

Void in Mixture (VIM). The total volume of air between the aggregates covered after the compaction process was an understanding of the VIM. The magnitude of this VIM value had an effect on the mixture durability, where the VIM value was related to the void in mineral aggregates (VMA) and the void filled with asphalt (VFA). Figure 3 showed the comparison of the VIM value at each asphalt content with the gypsum filler level, where the addition of gypsum filler results in the VIM value that was getting bigger, alkaline was caused by more asphalt dry than filler. This gave results with previous studies where the gypsum content used was 5–9% [11]. The VIM values were too high because the mixture easily oxidizes and cracks when traffic loading was applied. If the road was too low bleeding, the VIM value of the AC-WC mixture was limited to a minimum of 3% and a maximum of 5%.

Void in Aggregate Minerals (VMA). The increase in the level of asphalt used in the mixture will decrease up to reaches the minimum point and will increase again

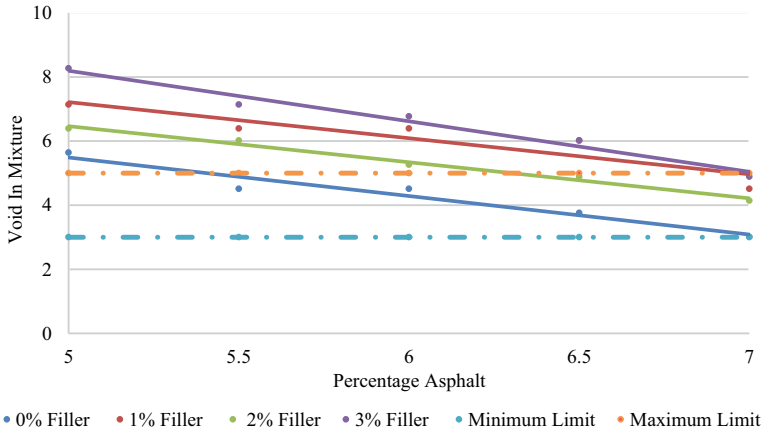


Fig. 3 Relationship between VIM and asphalt content

with the addition of asphalt content. This was because the asphalt filled the void between the aggregates so that the void could not be filled by asphalt. Based on Fig. 4, the increase in the content of the gypsum filler resulted in the VMA value tending to increase, this indicated that the gypsum filler did not fill the gaps between the aggregate particles, where the asphalt which served as a cover also filling the voids between the aggregate particles. The smaller VMA value indicated that the mixture had more durability because high VMA could cause the mixture to be susceptible to deformation so that 1% gypsum content had better durability than other gypsum levels.

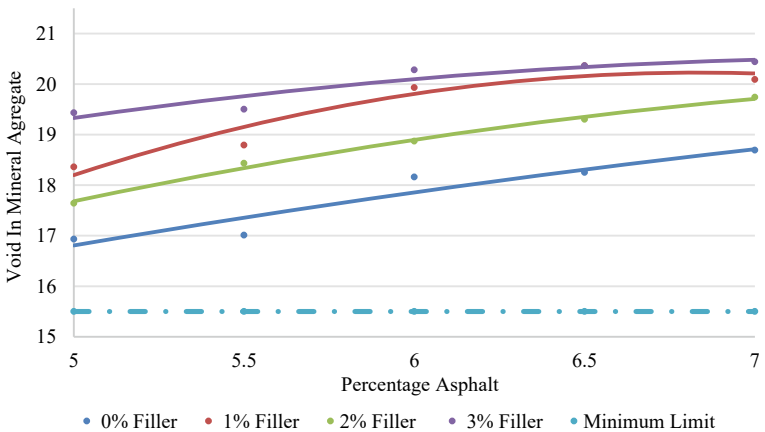


Fig. 4 Relationship between VMA and asphalt content

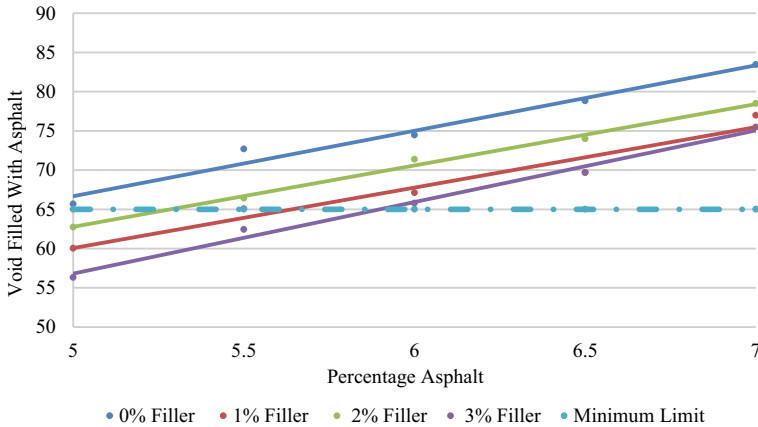


Fig. 5 Relationship between VFA and asphalt content

Void in Filled Asphalt (VFA). Asphalt content and the film thickness can be expressed in terms of the volume of mixed asphalt, the relationship between VFA and the increase in asphalt content showed that the VFA value tended to be greater with increasing asphalt content. In Fig. 5, it can be seen that the addition of gypsum filler results in the VFA value was getting smaller meaning that in the 3% gypsum filler mixture the void in the aggregate minerals was filled with less bitumen than the 1% gypsum filler mixture. The mixture with the higher VFA value is 1% gypsum filler which indicates that this mixture can fill the voids in the aggregate larger than the mixture with 3% gypsum filler.

Stability. One of the Marshall empirical values is the stability value, with direct measurement from the test when the test object is loaded with the Marshall test instrument. The stability value is influenced by several factors, including aggregate grading, bitumen content, internal friction of aggregate particles, interlocking and asphalt adhesion. Figure 6 shows the stability comparison for each mixture, where the addition of gypsum filler to the asphalt mixture resulted in a decrease in the stability value, due to the gypsum filler which affected the adhesion of the asphalt to the aggregate. The addition of gypsum filler cannot fill the voids in the mixture so that the bonds that occur between the aggregates are reduced.

Flow. Flow is a function of the stiffness of the binder and the content of the asphalt mixture, which is one of the empirical parameters that states the change in the plastic shape of the mixture due to loading. The addition of asphalt content will result in the aggregate being covered by asphalt, which results in interlocking between aggregates and causes an increase in melt value. Figure 7 shows that with the increase in the percentage of gypsum, the flow value becomes smaller so that the 1% gypsum mixture has a more flexible behavior than the 3% gypsum content.

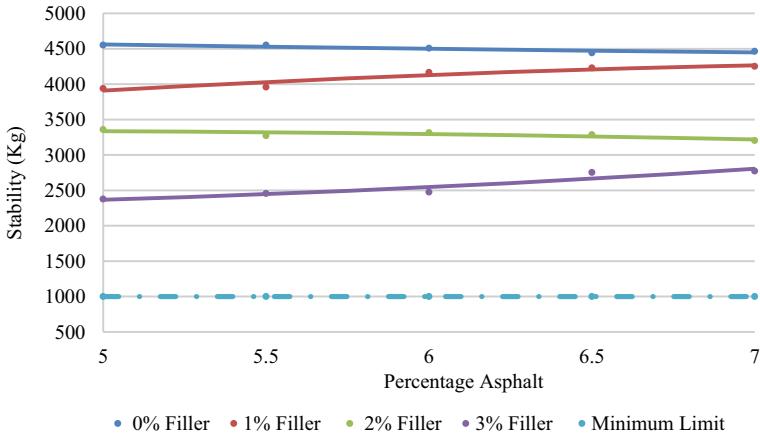


Fig. 6 Relationship between stability and asphalt content

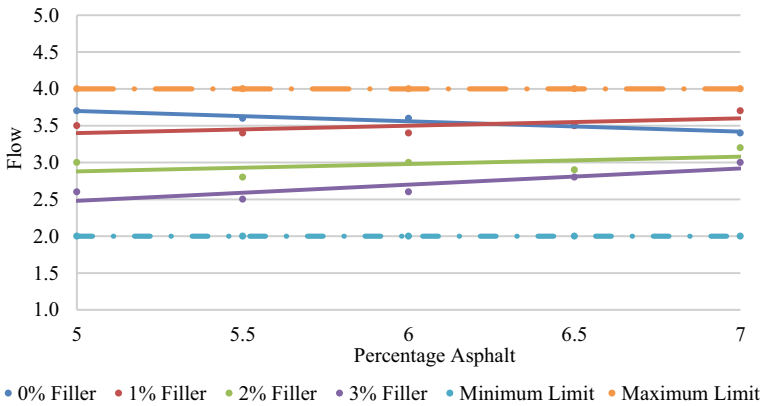


Fig. 7 Relationship between flow and asphalt content

Marshall Quotient. The Marshall Quotient (MQ) value is an approach to the level of stiffness and flexibility of the mixture, where the greater the MQ value of the mixture, the stiffer it is and the other hand the lower it is, the more flexible it is. Based on Fig. 8 the addition of gypsum filler causes the MQ value to be smaller so that the mixture is more flexible, this is because the flow value in the asphalt mixture with 3% gypsum content is the lowest compared to other mixtures.

Optimum Asphalt Content. Optimum Asphalt Content (OAC) is asphalt content that produces a mixture that fulfills all the elements of the Marshall parameter. Figure 9 shows that in general, the addition of filler resulted in a decrease in OAC in the gypsum filler 2% then it was added back to the 3% gypsum filler, with the

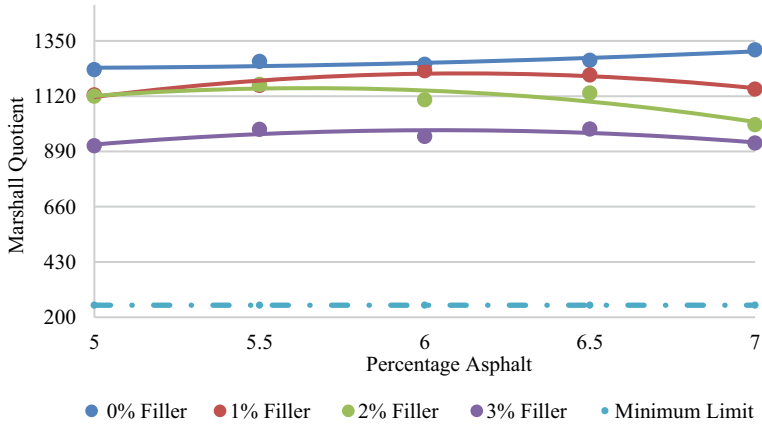


Fig. 8 Relationship between Marshall quotient and asphalt content

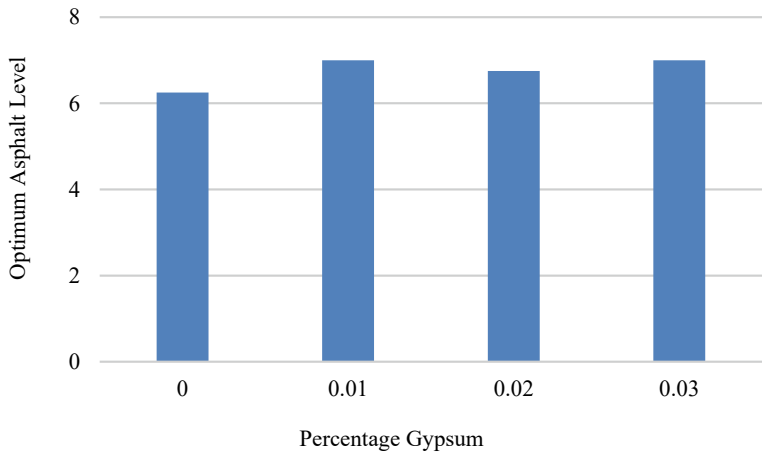


Fig. 9 Optimum asphalt content

optimum asphalt content obtained in this study was 6.25–7.0%. Based on the case, it can indicate that using filler gypsum needs more asphalt content with the high VIM value and the lower VFA value so that the thick film asphalt is lower than the mixture without using gypsum filler. It can be seen in Fig. 10.

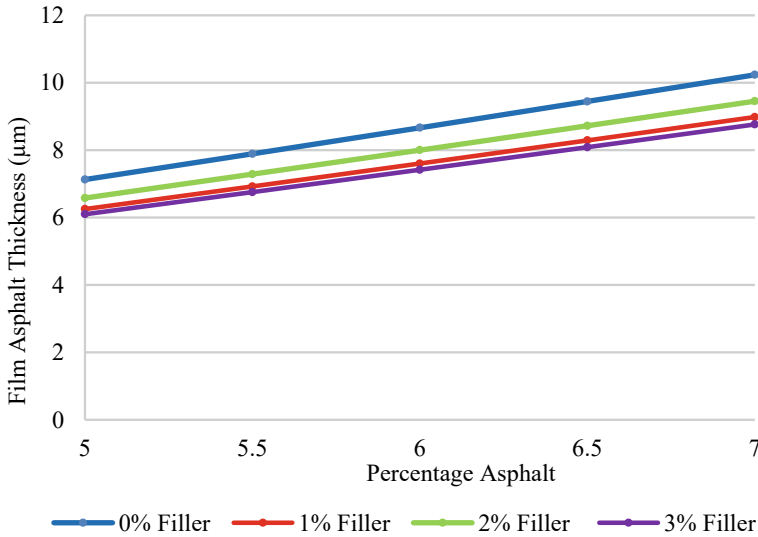


Fig. 10 Relationship between film asphalt thickness and filler gypsum

4 Conclusion

From the testing and analysis carried out in this study, the following conclusions are obtained:

1. The characteristics of the material used in this study met the General Bina Marga requirements in 2018 division 6 with the type of layer (AC-WC), where the gradation used includes the intermediate value of the gradation (AC-WC) with the mix design used for an aggregate of 1–2% for 15%, screening fraction is 24% and rock ash for 61%.
2. The addition of gypsum powder as a filler in the asphalt mixture to the volumetric characteristics can increase the VIM and VMA values, as well as decrease the VFA value. This indicated that the gypsum filler does not remove gypsum among aggregate particles so that it was filled with asphalt resulting in 1% more gypsum mix and gypsum mixture. Meanwhile, empirical testing with Marshall resulted in a decrease in stability and flow values.
3. The use of gypsums powder as a filler in polymer asphalt modification can accelerate the stiffening of the asphalt. It can be seen from a decrease in asphalt temperature then the asphalt is more flexible which is an indicator of resistance to deformation damage. On the other hand, the specific gravity of the asphalt mixture decreased because of the greater percentage of slack in the mixture causing its durability to be reduced.

References

1. Bethary RT, Subagio BS, Rahman H, Suaryana N (2019) Effect of recycled materials on marshall performance of hot asphalt mixture (HMA-RAP). *IOP Conf Ser: Mater Sci Eng* 508:012048
2. Silondae S, Muthalib HAA, Ernawati (2016) Keterkaitan jalur transportasi dan interaksi ekonomi kabupaten konawe utara dengan kabupaten/kota sekitarnya. *Jurnal Progres Ekonomi Pembangunan* 1:49–64
3. Harun-Or-Rashid GM, Islam MM (2020) A review paper on: effect of different types of filler materials on marshall characteristics of bitumen hot mix. *Int J Mater Sci Appl* 9(3):40–45. <https://doi.org/10.11648/j.ijmsa.20200903.11>
4. Eisa MS, Basiouny ME, Youssef A (2018) Effect of using various waste materials as mineral filler on the properties of asphalt mix. *Inno Infrastruct Solutions* 3:27. <https://doi.org/10.1007/s41062-018-0129-4>
5. Qiu Y (2007) Design and performance of stone mastic asphalt in Singapore conditions. Dissertation, Nanyang Technological University
6. Lau HH, Whyte AA (2007) A construction waste study for residential projects in Miri, Sarawak. In: *Proceeding of the conference on sustainable building South East Asia*, p 312–318
7. Yahya K, Boussabaine AH (2006) Eco-costing of construction waste. *Manage Environ Qual: Int J* 17:6–19
8. Do HS, Mun PH, Keun RS (2008) A study on engineering characteristics of asphalt concrete using filler with recycled waste lime. *Waste Manage* 28(1):191–199. <https://doi.org/10.1016/j.wasman.2006.11.011>
9. Hasmiati H, La Ode M (2014) Mix design asphalt concrete wearing course (AC-WC) dengan menggunakan fly ash batu bara sebagai pengganti filler. *STABILITA Jurnal Ilmiah Teknik Sipil* 2(1):133–144
10. Bethary RT, Rahman H (2019) Effect of slag and recycled materials on the performance of hot mix asphalt (AC-BC). *J Civ Eng* 26(1):1–9
11. Auditia BA, Rendih ED, Rachmansyah HHM (2018) Pengaruh Penggunaan Bubuk Gypsum Sebagai Filler Dalam Campuran Aspal. *Jurnal Teknik dan Ilmu Komputer* 7(26):149–155
12. Alpius KSW, Mangontan R (2020) The effect of the use of gypsum waste as a filler substitution on stone matrix asphalt coarse. *IOP Conf Ser: Mater Sci Eng* 1088:012097
13. Rombot P, Kaseke OH, Manoppo MRE (2015) Kajian kinerja campuran beraspal panas jenis lapis aspal beton sebagai lapis aus bergradasi kasar dan halus. *Jurnal Sipil Statik* 3(3):190–197
14. Nurlaily I, Rahardjo B (2017) Pengaruh Lama Perendaman Air Hujan Terhadap Kinerja Laston (Ac-Wc) Berdasarkan Uji Marshall. *Bangunan* 22(1):1–12
15. Sengoz B, Isikyakar G (2008) Analysis of styrene-butadiene-styrene polymer modified bitumen using fluorescent microscopy and conventional test methods. *J Hazard Mater* 150(2):424–432. <https://doi.org/10.1016/j.jhazmat.2007.04.122>
16. Yildirim Y (2007) Polymer modified asphalt binders. *Constr Build Mater* 21(1):66–72. <https://doi.org/10.1016/j.conbuildmat.2005.07.007>
17. Intari DE, Fathonah W, Kirana FW (2018) Analisis karakteristik campuran laston (HRS-WC) akibat redaman air laut pasang (ROB) dengan aspal modifikasi polimer starbit E-55. *Fondasi: Jurnal Teknik Sipil* 7(2):53–62
18. Kementerian Pekerjaan Umum (2018) Spesifikasi umum untuk pekerjaan konstruksi jalan dan jembatan. Bina Marga, Jakarta
19. Sinaga S (2009) Pembuatan papan gipsium plafon dengan bahan pengisi limbah padat pabrik kertas rokok dan perekat polivinil alkohol. Thesis, Universitas Sumatera Utara

Resistance of Modified Concrete-Wearing Course Mixture Using LDPE Polymer Against Damage Due to Water Immersion



Indah Handayasari, Dyah Pratiwi Kusumastuti,
and Arief Suardi Nur Chairat

Abstract Damage that occurs on the pavement can be in the form of permanent deformation, cracks due to temperature changes, material damage and material detachment. This research tested the resistance of the Asphalt Concrete Wearing Course (AC-WC) mixture using a plastic bag of LDPE (Low Density Polyethylene) polymer type against water through immersion in water with a temperature of 60 °C for 30 min, 24, 48 and 72 h with a continuous system and variations in LDPE polymer plastic content. by 0, 5, 7 and 9%. The results of the analysis show that the use of LDPE polymer plastic in the AC-WC mixture can increase the resistance to damage to the mixture due to continuous water immersion by reducing the retained strength index value and increasing the remaining strength index value with increasing the duration of immersion.

Keywords Retained strength index · Remaining strength index · Concrete wearing course

1 Introduction

One of the efforts to produce asphalt that has a high level of durability is the use of various modifications to the asphalt by utilizing synthetic polymers as a mixture. This is because synthetic polymers are artificial polymers that contain thermoplastic chemical elements so that they have high elasticity and binding capacity. Asphalt modification using polymeric materials obtained from a mixture of asphalt particles

I. Handayasari (✉) · D. P. Kusumastuti
Study Program of Civil Engineering, Institut Teknologi PLN, West Jakarta, Indonesia
e-mail: indah.handayasari@itpln.ac.id

A. S. N. Chairat
Study Program of Mechanical Engineering, Institut Teknologi PLN, West Jakarta, Indonesia

© The Author(s), under exclusive license to Springer Nature Singapore Pte Ltd. 2022
H. A. Lie et al. (eds.), *Proceedings of the Second International Conference of Construction, Infrastructure, and Materials*, Lecture Notes in Civil Engineering 216,
https://doi.org/10.1007/978-981-16-7949-0_36

with polymer additives is known to optimize the properties of asphalt. Polymers are able to increase the level of pavement durability from various types of damage, such as permanent deformation, cracks due to temperature changes, material damage and material release [1]. Modification of asphalt using polymer waste in the asphalt mixture to withstand extreme weather shows the results that this type of polymer can be used and provides good durability values [2]. The use of basalt material with a 60/70 penetration asphalt concrete layer with the additive of used plastic bag additives meets the general specifications of asphalt pavement in [3] so that in field application, it is able to withstand traffic loads [4]. From the results of [5] analysis, the addition of plastic bag waste to the AC-WC asphalt mixture can improve the quality of the mixture, which can increase the strength of the aggregate against abrasion and reduce the absorption and have a higher strength to withstand loads than the asphalt mixture without waste Plastic.

This study uses a laboratory-scale test approach by testing the resistance of the Asphalt Concrete Wearing Course (AC-WC) mixture using a plastic bag which is a type of LDPE (Low Density Polyethylene) polymer against water through immersion in water with a temperature of 60 °C for 24, 48 and 72 h with a continuous system and determination. Strength evaluation parameter after immersion or residual strength index. Where the addition of variations in the content of LDPE polymer plastic bags of 0, 5, 7 and 9% at the optimum asphalt content of 5.9%.

2 Durability

One of the performance parameters of the asphalt concrete mixture is durability. To get good durability, usually high asphalt content is used. However, if the asphalt mixture with high asphalt content is always submerged in water, the road will gradually suffer damage. The method used in evaluating the effect of water on the asphalt mixture with the Marshall immersion test in which the stability of the test object is determined by immersion in water at a temperature of 60 °C. The ratio of the immersed stability to the standard stability is expressed in percent and is called the Index Retained Strength, which is calculated in Eq. 1.

$$IRS = \left[\frac{MSi}{MSs} \right] \times 100 \quad (1)$$

IRS = Index Retained Strength (%)

MSi = Marshall stability after immersion for 24, 48, 72 h at a temperature of ±60 °C, (kg)

MSs = Standard Marshall stability in immersion for 30 minutes at 60 °C, (kg).

As shown in Table 1 for the specifications of the asphalt mixture based on the provisions of Bina Marga [6], the IRS value must be greater than 90%.

Table 1 Concrete asphalt mixture requirements [6]

Properties		Asphalt concrete		
		WC	BC	Base
Number of collisions per plane		75	75	112
The ratio of particles passed the 0.075 mm sieve with the effective asphalt content	Min	0.6		
	Max	1.2		
VIM (%)	Min	3.0		
	Max	5.0		
VMA (%)	Min	15	14	13
VFB (%)	Min	65	65	65
Marshall Stability (kg)	Min	800		1800
	Max	–		–
Flow (mm)	Min	2		3
	Max	4		6
Marshall Quotient (kg/mm)	Min	250		300
Remaining Marshall Stability (%) after immersion for 24 h, 60 °C	Min	90		
Void in the mixture (%) at refusal density	Min	2		

Durability modification [7] has developed a single parameter that describes the longevity condition of a hot asphalt mixture after a series of immersion periods. This parameter is called the Durability Index, which consists of two types, namely the first durability index and the second durability index.

First Durability Index The first index is defined as the successive amount of slope of the durability curve, which is expressed in Eq. 2.

$$r = \sum_{i=0}^{n-1} \frac{S_i - S_{i+1}}{t_{i+1} - t_i} \quad (2)$$

r = The value of the decrease in strength (%) on the first durability index.

S_0 = Absolute value of initial strength.

S_i = Percent strength remaining at time t_i .

S_{i+1} = Percent strength remaining at time t_{i+1} .

t_i, t_{i+1} = immersion time (starting from the beginning of the test).

Second Durability Index The second index is defined as the area of average strength loss between the durability curve with the line $S_0 = 100\%$, which is stated in Eq. 3.

$$a = \frac{1}{t_n} \sum_{i=1}^n a_1 = \frac{1}{2t_n} \sum_{i=0}^{n-1} (S_i - S_{i+1}) [2t_n - (t_i + t_{i+1})] \quad (3)$$

a = The value of the decrease in strength (%) on the second durability index.

t_n = immersion time (last).

S_1 = Percent strength remaining at time t_1 .

S_{i+1} = Percent strength remaining at time t_{i+1} .

t_i, t_{i+1} = immersion time (starting from the beginning of the test).

A positive value of (a) indicates a loss of strength, while a negative value represents an increase in strength. By definition, $a < 100$ so that to express the percentage strength of one day remaining (Sa) is stated in Eq. 4.

$$Sa = (100 - a) \quad (4)$$

Sa = Percent strength remaining at second durability index (%).

3 Results and Discussion

Testing the quality of the material used in the AC-WC mixture consists of testing the asphalt, coarse aggregate, fine aggregate and filler.

3.1 Asphalt Test

The results of tests carried out on 60/70 penetration asphalt can be seen in Table 2.

Table 2 Asphalt testing results

Test	Unit	Reference	Terms	Results	Information
Apparent Density	gr/cc	SNI 06-2442-2011	≥ 1	1.038	Fulfilled
Flash point	°C	SNI 2433-2011	≥ 232	360	Fulfilled
Soft point	°C	SNI 06-2434-2011	≥ 48	51	Fulfilled
Penetration	0.1 mm	SNI 06-2456-2011	60–70	63.1	Fulfilled
Ductility	Cm	SNI 2432:2011	≥ 100	100	Fulfilled

3.2 Coarse Aggregate Test

The results of tests carried out on coarse aggregate can be seen in Table 3. Based on the test results, it was found that the coarse aggregate material had met the specifications in accordance with the standards used in the inspection, namely Indonesia National Standard SNI 1969:2016.

3.3 Fine Aggregate Test

The results of tests carried out on coarse aggregate can be seen in Table 4. The standard used in examining specific gravity and absorption of fine aggregates is SNI 1970:2016.

3.4 Filler Test

The test for the filler sieve analysis used SNI ASTM C 136:2012. Based on the results of the analysis, the filler sieve met the standard requirements, namely that the minimum passing percentage of the No. 200 filter was 75%, with the percentage value of passing the No. 200 filter of 91.24%. To test the specific gravity of the filler following the AASHTO T-89-81 reference and from the test results obtained the filler density value of 3.045 gr/cc.

3.5 The Resistance of the AC-WC Mixture Against Continuous Water Immersion

The resistance of the AC-WC mixture with the addition of variations in the levels of LDPE polymer plastic bags were 0, 5, 7 and 9%. Where the test object is immersed in water with a temperature of 60 °C with immersion duration for 24, 48 and 72 h. The results of durability testing can be seen in Table 5.

Table 3 Coarse aggregate testing results

Test	Unit	Terms	Results		Information
			Coarse	Medium	
Abrasion	%	≤ 40	16.75	20.32	Fulfilled
Bulk specific gravity	gr/cc	≥ 2.5	2.607	2.597	Fulfilled
SSD specific gravity	gr/cc	≥ 2.5	2.633	2.634	Fulfilled
Apparent density	gr/cc	≥ 2.5	2.677	2.697	Fulfilled
Absorption	%	≤ 3	0.997	1.425	Fulfilled

Table 4 Fine aggregate testing results

Test	Unit	Terms	Results	Information
Bulk specific gravity	gr/cc	≥ 2.5	2.507	Fulfilled
SSD specific gravity	gr/cc	≥ 2.5	2.563	Fulfilled
Apparent density	gr/cc	≥ 2.5	2.645	Fulfilled
Absorption	%	≤ 3	2.208	Fulfilled

Table 5 Asphalt mixture durability test results

Mixed variations	Terms	Immersion duration (h)			
		0.5	24	48	72
		<i>Stability (Kg)</i>			
0% LDPE	≥ 800	970.791	890.239	871.182	803.092
5% LDPE		1034.356	986.362	963.901	956.360
7% LDPE		1018.982	948.602	940.032	931.745
9% LDPE		990.828	919.201	907.878	899.344
		<i>IRS (%)</i>			
0% LDPE	≥ 90	100.00	91.70	89.74	82.73
5% LDPE		100.00	95.36	93.19	92.46
7% LDPE		100.00	93.09	92.25	91.44
9% LDPE		100.00	92.77	91.63	90.76
<i>First Durability Index</i>		<i>Decrease in strength, r (%)</i>			
0% LDPE		00.00	0.35	0.43	0.72
5% LDPE		00.00	0.19	0.28	0.31
7% LDPE		00.00	0.29	0.32	0.36
9% LDPE		00.00	0.31	0.35	0.38
<i>Second Durability Index</i>		<i>Decrease in strength, a (%)</i>			
0% LDPE		00.00	5.48	6.95	12.39
5% LDPE		00.00	3.06	4.61	5.41
7% LDPE		00.00	4.56	5.25	6.14
9% LDPE		00.00	5.11	5.67	6.46
		<i>Remaining Strength, Sa (%)</i>			
0% LDPE		100.00	94.52	93.05	87.61
5% LDPE		100.00	96.94	95.39	94.59
7% LDPE		100.00	95.44	94.75	93.86
9% LDPE		100.00	94.89	94.33	93.54

Tests conducted showed that the stability value decreased along with the longer the asphalt mixture was submerged in water. The decrease in the stability value of the asphalt mixture with 0% LDPE polymer plastic content after soaking was 17.27%, namely from the initial stability of 970.791–803.092 kg. Likewise, a decrease in the value of stability occurred in the asphalt mixture with 5%, 7% and 9% content of LDPE polymer plastic. After soaking the mixture with the duration of continuous immersion, the stability value decreased by 7.54%, 8.56% and 9.23%, respectively. Decreased stability or failure of the mixture was associated with loss of adhesion or stripping, which is in line with the results stated [8], stated that the decrease in the value of the stability of the mixture was due to the immersion process carried out. The percentage reduction that occurred in the asphalt mixture using LDPE polymer plastic was lower than that of the asphalt mixture without LDPE polymer plastic. It can be said that asphalt mixtures with LDPE polymer plastics have more resistance to continuous immersion compared to asphalt mixtures without LDPE polymer plastics.

Based on the results in Table 5 and Fig. 1 shows that the IRS value of immersion in a continuous pattern results in a decreasing value with increasing immersion duration either with or without using LDPE polymer plastic. The IRS value on the variation of the LDPE polymer type plastic content of 0% gave a greater reduction than the IRS value of the asphalt mixture using LDPE polymer type plastic. It is known from the results of testing the IRS value at the duration of immersion of 48 h and 72 h continuously in the asphalt mixture with 0% LDPE polymer plastic content that cannot meet the requirements for a minimum IRS value of 90% according to Bina Marga 2018 provisions, and Figs. 2 and 3 for the value of the decrease in strength at the first durability index (r) and the value of the decrease in strength at the second durability index (a) increased after immersion for all variations of the LDPE polymer plastic content while the remaining strength percent (Sa) in Table 5 and Fig. 4 give a slower reduction result than without LDPE polymer plastic.

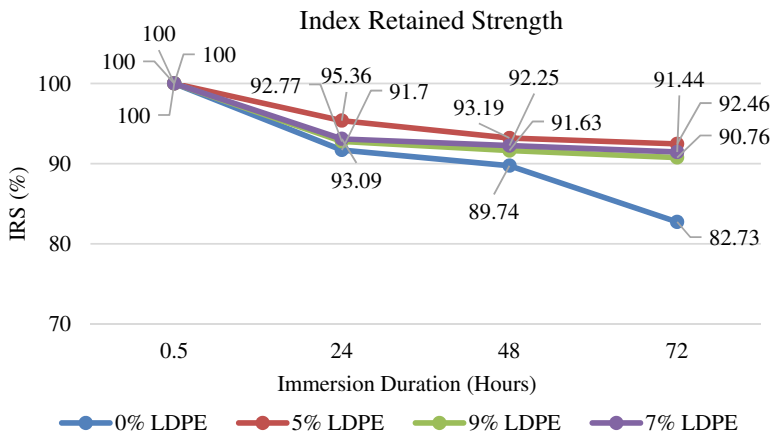


Fig. 1 Index retained strength value

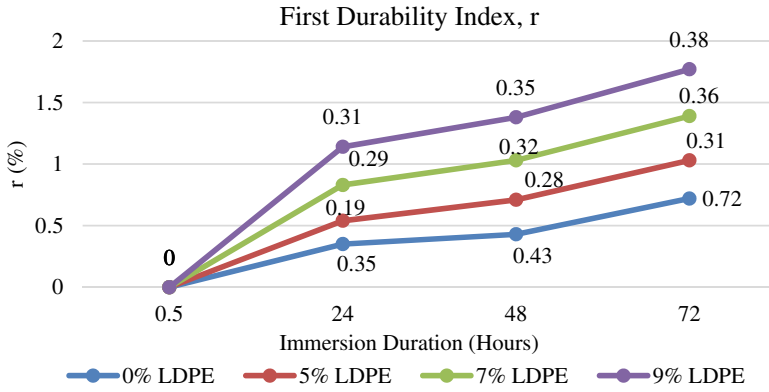


Fig. 2 First durability index value (r)

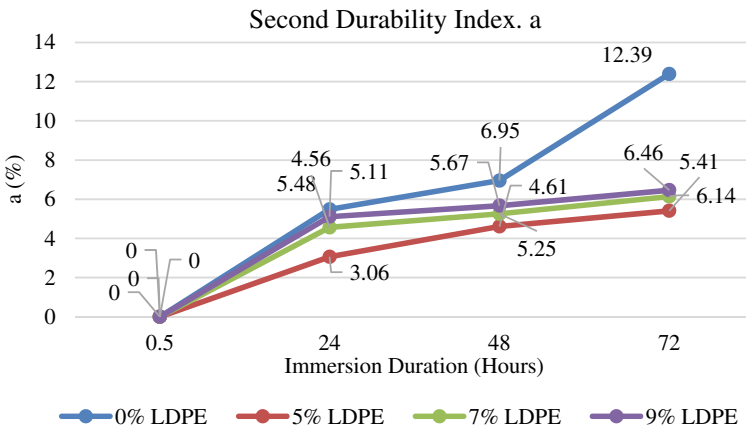


Fig. 3 Second durability index value (a)

The effect of the duration of immersion on the AC-WC asphalt mixture using LDPE polymer plastics showed a decreasing pattern that tended to be linear in the IRS and Sa values. The longer the immersion, the greater the reduction in IRS in the continuous immersion pattern. In addition, the use of LDPE polymer results in better Index Retained Strength and remaining strength than without the use of LDPE, so it can be stated that the LDPE polymer used in AC-WC smoke mixtures can reduce strength loss compared to using only pure asphalt.

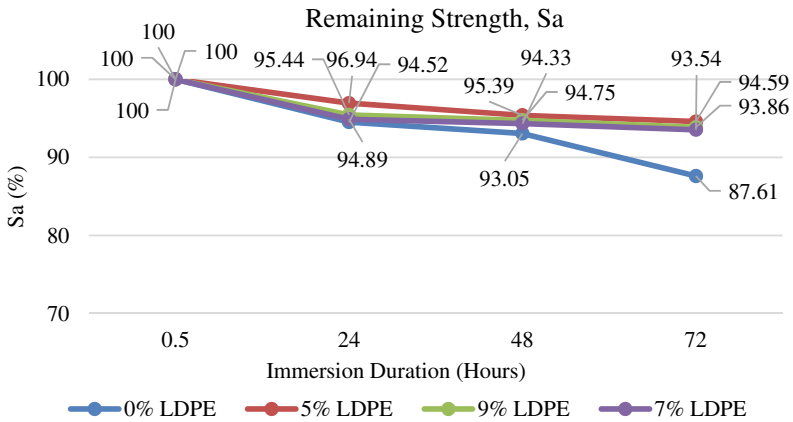


Fig. 4 Remaining strength value

4 Conclusions

Based on the analysis of the test results, it can be concluded that the addition of LDPE polymer type plastic can increase the stability of the AC-WC mixture. The use of LDPE polymer plastic in the AC-WC mixture can increase the resistance to damage to the mixture due to continuous water immersion, namely reducing the Index Retained Strength value and increasing the remaining strength index value with increasing the duration of immersion.

References

1. Yildirim Y (2007) Polymer modified asphalt binders. *Constr Build Mater.* <https://doi.org/10.1016/j.conbuildmat.2005.07.007>
2. Yildirim Y (2007) Polymer modified asphalt binders. *Constr Build Mater* 21:66–72
3. Kementerian Pekerjaan Umum (2010) Spesifikasi umum untuk pekerjaan konstruksi jalan dan jembatan (revisi 3). Bina Marga, Jakarta
4. Fitri S, Saleh SM, Isya M (2018) Pengaruh Penambahan Limbah Plastik Kresek Sebagai Substitusi Aspal Pen 60/70 Terhadap Karakteristik Campuran Laston AC-BC. *J Tek Sipil* 1:737–748
5. Susanto I, Suaryana N (2019) Evaluasi kinerja campuran beraspal lapis aus (AC-WC) dengan bahan tambah limbah plastik kresek. *J Apl Tek Sipil* 17:27
6. Kementerian Pekerjaan Umum (2018) Spesifikasi umum untuk pekerjaan konstruksi jalan dan jembatan. Bina Marga, Jakarta
7. Craus J, Ishai I, Sides A (1981) Durability of bituminous paving mixtures as related to filler type and properties. In: *Association of asphalt paving technologists proceedings*, pp 291–318
8. Nahyo N, Sudarno S, Setiadji BH (2019) Durabilitas campuran hot rolled sheet-wearing course (hrs-wc) akibat rendaman menerus dan berkala air rob. *J Tek Sipil* 13(1):124–135

Experimental Study on the Self-healing Ability of Wearing Course-Asphalt Concrete Mixes Reinforced with Steel Particles



Anissa Noor Tajudin , Arif Sandjaya, Daniel Christianto ,
and M. Bagas Haris Kurniawan

Abstract The self-healing method is one of the most recent technologies used to reduce road distress. One method to accelerate the healing process of asphalt is by using conductive materials in the mix and heating it with electromagnetics. Various materials are used as heat conductors, such as carbon-based fibers and nanofibers, conductive modified bitumen and metal particles. This research uses steel fiber for the Asphalt Concrete Wearing Course (AC-WC). Steel particles were added to the asphalt concrete mixture with varying amount of 0, 0.25, 0.5, 0.75, 1% to the mixture weight. The self-healing test was carried out with a three-point bending test and microwave heating for five cycles to see the healing ratio of each variation. To understand each variation's healing properties, the heating was done for 20, 40 and 60 s. The results showed that the pavement mixture using steel fibers was successful in the self-healing method test. The research results on the mixture with 0% steel particles proved to have self-healing ability but did not give results as good mixtures using 0.25, 0.5, 0.75 and 1% of steel particles.

Keywords Self-healing pavement · Steel fiber · AC-WC · Temperature sensitivity

A. N. Tajudin (✉) · A. Sandjaya · D. Christianto · M. B. H. Kurniawan
Universitas Tarumanagara, Jakarta 11140, Indonesia
e-mail: anissat@ft.untar.ac.id

A. Sandjaya
e-mail: arifs@ft.untar.ac.id

D. Christianto
e-mail: danielc@ft.untar.ac.id

1 Introduction

1.1 Background

Many factors can result in pavement distress. Temperature, humidity and temperature on humidity are the three main factors that must be considered in pavement design [1]. High temperatures can result in decreasing asphalt stiffness, while stiffness will increase at low temperatures. Environmental factors also influence the nature of the pavement.

An uncontrolled increase in traffic volume can also accelerate pavement damage because the structure or subgrade can no longer withstand loads that exceed its strength. The most common pavement damage is cracking. Cracks are a type of damage that is often ignored because they do not significantly affect comfort and safety while driving. However, cracks that are not treated immediately can develop into potholes because water can enter the gap and aggravate the damage.

Various new methods have been developed to repair damaged roads easily and quickly. One of them is by utilizing asphalt's ability to self-heal. The self-healing ability of asphalt cannot occur instantly at ambient temperature, while the road is constantly traversed by vehicles and is exposed to the environment. It is also risky to do a temporary closure of cracked locations because this will result in congestion. Due to these problems, many researchers are interested in developing mixtures and methods to accelerate the self-healing process.

Further innovations have been developed to reduce the asphalt viscosity by several methods, such as heating the material or releasing microencapsules into the cracks. Various materials are used as heat-conductors.

Although research on self-healing has been widely carried out, especially in developed countries in the last ten years, such research is still limited in Indonesia. Thus, this research aims to study the temperature characteristic and self-healing ability using steel fibers as a conductor material with a mixture of aggregates and asphalt commonly used in Indonesia.

1.2 Self-healing Mechanism in Pavement Mixtures

Increasing the temperature of mastic asphalt and asphalt concrete can increase the healing rate [2, 3]. Further innovations have been developed to reduce viscosity by several methods, such as heating the material by induction and microwaves [4, 5], infrared radiation [6], or by releasing the microencapsulates into the cracks [7, 8].

Various materials are used as heat conductors, such as carbon-based fibers and nanofibers [9], conductive modified bitumen [10] and metal particles of waste or commercial origin [11].

Internal pores and crack structure are the main factors in understanding service life extension in hot mix asphalt in thermal mixtures [12]. Further research was

conducted to explore variables that could affect the healing ability of asphalt mixtures, such as heating characteristics, induced heating efficiency [13], mixing and aging [14] and bitumen type [11].

1.3 Self-healing Process with Various Heating Methods

The induction heating method to speed up the asphalt recovery process requires a conductive material to be exposed to electromagnetic waves in the form of Kilohertz. This condition will induce an electric current into the conductive material so that the temperature increases. The heat energy from the conductive materials diffuses into the asphalt mixture so that the asphalt temperature increases. This technique can restore cracked samples to up to 80% of their initial strength [3].

The second method to increase the temperature of the asphalt mixture is by exposure to electromagnetic waves in the form of Megahertz generated by microwave. Microwave heating will affect the moisture and asphalt in the mixture by causing internal friction to increase the temperature. If there are conductive particles in it, then microwave radiation can accelerate the temperature of the mixture. This technique has the potential to be further developed [15].

2 Research Method

2.1 Self-healing Testing Process

The cylindrical Marshall sample is split into four semi-cylindrical samples and heated by microwave for three different heating durations: 20, 40 and 60 s. The various content of steel fiber added are 0, 0.25, 0.5, 0.75% and 1% of the total aggregate weight (1200 g), with an asphalt content of 5.5% for all mixtures. The mixture used is Asphalt Concrete-Wearing Course (AC-WC). The self-healing and testing processes are carried out as follows:

1. All samples are coded according to the steel fiber content.
2. Samples are then stored at -20 ± 2 °C (to produce uniform cracks).
3. The sample is then split into two, using a three-point bending test. The ultimate load is measured when the sample is split and recorded as F0.
4. The split samples are stored at room temperature for two hours. Then the two sides are combined and then heated for a particular duration: 20, 40 and 60 s, using a microwave. The thermal camera is used to record the temperature surface after the heating process.
5. The samples are stored again until reaching room temperature.
6. Then step two is repeated for five cycles.

7. The ultimate load that occurs in each cycle is recorded as F_a .
8. The healing ratio of the sample (Sh) is obtained by Eq. 1.

$$Sh = \frac{F_a}{F_0} \times 100\% \quad (1)$$

2.2 Temperature Sensitivity Test

A thermal camera measured the change in temperature of the sample after being heated by microwave. Measurements were carried out after three heating processes: 20, 40 and 60 s. Figure 1 shows the points for checking the temperatures using a thermal camera.

3 Results and Discussion

3.1 Temperature Characteristics of Mixtures

The average temperature from five checkpoints (Fig. 1) and the cooling times measured from the post-heating until the sample reaches room temperature (25 °C) are presented in Table 1.

Asphalt mixtures with higher steel fiber content generally achieve higher surface temperatures. However, the sample with 1% steel fiber did not get the highest surface temperature value. This was caused by poor fiber distribution in the asphalt mixture with 1% steel fiber, resulting in heating spots in certain zones. The samples with 0.75 and 0.5% steel fiber reached the highest surface temperature for a heating time of 60 s, as they presented a better fiber distribution in the asphalt mixture.

Fig. 1 Temperature checkpoints

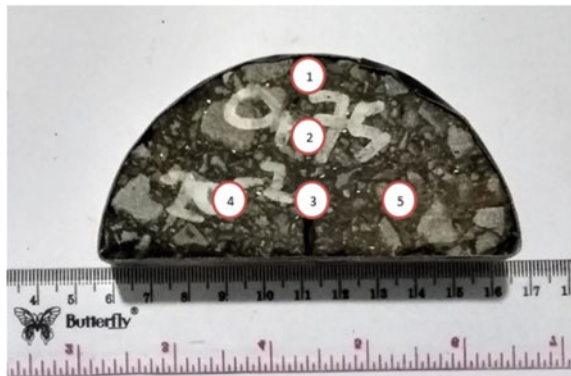


Table 1 Temperature characteristics

Steel fiber content (%)	Heating time (s)	Average surface temperature (°C)	Cooling time (min)
0	20	55.4	46
	40	82.8	53
	60	93.8	59
0.25	20	62.4	47
	40	87.5	54
	60	94.2	63
0.50	20	58.7	50
	40	89.4	63
	60	96	66
0.75	20	63.4	52
	40	96.4	65
	60	99.6	67
1	20	54.4	58
	40	86.4	71
	60	97.4	76

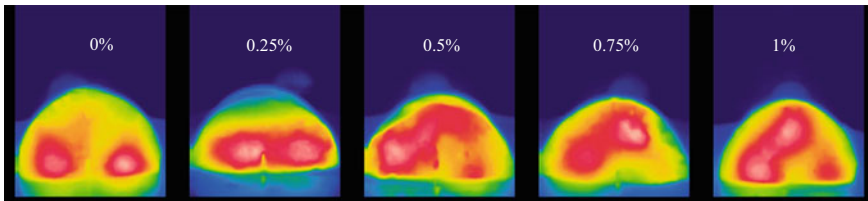


Fig. 2 Thermal camera photos after 60 s of heating

Regarding the general observable cooling results, the longest cooling time was recorded after heating times of 60 s, while the shortest cooling time was shown after 20 s of heating. This result is related to the temperature reached by the sample. Thus, the sample without steel fiber reached the lowest temperature and took a shorter time to cool, whereas the sample with high steel fiber content reached the highest surface temperature and took longer. The visual of heat distribution can also be seen in Fig. 2, where blue is the coolest and white is the hottest.

3.2 The Effect of Heating Time on the Ability to Self-healing

The results of the data obtained from self-healing tests in five cycles, with variations in the duration of heating and with various levels of steel fiber, were analyzed in the

Table 2 Healing ratio on five cycles

Steel fiber content (%)	Heating time (s)	Healing ratio on a specific cycle (%)				
		1	2	3	4	5
0	20	19.5	18.2	16.9	13.6	13.0
	40	36.5	35.9	34.8	28.2	27.1
	60	40.8	38.4	36.4	33.4	33.1
0.25	20	28.3	25.5	22.6	22.6	17.9
	40	50.3	49.7	49.2	49.2	49.2
	60	66.9	62.5	56.9	51.6	49.6
0.50	20	25.4	24.3	22.6	21.5	16.9
	40	43.3	40.9	39.6	36.6	35.4
	60	58.5	54.6	51.1	45.9	44.5
0.75	20	25.1	23.0	22.5	17.6	13.4
	40	41.4	40.2	37.3	36.1	31.4
	60	57.0	54.3	47.7	45.7	43.0
1	20	21.7	19.6	17.1	13.9	13.2
	40	38.8	38.0	35.4	28.3	27.4
	60	55.8	49.7	47.3	44.8	38.2

form of a healing ratio, namely the comparison of the strength of the test object after the healing process per cycle with the strength of the initial test. The strength of the specimens was obtained by a 3-point bending test on samples that have been conditioned at a $-20\text{ }^{\circ}\text{C}$ for ± 24 h. The healing ratios for each heating time are presented in Table 2 and Figs. 3, 4, and 5.

The cracked test sample is first heated in a microwave and then re-cracked for up to five cycles. The healing performance of the sample is defined as the three-point bending strength of the test sample after curing. It can be observed that the healing ratio decreases with increasing cycles. For example, the healing ratio with 0.25% steel fiber in 20 s heating time reaches 23.38%, the highest healing data for an average of five cycles of healing ratio. It can be seen that, in general, the rate of healing ratio is lower when the fiber percentage is higher. This is because the temperature reached by the asphalt in the steel fiber mixture is significantly higher than the temperature reached by the asphalt in the fiberless mixture, resulting in better thermal conductivity.

In addition, in the case of a heating time of 20 s, the number of cycles of the healing ratio has no significant effect on the healing rate of the sample. On the other hand, with longer heating times (40 and 60 s), it can be observed that the rate of healing ratio decreases with the increasing number of cycles. After the first and fifth cycles, each variation of the steel fiber content can be damaged due to the high temperature reached by the asphalt sample when heated for a long time. This behavior was also observed in a previous study that showed that microwave heating could change the internal structure of the asphalt mixture, causing the aggregate

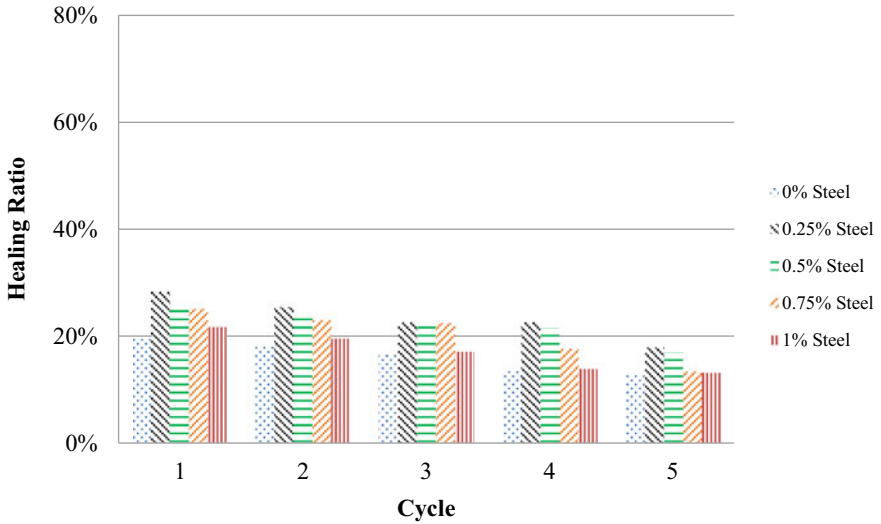


Fig. 3 Healing ratio in 20 s heating time

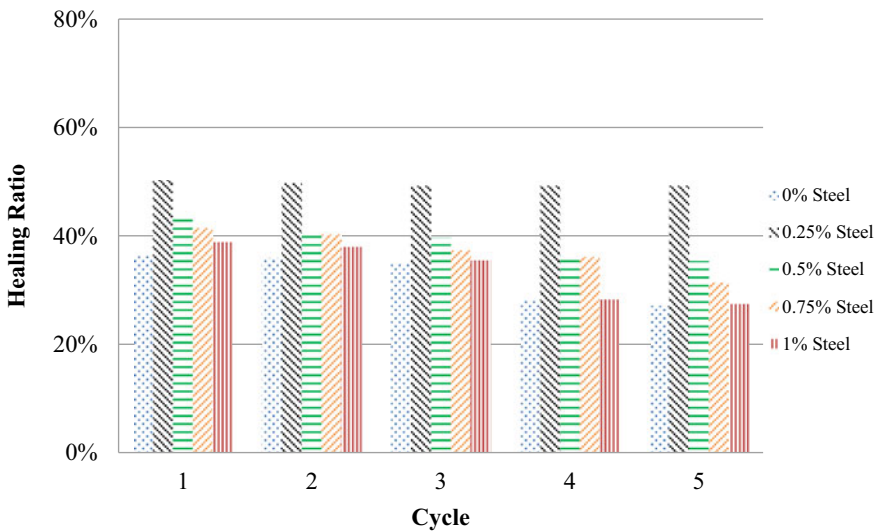


Fig. 4 Healing ratio in 40 s heating time

position in the sample to change. Moreover, the repetitive heating process can fasten the short-term aging process of asphalt mixture.

The variation of 1% steel fiber reaches the lowest healing ratio in all heating times. This happens because of the poor distribution of the steel fiber, which leads to poor heating distribution. The variation of 0.5 and 0.75% steel shows a lower and

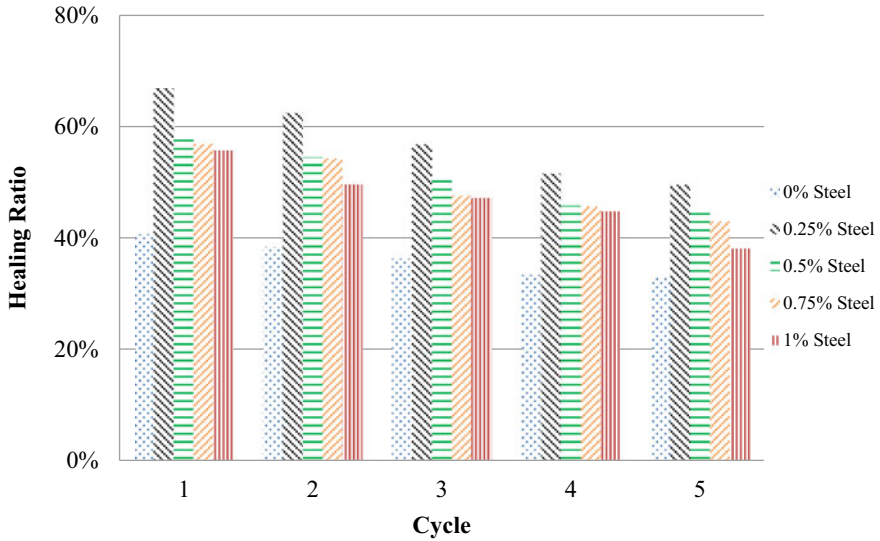


Fig. 5 Healing ratio in 60 s heating time

significant difference than the result from the variation of 0.25% steel. This happens because the higher steel fiber content leads to a very high temperature, damaging the asphalt, thus resulting in more significant strength loss. The highest healing ratio is found in the variation of 0.25% of steel fiber which is 66.9%.

The healing ratio only shows the post cracked strength compared to the initial strength. The ability of pavement to withstand traffic cannot be seen from this experiment. However, this method aims to be done on hairline cracks at the earliest stage of pavement distress that does not significantly impact structural strength. The crucial purpose of this study is to find the best maintenance method at the early stage of distress and prevent the hairline cracks from becoming a pothole.

3.3 The Visual Observation of the Self-healing Process

The observations of various cracks that are self-healed by microwave radiation, where cracks are completely closed or partially closed, show that the duration of heating in the microwave is a very influential factor in asphalt recovery. In the 20 s of heating, healing only occurred on the partial part of the sample. Meanwhile, in the 40 s and 60 s, the crack has been entirely healed to visual observation. The visuals of the cracks before and after the heating process are shown in Figs. 6, 7, and 8.

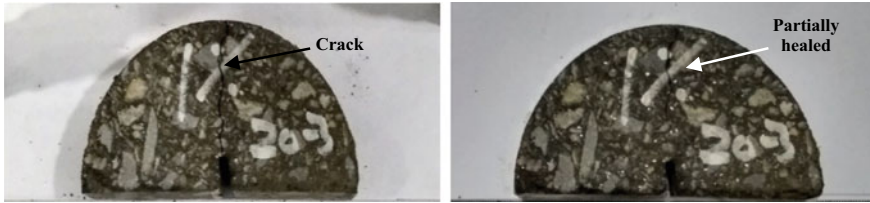


Fig. 6 Crack condition before (*black arrow*) and after (*white arrow*) 20 s of heating

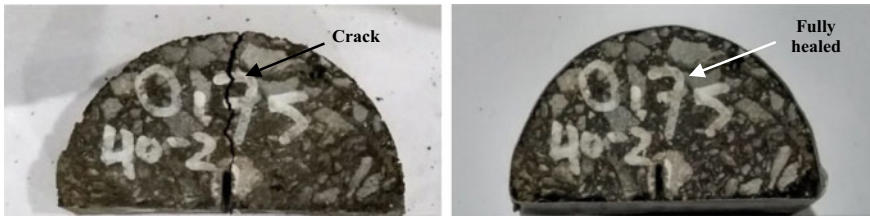


Fig. 7 Crack condition before (*black arrow*) and after (*white arrow*) 40 s of heating

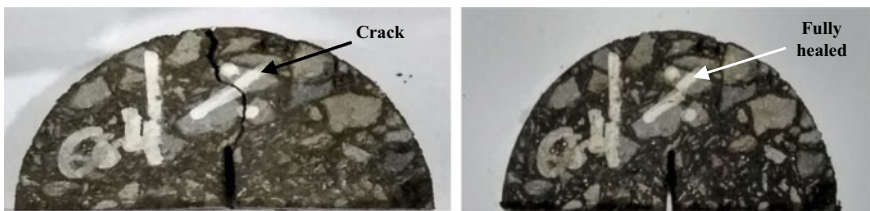


Fig. 8 Crack condition before (*black arrow*) and after (*white arrow*) 60 s of heating

4 Conclusion

1. The self-healing results show that the highest healing ratio is 0.25% steel fiber content variation. The results at the 5th cycle obtained for 20 s show a healing ratio of 17.9%, 49.2% for 40 s of heating and 49.6% for 60 s of heating.
2. 0% steel fiber content was successful in self-healing but not as good as samples with steel fibers due to the absence of additional conducting material.
3. Testing using a thermal camera showed that the maximum temperature was found in the sample with steel fibers of 0.75% in all heating times. The results obtained are 63.4 °C for 20 s of heating, 96.4 °C for 40 s of heating and 99.58 °C for 60 s of heating.
4. The percentage of healing rate decreases with the addition of steel fiber content in the AC-WC mixture.

5. On visual observation of the self-healing process, the crack is only partially closed after 20 s of heating time. In contrast, the crack is completely closed after 40 s and 60 s of heating time.

References

1. Mallick RB, Sakulich A, Chen BL, Bhowmick S (2013) Insulating pavements to extend service life. In: Kringos N, Birgisson B, Frost D, Wang L (eds) *Multi-scale modeling and characterization of infrastructure materials*. RILEM Bookseries, vol 8. Springer, Dordrecht, pp 219–236
2. García A (2012) Self-healing of open cracks in asphalt mastic. *Fuel* 93:264–272
3. García A, Bueno M, Norambuena-Contreras J, Partl MN (2013) Induction healing of dense asphalt concrete. *Constr Build Mater* 49:1–7
4. Norambuena-Contreras J, García A (2016) Self-healing of asphalt mixture by microwave and induction heating. *Mater Des* 106:404–414
5. Menozzi A, Garcia A, Partl MN, Tebaldi G, Schuetz P (2015) Induction healing of fatigue damage in asphalt test samples. *Constr Build Mater* 74:162–168
6. Ajam H, Lastra-González P, Gómez-Meijide B, Airey G, Garcia A (2017) Self-healing of dense asphalt concrete by two different approaches: electromagnetic induction and infrared radiation. *J Test Eval* 45(6):20160612
7. Tabaković A, Schuyffel L, Karač A, Schlangen E (2017) An evaluation of the efficiency of compartmented alginate fibres encapsulating a rejuvenator as an asphalt pavement healing system. *Appl Sci* 7(7):647
8. Al-Mansoori T, Norambuena-Contreras J, Garcia A (2018) Effect of capsule addition and healing temperature on the self-healing potential of asphalt mixtures. *Mater Struct* 51(2):1–12
9. Yoo DY, Kim S, Kim MJ, Kim D, Shin HO (2019) Self-healing capability of asphalt concrete with carbon-based materials. *J Market Res* 8(1):827–839
10. Pérez I, Agzenai Y, Pozuelo J, Sanz J, Baselga J, García A, Pérez V (2016) Self-healing of asphalt mixes, containing conductive modified bitumen, using microwave heating. In: *Proceedings of 6th euraspphalt & eurobitume Congress, Czech Republic, June 2016*
11. Ajam H, Gómez-Meijide B, Artamendi I, Garcia A (2018) Mechanical and healing properties of asphalt mixes reinforced with different types of waste and commercial metal particles. *J Clean Prod* 192:138–150
12. Salih S, Gómez-Meijide B, Aboufoul M, Garcia A (2018) Effect of porosity on infrared healing of fatigue damage in asphalt. *Constr Build Mater* 167:716–725
13. Liu Q, Chen C, Li B, Sun Y, Li H (2018) Heating characteristics and induced healing efficiencies of asphalt mixture via induction and microwave heating. *Materials* 11(6):913
14. Norambuena-Contreras J, Yalcin E, Garcia A, Al-Mansoori T, Yilmaz M, Hudson-Griffiths R (2018) Effect of mixing and ageing on the mechanical and self-healing properties of asphalt mixtures containing polymeric capsules. *Constr Build Mater* 175:254–266
15. Norambuena-Contreras J, Gonzales-Torre I (2017) Influence of the microwave heating time on the self-healing properties of asphalt mixtures. *Appl Sci* 7(10):1076

The Use of Gauss-Jordan Elimination Method in Determining the Proportion of Aggregate Gradation



Bagus Hario Setiadji, Supriyono, and Amelia Kusuma Indriastuti

Abstract The determination of the proportion of combined aggregate gradation is an important step in the manufacture of asphalt mixtures, so this step needs to be performed carefully. Today, the determination of the proportion of combined aggregates is mainly done by trial and error or the graphical method, which often gives inaccurate results. In this study, the determination of the combined aggregate gradation proportion was carried out using the Gauss-Jordan elimination method to find the best solution by solving a set of linear equations formed from several aggregate grading groups. This study indicated that the Gauss-Jordan method provides good guidance in determining a single unique aggregate gradation proportion. The results of the iteration of this method can also show the trend of the characteristics of the combined gradation that can improve the understanding of the aggregate gradation used.

Keywords Gauss-Jordan elimination · Aggregate gradation · Combined aggregate proportion

1 Introduction

In the manufacture of hot mix asphalt, the determination of the proportion of the combined aggregate gradation is an important process, which can determine the properties of the resulting asphalt mixture. Determination of this proportion is generally carried out analytically or graphically. Many studies have been carried out related to this method of determining proportions [1–6]. The methods used include: (i) the simplest methods, namely the trial-and-error method; (ii) mathematical methods by substitution and elimination; (iii) the use of optimization techniques

B. H. Setiadji (✉) · Supriyono · A. K. Indriastuti
Diponegoro University, Semarang, Indonesia
e-mail: bhsetiadji@ft.undip.ac.id

© The Author(s), under exclusive license to Springer Nature Singapore Pte Ltd. 2022
H. A. Lie et al. (eds.), *Proceedings of the Second International Conference of Construction, Infrastructure, and Materials*, Lecture Notes in Civil Engineering 216, https://doi.org/10.1007/978-981-16-7949-0_38

431

such as the least square method, linear and nonlinear programming; and (iv) graphical methods such as triangular or rectangular chart methods.

Each method has advantages and disadvantages, such as the trial-and-error method, which is the easiest but contains high uncertainty; the mathematical method is generally very accurate but often requires a reasonably long calculation time. In contrast, the graphical method has the advantage of being easy to work with, but the results are sometimes not accurate.

In this research, a mathematical method known as the Gauss-Jordan method is used to solve the blended aggregate problem, which is generally formulated in a set of linear equations with n unknowns. This method is one of the most accurate methods in determining the solution and is supported by the ease of operation so that the Gauss-Jordan method is expected to be widely used in determining the proportion of combined aggregates. In addition, this study also aims to evaluate the trend generated by a series of iterations of the Gauss-Jordan method on a specific aggregate gradation.

2 Gauss-Jordan Elimination Method

In determining the combined aggregate gradation, ones have two common options, i.e., using analytical methods or graphical methods. The analytical method, in the form of linear equations, generally is written Eqs. 1 and 2.

$$\sum_{i=1}^n \sum_{j=1}^n a_{ij} \cdot x_i = b_i \quad (1)$$

$$\sum_{i=j=1}^n a_{ij} = b_i \quad (2)$$

in which: a_{ij} is the i th percentage (by weight) of aggregate gradation j passing certain sieve size, x_i is the sought proportion of aggregate gradation j ; b_i is the percentage (by weight) of combined aggregate retained on certain sieve size.

The value n represents the number of unknown, i.e., the proportion of aggregate gradation used to produce target gradation that complies with the specification. To determine a single unique solution of the unknown, one has to use the number of a linear equation similar to the number of unknown. Many techniques can solve a linear system problem; one of them is the Gauss elimination method. The Gauss elimination method systematically implements elementary row operations to a linear system to convert the system to upper triangular form and then back-substitute to obtain the solution. The improved method, namely Gauss-Jordan elimination, has increased the technique's effectiveness by conducting the elementary row operations to upper and lower triangular forms simultaneously.

Coupled with the use of a computer, it could be double the speed to obtain the solution.

Adenegan and Aluko [7] briefly provided that the procedure of Gauss Jordan elimination is as follows.

1. Write the normal matrix into the augmented matrix $[A/b]$.
2. Use elementary row operation on the augmented matrix $[A/b]$ to transform A into diagonal form.
3. Divide the diagonal elements and a right-hand side's element in each row by the diagonal elements in the row, and this will make the diagonal elements equal to one.

The problem encountered if there is a zero located on the diagonal of matrix A ; then it could be switched the rows until a non-zero is in that element. If there is no possibility to find another non-zero, then stop because the system has either infinite or no solution.

The implementations of the above procedure to a 4×4 matrix are shown in Eqs. 3–7.

$$\begin{pmatrix} a_{11} & a_{12} & a_{13} & a_{14} \\ a_{21} & a_{22} & a_{23} & a_{24} \\ a_{31} & a_{32} & a_{33} & a_{34} \\ a_{41} & a_{42} & a_{43} & a_{44} \end{pmatrix} \begin{pmatrix} x_1 \\ x_2 \\ x_3 \\ x_4 \end{pmatrix} = \begin{pmatrix} b_1 \\ b_2 \\ b_3 \\ b_4 \end{pmatrix} \tag{3}$$

Step a The matrix in Eq. 3 can be written in an augmented matrix $[A/b]$ as shown in Eq. 4.

$$\left(\begin{array}{cccc|c} a_{11} & a_{12} & a_{13} & a_{14} & b_1 \\ a_{21} & a_{22} & a_{23} & a_{24} & b_2 \\ a_{31} & a_{32} & a_{33} & a_{34} & b_3 \\ a_{41} & a_{42} & a_{43} & a_{44} & b_4 \end{array} \right) \tag{4}$$

Step b Use the elementary row operation on the matrix $[A/b]$ to make the diagonal of the matrix equals to one. To do so, eliminate x_1 from the 2nd, 3rd, and 4th row by subtracting the element on that row with the multiplication of the element x_1 from the 1st row and the following ratio $m_{21} = a_{21}/a_{11}$, $m_{31} = a_{31}/a_{11}$, and $m_{41} = a_{41}/a_{11}$, respectively (Eq. 5).

$$\left(\begin{array}{cccc|c} a_{11} & a_{12} & a_{13} & a_{14} & b_1 \\ 0 & a_{22}^{(2)} & a_{23}^{(2)} & a_{24}^{(2)} & b_2^{(2)} \\ 0 & a_{32}^{(2)} & a_{33}^{(2)} & a_{34}^{(2)} & b_3^{(2)} \\ 0 & a_{42}^{(2)} & a_{43}^{(2)} & a_{44}^{(2)} & b_4^{(2)} \end{array} \right) \tag{5}$$

in which: $a_{22}^{(2)} = a_{22} - a_{12} \cdot m_{21}$; $b_2^{(2)} = b_2 - b_1 \cdot m_{21}$; the other elements follow similar calculation pattern.

The subsequent elimination is for x_2 , especially on the first, third, and fourth rows by subtracting the element on that rows with the multiplication of the element x_2 from the 2nd row and the ratio $m_{12} = a_{12}/a_{22}$, $m_{32} = a_{32}/a_{22}$, and $m_{42} = a_{42}/a_{22}$, respectively (Eq. 6).

$$\left(\begin{array}{cccc|c} a_{11}^{(3)} & 0 & a_{13}^{(3)} & a_{14}^{(3)} & b_1^{(3)} \\ 0 & a_{22}^{(2)} & a_{23}^{(2)} & a_{24}^{(2)} & b_2^{(2)} \\ 0 & 0 & a_{33}^{(3)} & a_{34}^{(3)} & b_3^{(3)} \\ 0 & 0 & a_{43}^{(3)} & a_{44}^{(3)} & b_4^{(3)} \end{array} \right) \tag{6}$$

where $a_{33}^{(3)} = a_{33}^{(2)} - a_{23} \cdot m_{32}$; $b_1^{(3)} = b_1 - b_2^{(2)} \cdot m_{12}$; the others follow similar calculation pattern.

Repeat this elimination procedure until only the diagonal elements of A contains non-zero elements.

Step c Divide the non-zero elements and the corresponding b element on each row with the diagonal element on that row (Eq. 7).

$$\left(\begin{array}{cccc|c} 1 & 0 & 0 & 0 & b_1/a_{11} \\ 0 & 1 & 0 & 0 & b_2/a_{22} \\ 0 & 0 & 1 & 0 & b_3/a_{33} \\ 0 & 0 & 0 & 1 & b_4/a_{44} \end{array} \right) \tag{7}$$

3 Research Methodology

The methodology of this work can be summarized into four steps as follows.

1. Preparing and testing the aggregate properties
 Four groups of aggregate, i.e., two coarse-aggregates and two fine-aggregates, were collected from a local quarry, and they were tested to determine the properties before they were sieved to know the gradation. The properties of the aggregate were tested based on the Indonesian National Standard (SNI) and the results obtained have to comply with the specification of Directorate General of Highways year 2018 version 2 [8].
2. Sieving the aggregate materials
 Once the properties of the aggregates can fulfill the specification, the aggregates were prepared for sieving. In this work, the aggregate was assumed to be used for asphalt mixture AC-WC (asphalt cours—wearing course). Each group of aggregates was a sieve, and the result was checked against the specification of Directorate General of Highways year 2018 version 2 [8].

3. Conducting analysis using Gauss-Jordan elimination method

Four aggregate gradations were blended to obtain the target gradation; therefore, four unknowns were to be solved, i.e., x_1 to x_4 . According to Eqs. 1 and 2, three equations were selected based on Eq. 1, and the last equation adopted Eq. 2. There were nine sieve sizes, and three sieve sizes were used in each Gauss-Jordan elimination iteration; therefore, by using the combination formula, there were 84 Gauss-Jordan elimination iterations.

4. Evaluating the results

The analysis results were evaluated by considering whether the target gradation can be achieved for each aggregate proportion produced and the trend of the combined gradation against the specification used.

4 Results and Analysis

The aggregate is required to be tested first to ensure that the aggregate can be used for the next step. As mentioned in Sect. 3, there were four groups of aggregate, i.e., two of them were coarse aggregate (Grad-A and Grad-B), and the rest were fine aggregate (Grad-C and Grad-D). The results of the property test are shown in Table 1.

Table 1 shows that all aggregate properties could fulfill the specification used, the Specification of Directorate General of Highways Year 2018 ver. 2 [8]. It means that both coarse and fine aggregates can be used for the next test, i.e., sieve test.

The asphalt mixture used in this study, i.e., asphalt concrete—wearing course (AC-WC), is a mixture with a dense-graded aggregate gradation. It requires ten

Table 1 Results of the property tests of the aggregate

Types of aggregate	Property of aggregate	Results	Specification
Coarse aggregate	Los Angeles abrasion value	14.59	Min. 40%
	Bulk specific gravity of aggregate of Grad-A	2.667	Min. 2.5
	Bulk specific gravity of aggregate of Grad-B	2.634	Min. 2.5
	Absorption of aggregate of Grad-A	1.209	Max. 3%
	Absorption of aggregate of Grad-B	1.406	Max. 3%
Fine aggregate	Bulk specific gravity of aggregate of Grad-C	2.611	Min. 2.5
	Bulk specific gravity of aggregate of Grad-D	2.617	Min. 2.5
	Absorption of aggregate of Grad-C	1.922	Max. 3%
	Absorption of aggregate of Grad-D	1.096	Max. 3%

Table 2 Different aggregate gradations were used in this study

Sieve sizes		Percentage of passing sieve size				
No.	mm	Grad-A	Grad-B	Grad-C	Grad-D	Spec
¾"	19	100	100	100	100	100
½"	12.5	28.71	100	100	100	90–100
3/8"	9.5	3.35	90.36	100	100	77–90
4	4.75	0.76	23.94	100	100	53–69
8	2.36	0.56	3.70	82.80	90.23	33–53
16	1.18	0.48	2.10	55.34	74.31	21–40
30	0.6	0.44	1.79	34.68	55.10	14–30
50	0.3	0.41	1.62	24.08	36.23	9–22
100	0.15	0.33	1.23	11.94	20.28	6–15
200	0.075	0.24	0.84	6.72	6.00	4–9

aggregate sieve sizes with the maximum aggregate size is no. ¾" (or the nominal maximum aggregate size/NMAS is ½"). The results of the sieve test for four groups of aggregates (Grad-A to Grad-D) are depicted in Table 2.

Table 2 shows that none of the groups of aggregate could fulfill the specification. It is indicated that a blend of that four gradations was required to obtain the target gradation that complies with the specification. It is possible to determine the proportion of the four gradations by using the trial-and-error method, but for a particular case, it is not easy to find the exact solution and is also time-consuming.

In this work, the Gauss-Jordan elimination method is proposed. The work only needs simple software such as an Excel spreadsheet. It has to be admitted that this method required much work in the beginning. It included: (i) developing the template of the calculation of the Gauss-Jordan method using Eqs. 4–7. It needed three linear equations of Eq. 1 selected in a systematic way among nine possible percentages of aggregate passing certain sieve size (Table 2) and one another equation of Eq. 2; (ii) calculating the combined gradation using the proportion x_i produced by point (i); and (iii) checking whether the target gradation is achieved by examining the percentage of aggregate passing of each sieve size against the specification. It is beneficial if all calculation cells in the spreadsheet are linked to the master table (see Table 2) because the proportion calculation will be conducted directly if there is an update on the master table in the future.

As mentioned in Sect. 3, Gauss-Jordan elimination was iterated as many as 84 times in this work to enable checking the possibility of the combination of three among nine aggregate sieve sizes to produce a correct proportion. The selection of three aggregate sizes to form a combination was conducted systematically to make it easier for the analysis. A result indicated a criterion of a correct proportion that

none of the proportions was less than zero and more than 1. Among all possible combinations of aggregate sieve sizes in this work, only 15 combined gradations can produce correct proportions. Together with some incorrect proportions (i.e., negative proportions and proportion more than 1, indicated by bold letters), some of them were selected randomly and presented in Tables 3 and 4. In Tables 3 and 4, all proportion is denoted in percentage unit.

The combined gradation (stated as CGrad) in Tables 3 and 4 are divided into two parts: the combined gradation with correct proportions (CGrad-4 to CGrad-7) and the rest are the combined gradation with incorrect proportions (CGrad-1 to CGrad-3, and CGrad-8 to CGrad-10). The CGrads on the left of the table are the ones with the most combinations of coarse aggregate; the CGrads on the right of the table are the ones with the most combinations of fine aggregates. The combined gradation with correct proportions generally has a relative balance of a combination of coarse and fine aggregates.

Beside correct proportions, the target gradations have to produce a good result, i.e., it could fulfill the specification. Unfortunately, as seen in the tables, none of the combined gradation can produce good results. The four gradations with correct proportions (CGrad-4 to CGrad-7) in the table are the ones that has less deviation against the specification.

It is not too surprising to know this result because all combined gradations obtained in this work are only a small part of a substantial possible combination that could be produced by using the analytical method. It means that Gauss-Jordan

Table 3 The five combined gradations were used firstly in this study

Sieve No.	Percentage passing sieve size					Specification
	CGrad-1	CGrad-2	CGrad-3	CGrad-4	CGrad-5	
	$x_1 = 7$	$x_1 = 7$	$x_1 = 7$	$x_1 = 7$	$x_1 = 7$	
	$x_2 = 101$	$x_2 = 101$	$x_2 = 42$	$x_2 = 42$	$x_2 = 44$	
	$x_3 = -623$	$x_3 = -120$	$x_3 = 60$	$x_3 = 33$	$x_3 = 35$	
$x_4 = 616$	$x_4 = 112$	$x_4 = -10$	$x_4 = 18$	$x_4 = 14$		
3/4"	100.0	100.0	100.0	100.0	100.0	100
1/2"	95.0	95.0	95.0	95.0	95.0	90-100
3/8"	83.5	83.5	89.2	89.2	88.9	77-90
4	16.3	16.3	61.0	61.0	59.3	53-69
8	43.0	5.6	43.0	45.0	43.0	33-53
16	114.6	19.1	27.2	32.4	30.5	21-40
30	124.8	22.0	16.5	22.0	20.5	14-30
50	74.6	13.4	11.8	15.1	14.1	9-22
100	51.7	9.7	5.8	8.1	7.5	6-15
200	-4.1	-0.5	3.9	3.7	3.6	4-9

CGrad-1, CGrad-2, CGrad-3, CGrad-4, and CGrad-5 were determined using all gradation with sieve no. 1/2", 3/8", no. 8; 1/2", 3/8", no. 30; 1/2", no. 4, no. 8; 1/2", no. 4, no. 30; and 1/2", no. 8, no. 16, respectively

Table 4 The other combined gradations were used in this study

Sieve No.	Percentage passing sieve size					Specification
	CGrad-6	CGrad-7	CGrad-8	CGrad-9	CGrad-10	
	$x_1 = 14$	$x_1 = 13$	$x_1 = -4$	$x_1 = -37$	$x_1 = -196$	
	$x_2 = 33$	$x_2 = 45$	$x_2 = 57$	$x_2 = 99$	$x_2 = 256$	
	$x_3 = 51$	$x_3 = 11$	$x_3 = 25$	$x_3 = -4$	$x_3 = 19$	
$x_4 = 2$	$x_4 = 31$	$x_4 = 22$	$x_4 = 41$	$x_4 = 21$		
3/4"	100.0	100.0	100.0	100.0	100.0	100
1/2"	90.2	91.0	103.1	126.1	239.9	90–100
3/8"	83.5	83.5	98.7	125.8	264.9	77–90
4	61.0	53.4	61.0	61.0	99.8	53–69
8	45.3	39.3	43.0	37.6	43.0	33–53
16	30.5	30.5	31.6	30.5	30.5	21–40
30	19.5	22.0	22.0	23.0	21.8	14–30
50	13.6	14.8	15.0	15.5	15.5	9–22
100	7.0	8.3	8.2	9.0	9.0	6–15
200	3.9	3.0	3.5	3.0	4.2	4–9

CGrad-6, CGrad-7, CGrad-8, CGrad-9, and CGrad-10 were determined using all gradation with sieve no. and 3/8", no. 4, no. 16; 3/8", no. 16, no. 30; no. 4, no. 8, no. 30; no. 4, no. 16, no. 50; and no. 4, no. 16, no. 50, respectively

elimination is only a method that assists ones in indicating correct proportions. If the proportion(s) cannot produce the target gradation that fulfills the specification, an adjustment has to be conducted by changing the proportion slightly based on the combined gradation obtained. For example, CGrad-6 is the best combined gradation produced by Gauss-Jordan in this study, although the gradation cannot produce a good result. By changing x_1 from 14 to 12%, and x_3 from 51 to 53% while the rest

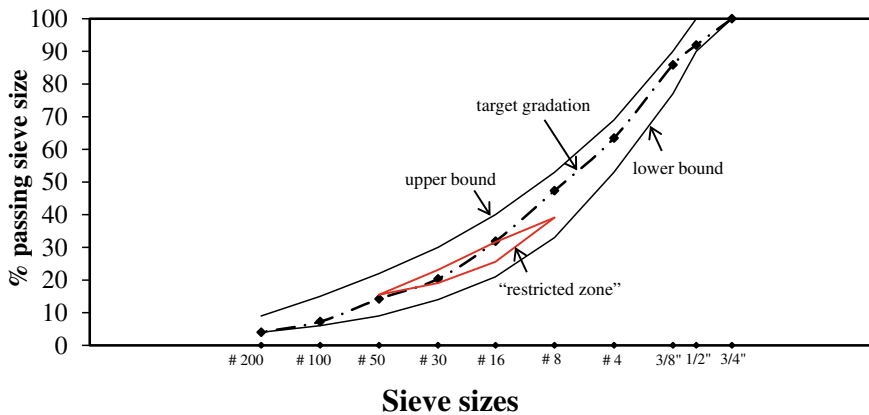


Fig. 1 Plotting of the selected combined gradation against the specification

remains the same, all combined gradation now can fulfill the specification. Further examination can be carried out by plotting the combined gradation produced using correct proportions against the specification (see Fig. 1).

Although “restricted zone” (the area with the red line in Fig. 1) is omitted in Indonesian specification, the knowledge of this area is useful to help one in determining a better aggregate gradation. According to Al-Khateeb et al. [9], the crossover-through-restricted-zone curve (the target gradation in Fig. 1) could be more susceptible to permanent deformation (rutting). A below-restricted-zone curve is preferable to provide sufficient voids for a more long-lasting asphalt mixture.

In addition, using many iterations of Gauss-Jordan, one also can analyze the trend produced. For example, it is more challenging to obtain target gradation with the percentage of coarse aggregate higher than that of fine aggregate. The combined gradation with higher coarse aggregate proportions or $x_1 + x_2 > x_3 + x_4$ (i.e., CGrad-5 and CGrad-7) has a lower percentage passing sieve no. 200 than those of gradation with higher fine aggregates (i.e., CGrad-4 and CGrad-6).

5 Conclusions

This paper presented a systematical method, i.e., Gauss-Jordan elimination, to determine the proportion of aggregate gradation mathematically. To do so, a dense graded aggregate gradation consisted of four groups of aggregate was used in this study. Eighty-four iteration was conducted by systematically selecting three of nine possible aggregate sieve sizes plus one proportion summation to produce four linear equation systems that will be solved using Gauss-Jordan elimination. The results indicated that the Gauss-Jordan method could produce many benefits in solving the blended aggregate problems. Although this method did not always produce a good result that complies with the specification, the solution obtained can still be used as guidance to determine a single unique solution of the aggregate proportion. In addition, the iteration of the method may also show the trend of the characteristics of the combined gradation that can improve the understanding of the aggregate gradation used.

References

1. Popovics S (1973) Methods for the determination of required blending proportions for aggregates. Highway Res Rec 441:65–75
2. Lee DY (1973) Review of aggregate blending techniques. In: Proceedings of 52nd annual meeting of the highway research board, Washington District of Columbia, p 111–127
3. Fadhil TH (2015) Selecting the optimum graphical method to find aggregate blend proportions in the production of HMA. Eng Technol J 33(7):1636–1655
4. Sarsam SI (2015) Modelling asphalt concrete mix design using least square optimization. Int J Math Comput Sci 1(1):1–4

5. Ramu P, Sarika P, Kumar VP, Sravana P (2016) Analytical method for asphalt concrete job mix formula design. *Int Res J Eng Technol* 3(10):927–932
6. Singh P, Walia GS (2014) Review of optimization methods for aggregate blending. *Int J Adv Res Civil, Struct Environ Infra Eng Dev* 1(3):1–9
7. Adenegan KE, Aluko TM (2012) Gauss and gauss jordan-elimination methods for solving system of linear equations: comparisons and applications. *J Sci Sci Educ, Ondo* 3(1):97–105
8. Badan Pengurus Jalan Tol (2000) Spesifikasi badan pengurus jalan tol revisi tahun 2018. Kementerian Pekerjaan Umum, Jakarta
9. Al-Khateeb GG, Ghuzlan KA, Al-Barqawi MO (2017) Effect of superpave restricted zone on volumetric and compaction properties of asphalt mixtures. *Int J Pavement Res Technol* 10 (6):488–496

Conceptual System Model Dynamic OSH Performance Improvement of Building Construction Projects



Feri Harianto, Nadjadji Anwar, I Putu Artama Wiguna,
and Erma Suryani

Abstract In Indonesia, construction projects have a high risk of work accidents. The human factor is the cause of work accidents. For example, most workers have low safety awareness. Therefore, the workforce has a significant role in reducing the risk of work accidents. This study aims to build a conceptual model for improving the performance of Occupational Safety and Health (OSH) building construction projects based on behavior and understanding of workplace safety. This research method uses a dynamic system, choosing a dynamic system because this method can explain complex systems over time, time delays and looping between variables. OSH behavior, understanding and performance variables form the dynamic system model to improve OSH performance. Concept scenarios for developing a dynamic system model are financial incentives, OSH training and patrol frequency. This research was conducted in a high-rise building construction project in Surabaya. The results of this study are the dynamic system modeling for improving safety performance into a sub-model of understanding construction OSH, sub-model of building OSH behavior and sub-model of building OSH performance. Meanwhile, the scenario for improving OSH performance is providing financial incentives, training and increasing the frequency of safety patrols.

Keywords Training · Behavior · Performance · Occupational safety

F. Harianto (✉) · N. Anwar · I. P. A. Wiguna
Department of Civil Engineering, Faculty of Civil, Planning, and Geo Engineering, Institut
Teknologi Sepuluh Nopember, Surabaya, Indonesia
e-mail: feriharianto69@gmail.com

I. P. A. Wiguna
e-mail: artama@ce.its.ac

E. Suryani
Department of Information Systems, Faculty of Intelligent Electrical and Informatics
Technology, Institut Teknologi Sepuluh Nopember, Surabaya, Indonesia
e-mail: erma@is.its.ac.id

1 Introduction

Limited time for construction projects, workers experience physical and psychological pressure in carrying out their work, so that workers tend to show unsafe behavior at work [1, 2]. In addition, many company leaders are still oriented towards productivity targets. And short-term financial performance so that safety and health efforts are neglected so that the company is inconsistent in implementing an occupational safety and health management system. Therefore, the implementation of a construction project has a very high risk of work accidents [3–6].

Unsafe behavior and conditions are the root causes of accidents. The cause of accidents is 88% due to dangerous behavior, 10% hazardous conditions and 2% could not be prevented [7]. Most of the construction workers in Indonesia have low awareness and knowledge of work safety. Poor OSH communication in the work environment, such as the number of work accidents due to a lack of good OSH communication and reporting of work accidents to the company [8]. Behavior-based work safety is effective in preventing accidents [9, 10].

Occupational Safety and Health (OSH) training for construction projects enhances workers' knowledge. An effective OSH training program is an essential part of the OSH management system [11]. The impact of OSH training is to improve the performance of OSH construction projects and reduce the rate of work accidents [12–15]. An effective work safety program can minimize occupational accidents [16].

Worker's behavior is the most significant cause of work accidents, so worker behavior is the primary variable shaping the OSH performance improvement model [17]. The understanding of occupational safety and health can shape worker safety behavior. Occupational safety and health can be realized through OSH training, OSH patrols, and providing OSH financial incentives [18]. This study aims to develop a workplace safety performance model using a dynamic system to reduce workplace accidents.

2 Literature Review

2.1 *Dynamic System Models*

The model shows a representation in a real-life system that focuses on the problem with a particular formal language. Model development usually uses basic principles, including the validity of the model is then tested with sample data to produce a valid model. Simulation is the process of designing a model of a real system followed by the implementation of experiments on the model to study behavior [19]. The variables in the dynamic system model consist of level, rate, and auxiliary. The level variable is the accumulation of flow over time and the rate variable is the rate that determines the incoming or outgoing flow, while the auxiliary is an

auxiliary variable that simplifies the relationship between variables. In addition to variables, there are parameters and constants. Parameters are inputs for rate and auxiliary; parameters have fixed values at certain times but can change at other times. In comparison, the constant has a fixed value throughout the simulation period.

2.2 Occupational Safety Behavior

Attitude is a reaction of someone who is still closed to an object or stimulus. A person's attitude is a tendency to do certain behaviors [20]. The foreman's leadership influences workers' OSH attitude, punishment in reprimands, salary cuts, and dismissal [7, 21]. Dangerous behavior is synonymous with harmful behavior. The opposite of risky behavior is safety behavior. Dangerous work behavior such as:

- Do not use personal protective equipment,
- Lack of communication between friends and leaders,
- Using the equipment not according to the procedure,
- Joking at work,
- Not concentrating on work,
- Not obeying safety signs,
- Do not interfere with the operation of dangerous equipment. In principle, risky behavior encourages the risk of work accidents [22].

The OSH understanding variables and safety behavior variables OSH can form the concept of modeling OSH performance improvement. The knowledge of OSH through training shows a significant relationship with project safety performance [18]. The comfort of space influence to process of OSH training [23]. Understanding through occupational safety training can improve work safety behavior [24]. Improving work safety performance can be achieved by focusing on unsafe behavior at construction sites [17]. Meanwhile, OSH performance measures depend on the number of work accidents, the number of sick workers and the number of workdays lost.

3 Research Methodology

Dynamic systems modeling begins with building a system conceptualization based on the research problem. To conceptualize the system, then define the boundaries of the system. After that, make a causal pie chart. In making a stock-flow diagram based on the causal loop diagram, a validated structural model. After the conceptualization of the system is formed, then formulate a model, then perform a model

Table 1 The OSH performance model variable

Internal variable	External variable	References
Comfort space	Room temperature, space area, light, wall color	[23, 25]
Understanding OSH	Level of education, training duration, easy of transfer course material	[3, 26]
Worker characteristics	Age, level of education, length of working	[3, 27, 28]
OSH commitment	OSH posters, safety infrastructure, first aid, OSH regulation	[29, 30]
Patrol frequency	The attitude of OSH workers	[31, 32]
Infrastructure structure		[33]
Punishment		[7]
Using of PPE		[29]
Using an id card		[31]
Standard operating procedure		[29]
OSH communication		[34]
Responsive to occupational safety		[31]
Safety leadership foreman		[35]
Government OSH regulation		[32]

simulation. The simulation model has good validity if the error rate is less than 5% and the variation error is less than 30%.

Human OSH behavior and understanding improve OSH performance [17, 18]. The basis for compiling the variable understanding of OSH and OSH safety behavior is shown in Table 1.

4 Analysis and Discussion

Figure 1 shows sub-model 1 the causal loop diagram of occupational safety understanding, the understanding of OSH training participants influenced by the comfort of space, level of education, duration or length of training and the ease or clarity of the delivery of OSH training materials [3, 17, 26]. Room comfort influence by wall color, light, space area and room temperature or temperature [23, 25].

Figure 2 shows sub-model 2 the causal loop diagram of occupational safety behavior, describes four balancing conditions, namely B1, B2, B3, and B4. The B3 balancing condition shows that punishment (warning, payroll deduction, dismissal) increases workers' work following the SOP. In contrast, workers who work in harmony with SOP reduce penalties [21, 36]. The condition for balancing B4 shows

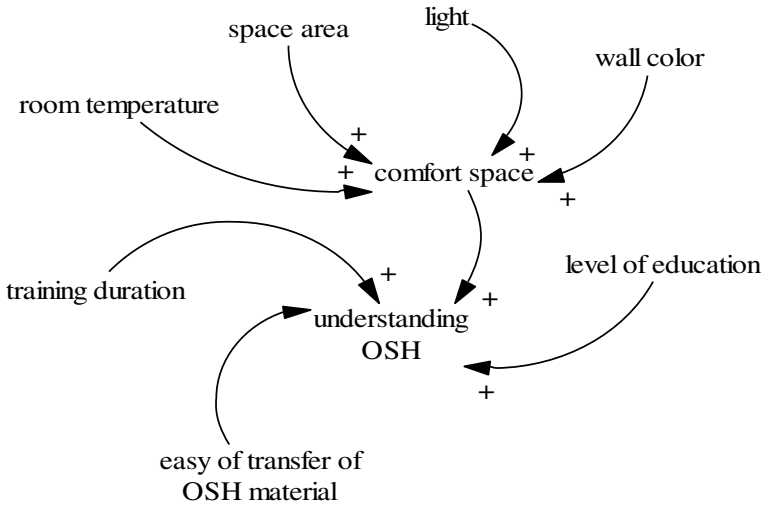


Fig. 1 Sub-model 1 the causal loop diagram of occupational safety understanding

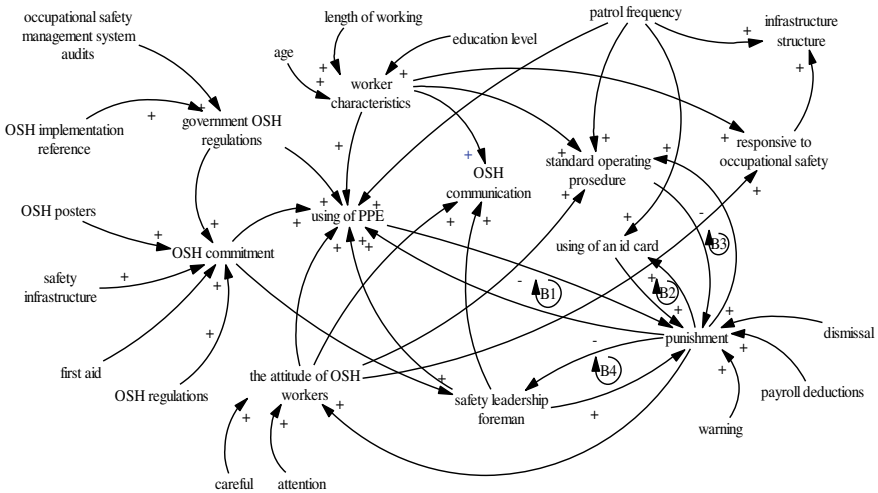


Fig. 2 Sub-model 2 the causal loop diagram of occupational safety behavior

that the foreman’s safety leadership actively decreases the worker’s punishment, while the worker’s sentence makes the foreman’s safety leadership work actively [37]. The conditions for balancing B2 and B1 show that punishment makes workers disciplined in identity cards. The use of PPE, in contrast to the use of identity cards and PPE in a disciplined manner, reduces the form of punishment [19, 36].

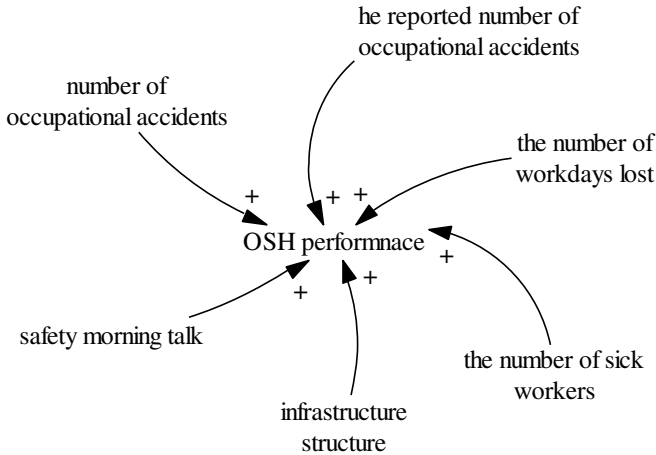


Fig. 3 Sub-model 3 the causal loop diagram of occupational safety performance

Figure 3 shows sub-model 3 the causal loop diagram of the occupational safety performance sub-model measure by the number of reported work accidents, the number of work accidents, the number of sick workers and the number of lost workdays. The OSH performance of a building construction project is influence by the safety morning talk and infrastructure structures.

The dynamic system modeling scenario to improve the safety and health performance of the building construction project proposed in this study is the parameter and structural scenario. The proposed parameter scenario is patrol frequency [38, 39]. At the same time, the structural scheme proposed in this study is the provision of incentives and OSH training [13, 40].

5 Conclusion

Behavioral variables and an understanding of worker safety can form a model for improving OSH performance in construction project implementation. OSH training can provide a sense of work safety. To improve safety performance in this modeling scenario, provide financial incentives, training and increase the frequency of safety patrols. With good understanding and safety behavior, it can minimize workplace accidents.

References

1. Bronkhorst B (2015) Behaving safely under pressure: the effects of job demands, resources, and safety climate on employee physical and psychosocial safety behavior. *J Safety Res* 55:63–72
2. Poon SW, Rowlinson SM, Koh T, Deng Y (2013) Job burnout and safety performance in the Hongkong construction industry. *Int J Constr Manage* 13(1):69–78
3. Zhou Q, Fang D, Wang X (2008) A method to identify strategies for the improvement of human safety behavior by considering safety climate and personal experience. *Saf Sci* 46(10):1406–1419
4. Mouleeswaran K (2014) Evaluation of safety performance level of construction firms in ABD around Erode zone. *Int J Inno Res Sci Eng Technol* 3(1):1586–1594
5. Andolfo C, Sadeghpour F (2015) A probabilistic accident prediction model for construction sites. *J Proc Eng* 123:15–23
6. Zahoor H, Chan AP, Gao R, Utama WP (2017) The factors contributing to construction accidents in Pakistan: their prioritization using the delphi technique. *Eng Constr Archit Manag* 24(3):463–485
7. Guo BH, Goh YM, Wong KL (2018) A system dynamics view of a behavior-based safety program in the construction industry. *J Safety Res* 104:73–81
8. Ramli S (2009) *Sistem Manajemen Keselamatan dan Kesehatan Kerja OHSAS 18001* Dian Rakyat, Jakarta
9. Chen D, Tian H (2012) Behavior-based safety for accidents prevention and positive study in China construction project. *J Proc Eng* 43:528–534
10. Choudhry RM (2014) Behavior-based safety on construction sites: a case study. *Accid Anal Prev* 70:14–23
11. Demirkesen S, Arditi D (2015) Construction safety personnel's perceptions of safety training practices. *Int J Project Manage* 33(5):1160–1169
12. Bahn S, Barratt-Pugh L (2014) Safety training evaluation: the case of construction induction training and the impact on work-related injuries in the Western Australian construction sector. *Int J Training Res* 12(2):148–157
13. Başağa HB, Temel BA, Atasoy M, Yıldırım İ (2018) A Study on the effectiveness of occupational health and safety training of construction workers in Turkey. *Saf Sci* 110:344–354
14. Jafari MJ, Gharari M, Kalantari S, Omidi L, Asadolah Fardi G (2014) The influence of safety training on safety climate factors in a construction site. *Int J Occup Hygiene* 6(2):81–87
15. Okoye PU, Okolie KC (2014) Exploratory study of the cost of health and safety performance of building contractors in South-East Nigeria British. *J Environ Sci* 2(1):21–33
16. Chen Q, Jin R (2012) Safety site commitment to enhance jobsite safety management and performance. *J Constr Eng Manag* 138(4):509–519
17. Wu X, Liu Q, Zhang L, Skibniewski MJ, Wang Y (2015) Prospective safety performance evaluation on construction sites. *Accid Anal Prev* 78:58–72
18. Jazayeri E, Liu H, Dadi GB (2018) Creating a safety training and competence model for construction craft professionals. In Conference: construction congress 2018 ASCE
19. Suryani E (2006) *Pemodelan Simulasi*. Graha Ilmu, Yogyakarta
20. Wawan A, Dewi M (2010) *Teori dan Pengukuran Pengetahuan, sikap, dan Perilaku Manusia*. Nuha Medika, Yogyakarta
21. Trevino LK, Ball GA (1992) The social implications of punishment unethical behavior: observers' cognitive and affective reactions. *J Manag* 18(4):751–768
22. Winarsunu T (2008) *Psikologi Keselamatan Kerja UMM*, Malang
23. Satwiko P (2003) *Fisika Bangunan I* Andi, Yogyakarta
24. Jafari MJ, Gharari M, Ghafari M, Omidi L, Kalantari S, Asadolah-Fardi G (2014) The influence of safety training on safety climate factors in a construction site. *Int J Occup Hygiene, Iranian Occup Hygiene Asso* 6:81–87

25. Darmaprawira WAS (2002) *Warna: Teori dan Kreativitas Penggunaannya*. ITB, Bandung
26. Lawton R, Parker D (1998) Individual differences in accident liability: a review and integrative approach. *Hum Factors* 40(4):655–671
27. Wang B, Wu C, Kang L, Reniers G, Huang L (2018) Work safety in China's thirteenth five-year plan period (2016–2020): current status, new challenges, and future tasks. *Saf Sci* 104:164–178
28. Wang Y, Goodrum PM, Haas CT, Glover RW (2008) Craft training issues in American industrial and commercial construction. *J Constr Eng Manag* 134(10):795–803
29. Lingard H (2002) The effect of first aid training on Australian construction workers' occupational health and safety knowledge and motivation to avoid work-related injury or illness. *Constr Manag Econ* 20(3):263–273
30. Yahya K, Hasan AM, Ebrahim H, Narmin HR, Amir HB (2014) Structural modeling of safety performance in construction industry. *Iran J Public Health* 43(8):1099–1106
31. Zhang M, Fang D (2013) A cognitive analysis of why Chinese scaffolders do not use safety harnesses in construction. *Constr Manag Econ* 31(3):207–222
32. Yu QZ, Ding LY, Zhou C, Luo HB (2014) Analysis of factors influencing safety management for metro construction in China. *Accid Anal Prev* 68:131–138
33. Farmakis PM, Chassiakos AP (2017) Dynamic multi-objective layout planning of construction sites. *Proc Eng* 196:674–681
34. Ismail Z, Doostdar S, Harun Z (2012) Factors influencing the implementation of a safety management system for construction sites. *Saf Sci* 50(3):418–423
35. Gunawan FA (2013) *Safety leadership*. Dian Rakyat, Jakarta
36. Arvey RD, Ivancevich JM (1980) Punishment in organization: a review, propositions, and research suggestions. *Acad Manag Rev* 5(1):123–132
37. Tremblay M, Vandenberghe C, Doucet O (2013) Relationships between leader-contingent and non-contingent reward and punishment behaviors and subordinates' perceptions of justice and satisfaction, and evaluation of moderating implement of trust propensity, pay level and role ambiguity. *J Bus Psychol* 28:233–249
38. Zohar D, Luria G (2003) The use of supervisory practices as leverage to improve safety behavior: a cross-level intervention model. *J Safety Res* 34(5):567–577
39. Fang D, Jiang Z, Zhang M, Wang H (2015) An experimental method to study the effect of fatigue on construction workers' safety performance. *Saf Sci* 73:80–91
40. Alarcón LF, Acuña D, Diethelm S, Pellicer E (2016) Strategies for improving safety performance in construction firms. *Accid Anal Prev* 94:107–118

Experiment the Effect of Providing Monetary Incentives and Safety Patrols on Work Safety Behavior in Construction Project Implementation



Feri Harianto, Nadjadji Anwar, I Putu Artama Wiguna,
and Erma Suryani

Abstract The process of implementing a construction project has a high risk of work accidents. The risk of work accidents is due to the limited project implementation time, low human resources and weak work safety management system. For this reason, efforts should be made to minimize the risk of accidents. Therefore, the role of workplace safety management is essential. One form of policy in occupational safety management is patrols and the provision of financial incentives for work safety. This study aims to determine the effect of safety patrols and the provision of financial incentives on safety behavior. This research method is quasi-experimental with a 2×2 factorial design, with the respondents being workers. The number of samples is 20 respondents. Sampling using purposive sampling. The treatment of this research is the provision of financial incentives and safety patrols. The analysis in this study used a two-way ANOVA. The result of this study is that there is a significant effect between safety patrol and the provision of financial incentives (together) on work safety behavior. On the other hand, what is quite impactful is the provision of financial incentives.

Keywords Financial incentives · Safety · Monitoring · Behavior

F. Harianto (✉) · N. Anwar · I. P. A. Wiguna
Department of Civil Engineering, Faculty of Civil, Planning, and Geo Engineering,
Institut Teknologi Sepuluh Nopember, Surabaya, Indonesia
e-mail: feriharianto69@gmail.com

I. P. A. Wiguna
e-mail: artama@ce.its.ac

E. Suryani
Department of Information Systems, Faculty of Intelligent Electrical and Informatics
Technology, Institut Teknologi Sepuluh Nopember, Surabaya, Indonesia
e-mail: erma@is.its.ac.id

1 Introduction

The implementation of construction projects limited time and workers do not understand work safety and lack of OSH communication and low awareness of work safety has implications for a high risk of work accidents in construction projects [1–4]. The death rate in the construction industry is relatively high compared to other sectors. Therefore, it is necessary to make efforts to lead to zero accidents [5]. Worker safety performance dramatically affects the results of construction project safety performance [6]. The effectiveness of occupational safety supervision in construction projects is essential in influencing work safety [7, 8]. Supervisors have an important role in occupational safety management. Supervisor finances have an impact on worker safety. The financial supervisor, for example, frequently visits workplaces and safety communications [9–11]. The interactions between workers and supervisors often influence workers' safety attitudes and finances [6, 12]. Supervisory situational violations are more socially influential than routine safety violations to workers on construction projects. Workers with less work experience are more likely to commit frequent violations, besides workers with less education tend to commit situational safety violations [10].

Providing financial incentives motivates workers to behave safely [13, 14]. Providing financial incentives and rewards can most effectively reduce the rate of work accidents [15]. In the same study [16], there is a significant relationship between financial incentives and work safety performance. Based on this explanation, research on work safety behavior uses a survey method with the main parameter being worked safety management. At the same time, the main factor of work safety is primarily determined by workers' behavior. Therefore, this study uses an experimental method with safety behavior parameters with work safety supervision treatment and financial incentives. Good work safety behavior encourages the improvement of work safety performance. Therefore, this study aims to determine the effect of monitoring and financial incentives on work safety behavior in construction projects.

2 Literature Review

2.1 Occupational Safety Supervision

The effectiveness of supervision carried out by supervisors has an essential role in occupational safety management. Good safety management will undoubtedly improve safety performance [10, 11, 17]. An occupational safety program is impact control, direct cause control and root cause control. One form of direct cause control is supervision or inspection of occupational safety. Occupational safety officers carry out this activity. The essential thing in occupational safety supervision, that time it is found unsafe or non-standard conditions in the workplace,

it needs to be corrected. If the dangerous condition is high, it is necessary to carry out a risk analysis and this is to find out the root cause of the hazardous situation. It helps in improving the safety management system [18].

2.2 Providing Occupational Safety Incentives

To a large extent, human financial can become more robust when it has potential consequences. On the contrary, its weakness if human finances have adverse effects. Therefore, a good understanding is needed in managing safe behavior in the workplace [19]. Providing financial incentives and rewards to workers reduces the workplace's accident rate [9, 16]. Therefore, the provision of financial incentives for workers who behave in safety at work, for example, wearing personal protective equipment, working according to procedures, not joking while working, etc.

2.3 Occupational Safety Behavior

Attitude is a reaction of someone who is still closed to an object or stimulus—the attitude of someone who tends to do certain behaviors [20]. Behavior is a form of a person's attitude. Dangerous behavior is synonymous with harmful behavior. Human behavior that deviates from what it should be has the potential to reduce work safety. This cause occurs in the workplace due to internal and external factors. Internal factors exist in human behavior, while external factors are due outside of the action, such as work, organizational environment, equipment design and social environment [18]. Several studies show that 80–90% are caused by humans' mistakes and violations [21]. In principle, risky behavior encourages the risk of work accidents [19]. The human factor has an essential role in occupational safety. The fundamental cause of work accidents is dangerous behavior in the form of mistakes made by humans. The habit of humans behave unsafely causes them to expose to a very high risk of work accidents.

3 Research Methodology

This study used a quasi-experimental method, the research design was chosen because the control of non-experimental variables was not so strict and the sample determination was not randomized. This quasi-experiment used a 2×2 factorial design, with five people per group observed [22] so that the total number of samples as respondents was 20 people (standard error data must be normally distributed).

Sampling as respondents using purposive sampling. The respondents of this research are workers. The treatment given in this quasi-experiment provides

financial incentives [8, 13, 15, 16] and safety patrols [7, 8]. Both treatments function as independent variables, while the dependent variable is financial incentives. symbol of existing condition = 1, safety patrol = 2, financial incentive = 3 and safety patrol and financial incentive = 4. The variable that is measured is the variable of work safety behavior. Collecting data in this study using a questionnaire, the measurement scale used in the questionnaire is a Likert scale with weights 1 = not always, 2 = sometimes, 3 = almost always and 4 = always. The analysis used is two-way ANOVA. Standard error data must be normally distributed. The research location is in the terraced building construction project of Mawar Saron Church. The questionnaire lattice is as in Table 1. The criteria for assessing work safety behavior are as in Table 2. The hypothesis in this study are:

- Hypothesis 1
 - Ho: There is no difference in work safety behavior in existing conditions with the safety patrol.
 - H1: There are differences in work safety behavior in existing conditions with safety patrols.
- Hypothesis 2
 - Ho: There is no difference in safety behavior in existing conditions with the existence of financial incentives.
 - H1: There are differences in work safety behavior in existing conditions with the existence of financial incentives.
- Hypothesis 3
 - Ho: There is no difference in safety behavior in existing conditions with the interaction of safety patrols and financial incentives.

Table 1 Work safety behavior indicators

Indicator	References
Using of personal protective equipment	[23–25]
Occupational safety communication	[11, 25–27]
Using of tools according to the procedure	[25, 28]
No kidding	[25, 29]
Report unsafe situation	[11, 27]
Don't touch	[25, 29, 30]
Walking according to the specified path	[8, 30]
Concentration on work	[20, 28, 30]
Obey safety signs	[8, 29]
Don't play with work equipment	[25, 29, 30]
It doesn't interfere with the operation of dangerous tools	[25, 29, 30]

Table 2 Criteria of safety financial assessment

Size	Criteria
1.00–1.75	Not always
1.76–2.50	Sometimes
2.51–3.25	Almost always
3.26–4.00	Always

- H1: There are differences in work safety behavior in existing conditions with the interaction safety patrols and financial incentives.
- Hypothesis 4
 - Ho: There is no difference in safety behavior with safety patrols and financial incentives.
 - H1: There are differences in work safety behavior with safety patrols and financial incentives.
- Hypothesis 5
 - Ho: There is no difference in work safety behavior with safety patrol and the interaction between safety patrol and financial incentives.
 - H1: There are differences in work safety behavior with the safety patrol and the interaction between safety patrol and financial incentives.
- Hypothesis 6
 - Ho: There is no difference in safety behavior with financial incentives and safety patrol-financial incentive interactions.
 - H1: There are differences in safety behavior with financial incentives and safety patrol-financial incentive interactions.

4 Results and Discussion

In Table 3, the average variable of work safety behavior in safety patrol treatment, financial incentives and their interaction has an increasing trend. Compared to the existing conditions in the patrol safety treatment, the average is relative and the standard deviation is the same. The average of the four states is 3.103. In the homogeneity test of work safety behavior variables using Leneve’s trial, the results are as in Table 4, which explains that the safety behavior variables have similar variations (sig. 0.520 > 0.05). The normality test in Table 5 illustrates that the residual standards for safety behavior variables are normally distributed (sig. 0.637 > 0.05).

Table 6 explains that the overall experimental treatment (safety patrol, financial incentives and the interaction of both treatments) affects work safety behavior

Table 3 Descriptive of safety behavior variable

Treatment	Mean	Std. deviation	N
1	2.8160	0.12582	5
2	2.9840	0.12542	5
3	3.2600	0.08775	5
4	3.3520	0.08643	5
Total	3.1030	0.24092	20

Table 4 Homogeneity test of safety behavior variable

F	df1	df2	Sig.
0.784	3	16	0.520

Table 5 Test of normality for safety behavior

	Shapiro–Wilk		
	Statistic	df	Sig.
Standardized residual for safety behavior	0.964	20	0.637

(sig. 000 < 0.05) with the sum of squares of the model of 0.916 while the mean square is 0.305. Work safety behavior variables can be explained by the three experimental treatments of 0.799. The model courts describe the total effect of experimental treatment, while the mean square represents the average effect of experimental treatment.

In Table 7, the Tukey HSD and Bonferroni test results explain that hypothesis 1 is that there is no difference in work safety behavior in existing conditions and safety patrol treatment (sig. 0.106 > 0.05) or (sig. 0.155 > 0.05). The absence of evidence for hypothesis 1 illustrates that workers who are not self-disciplined in work safety behavior and lack supervisor support in safety patrols will increase work accidents. Therefore, worker participation in workplace safety behavior is significant [17, 31].

Table 6 Test of between-subjects effects

Source	Type III: sum of squares	df	Mean square	F	Sig
Corrected model	0.916 ^a	3	0.305	26.133	0.000
Intercept	192.572	1	192.572	16,483.816	0.000
Treatment	0.916	3	0.305	26.133	0.000
Error	0.187	16	0.012		
Total	193.675	20			
Corrected total	1.103	19			

^aR Squared = 0.831 (Adjusted R Squared = 0.799)
 Computed using alpha = 0.05

Table 7 Multiple comparisons

	(I) Treatment	(J) Treatment	Mean difference (I - J)	Std. error	Sig.
Tukey HSD	1	2	-0.1680	0.06836	0.106
		3	-0.4440*	0.06836	0.000
		4	-0.5360*	0.06836	0.000
	2	1	0.1680	0.06836	0.106
		3	-0.2760*	0.06836	0.005
		4	-0.3680*	0.06836	0.000
	3	1	0.4440*	0.06836	0.000
		2	0.2760*	0.06836	0.005
		4	-0.0920	0.06836	0.549
	4	1	0.5360*	0.06836	0.000
		2	0.0368*	0.06836	0.000
		3	0.0920	0.06836	0.549
Bonferroni	1	2	-0.1680	0.06836	0.155
		3	-0.4440*	0.06836	0.000
		4	-0.5360*	0.06836	0.000
	2	1	0.1680	0.06836	0.155
		3	-0.2760*	0.06836	0.006
		4	-0.3680*	0.06836	0.000
	3	1	0.4440*	0.06836	0.000
		2	0.2760*	0.06836	0.006
		4	-0.0920	0.06836	1.000
	4	1	0.5360*	0.06836	0.000
		2	0.3680*	0.06836	0.000
		3	0.0920	0.06836	1.000

*The mean difference is significant at the 0.05 level

Table 7 explains that hypothesis 2 and hypothesis 3 prove a substantial difference in safety behavior between existing conditions and conditions with treatment (sig. $0.00 < 0.05$). The means that the role of financial incentives and the interaction of the two experimental treatments play a role in working safety behavior for workers [14–16]. Hypothesis 4 and hypothesis 5 prove a significant difference in safety behavior in the conditions with the treatment of safety patrols and financial incentives and the interaction conditions of the two treatments ($0.00 < 0.05$). The means that the experimental treatment of providing financial incentives and the interaction of the two treatments can improve work safety behavior [10, 13]. Table 7 Tukey HSD test results (sig. $0.549 > 0.05$) and Bonferroni (sig. $1.00 > 0.05$) explained that hypothesis 6 was proven that there was no difference in safety behavior in the conditions of financial incentive treatment and the interaction between the two treatments. The overall hypothesis explains that work safety management policies in financial incentives and safety patrols need to be carried out

in construction projects to increase work safety behavior to decrease workplace accidents. The reduction in the number of work accidents will improve safety performance in construction projects [6].

5 Conclusions

Based on the results and discussion, it can be concluded that the provision of safety patrol treatment is not effective in increasing safety behavior. Still, safety patrol–financial incentives together affect increasing work safety behavior. On the other hand, the provision of financial incentive treatment impacts improving work safety behavior. The provision of financial incentives is more important than the provision of work safety patrol treatment. Policy Provision of incentives and work safety patrols need to be carried out simultaneously. Therefore, this policy requires project management support in the implementation of construction projects. So that the occurrence of work accidents can be minimized, with a minimum of work accidents, work safety performance will also increase.



References

1. Bronkhorst B (2015) Behaving safely under pressure: the effects of job demands, resources, and safety climate on employee physical and psychosocial safety financial. *J Saf Res* 55:63–72
2. Ramli S (2009) *Sistem Manajemen Keselamatan dan Kesehatan Kerja OHSAS 18001*. Dian Rakyat, Jakarta
3. Zhou Q, Fang D, Wang X (2008) A method to identify strategies for the improvement of human safety financial by considering safety climate and personal experience. *Saf Sci* 46 (10):1406–1419
4. Mouleeswaran K (2014) Evaluation of safety performance level of construction firms in ABD around Erode zone. *Int J Inno Res Sci Eng Technol* 3(1):1586–1594
5. Zaira MM, Hadikusumo BH (2017) Structural equation model of integrated safety intervention practices affecting the safety behavior of workers in the construction industry. *Saf Sci* 98:124–135
6. Lingard H, Ron W, Patrick C (2011) Development and testing of hierarchical measure of project OHS performance engineering. *Constr Arch Manage* 18(1):30–49
7. Han S, Saba F, Lee S, Mohamed Y, Peña-Mora F (2014) Toward an understanding of the impact of production pressure on safety performance in construction operations. *Accid Anal Prev* 68:106–116
8. Xia N, Griffin MA, Wang X, Liu X, Wang D (2018) Is there agreement between worker self and supervisor assessment of worker safety performance? an examination in the construction industry. *J Safety Res* 65:29–37
9. Fleming M (2001) *Effective supervisory safety leadership behaviors in the offshore oil industry* HSE, Norwich
10. Liang H, Zhang S (2019) Impact of supervisors safety violations on an individual worker within a construction crew. *J Saf Sci* 120:679–691

11. Huang YH, Sinclair RR, Lee J, McFadden AC, Cheung JH, Murphy LA (2018) Does talking the talk matter? effects of supervisor safety communication and safety climate on long-haul truckers. *Saf Perform Acci Anal Prevention* 177:357–367
12. Fang D, Jiang Z, Zhang M, Wang H (2015) An experimental method to study the effect of fatigue on construction workers' safety performance. *J Saf Sci* 73:80–91
13. Teo EA, Ling FY, Ong DS (2005) Fostering safe work financial in workers at construction sites engineering. *J Constr Arch Manage* 12(4):410–422
14. Manjula NHC, De Silva N (2014) Factors influencing safety behavior of construction workers. In: *The third world construction symposium: sustainability and development in built environment*, Colombo, 20–22 June 2014
15. Alarcón LF, Acuña D, Diethelm S, Pellicer E (2016) Strategies for improving safety performance in construction firms accident. *Anal Prevent* 94:107–118
16. Goodrum PM, Gangwar M (2004) Safety incentives: a safety of their effectiveness in construction. *Prof Saf* 49(7):24–34
17. Guo M, Liu S, Chu F, Ye L, Zhang Q (2019) Supervisory and coworker support for safety: buffers between job insecurity and safety performance of high-speed railway drivers in China. *Saf Sci* 117:290–298
18. Gunawan FA, Waluyo (2015) *Risk-based behavioral safety*. Gramedia Pustaka Utama, Jakarta
19. Winarsunu T (2008) *Psikologi Keselamatan Kerja*. UMM, Malang
20. Wawan A, Dewi M (2010) *Teori dan Pengukuran Pengetahuan, Sikap, dan Perilaku Manusia*. Nuha Medika, Yogyakarta
21. Lawton R, Parker D (1998) Individual differences in accident liability: a review and integrative approach. *J Human Factors Ergon Soc* 40:655–671
22. Alwi I (2012) Kriteria Empirik Dalam Menentukan Ukuran Sampel Pada Pengujian Hipotesis Statistika dan Analisis Butir. *Jurnal Formatif* 2(2):140–148
23. Ammad S, Alaloul WS, Saad S, Qureshi AH (2020) Personal protective equipment (PPE) usage in construction projects: a scientometric approach. *J Build Eng (JOBE)* 35:102086
24. Rafiq MC (2014) Financial-based safety on construction sites: a case study. *Accid Anal Prev* 70:14–23
25. Sawacha E, Naoum S, Fong D (1999) Factors affecting safety performance on construction sites. *Int J Project Manage* 17(5):309–315
26. Edirisinghe R, Lingard H (2016) Exploring the potential for the use of video to communicate safety information to construction workers: case studies of organizational use. *Constr Manag Econ* 34(6):366–376
27. Chen D, Tian H (2012) Financial-based safety for accidents prevention and positive study in China construction project. *J Proc Eng* 43:528–534
28. Masood R, Mujtaba B, Khan MA, Mubin S, Shafique F, Zahoor H (2014) Investigation for safety performance indicators on construction projects. *Sci Int* 47:1403–1408
29. Babajide T, Francis EF, Alistair G (2015) Behaviour based safety (BBS): a construction industry's perspective. In: *Proceedings of international health and safety conference (Belfast: Northern Ireland/EEI)*, p 181
30. Iumba R (2014) Spatial analysis of construction accidents in Kampala, Uganda. *Saf Sci* 64:109–120
31. Yanar B, Lay M, Smith PM (2019) The interplay between supervisor safety support and occupational health and safety vulnerability on work injury. *J Saf Health Work* 10(2):172–179

Development of Activity-Based Safety Plan for Precast Parapet Panel Work in Elevated Construction



Pungky Dharma Saputra , Anasya Arsita Laksmi ,
Nina Purwanti , and Muhammad Hamzah Fansuri 

Abstract One of the infrastructures being developed is the construction of railways such as MRT Jakarta. The use of precast parapet panels is still relatively new in Indonesia and it is used in MRT Jakarta. Because the installation requires lifting work, there is a very dangerous risk that the precast parapet will fall. The purpose of this research is to develop an activity-based safety plan in precast parapet panel works. The first stage was identifying safety risks by asking for expert validation, the second stage was surveying for safety risk assessment, and the last stage was surveying for safety objectives and programs by distributing questionnaires. The project sample was MRT Jakarta Contract Package (CP) 103 project. The results will be developed based on the regulation. The potential hazard is parapet panel falls with a risk rating is 15 and categorized as high-risk level. There are 5 risk controls to reduce the risk are lifting calculation, rigging and wire sling check, equipment check and audit, operator training and certification, and the last are creating, socializing, and evaluating Standard Operating Procedure (SOP). The safety plan is developed from the risk controls in the form of safety objectives and safety programs.

Keywords Safety plan · Activity · Safety risks · Precast parapet work

1 Introduction

The acceleration of infrastructure development in Indonesia shows very rapid progress. This is following government policies to accelerate infrastructure development [1]. One of the infrastructures being developed is the construction of railways that are capable of carrying out rapid mass transfers, such as the Jakarta Mass Rapid Transit (MRT) since 2013 until now [2]. The construction of the MRT

P. D. Saputra (✉) · A. A. Laksmi · N. Purwanti · M. H. Fansuri
Department of Civil Engineering, Faculty of Military Engineering, Republic of Indonesia
Defense University, Bogor, Indonesia
e-mail: ir.pungky@gmail.com

Jakarta which has been under development consists of elevated construction and underground construction [2]. The superstructure of the elevated construction that has been developed uses a precast box girder as the main beam and precast parapet panels as safety railings.

The use of precast parapet panels is still relatively new in Indonesia because only a few projects have applied it, such as the MRT Jakarta Contract Package (CP) no. 101, 102, and 103. The use of parapet precast is considered to be one of the advantages in terms of ease of installation, quick implementation, cost-effectiveness, and better quality [3]. On the other hand, the use of parapet precast also poses a safety risk due to the use of lifting and transportation equipment and having to work at a height [4, 5]. The construction method was using a truck-mounted crane to lift and install the precast parapet at a location that has been determined according to the construction drawing. The illustration of the construction method is in Figs. 1, 2, and 3.

A work accident due to the fall of the precast parapet panel has occurred at the MRT Jakarta project in 2017. The chronology of the accident was when a 3 tons Overhead Catenary System (OCS) parapet was lifted to be installed using a truck-mounted crane on the bridge deck, but there was a hydraulic problem in the crane boom, causing the Overhead Catenary System (OCS) parapet to fall from a height and hit motorbikes and cars passing under it [6]. The losses caused by this accident were one motorcycle unit was badly damaged, one car was slightly damaged and one person was slightly injured [6] (see Figs. 4 and 5). Even though this was the first time this work has been done and inexperienced, the accident cannot be tolerated. From the incident, this accident can be used as a lesson to improve the construction safety management system in projects that use precast parapet panels.

As we all know that construction causes many deaths because it is a dangerous industry [8, 9]. Moreover, the project is a big, complicated and difficult project and this is a factor that can cause many work accidents [10, 11]. The impact is also very large for the project, namely poor performance starting from cost performance, quality, time and other adverse impacts [12].

Fig. 1 Construction method [7]



Fig. 2 Construction method [7]



Fig. 3 Parapet installation [7]

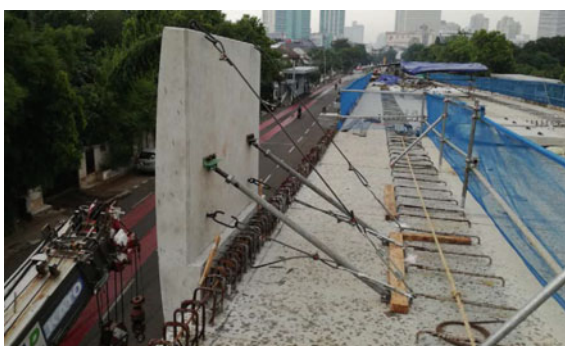


Fig. 4 Evacuation process [6]

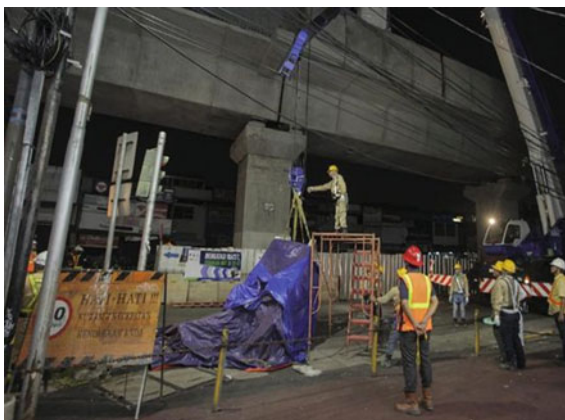


Fig. 5 Evacuation process [6]

The solution to solve the problems that arise is to develop a better construction safety plan [11, 13]. The safety plan is developed based on the activities in the work breakdown structure [11, 13]. Then make the identification of hazards that affect safety, risk assessment and determine risk control [11, 13]. Safety objectives and programs are also developed to ensure the implementation of safety at construction sites [11, 13].

There have been many previous studies regarding the development of construction safety plans in various types of buildings ranging from irrigation [14], dams [15], airports [16], seaports [17] and stadiums [18]. Research on the development of an elevated and bridge construction safety plan has also been carried out [5, 6, 11, 19], but the planning is still general and has not been detailed in the work package level. This study tries to complement previous studies, which aim to develop a safety plan for the construction of precast parapet panel work based on activity. Because activities are a very important basis for the implementation of construction, such as safety planning [20] and each activity has its respective potential hazards [19], which are identified and assessed for risk [4, 5, 13]. Activities are identified from the work breakdown structure [21]. The work breakdown structure used in this study is the work breakdown structure of the precast parapet that has been developed previously [22].

This research has positive implications for the safety development of elevated or bridge construction. This research also refers to the new construction safety regulations so that it is more updated, applicable and can be used as a reference for future similar projects. And it is very useful to decrease fatal accidents.

2 Methodology

This research was classified as quantitative survey research and designed in 3 stages (Fig. 6). The first stage was identifying safety risks by asking for expert validation, the second stage was surveying for safety risk assessment and the last stage was surveying for safety objectives and programs. The project sample was MRT Jakarta Contract Package (CP) 103 project. The variables were safety risks (X1), safety risks level (X2), risks controls (X3), safety objectives (X4), safety programs (X5). The closed questionnaire was distributed to the experts to get their opinions and to the respondents to assess the risk rating. The profile of five experts was requested to validate the safety risks show in Table 1.

The survey of risk assessment was conducted on the 50 construction and safety engineers. The respondents were engineers should have requirements minimum ten years working experience in elevated construction such as elevated road, bridge, flyovers, etc., minimum bachelor degree in education, minimum qualified and certified as a junior safety engineer, respondents should be actively involved in the project or a stakeholder of the projects (owner, consultant, contractor, or subcontractor).

Table 1 shows that the experts were from Japan, the Philippines, and Indonesia. The experts were the Project Manager, Deputy Project Manager, Site Manager, Chief of Engineer, and Engineering Manager. The working experience of the experts starts from 17 to 30 years. And the education of the experts was master and bachelor degree in engineering.

The analysis of safety risk assessment (R) was conducted by multiplying the probability value (P) and impact value (I) following the Eq. 1.

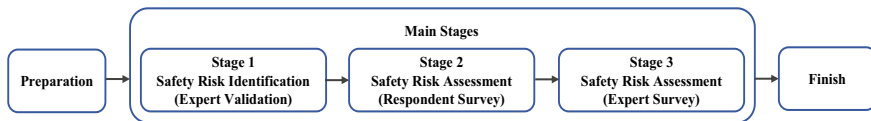


Fig. 6 Stages of the research

Table 1 Profile of experts

No.	Expert	Country of origin	Position	Working experience	Education
1	Expert 1	Japan	Project Manager	30 Years	Master Degree
2	Expert 2	Japan	Deputy Project Manager	25 Years	Master Degree
3	Expert 3	Japan	Site Manager	37 Years	Bachelor Degree
4	Expert 4	Philippines	Chief of Engineer	18 Years	Master Degree
5	Expert 5	Indonesia	Engineering Manager	17 Years	Bachelor Degree

		Impact				
		Very Low	Low	Med	High	Very High
Probability		1	2	3	4	5
Almost Never	1	1	2	3	4	5
Unlikely	2	2	4	6	8	10
Might	3	3	6	9	12	15
Very Possible	4	4	8	12	16	20
Almost	5	5	10	15	20	25

Fig. 7 Matrix of the risk level [23]

$$R = P \times I \tag{1}$$

The result of the calculation of the risk level or combination of the probability value and impact value can be seen in the matrix of risk level in Fig. 7. According to the regulation, the results of the calculation can be categorized qualitatively, the green color show low-risk level category with risk rating 1–4, the yellow color show the medium risk level with risk rating 5–12 and the red color shows the high-risk level with risk rating 15–25 [23].

3 Results and Discussions

3.1 Characteristics of Respondents

The total sample of respondents was 50 engineers. The manager position was 11 samples (22%), the assistant manager/senior engineer position was 13 samples (26%) and the engineer/staff position was 26 samples (52%). The engineer who had 10–15 years of experience were 38 samples (76%), 16–20 years of experience were 10 samples (20%) and more than 20 years were 2 samples (4%). The level of education of the respondents were 3 samples for diploma degree (6%), 41 samples for bachelor degree (82%), and 6 samples for master degree (12%). The involvement of respondents in the projects was 3 samples of the project owner (6%), 3

samples of supervision consultants (6%), 32 samples of contractors (64%), and 12 samples of subcontractors (24%). The detail of the characteristics of respondents is shown in Figs. 8, 9, 10, and 11.

Fig. 8 Characteristics of respondents by position

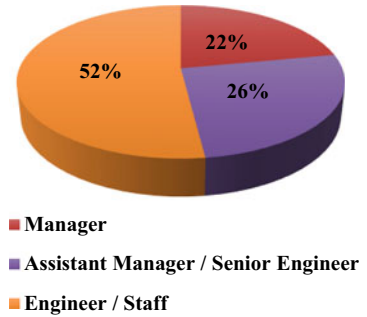


Fig. 9 Characteristics of respondents by working experience

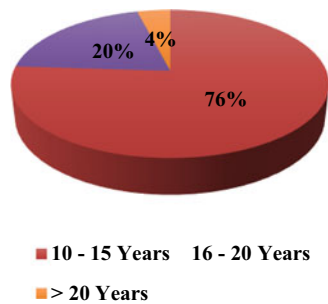


Fig. 10 Characteristics of respondents by education

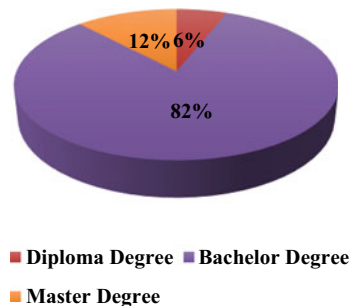
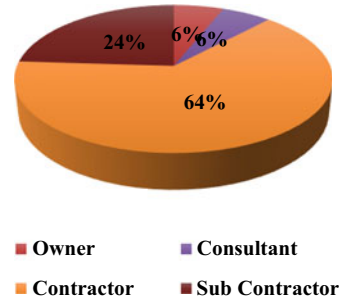


Fig. 11 Characteristics of respondents by project involvement



3.2 Identification of Hazards, Assessment of Risk, and Assigning Risk Control

Identification of hazards is carried out based on activities in the previously developed work breakdown structure [22]. And it is very important [11]. The precast parapet activities in the level 5 work breakdown structure are preparation, surveying of the position, installation of adjustment material, shifting precast parapet panel to deck slab, distributing precast parapet panel, installing precast parapet panel, installing rebar for concrete stitch, installing formwork for concrete stitch, sealing work, casting of concrete, dismantling of formwork and finishing work [22].

The experts have validated the hazards which had been identified. The result of expert validation analysis shows that all experts agree to all identified safety risks with a value of more than 80% agree. Then the data of survey results were analyzed with descriptive statistics. The result of the homogeneity test to the position, working experience, and education characteristics shows that the sig. >0.05, meaning the data was homogenous and there is no difference in respondents' perceptions of the questionnaire based on characteristics. The results of the normality test for the assessment of safety risk probability and safety risk impact show that the sig. >0.05 meaning the data does not distribute normally. Hence the conclusion of safety risk probability and safety risk impact use the median value. Then the median value is operated in the risk level formula above.

The case study is precast parapet installation activity because it is dangerous. After all, it is lifting works [4, 5]. The potential hazard of installing the precast parapet is parapet panel falls because it is similar to the girder erection which lifting the heavy load [4, 5]. The value of safety risk probability is 3, according to the regulation [23], meaning the probability might happen (see Fig. 7) and the value of safety risk impact is 5, according to the regulation [23], meaning the impact is very high (see Fig. 7). The risk rating is 15 and categorized as high-risk level according to the regulation (see Table 2 and Fig. 7).

Table 2 Identification of hazards, assessment of risks, and assigning risk controls

WBS level 5 activities	Potential hazards	Probability	Impact	Risk rating	Risk level	Risk controls	
Precast parapet installation	Parapet panel fall down	3	5	15	High	1	Lifting calculation
						2	Rigging and wire sling check
						3	Equipment check and audit
						4	Operator training and certification
						5	Creating, socializing, and evaluating standard operating procedures (SOP)

3.3 Safety Plan Development

The safety plan development consists of safety objectives and safety programs. In developing a safety plan, risk control is the basis for its development [5, 11]. According to the most updated regulation in construction safety, the safety objectives are broken down to the description and measurements and the safety program is broken down to the activities, resources, schedule, monitoring, achievement indicators, and person in charge [23]. The detailed safety plan developed according to the regulation is shown in Tables 3 and 4.

Table 3 Safety objective for precast parapet installation (WBS level 5 activity) against parapet panel falling down as the potential hazard

Risk controls	Objectives	
	Description	Measurements
Lifting calculation	The parapet precast does not fall down	Protected workers
Rigging and wire sling check	The rigging is not untied and the wire sling is not broken	Wire sling condition is good and rigging is right and strong
Equipment check and audit	The equipment is not damaged, the hydraulics do not leak, and can be used according to their function properly	Equipment is in good condition and stable
Operator training and certification	Competent operator	Operators can operate equipment and carry out lift and transport work
Creating, socializing, and evaluating standard operating procedures (SOP)	Workers follow standard operating procedures (SOP) and work instruction (WI)	Documents, Induction, Directions, Meetings, Training, Banner, Information Boards

Table 4 Safety program for precast parapet installation (WBS level 5 activity) against parapet panel falling down as the potential hazard

Program					
Activities	Resources	Schedule	Monitoring	Achievement indicator	PIC
Supervision and checking of calculations	Bridge lifting expert	Before work activity date	Lifting report and Safety report	The calculation is correct and applicable	Engineering Manager
Inspection and audit	Rigging expert and safety officer	Along with the work activity date	Periodic checklist report and safety report	There is no injury to workers	Safety officers, Supervisors, QC Engineer
Inspection and audit	Mechanics and safety officer	Along with the work activity date	Periodic checklist report and safety report	There is no injury to workers	Mechanics, operators, and safety officer
Training and certification	Operator and safety officer	Along with the work activity date	Operator license and safety report	There is no injury to workers	Operators and safety officers
Safety talk, safety meeting, and toolbox meeting	Supervisor, engineer, safety officer, workers, written publications	Along with the work activity date	Supervisory report per term of work/ Safety report	There is no injury to workers	Safety officers, Supervisors, QC Engineer

4 Conclusion

Precast parapet panel activity in precast parapet work has a potential hazard, that is parapet panel fall with the risk rating is 15 and categorized as high-risk level. There are five risk controls to reduce the risk are lifting calculation, rigging and wire sling check, equipment check and audit, operator training and certification, and lastly are creating, socializing, and evaluating standard operating procedures (SOP). The safety plan is developed from the risk controls in the form of safety objectives and safety programs based on the regulation. This research can be a reference for making safety plans in other various construction and it and needs to be investigated more deeply. The positive implication of this research is to provide input to the main stakeholders of the construction project in carrying out good safety planning to prevent and reduce fatal incidents.

Acknowledgements The author would like to show gratitude to stakeholders of the project for giving permission and supporting this research.

References

1. Presiden Republik Indonesia (2017) Peraturan Presiden Republik Indonesia Nomor 58 Tentang Perubahan atas Peraturan Presiden Nomor 3 Tahun 2016 Tentang Percepatan Pelaksanaan Proyek Strategis Nasional. Negara Republik Indonesia, Indonesia
2. PT MRT Jakarta (2020) Sejarah PT mass rapid transit (MRT) Jakarta. <https://jakartamrt.co.id/id/sejarah>. Accessed 21 Oct 2020
3. Elliot KS (2002) Precast concrete structures. Butterworth-Heinemann, Oxford
4. Putra ASP, Latief Y (2020) Analysis of safety cost structure in infrastructure project of cable stayed bridge based on work breakdown structure (WBS). IOP Conf Ser: Mater Sci Eng 830:022075
5. Saputra PD, Latief Y (2020) Analysis of safety cost structure in infrastructure project of precast of precast concrete bridge based on work breakdown structure (WBS). IOP Conf Ser: Mater Sci Eng 830:022074
6. CNN Indonesia (2017) Kronologi Jatuhnya Beton Proyek MRT Menimpa Pengendara. <https://www.cnnindonesia.com/nasional/20171104154444-20-253464/kronologi-jatuhnya-beton-proyek-mrt-menimpa-pengendara>. Accessed 21 Oct 2020
7. OSJ-JV (2017) Method statement for precast parapet construction OSJ-103-CMN-MST-STR-0079 Rev D. OSJ-JV, Jakarta
8. Haadir SA, Panuwatwanich K (2011) Critical success factors for safety program implementation among construction companies in Saudi Arabia. Proc Eng 14:148–155
9. Ramli A, Akasah ZA, Masirin MIM (2014) Factors contributing to safety and health performance of Malaysian low-cost housing: partial least squares approach. Res J Appl Sci Eng Technol 7(21):4612–4620
10. Cheng EWL, Li H, Fang DP, Xie F (2004) Construction safety management: an exploratory study from China. Constr Innov 4(4):229–241
11. Saputra PD, Latief Y (2020) Development of safety plan based on work breakdown structure to determine safety cost for precast concrete bridge construction projects. case study: girder erection with launching gantry method. Civil Eng Arch 8(3):297–304
12. Chan APC, Wong FKW, Chan DWM, Yam MCH, Kwok AWK, Lam EWM, Cheung E (2008) Work at height fatalities in the repair, maintenance, alteration, and addition works. J Constr Eng Manag 134(7):527–535
13. Fitriani R, Latief Y (2019) A conceptual framework of cost of safety model in infrastructure project based on work breakdown structure (WBS) to improve safety policy in Indonesia. IOP Conf Ser: Mater Sci Eng 650:012003
14. Tamara A, Latief Y, Machfudiyanto RA (2020) The development of safety plan to improve OHS (occupational health and safety) performance for construction of irrigation channel based on WBS (work breakdown structure). IOP Conf Ser: Earth Environ Sci 426:012016
15. Wardahni NI, Latief Y, Machfudiyanto RA (2020) Development of safety plan to improve OHS (occupational health and safety) performance for construction of dam (supporting infrastructure) based on WBS (work breakdown structure). IOP Conf Ser: Earth Environ Sci 426:012017
16. Sitohang D, Latief Y, Riantini LS (2019) Development of risk-based work breakdown structure (WBS) standard to improve scheduling planning of airport construction work. IOP Conf Ser: Earth Environ Sci 258:012052
17. Susiawan TA, Latief Y, Riantini LS (2019) Development of WBS (Work Breakdown Structure) risk-based standard for safety planning at seaport project. J Phys: Conf Ser 1360:012007
18. Amin JT, Sagita L, Latief Y (2020) Work breakdown structure (WBS) dictionary and checklist development of stadium architectural and interior works for safety planning. IOP Conf Ser: Mater Sci Eng 930:012006
19. Nicodemus AM, Latief Y (2021) Identify of occupational health and safety (OHS) cost component for flyover project by developing of safety plan based on work breakdown

- structure (case study: erection girder using tandem crane). IOP Conf Seri: Mater Sci Eng 1098:022048
20. Latief Y, Nurdiani D, Supriadi LSR (2019) Development of work breakdown structure (WBS) dictionary for the construction works of lower structure steel bridge. MATEC Web Conf 258:02003
 21. Project Management Institute (2016) Construction extension to the project management body of knowledge guide. Project Management Institute, Pennsylvania
 22. Saputra PD (2021) Identification of precast parapet work activities in elevated railway construction. Appl Res Civil Eng Environ (ARCEE) 2(2):52–61
 23. Kementerian Pekerjaan Umum dan Perumahan Rakyat (2021) Peraturan Menteri Pekerjaan Umum dan Perumahan Rakyat Republik Indonesia Nomor 10 Tahun 2021 tentang Pedoman Sistem Manajemen Keselamatan Konstruksi. Kementerian Pekerjaan Umum dan Perumahan Rakyat, Jakarta

Game Theory Approach for Risk Allocation in Public Private Partnership



Adhika Nandi Wardhana, Farida Rachmawati, and Erwin Widodo

Abstract Public Private Partnership (PPP) is a cooperation between public and private sectors in which all stakeholders develop mutual products and services. Risk management is important in this collaboration, considering that there must be an equal relationship between the two parties. Several studies have been carried out in allocating the level of PPP risk in various projects such as toll roads, buildings and other manufactures. One of the risk allocation tools used in those studies was game theory. The game theory consists of players, strategy and pay-off. Where each component of this method is different in each paper but still within the scope of risk allocation. This study is aimed to discuss the use of game theory for risk allocation and to describe the strategy and pay-off of previous studies. This study focuses on the similar and specific aspects of each paper.

Keywords Construction management · Game theory · Risk allocation

1 Introduction

Public–private partnerships (PPPs) are long-term integrated contracts between government and investors that are used for the provision of public infrastructure. Infrastructure that has been built recently must have the nature or purpose of sustainability, integration which includes environmental health, social justice and economic vitality that will create a thriving, healthy, diverse and resilient society for

A. N. Wardhana (✉) · F. Rachmawati
Department of Civil Engineering, Institut Teknologi Sepuluh Nopember, Surabaya, Indonesia
e-mail: adhika.wardhana24@gmail.com

E. Widodo
Department of Industrial Engineering, Institut Teknologi Sepuluh Nopember, Surabaya,
Indonesia

© The Author(s), under exclusive license to Springer Nature Singapore Pte Ltd. 2022
H. A. Lie et al. (eds.), *Proceedings of the Second International Conference of Construction, Infrastructure, and Materials*, Lecture Notes in Civil Engineering 216, https://doi.org/10.1007/978-981-16-7949-0_42

471

this generation and future generations is the goal of sustainability [1, 2]. The practice of sustainability recognizes how these issues are interconnected and require a systems approach and an acknowledgment of complexity. Sustainable development is one of the biggest global challenges today. It is not surprising that sustainability is increasingly recognized in the field of public procurement, as can be seen by various policies in various countries such as Europe, America, Asia, etc. The need for risk locations in a sustainable PPP needs to be considered [3]. Project in California has a problem in managing their water efficiency due to demographic pressure, declining financial and technical support at the state and federal level, climatic stress and outdated water management systems. They were implementing PPP to mobilize resources, provide technical expertise and share project risks. But many studies said the goal of the private sector is maximizing their profit that can reduce their quality of service. So the role of the private sector in partnership to supporting sustainability and resilience by examining the distribution of project risks is needed.

PPP has a complex risk, where the activities didn't focus on self because other participants joined our activities that can impact our benefit, their benefit, or both parties. Risk management is used to reduce the level of occurrence of the risk that occurs and the impact that will be caused by activity in the project. Understanding and explaining the risk perceptions of stakeholders is very important in carrying out this collaboration. Systems theory regarding the analytical distinction between 'internal risk' and 'external hazard' is a key concept for understanding whether stakeholders will take action or not [4]. While the perception of 'external harm' will not lead to action, the perception of 'internal risk' encourages stakeholders to take action. The challenge to provide one clear definition of the term risk is the concept of risk management [5]. The similarities among all risk concepts are: the possible and chosen actions might be different. All definitions of risk contain three elements: the impact or outcomes from humans action, the likelihood of occurrence (uncertainty) and the value of combination from both elements [6].

Game theory has a function as a method that allows for modeling such as bargaining and negotiation among rational decision makers [7], which has been applied to many critical problems, including negotiation, finance, imperfect markets, etc. [8]. Frequent conflicts between the government and private investors, especially in situations that can harm related parties, game theory can explain the mechanisms of competition and cooperation and provide solutions to these mechanisms [9]. This method is very suitable to be applied to PPP projects where there are usually conflicts between the government and investors, especially in risk allocation. This study will discuss several studies on game theory as a tool for PPP risk allocation and the scope of risks that have been studied using this method.

2 Conceptual Background

2.1 Risk Allocation

Verifying resilience to the definition of risk over time is necessary because this definition is changing and becoming increasingly complex with respect to a subject. The concept of risk is very important for starting a consistent discussion about an issue. In individuals or groups, it is necessary to have risk management in order to avoid the loss or impact of each action for both individuals and groups [10]. Increasing success probability in complex, multidisciplinary and challenging activities in managing projects and developing products is the goal of risk management activities. [11]. Thus, it is indispensable for any business environment such as a PPP project because risks can affect both results and processes and this is very important to ensure the achievement of strategic objectives. According to Berto, procedures in risk management consist of risk identification, risk assessment and risk treatment carried out sequentially during the risk management process, accompanied by a risk review and continuous risk monitoring [12].

A study from China shows that risks arise from a variety of sources, including capital budgets, construction time, construction costs, operating costs, politics and policies, market conditions, the credibility of cooperation and the economic environment [13]. Generally, each risk must be allocated to the party best able to manage it and at the lowest cost [14]. But this does not mean that all risks have to be left to the private sector but to minimize the total costs of managing the public and private sectors. So that risk allocation, such as risk transfer to third parties or sharing between the government and the private sector, is needed in the partnership scheme.

2.2 Game Theory Approach

Game Theory (GT) is a mathematical method model that describes the interaction between two or more rational players. GT can be used in order to face a group of players who act with self-interest so as to maximize their profits [15]. In other words, this method is used to find the best or win-win solution for conflicting interests [16, 17].

The decision making on risk allocation carried out in a partnership can be in the form of financial risk, construction risk, environmental risk and social risk. Game theory is a quantitative decision-making tool. Financial risks can be easily analyzed using this method, as for the financial risks commonly faced in partnerships, such as the renegotiation of excess income [18] or renegotiation of risks that cause financial losses [19]. Allocation of risks for construction, environmental and social risks can also be done by using the game theory method, namely by giving the magnitude of the impact, the chance of risk, which results in risk value [16]. The objects of decision making using this method also vary, such as in transportation [18–20],

irrigation/sewage [21, 22], buildings [23, 24], etc. are usually carried out in the construction industry.

3 Result and Discussion

3.1 Result

This research is to analyze the game theory approach for risk allocation on PPP from previous studies. Various sources from journals are analyzed in this study. There are 7 publication journals published from 2016 to 2020 [16, 18, 20–24]. The literature review has been analyzed from it that listed in Tables 1 and 2. Table 1 shows the mapping result from the analyzed paper based on the structure or formula for the game theory model and Table 2 shows the mapping result from the usability of risk allocation in many sectors of risk, case studies on many infrastructures and additional methods to achieve the goal of many research.

3.2 Discussion

Judging from previous research, a mapping diagram is formed. A mapping diagram is a group of previous research based on data sources and types of research. All

Table 1 Theoretical mapping on many research (game theory variables)

Source	Input		
	Participants	Strategies	Pay-off
[20]	Government, investor	MRG, project period	Calculated NPV each implemented strategies
[18]	Government, investor	Investor behaviour, government behaviour	Sum of investor revenue and government subsidies with the standard of MRG
[21]	Government, investor	Government surplus ratio, investor surplus ratio	Calculated surplus revenue between government and investor each turn
[16]	Government, investor	Public risk ratio, private risk ratio	Calculated risk value between public and private sector each turn
[23]	Contractor, contractor competitors	Contractor experience, strategies implemented	Actual cost or bidding estimation
[22]	Client, contractor	Risk allocation percentage	Contractor cost
[24]	Local government, SPV	Enhancing cooperation or not	Project cost

Table 2 Theoretical mapping on many research (usability)

Source	PPP object	Risk subject	Extra method	Result
[20]	Highway	Project cost	NPV, monte carlo	Optimal period time and MRG for the project, but the result can't be implemented on a social project
[18]	Highway	Material quality, project cost	–	Relation between MRG with investor effort that affects project quality
[21]	Sewage disposal	Project cost	–	The surplus allocation is directly proportional to the stakeholder power status in the coalition and is inversely proportional to the negotiation rate losses
[16]	Combined cooling heating and power (CCHP)	General risk (economic, finance, social, environment, political, etc.)	Corrected item total correlation (CITC)	The dominant position holder is determined by the degree of asymmetric information. In the bargaining process, the public sector usually has a stronger position. Therefore, more risk will be transferred to the private sector
[23]	Building	Project cost	–	Skepticism of an inexperienced contractor can create a fear of losing a high investment. This could leave them behind the opportunity to participate in the tender. Mechanisms to increase competition, such as providing incentives, need to be considered to strengthen competition
[22]	Pipeline	Project cost	System dynamic	It is a continuation of the previous SD-based model. The result is a share of the profit from lowering contractor costs
[24]	Bridge island tunnel	Project cost	Numerical simulation	The benefit allocation and punishment mechanisms are positively associated with increased cooperation between government and private investors

Table 3 Risk allocation mapping

Risk allocation	Research article
Engineering design	[16, 21–23]
Procurement	[18, 20–24]
Construction	[21]
Project management	[16, 21, 23]
Physical	[20, 21]
Financial	[16, 18, 20–24]
Social	[21]
Political	[21]

research data are quantitative model analysis. The mapping diagram can be seen in Table 3, which what risk allocation that the past research analyzed. Risk involvement in project life cycle Table 3 [25] and types of risks involved in commercial activities Table 3 [26]. Mulholland and Christian (1999) categorizing risk: engineering design (site investigation, design criteria and engineering estimates), procurement (material, manufacture process and vendor performance), construction (resource planning, construction mistakes and weather effects), project management (management experience, project procedure and resource control) [25].

4 Conclusion

The game theory approach for risk allocation in research is often used on financial problems. This occurs due to several factors such as competition for prospective contractors in tenders, renegotiation in cooperation, or efforts issued by stakeholders in a project. The use of game theory in general risk allocation still only one research conducted that discusses risk in general, whereas game theory is a mathematical method of solving problems between conflicting parties. With this paper, we hoped that there would be research on the use of the game theory approach for risk allocation in general, not only focusing on financial risk, which will help stakeholders in the project to establish a sustainable collaboration in the future.

References

1. Hueskes M, Verhoest K, Block T (2017) Governing public–private partnerships for sustainability: an analysis of procurement and governance practices of PPP infrastructure projects. *Int J Project Manage* 35(6):1184–1195
2. Lenferink S, Tillema T, Arts J (2013) Towards sustainable infrastructure development through integrated contracts: experiences with inclusiveness in Dutch infrastructure projects. *Int J Project Manage* 31(4):615–627

3. Nizkorodov E (2021) Evaluating risk allocation and project impacts of sustainability-oriented water public-private partnerships in Southern California: a comparative case analysis. *World Dev* 140:105232. <https://doi.org/10.1016/j.worlddev.2020.105232>
4. Luhmann N (1993) *Risk: a sociological theory*, 4th edn. A. de Gruyter, Berlin
5. Aven T, Renn O (2010) *Risk management and governance: concepts, guidelines and applications*. Springer, Berlin
6. Renn O, Walker KD (eds) (2008) *Global risk governance*, vol 1. Springer, Netherlands, Dordrecht
7. Miller D, Watson J (2013) A theory of disagreement in repeated games with bargaining. *Econometrica* 81(6):2303–2350. <https://doi.org/10.3982/ecta10361>
8. Farrell J, Maskin E (1989) Renegotiation in repeated games. *Games Econom Behav* 1(4):327–360. [https://doi.org/10.1016/0899-8256\(89\)90021-3](https://doi.org/10.1016/0899-8256(89)90021-3)
9. Narahari Y (2014) *Game theory and mechanism design*. World Scientific, Singapore
10. Power M (2004) *The risk management of everything: rethinking the politics of uncertainty*, 1st edn. Demos, London
11. Oliva FL (2016) A maturity model for enterprise risk management. *Int J Prod Econ* 173:66–79
12. Berto L, Favaretto T, Sietta A (2013) Seismic risk mitigation technique for art objects: experimental evaluation and numerical modelling of double concave curved surface sliders. *Bull Earthq Eng* 11(5):1817–1840. <https://doi.org/10.1007/s10518-013-9441-8>
13. Chan AP, Yeung JF, Yu CC, Wang SQ, Ke Y (2011) Empirical study of risk assessment and allocation of public-private partnership projects in China. *J Manag Eng* 27:136–148
14. Ke Y, Wang S, Chan AP (2010) Risk allocation in public-private partnership infrastructure projects: comparative study. *J Infrastruct Syst* 16:343–351
15. Wu CK (2018) A game theory approach for assessing risk value and deploying search-and-rescue resources after devastating tsunamis. *Environ Res* 162:18–26
16. Li Y, Wang X, Wang Y (2017) Using bargaining game theory for risk allocation of public-private partnership projects: insights from different alternating offer sequences of participants. *J Constr Eng Manag* 143:04016102. [https://doi.org/10.1061/\(ASCE\)CO.1943-7862.0001249](https://doi.org/10.1061/(ASCE)CO.1943-7862.0001249)
17. Khallaf R, Naderpajouh N, Hastak M (2018) Modeling three-party interactional risks in the governance of public-private partnerships. *J Manag Eng* 34(6):04018040. [https://doi.org/10.1061/\(asce\)me.1943-5479.0000646](https://doi.org/10.1061/(asce)me.1943-5479.0000646)
18. Wang Y, Gao HO, Liu J (2019) Incentive game of investor speculation in PPP highway projects based on the government minimum revenue guarantee. *Transp Res Part A: Policy Practice* 125:20–34
19. Medda F (2007) A game theory approach for the allocation of risks in transport public private partnerships. *Int J Project Manage* 25(3):213–218
20. Jin H, Liu S, Sun J, Liu C (2021) Determining concession periods and minimum revenue guarantees in public-private-partnership agreements. *Eur J Oper Res* 291(2):512–524
21. Liang Q, Hu H, Wang Z, Hou F (2019) A game theory approach for the renegotiation of public-private partnership projects in Chinese environmental and urban governance industry. *J Clean Prod* 238:117952. <https://doi.org/10.1016/j.jclepro.2019.117952>
22. Nasirzadeh F, Mazandaranzadeh H, Rouhparvar M (2016) Quantitative risk allocation in construction projects using cooperative-bargaining game theory. *Int J Civ Eng* 14(3):161–170. <https://doi.org/10.1007/s40999-016-0011-8>
23. De Clerck D, Demeulemeester E (2016) Creating a more competitive PPP procurement market: game theoretical analysis. *J Manag Eng* 32(6):04016015. [https://doi.org/10.1061/\(ASCE\)ME.1943-5479.0000440](https://doi.org/10.1061/(ASCE)ME.1943-5479.0000440)

24. Li L, Li Z, Jiang L, Wu G, Cheng D (2018) Enhanced cooperation among stakeholders in PPP mega-infrastructure projects: a China study. *Sustainability* 10(8):2791. <https://doi.org/10.3390/su10082791>
25. Mulholland B, Christian J (1999) Risk assessment in construction schedules. *J Constr Eng Manag* 125(1):8–15. [https://doi.org/10.1061/\(ASCE\)0733-9364\(1999\)125:1\(8\)](https://doi.org/10.1061/(ASCE)0733-9364(1999)125:1(8))
26. Edwards L (1995) *Practical risk management in the construction industry*. Thomas Telford, Heron Quay

Analysis of Change Orders Based on the Type of Road Construction



Mega Waty  and Hendrik Sulistio 

Abstract Change Order is a written and valid work order that changes the scope of the original contract, with compensation agreed upon by the owner and contractor. Changes can be in the form of adding or reducing the scope of work, material changes, or schedule changes. The Change Order that occurred in Banten Province stated the value of the percentage change order for various works on road projects expressed in the type of road construction. The changes that occur are job changes due to added work and changes due to less work. The purpose of this study is to determine the type of road construction that occurs in 5 change order contracts for road construction projects and the results are the largest changes in the type of drainage work construction, both the changes themselves and changes to additional work. Changes due to work are less in the largest type of construction in Condition Returns and Minor Works.

Keywords Change order · Road construction project · Banten

1 Introduction

Change Order is a common thing that often occurs in construction projects. Almost all existing projects always have change orders, both government projects and private projects. During the implementation of a construction project, these changes can occur either from the contractor or the owner [1]. A Change Order is a written and legal work order that changes the scope of the original contract, with compensation that has been agreed upon by the owner and the contractor. Changes can be in the form of adding or reducing the scope of work, changing materials, or changing schedules [2].

M. Waty (✉)

Civil Engineering Undergraduate Program, Universitas Tarumanagara, Jakarta, Indonesia
e-mail: mega@ft.untar.ac.id

H. Sulistio

Civil Engineering Doctoral Program, Universitas Tarumanagara, Jakarta, Indonesia

Goudreau [3] reports that there are five keys that burden the project, namely: payment, authority, change orders, schedule of work and contract documents.

The main cause of delays in 130 projects in Jordan was change orders [4]

Change Order causes costs to cause contract items to swell, planning errors and negligence, as well as changes in scope which can be reduced by sharpening the final results of planning [5].

Research by Sulistio and Waty [1] shows that the percentage of change orders occurred at 28.26% of projects in East Kalimantan in excavation and embankment works on road pavement projects. Research by Waty and Sulistio [6] states that the Change Order effect from the calculation of Change Order for road projects in Banten is: delaying the project completion date, cost overruns, generating claims and disputes, affecting performance and work morale and most contractors incur additional costs.

The average percentage of jobs that experience the biggest change orders in road construction projects that occur in Banten is U-shaped channel work type DS 1 (19.64%) in Waty and Sulistio's research [6]. Seeing the large percentage of change orders in Banten Province, the authors want further researching the types of road construction that occurred in Banten Province, which originated from the contract change orders that occurred.

2 Methodology

The object of research regarding changes in the type of road construction occurred as a result of change orders carried out in Banten Province. The road project is one of the prioritized infrastructure projects in Banten Province. Of course, it is very necessary to pay attention to the infrastructure that continues to be built as well as Banten province as the closest province to DKI Jakarta, which has a fairly large percentage of change orders in previous studies.

2.1 Data Collection

The research data were obtained from the Public Works Office of Banten Province. In total, the researchers obtained five real project data consisting of 2018 which were analyzed in hard copy and soft copy. The real data is in the form of a contract addendum containing the change order contract. In five projects, there were quite a lot of project changes. This study focuses on the change order contract addendum, which contains project changes and the reasons for the changes and is presented in each change order note, including the following relevant information:

- Changes in overall costs and times;
- Changes in the cost per specific work item;

- Original contract value;
- Type of construction;
- Project description; and
- The reason for each change order.

2.2 Data Analysis Method

The data analysis method consists of 5 change order contract data in 2018 at the Banten Province project in the form of project construction change data. The calculation of the change order contract is in the form of additional work changes and fewer work changes in the change order contract that you can see below:

1. Change Order Ratio (COR)

This index measures the total cost of the variants of the project where Change orders occur.

$COR = (the\ amount\ of\ added\ and\ less\ value\ for\ the\ project.\ Change\ order / original\ contract\ price) \times 100\%$

2. Change Order Ratio in Addition (CORA)

This index measures the total cost of the variants of the project where change orders occur.

$CORA = (the\ amount\ of\ added\ and\ less\ value\ for\ the\ project.\ Change\ order / original\ contract\ price) \times 100\%$

3. Change Order Ratio in Subtraction (CORS) [7]

This index measures the ratio of the total subtraction achieved in change order projects were carried out.

$CORS = (the\ amount\ of\ work\ value\ was\ less\ than\ the\ projects\ performed\ change\ order / original\ contract\ price) \times 100\%$

Based on this data, we can find the type of road construction which consists of 11 construction works based on the 2018 Bina Marga specifications [8].

3 Result and Discussion

3.1 Acquisition of Data

After data collection, five real data were obtained from road projects in Banten Province. Of the five projects obtained, all of which are budget projects from 2018. Of the five projects, the results are as in Table 1.

Table 1 Project based on balance and addition of budget

No.	Project	Contract	Contract add	Year	Information
1	Road 1	17,891,881,000	17,891,881,000	2018	Balance budget
2	Road 2	28,501,187,000	30,841,291,000	2018	Additional budget
3	Road 3	11,790,233,000	12,969,256,000	2018	Additional budget
4	Road 4	2,647,761,000	2,890,502,000	2018	Additional budget
5	Road 5	7,322,434,000	8,022,434,000	2018	Additional budget

3.2 Calculation of the Percentage Change Order for the Banten Road Project

The percentage of Change Order is calculated based on COR, CORA and CORS. Project COR calculation is the ratio of calculating changes in the form of additional funds or reduction of funds or addition of work items or reduction of work items or removal of work items or addition of new work items.

The change order contract can be used to see work that has changed orders which are divided into types of road construction and for daily work items that do not exist, what is used in this study are [8]:

1. Drainage Work
2. Earthworks
3. Road Shoulder Pavement Widening Work
4. Cement Concrete Works
5. Structural Work
6. Asphalt Work
7. Works Restoring and Minor Works
8. Maintenance of Routine Work which consists of
9. Routine Maintenance Work
10. SKH2.10A Road Performance Maintenance
11. SKH 2.10 B Bridge Performance Maintenance.

Road Project Work Change Analysis (COR). COR calculation [7]

Change Order Ratio (COR). This index measures the total cost of the variants of the project where Change orders occur. $COR = (\text{the amount of added and less value for the project. Change order/original contract price}) \times 100\%$

1. Total COR of Each Road Project

Total project COR calculation is the total COR calculation on the project as a whole, which is contained in 10 construction work items which when totaled, will get the total COR value, as can be seen in Table 2.

Table 2 COR total of each project

Project total COR value	Project name
25.13	1
23.12	2
93.44	3
8.66	4
20.91	5

Table 3 COR total of the entire road project

Type of constructions	COR
Div. 2 Drainage work	42.50
Div. 3 Earth work	7.01
Div. 4 Road shoulder pavement widening work	3.83
Div. 5 Cement concrete work	7.37
Div. 6 Asphalt work	36.82
Div. 7 Structural work	33.0
Div. 8 Works restoring and minor works	34.42
Div. 10 Routine maintenance work	0
SKH2.10A Road performance maintenance	6.24
SKh1-10b Bridge performance maintenance	0.04
Total	171.27

2. Total COR of All Road Projects and COR Average Projects

The total COR of all projects resulted in the largest change order change value in 5 projects was 42.50% for asphalt work and the smallest change in 5 projects was road shoulder widening work 3.83%, so that the total change in 5 projects was 171.27% which occurs because the condition of the project field changes which causes changes in work on the project as in Table 3. Changes in the average change order in all construction projects can be seen in Table 4. The smallest chance of change order in the type of bridge performance maintenance construction was 0.045% and the bigger is Drainage Work was 38.90%.

Change Order Ratio in Addition (CORA) [7]. This index measures the ratio of the total work added to projects that are experiencing change orders. CORA = (the amount of the added value of the project that underwent a change of order/original contract price) × 100%

1. Change Order Ratio in Addition (CORA) Total of each Project

CORA total project is a change of work plus the overall change order in one project package, which can be seen in Table 5 on each road project. CORA Total for each project resulted in the largest value of change in Road Project 3 at 51.49% and the smallest on Project 4 at 5.562% that you can see in Table 5. CORA Total Project of 51.49% occurred due to changes in project field conditions which led to changes in work on the project. The conditions in the project field have changed because

Table 4 Project average COR

Type of construction	Average COR
Div. 2 Drainage work	38.90
Div. 3 Earth work	1.95
Div. 4 Road shoulder pavement widening work	0.97
Div. 5 Cement concrete work	0.66
Div. 6 Asphalt work	17.07
Div. 7 Structural work	11.85
Div. 8 Works restoring and minor works	9.86
Div. 10 Routine maintenance work	
SKh-2.10a Road performance maintenance	6.24
SKh1-10b Bridge performance maintenance	0.04

usually project planning was carried out in the previous year and changed regulations which resulted in changes in work. It occurs because the state of the project field changes, which causes changes to work on the project. Changes of 51.49% are not allowed according to Peraturan Presiden No. 54 of 2010 Article 87 [9], only 10% chance of work is permitted.

2. CORA Total of All Road Projects and CORA of Project Average

Changes in work added to change orders for five projects in Table 5 consist of the smallest amount of 0.05% to Cement Concrete work and the largest percentage in Structural Work is 24.74%, so that the total change in added work of 102.97% occurs due to field conditions. Project changes that cause changes to the work on the project. The average CORA of the project also experienced the same thing, namely the type of construction of drainage works experienced the largest change order of 37.72 0% and the smallest change of change order was in the type of bridge performance maintenance construction of 0.045% that can be seen on Table 6.

Change Order Ratio in Subtraction (CORS) [7]. This index measures the ratio of the total subtraction achieved in Change order projects were carried out. $CORS = (the\ amount\ of\ work\ value\ was\ less\ than\ the\ projects\ performed\ Change\ order / original\ contract\ price) \times 100\%$ CORS Total of each Project.

CORS Total Project is a change of work less a project in each project. The CORS Total Project resulted in the largest value of change in Project number 3,

Table 5 CORA Total of each project

Total CORA (%)	Project name
12.800	1
23.848	2
51.49	3
5.562	4
9.275	5

Table 6 CORA total of all road project

Type of construction	Amount (%)
Div. 2 Drainage work	41.91
Div. 3 Earth work	3.82
Div. 4 Road shoulder pavement widening work	2.63
Div. 5 Cement concrete work	0.05
Div. 6 Asphalt work	10.50
Div. 7 Structural work	24.74
Div. 8 Works restoring and minor works	12.14
Div. 10 Routine maintenance work	
SKh-2.10a Road performance maintenance	7.15
SKh1-10b Bridge performance maintenance	0
Total	102.97

Table 7 CORS total for each project

Total CORS	Project name
12.28	1
2.35	2
42.31	3
0	4
9.92	5

amounting to 42.31% and the smallest in Project number 4 by 0%. The total project CORS of 42.31% occurred due to changes in project field conditions which led to changes in work on the project that can be seen in Table 7.

CORS Total of all Road Projects and Average CORS of Projects. The calculation of work lacking change orders in 5 projects (all projects) at the smallest is 0% for bridge performance maintenance work and the largest fewer work changes in the condition restoration work and minor work as the highest less work change, namely 23.39% that can be seen on Table 8 and total change is 66.87% that can be seen on Table 8.

The average change in a change order for all construction projects was obtained with the largest result in drainage work of 15.515% and the smallest change in a change order for the bridge maintenance construction type of 0.045% that can be seen on Table 9.

Table 8 CORS total of all road projects

Type of construction	Amount (%)
Div. 2 Drainage work	15.74
Div. 3 Earth work	3.19
Div. 4 Road shoulder pavement widening work	1.19
Div. 5 Cement concrete work	1.87
Div. 6 Asphalt work	12.03
Div. 7 Structural work	8.25
Div. 8 Works restoring and minor works	23.39
Div. 10 Routine maintenance work	
SKh-2.10a Road performance maintenance	1.20
SKh1-10b Bridge performance maintenance	0
Total	66.87

Table 9 Average CORS project

Type of construction	Average CORS (%)
Div. 2 Drainage work	15.515
Div. 3 Earth work	1.368
Div. 4 Road shoulder pavement widening work	0.599
Div. 5 Cement concrete work	0.941
Div. 6 Asphalt work	9.732
Div. 7 Structural work	4.277
Div. 8 Works restoring and minor works	10.543
Div. 10 Routine maintenance work	
SKh-2.10a Road performance maintenance	1.198
SKh1-10b Bridge performance maintenance	0.045

4 Conclusion

Analysis of change order for road construction projects in Banten based on the type of road construction derived from the calculation and analysis of change order contracts, both the average and the total obtained are:

1. Biggest work Change on Drainage work
2. Work changes added to the largest change order for Drainage jobs
3. Work changes are less the biggest change order on work Restore Conditions and Minor Work.

5 Suggestion

Pay more attention to the type of construction work, Drainage and Restoration of Conditions and Works so that in the following year change orders can be reduced.


Acknowledgements We would like to thank the Institute for Research and Community Service of Tarumanagara University which has helped fund this research.

References

1. Sulistio H, Waty M (2008) Analysis and evaluation change order in flexible pavement (case study: road projects in East Kalimantan). *Media Komunikasi Teknik Sipil* 16(1):31–47
2. Lim M (2013) *Analisa change order pada Proyek Perkerasan Jalan*. Thabi' Press, Bandung
3. Goudreau H (2021) The five key elements of every construction contract—forget them and you're in trouble!. http://www.hgassociates.com/article_contracts.html. Accessed 29 Aug 2021
4. Al-Momani AH (2000) Construction delay: a quantitative analysis. *Int J Project Manage* 18(1):51–59
5. Taylor TR, Uddin M, Goodrum PM, McCoy A, Shan Y (2012) Change orders and lessons learned: knowledge from statistical analyses of engineering change orders on Kentucky highway projects. *J Constr Eng Manag* 138(12):1360–1369
6. Waty M, Sulistio H (2020) Perhitungan change order proyek jalan di banten. *Jurnal Muara Sains, Teknologi, Kedokteran dan Ilmu Kesehatan* 4(2):211–220
7. Hsieh TY, Lu ST, Wu CH (2004) Statistical analysis of causes for change orders in metropolitan public works. *Int J Project Manage* 22(8):679–686
8. Direktorat Jendral Bina Marga (2018) *Spesifikasi Umum 2018*. Direktorat Jendral Bina Marga, Departemen Pekerjaan Umum, Jakarta
9. Republik Indonesia R (2010) *Peraturan Presiden Republik Indonesia Nomor 54 Tahun 2010 Tentang Pengadaan Barang/Jasa Pemerintah*. Sekretariat Kabinet RI, Jakarta

Implementation of Occupational Safety and Health Management Systems During COVID-19 Pandemic on High-Rise Building Construction Projects



Alexsander Martin and Mega Waty 

Abstract Indonesia is one from many countries that is struck by the COVID-19 virus pandemic. Indonesia still needs to recover from economy crisis caused by the pandemic. Indonesia's evolvement can be seen from their development in their infrastructure during the COVID-19 pandemic. The Occupational Safety and Health (OHS) Management System is a crucial part of the contractor organization's management system that is used to implement and develop OHS policies in all of the existing development project. In this research study, it will discuss about the application of OHS management systems in high-rise building projects during the COVID-19 pandemic. The result from the analysis and calculation in this research are compared with the Minister of Public Works Regulation No. 9/2008 regarding the Management System and Work Safety and the Instruction of the Minister of PUPR No. 2/IN/M/2020 concerning about the Protocol to Prevent the Spread of Corona Virus Disease 2019 (COVID-19) in the implementation of construction services. In its implementation, the OHS Management System is divided into 3 important parts, namely the Implementation and Operation of OHS Activities, OHS Evaluation/Inspection and OHS Management Review. The implementation of OHS Management System during the COVID-19 pandemic in high-rise building was obtained 77.09% (Good Enough).

Keywords COVID-19 · Occupational safety and health management system · High-rise building projects

A. Martin (✉) · M. Waty

Civil Engineering Undergraduate Program, Universitas Tarumanagara, Jakarta, Indonesia
e-mail: alexsander.325170001@stu.untar.ac.id

© The Author(s), under exclusive license to Springer Nature Singapore Pte Ltd. 2022
H. A. Lie et al. (eds.), *Proceedings of the Second International Conference of Construction, Infrastructure, and Materials*, Lecture Notes in Civil Engineering 216, https://doi.org/10.1007/978-981-16-7949-0_44

489

1 Introduction

The ongoing global pandemic, which is caused by the Corona Virus Disease 2019 (COVID-19) that has been going on for the past year, is causing significant shocks to Indonesia's economic system. The construction services industry, which is one of the economy's main drivers, is also affected by the pandemic. The Occupational Health and Safety Management System is an important part of the contractor organization's management system that is used to implement and develop occupational safety and health policy on every existing construction project [1].

To ensure the quality of construction workers in the middle of the pandemic, the Director General of Construction Development issued circular letter No. 107/SE/Dk/2020 outlining guidelines for the development of competence for construction workers in the New Normal Period [2].

In the middle of a pandemic, competency development must continue while also following health procedures and minimizing the risk of COVID-19 spread. COVID-19 is an extremely contagious virus that can be spread through direct or indirect physical contact [3].

2 Literature Review

2.1 Occupational Health and Safety Management System

The occupational safety and health management system is part of the organization's management system that is used to develop and implement (Occupational Health and Safety) OHS policies and manage risks [4].

According to Government Regulation No. 50 of 2012 the objectives of the occupational safety and health management system are:

1. Improving the effectiveness of occupational safety and health protection that is planned, measurable, structured and integrated.
2. Prevent and reduce workplace accidents and occupational diseases by involving elements of management, workers/laborers and/or trade/labor unions.
3. Creating a safe, comfortable and efficient workplace to boost productivity.

2.2 Implementation of the Construction Occupational Safety and Health Management System During the COVID-19 Pandemic

Many jobs were disrupted by the COVID-19 pandemic, including those in the construction services sector. Various adjustments to the implementation of existing

work activities are required during this pandemic. Adjustments to the Occupational Health and Safety Management System in the field are required in the construction services sector so that work activities can continue.

The COVID-19 Prevention Protocol on Construction Projects in the field issued by [5] is as follows:

1. The Task Force distributed or installed flyers, both digital and physical, on the appeals/recommendations for preventing COVID-19, such as handwashing and wearing masks, in strategic areas throughout the project field.
2. The Task Force, together with the Medical Officers, must provide explanations, recommendations, campaigns and promotions of COVID-19 prevention techniques in every morning safety education activity (safety morning talk).
3. The Task Force forbids anyone (managers, engineers, architects, employees/staff, foremen, workers and project guests) from coming to the project site if they are unwell with a temperature above 38 °C.
4. Medical officers carry out body temperature measurements to all workers and employees together with the Project Security Staff and Security Officers every morning, afternoon and evening.

If it is found that managers, engineers, architects, employees/staff, foremen and workers in the project field are exposed to the COVID-19 virus, the Medical Officers assisted by the project Security Officers will evacuate and spray disinfectants on the premises, facilities, handles and work equipment.

2.3 Government Way to Overcome COVID-19 Pandemic in the Construction Services Sector

The Indonesian Contractors Association (ICA) revealed that the construction sector in Indonesia experienced a slowdown during the COVID-19 pandemic and needed fast handling [6].

The government's initial step in overcoming this pandemic problem is by issuing Ministerial Instruction No. 02/IN/M/2020 regarding the Protocol to Prevent the Spread of COVID-19 on March 27, 2020, the contents of which are as follows:

1. Establishment of a COVID-19 prevention task force.
2. Identification of potential COVID-19 hazards in the field.
3. Provision of Health Facilities in the field.
4. Implementation of COVID-19 Prevention in the field.

3 Research Methods

3.1 Research Sites

The location used to carry out this research covers the Greater Jakarta area. This location was chosen due to the high level of development in the area around the capital.

3.2 Research Procedure

In general, the procedures carried out in this study are as follows:

1. The first stage in this research is to determine the research covers for the projects that will be used.
2. The data obtained will next be put to the test using a validity and reliability test.
3. The validity and reliability tests in this study use the SPSS program.
4. If the data is valid and reliable, then research can continue to the calculation stage using the quantitative method.
5. After the data is calculated, then the results of the calculation will be displayed in the form of a pie chart.
6. Then do the analysis of the results of the pie chart.
7. The final stage of this research is to come to a conclusion about the calculations' results. Following that, conclusions will be drawn that will be valuable to engineers.

3.3 Research Variable

The following are the variables used in the study, which can be seen in Table 1.

4 Result and Discussion

The collected data from respondents will be put into the SPSS program. The data will be tested for validity and reliability in this program and if the data passes those two criteria, it will be processed using quantitative methods.

Table 1 Research variable

Variable	Factors for occupational safety and health management system	Source
X1	Have all dangerous parts of the equipment been marked	[7]
X2	Has the construction company leader taken primary responsibility for OHS and OHS management systems	[7]
X3	Does the company provide training and education for every employee to act safely in completing work	[7]
X4	Have the required documents and OHS guidelines been provided?	[7]
X5	Does the company make provisions to effectively communicate occupational safety and health information	[8]
X6	Does the company make rules to get expert opinion and advice	[8]
X7	Does the company provide a hand purifier (water, soap and hand sanitizer) and mask in the field	[9]
X8	Does the company provide education about COVID-19 in the field?	[9]
X9	Does the company carry out routine temperature checks every morning, afternoon and evening in the field	[9]
X10	Does the company carry out regular spraying of disinfectants throughout the premises, facilities and work equipment	[9]
X11	Is there any use of tools or clothes that are still shared	[9]
X12	Are the equipment and testing methods used adequately	[7]
X13	Are records of inspections, testing and monitoring well maintained	[7]
X14	OHS Management System audits are conducted periodically to determine the effectiveness of the implementation of the OHS Management System	[8]
X15	Audit results are used by management in the management review process	[8]
X16	Does the management conduct periodic reviews of the occupational safety and health management system	[7]
X17	Has there been a review of the evaluation of the implementation of the OHS policy	[7]
X18	Is there a review of the OHS goals, objectives and performance	[7]
X19	Is a review of the findings of the occupational safety and health management system audit conducted?	[7]
X20	Is there a review of the evaluation of the effectiveness of the implementation of the occupational safety and health management system	[7]

Table 2 Validity test results

Variable		r value
X1	Pearson correlation	0.476
X2	Pearson correlation	0.523
X3	Pearson correlation	0.393
X4	Pearson correlation	0.393
X5	Pearson correlation	0.694
X6	Pearson correlation	0.461
X7	Pearson correlation	0.483
X8	Pearson correlation	0.526
X9	Pearson correlation	0.531
X10	Pearson correlation	0.389
X11	Pearson correlation	0.585
X12	Pearson correlation	0.496
X13	Pearson correlation	0.656
X14	Pearson correlation	0.688
X15	Pearson correlation	0.478
X16	Pearson correlation	0.852
X17	Pearson correlation	0.894
X18	Pearson correlation	0.854
X19	Pearson correlation	0.841
X20	Pearson correlation	0.814

4.1 Validity Test

In this validity test, only 20 from 33 questions can be called valid. The data can be valid is when the r results from the test have passed the r table (0.344). The data from validity test results can be seen in Table 2.

4.2 Reliability Test

Data that passed the validity test will be tested for reliability test. The data can be reliable is when the Cronbach Alpha result from the test has passed 0.6. This means that the questionnaire data from the results of this study are reliable. The results of the reliability of this study are good because they are in the range of 0.8–1. The data from reliability test results can be seen in Table 3.

Table 3 Reliability test result

Cronbach's Alpha	N of items
0.904	20

4.3 Percentage Result of the Occupational Health and Safety Management System Implementation

Analysis result of the implementation of the occupational safety and health management system during the COVID-19 pandemic on high-rise building projects can be seen in Table 4.

According to the occupational safety and health management system during the COVID-19 pandemic, all activities for high-rise building projects reached a value of 77.1%, indicating that the implementation has been handled effectively. This can be seen from the regulations:

- Good, if the assessment results reach >85%
- Pretty good, if the assessment results reached 60–85%
- Not good, if the assessment results reach <60%.

Table 4 Questionnaire percentage results

No.	Yes (%)	No (%)	Total (%)
<i>The implementation and operation of OHS activities</i>			
X1	69.7	30.3	100
X2	87.9	12.1	100
X3	78.8	21.2	100
X4	78.8	21.2	100
X5	87.9	12.1	100
X6	57.6	42.4	100
X7	90.9	9.1	100
X8	90.9	9.1	100
X9	72.7	26.3	100
X10	45.5	54.5	100
X11	48.5	51.5	100
<i>OHS evaluation/inspection</i>			
X12	84.8	15.2	100
X13	90.9	9.1	100
X14	81.8	18.2	100
X15	84.8	15.2	100
<i>OHS management review</i>			
X16	72.7	26.3	100
X17	78.8	21.2	100
X18	69.7	30.3	100
X19	69.7	30.3	100
X20	69.7	30.3	100
Average (%)	77.1	22.9	100

Table 5 Classification table based on research section

Research section	Percentage (%)	Classification
Implementation and operation of OHS activities	73.5	Pretty good
OHS evaluation/inspection	85.6	Good
OHS management overview	72.1	Pretty good

5 Conclusion

Based on the results of research that has been carried out on the Implementation of Occupational Health and Safety Management Systems During the COVID-19 Pandemic in high-rise construction projects, there are three parts of research in determining the success of implementing Occupational Health and Safety Management Systems, which can be seen in Table 5.

Several findings from the research conducted on the three sections above reveal that the implementation of the OHS management system in high-rise building construction projects during the COVID-19 pandemic has been carried out relatively well, with an average percentage of 77.1%. However, being relatively well or good is not enough to make the construction environment safer. In order to create a safer environment, safety protocols such as using a mask are required.

References

1. Purwanto A (2021) Ekonomi Indonesia pada masa pandemic COVID-19: Potret dan strategi pemulihan 2020–2021. <https://kompaspedia.kompas.id/baca/paparan-topik/ekonomi-indonesia-pada-masa-pandemi-covid-19-potret-dan-strategi-pemulihan-2020-2021>. Accessed 13 Feb 2021
2. Tresnawati D (2020) Upaya pemenuhan target sertifikasi tenaga kerja konstruksi dalam periode tatanan kehidupan baru. *Buletin Konstruksi* 4:7–9
3. Jati A (2020) 2 Cara Penularan Virus Corona COVID-19, Langsung dan Tidak Langsung. <https://www.liputan6.com/bola/read/4215173/2-cara-penularan-virus-corona-covid-19-langsung-dan-tidak-langsung>. Accessed 13 Feb 2021
4. British Standards Institute (2007) BS OHSAS 18001:2007: occupational health and safety managements systems-requirements. British Standards Institute, London
5. Kementerian Pekerjaan Umum (2020) Protokol pencegahan COVID-19 di Proyek Konstruksi. <https://covid19.go.id/p/protokol/kemen-pupr-protokol-pencegahan-covid-19-di-proyek-konstruksi>. Accessed 20 Feb 2021
6. Fitriani R (2020) Mengintip panduan pengendalian COVID-19 sektor konstruksi oleh OSHA. *Buletin Konstruksi* 4:4–6
7. Bramantya D (2016) Penerapan sistem manajemen keselamatan kerja di lingkungan proyek pembangunan MIDTOWN hotel Samarinda. *Kurva S Jurnal Mahasiswa* 1(1):51–66
8. International Labour Organization (2021) Occupational safety and health management in the construction sector. International Labour Organization, Geneva
9. Kementerian Pekerjaan Umum (2020) Instruksi Menteri No.2/IN/M/2020. Kementerian Pekerjaan Umum, Jakarta

Developing Knowledge Management Strategy to Improve Project Communication in Construction of Coal Mining Infrastructure: A Conceptual Study



Alfandias Seysna Putra, Leni Sagita Riantini, and Mohammad Ichsan

Abstract Construction delays are a critical phenomenon and occur in many construction industries, including construction projects in mining companies. The most significant factor is poor communication between stakeholders, with an average severity of 60.89% affecting the success of the project. The phenomenon that occurs in mining companies, this study conducted in a mining contractor company, that the organization responsible for infrastructure management only has one supervisor with basic construction knowledge, so there is a gap of knowledge and competency between organization members that causes weak supervision and causes delay project. Previous studies suggest that knowledge management can affect project performance and improve communication with knowledge alignment within organizations. This study proposes an integrated conceptual research model to identify how knowledge management activities can be managed effectively to increase the level of project knowledge in the owner's organization to improve project communication, as well as examine the correlation between project communication and project time performance with the mediation of knowledge management in coal mining construction projects.

Keywords Project management · Project communication · Project time performance · Infrastructure project · Mining

A. S. Putra (✉) · L. S. Riantini
Civil Engineering Department, Faculty of Engineering, University of Indonesia, Depok,
Indonesia
e-mail: alfandias.seysna@ui.ac.id

M. Ichsan
Management Program, Binus Business School Undergraduate Program, Binus University,
Jakarta, Indonesia

1 Introduction

The coal mining industry is one of the strategic industries in Indonesia where the company’s operations are greatly influenced by the dynamic reference price of coal. Based on data from the Ministry of Energy and Mineral Resources, during 2013–2020, the coal reference price decreased in 2014–Mid 2016 to \$50/ton, then the price recovery in 2017–2019 and a decline again in 2020 [1]. The dynamics of coal prices greatly influence the company’s decision to invest in human resources and infrastructure to support mining operations. PT X is a coal mining contractor company in Indonesia that was founded in 2003 which also experienced a critical condition due to the decline in coal prices in 2016. Infrastructure projects to support mining operations consist of workshops, warehouses, offices, employee mess and facilities, pedestrian bridges, weighbridges, places of worship, lightning distribution towers, and supporting buildings in the mine. The dynamic development of infrastructure investment, which increases and decreases in investment every year, makes all project supervisors need to be more intense in monitoring in terms of time, quality, and work safety. Because the fulfillment of this infrastructure greatly affects mining operations.

Time delay in construction projects is a critical phenomenon and occurs in many construction industries around the world [2], 70% of construction projects have experienced delays in terms of time with an average time delay ranging from 10 to 30% of the duration of the contract [3]. This is following the phenomenon of delays that occurred in the infrastructure project of PT X which experiences delays every year and tends to increase as displayed on Fig. 1. The largest percentage of project delays in the time of 1–15 days (45%) and 16–30 days (24%), exceeds the maximum limit of the Key Performance Indicator (KPI) of the infrastructure team, which is 14 days of delay as presented on Fig. 2. This has an impact on the delay in the operational process of the related user because after the infrastructure facility is completed, the user still needs to procure other operational facilities such as the procurement of tables, chairs, stationery, and others needed for daily operations. So that if the infrastructure development process is late, it will have a domino impact on company operations.

Project communication has a significant portion in influencing project delays. Sanni-Anibire et al. [4]; El-Razek et al. [5]; and Akram Akhund et al. [6] stated that poor site organization and coordination with various parties/stakeholders were the

Fig. 1 PT X infrastructure project data 2016–2019

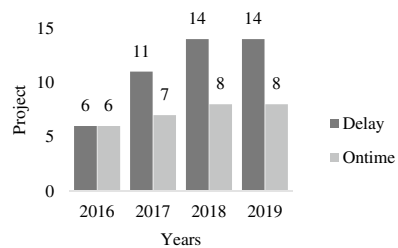
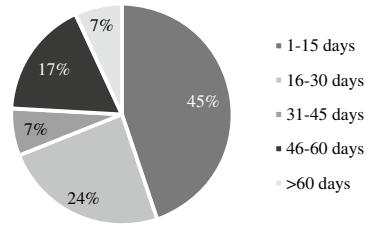


Fig. 2 Percentage of PT X project delayed 2016–2019



dominant factors in project delays. Communication and planning factors are very important to the timeliness of project completion. Poor communication has a quite significant impact. According to Gamil et al. [7], Gamil and Rahman [8], poor communication, lack of, and substandard is one of the main factors for project delays with average severity. 60.89% and harmed the success of the project.

When viewed from the cause, poor communication was caused by the lack of knowledge of stakeholders about the project, the staff was inexperienced, the choice of language that leads to miscommunication and stakeholder identification problem [9]. Another study that examines the causes of the poor communication of the project, said that the lack of effective communication between the parties, effective communication systems, and media are bad, and the low-level communication skills become the dominant cause of the poor communication on the construction project [8].

The phenomenon that occurs in PT X that the communication between the supervisors of PT X and the executing contractor encountered a problem when the main supervisor (Civil Construction Group Leader) was on field leave. On a roster basis at a mining company, employees have the right to leave the field for two weeks after working at the job site for eight weeks. So that in the duration of the main supervisor’s field leave, the project supervisory responsibilities are replaced by other functions in one department such as Human Capital Officer, General Service Officer, Payroll Officer and Comdev Officer. This created a communication problem between the project and the contractor because the replacement supervisor did not have the competence and basic knowledge of project construction and supervision.

This competency and knowledge gap resulted in the ineffective project supervision process because the replacement supervisor did not know about construction and project supervision. This phenomenon can be avoided if there is a knowledge management strategy that is in line with the fulfillment of minimum knowledge and competencies for all functions in the infrastructure project supervisory team. Dalkir [9] states that Knowledge Management is a management strategy with an integrated collaborative approach to create, acquire, organize, access, and use company intellectual assets. Construction projects are knowledge-intensive activities where a lot of knowledge is involved and can produce new knowledge [10].

Therefore, optimization of communication with uniform knowledge about the project in the project supervisory organization with a knowledge management

system is needed to improve the quality of communication between project supervisors and contractors and improve delays in mining infrastructure projects.

1.1 Research Objective

The objective of this study is to define a framework for a knowledge management system strategy that describes the variants of project communication factors that affect project time performance. This study also proposes a baseline for analyzing communication factors and their correlation in future empirical research.

2 Literature Review

2.1 Management of Infrastructure Project in Mining Company

Construction projects in mining are divided into two criteria based on the project value, namely projects above Rp. One hundred million with the procurement process at the Head Office and projects under 100 million with the procurement process at Jobsite. Most of the new infrastructure development projects are projects over 100 million, with the procurement process being carried out at the Head Office after the winner of the job supervision process is determined by the Jobsite team. Infrastructure project management consists of five stages, starting from project initiation, namely user requests related to infrastructure building needs, the project planning process, namely design, real cost estimate, and budget approval, the execution process, namely job package tenders, making work contracts, and Pre-Job Activity and Kick. Off Meeting, the monitoring and control process carried out at the project site by the project supervisory team at Jobsite, to the closing process, namely handover from the contractor to the project supervisory team, evaluation of contractor performance, and handover of buildings to building users.

The organizational structure used in infrastructure projects in PT X is a functional organization model in which the field supervisors are responsible for monitoring and reporting related to the respective functional work at Head Office. So, within its organizational structure no owner Project Manager of the organization for each project, all project managers are centralized at Head Office. And the supervisor at the job site organization consisting of several functional which later merged into one department, where the department is responsible for the implementation and supervision of construction projects.

Therefore, there are several challenges faced, including starting from the initiation process, namely the request from the user regarding the need for infrastructure buildings to the General Service and Infrastructure Department at the Head Office

or HCGS Department at Jobsite, then requests are processed in the form of designs and real cost estimate for review and then evaluate the availability of the budget, if the budget is available and the application has been approved, it will enter the pre-qualification and tender preparation process. Then the bidding process is conducted by the provision, if the value is above 100 million, the project tender process is carried out at the Head Office, whereas if the value of the project is under 100 million, the bidding process is conducted in Jobsite. After determining the winning bidder, then be made to the employment contract the contractor, and the Pre-Job Activity and Kick-Off Meeting.

2.2 Project Time Performance

By definition, a project is a temporary endeavor undertaken to create a product, service, or unique outcome [11]. The temporary nature of projects indicates that the project has a time limit for the duration of the work that will be completed when one or more of the project objectives are achieved. The project is also in the process of achieving the result is limited by the three major aspects of cost, schedule, and quality that must be met. One common cause of loss of productivity in construction activity is the low level of performance due to the time delay. Delays in the construction project have a lot of negative impact on overall project success both on the client/owner and the contractor, ranging from disputes, cost overruns and time, loss of productivity and income, up to termination of the contract [12–14].

Delays can be defined as a situation where the time of project completion was delayed for reasons that may be related to the owner of the work, consultants, and contractors [15]. According to Lo et al. [16] and Trauner et al. [17] that “delay is a situation when an event occurs at a slower than expected or not as planned, take place outside the agreed date in the contract”. “Time delays on projects frequently occur in all phases of a construction project and consequently increase the total project duration” [18]. This is a serious thing to be noticed in the time control on construction work for each day of delay accounts for a significant revenue loss and is unrecoverable [19].

Several previous studies have also examined the causes of delays in construction projects and their impact on construction performance. Globally, the three biggest causes of project delays are financial, communication, and delivery aspects [4, 7]. Research conducted by Sanni-Anibire et al. [4] confirms that the most significant group that causes delays is related to financing. This occurs due to delays in project owner approval of the work that has been done. Ideally, approval can be made if the project owner has carried out a complete inspection and carried out tests to compare with the required specifications, but this is often constrained by poor coordination between the contractor and the project owner, inadequate supervision, inspection, and testing procedures by the project owner, low/traditional communication systems and media, lack of knowledge of project owners about project management, and inexperienced owner staff [4, 6, 8, 19, 20].

2.3 *Project Communication*

Communication is an important aspect of the implementation of construction projects. In construction projects, information is scattered highly specialized and varied given the number of actors involved in all of the construction processes. Communication is the exchange of information between people. This interaction is determined by the rules and norms of social behavior because people are going to translate the meaning and use such information [21, 22].

Previous studies were dealing with project communication management from the perspective of the contractor's project manager, while the perspective of the client/owner as stakeholders are rarely discussed. The perspective of stakeholders requires project management to be more responsive to the external environment forces them to engage in the analysis of the situation and expand their understanding of the project and other stakeholders from external parties [23, 24].

Communication needs in each phase vary, the conceptual phase focusing on the content and recent project, setting rules and objectives of the project [25], the phase of the implementation focused on the explanation of the purpose and objectives of the project and the motivation of the team [26], while the phase of the post-project focus on ensuring the exchange of information related to the activities and results of project documentation between the parties [27]. According to Larson and Gray [28], some core questions need to be answered in Risk Management to create a communication channel communication that is required by the team, among others, (1) what information should be collected and communicated? (2) When this information should be collected and communicated? (3) Who are the recipients of the information? (4) The method for collecting, storing, and communicating information? (5) Restriction of access to information?.

Critical Success Factor of the Project Communication From a project management perspective, critical success factors are characteristics, conditions, or variables that can have a significant impact on project success if properly maintained, maintained, or managed [29]. Delays caused by bad communication can be a slow flow of information, communication channels are not appropriate, the wrong design, wrong interpretation, rework, and more [12, 30–32].

Gamil and Rahman [8] state that the lack of effective communication between the construction occurs 17 times in the different literature after the system and communication platforms that are less effective have taken place ten times, and poor communication skills occurred nine times. Meanwhile, according to Hussain et al. [20], the linguistic barrier, the lack of feedback, poor communication management, and project management skills are poor have the highest repetition frequency of previous studies. It shows that the categories of communication systems, knowledge and skills, and language and culture is the dominant category of successful communication projects.

2.4 Relationship Project Communication on Project Time Performance

Several studies and arguments regarding the relationship between communication and project performance indicate that aspects of communication, information sharing, and coordination are important in the success of the project. Abuhussein et al. [33] stated that the area of project management that most influences project performance is communication management. Communication occurs at any time during the project and affects the relationship between project members and individual commitments in supporting and promoting project success. This shows that project communication is a significant predictor of project performance [34]. In the research of Khattak et al. [35], the perception of project members towards information equality can foster open communication which can increase task assignment which has implications for improving project performance. Assignment of tasks facilitates the division of responsibilities for project coordination and control [36]. Other indicators that affect the effectiveness of communication include the accuracy of the information, constraints and distortions of the information submitted, the suitability of information delivery time, as well as incomplete information in the setting report which disrupts the communication process which affects the project performance [37]. In the context of the project owner (owner) needs to carry out communication management because his involvement has a significant impact on project performance, especially in overseeing the results of work under the contract and reducing the level of project uncertainty [38, 39].

H1: Project communication positively influenced the project time performance.

2.5 Knowledge Management as Mediating Variable

In construction projects, Knowledge Management is a discipline that promotes an integrated approach in the creation, capture, sharing, and reuse of knowledge from certain fields obtained from previously carried out projects [40]. Knowledge Management is also defined as a process where knowledge is acquired, created, communicated, distributed, applied, and effectively used and managed to reach the needs of organizations that appear [41–43]. To describe the process of knowledge systematically, the author adopts the work of Nonaka and Takeuchi [44], i.e., the SECI Model. The reasons for choosing the SECI Model include (1) their work has been widely accepted in management fields such as organizational learning, crowdfunding, new product development, and information technology; (2) The process is carried out includes not only the creation of knowledge but also the transfer of knowledge [45].

The stakeholder knowledge factor, in this case, the project owner, is very important and becomes a significant factor in project communication that affects construction failure [20]. Previous research stated that knowledge management

systems help disseminate and equalize perceptions related to project knowledge, form a balance of project members' contributions, and increase the competence of project members so that the communication aspect can be improved with equal levels of knowledge possessed by all stakeholders [46, 47]. These aspects of project communication help employees to understand the process and be guided by the culture of the organization, and the provision of environmental and technology as a knowledge management system can encourage organizations (employees) to learn and apply new knowledge in project management in the future [48].

Existing research states that knowledge management systems can improve organizational performance by disseminating and equating perceptions regarding project knowledge and understanding customer needs and wants [49]. With the knowledge management system, the capacity to receive knowledge of team members will increase so that it also affects project performance improvement [50]. Reich et al. [51] stated that knowledge management is important for project performance by mediating the knowledge alignment process. Alignment of knowledge is carried out by gathering comprehensive knowledge and specialist knowledge according to the needs of the project. Practical knowledge management assists team members in transferring new knowledge to practice and also improves project performance by gaining a better understanding of project knowledge [52]. Applications that can be used for knowledge management include e-mail, social media, and IT-based document management systems. The knowledge variable that will be managed is related to communication and project coordination that occurs in the project life cycle, referring to the applicable SOPs relating to the role of the project owner and interventions that can be carried out by the project owner organization.

Taking into account the above factors, it can be the basis for measuring the effect of mediation on the relationship of knowledge management and project communication project time performance.

H2: Project Communication Factors influence to become Knowledge Management input.

H3: Knowledge Management Process influences Project Time Performance.

3 Methodology/Materials

This conceptual study area refers to the construction project published literature related to project communication, knowledge management, and project time performance. All publications that match the keywords are included in the literature. The literature study provides empirical articles relating to construction project communication, knowledge management in construction projects as well as project time performance. This study did not include statistical analysis as a major shipment of this article is the conceptual framework in the form of research models and related variables.

3.1 Methodology

The method used for the PT X case study in this article is a desktop study using previous research studies that are relevant from various journals, scientific articles, books, and secondary data from PT X is a mining company that conducted research. This study took a three-step approach consisting of (1) identifying academic journals, (2) collecting, submitting, and filtering relevant articles, then (3) establishing a research model.

Identify Academic Journal Initiative action identifies academic journals that involve material for this research. Table 1 shows the results of the journal information summarized in the process of research include project communication variables.

Collect, Review, and Filter Relevant Article The conceptual study in this research uses academic and public databases such as google scholarships and Mendeley

Table 1 Summary of the variable causes of poor communication of the project

Communication variables	Causative factor	References
Communication system	<ul style="list-style-type: none"> - Lack of communication platforms and systems - The communication channel is not right - The flow of information is slow between the parties - Ineffective reporting system - Submission of inaccurate information 	[8, 31, 32, 53]
Knowledge and skills	<ul style="list-style-type: none"> - Poor communication skills - Have different levels of Education - Have different skill levels - Poor project management skills - Lack of training - Lack of knowledge of the project - The difference in experience - Inexperienced stakeholders - Bad feedback 	[5, 8, 31, 53]
Language and culture	<ul style="list-style-type: none"> - Cultural differences - Language difference - Differences in personal perception 	[20, 22, 32]
Project communication plan	<ul style="list-style-type: none"> - Poor role clarity - Bad stakeholder identification - Unclear project objectives - Lack of a communication plan - Lack of communication during the early stages of the contract - Lack of communication procedures - Instructions or incorrect technical information 	[8, 32]
Project organizations	<ul style="list-style-type: none"> - Weak organizational structure - Multi-organizational interactions 	[8, 53]

search engines for an abroad approach. Subsequently conducted a literature search of the individual publisher of several international journals and proceedings as Elsevier, Emerald, ASCE, Taylor. Screening journals are used for literature studies by reviewing abstracts and keywords to check the research relevance index. Only publications related to the study were subject to literature analysis.

Data Analysis The analysis is divided into two categories, namely: (1) academic analysis that includes the publication of journals and international conferences, and (2) non-academic analysis covering the relevant report from the Institute, theses, and dissertations, as well as general articles that are relevant and reliable.

4 Result and Findings

Based on the literature review mentioned above, project communication is identified and specifically influenced by five variables, including (1) communication system, (2) knowledge and skills, (3) language and culture, (4) project communication plan, and (5) project organization, which has an influence on project performance and knowledge management as a source of knowledge. Knowledge management also influences project performance, specifically with the SECI model, integration and generalization of stakeholder knowledge can be carried out which has an impact on project performance so that the proposed conceptual model is where project management works as a mediator of project communication with project time performance with the SECI model (Fig. 3).

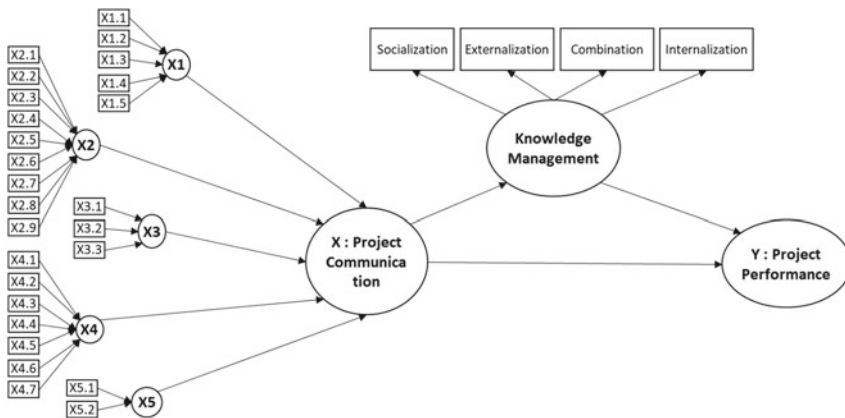


Fig. 3 Knowledge management as a mediator variable

5 Conclusion

The study developed and presented in this paper proposes a possible relationship between the project communication process, knowledge management, and project performance. Many previous studies conducted have shown that knowledge management in construction projects has a positive impact on project performance by equating project understanding and knowledge among all team members in the project organization. Knowledge management is also needed to increase the success rate of the project, and any variable influencing project communication can be developed into an input in the knowledge management process. This study also presents the perspective of the project supervisory organization from the owner, that knowledge management as a mediator function can be developed to improve project communication of supervisory team members that have an impact on project performance.

For further research, the relationship and correlation between independent and dependent variables and moderating variables need to be analyzed using empirical tests where there are several forms of test models such as structural equation models and partial least squares. Further studies need to be carried out test models are most appropriate.

References

1. Kementrian Energi dan Sumber Daya Mineral (2021) Harga acuan. https://www.minerba.esdm.go.id/harga_acuan. Accessed 26 Dec 2020
2. Aliniatwe H, Apolot R, Tindiwensi D (2013) Investigation into the causes of delays and cost overruns in Uganda's public sector construction projects. *J Constr Dev Countries* 18(2):33–47
3. Assaf SA, Al-Hejji S (2006) Causes of delay in large construction projects. *Int J Project Manage* 24(4):349–357. <https://doi.org/10.1016/j.ijproman.2005.11.010>
4. Sanni-Anibire MO, Zin MR, Olatunji SO (2020) Causes of delay in the global construction industry: a meta analytical review. *Int J Constr Manag*. <https://doi.org/10.1080/15623599.2020.1716132>
5. Abd El-Razek ME, Bassion HA, Mobarak AM (2008) Causes of delay in building construction projects in Egypt. *J Constr Eng Manag* 134(11):831–841. [https://doi.org/10.1061/\(asce\)0733-9364\(2008\)134:11\(831\)](https://doi.org/10.1061/(asce)0733-9364(2008)134:11(831))
6. Akhund MA, Khoso AR, Memon U, Khahro SH (2017) Time overrun in construction projects of developing countries. *Imp J Interdiscip Res* 3(4):1–6
7. Gamil Y, Ismail AR, Nagapan S (2019) Investigating the effect of poor communication in terms of cost and time overruns in the construction industry. *Int J Constr Supply Chain Manage* 9(2):94–106. <https://doi.org/10.14424/ijcscm902019-94-106>
8. Gamil Y, Rahman IA (2017) Identification of causes and effects of poor communication in construction industry: a theoretical review. *Emerg Sci J* 1(4):239–247. <https://doi.org/10.28991/ijse-01121>
9. Dalkir K (2005) Knowledge management in theory and practice. Elsevier Butterworth-Heinemann, Burlington. <https://doi.org/10.4324/9780080547367>

10. Ganiyu SA, Egbu CO, Cidik MSM (2018) Knowledge management and BIM practices: towards a conceptual BIM-knowledge framework. In: Psychon international conference, Wolverhampton, UK, December 2018
11. Project Management Institute (2017) A guide to the project management body of knowledge, 6th edn. Project Management Institute Inc., Pennsylvania
12. Sambasivan M, Soon YW (2007) Causes and effects of delays in Malaysian construction industry. *Int J Project Manage* 25(5):517–526. <https://doi.org/10.1016/j.ijproman.2006.11.007>
13. Santoso DS, Soeng S (2016) Analyzing delays of road construction projects in cambodia: causes and effects. *J Manag Eng* 32(6):1–11. [https://doi.org/10.1061/\(asce\)me.1943-5479.0000467](https://doi.org/10.1061/(asce)me.1943-5479.0000467)
14. Tumi SAH, Omran A, Pakir AHK (2009) Causes of delay in construction industry in Libya. In: The international conference on economics and administration, University of Bucharest, Romania, 14–15 Nov 2009
15. Aibinu AA, Jagboro GO (2002) The effects of construction delays on project delivery in Nigerian construction industry. *Int J Project Manage* 20:593–599. [https://doi.org/10.1016/s0263-7863\(02\)00028-5](https://doi.org/10.1016/s0263-7863(02)00028-5)
16. Lo TY, Fung IW, Tung KC (2006) Construction delays in Hong Kong civil engineering projects. *J Constr Eng Manage* 132(6). [https://doi.org/10.1061/\(ASCE\)0733-9364\(2006\)132:6\(636\)](https://doi.org/10.1061/(ASCE)0733-9364(2006)132:6(636))
17. Trauner TJ, Lowe JS, Furniss BJ, Manginelli WA, Nagata MF (2009) Construction delays: understanding them clearly, analyzing them correctly second edition. Butterworth-Heinemann. <https://doi.org/10.1016/B978-1-85617-677-4.X0001-3>
18. Yang J-B, Ou S-F (2008) Using structural equation modeling to analyze relationships among key causes of delay in construction. *Can J Civ Eng* 35(4):321–332. <https://doi.org/10.1139/L07-101>
19. Memon AH, Abdul Rahman I, Abdullah MR, Aziz AAA (2011) Time overrun in construction projects from the perspective of project management consultant (PMC). *J Surv Constr Property* 2(1):1–13. <https://doi.org/10.22452/jscp.vol2no1.4>
20. Hussain MA, Othman AAE, Gabr HS, Aziz TA (2018) Causes and impacts of poor communication in the construction industry. In: 2nd International conference: sustainable construction and project management-sustainable infrastructure and transportation for future cities, Egypt, 16–18 Dec 2018
21. Gayeski DM (1993) Corporate communication management: the renaissance communicator in information-age organizations. Focal Press
22. Gomez-ferrer AP (2017) Communication problems between actors in construction projects. Thesis, AALTO University
23. Parker DW, Kunde R, Zappetella L (2017) Exploring communication in project-based interventions. *Int J Product Perform Manag* 66(2):146–179. <https://doi.org/10.1108/ijppm-07-2015-0099>
24. Welch M, Jackson PR (2007) Rethinking internal communication: a stakeholder approach. *Corp Commun: Int J* 12(2):177–198. <https://doi.org/10.1108/13563280710744847>
25. Katzenbach JR, Smith DK (1993) The discipline of teams. *Harvard Business Review*, March–April 1993
26. Mukherjee D, Lahiri S, Mukherjee D, Billing TK (2012) Leading virtual teams: how do social, cognitive, and behavioral capabilities matter? *Manag Decis* 50(2):273–290. <https://doi.org/10.1108/00251741211203560>
27. Turkulainen V, Aaltonen K, Lohikoski P (2015) Managing project stakeholder communication: the qstock festival case. *Proj Manag J* 46(6):74–91. <https://doi.org/10.1002/pmj.21547>
28. Larson EW, Gray CF (2011) Project management: the managerial process, 5th edn. McGraw-Hill/Irwin, New York
29. Milosevic D, Patanakul P (2005) Standardized project management may increase development projects success. *Int J Project Manage* 23:181–192. <https://doi.org/10.1016/j.ijproman.2004.11.002>

30. Love PED, Li H (2000) Quantifying the causes and costs of rework in construction. *Constr Manag Econ* 18(4):479–490. <https://doi.org/10.1080/01446190050024897>
31. Tipili LG, Ojeba PO, Ilyas SM (2014) Evaluating the effects of communication in construction project delivery in Nigeria. *Global J Environ Sci Technol* 2(5):2360–7955
32. Dainty A, Moore D, Murray M (2006) *Communication in construction: theory and practice*. Routledge, London. <https://doi.org/10.4324/9780203358641>
33. Abuhussein R, Hyassat M, Sweis R, Alawneh A, Al-Debeie M (2016) Project management factors affecting the enterprise resource planning projects' performance in Jordan. *J Syst Inf Technol* 18(3):230–254. <https://doi.org/10.1108/jisit-03-2016-0020>
34. Ahimbisibwe A, Nangoli S (2012) Project communication, individual commitment, social networks, and perceived project performance. *J Afr Bus* 13(2):101–114. <https://doi.org/10.1080/15228916.2012.693436>
35. Khattak SM, Iqbal MZ, Ikramullah M, Raziq MM (2020) The mechanism behind informational fairness and project performance relationship: evidence from Pakistani construction organizations. *Int J Product Perform Manag* 70:151–178. <https://doi.org/10.1108/ijppm-04-2019-0164>
36. Ko D-G, Lee G, Keil M, Xia W (2019) Project control, coordination, and performance in complex information systems outsourcing. *J Comput Inf Syst* 61(3):256–266. <https://doi.org/10.1080/08874417.2019.1606687>
37. Kwofie TE, Aigbavboa CO, Machethe SO (2019) Nature of communication performance in non-traditional procurements in South Africa. *Eng Constr Archit Manag* 26(10):2264–2288. <https://doi.org/10.1108/ecam-02-2018-0044>
38. Chou J-S, Yang J-G (2013) Evolutionary optimization of model specification searches between project management knowledge and construction engineering performance. *Expert Syst Appl* 40(11):4414–4426. <https://doi.org/10.1016/j.eswa.2013.01.049>
39. Karlsten JT (2010) Project owner involvement for information and knowledge sharing in uncertainty management. *Int J Manag Proj Bus* 3(4):642–660. <https://doi.org/10.1108/17538371011076091>
40. Lin Y-C, Lee HY (2012) Developing project communities of practice-based knowledge management system in construction. *Autom Constr* 22:422–432. <https://doi.org/10.1016/j.autcon.2011.10.004>
41. Alavi M, Leidner DE (2001) Review: knowledge management and knowledge management systems: conceptual foundation and research issues. *MIS Q* 25(1):107–136. <https://doi.org/10.2307/3250961>
42. Bhatt GD (2001) Knowledge management in organizations: examining the interaction between technologies, techniques, and people. *J Knowl Manag* 5(1):68–75. <https://doi.org/10.1108/13673270110384419>
43. Karamente K, Aduwo JR, Mugejjera E, Lubega J (2009) Knowledge management frameworks: a review of conceptual foundations and a KMF for IT-based organizations *Information Technology* p 35–57
44. Nonaka I, Takeuchi H (1995) *The knowledge-creating company: how Japanese companies create the dynamics of innovation*. Oxford University Press, England
45. Choi B, Lee H (2002) Knowledge management strategy and its link to knowledge creation process. *Expert Syst Appl* 23:173–187. [https://doi.org/10.1016/s0957-4174\(02\)00038-6](https://doi.org/10.1016/s0957-4174(02)00038-6)
46. Shatti LA, Bischoff JE, Willy CJ (2017) Investigating the effectiveness of team communication and the balance of member contributions on knowledge acquisition. *Knowl Manag Res Pract* 16(1):51–65. <https://doi.org/10.1080/14778238.2017.1405775>
47. Yap JBH, Skitmore M (2020) Ameliorating time and cost control with project learning and communication management: leveraging on reusable knowledge assets. *Int J Manag Proj Bus* 13(4):767–792. <https://doi.org/10.1108/ijmpb-02-2019-0034>
48. Sekar G, Viswanathan K, Sambasivan M (2018) Effects of project-related and organizational-related factors on five dimensions of project performance: a study across the construction sectors in Malaysia. *Eng Manag J* 30(4):247–261. <https://doi.org/10.1080/10429247.2018.1485000>

49. Haider SA, Kayani UN (2020) The impact of customer knowledge management capability on project performance-mediating role of strategic agility. *J Knowl Manag* 25:298–312. <https://doi.org/10.1108/jkm-01-2020-0026>
50. Popaitoon S, Siengthai S (2014) The moderating effect of human resource management practices on the relationship between knowledge absorptive capacity and project performance in project-oriented companies. *Int J Project Manage* 32(6):908–920. <https://doi.org/10.1016/j.ijproman.2013.12.002>
51. Reich BH, Gemino A, Sauer C (2014) How knowledge management impacts performance in projects: an empirical study. *Int J Project Manage* 32(4):590–602. <https://doi.org/10.1016/j.ijproman.2013.09.004>
52. Yang L-R, Chen J-H, Wang H-W (2012) Assessing impacts of information technology on project success through knowledge management practice. *Autom Constr* 22:182–191. <https://doi.org/10.1016/j.autcon.2011.06.016>
53. Rahman IA, Memon AH, Karim ATA (2013) Significant factors causing cost overruns in large construction projects in Malaysia. *J Appl Sci* 13(2):286–293. <https://doi.org/10.3923/jas.2013.286.293>

Portable Structure for Post-disaster Temporary Shelter



Bayu Ariaji Wicaksono, Dalhar Susanto, and Emirhadi Suganda

Abstract This paper aims to review about application of portable structures for post-disaster temporary shelter. Appropriateness in applying portable structures as temporary shelters are observed based on parameters such as ease in availability and also user's comfort. The data in this paper were derived based on literature studies by examining the theory about post-disaster temporary shelter, design requirements, and portable structure by showing some examples that have been developed. The most important aspects in the assessment are ease and speed in moving and also erecting process, but without ignoring the user well-being. According to the review's results, a deployable scissors structure is the most suitable to apply as a temporary shelter. It is because of the simple structure system which is joining each bar with hinged in the middle and the end, so the movement of one bar will affect the other bars and result in structure transformation from a small closed compact configuration to the large open. This structure has some advantages, like being easily stowed, erected, and sustainable. In the case of sustainability, this structure can accommodate various temporary activities. Moreover, the bar components can be reused as materials for the next development in the recovery process.

Keywords Temporary shelter · Portable structure · Deployable · Scissors · Simply structure system

1 Introduction

Indonesia is a disaster-prone country, it is due to its geographic location along the pacific ring of fire and also the hydrological condition. This results in natural disasters like earthquakes, volcanic eruptions, tsunami, floods, landslides, etc. [1]. Data from Indonesia National Disaster Management Authority (BNPB) shows there are 2,952 disasters that happened during January–December 2020, and it has caused

B. A. Wicaksono (✉) · D. Susanto · E. Suganda
Department of Architecture, Universitas Indonesia, Depok 16424, Indonesia
e-mail: bayu.ariajiw@gmail.com

© The Author(s), under exclusive license to Springer Nature Singapore Pte Ltd. 2022
H. A. Lie et al. (eds.), *Proceedings of the Second International Conference of Construction, Infrastructure, and Materials*, Lecture Notes in Civil Engineering 216, https://doi.org/10.1007/978-981-16-7949-0_46

511

the damage of almost 42,762 houses [2]. Since the people can't stay in their houses, it requires them to stay in disaster relief shelters to obtain protection, safety, comfort, and security [3]. In the first phase, people will stay in an emergency shelter. In providing this facility don't need to construct a temporary building because it only refers to the aftermath of the disaster. Therefore, they will use existing building space like a public or social facility. Due to the limitation of this facility, such as space and privacy, people will be moved to the temporary shelter. This facility is designed to suit family or group size, so it can provide privacy and more space to carry out simple activities and ensure them to rest in good condition for recover their emotional and psychological [4]. An emergency situation requires the facilities must be available as soon as possible. In this context, flexible architecture can be an instant solution to answer that problem is because the characters of flexible architecture are dynamic rather than stagnant. They are possible for moving and transforming to be used in different functions [5]. In order to achieve it, the building must be applied portable structure because the building will be lighter and also able to through assembling and also mechanisms systems of the components, so it allows the building to be stowed and moved by vehicles and time-efficient for erecting process in different locations [6]. Considering the special behavior of the structure and its advantages in accommodating sheltering facilities during emergency situations. This paper aims to discuss the most suitable type of portable structure to apply as a temporary shelter.

2 Temporary Shelter and Portable Structure

2.1 Temporary Shelter

Temporary shelter is an instant facility for sheltering that prioritizing speed and costs efficiency in construction and also have a limited lifetime [7]. The refugees stay in this facility only for a short time, just a few weeks after the disaster [4]. Although speed is the most important aspect, we must consider the human aspect. Temporary shelter is more than just a facility. It is a process for helping rehabilitation, both psychological and mental [3]. As seen on Tables 1 and 2 [4], there are some requirements in providing temporary shelter as temporary accommodation.

2.2 Temporary Shelter with Portable Structure

Portable structures are designed with prioritizing mobility and efficient aspects. It allows the building to move easily and is also time-efficient in the erection process to a different location. It will be a good solution functionally, structurally, and spatially in an emergency situation. Flexible Architecture with portable structure classified according to the configuration of products and erection process. There are

Table 1 Requirements for temporary shelter: designing for people, adequate dimensions, local-oriented design, comfort, and easy to transport [4]

Requirements	Explanation
Designing for People	Feeling like home. It will make the refugees comfortable psychologically and mentally, e.g., gathering with their family, doing the daily activities, also getting privacy. According to the aforementioned, temporary shelter must be designed only for groups or families [3]
Adequate dimensions	Space dimensions affect comfort in movement. According to International Federation of Red Cross and Red Crescent Societies [7], the minimum area for one person is 3.5 m ² , and the building minimum for covering space is 18 m ² , it allows five people to live there, and also the headroom minimum 2.4 m [8]
Local-oriented design	A shelter with a local-oriented design will be more efficient because it uses local material and construction methods. But if it is not possible, it must be imported from other areas and using modern technology
Comfort	Comfort aspects in temporary shelter include thermal comfort, lighting, and ventilation, either natural or artificial. Because this paper just give an overview based on literature review, the author just explain according to the technical product specification
Easy to transport	Due to the Limited access in reaching for disaster areas, the shelter should be designed small and lightweight to adjust the capacity of the vehicle, e.g., trailer truck or pickup car

ready-made units, demountable, and deployable [12]. To easy understanding the explanation, the author will show some examples of temporary shelters with portable structures.

Ready-Made Units This building configuration carries to the locations as one piece ready-to-use unit without requiring an assembly process. It is good as a very instant solution, but the most disadvantage of this type is the limited area. It is because of the limited capacity of the vehicle to carry them [13]. But in some cases, the unit can be separated into big components. One of the examples shown in this paper is Exo Shelter by Michael McDaniel are displayed on Fig. 1 [14]. These shelter components are separated as building envelopes and floor components. It can be assembled using a magnetic system. Separating the building envelopes will allow them to be stacked like a cup of coffee to save space in the shipping process. The building form is a trapezoid, where the walls and roof are sloping. From that form, it will be easier to stack. This shelter covers a 6.76 m² area with headroom 3 m, and it has a capacity for four people with a layout of leveling bunk beds. If the room is used for other functions, the bunk bed can be folded to the wall. The latest technology from this shelter is to allow electric supply from portable power generators, so it allows the refugees to use it for lighting, charging a gadget, and also get an air conditioner. This shelter has no ventilation system that can be opened but can allow natural lighting.

Demountable It consists of components that allow being assembled and disassembled with dry-system [15] and packaging in separated small components, it

Table 2 Requirements for temporary shelter: simple construction, flexibility, long term option, durability, protection, outdoor space, and non-pollutant solution [4]

Requirements	Explanation
Simple construction	Easy and fast in erecting process. It can be done with non-professional people also minimum auxiliary equipment. Because if the construction system of shelter is complex, it requires more training and resources to erect the shelter and potential to delay [3]
Flexibility	It allows users to modified their shelter unit either space or form according to the function and user members. e.g., unit expansion and adjusting layout space
Long term option	The chance to reuse shelter unit also the component for different function
Durability	Because the portable structure in this paper uses modern material and technology, it is possible to use it for a few weeks. And it can be reused for another emergency situation
Protection	Shelter as a weather shield. It gives some protection to the user from snow, wind, or other climates. One requirement in a tropical climate like Indonesia, the shelter must respond to the rain. So the roof must be gable or curve [9]
Outdoor space	The outdoor area between shelters can be used as a social facility and other activities. According to the Sphere project [10], the minimum distance for each temporary shelter unit is 2 m or twice the height of the building because it's about fire safety risk
Non-pollutant solution	In minimizing pollution, the building must adopt a sustainable aspect. In the case of eco-friendly materials and constructions, it enables them to reuse and recycle. Basically, a portable structure is a sustainable architecture. It is because the prefabricated material will minimize waste and site impact during the construction process. Also, upgrading and improving shelters is cheaper than moving from phase to phase [11]



Fig. 1 a Separating component between building envelope and floor, b stacked building envelope like a cups of coffee, c bunk bed inside the shelter [14]

will be more efficient in the logistic process. In Indonesia, National Disaster Management Authority (BNPB) is using tents as temporary shelters for refugees as shown on Fig. 2. It's a dome configuration tent that consists of configurable stainless steel pipe and polyester fabric as building envelope, and it covers a 20.25 m² area and suits four people [16]. For the headroom, according to the information from the tent factory, it is almost 3 m. These tent components can be disassembled, folded, and packaged in 650 D polyester bags with small dimensions. Another

example of demountable is a shelter that consists of a modular panel and metal frame, a better shelter by IKEA presented on Fig. 2 [17]. It has been used in several countries to accommodate refugees of disasters, both natural or conflicts, and also to use as an emergency health facility during pandemic Covid-19. With area 17.49 m² and headroom 2.83 m, it suits five people. This facility also using solar panels as the electrical resource and can be packaged in a box with dimensions 2.020 m 1.090 m × 0.52 m (L × W × H).

Deployable Deployable is a structure that consists of the components that have been integrated with mechanisms, that it allows transforming from small compact configuration to wide compact also stable and effective in carrying load [18]. The mechanisms are kinetic and air-supported, for architectural application, the structure is composed of components like bar, panel, and membrane [18]. The first type is kinetic mechanisms, and the components connect with a hinge. In structure with bar component, it consists of many bars. One of the simplest mechanisms and also multi-purpose is a scissors structure. Which are consists of two bars connected by a revolute joint in the middle also the end of the bar. One movement of the bar can affect the other bars, so it can be a wide, stable structure. One of the scissors configurations is barrel vault, and it can give protection from the weather by adding membrane to the structure can be seen from Fig. 3. The uniqueness of this structure is that it can be folded into a small configuration. Previous research shows that in the open configuration, it covers 20.2 m² area, headroom 3 m, and can accommodate five people. In folding condition, the dimension are 0.9 m × 1.7 m 0.5 m (L × W × H) [19]. Another type with kinetic mechanisms consists of panel components. The panels are connected by hinged, and the panel plays the role of supporting structure and roof. This structure also can be folded, but it is much bigger and also heavy because of the dimension of the panel [18]. An example of the project with that system is a folded house from china with an area of 27.25 m² and headroom 2.415 m is presented on Fig. 4. In folding condition, it has dimensions 4.89 m × 2.52 m (L × W), the folded dimensions are affected by the dimension of panel components [20]. The second type, also the last type of deployable structure, is pneumatic, which is composed of a membrane and can be erected by filling the air using an air compressor. An example of a pneumatic system in this paper is displayed on Fig. 5, a product that is sold in the market with a cover area of 29 m² and headroom 2.6 m. Because all of the components are membrane, it will be more elastic and can be folded in very small configuration [21].

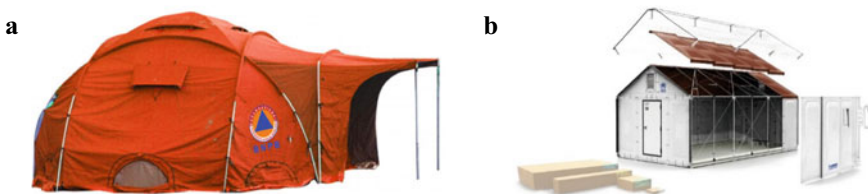


Fig. 2 a Dome tent [16], b shelter consists of plastic panel [17]

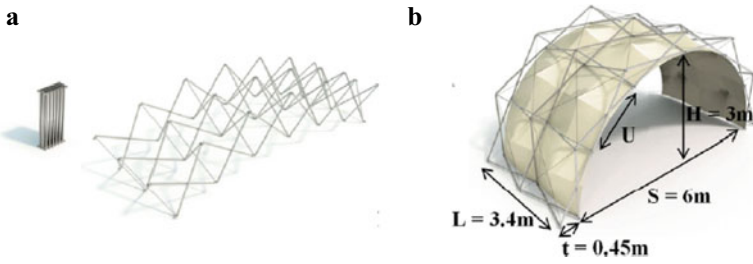


Fig. 3 a Scissors mechanism [19], b additional membrane for stiffness and cover [19]

Fig. 4 The structure consists of panel components and foldable mechanisms [20]

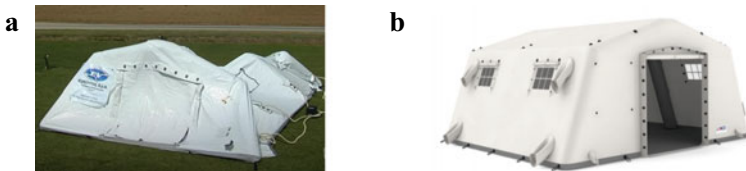


Fig. 5 a Erection process in pneumatic structure [22], b building erected [21]

3 Discussions

This chapter will assess a portable structure according to the design requirements of a temporary shelter as displayed on Tables 3 and 4. Through this assessment, it will result in the most suitable portable structure system for emergencies.

From Tables 3 and 4, we can see that portable structures and their examples have advantages in terms of ease of moving and assembling. Among them, the type of portable structure that can achieve temporary shelter design requirements are demountable and deployable. It is because the building can achieve minimum space dimensions and also can be packaged in one pack of small components, so it will be easy to stow and transport. Packaging is an important aspect because access in post-disaster situations is limited, so it can affect the ability of vehicles to ride on the road. According to the case study, the most efficient buildings in case of easy carrying with the small vehicle are tent, better shelter, scissors structure, and pneumatic. In case of allowing more opportunity to use for other functions and space arranging, all types must be applying a square floor plan. Among them also,

Table 3 Portable structure assessment according to the requirements: designing for people, adequate dimensions, protection, simple construction system

Parameter	Ready-made units	Demountable	Deployable
Designing for people	Minimum space and arranged layout (Bunk bed installation), only can accommodate limited function interchangeably	Open plan space can accommodate more functions according to the users' needs and it can be used simultaneously	
Adequate dimensions	Area less than the minimum requirement, it is not comfortable for human movement	They are made based on the minimum requirement, so they will be comfortable for human movement	
Protection	Gable roof	<ul style="list-style-type: none"> - Tent with curved roof - Bettershelter with gable roof 	<ul style="list-style-type: none"> - Scissors structure with curved roof - Foldable panel with a flat roof - Pneumatic with gable roof
Simple construction system	Only need to stick the building envelope with the floor component using a magnetic system	Assembling separated components with a dry system	<ul style="list-style-type: none"> - Since components of scissors structure are bar and connected by the hinge joint. It will be easy to erect only with three people [19] - Deployable structure foldable panel, the components are integrated with hinge joint, but because the dimension is big, It needs a mobile crane to unload and for erecting need more people because the panel is heavy. And for pneumatic type is need to use the air compressor and building can be erecting itself automatically

the one that has the advantage in terms of ease and speed in the assembly also possible for space expansion is scissors structure, because the bar components have been connected by hinges and integrated with the kinetic system that enables the construction process is only by folding and can be done by hand-operated and non-skilled personnel also we can add more scissors portal to add more space. If it is no longer used as a temporary shelter, all of the temporary shelters can still be

Table 4 Portable structure assessment according to the requirements: easy to transport, flexibility, long term option, comfort, durability, outdoor space, and non pollutant solution

Parameter	Ready-made units	Demountable	Deployable
Easy to transport	Must be carried with a trailer truck	Able to carry with a small truck or pickup car	Both scissors and pneumatic mechanisms can be carried with a small truck or pickup cars But for the foldable panel, it must be carried with a trailer truck due to its big panel's dimension
Flexibility	The flexibility aspect is only in arranging space-layout, but it is limited, and for space expansion, more shelter units must be added [14]	For both tent and bettershelter, because the layout is open, it can be free to arrange. But only better shelter that can be expanded	Due to the open layout in scissors mechanism, foldable panel, and pneumatic. The unit layout is free to arrange. But among the three units, only scissors can be expanded with a simple solution by adding more scissors portals [19]
Long term option	The shelter unit can accommodate other functions, but it is very limited due to the small area causes limited arranging of the layout and also space to save the stuff. For sustainability reasons, reusing the components directly for other functions is limited, e.g., only door and bunk bed and other small parts. But for reusing big components like building enclosure needs more recycling process	Because the tent form is a dome and has a circle layout, it causes limited to rearrange the space. It's very different with better shelter, considering the square layout and perpendicular wall, it will be more variant in arranging the space. But for reusing components, both tent and bettershelter only bar components can use directly, and the others need more process for recycling and reuse	Because the floor plan in scissors mechanism, foldable panel, also pneumatic is square, it will be easier to rearrange the layout and reuse it for other functions. But only in the scissors mechanism that almost all of the components can be reused directly because their components are still intact and multifunction [19] In pneumatic and foldable panel need to advance process for reuse component
Comfort	The Source of lighting and ventilation can be artificial or natural. But, ventilation relies more on the air conditioner. It is because the window cannot be open if we want to use natural	More in artificial lighting, because the window is small. But the ability of window can be opened, and it allows natural ventilation	According to the reference about shelter with scissors structure, it just only explains the membrane as a wall and roofing. They do not provide doors and windows. So it can't be

(continued)

Table 4 (continued)

Parameter	Ready-made units	Demountable	Deployable
	ventilation. It is simply by opening the door		explained in this paper [19] For pneumatic and foldable panels, they have small windows that can be open, but for lighting, they will be better by using artificial lighting
Durability	Durable for several weeks		
Outdoor space	The shelter position must fit the standard distance. But for further expanded, each refugee must discuss it first to avoid violation of the distance rule		
Non-pollutant solution	Due to the components are prefabricated, they are truly sustainable in terms of the construction process and minimizing site impact. But for pneumatic type and also foldable panels. They are less sustainable because they need auxiliary tools for the erection process like an air compressor and mobile crane, which need electrical power to operate them		

used to accommodate other temporary functions. In the case of sustainability aspects, almost all of the components of portable structures can still be reused for other development.

4 Conclusions

Flexible architecture with portable structures is an instant solution for the post-disaster temporary sheltering facility. But in designing them, we need to consider the minimum requirements. Because it is not just the product but a process. The most important aspect to achieve is movability, rapid erection process, comfortable space, and less negative impact to the environment. Among them, deployable scissors structure almost fulfills all aspects in the requirements, because its behavior can be transformed from small configuration to wide configuration, it will be easy to stow and transport. And also, due to the components are connected with a hinged joint and integrated with the kinetic system, it allows easy and rapid erection with non-professional people. In the case of sustainability aspect, that is the minimum damage to the site, minimal material waste, and also the components can be reused directly for other functions. Besides its advantages, the deployable scissors structure also has disadvantages that need to be further developed in terms of energy resources for electrical, also a windows system to allow natural lighting and ventilation.

References

1. Yanuarto T, Pinuji S, Utomo AC, Satrio IT (2019) Buku saku tanggap tangkas tangguh menghadapi bencana (4th ed). Pusat Data Informasi dan Humas BNPB, Jakarta Timur
2. Bidang Informasi (2021) Kejadian bencana tahun 2020. <https://bnpb.go.id/infografis/kejadian-bencana-tahun-2020>. Accessed 21 March 2021
3. Bashawri A, Garrity S, Moodley K (2014) An overview of the design of disaster relief shelters. *Proc Econ Fin* 18:924–931. [https://doi.org/10.1016/s2212-5671\(14\)01019-3](https://doi.org/10.1016/s2212-5671(14)01019-3)
4. Félix D, Monteiro DV, Branco JM, Bologna R, Feio A (2014) The role of temporary accommodation buildings for post-disaster housing reconstruction. *J Housing Built Environ* 30(4):683–699. <https://doi.org/10.1007/s10901-014-9431-4>
5. Anas DM, Khan S, Nisar Z (2017) Flexible architecture: optimization of technology and creativity. *Int J Eng Technol* 9:510–520. <https://doi.org/10.21817/ijet/2017/v9i3/170903s078>
6. Cerrahoglu M, Maden F (2020) A review on portable structures. In: ATI 2020 “Smart Cities and Smart Building”. The international symposium of architecture, technology and innovation, Yaşar University, Izmir, Turkey, 25–28 Aug 2020
7. International Federation Red Cross and Red Crescent Societies (2013) Post-disaster shelter: ten designs. International Federation of Red Cross, Geneva
8. Palang Merah Indonesia (2019) Panduan shelter untuk kemanusiaan. Kementerian Sosial Republik Indonesia, Indonesia
9. Prasetyo YH, Astuti S (2017) Ekspresi bentuk klimatik tropis arsitektur tradisional nusantara dalam regionalisme. *Jurnal Permukiman* 12(2):80–93
10. Sphere Association (2018) The sphere handbook: humanitarian charter and minimum standards in humanitarian response. Practical Action Publishing, United Kingdom
11. United Kingdom’s Department for International Development, International Organization for Migration, Swedish International Development Cooperation Agency (2012) Transitional shelter guidelines. Shelter Center. www.sheltercentre.org
12. Krishnan S, Liao UY (2019) Integrating shelter design and disaster education in architectural curriculum. In: 126th Annual conference and exposition American Society for Engineering Education, Tampa Convention Centre, 16–19 June 2019
13. Kronenburg R (2008) Portable architecture: design and technology. Birkhäuser. <https://doi.org/10.1007/978-3-7643-8325-1>
14. Inhabitat (2011) Reaction housing system: a rapid response flat-pak emergency shelter. <https://inhabitat.com/reaction-housing-system-a-rapid-response-flat-pak-emergency-shelter/>. Accessed 19 April 2021
15. De Temmerman N, Mira LA, Vergauwen A, Hendrickx H, De Wilde WP (2012) Transformable structures in architectural engineering. In: 6th International conference on high performance structures and materials, New Forest, 19–21 June 2012, HPSM 2012, vol 124, p 457–468
16. Badan Nasional Penanggulangan Bencana Editorial (2020) Standar spesifikasi teknis minimal peralatan penanggulangan bencana. Badan Nasional Penanggulangan Bencana, Jakarta Timur
17. Fairs M (2017) IKEA refugee shelter to be redesigned following safety fears and design flaws. <https://www.dezeen.com/2017/04/27/ikea-unhcr-refugee-better-shelter-redesign-safety-fears-flaws/>. Accessed 19 April 2021
18. Adhrover ER (2015) Deployable structures. Laurence King Publishing, London
19. Mira LA, Thrall AP, De Temmerman N (2014) Deployable scissors arch for transitional shelters. *Autom Constr* 43:123–131. <https://doi.org/10.1016/j.autcon.2014.03.014>

20. DeepBlue Smarthouse (2021) Portable emergency shelter. <https://smarthousing.cn/oldsite/supplier-39227-portable-emergency-shelter.html>. Accessed 19 April 2021
21. Lanco (2021) AZF 29 self-erecting tents. <https://www.lanco-tents.com/azf-29>. Accessed 19 April 2021
22. Losberger De Boer Deutschland (2013) Rapid deployment tent/inflatable tent/self erecting tent/rescue tent/hospital tent TAG. <https://www.youtube.com/watch?v=3LfJrmHF5NE>. Accessed 19 April 2021

Concrete Damage Risk Rating Examination to Existing Buildings



Henny Wiyanto, Reagen Yocom, and Glen Thenaka

Abstract Building assessment is a measure that has to be taken by building management to the existing building or operational building because it is very critical to the safety and comfort of the building's users. One of the commonly used building assessment methods is visual assessment. Visual assessment is a non-destructive concrete assessment that is done to identify and define different concrete conditions, which can be seen during its' lifetime. Concrete damage assessment is done to estimate the risk rating of concrete damage against the existing building structures. The risk assessment process is done in three steps: risk identification, risk analysis, and risk evaluation. There are three risk ratings: low, medium, and high. Risk rating examination of the existing building is determined based on the concrete damage type and condition rating value on the building structure element, concrete damage frequency on the building, and critical weight of the building structure element. Risk rating examination results of concrete damage are used to determine priorities building structure element repair.

Keywords Concrete damage · Risk rating · Visual assessment · An existing building

1 Introduction

Concrete damage on reinforced concrete structures cannot be avoided. This is caused by a lot of factors, one of which is poor construction implementation and low material quality. As time goes on, existing building usage also predominantly affects

H. Wiyanto (✉) · R. Yocom · G. Thenaka
Department of Civil Engineering, Faculty of Engineering, Universitas Tarumanagara, Jakarta 11440, Indonesia
e-mail: hennyw@ft.untar.ac.id

the building's condition. Improper building usage will cause physical damage to the building itself. Building usage is the act of using a building according to its' intended function [1, 2]. Oftentimes, building management or owners neglect the building's condition and do not perform proper building assessments because of cost factors. Even though building condition assessment can lower the risk of further building damage, which severely endangers the building's users, that is very risky towards the safety and comfort of building users. Building condition assessment is done with assessment towards concrete damage condition, which is done to estimate the risk of structural and non-structural damage in order to perform building reparation. According to ISO 31000:2009 [3], the risk assessment process is done with three steps: risk identification, risk analysis, and risk evaluation. The search for references about building condition rating has been performed from multiple sources, which are [4–21]. Based on that problem, the risk assessment needs to be done towards concrete damage to the existing building structure.

2 Method

Concrete damage risk rating examination to the existing building is performed in the following steps.

2.1 Risk Identification

Concrete damage risk identification is a step to identify the amount and location of concrete damage on a building structure that can lower a building's functionality. Concrete damage location is divided into four structure elements: shear wall, column, beam, and slab. Concrete damage identification is made using visual assessment.

2.2 Risk Analysis

Concrete damage risk analysis is a step done to assess risk towards the concrete damage types that have already been identified according to the damage amount and location. Damage location affects the structure element critical weight. The amount of concrete damage describes the damage frequency of a damage type on the building.

Concrete damage risk assessment is done with the following steps:

Determining Concrete Damage Type and Condition Rating Based on concrete damage type and condition rating search results for building from multiple

Table 1 Concrete damage type and condition rating [20]

No.	Damage type	Condition rating
1	Craze crack	2.54
2	Mapping crack	3.00
3	Random cracks	3.36
4	Delamination	3.25
5	Pop-outs (small)	2.75
6	Pop-outs (medium)	2.93
7	Pop-outs (large)	3.36
8	Scaling (light)	2.53
9	Scaling (medium)	2.88
10	Scaling (severe)	3.13
11	Scaling (very severe)	3.47
12	Spall (small)	2.86
13	Spall (large)	3.40

references, namely [4–18, 22–24], concrete damage type and condition rating are determined for existing buildings in Indonesia by Wiyanto et al. in [19, 20] as in Table 1.

Criteria and measures for each concrete damage condition rating are as shown in Table 2.

Determining Concrete Damage Frequency Concrete damage frequency is determined based on the amount of damage done to the building. Damage frequency is determined using three criteria based on Table 3.

Determining Concrete Damage Risk Rating The concrete damage risk rating is determined based on concrete damage condition rating and concrete damage frequency using Eq. 1.

Table 2 Criteria and measure for each concrete damage condition rating [19, 20]

Condition rating	Description	Criteria	Measure
1	Very good	No damage	No repairs are needed, but still needs maintenance
2	Good	Light damage	Needs reparation in the field of routine maintenance
3	Medium	Medium damage	Immediately needs further assessment or testing and or reparation
4	Bad	Heavy damage	Needs structure strengthening or weight reduction
5	Very bad	Very heavy/ critical damage	It cannot be maintained or demolished

Table 3 Damage concrete frequency

Rating	Frequency
1	Rare (R)
2	Moderate (M)
3	Common (C)

$$RR_{se} = \frac{\sum CI \times f_{cd}}{n_{cd}} \tag{1}$$

RRse is the concrete damage risk level of each structure element, CI is the concrete damage condition rating, fcd is the concrete damage frequency, and ncd is the amount of damage done.

Determining Building Damage Risk Rating Building damage risk rating is determined based on concrete damage risk rating and damage location. Concrete damage location is divided into four structure elements, each with its own critical weight. Based on structure element critical weight search results for buildings from multiple references, namely [9–13, 21], structure element critical weight for existing buildings is determined by Wiyanto et al. in [19, 20], such as in Table 4.

Building damage risk rating is determined using Eq. 2.

$$SR = \frac{\sum RR_{se} \times w_{se}}{\sum w_{se}} \tag{2}$$

SR is the building’s damage risk rating, and wse is the structure element critical weight, as shown in Table 4. Based on the building’s damage risk rating value, concrete damage risk rating can be described by referring to Table 5.

2.3 Risk Evaluation

Concrete damage risk evaluation is a step used to determine priority towards risk on a building so that further measures can be taken according to the risk rating. This is done in order to maintain and repair a building to increase safety and comfort for the building’s users.

Table 4 Structure element critical weight [19, 20]

Structure element	Critical weight
Shear wall (SW)	1
Column (C)	1
Beam (B)	0.7
Slab (S)	0.5

Table 5 Concrete damage risk rating

Rating	Risk	Criteria
1	Low	$S < 5$
2	Medium	$5 \leq S < 10$
3	High	$10 \leq S \leq 15$

3 Results and Discussion

Assessment is applied to an existing high-rise building. Concrete damage risk rating assessment is done based on visual assessment on a 13-year-old 13-story parking building. Assessment is initiated with damage type examination, which is done on each building structure element, and condition rating of each damage. The results of concrete damage examination and condition rating assessment can be seen in Table 6.

Table 6 Parking building concrete damage type and condition rating

No.	Damage type	Element	Condition rating
1	Craze crack	C	2.54
2	Mapping crack	S	3.00
3	Scaling (very severe)	B	3.47
4	Spall (small)	B	2.86
5	Spall (small)	SW	2.86
6	Random Cracks	S	3.36
7	Scaling (light)	S	2.53
8	Scaling (severe)	S	3.13
9	Scaling (light)	S	2.53
10	Random cracks	C	3.36
11	Spall (large)	C	3.40
12	Pop-outs (medium)	B	2.93
13	Scaling (medium)	B	2.88
14	Spall (small)	C	2.86
15	Spall (small)	S	2.86
16	Spall (small)	B	2.86
17	Spall (small)	B	2.86
18	Scaling (very severe)	B	3.47
19	Scaling (light)	C	2.53
20	Spall (small)	C	2.86
21	Spall (small)	B	2.86
22	Scaling (severe)	B	3.13
23	Random cracks	S	3.36
24	Spall (small)	B	2.86
25	Spall (small)	B	2.86
26	Delamination	C	3.25
27	Scaling (very severe)	C	3.47
28	Random cracks	B	3.36

Table 7 Parking building concrete damage frequency

No.	Damage type	Frequency	Rating
1	Craze crack	R	1
2	Mapping crack	R	1
3	Scaling (very severe)	R	1
4	Spall (small)	C	3
5	Random cracks	R	1
6	Scaling (severe)	R	1
7	Scaling (light)	R	1
8	Spall (large)	R	1
9	Pop-outs (medium)	R	1
10	Scaling (medium)	R	1
11	Delamination	R	1

Based on the damage types that are identified in the visual assessment, concrete damage frequency on that building is determined. Damage frequency from each damage can be seen in Table 7.

Concrete damage risk rating of each structural element is determined based on concrete condition rating assessment results and the concrete damage frequency on the building. The risk rating assessment of each structural element can be seen in Table 8.

The parking building's structural damage risk rating is determined based on the concrete damage risk rating of each structure element, with the structure element's critical weight. Parking building structure damage risk rating assessment can be seen in Table 9.

Building damage risk rating is determined referring to Table 5. A risk rating of 5.95 shows that the parking building's concrete damage risk rating is 2, which is the medium rating. Medium risk means that further examination and reparation measures need to be done on the building. From the risk rating, it can be shown that the shear wall and beam elements are the highest priority for examination and reparation measures.

Table 8 Parking building concrete damage risk rating

No.	Damage type	Condition rating	Frequency rating	Risk rating
<i>Shear wall</i>				
1	Spall (small)	2.86	3	8.58
			RR_{sw}	8.58
<i>Column</i>				
1	Craze crack	2.54	1	2.54
2	Random cracks	3.36	1	3.36
3	Spall (large)	3.40	1	3.40
4	Spall (small)	2.86	3	8.58
5	Scaling (light)	2.53	1	2.53
6	Spall (small)	2.86	3	8.58
7	Delamination	3.25	1	3.25
8	Scaling (very severe)	3.47	1	3.47
			RR_{ct}	4.46
<i>Beam</i>				
1	Scaling (very severe)	3.47	1	3.47
2	Spall (small)	2.86	3	8.58
3	Pop-outs (medium)	2.93	1	2.93
4	Scaling (medium)	2.88	1	2.88
5	Spall (small)	2.86	3	8.58
6	Spall (small)	2.86	3	8.58
7	Scaling (very severe)	3.47	1	3.47
8	Spall (small)	2.86	3	8.58
9	Scaling (severe)	3.13	1	3.13
10	Spall (small)	2.86	3	8.58
11	Spall (small)	2.86	3	8.58
12	Random cracks	3.36	1	3.36
			RR_{bm}	5.89
<i>Slab</i>				
1	Mapping crack	3.00	1	3.00
2	Random cracks	3.36	1	3.36
3	Scaling (light)	2.53	1	2.53
4	Scaling (severe)	3.13	1	3.13
5	Scaling (light)	2.53	1	2.53
6	Spall (small)	2.86	3	8.58
7	Random cracks	3.36	1	3.36
			RR_{sl}	3.78

Table 9 Parking building damage risk rating

No.	Structure element	Risk rating	Critical weight	$RR_{se} \times w_{se}$
1	Shear Wall	8.58	1	8.58
2	Column	4.46	1	4.46
3	Beam	5.89	0.7	4.12
4	Slab	3.78	0.5	1.89
		\sum	3.2	19.05
		SR	5.95	

4 Conclusion

The building damage risk rating resulted from damage type assessment based on visual to existing buildings can be used to describe risk criteria. The risk rating value can describe concrete damage risk towards building structure, so it can be used to determine priorities for the measures that will be done to the building. These measures can be in the form of building maintenance, destructive testing, and building reparation. This risk rating assessment method can be applied to existing buildings in order to determine building structure element reparation priority.

References

1. Republik Indonesia (2002) Undang-undang Republik Indonesia nomor 28 tahun 2002 tentang bangunan gedung. Kementerian Riset, Teknologi, dan Pendidikan Tinggi, Jakarta
2. Republik Indonesia (2005) Peraturan pemerintah Republik Indonesia nomor 36 tahun 2005 tentang peraturan pelaksanaan undang-undang nomor 28 tahun 2002 tentang bangunan gedung. Kementerian Riset, Teknologi, dan Pendidikan Tinggi, Jakarta
3. ISO/TC 262 Risk management (2009) ISO 31000:2009 Risk management—principle and guidelines. International Organization for Standardization, Geneva, Switzerland
4. Aparicio AC, Casas JR, Cruz PJS (2003) Deterioration and structural performance of reinforced concrete beams. In: The 3rd international workshop LCC03/IABMAS, Lausanne, Switzerland, 24–26 March 2003
5. Shohet IM (2003) Building evaluation methodology for setting maintenance priorities in hospital buildings. *Constr Manage Econ J* 21(7):681–692. <https://doi.org/10.1080/0144619032000115562>
6. Znidaric J, Perus I (1998) Condition rating methods for concrete structures. In: CEB bulletin No. 243: strategies for testing and assessment of concrete structure affected by reinforcement corrosion, p 155–168
7. Coronelli D (2007) Condition rating of RC structures: a case study. *J Build Apprais* 3(1):29–51. <https://doi.org/10.1057/palgrave.jba.2950057>
8. Pedro JACBO, Paiva JAVP, Vilhena AJDSM (2008) Portuguese method for building condition assessment. *Struct Surv* 26(4):322–335. <https://doi.org/10.1108/02630800810906566>
9. Mitra G, Jain KK, Bhattacharjee B (2010) Condition assessment of corrosion-distressed reinforced concrete buildings using fuzzy logic. *J Perform Constr Facil* 24(6):562–570. [https://doi.org/10.1061/\(asce\)cf.1943-5509.0000137](https://doi.org/10.1061/(asce)cf.1943-5509.0000137)

10. Jain KK, Bhattacharjee B (2012) Visual inspection and condition assessment of structures (VICAS): an innovative tool for structural condition assessment. *Int J 3R's* 3(1):349–357
11. Jain KK, Bhattacharjee B (2012) Application of fuzzy concepts to the visual assessment of deterioration reinforced concrete structure. *J Constr Eng Manage* 138(3):399–408. [https://doi.org/10.1061/\(ASCE\)CO.1943-7862.0000430](https://doi.org/10.1061/(ASCE)CO.1943-7862.0000430)
12. Tirpude NP, Jain KK, Bhattacharjee B (2014) Decision model for repair prioritization of reinforced-concrete structures. *J Perform Constr Facil* 28(2):250–256. [https://doi.org/10.1061/\(ASCE\)CF.1943-5509.0000427](https://doi.org/10.1061/(ASCE)CF.1943-5509.0000427)
13. Pragalath H, Seshathiri S, Rathod H, Esakki B, Gupta R (2018) Deterioration assessment of infrastructure using fuzzy logic and image processing algorithm. *J Perform Constr Facil* 32(2):1–13. [https://doi.org/10.1061/\(asce\)cf.1943-5509.0001151](https://doi.org/10.1061/(asce)cf.1943-5509.0001151)
14. Wijaya MGW, Wahyuni E, Iranata D (2014) Assessment kerentanan bangunan beton bertulang pasca gempa. *Jurnal Teknik Pomits* 1(1):1–6
15. Hamdia KM, Arafa M, Alqedra M (2018) Structural damage assessment criteria for reinforced concrete buildings by using a fuzzy analytic hierarchy process. *Underground Space* 3(3):243–249. <https://doi.org/10.1016/j.undsp.2018.04.002>
16. Leite FM, Volsse RA, Roman HR, Saffaro FA (2020) Building condition assessment: adjustments of the building performance indicator (BPI) for university buildings in Brazil. *Ambiente Construído* 20(1):215–230. <https://doi.org/10.1590/s1678-86212020000100370>
17. American Society of Civil Engineers, Agency FEMA (2000) FEMA 356/November 2000: prestandard and commentary for the seismic rehabilitation of buildings. American Society of Civil Engineers, Reston, Virginia
18. Wiyanto H, Chang J, Dennis J (2020) Concrete structure condition rating in Buildings with non-destructive testing. *IOP Conf Ser: Mater Sci Eng* 852:012058; In: The 2nd Tarumanagara international conference on the applications of technology and engineering 2019, Jakarta, Indonesia, 21–22 Nov 2019. <https://doi.org/10.1088/1757-899X/852/1/012058>
19. Wiyanto H, Lie D, Kurniawan J (2019) Critical index determination method on visual assessment of concrete damage for buildings. *IOP Conf Ser: Mater Sci Eng* 508:012003; In: Tarumanagara international conference on the applications of technology and engineering, Jakarta, Indonesia, 22–23 Nov 2018. <https://doi.org/10.1088/1757-899X/508/1/012003>
20. Wiyanto H, Makarim CA, Gondokusumo O (2020) Condition rating examination based on visual assessment of concrete damage caused by poor implementation. *Tech Rep Kansai Univ* 62(09):5861–5870
21. Pushpakumara BHJ, Silva S, Silva GHMJS (2017) Visual inspection and non-destructive tests-based rating method for concrete bridges. *Int J Struct Eng* 8(1):74–91. <https://doi.org/10.1504/ijstructe.2017.081672>
22. American Society of Civil Engineers (2000) Guideline for structural condition assessment of existing buildings. American Society of Civil Engineers, Reston, Virginia, United State
23. American Concrete Institute Committee 201 (2008) Guide for conducting a visual inspection of concrete in service. American Concrete Institute, Farmington Hills, U.S.A.
24. Wiyanto H (2020) Penerapan soft system methodology pada metode penilaian kerusakan beton secara visual. *Jurnal Media Komunikasi Teknik Sipil* 26(1):52–60

A Literature Review of Life Cycle Costing of Dam Asset Management



Ismi Astuti Anggraini, Ayomi Dita Rarasati,
and R. Jachrizal Sumabrata

Abstract The increasing demand for water from various sectors such as industry, domestic, agriculture has led to an increase in the need for investment to develop water resources infrastructure, particularly dams. The dam is one of the infrastructures that have a long service life. It requires proper management to maximize its use which is also comparable to the costs incurred. The Life Cycle Cost (LCC) method is one method that can be used to estimate the cost during the operation of the dam. It considers the financial costs at different life cycle stages, including capital costs, costs of operational, maintenance costs, replacement and rehabilitation costs, demolition, and residual costs. Life Cycle Costing is an inseparable part of decisions about financially expensive investments. LCC works by calculating the life cycle length, future costs, discount rate, and inflation. This study aims to define the integration of the life cycle costs and the management of dam assets. The author used a literature review method from 28 compatible literature. By applying LCC to the dam, the cost of each stage of the dam's service life can be determined to obtain economic financing.

Keywords Asset management · Dam · Life cycle cost

1 Introduction

The dam is designed to store water for social purposes such as flood control, irrigation, water supply, energy generation, entertainment, and environmental protection. Dam can give many advantages but also the potential threats to public safety cannot be ignored [1]. After the dam's completion, the dam's safety will be affected by changes in time, maintenance, and operating conditions. Only through continuous maintenance, inspection, and evaluation will it be known of the changes

I. A. Anggraini (✉) · A. D. Rarasati · R. J. Sumabrata
Civil Engineering Department, Faculty of Engineering, Universitas Indonesia, Depok,
Indonesia
e-mail: ismi.astuti@ui.ac.id

© The Author(s), under exclusive license to Springer Nature Singapore Pte Ltd. 2022
H. A. Lie et al. (eds.), *Proceedings of the Second International Conference of Construction, Infrastructure, and Materials*, Lecture Notes in Civil Engineering 216, https://doi.org/10.1007/978-981-16-7949-0_48

533

that caused the dam safety. If we consider the life of a building to be decades, assessing project alternatives only in terms of investment costs would be too narrow and insufficient. A structure can be exposed to several conditions during its operating cycle, which have different consequences. In general, the structure's life cycle management activities can be divided into several types, e.g., inspection, monitoring, maintenance, and repair (IMMR) [2]. Maintenance operating costs is an essential part of the investment over the life cycle. Dam asset management must be a severe concern in order to maximize its utilization. Life Cycle Costing (LCC) is an inseparable part of making decisions on financially expensive investments.

The principles and approaches of Life Cycle Costing (LCC) have had a significant influence on the field of civil infrastructure. The principles and methods of LCC are explored in this paper, with a focus on the dam. Life Cycle Costing is an analysis method that improves the estimation of many different investment options total long-term economic feasibility [3]. The relationships between several success indicators are explored. LCC requires the identification of all materials and processes used in each phase [4]. The LCC analysis is formulated to consider the socio-economic consequences of structural collapse and the minimize of lifetime maintenance costs. The Life Cycle Costing can be applied to the whole project or its parting [5].

To offer greater transparency, LCC considers both user costs (e.g., decreased flexibility at project location) as well as agency costs related to planned operations, such as potential annual repairs and reconstruction, when calculating the cost of a dam infrastructure. Both expenses are typically discounted and added up to arrive at a current-day valuation known as Net Present Value (NPV). A life cycle model is typically combined with the overall cost of ownership to give the operator, or more specifically the owner of the entire concept, a more sophisticated and reliable costing model [6].

A primary reason presented was an overestimation of the value of creating datasets for expense storage and repair to help any potential costs. However, it was discovered that the risks of maintaining these datasets outweighed the advantages. Users inserted outdated records, cost statistics became out-of-date, and it was impossible to directly use historical data for a component due to various types, vendors, and technical advances, to name a few issues with databases [6]. Future expenditures become imaginary when funding is not saved or set aside, in contrast to capital investment, which has actual budget constraints. Furthermore, various organizations are frequently in charge of investing and maintaining equipment, with different budgets, reducing the ability to consider life cycle costs. There are many reasons why the practical use of life cycle costing has been restricted due to the methodology's scope [7]. However, it is worth noting that the advantages of life cycle costing are not so much about the direct quantification of life cycle costs as they are in the way of reasoning about how to reduce overall expense over the asset's life cycle.

2 Objective

The construction of dams pursues several goals in ecological, social-economic terms. Since the focus of this paper is on the economic value of dams throughout their lifetime, economic considerations primarily determine the limits of the scope of the study. This study aims to determine the integration of life cycle costing and dam asset management and its benefit. Dams are one of the infrastructures that are designed for a long service life. Taking into account the life cycle costs of a dam can reduce overall costs during dam operation and optimize the budget reserved for dam management. The contribution of this literature knowledge is to add to the financing terms of asset management in the dam with the estimated costs over the life cycle of the dam.

3 Methods

The authors gathered publications for this review using Scopus as the central archive for scientific journals. The keywords used were “Life Cycle Costing”, “Life Cycle Cost Infrastructure”, “Dam Maintenance”, “Management Asset of Dam”, “Life Cycle Management”, and the publications chosen were academic and conference papers written over summaries and combining pre-determined keywords to filter out ancient documents from the search results. The publication years of papers were set limited from 2012 to 2021. There are 37 papers that are thought to be important to the subjects we covered. Then the text should be read in its entirety for the second screening. After the second screening, nine papers were not chosen to be addressed. As a result, 28 papers will be addressed and clustered based on life cycle costing and dam asset management. Several works of literature from other infrastructure sectors are also used to support this review.

4 Result and Discussion

Life Cycle Cost is an analysis method that refers to all the costs related to construction, operational, and project maintenance on a specific period [8]. LCC is handling all cash flow during the determined duration [6]. The LCC method considers the financial costs at different stages of the life cycle, including investment costs (i.e., initial construction materials, manpower, and indirect costs), cleaning, maintenance, replacement, and energy costs during the use phase, and also demolition and residual costs [9]. From a statistical point of view, the stochastic life cycle performance integrates the time-dependent behavior of structures affected by external shocks, maintenance, and functionality. Both uncertainties regarding the performance of the existing infrastructure and the damage quantification were taken

into account using stochastic analysis. One of the stochastic approaches used also took into account the epistemic nature of risk analyzes, which focus on the costs of maintaining reliable containment after an accident, and shows that maintenance and operational safety will become an economic issue for the affected communities in the coming decades. For such maintenance work was underlined by modeling approaches that clarify that the safety of the local population and the reliability of the infrastructure can only be guaranteed with high reliability if the maintenance work is carried out at regular intervals [10]. The LCC process typically includes the following steps: planning the LCC analysis (e.g., the definition of objectives), selecting and developing the LCC model (e.g., structuring cost breakdowns, identifying data sources and possibilities), applying the LCC model, and documenting and reviewing the LCC Results [11, 12]. The prices of manpower, fuel, materials, and parts can vary significantly from year to year and depend on location, market, and quality. The lack of quantitative advantages (such as the decrease in accidents and opportunity costs) makes it possible to evaluate infrastructure projects in a way that minimizes costs [13]. Due to inflation, the currency's value will be different nowadays and within the future [14]. Life Cycle Cost Analysis can be used to compare the advantages of different planting systems in terms of water consumption, energy, and environmental pollution [15].

The dam project can be divided into the following sections: feasibility study and planning (phase one), construction (phase two), and operation (phase three). A conceptual error probability and risk assessment were developed for each stage [1]. A high failure rate characterizes the initial construction and fills cycle, but at the end of this interval, the structure failure rate stabilizes. During the operation of the dam, damage with strong influence will occur [16]. Hence it is important to optimize the maintenance and operational costs of the dam during its regular operation.

The Life Cycle Cost method uses current spent costs and costs incurred in the future. The calculation time value of money is needed due to guarantee all the comparable values. LCC works by calculating the life cycle length, future costs, discount rate, and inflation. The most appropriate and most commonly used approaches to estimate LCC are Net Present Value (NPV) and Equivalent Annual Cost (EAC) [8].

4.1 Calculation Data

The efficiency of the LCC is highly dependent on the set of records used to carry out structural evaluations [17]. According to [11], the data required for the calculation and analysis of LCC can be classified into three groups:

1. Data for the converting costs spent during the life cycle to their present value, the so-called discount rate, inflation rate, length of the period analyzed.
2. Cost data, i.e., costs in the specified structure, life cycle phases.

3. Other data include the quality of buildings and structures, intensity and method of use, and technical parameters.

In LCC analysis, the life span of the dam or other structure and its equipment is distinguished from the length of the analyzed period. The dam is specific because their long technical life usually exceeds their moral or economic life.

Through years of continual use and responses to environmental consumption and environmental conditions, infrastructure, like all forms of capital spending, will become redundant. These aging infrastructures would need periodic repairs, modernization, and reconstruction of whole or sections in order to maintain operations. At maximum, annual repair and modernization costs range from 2 to 20% or more, based on a variety of factors such as the scale, structure, and capability of the facility, as well as the fit for purpose, configuration, materials, construction efficiency, and, most significantly, how it performs and retains [4]. These operating expense pieces are investments that can last 20–30 years or more. Especially in infrastructure, the operating period is very long. It is also likely that the total capital investment on infrastructure over its lifetime would be much higher than the initial capital expenditure. Furthermore, we do not see enough of this kind of study when constructing our asset, region, or megaproject. There is a pressing need to investigate this and maximize the spending on infrastructure over its whole life cycle. In this case, a Life Cycle Cost Analysis (LCCA) is especially useful in ensuring the cost-effectiveness of an infrastructure project [18].

In infrastructure projects such as dams, technical solutions are used in LCC calculations to estimate costs and gaps or lack economic data [19]. Therefore, the error is caused by incomplete data and incorrect judgment. It can cause considerable calculation errors. To ensure Asset Performance, it is critical to replace equipment at the appropriate time, according to best practices, company policies, and vendor guidelines. As a result, before incurring actual costs, efficient capital planning will increase reliability through time and money [11]. Cost reductions can also be achieved by standardizing sourcing practices, smoothing out prices, and avoiding widespread adoption through procuring assets from supply chain partners. Reduced complexity in cost planning will lead to improved asset efficiency and less instability and risk to the enterprise, so the goal is to boost stakeholder trust [20]. Dam infrastructure will benefit from life cycle cost analysis. These ventures make use of capital investment, which is the upfront expense of building or providing a piece of infrastructure. Stated, it is the cost of constructing the preferred infrastructure. Another consideration of infrastructure construction is running expenses, including a variety of expenses such as utility, manpower, insurance, facilities, health, and regular and scheduled maintenance [21]. The cost of disposal is perhaps another critical aspect of LCC.

Another aspect of the LCC that has received little attention is its ability to guarantee long-term dam operational efficiency. LCC continues to be limited and undeveloped during the life span of an object or property [18, 22]. Because of this, LCC is not often thought of as a reliable budgeting mechanism. One explanation may be a lack of comprehensive research spanning all aspects of an asset's life

cycle, although life cycle costing in principle covers all costs at all points of the dam life cycle. The use of LCC should be widespread in the portfolio's economic life [21]. In reality, the LCC is used for asset financial process improvement. The procedure aids in the tracking of the asset's gross domestic product in addition to expectations.

As previously mentioned, LCC has progressed from a project assessment mechanism to a more holistic way of integrating sustainable growth elements across various industries. LCC may be seen as part of a larger system for sustainable growth. Three interconnected sustainability aspects make up the system (economic, environmental, social) [6]. Economic sustainability is derived from the public finance system, which employs financial and economic analysis of investments. Externalities system (again, from public benefit and public finance) is used to ensure environmental protection. Environmental responsibility is based on a public policy system that places a premium on service access, governance, and social justice. These two parts are linked by operational policies where the system's performance affects the economic cost and vice versa. Therefore, the LCC of dam projects can be tied to their performance over the life cycle based on a change in operational policy and monitoring of the resulting changes to the system [19].

4.2 Determination of Costs Estimates

Costs incurred during the life cycle are different. Since the timing of costs is different, this needs to be reflected in the LCC calculations [23]. This purpose uses the most common techniques of determining the Net Present Value and time value of money, which are expressed in the form of discount rates and depend on inflation, capital costs, investment opportunities, and personal consumption choice. The discount rate controls the present value of life cycle costs. Variations in the discount rate change the impact of maintenance, operation, and end-of-life costs throughout the infrastructure's life cycle [23]. Therefore, identification of the discount rate is critical in calculating. Determining the correct discount rate is one of the limitations of the LCC study [23]. LCC changes significantly with changes in the discount rate.

It is also important to analyze The Life Cycle Inventory (LCI) that consists of all the materials, fuels, and energy needed to construct and maintain the system [24]. Some components are prone to damage to dam infrastructure, like spillway gates, hydraulic gates, dam instruments, etc. LCC analysis is based on many input costs, and the rest usually requires significantly different information for the cost calculation of the dam project life cycle phase. The total cost of the economic life cycle is usually considered with market applications. The LCC analysis includes all costs to be assessed. The cost usually includes the tendered amount (investment price) and the minimum costs of energy. However, maintenance and other related costs are often required in the demand information [25]. Operational costs represent costs that arise at the operating stage of the dam. The residual value of the structure

depends on the decision to destroy, where the materials can be recycled or reconstructed to allow the reuse of structural components [23]. In the dam infrastructure, which is concrete construction, it can be considered that there is no residual value.

The life cycle of a dam generally consists of two stages: the project, design, and construction stage, and the service and demolition stage. All explicit funds that are consumed in these two stages are called direct costs. The negative technical impacts on society and people in these two stages are indirect costs, such as environmental pollution and displacement of residence. Direct costs can be divided into the following sections: initial costs, detection costs, reinforcement costs, failure costs, and residual project value [18].

Initial Costs The cost required to complete the water conservation project construction. That is, the funds spent in the project, design, and construction stages. The manpower and material resources in the construction phase are all construction costs. According to industry standards, planning and design costs are considered a percentage of construction costs, generally 3–5% [18]. The costs at this stage are related to the costs of the construction company. These costs include the manpower required in extracting and manufacturing materials and the cost of transporting them to the construction site [26]. In construction projects of the dam, feasibility studies and preliminary tests will bring considerable costs, exceeding the construction time. Therefore, these costs are part of LCC [19].

Detection Costs A water conservation project service phase, required to monitor and detect structures. Safety problems and potential hazards in a project can be identified mostly through detection or patrol [18].

Reinforcement Costs Maintenance costs of the dam are included in this cost. They have performed before the structural reliability is reduced to the minimum value permitted by the standard. Maintenance measures are taken to reduce the likelihood of engineering failures and extend service time to ensure the safe operation of the infrastructure. The maintenance procedure includes four work processes, such as engineering failure investigation, maintenance plan design, construction quality control, and acceptance [18]. The single maintenance cost is the sum of the four process costs. Over time, when the structure's performance is reduced to the minimum allowable requirements or the dam's safety is threatened, action must be taken to strengthen the structure to improve performance and ensure safe project operation. In the final stages of structural life, measures must be taken to slow the breakdown rate and effectively reduce maintenance costs. The maintenance of the dam must be constantly adapted to changing conditions throughout its life cycle. The operator and the state must closely monitor it to ensure public safety in practical management [16]. The engineering component upgrade can restore the structure's performance to the original construction level, which can improve the structure's performance and slow the speed of failure down [18].

Failure Costs Cost of losses caused by accidents in water conservation projects. A serious accident will result in the loss of life and the safety of the property of the downstream community. Minor accidents will result in structural failure and loss of benefits. Apart from causing direct loss of economic property, serious accidents will also negatively impact society and the environment, resulting in indirect losses. During the project's life, inspection and maintenance aim to minimize the possibility of dam failure. However, it is impossible to ensure the absolute safety of the project [18].

Residual Project Value The project's life is t years and cannot be used after T years, but there is still a residual value. In general, concrete structures have no residue. The value and cost of demolition are usually estimated to correspond to a percentage of the initial construction cost [18].

One aspect of LCC that has not been thoroughly studied is its potential to ensure sustainable service delivery [15]. The lack of comprehensive analysis covering all phases of an asset's life could be one reason the LCC is not necessarily seen as a good budgeting tool [27]. Although life cycle costs theoretically include all costs in different life cycle phases. The implementation of LCC must be extended over the life of the asset. The process helps to monitor the relationship between the economic performance of the asset and the expectations set at the project beginning, and maintain or extend the useful life of the assets or system, to maintain a certain level of performance, such as control slippage and maintain the sustainability of dam services. Ultimately, this can ensure that the number of system failures is reduced, costs are minimized, system efficiency, financial stability, and service sustainability are improved. Generally, the reliability design literature often reports the basic probabilistic cost optimization in the maintenance strategy, but there is usually a lack of cost accounting. The cost of failure is compared with the cost of preventive maintenance to find the best preventive or corrective maintenance strategy [28]. Based on the asset's value to the community and the best time when such an event occurs, LCC can be used in this decision-making process to assess the feasibility of repair or replacement. It is significant for asset owners, asset managers, and service providers.

5 Conclusion

Based on the discussion above, we can conclude that as one of the infrastructures with long service life, the application of the LCC on the dam will help map the costs at each phase of the dam's life cycle. So that more economical financing is obtained. LCC implementations use capital investment, which is the upfront cost to build or provide infrastructure. This includes operational costs, covering various costs such as utilities, manpower, insurance, facilities, health, and routine and scheduled maintenance. Another benefit of applying LCC on the dam is that it can minimize dam failures due to limited costs or errors in dam maintenance.

References

1. Lin C-H, Lin C-P, Hung Y-C, Chung C-C, Wu P-L, Liu H-C (2018) Application of geophysical methods in a dam project: life cycle perspective and Taiwan experience. *J Appl Geophys* 158:82–92. <https://doi.org/10.1016/j.jappgeo.2018.07.012>
2. Zhang WH, Lu DG, Qin J, Faber MH (2019) Life cycle management of structural systems based on the optimal SHM strategy by Vol analysis. In: Proceedings of the 13th international conference on applications of statistics and probability in civil engineering, vol 194, ICASP13-MS32. ICASP 2019, Seoul, Republic of Korea, 26–30 May 2019
3. Babashamsi P, Yusoff NIM, Ceylan H, Nor NGM, Jenatabadi HS (2016) Evaluation of pavement life cycle cost analysis: review and analysis. *Int J Pavement Res Technol* 9(4):241–254. <https://doi.org/10.1016/j.ijprt.2016.08.004>
4. Moins B, France C, Van den bergh W, Audenaert A (2020) Implementing life cycle cost analysis in road engineering: a critical review on methodological framework choices. *Renew Sustain Energy Rev* 133:110284. <https://doi.org/10.1016/j.rser.2020.110284>
5. Shahata K, Zayed T (2013) Simulation-based life cycle cost modeling and maintenance plan for water mains. *Struct Infrastruct Eng* 9:403–415. <https://doi.org/10.1080/15732479.2011.552509>
6. Sun Y, Carmichael DG (2017) Uncertainties related to financial variables within infrastructure life cycle costing: a literature review. *Struct Infrastruct Eng* 14(9):1233–1243. <https://doi.org/10.1080/15732479.2017.1418008>
7. Pan Y, Shang Y, Liu G, Xie Y, Zhang C, Zhao Y (2021) Cost-effectiveness evaluation of pavement maintenance treatments using multiple regression and life-cycle cost analysis. *Constr Build Mater* 292:123461. <https://doi.org/10.1016/j.conbuildmat.2021.123461>
8. Heralova RS (2017) Life cycle costing as an important contribution to feasibility study in construction projects. *Proc Eng* 196:565–570. <https://doi.org/10.1016/j.proeng.2017.08.031>
9. Trigaux D, Wijnants L, Troyer FD, Allacker K (2017) Life cycle assessment and life cycle costing of road infrastructure in residential neighbourhoods. *Int J Life Cycle Assess* 22:938–951
10. Cánovas JAB, Stoffel M, Corona C, Schraml K, Gobiet A, Tani S, Sinabell F, Fuchs S, Kaitna R (2016) Debris-flow risk analysis in a managed torrent based on a stochastic life-cycle performance. *Sci Total Environ* 557–558:142–153. <https://doi.org/10.1016/j.scitotenv.2016.03.036>
11. Heralova RS (2014) Life cycle cost optimization within decision making on alternative designs of public buildings. *Proc Eng* 85:454–463. <https://doi.org/10.1016/j.proeng.2014.10.572>
12. Yu B, Lu Q, Xu J (2013) An improved pavement maintenance optimization methodology: integrating LCA and LCCA. *Transp Res Part A: Policy Practice* 55:1–11. <https://doi.org/10.1016/j.tra.2013.07.004>
13. Heidari MR, Heravi G, Esmaeli AN (2020) Integrating life-cycle assessment and life-cycle cost analysis to select sustainable pavement: a probabilistic model using managerial flexibilities. *J Clean Prod* 254:120046. <https://doi.org/10.1016/j.jclepro.2020.120046>
14. Huang L, Liu Y, Krigsvoll G, Johansen F (2018) Life cycle assessment and life cycle cost of university dormitories in the Southeast China: case study of the university town of Fuzhou. *J Clean Prod* 173:151–159. <https://doi.org/10.1016/j.jclepro.2017.06.021>
15. Reddy VR, Kurian M (2015) Life-cycle cost analysis of infrastructure projects. In: Kurian M, Ardakanian R (eds) *Governing the nexus: water, soil and waste resources considering global change*. Springer International Publishing, Cham, pp 105–127
16. Titova TS, Longobardi A, Akhtyamov RG, Nasyrova ES (2017) Lifetime of earth dams. *Mag Civil Eng* 1:34–43. <https://doi.org/10.18720/MCE.69.3>
17. Mitropoulou CC, Lagaros ND, Papadrakakis M (2015) Generation of artificial accelerograms for efficient life-cycle cost analysis of structures. *Eng Struct* 88:138–153. <https://doi.org/10.1016/j.engstruct.2015.01.029>

18. Su H, Gao J, Wen Z (2020) Life cycle cost optimisation model for design and reinforcement of dams based in fuzzy clustering and a backtracking search algorithm. *Struct Infrastruct Eng* 17:1257–1270. <https://doi.org/10.1080/15732479.2020.1802602>
19. Vahdat-Aboueshagh H, Nazif S, Shahghasemi E (2014) Development of an algorithm for sustainability based assessment of reservoir life cycle cost using fuzzy theory. *Water Resour Manage* 28:5389–5409. <https://doi.org/10.1007/s11269-014-0808-7>
20. Jansen BW, van Stijn A, Gruis V, van Bortel G (2020) A circular economy life cycle costing model (CE-LCC) for building components. *Resour Conserv Recycl* 161:104857. <https://doi.org/10.1016/j.resconrec.2020.104857>
21. Frangopol DM, Saydam D, Kim S (2012) Maintenance, management, life-cycle design and performance of structures and infrastructures: a brief review. *Struct Infrastruct Eng* 8(1):1–25. <https://doi.org/10.1080/15732479.2011.628962>
22. Plebankewicz E, Zima K, Wiczorek D (2019) Original model for estimating the whole life costs of buildings and its verification. *Arch Civ Eng* 65:163–179. <https://doi.org/10.2478/ace-2019-0026>
23. Illankoon IMCS, Tam VWY Le KN, Wang JY (2018) Life cycle costing for obtaining concrete credits in green star rating system in Australia. *J Clean Prod* 172:4212–4219. <https://doi.org/10.1016/j.jclepro.2017.11.202>
24. Fathollahi A, Coupe SJ (2021) Life cycle assessment (LCA) and life cycle costing (LCC) of road drainage systems for sustainability evaluation: quantifying the contribution of different life cycle phases. *Sci Total Environ* 776:145937. <https://doi.org/10.1016/j.scitotenv.2021.145937>
25. Spickova M, Myskova R (2015) Costs efficiency evaluation using life cycle costing as strategic method. *Proc Econ Fin* 34:337–343. [https://doi.org/10.1016/s2212-5671\(15\)01638-x](https://doi.org/10.1016/s2212-5671(15)01638-x)
26. Cuéllar-Franca RM, Azapagic A (2014) Life cycle cost analysis of the UK housing stock. *Int J Life Cycle Assess* 19:174–193
27. Kambanou ML (2020) Additional uses for life cycle costing in life cycle management. *Procedia CIRP* 90:718–723. <https://doi.org/10.1016/j.procir.2020.01.128>
28. van den Boomen M, Schoenmaker R, Wolfert ARM (2018) A life cycle costing approach for discounting in age and interval replacement optimisation models for civil infrastructure assets. *Struct Infrastruct Eng* 14(1):1–13. <https://doi.org/10.1080/15732479.2017.1329843>

An Explorative Study to Public Rental Housing's Tenants Using Importance Performance Analysis



Indira Surya Kumala and Farida Rachmawati 

Abstract Due to land scarcity and high land price in the city center or the area close to workplace, has led local government to build public rental housing. It is also expected to be the pathway to home ownership. This study aimed to determine tenants satisfaction based on the conformity between the desired expectations and the reality received by the tenants of the public rental housing called Rusunawa. There were three indicators: Building Performance Evaluation (BPE), maintenance quality and service quality (servqual). However, this paper only focuses on service quality (servqual) as this paper will contribute to the improvement of Rusunawa services on the invisible side. This study identified 12 attributes. Data were collected by distributing questionnaires with a total of 231 tenants who were accepted in four Rusunawa with different building ages. In this study, the Importance Performance Analysis (IPA) method is used to produce a Cartesian diagram that can describe four quadrants where quadrant I contains service quality attributes which are a priority to be repaired in order to improve the quality of existing Rusunawa and as an evaluation material for the construction of a new Rusunawa.

Keywords Tenants satisfaction · Public rental housing · Servqual · Importance and performance analysis

1 Introduction

Land scarcity in the urban area and increasing population have resulted in complex problems as a result of horizontal development so that more low-income people are homeless [1, 2]. The housing backlog problem has dominated the housing policy made by the Indonesian government to prioritize low-income people by paying attention to aspects of housing affordability [3]. For this reason, a solution is needed to accommodate a large population with less land area by developing vertically so

I. S. Kumala (✉) · F. Rachmawati
Department of Civil Engineering, Institut Teknologi Sepuluh Nopember, Surabaya, Indonesia
e-mail: indirasuryakumala25@gmail.com

© The Author(s), under exclusive license to Springer Nature Singapore Pte Ltd. 2022
H. A. Lie et al. (eds.), *Proceedings of the Second International Conference of Construction, Infrastructure, and Materials*, Lecture Notes in Civil Engineering 216, https://doi.org/10.1007/978-981-16-7949-0_49

543

that saving land is one of the efforts in sustainable development [1, 2]. Sustainable development can be achieved if the building can maintain its quality, save costs in the short and long term, the conditions inside the building and the environment are good, durable, low maintenance costs, environmentally friendly [4]. The focus on sustainable development for low-income communities is to increase the balance between the need to seek business profits without sacrificing the environment and the needs of society [4].

Many problems that arise in the post-occupancy of vertical houses include slum occupancy, and residents do not have an awareness of caring for, noise, lack of privacy, inadequate public facilities so that the quality of life of the residents decreases [2]. Low-income people often complain that the buildings they live in are not designed to fit their needs and meet their expectations even though building planners have tried to design according to predetermined requirements. This is a misunderstanding on both sides so that feedback from the tenants is needed after the building is completed as an evaluation material [4, 5]. Understanding tenants needs can be used as a guide to determine more effective resources by adjusting to the occupants' needs in evaluating the performance of a building [6].

Currently, many efforts are being made to carry out maintenance and repairs only by considering tenants' input. In other words, the management considers a lot from a technical point of view without considering whether the tenants are completely satisfied with the services provided or not [7]. Maintenance in service quality does not only see the results, namely the maintenance product but also the process, namely the way of service in maintenance. Service quality is a technical quality that is what tenants actually receive during interactions with service providers and functional quality, namely technical results [3]. Complaints raised in service provision can be a profitable strategy because they provide benefits to all stakeholders, can save costs and reduce repetitive work [8]. The importance of measuring service quality, among others, is to ensure that tenants' needs are met, provide benchmarks, set standards for comparison, get a picture of resource allocation, and can provide feedback [9] Lack of attention to measuring attributes in the service delivery process can have an impact on the final result, namely building quality and building age so that this study aims to identify the priority service quality attributes to get improvements in the evaluation of tenants satisfaction based on the age of the building using Importance Performance Analysis which includes gap analysis and quadrant analysis.

2 Research Theory and Methods

2.1 Tenant Satisfaction

The paradigm of "satisfaction" has revolutionized almost every formation of an organization which has become an attitude in ensuring the highest service delivery to manage one's expectations [10]. Tenants satisfaction is an evaluative assessment

after the occurrence of certain interactions that depend on past experiences. In other words, quality takes precedence for residents therefore it is not only based on the predetermined specifications but also on user perceptions [11]. In terms of service quality, host feedback can be positive (praise or suggestion) or negative (complaint). Most studies focus on negative feedback because it is a problem that must be solved [12]. Responding to tenant complaints is a targeted operational effort to find solutions to negative tenant feedback and the quality of post-complaint service should also be considered [13]. Lack of interaction between the service provider and tenants causes dissatisfaction. This shows that service providers need to pay attention to tenants feedback so that solutions can be found and immediately addressed [14]. Good communication with tenants is an effective tool to collect tenant feedback and trained employees affect the performance of service providers [15]. It is very important for service providers to know which service attributes add value and increase satisfaction and which meet only minimum requirements and minimize dissatisfaction [16]. Measurement of service attributes contributes more to the delivery of effective and efficient services related to property maintenance to meet tenants expectations which result in tenants feedback regarding satisfaction assessments used for building quality, which results in benchmarks in improving service quality in multi-story tenants buildings [8].

2.2 *Service Quality*

Employees or physical resources or goods or service provider systems as a solution to solving customer problems [3]. Service quality is the difference between the desired expectations and the service perceived by the tenants. If the services provided are less than expected, the tenants will be dissatisfied. Perception is an influencing factor to consider to compare between satisfaction and services provided [17]. Service quality is an abstract and elusive construct because of three features unique to services: intangibility, heterogeneity and inseparability of production and consumption [3, 17]:

- The first feature of services is intangibility, where it is not only the quality of maintenance results that is a concern but also the quality of service for tenants. Paying attention to service quality makes it difficult to reach the target tenants' expectations because service quality is intangibility so that it cannot be measured and standardized. This causes service providers to find it difficult to understand how tenants value service and evaluate service quality.
- The second feature of services is the heterogeneity in which services are considered heterogeneous in that the variation in performance can occur from producer to producer and from tenants to tenants. The services examined involve individuals from different categories so that they appear heterogeneous. Service quality evaluation depends on the maintenance services provided by the service provider.

- The third feature of services is the inseparability of production and consumption, where the quality occurs during service delivery, namely the interaction between residents and service providers. Service quality occurs by the interaction of the three parties, namely the owner, tenant and service provider.

With respect to the Total Maintenance Scheme, the above review on three features of services suggests three underlying themes:

- Service Quality is not evaluated on the end result of product maintenance quality alone.
- Perceptions of service quality resulted from a comparison of tenants expectations with perceived service performance.
- The quality evaluation is not only based on service quality results but also evaluates the service delivery process, namely the interaction between tenants and service providers.

2.3 *SERVQUAL*

SERVQUAL is a model that measures the difference between expectations and perceptions regarding service [15, 17] which focuses on tenants satisfaction as the main driver for creating service improvements, productivity and profit optimization [7]. But *SERVQUAL* cannot consider the dynamics of growing expectations and focuses only on the service delivery process but not on the results of service delivery so it cannot accurately measure the end result of the service delivered [10, 15]. Parasuraman et al. [17] identified five broad dimensions, namely tangibles, reliability, responsiveness, assurance, and empathy which are widely applied to measure service quality. The following five dimensions are modified as follows to fit the context of the total maintenance scheme [17, 18]:

- Tangibility: physical facilities, equipment and appearance of personnel
- Reliability: ability to perform the promised service dependably and accurately
- Responsiveness: willingness to help customers and provide prompt service
- Assurance: knowledge and courtesy of employees and their ability to inspire trust and confidence
- Empathy: caring, individualized attention the firm provides for its customers.

Service quality gap (gap) is the difference between tenants' expectations and perceptions of services that illustrates the level of satisfaction as presented on Eq. 1 [8].

$$\text{Service Quality Score} = \text{Average expectation score} - \text{Average perception score} \quad (1)$$

2.4 Research Methods

Based on the literature review identified 12 attributes derived from service quality can be seen in Table 1. Primary data was obtained from respondents’ assessment of the interests and performance using a questionnaire with a Likert scale of 1–5. Type scale (1 representing “not important”, 2 representing “very important”, 3 representing “important”, 4 representing “important”, and 5 representing “very important”). The population in Penjaringansari II is 288 tenants, Wonorejo II is 192 tenants, Grudo is 100 tenants, and Gunung Anyar is 65 tenants. For sample determination, the solving formula is used as displayed on Eq. 2 [19].

$$n = \frac{N}{1 + N(e)^2} \tag{2}$$

where n = sample size, N = population size, E = margin of error or maximum error measured (assuming 10% = 0.1). So that a total sample of 231 respondents of public rental housing was obtained, 75 respondents from Penjaringansari II, 66 respondents from Wonorejo II, 50 respondents from Grudo, and 40 respondents from Gunung Anyar using incidental sampling with the consideration that they are the original residents of the flats who live in public rental housing every day. Data

Table 1 Identification of research variables for service quality criteria assessment

Variables	Code	Attribute
Tangibles [20]	t1	Service providers explain the information needed by tenants correctly
	t2	Service providers maintain the cleanliness and tidiness of the work area
Empathy [20–22]	e1	Service providers understand the needs of the tenants
	e2	Service providers have effective operating hours
Responsiveness [20–23]	r1	Service providers respond to requests and complaints of tenants quickly and precisely
	r2	Service providers are available when there are special requests from tenants
Reliability [20–23]	re1	Service providers respond to requests from tenants according to the promised time
	re2	Public rental housing prices are in accordance with the facilities provided
	re3	The terms of acceptance as tenants are carried out in accordance with the applicable regulations
	re4	The rules of the public rental housing were strictly enforced
Assurance [20, 21]	as1	Service providers have knowledge and skills in dealing with complaints
	as2	Service provider ensures that the rental duration is in accordance with the duration stated in the rental contract

were analyzed using the Importance Performance Analysis including Gap Analysis and Quadrant Analysis. The research variables for service quality criteria assessment are as displayed on Table 1.

3 Result and Analysis

3.1 Gap Analysis of 12 Servqual Attributes

The gap is the difference between X (the tenants' expectations) and Y (the tenants' perceived reality). Based on Tables 2 and 3, it can be seen that all gaps are negative, which means that none of the attributes meet the expectations of the occupants [24]. It was found that the biggest gap in public rental housing named: (1) Penjaringansari II is attribute r1 (Service provider respond to requests and complaints of tenants quickly and precisely) = -1.55 (2) Wonorejo II is attribute re1 (Service provider respond to requests from tenants according to the promised time) = -1.26 (3) Grudo is attribute r1 (Service provider respond to requests and complaints of tenants quickly and precisely) = -1.02 and (4) Gunung Anyar is attributed re4 (The rules of the public rental housing were strictly enforced) = -2.10 . While the smallest gap occurs in the same attribute is the attribute re2 (Public rental housing prices are in accordance with the facilities provided) which is found in the public rental housing named (1) Penjaringansari II = -0.48 (2) Wonorejo II = -0.42 (3) Grudo = -0.10 and (4) Gunung Anyar = -0.40 . The bigger the gap that occurs, the worse the assessment of the attributes of the research or the less fulfilled the expectations of tenants of public rental housing for the perceived reality. The smaller the gap that occurs, the better the assessment of the attributes of the research or the fulfillment of the expectations of tenants of public rental housing regarding the perceived reality [24]. The gap between importance and performance in four public rental housing is also interpreted on a radar chart. As shown in Figs. 1, 2, 3, and 4. It can be seen that the Grudo Public Rental Housing radar chart which has a line of importance and performance that coincides or is close to each other and the opposite occurs in Penjaringansari II and Gunung Anyar.

3.2 Quadrant Analysis

The determination of the quadrant comes from the cartesian diagram depiction. Where is Quadrant I (low performance, low and high importance), which means the main attribute that is emphasized more by tenants, but the performance of the public rental housing has not satisfied the tenants so it is "Concentrate here". Quadrant II (high performance and high importance), which means that the main attribute that

Table 2 Gap analysis of 12 Servqual attributes for Penjaringan II and Wonorejo II

Code	Penjaringan II				Wonorejo II			
	X	Y	Gap	%	X	Y	Gap	%
t1	3.85	4.49	-0.64	86	3.70	4.41	-0.71	84
t2	3.63	4.56	-0.93	81	3.53	4.55	-1.02	78
e1	3.41	4.44	-1.03	77	3.38	4.45	-1.08	76
e2	3.60	4.39	-0.79	84	3.82	4.29	-0.47	89
r1	3.09	4.64	-1.55	67	3.47	4.67	-1.20	74
r2	3.03	4.55	-1.52	67	3.65	4.24	-0.59	86
re1	3.29	4.63	-1.33	71	3.33	4.59	-1.26	73
re2	4.05	4.53	-0.48	89	4.08	4.50	-0.42	91
re3	4.04	4.61	-0.57	88	3.79	4.58	-0.79	83
re4	3.84	4.59	-0.75	84	3.79	4.56	-0.77	83
as1	3.60	4.53	-0.93	84	3.61	4.48	-0.88	80
as2	3.80	4.47	-0.67	85	3.76	4.44	-0.68	85
Mean suitability	80				82			

Table 3 Gap analysis of 12 Servqual attributes for Grudo and Gunung Anyar

Code	Grudo				Gunung Anyar			
	X	Y	Gap	%	X	Y	Gap	%
t1	3.98	4.32	-0.34	92	3.78	4.38	-0.60	86
t2	3.96	4.34	-0.38	91	3.48	4.53	-1.05	77
e1	3.86	4.30	-0.44	90	3.18	4.50	-1.33	71
e2	3.76	4.36	-0.60	86	3.33	4.45	-1.13	74
r1	3.44	4.46	-1.02	77	3.50	4.53	-1.03	77
r2	3.58	4.12	-0.54	87	3.78	4.25	-0.48	89
re1	3.58	4.44	-0.86	81	3.73	4.43	-0.70	84
re2	4.38	4.48	-0.10	98	4.20	4.60	-0.40	91
re3	4.12	4.34	-0.22	95	3.98	4.43	-0.45	90
re4	4.04	4.42	-0.38	91	2.70	4.55	-1.85	59
as1	3.58	4.30	-0.72	83	3.40	4.38	-0.98	78
as2	4.14	4.26	-0.12	97	3.85	4.38	-0.53	88
Mean suitability	89				80			

the tenants emphasize is the performance of the public rental housing that has satisfied the tenants so that it is “Keep up the good work”. Quadrant III (high performance and low importance), which means that the main attributes of the tenants are not emphasized, but the performance of the public rental housing has exceeded the tenants’ expectations so that it is a ‘Possible overkill’. Quadrant IV (low performance and low importance), which means that the main attributes that tenants will not pay attention to and the performance of the public rental housing has not satisfied tenants so it is a ‘Low priority’ [24]. Quadrant I contain attributes that must

Fig. 1 Radar chart Penjaringansari II

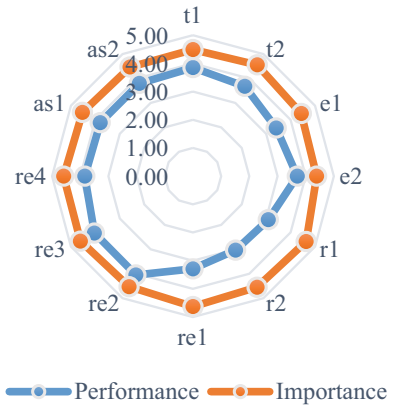


Fig. 2 Radar chart Wonorejo II

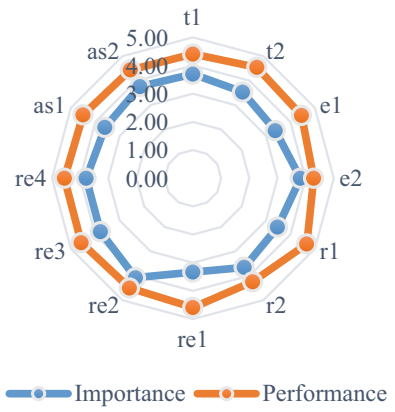


Fig. 3 Radar chart Grudo

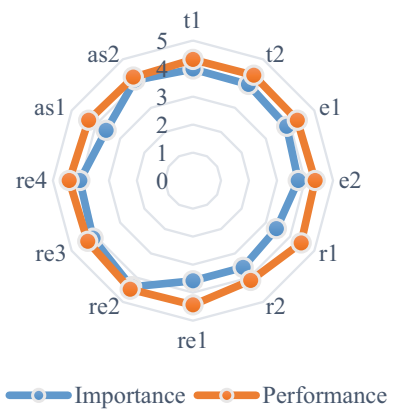
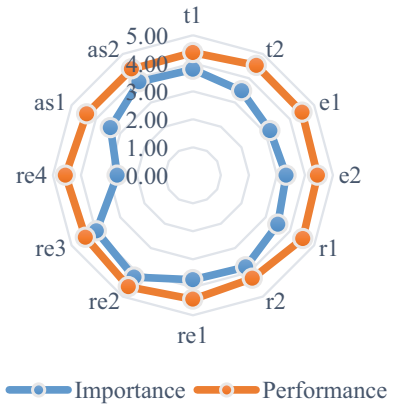


Fig. 4 Radar chart Gunung Anyar



be corrected immediately. Based on Figs. 5, 6, 7, and 8 in the public rental housing named (1) Penjaringanansari II there are five attributes, namely t1, e2, re2, as1, as2. (2) Wonorejo II has four attributes, namely t2, r1, re1, as1. (3) Grudo has three attributes, namely e2, r1, re1. (4) Gunung Anyar Flats has five attributes, namely t2, e1, e2, r1, re4. The lowest attribute assessment of Quality Service are

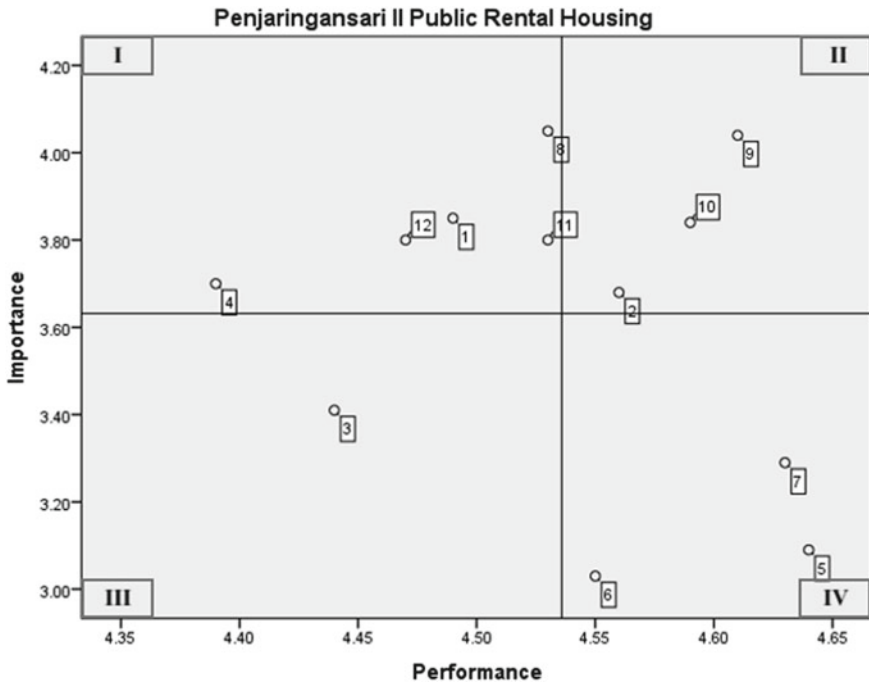


Fig. 5 Importance performance analysis of Pejaringanansari II public rental housing

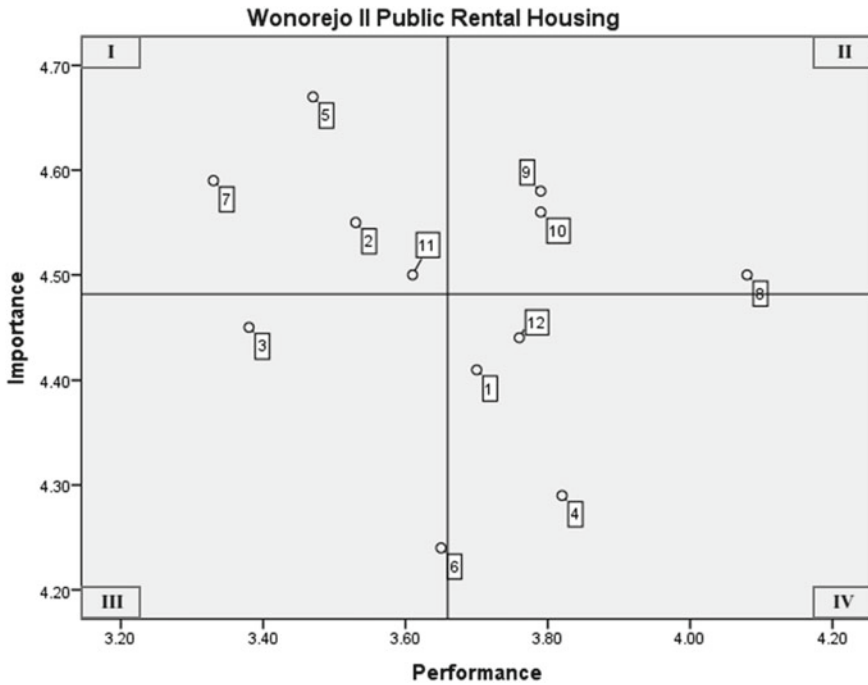


Fig. 6 Importance performance analysis of Wonorejo II public rental housing

Penjaringansari II and Gunung Anyar flats with five attributes that are in Quadrant I. For the results of Quadrant II, III, and IV can be seen from Tables 2 and 3). It can be seen that the attribute that is always in quadrant I of the four public rental housings is the reliability attribute with code (re). In line with the theory that in terms of measuring customer perceptions of service quality, reliability is considered as one of the core dimensions. Customers may expect to do business again with such an organization, which is renowned for keeping their promises. Consequently, customer reliability expectations should be well studied by all service providers [21].

4 Conclusion

This study aimed to identify the tenants satisfaction attributes of public rental housing in Surabaya which are the priority to be improved. The literature review was used to obtain 12 attributes of residence satisfaction based on Service Quality using the Servqual dimension. The questionnaire was distributed to a total of 231 tenants containing the assessment of the satisfaction of living in four public rental housing which represent different building ages, namely Gunung Anyar Public Rental Housing representing 0–5 years, Grudo Public Rental Housing representing



Fig. 7 Importance performance analysis of Grudo public rental housing

6–10 years, Wonorejo II Rental public Housing representing 11–15 years, and Penjaringansari II Public Rental Housing representing 15–20 years the results show that Penjaringansari II, namely attributes t1, e2, re2, as1, as2 and Gununganyar namely attribute t2, e1, e2, r1, re4 which have the lowest service quality attribute ratings because they have five attributes that are in quadrant I ‘Concentrate here’ which is a group of attributes that are a priority to be fixed. When there are many complaints about the quality of maintenance and quality of buildings that are ignored, it can cause the quality of maintenance and the quality of the building to decline which is the result of poor service quality delivery that can affect the age of the building. This shows that a public rental housing with a building age at least does not necessarily have a high level of service quality attribute rating because it depends on the services provided. Future research can close other research gaps by formulating improved strategies, especially for areas in the main concentrated quadrant. So, it can be used as an evaluation material for stakeholders to consider and make policies.

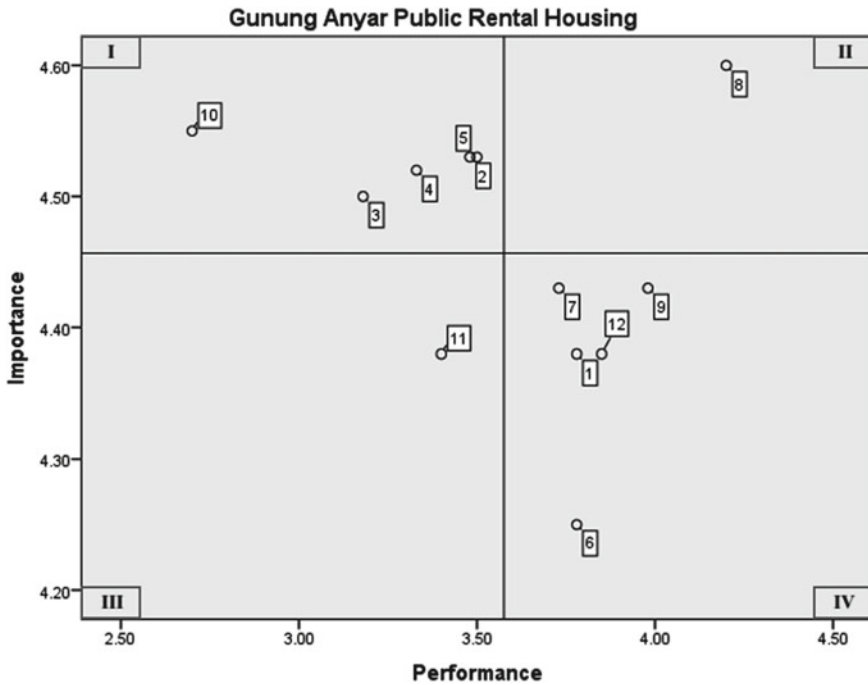


Fig. 8 Importance performance analysis of Gunung Anyar public rental housing

References

1. Zuashkiani A, Rahmandad H, Jardine AKS (2011) Mapping the dynamics of overall equipment effectiveness to enhance asset management practices. *J Qual Maint Eng* 17:74–92. <https://doi.org/10.1108/13552511111116268>
2. Ibem EO, Opoko AP, Adeboye AB, Amole D (2013) Performance evaluation of residential buildings in public housing estates in Ogun State, Nigeria: users' satisfaction perspective. *Front Arch Res* 2:178–190. <https://doi.org/10.1016/j.foar.2013.02.001>
3. Lai AWY, Lai WM (2013) Users' satisfaction survey on building maintenance in public housing. *Eng Constr Archit Manag* 20:420–440. <https://doi.org/10.1108/ECAM-06-2011-0057>
4. Seshadhri G, Paul VK (2018) Validation and ranking of user requirement related building performance attributes and sub attributes for government residential buildings. *Facilities* 36:638–656. <https://doi.org/10.1108/F-09-2017-0094>
5. Karim HA (2009) The satisfaction of residents on community facilities in Shah Alam, Malaysia. *Asian Social Sci* 4:131. <https://doi.org/10.5539/ass.v4n11p131>
6. Iriansyah N (2011) A Need for affordable housing in Banda Aceh, Indonesia. In: Proceedings of the annual international conference Syiah Kuala University 2011, vol 1(2):189–193, Banda Aceh, Indonesia, 29–30 Nov 2011
7. Olanrewaju AA (2013) Revealing the service gaps in building maintenance service delivery: balancing providers' perspectives with users' perspectives. *Int J Built Environ Asset Manage* 1:121. <https://doi.org/10.1504/IJBEAM.2013.056952>

8. Olanrele OO, Thontteh EO (2014) FM service delivery and quality service measurement in public high rise residential buildings in Nigeria: the use of SERVQUAL and satisfaction index. *J Manage Sustain* 4:145. <https://doi.org/10.5539/jms.v4n3p145>
9. Harris PJ, Mongiello M (2001) Key performance indicators in European hotel properties: general managers' choices and company profiles. *Int J Contemp Hosp Manag* 13:120–128. <https://doi.org/10.1108/09596110110388909>
10. Karunasena G, Vijerathne D, Muthmala H (2018) Preliminary framework to manage tenant satisfaction in facilities management service encounters. *Facilities* 36:171–194. <https://doi.org/10.1108/f-05-2016-0050>
11. Vinagre MH, Neves J (2008) The influence of service quality and patients' emotions on satisfaction. *Int J Health Care Qual Assur* 21:87–103. <https://doi.org/10.1108/09526860810841183>
12. Wirtz J, Tambyah SK, Mattila A, Goh JEP (2010) Organizational learning from customer feedback received by service employees: a social capital perspective. *J Serv Manage* 21(3). <https://doi.org/10.1108/17575811080000440>
13. Vos JFJ, Huitema GB, de Lange-Ros E (2008) How organisations can learn from complaints. *TQM J* 20(1):8–17. <https://doi.org/10.1108/09544780810842866>
14. Deuble MP, de Dear RJ (2014) Is it hot in here or is it just me? Validating the post-occupancy evaluation. *Intell Build Int* 6:112–134. <https://doi.org/10.1080/17508975.2014.883299>
15. Abisuga AO, Wang CC, Sunindijo RY (2020) Facility managers' responses to user post-occupancy feedback: a conceptual framework. *Facilities* 38:481–499. <https://doi.org/10.1108/f-10-2018-0119>
16. Negi R (2009) Determining customer satisfaction through perceived service quality: a study of Ethiopian mobile users. *Int J Mobile Mark* 4(1):31–38
17. Parasuraman A, Zeithaml VA, Berry L (1988) SERVQUAL: a multiple-item scale for measuring consumer perceptions of service quality. *1988* 64(1):12–40
18. Abdellatif MA, Othman AAE (2006) Improving the sustainability of low-income housing projects: the case of residential buildings in Musaffah commercial city in Abu Dhabi. *Emirates J Eng Res* 11(2):47–58
19. Sugiyono P (2010) *Metode Penelitian Bisnis* (15th ed). Alfabeta, Bandung
20. Lai JH (2012) Analytical assessment and comparison of facilities management services for residential estates. *Int J Strateg Prop Manag* 16:236–253. <https://doi.org/10.3846/1648715x.2012.682183>
21. Bashir S, Sarki IH, Samidi J (2012) Students' perception on the service quality of Malaysian Universities' hostel accommodation. *Int J Bus Soc Sci* 3(15):213–222
22. Radder L, Han X (2009) Service quality of on-campus student housing: a South African experience. *Int J Econ Bus Res* 8(11):107–120. <https://doi.org/10.19030/iber.v8i11.3190>
23. Oladapo AA (2006) A study of tenants' maintenance awareness, responsibility and satisfaction in institutional housing in Nigeria. *Int J Strateg Prop Manag* 10:217–231. <https://doi.org/10.3846/1648715x.2006.9637554>
24. Lin S-P, Chan Y-H, Tsai M-C (2009) A transformation function corresponding to IPA and gap analysis. *Total Qual Manage Bus Excellence* 20(8):829–846. <https://doi.org/10.1080/14783360903128272>

Modeling of Conceptual Framework to Understand Stakeholders' Awareness in Construction Industry in Thailand Affected by the 3rd Wave of COVID-19 Pandemic



Nattasit Chaisaard and Grit Ngowtanasuwan

Abstract The latest 3rd wave of COVID-19 pandemic is occurring globally from 2020 to 2021 without any sign of significant diminishing. More variants of coronavirus 2019 mutation have been found in Thailand, together with a high mortality rate. While vaccination, an important national agenda, could not yet control the pandemic, the pandemic has caused difficult circumstances in labor-intensive industries, especially the construction industries. Consequently, the researchers became interested in studying the conceptual framework to understand stakeholders' awareness in the Thai construction industry affected by the 3rd wave of the COVID-19 pandemic, especially during April–May 2021. And hence did as follows. At first, the researchers studied literature reviews from various academic articles and online databases and gathered information through in-depth interviews via collaboration tools such as the Microsoft team and zoom applications in communicating with thirteen experienced construction practitioners. Secondly, the researchers validated the information and developed a conceptual framework model of stakeholders' awareness in the construction industry in Thailand. In the model, the researchers found that the pandemic changed the attitudes of Thai practitioners, both confident and satisfaction attitudes, affected working practices, and necessitated stakeholders to assess effects on construction projects and formulate future policies and practical measures at executive and operational levels.

Keywords Conceptual framework • Stakeholders' awareness • COVID-19 pandemic

N. Chaisaard (✉)

Construction Management Program, School of Management Science, Sukhothai Thammathirat Open University, Nonthaburi 11120, Thailand
e-mail: nattasit.chaisaard@gmail.com

G. Ngowtanasuwan

Construction Management Program, Faculty of Architecture, Urban Design and Creative Arts, Mahasarakham University, Maha Sarakham 44150, Thailand

1 Introduction

The COVID-19 pandemic has been a major global health crisis for decades. Apart from the unprecedented number of deaths and hospitalizations, the plague has resulted in economic slowdowns, extensive business disruptions, and significant adversities [1, 2]. Yet another pathogenic HCoV (human coronavirus) initially found in December 2019 next to SARS-CoV and MERS-CoV (the Middle East Respiratory Syndrome coronavirus), the novel coronavirus, “Coronavirus disease (COVID-19)”, was first recognized in Wuhan, the People’s Republic of China with unprecedented rates of infection and death so high that Public health authorities and World Health Organization, WHO, initiated preparedness and response activities [3, 4]. March 11, 2020, WHO designated “coronavirus disease 2019” (COVID-19) to be a global pandemic [5, 6] and found it could be infectious even before the significant symptoms appear [7]. However, based on currently available data, people who have symptoms account for the majority of virus spread. Then a new ripple, the 3rd wave of the pandemic, is occurring globally throughout the year 2020 to 2021, especially in Thailand between April and May 2021, without any sign of significant diminishing. Although globally, WHO has declared vaccination an important mission toward herd immunity of the world’s population, still many countries, particularly Asian and Southeast Asian countries continue to extremely experience the pandemic with high mortality rates for several consecutive months since last year. Especially in India, as of late May 2021, there were more than 27,367,935 people infected with COVID-19 [8], with the total mortality rate high over 315,263. ASEAN countries such as Singapore, Malaysia, and Thailand have all suffered such severe consequences. Particularly Thailand, although it could control the situation well in the early period of the pandemic last year in 2020, has been hit by the new 3rd wave of the pandemic from early April 2021. Also, the new variants from coronavirus 2019 mutation are defined and classified as follows: (1) variant of interest, (2) variant in concern, and (3) variant of high consequence. Specifically, a variant of interest requires appropriate public health actions such as enhanced sequencing-based surveillance, boosted laboratory characterization, or epidemiological investigations to assess the extent of viral spreads, the severity of disease, and the efficacy of therapeutics and currently authorized vaccines [9]. While the viral mutations spread quickly and easily across Asian countries, particularly Thailand, where outbreaks of many strains have been found. According to the report from the Department of Disease Control (DDC) in Thailand, as the latest May 27, 2021, there were 920 deaths, 143,280 infected patients, 50,595 of which were in the public health system [10]. Apart from the widespread health crisis, the COVID-19 pandemic has resulted in a nationwide economic downturn in Thailand together with realms of socio-economic and cultural impacts [11]. Like other countries, Thailand has faced the same problems precisely from the massive shrinkage of demand in the economy that disrupts airlines, restaurants, service businesses, manufacturing, and retail industries, particularly high labor-intensive industries like construction industries. Thai stakeholders such as project owners or

investors, end-users, architect and engineer (A/E) designers, construction project consultants, supervisors, technicians, and important parties, particularly contractors, are directly and indirectly impacted by the COVID-19 pandemic. So, the researchers have planned to study literature reviews from various published articles of both international and domestic contexts for clearer understanding and meanwhile gathered information through in-depth interviews via the collaboration tools such as Microsoft team and zoom applications to communicate with thirteen experienced construction practitioners. And then developed a conceptual framework to understand awareness of stakeholders in the Thai construction industry affected by the 3rd wave of COVID-19 pandemic from April 2021—present. While collecting necessary information by prompt in-depth interviews, the researchers compared the finding to the research articles, and online databases earlier studied to create and modify a model. In the model, the researchers found that the pandemic changed the attitudes of Thai practitioners, both confident and satisfaction attitudes, affected working practices, and necessitate stakeholders to assess effects on construction projects and formulate future policies and practical measures at executive and operational levels.

2 Research Background

The COVID-19 pandemic has put labor-intensive industries at much risk that practitioners in the construction industries around the world are facing high probabilities of COVID-19 transmission. Their knowledge, particularly attitudes, and practices (KAP), are so critical to prevent virus spread [12] that the practitioners in China generally have optimistic attitudes in battling against the COVID-19 contagion and are satisfied with the Chinese governments' contingency measures [12]. Thus the researchers needed to explore further in the context of the Thai construction industry for better understanding by contrasting political, economic, and cultural aspects. Whereas both Chinese and typical Thai practitioners in Thailand tend to actively take preventive measures such as checking body temperature, wearing face masks, and keeping safe social distance continually [4, 12], the researchers need to study more about the actual practices, particularly in identifying and adopting safety measures recommended for the safe operation of construction workplaces. The taskforce staff continuously updates the operational plan, offers practical guidance to the site leadership on work management in construction workplaces, and determines the acceptance of safety measures presented to workers and site personnel on the safety risk of COVID-19 and safety management [1]. Whether such procedures are carried out in Thailand, the researchers need to explore the real in-depth practices in the Thai construction industry by following the guidelines [1, 4, 12, 13] on contract management practices and procedures on various waiver compensation. Those guidelines are as follows: (1) strict access to an organization or workplace, (2) operation in an organization or workplace still are limited due to worker density, (3) verified attendance records, (4) coordination and

communication by smart devices and applications to avoid confrontation, (5) standard setup and organization of working condition, (6) adequate public communication and recommendation especially on working procedures for those in work units and places. There are general measures in maintaining the social distancing between individuals, wearing face masks along with temperature measurements, and other special measures and requirements such as determination of working zone, the entry and exit routes in construction site, disinfectant spray with the dedicated station for hand cleansing, ventilation system setup, the organization in the dining area, toilets, building-material storage, and waste sort-out, etc. Since almost the entire construction industry in Thailand employs migrant workers from neighboring countries such as Cambodia, Myanmar, and Laos, such migrant workers must be strictly inspected in conjunction with firm procedures. Focusing on common points with possible impacts in the international context [1, 12], the researchers modified the information to the context of the Thai construction industry and conducted an in-depth interview to confirm consistency. The information from the interview was compiled and revised to create a conceptual framework as defined by [14, 15] and used to form a network of conceptual diagrams to provide a comprehensive understanding of the phenomenon being studied. The conceptual framework consists of factors and indicators that affect each other within the framework [14]. There are eight steps in formulating a conceptual framework as follows: (1) mapping the selected data sources, (2) extensive reading and categorizing the selected data, (3) identifying and naming concepts, (4) deconstructing and categorizing concepts, (5) integrating concepts, (6) synthesis and re-synthesis to finalize the best approach, (7) validating the conceptual framework, (8) rethinking the conceptual framework.

3 Research Method

First, an in-depth interview technique [16] is applied to develop the conceptual framework model to understand the awareness of stakeholders in the construction industry in Thailand impacted by the 3rd wave of the COVID-19 pandemic. The method was as follows:

3.1 Identification of the Factors

First, the researchers studied, assessed factors and related variables in related works of literature such as academic articles and online databases, and associated the data from informal talks with experienced practitioners to compile all relevant factors to be collected and grouped.

3.2 *Validation of the Factors*

The researchers confirmed the listed factors with thirteen experienced construction practitioners in related fields by an in-depth interview technique. The experienced practitioners selected based on their professional experiences were as follows:

- Five construction project directors and/or managers with more than 20 years of experience in the Thai construction industry.
- Three experienced practitioners from construction consultancy companies.
- Four experienced practitioners working as project supervisors from government agencies.
- One experienced practitioner from an academic institution.

An in-depth interview is not only one of the most effective qualitative methods for people, in this research, the experienced practitioners, to voice their personal feelings, opinions, and experiences, but also gives an opportunity to gain insight into how people interpret and order the world [16]. The researchers conducted the interview via the collaboration tools such as the Microsoft team and zoom applications, observed the causal explanations, after saturated, sought consistency with opinion confirmation, and then constructed the conceptual framework in the next step.

3.3 *Drafting the Conceptual Framework*

The researchers compared the results from the in-depth interviews of thirteen experienced practitioners with the data from related literature to create saturated contents, drew nodes and arrows between each factor to create the first draft of a conceptual framework, reconfirmed the first draft with some of the thirteen experienced practitioners for validation, and categorized the validated factors to create the final conceptual framework.

4 Results

Opinions from thirteen experienced practitioners are arranged in sequential order of factors starting from (1) attitude of the respondents, confident and satisfaction attitudes, that caused (2) affected practices during the pandemic leading to (3) effect assessment on construction projects by stakeholders in various construction industries as itemized in Tables 1, 2, 3, and 4.

Tables 1, 2, 3, and 4 show each confirmed factor and its measurement as follows: ATT, attitude of practitioners, categorized into two sub-factors, (1) CATT, confident attitude, consisted of 3 items (CATT1–CATT3), (2) SATT, satisfaction

Table 1 Confirmed factors (attitude of respondents: confident attitude) in conceptual framework and their measurement items

Factor	Item
Attitude of respondents (ATT) Confident attitude (CATT)	CATT1: I always felt anxiety and a lack of confidence at contacting coronavirus (COVID-19) through my routine operations CATT2: I feel tired of working during the COVID-19 pandemic CATT3: Since construction activities require interaction with others. I believe that my colleagues and staffs in my organization have a chance to contact COVID-19

Table 2 Confirmed factors (attitude of respondents: satisfaction attitude) in conceptual framework and their measurement items

Factor	Item
Attitude of respondents (ATT) Satisfaction attitude (SATT)	SATT1: My agency executives are focused and well prepared against the 3rd wave of the COVID-19 pandemic with regularly reminding of policies, plans, and preventive measures SATT2: My organization gives priority to personnel by providing additional materials and supplies such as body temperature monitoring devices, hand sanitizers, face masks, etc. SATT3: I am willing to cooperate with my organization’s policies on safety and hygiene reasons for myself, my colleagues, and my agencies SATT4: My organization is affected by the management policy of government agencies to confront the 3rd wave of coronavirus pandemic crisis SATT5: During the 3rd wave of outbreak, my organization encourages staff and workers to reserve vaccination against COVID-19 according to government policy, to which I am willing to cooperate SATT6: I can work efficiently without any problems or obstacles during the 3rd wave of the COVID-19 pandemic

attitude, consisted of 6 items (SATT1–SATT6); PRA, affected practice during the pandemic, consisted of 10 items (PRA1–PRA10); EFF, effect assessment in construction projects from the stakeholders’ viewpoints, consisted of 15 items (EFF1–EFF15) respectively. Afterward, all factors and their measurement items were used to construct the conceptual framework shown in Fig. 1. Consequently, the extended framework included more details on items, variables, and their indicators shown in Fig. 2.

Table 3 Confirmed factors (affected practice) in conceptual framework and their measurement items

Factor	Item
Affected practice (PRA)	<p>PRA1: Contract management and project operations are compensated (e.g., extension period, abstinence, or reduction of the penalty fee)</p> <p>PRA2: Operation in an organization or workplace is still limited by rules on crowd gathering, worker density, and attendance record</p> <p>PRA3: To coordinate and communicate without confrontation, smart devices and applications are definitely used to support remote operations</p> <p>PRA4: Organizing and setting standards of working conditions in workplaces are tidier than usual</p> <p>PRA5: Adequate public communication and recommendation, especially on working procedures for those in working units and places</p> <p>PRA6: There are strict measures in maintaining the social distancing between individuals, wearing face masks along with temperature measurements, etc. Maintaining hygiene in units or workplaces is performed according to recommendations from government agencies</p> <p>PRA7: There are other special measures. For instance, a determination of working zone, the entry and exit routes in construction site, disinfectant spray with the dedicated station for hand cleansing, ventilation system setup, the organization in the dining area, toilets, building-material storage, and waste sort-out, etc.</p> <p>PRA8: There is a strict screening of people in the organization or workplace. Those not involved are not permitted into the working area</p> <p>PRA9: Migrant workers are subject to rigorous scrutiny and working regulation by cooperating with government agencies</p> <p>PRA10: Due to the volatility and uncertainty from the new potential surge, unusual construction operation will continue in conjunction with the hygiene system of the workplace in the future</p>

5 Conclusions

To model a conceptual framework to understand the awareness of stakeholders in the construction industry in Thailand affected by the 3rd wave of COVID-19 pandemic, the researchers studied factors related to attitudes of the stakeholders and identified various factors from the related theories and literature reviews from numerous sources of articles and online databases, most of which are recent, previous studies in the year 2020 to 2021. Then confirmed the factors with thirteen experienced construction practitioners in related fields using the in-depth interview technique, investigated and categorized the saturated opinions of thirteen experienced practitioners to create the conceptual framework shown in Fig. 2 with attitudes of the respondents, confident and satisfaction attitudes, and affected practices of the stakeholders referred from [1, 4, 12]. All The factors were shown in Tables 1, 2, 3, and 4 respectively: ATT, attitudes of practitioners, categorized into two sub-factors, (1) CATT, confident attitude, consisted of 3 items (CATT1–CATT3), (2) SATT, satisfaction attitude, consisted of 6 items (SATT1–SATT6); PRA, affected practices during the pandemic, consisted of 10 items (PRA1–PRA10);

Table 4 Confirmed factors (effect assessment in construction projects) in conceptual framework and their measurement items

Factor	Item
Effect assessment in construction projects (EFF)	<p>EFF1: Effect on disruption on construction activities</p> <p>EFF2: Effect on labor shortages</p> <p>EFF3: Effect on working period</p> <p>EFF4: Effect on construction cost overrun</p> <p>EFF5: Effect on the quality of work from construction operation</p> <p>EFF6: Effect on the financial aspect (accruals, delays, delays in settlement of trade debt, late payment, and others)</p> <p>EFF7: Effect on material and equipment shortage</p> <p>EFF8: Effect on price hikes and fluctuations of construction materials and equipment</p> <p>EFF9: Effect on construction planning and scheduling of working duration and/or project implementation</p> <p>EFF10: Effect on inconvenient transportation, especially labor movement across country and provinces according to the order of the Center for COVID-19 Situation Administration during the outbreak</p> <p>EFF11: Effect on construction contract management and/or contracts related to the construction transactions and activities</p> <p>EFF12: Effect on activities during operations as well as scheduled work completion</p> <p>EFF13: Effect on confidence on construction occupations impacted by economic, social conditions and the future uncertainty</p> <p>EFF14: Effect on innovation and technology that will transform the construction industry and working context in the future</p> <p>EFF15: Effect on the expectation of continual change adapting to the future under the next normal's working culture and post-COVID-19 working context</p>

EFF, effect assessment in construction projects from the stakeholders' viewpoints, consisted of 15 items (EFF1–EFF15). Afterward, the researchers drew a network diagram from effect assessment, the attitude of the respondents, and affected practice to create a conceptual framework of the awareness of stakeholders in the construction industry in Thailand affected by the 3rd wave of COVID-19 pandemic. Whereas all factors and their measurement items were used to construct the conceptual framework as shown in Fig. 1, the extended framework included more details of items, variables, and their indicators shown in Fig. 2, respectively. This improved and expanded framework will be used in quantitative analysis to determine and formulate future policies and practical measures for Thai construction stakeholders at the executive and operational levels.

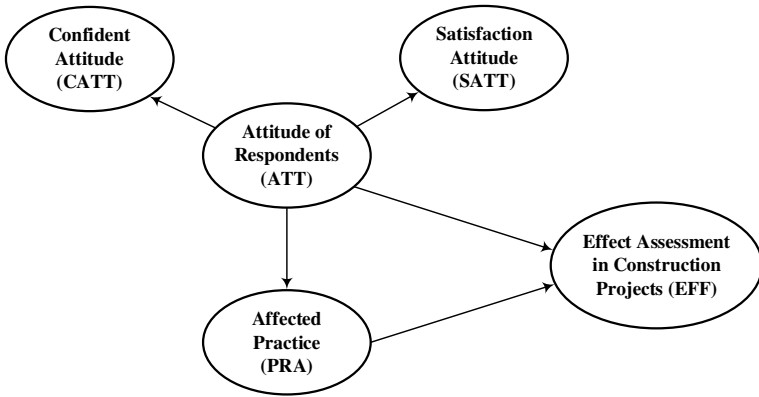


Fig. 1 Conceptual framework of the awareness of stakeholders in construction industry in Thailand affected by the 3rd wave of COVID-19 pandemic

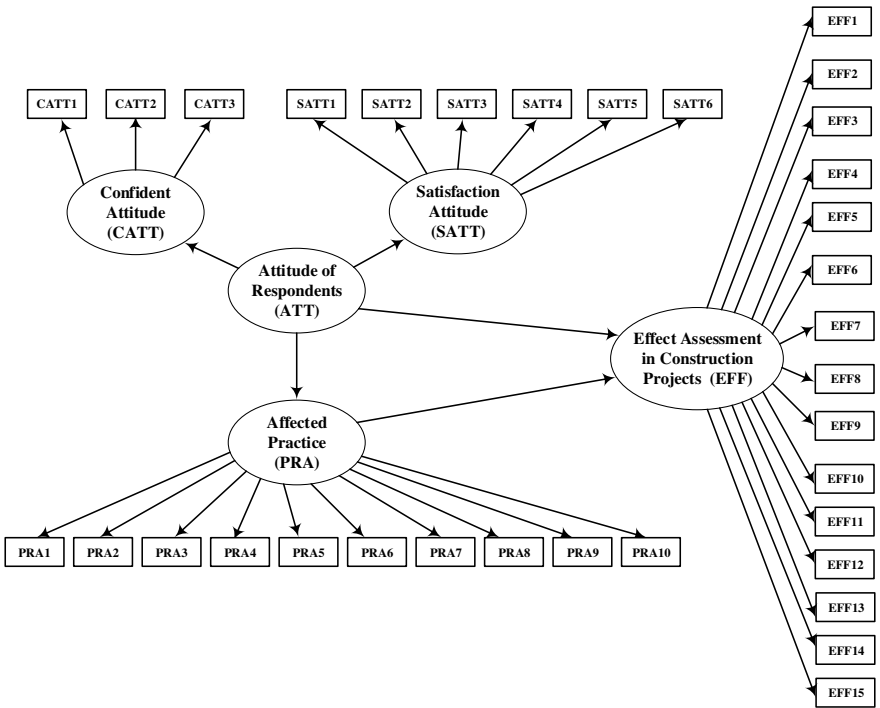


Fig. 2 Detailed conceptual framework

References

1. Alsharaf A, Banerjee S, Uddin SM, Albert A, Jaselskis E (2021) Early impacts of the COVID-19 pandemic on the United States construction industry. *Int J Environ Res Public Health*. <https://doi.org/10.3390/ijerph18041559>
2. Ruiz Estrada MA (2020) COVID-19: economic recession or depression? *SSRN Electron J*. <https://doi.org/10.2139/ssrn.3575881>
3. Zhu N, Zhang D, Wang W et al (2020) A novel coronavirus from patients with pneumonia in China, 2019. *N Engl J Med*. <https://doi.org/10.1056/NEJMoa2001017>
4. Chaisaard N, Ngowtanasuwan G, Doungpan S (2020) A review of construction project management guidelines under the impact of COVID-19 epidemic dispersal: a case study of Thai construction projects. In: SUT international virtual conference on science and technology, Nakhon-Ratchasima, Thailand, 28 Aug 2020
5. Ranney ML, Griffeth V, Jha AK (2020) Critical supply shortages—the need for ventilators and personal protective equipment during the Covid-19 pandemic. *N Engl J Med*. <https://doi.org/10.1056/nejmp2006141>
6. Hansen S (2020) Does the COVID-19 outbreak constitute a force majeure event? A pandemic impact on construction contracts. *J Civil Eng Forum* 6:201. <https://doi.org/10.22146/jcef.54997>
7. Rothe C, Schunk M, Sothmann P et al (2020) Transmission of 2019-nCoV infection from an asymptomatic contact in Germany. *N Engl J Med* 382(10):970–971. <https://doi.org/10.1056/nejmc2001468>
8. Worldometer (2021) Coronavirus cases. <https://www.worldometers.info/coronavirus/#countries>. Accessed 26 May 2021
9. Centers for Disease Control and Prevention (2021) SARS-CoV-2 variant classifications and definitions. <https://www.cdc.gov/coronavirus/2019-ncov/variants/variant-info.html#Interest>. Accessed 27 May 2021
10. DDC OpenData (2021) Covid-19 Thailand situation report. <https://covid19.ddc.moph.go.th/>. Accessed 27 May 2021
11. Review Board (2021) Introduction to socio-economic impact assessment. https://reviewboard.ca/upload/ref_library/SEIA_Guidelines_Chapter_2.pdf. Accessed 30 May 2021
12. Zheng L, Chen K, Ma L (2020) Knowledge, attitudes, and practices towards COVID-19 among construction industry practitioners in China. *Front Public Health*. <https://doi.org/10.3389/fpubh.2020.599769>
13. Gamil Y, Alhagar A (2020) The impact of pandemic crisis on the survival of construction industry: a case of COVID-19. *Mediterr J Soc Sci* 11:122. <https://doi.org/10.36941/mjss-2020-0047>
14. Jabareen Y (2009) Building a conceptual framework: philosophy, definitions, and procedure. *Int J Qual Methods* 8(4):49–62. <https://doi.org/10.1177/160940690900800406>
15. Ngowtanasuwan G (2020) Modeling of conceptual worker engagement framework for construction projects in Thailand. In: 2nd International conference on civil and environmental engineering technologies, University of Kufa, Najaf, Iraq, 10–11 June 2020; IOP Conf Ser: Mater Sci Eng 888. <https://doi.org/10.1088/1757-899X/888/1/012083>
16. Milena ZR, Dainora G, Alin S (2008) Qualitative research methods: A comparison between focus-group and in-depth interview. In: *Annals of faculty of economics, University of Oradea*, vol 4, p 1279–1283

A Literature Review on Healthy Buildings Based on Various Perspectives



Louferinio Royanto Amatkasmin, Mohammed Ali Berawi ,
and Mustika Sari 

Abstract Existing healthy building standards and guidelines are based on the dose exposure point of view, where certain doses of safe or comfortable exposure to light, sound, air quality, water quality and indoor temperature are established. This poses a substandard outlook of designing a healthy indoor environment which is defined by more than just levels of exposure that are safe. This research presents a literature review that provides a new outlook on healthy building which is more user-centric and improves occupant quality of life by considering the mental and physical health effects, and the effect of the built environment on its occupants. Literature was collected on indoor environmental quality parameters: indoor air quality, thermal comfort, visual comfort, and acoustic comfort in relation to different perspectives. The current body of knowledge still needs more research on specific health effects of buildings on occupants in order to augment existing standards and guidelines. Literature shows that there is a surge of awareness that the buildings we utilize have a tremendous hold on our health and life quality. In the future a shift in mindset and practice is essential to ensure further advancement in the construction industry.

Keywords Healthy building design · Indoor environmental quality · Built environment · Green building

L. R. Amatkasmin (✉) · M. A. Berawi · M. Sari
Civil Engineering Department, Faculty of Engineering, Universitas Indonesia, Jakarta, Indonesia
e-mail: loufirinio@hotmail.com

© The Author(s), under exclusive license to Springer Nature Singapore Pte Ltd. 2022
H. A. Lie et al. (eds.), *Proceedings of the Second International Conference of Construction, Infrastructure, and Materials*, Lecture Notes in Civil Engineering 216, https://doi.org/10.1007/978-981-16-7949-0_51

567

1 Introduction

Healthy building design strives to minimize the negative impacts on the environment and to maximize the positive impacts of health and well-being that buildings have on occupants. Although urbanization shows growing health costs and other social consequences, we should also consider the positive impact buildings can have on people as well as reducing the impact on our environment. A healthy building is a building that is designed to be supportive to: the well-being of its tenants and to the preservation of the environment [1]. Indoor environmental quality concerns are therefore a determining factor in the design and must be assessed to evade negative effects on the well-being and prosperity of its inhabitants. This does not just include the use of healthy materials in the design (with consideration of acoustic comfort, thermal comfort, pollution, etc.), but also promotes healthy living amongst occupants by means of education about living healthily. A study was done on educational building based healthy building design on three principles and main groups proving that work environment has a big impact on health [2]. The first principle is building placement on the site, landscape design, and connection to the entire city. The second principle is designing healthy buildings (from a big idea, construction, Mechanical, Electrical, and Plumbing (MEP), etc.). Lastly, the third is interior design and its influence on human health. For the literature review, emphasis will be placed upon the third principle; the design of a healthy building. In order to construct an orderly review, a systematic approach to section division is conducted based on three viewpoints: the perspective of the built environment, the dose exposure parameter, and the occupant or end-user effect [3]. This paper presents a state-of-the-art analysis of research in the area of healthy building design and occupant well-being in relation to indoor environment quality. The review of literature is narrowed down to the design of healthy spaces and how it influences the health of humans. Indoor environmental factors paired with the dynamic nature of occupants in different building situations make for a complex system. Existing healthy building standards (Leadership in Energy and Environmental Design (LEED), Building Research Establishment Environmental Assessment Method (BREEAM), WELL, etc.) and guidelines are based on the dose exposure point of view, where certain doses of safe or comfortable exposure to light, sound, air quality, water quality, and indoor temperature are set [3]. This poses a substandard outlook of designing a healthy indoor environment, which is defined by more than just levels of exposure that are safe. This new outlook which focuses not only on levels of 'safe' exposure to indoor environmental factors, but also includes the effects of the built environment on the occupant, and the mental and physical health effects on occupants which are not considered enough in standards and guidelines. Literature shows that there is still much more to be researched about the effects of buildings on human health. The paper further discusses the various threats and challenges emerging from research in this area to aid upcoming researchers in establishing a proper foundation. The discussion is focused on establishing a connection between Indoor Environmental Quality (IEQ) parameters with different

perspectives to consider for healthy building design. The next section consists of the methodology followed by the literature review, and the discussion section and conclusions closing the paper with possibilities for future research.

2 Methodology

The focus of the literature review is to document literature and analyze vital subjects derived from this study based on the perspective of the built environment, dose exposure to indoor environmental factors and occupant effect in various situations. Eventually, a way forward will be established for a more integrated approach to designing healthy indoor environments. For this study, identification of literature is carried out with the use of keywords for each point of view. The keywords used for the search were:

- Built environment: visual comfort, acoustic comfort, thermal comfort, and Indoor Air Quality ergonomics and design.
- Dose exposure: visual comfort, acoustic comfort, thermal comfort, and Indoor Air Quality paired with occupant effect.
- End-user or occupant effect: illnesses, physiological effect, illnesses, and psychological effect of the building on occupant well-being.

The articles were collected from ScienceDirect, Scopus, and Google Scholar. The bibliographies of these articles were then “snowballed” to further identify any relevant research that can contribute to the main thread. The collection of articles are based on the latest research available from the search engines to maintain an up-to-date view of current research. Finally, the analysis takes place where the papers are analyzed according to their respective topics that stand for the sections in this paper. The topics are: indoor air quality, thermal comfort, visual comfort, and acoustic comfort relating to the built environment, effects on occupants, and dose-response of occupants. The upcoming sections after the previous topics consist of relevant issues that impact healthy building design greatly. With the recent emerging trends of designing healthy buildings using healthy building guidelines, the discussion creates a way to establish the current state of challenges researchers are facing and help researchers propose a way forward. The discussion will help provide a more holistic view of how healthy spaces relate to healthy people.

3 Healthy Building from Different Viewpoints

Indicators for healthy building performance can be viewed from various different perspectives, a few to mention: the built environment (building and components), the occupant or end-user (illnesses, workability, symptoms), and the dose or

environmental parameter (concentrations of indoor air pollutants, indoor temperature, lighting intensity, ambient noise level) [3]. In order to have a more holistic approach towards assessing healthy buildings, we need to consider the complexity involved when relating human health to buildings. Standards and guidelines for healthy building are more focused on dose-related indicators rather than the in-depth consideration of the different viewpoints, which are integrated into the design process [4]. This may result in designers aiming to achieve the minimum requirements for indicators, possibly negating the consequences.

Health insurance costs reported across several references indicate that a sub-standard indoor environment is correlated with several health conditions and illnesses such as colds, headaches, respiratory illnesses, musculoskeletal disorders, back pain, and symptoms of SBS (sick building syndrome) [5]. Hence the importance of discussing the subject of human health and well-being from a built environment perspective as a topic that requires a substantial amount of field research and experimentation. Occupant well-being is correlated with the built environment due to the interaction of its users with systems that often case are solutions or problems depending on the degree of focus placed on their lifestyle and personal traits [6]. In order to successfully implement factors that are important for a healthy living environment, designers face many challenges. The Comfort Houses project discovered that analysis of the indoor environment and systems that are user-friendly (and consider patterns of human behavior) are a part of the design process for healthy building [6].

Research shows that design choices made in engineering and architecture contribute to the physical and mental effects imposed on occupants through the built structures they inhabit. The physical health problems that are caused by poor design and construction have been studied to a greater extent than the mental health problems [7]. Some indoor environmental parameters can be designed to extend more control to the occupants, which gives them more freedom to personalize according to their complicated individual needs. Thermal comfort (and visual comfort (glare control, zone lighting controls, etc.)) are two examples where engineered control can be provided to the user, improving their physical and mental health. The design of a healthy indoor environment, therefore, is not as marginal as attending to the physiological issues through increasing the rates of ventilation, improved ergonomics, sufficient and efficient lighting, heating and cooling systems [5], but also the psychological issues. Emerging trends in research address the psychological impact that design of spaces has on the mental health of occupants. Based on research done by Dunleavy et al. [8] on IEQ, more specifically, indoor air quality, thermal comfort, acoustic comfort, and visual comfort have been associated with psychological distress. Aboveground workspaces are found to have a higher negative psychological impact when indoor air quality, thermal comfort, and lighting are of poor quality. Underground workspaces, however, have a higher odds of psychological distress due to poor thermal comfort and acoustic comfort, as found by Dunleavy et al. Healthy building guidelines focused on these parameters may be helpful in countering the negative effects.

4 Indoor Air Quality

4.1 *From a Built Environment Perspective*

Research indicates that from a built environment perspective, ventilation systems, the condition and design of the building, and occupant behavior have a big impact on ventilation design. Occupant health depends on the quality of indoor air, and thus the amount and quality of air entering the building from the outdoors is a major concern. Designers address this concern by considering aspects like the heating, ventilation, and air conditioning (HVAC) system, airflow throughout between the spaces, user control of windows or doors, and systems for ventilating areas like kitchens and bathrooms [9–12]. Both designers and occupants play a major role in ensuring healthy indoor air. User-control over ventilation within the safe means, considering the balance between low and high ventilation rates, is a challenge that designers are facing today.

4.2 *From an Occupant/End-User Perspective*

Physiological Health Concerns According to Hoisington et al. [13], there are health concerns for buildings with both low and high rates of ventilation. Areas with low rates of ventilation can increase the build-up of carbon dioxide (CO₂) due to respiratory exhalation [14]. An excess amount of CO₂ can serve as a carrier for other indoor air pollutants that come from indoor activities like cleaning activities, cooking activities (air fresheners, combustion, household equipment), and from indoor materials (composite-wood materials, and flooring) and furnishings [15]. Furthermore, if there is an excess in moisture due to low ventilation, mold growth may occur and can be particularly worsened in areas like kitchens and bathrooms; its severity depending on occupant behavior [16]. Alternatively, high rates of ventilation have higher odds of introducing unsafe amounts of outdoor air pollutants into the indoors. These outdoor air pollutants include but are not limited to carbon monoxide, ozone, nitrogen oxides, and sulfur oxides [17]. High ventilation rates caused by the breach of the building façade does not only have higher odds of unsafe outdoor air pollutants indoors but also hold risks to pest intrusion, moisture, and bad thermal comfort [13]. Poor indoor air quality has been linked to SBS symptoms (such as headaches, irritated eyes, blocked nose), and reduced work performance. Therefore, designers need to provide satisfactory ventilation and thermal comfort (to mention the HVAC system) in order to support the health and productivity of its users [8].

Another indicator for indoor air quality is humidity, measured by Relative Humidity (RH), which has been shown to have a link to stress responses, physical activity, and sleep quality proven in one study which was conducted on a diverse group of study subjects in office buildings [18]. The workers were monitored on

their heart rate for three days consecutively, during which RH and temperature were measured in their workplaces. The study mentions the concern of the relaxation of thermal comfort standards on RH over the last 30 years, emphasizing that the initial accounts of American Society of Heating, Refrigerating and Air-Conditioning Engineers (ASHRAE) standards not possessing a lower limit for RH is false and that there is in fact proof of a lower limit. The study found that workers exposed to an environment with an RH of 30–60% experienced lower stress responses and better sleep quality than those outside the range (25% or less); suggesting that the range for RH should be narrower for optimal health (between 45 and 60%). According to one study higher rates of ventilation is correlated with negative physiological effects like asthma and asthma-like complaints, and persistent coughing [18]. Higher rates of ventilation may reduce the humidity in the building, affecting the relative humidity in indoors. Initial studies associated high or low RH with the development of health problems in occupants such as asthma, SBS, dry and irritated mucous membranes of the eyes and airways [19–21]. In addition, low RH increases the odds of infection, irritation, and fatigue from moisture reduction in the precorneal tear film of eyes, negative mental impacts associated with dehydration, and increased risks of contracting influenza [21–23]. Lastly, dry air conditions may be linked to increased levels of cortisol in the skin which in turn may result in the weakening of our immune system response [24].

Another study on Indoor Air Quality (IAQ) which was conducted on a sample of 148 office rooms across several European countries which relates concentrations of indoor air pollutants (volatile organic compounds) with reported health symptoms among workers, found that higher concentration of VOCs had higher odds of reporting health symptoms. The study concluded that xylenes were linked to headaches, tiredness and skin symptoms, ethylbenzene with eye irritation and respiratory symptoms, α -pinene with respiratory and heart symptoms, d-limonene with headaches and tiredness, and styrene with skin symptoms. Moreover, aldehydes like formaldehyde, acrolein, propionaldehyde, and hexanal were linked to respiratory, general symptoms, heart symptoms, and general SBS. Ozone was associated with almost all symptom groups [25].

Psychological Health Concerns There is a lack of research done on the topic of air quality indoors on psychological health, but there have been multiple studies on outdoor air pollutants relating to mental health. Even though it is of different sources, these studies may prove useful in providing some insight on the impact of air quality on psychological health. One literature review done by Hoisington et al. [13] has mentioned several studies (on men and women) conducted in countries like the US, China, and South Korea where unsafe amounts of exposure to air pollutants like SO_2 , NO_2 , CO, PM_{10} , $\text{PM}_{2.5}$ were linked to suicide, anxiety, and depression. Alongside this study, another study has proven that proper IAQ has been linked to lower levels of stress. This discovery was found due to occupants participating and producing feedback concerning the maintenance of the building ventilation system [8]. Arguably, occupant behavior and participation can play a big determining factor in the success of establishing proper IEQ in a building. The same study

estimated and compared the negative psychological impact of underground and aboveground workplaces, with repeated measures over time, concluded that underground workspaces are similar to aboveground workspaces in determining psychological distress [8]. Standards like the Regenerative Ecological, Social, and Economic Targets (RESET) air standard [26] are limited to minimal concentrations of particular air pollutants (particulate matter, total volatile air compounds, carbon-dioxide, and carbon-monoxide) which are considered 'safe'. But what is much less certain, is whether the plausibility of psychological distress is included within the standard. There are many other compounds which have proven to be linked to mental and physical health symptoms, not included within many existing guidelines and standards.

4.3 *The Dose Parameter*

Indoor air quality has an influence on the work-rate and well-being of occupants. Indoor air pollutants consist of, but are not limited, to carbon dioxide (CO₂), sulfur dioxide (SO₂), nitric oxide (NO), nitrogen dioxide (NO₂), volatile organic compounds (VOCs), semi-volatile organic compounds (SVOCs), levels of particulate matter (PM), and biological contaminants, all of which can affect both cognitive function and acts of learning [27]. In practice, ventilation and indoor CO₂ concentrations are used as a measure for the varying degrees of indoor air quality. An increase in CO₂ of 1000 ppm in educational buildings has shown an increase of student absences by 10–20% [28]. A study conducted by Sakellaris et al. [25] examined the association of indoor chemical air pollutants with SBS symptoms in office buildings. Across eight participating European countries and 167 office buildings, the methodology considered the known factors that SBS possess, which affect human health measured by some such as IEQ parameters (temperature, relative humidity, ventilation, light, noise), electromagnetic radiation, biological factors, IAQ/chemical compounds, as well as personal traits. Measurement results in the research above show that, among the indoor VOCs present in the office buildings, the highest quantities seemed to be: d-limonene 5.9–81 µg m⁻³, toluene 3.7–63 µg m⁻³, and a-pinene 3.2–68 µg m⁻³. Formaldehyde was the highest aldehyde amount discovered concerning indoor concentration, which was recorded to be between 10 and 48 µg m⁻³. Concentrations for O₃ and NO₂ were measured as 3.0 µg m⁻³ to 42 µg m⁻³ and 17 µg m⁻³ to 39 µg m⁻³, respectively. The study measured several VOCs linking the above mentioned d-limonene to general symptoms (symptoms of flu, headaches, languor, unusual tiredness) and heart problems, toluene to eye irritation and general symptoms, a-pinene to respiratory health problems, heart problems, and other general symptoms. Furthermore, formaldehyde is associated with general and respiratory symptoms, and NO₂ with general, eye irritation and skin conditions. The 'RESET' Air Standard for healthy residential buildings is a standard that helps monitor indoor air pollutants like particulate matter (PM_{2.5}), total volatile air compounds (TVOCs), carbon-dioxide

and carbon-monoxide (CO₂ and CO) as a representation of the performance of indoor air quality [26]. This is then used to educate and create awareness of indoor air quality on the environment and human health. However, judging from the literature review and a human health standpoint there are many more indoor air pollutants that need to be considered and monitored alongside the concentrations of PM_{2.5}, TVOCs, CO₂, and CO.

5 Thermal Comfort

5.1 *From a Built Environment Perspective*

It is now known that living in an environment with too high a temperature and level of humidity may cause moisture damage and fungal growth in the building [29]. Designers have to consider some of the same design aspects as before mentioned with indoor air quality, mainly the flow of air through the building, the HVAC system, and occupant control of windows and doors. For establishing thermal comfort, upholding standards of human health, and improving overall life quality, humans need the right temperature condition indoors, amongst other parameters [30]. Every person is unique when it comes to optimal thermal comfort which not only depends on the air parameters in the building (such as airspeed and temperature, mean radiant temperature] and RH), but also the individual metabolic rate or clothing insulation and the thermal adaptation ability [31, 32]. Predicted mean vote (PMV), predicted percentage dissatisfaction (PPD) model, adaptive thermal comfort model, and machine learning methods for thermal comfort are amongst the most popular models to predict the level of thermal comfort in a building [27].

A study by Yu et al. [33], researching the effect of occupant ventilation-behavior (OVb) in dormitories during leave, on indoor thermal comfort for intermittently heated space, found that occupants can drastically reduce the indoor thermal comfort level during periods of heating. The study proceeds to present two solutions. Firstly, decreasing the air change rate during periods of non-heating. Secondly, the use of automatic windows (for occupant control) alongside pre-heating is suggested for occupants who desire both indoor thermal comfort and ventilation. By functioning based on building parameters, air change rate, and outdoor mean temperatures, the automatic control system can do a number of things, such as: closing windows, pre-setting the temperature, and detecting the appropriate time to activate the heating system. The study suggests a setpoint of 3.3 h and 24 °C in case of low outdoor temperatures (e.g. 0 °C) in order to meet indoor thermal comfort requirements. In conclusion, occupants need to be aware and educated on the use of systems to obtain a complete understanding of the mechanisms in place to ensure their health. Full automation of the right living conditions of occupants is complex considering the individual requirements of each

person. Both designers and occupants play a major role in ensuring healthy thermal comfort. User-control is therefore, one of the main aspects for designers to place their focus on.

5.2 From an Occupant/End-User Perspective and Dose Perspective

Sub-optimal levels of temperature, specifically lower than acceptable temperatures, are linked with several physiological conditions like pneumonia, higher blood pressure, asthma, bronchitis, chronic headaches [30], and respiratory tract infection caused by a reduction in relative humidity [34]. Furthermore, psychological impacts of living in lower than acceptable temperatures include depression and anxiety disorders, amongst other stress-related psychological illnesses. On the opposite end, when exposed to conditions where the temperatures and humidity are too high, fungal growth may occur which is correlated with increased absenteeism, reduced worker productivity, and mortality [35, 36].

6 Visual Comfort

6.1 From a Built Environment Perspective

Human health is not just dependent on exposure to the proper lighting but also on non-visual factors like the textures of interior surfaces, design of spaces, décor, color, natural views, biophilia, along with many more non-light visual factors which may enhance cognitive functions and work productivity [37]. Humans have a calm and harmonious feeling when encountering, for example, the color green in the interior because of the association with nature [38]. Natural environments have the effect of restoring attention in humans, enhances work performances and satisfaction at the workplace [39]. Research has shown that access to natural landscapes results in higher odds of proficiency in reading and mathematics in students [40].

6.2 From an Occupant/End-User Perspective

Visual comfort provided by lighting is another parameter that can be controlled by designers in order to benefit occupants in the improvement of physical and mental health [41]. It is known that natural daylight is the better and more preferred source of light for occupants [42, 43]. Windows that provide natural daylight to working areas and have a view out are more desired by occupants [44]. Glare and thermal

discomfort provided by sub-standard lighting are associated with decreased productivity, increased absenteeism, and the choice to reduce exposure to the light source [45]. Light has the ability to trigger alertness and provide arousal; light has a direct influence on the natural process in humans (circadian rhythm) and the sleep quality and length. It is known that for people with neurodegenerative diseases and psychiatric disorders (schizophrenia, bipolar disorder, and autism), circadian rhythm correction has a positive impact on their ability to benefit from therapy and gain better control of their conditions of circadian abnormalities [13]. Timing and quantity of proper lighting have a big impact on the improvement of sleep quality and circadian rhythm correction [46]. It is therefore essential for designers to connect human health to lighting design because of its benefits towards healthy living. An example of faulty lighting design is the use of cool white fluorescent light which is able to disrupt the circadian rhythm of those exposed. On the contrary, the use of natural views and the right lighting exposure is able to reduce stress, decrease anxiety, and improve mood [47]. There is evidence suggesting that the use of bright light is effective as a therapeutic method (BLT) for treating the seasonal affective disorder and non-seasonal depression (chronic and antepartum depression, and bipolar disorder) [13].

6.3 *The Dose Parameter*

The quality of light is mostly determined by photometric variables (such as luminance, illuminance, color temperature, color rendering), glare, and light color temperature. Daylight supports natural processes in humans (circadian rhythm) and is the most satisfying, mainly due to how closely the color rendering matches the human visual response [48–50]. The study has shown that exposure to light through intrinsically photosensitive retinal ganglion cells called Melanopsin retinal ganglion cells (mRGCs), which are a part of a non-visual photoreception system, may have an enhancing effect on the alertness and performance of workers [51]. Furthermore, other non-visual lighting findings relating to variables like light exposure duration, timing, and spectrum distribution based on units of radiometric radiation have an influence on enhancing alertness, cognitive performance, and mood [52–54].

7 Acoustic Comfort

7.1 *From a Built Environment Perspective*

According to a recent study by Alonso et al. [55], there should be a more uniform and worldwide-wise acoustic requirements concept on external noise insulation, specifically for reference descriptors for façade sound insulation. Building façade

acoustic performance can be expressed in terms of the acoustic performance of the building components itself and the outdoor and indoor level of noise. The study found that proper acoustic retrofitting of façade windows can be enough to meet acoustic requirements worldwide with an external noise level of 60 dB(A) and suggests that strategies surrounding the quality of window design with respect to acoustic performance can provide a significant improvement the acoustic integrity of the building.

7.2 From an Occupant/End-User and Dose Parameter Perspective

A study by Dong et al. [56] concluded that an environment with high levels of noise (>90 dB(A)) have a detrimental effect on comfort and productivity, so much so that it has a higher influence than other indoor environmental quality parameters (like temperature, humidity, light, air quality, etc.) weighing the heaviest when it comes to the level of overall comfort. Environments with noise levels between 40 and 70 dB(A), although considered environments with daily noise, also have a negative influence on human body comfort and work productivity, even more so than music. The Environmental Noise Guidelines (ENG) published by the World Health Organisation provides recommended values for noise exposure, including for health, specifically sleep disturbance. It is mentioned that the noise level during sleep should not be more than 30 dB(A) for persistent noise and not more than 45 dB(A) in the case of momentary noise with a maximum of 55 dB(A) to avoid negative cardiovascular health impacts [57]. Furthermore, international studies have linked traffic noise to higher odds of ischemic heart disease whenever (Leq) 65 dB (A) is exceeded [58–60]. The assessment of façade sound insulation is a part of one of the five broad categories defined by the Guide Development Group (GDG) that focus on actions or interventions on environmental noise. In the case of building façade, path intervention is utilized by altering the path between source and receiver, or path control of the receiver through insulation [61, 62]. Designers can utilize path intervention through the insulation of dwellings, constructing barriers or a combination of both [63], providing healthy conditions for occupants [64].

8 Discussion

There is overwhelming evidence that suggests that buildings have a tremendous effect on human health, especially since humans spend most of their time indoors. Americans, for example, spend 90% of their time indoors, where concentrations of some air pollutants are twice or five times higher than the outdoors [65, 66]. We have gathered from research that most of the indoor pollutants come from the

interior of the building itself, with some of them originating from the outdoors. Several strategies exist to combat poor IAQ, to mention: control of the source of pollutants indoors (such as furnishings, wood composite materials, etc.), using air cleaners, and optimizing ventilation [67]. The IAQ parameter is much more complex after viewing it from different perspectives. Solutions do exist, but whether they are holistic in accordance with the previous perspectives presented is another question entirely. For example, a study on air cleaning of air-conditioned office buildings successfully developed an IAQ system connected to an air handling unit (AHU). The system decontaminates the air of TVOCs, converting them through oxidation into water-vapor and CO₂ [68]. Although CO₂ is considered harmless to human health, it is not exactly sustainable, as the carbon footprint of the building increases, it contributes more to greenhouse effect-related environmental issues. Alternatively, research shows that although green buildings possibly promote healthy IAQ, some green practices and products are known to compromise IAQ [69]. Rather than focusing on ventilation strategies, researchers should work on developing better practices for source control or air cleaning. A building is more energy-efficient when the building envelope is tighter and has lower rates of ventilation. However, this negatively influences human well-being [70]. Challenges and conflicts not only exist between human well-being, sustainable and green practices, but also between IEQ parameters. One challenge for example is designed using natural ventilation for the sake of thermal comfort, which can impair acoustic comfort by permitting more exposure to outdoor noise [71]. This exposure to outdoor noise causes some non-green certified buildings to have a higher acoustic comfort than green building certified buildings [72]. Maintaining the balance between human well-being and building performance with the addition of the challenges that rise when IEQ parameters are in conflict is a complicated task. Existing healthy building guidelines are not yet perfect, and do not include enough of the effect on occupants (mental and physical). Sustainable building design geared toward occupants and the environment may benefit both greatly (for example, cognitive function, productivity, physical and mental health) and environmental safety [73].

9 Conclusion

There is much more research needed that establish the effects of the built environment on mental health more firmly, including the aspects that improve the performance of occupants. Literature shows that there is a surge of awareness that the buildings we utilize have a tremendous hold on our health and life quality. A multidisciplinary approach is needed that involves health researchers, designers, computer engineers, and building scientists to not only experiment on the various specific outcomes of the built environment on overall human health, but also to automate and integrate these findings for the purpose of creating a truly holistic practice. In the future, a shift in mindset and practice is essential to ensure further

advancement in construction, starting with source control derived from an understanding of the balance between the three pillars of sustainability (economic, social, and environmental) and overall human health.

References

1. Levin H (1995) Building ecology: an architect's perspective on healthy buildings. In: Healthy buildings'95, Milan, Italy, 10–15 Sept 1995
2. Jutraž A, Štimac S (2015) How to design healthy building for healthy living? Place and technologies 2015. In: 2nd International academic conference, Nova Gorica, Slovenia, 18–19 June 2015
3. Bluysen P (2013) What do we need to be able to (re)design healthy and comfortable indoor environments? *Intell Build Int* 6:69–92. <https://doi.org/10.1080/17508975.2013.866068>
4. Bluysen P (2012) A different view on indoor environment: focus on people and situations rather than single-dose response relationships. In: 10th International conference on healthy buildings 2012, Brisbane, Australia, 8–12 July 2012
5. Loftness V, Hakkinen B, Adan O, Nevalainen A (2007) Elements that contribute to healthy building design. *Environ Health Perspec* 115(6). <https://doi.org/10.1289/ehp.8988>
6. Brunsgaard C, Heiselberg P, Knudstrup MA, Larsen TS (2011) Evaluation of the indoor environment of comfort houses: qualitative and quantitative approaches. *Indoor Built Environ* 21:432–451. <https://doi.org/10.1177/1420326x11431739>
7. Evans GW (2003) The built environment and mental health. *J Urban Health* 80(4):536–555
8. Dunleavy G, Bajpai R, Tonon AC, Cheung KL, Thach TQ, Rykov Y, Soh CK, Vries H, Car J, Christopoulos G (2020) Prevalence of psychological distress and its association with perceived indoor environmental quality and workplace factors in under and aboveground workplaces. *Build Environ* 175:106799. <https://doi.org/10.1016/j.buildenv.2020.106799>
9. Carrer P, Wargocki P, Fanetti A, Bischof W, Fernandes ED, Hartmann T, Kephelopoulos S, Palkonen S, Seppänen O (2015) What does the scientific literature tell us about the ventilation–health relationship in public and residential buildings? *Build Environ* 94:273–286. <https://doi.org/10.1016/j.buildenv.2015.08.011>
10. Seppänen OA, Fisk WJ, Mendell MJ (1999) Association of ventilation rates and CO₂ concentrations with health and other responses in commercial and institutional buildings. *Indoor Air* 9:226–252. <https://doi.org/10.1111/j.1600-0668.1999.00003.x>
11. Sundell J, Levin H, Nazaroff WW et al (2011) Ventilation rates and health: multidisciplinary review of the scientific literature. *Indoor Air* 21:191–204. <https://doi.org/10.1111/j.1600-0668.2010.00703.x>
12. Li Y, Leung GM, Tang JW et al (2007) Role of ventilation in airborne transmission of infectious agents in the built environment? A multidisciplinary systematic review. *Indoor Air* 17:2–18. <https://doi.org/10.1111/j.1600-0668.2006.00445.x>
13. Hoisington AJ, Stearns-Yoder KA, Schuldt SJ, Beemer CJ, Maestre JP, Kinney KA, Postolache TT, Lowry CA, Brenner LA (2019) Ten questions concerning the built environment and mental health. *Build Environ* 155:58–69. <https://doi.org/10.1016/j.buildenv.2019.03.036>
14. Allen JG, MacNaughton P, Satish U, Santanam S, Vallarino J, Spengler JD (2016) Associations of cognitive function scores with carbon dioxide, ventilation, and volatile organic compound exposures in office workers: a controlled exposure study of green and conventional office environments. *Environ Health Perspec* 124:805–812. <https://doi.org/10.1289/ehp.1510037>
15. Weschler CJ (2009) Changes in indoor pollutants since the 1950s. *Atmos Environ* 43(1):153–169. <https://doi.org/10.1016/j.atmosenv.2008.09.044>

16. Wargocki P, Sundell J, Bischof W et al (2002) Ventilation and health in non-industrial indoor environments: report from a European multidisciplinary scientific consensus meeting (EUROVEN). *Indoor Air* 12:113–128. <https://doi.org/10.1034/j.1600-0668.2002.01145.x>
17. Ben-David T, Waring MS (2018) Interplay of ventilation and filtration: differential analysis of cost function combining energy use and indoor exposure to pm 2.5 and ozone. *Build Environ* 128:320–335. <https://doi.org/10.1016/j.buildenv.2017.10.025>
18. Razjouyan J, Lee H, Gilligan B et al (2019) Wellbuilt for wellbeing: controlling relative humidity in the workplace matters for our health. *Indoor Air* 30(1):167–179. <https://doi.org/10.1111/ina.12618>
19. Rashid M, Zimring C (2008) A review of the empirical literature on the relationships between indoor environment and stress in health care and office settings. *Environ Behav* 40:151–190. <https://doi.org/10.1177/0013916507311550>
20. Mitchell CS, Zhang JJ, Sigsgaard T, Jantunen M, Liroy PJ, Samson R, Karol MH (2007) Current state of the science: health effects and indoor environmental quality. *Environ Health Persp* 115(6):958–964. <https://doi.org/10.1289/ehp.8987>
21. Wolkoff P, Kjaergaard SK (2007) The dichotomy of relative humidity on indoor air quality. *Environ Int* 33(6):850–857. <https://doi.org/10.1016/j.envint.2007.04.004>
22. Sterling EM, Arundel A, Sterling TD (1985) Criteria for human exposure to humidity in occupied buildings. In: ASHRAE's annual and winter conferences, Chicago, 1985; ASHRAE Trans 91(1):611
23. Wolkoff P (2018) The mystery of dry indoor air—an overview. *Environ Int* 121:1058–1065. <https://doi.org/10.1016/j.envint.2018.10.053>
24. Zhu G, Janjetovic Z, Slominski A (2013) On the role of environmental humidity on cortisol production by epidermal keratinocytes. *Exp Dermatol* 23:15–17. <https://doi.org/10.1111/exd.12275>
25. Sakellaris I, Saraga D, Mandin C et al (2020) Association of subjective health symptoms with indoor air quality in European office buildings: the OFFICAIR project. *Indoor Air* 31(2):426–439. <https://doi.org/10.1111/ina.12749>
26. RESET® (2019) Air standard for residential v1.0. https://reset.build/system/RESET_Air_Residential_v1_200803.pdf. Accessed 6 July 2021
27. Wang C, Zhang F, Wang J, Doyle JK, Hancock PA, Mak CM, Lin S (2021) How indoor environmental quality affects occupants' cognitive functions: a systematic review. *Build Environ* 193:107647. <https://doi.org/10.1016/j.buildenv.2021.107647>
28. Shendell DG, Prill R, Fisk WJ, Apte MG, Blake D, Faulkner D (2004) Associations between classroom CO₂ concentrations and student attendance in Washington and Idaho. *Indoor Air* 14(5):333–341. <https://doi.org/10.1111/j.1600-0668.2004.00251.x>
29. Dannemiller KC, Weschler CJ, Peccia J (2017) Fungal and bacterial growth in floor dust at elevated relative humidity levels. *Indoor Air* 27(2):354–363. <https://doi.org/10.1111/ina.12313>
30. Santamouris M, Alevizos SM, Aslanoglou L, Mantzios D, Milonas P, Sarelli I, Karatasou S, Cartalis K, Paravantis JA (2014) Freezing the poor-indoor environmental quality in low and very low income households during the winter period in Athens. *Energy Build* 70:61–70. <https://doi.org/10.1016/j.enbuild.2013.11.074>
31. Katafygiotou MC, Serghides DK (2014) Bioclimatic chart analysis in three climate zones in Cyprus. *Indoor Built Environ* 24(6):746–760. <https://doi.org/10.1177/1420326x14526909>
32. Quang TN, He C, Knibbs LD, de Dear R, Morawska L (2014) Co-optimisation of indoor environmental quality and energy consumption within urban office buildings. *Energy Build* 85:225–234. <https://doi.org/10.1016/j.enbuild.2014.09.021>
33. Yu J, Kang Y, Zhai ZJ, Zhong K (2020) Influences of occupant ventilation-behavior during off-periods on indoor thermal environment in intermittently heated buildings. *Build Environ* 186:107289. <https://doi.org/10.1016/j.buildenv.2020.107289>
34. Mäkinen TM, Juvonen R, Jokelainen J, Harju TH, Peitso A, Bloigu A, Silvennoinen-Kassinen S, Leinonen M, Hassi J (2009) Cold temperature and low humidity are associated with

- increased occurrence of respiratory tract infections. *Respir Med* 103(3):456–462. <https://doi.org/10.1016/j.rmed.2008.09.011>
35. Stafoggia M, Forastiere F, Agostini D et al (2006) Vulnerability to heat-related mortality. *Epidemiology* 17(3):315–323. <https://doi.org/10.1097/01.ede.0000208477.36665.34>
 36. Wargocki P, Wyon DP, Sundell J, Clausen G, Fanger PO (2000) The effects of outdoor air supply rate in an office on perceived air quality, sick building syndrome (SBS) symptoms and productivity. *Indoor Air* 10(4):222–236. <https://doi.org/10.1034/j.1600-0668.2000.010004222.x>
 37. World Green Building Council (2014) Health, wellbeing and productivity in offices: the next chapter for green building. https://www.worldgbc.org/sites/default/files/compressed_WorldGBC_Health_Wellbeing_Productivity_Full_Report_Dbl_Med_Res_Feb_2015.pdf. Accessed 7 June 2021
 38. Ou LC, Luo MR, Woodcock A, Wright A (2004) A study of colour emotion and colour preference. Part 1: colour emotions for single colours. *Color Res Appl* 29(3):232–240. <https://doi.org/10.1002/col.20010>
 39. Lottrup L, Stigsdotter UK, Meilby H, Claudi AG (2013) The workplace window view: a determinant of office workers' work ability and job satisfaction. *Landsc Res* 40(1):57–75. <https://doi.org/10.1080/01426397.2013.829806>
 40. Kweon BS, Ellis CD, Lee J, Jacobs K (2017) The link between school environments and student academic performance. *Urban Fores Urban Greening* 23:35–43. <https://doi.org/10.1016/j.ufug.2017.02.002>
 41. U.S. Green Building Council (2015) The health and design benefits of accessing daylight and views with dynamic glass. <https://www.usgbc.org/education/sessions/health-and-design-benefits-accessing-daylight-and-views-dynamic-glass-9831279>. Accessed 24 May 2021
 42. Heerwagen J, Heerwagen D (1986) Lighting and psychological comfort. *Light Des Appl* 6:47–51
 43. Veitch JA, Hine DW, Gifford R (1993) End users' knowledge, beliefs, and preferences for lighting. *J Inter Des* 19(2):15–26. <https://doi.org/10.1111/j.1939-1668.1993.tb00159.x>
 44. Chang CY, Chen PK (2005) Human response to window views and indoor plants in the workplace. *HortScience* 40(5):1354–1359. <https://doi.org/10.21273/hortsci.40.5.1354>
 45. Wulff K, Gatti S, Wettstein JG, Foster RG (2010) Sleep and circadian rhythm disruption in psychiatric and neurodegenerative disease. *Nat Rev Neurosci* 11:589–599. <https://doi.org/10.1038/nrn2868>
 46. Edwards L, Torcellini P (2002) A literature review of the effects of natural light on building occupants. In: National renewable energy laboratory. <https://www.nrel.gov/docs/fy02osti/30769.pdf>. Accessed 25 May 2021
 47. Ulrich RS (1981) Natural versus urban scenes: some psychophysiological effects. *Environ Behav* 13(5):523–556. <https://doi.org/10.1177/0013916581135001>
 48. Li DHW (2010) A review of daylight illuminance determinations and energy implications. *Appl Energy* 87:2109–2118. <https://doi.org/10.1016/j.apenergy.2010.03.004>
 49. Shahidi R, Golmohammadi R, Rizevandi ZP, Soltani A, Khoram NS, Kazemi R (2020) Study of daytime lighting at official rooms and its relation with personnel's cognitive performance, alertness, visual comfort and sleep quality. *J Ergon* 8(1):32–41. <https://doi.org/10.30699/jergon.8.1.32>
 50. Begemann SHA, van den Beld GJ, Tenner AD (1997) Daylight, artificial light and people in an office environment, overview of visual and biological responses. *Int J Ind Ergon* 20(3):231–239. [https://doi.org/10.1016/s0169-8141\(96\)00053-4](https://doi.org/10.1016/s0169-8141(96)00053-4)
 51. Daneault V, Dumont M, Massé É, Forcier P, Boré A, Lina JM, Doyon J, Vandewalle G, Carrier J (2018) Plasticity in the sensitivity to light in aging: decreased non-visual impact of light on cognitive brain activity in older individuals but no impact of lens replacement. *Front Physiol* 9:1557. <https://doi.org/10.3389/fphys.2018.01557>
 52. Li H, Wang H, Shen J, Sun P, Zhang S, Xie T, Zhang S, Zheng Z (2017) Non-visual biological effects of light on human cognition, alertness, and mood. In: *Light in nature VI*. <https://doi.org/10.1117/12.2272555>

53. Price LLA, Udovičić L, Behrens T et al (2019) Linking the non-visual effects of light exposure with occupational health. *Int J Epidemiol* 48:1393–1397. <https://doi.org/10.1093/ije/dyz131>
54. Bansal N, Prakash NR, Randhawa JS, Kalra P (2017) Effects of blue light on cognitive performance. *Int Res J Eng Technol* 4(6):2434–2442
55. Alonso A, Suárez R, Patricio J, Escandón R, Sendra JJ (2021) Acoustic retrofit strategies of windows in facades of residential buildings: requirements and recommendations to reduce exposure to environmental noise. *J Build Eng* 41:102773. <https://doi.org/10.1016/j.jobbe.2021.102773>
56. Dong X, Wu Y, Chen X, Li H, Cao B, Zhang X, Yan X, Li Z, Long Y, Li X (2021) Effect of thermal, acoustic, and lighting environment in underground space on human comfort and work efficiency: a review. *Sci Tot Environ* 786:147537. <https://doi.org/10.1016/j.scitotenv.2021.147537>
57. World Health Organization (2018) Environmental noise guidelines for the European region. <https://www.euro.who.int/en/publications/abstracts/environmental-noise-guidelines-for-the-european-region-2018>. Accessed 4 June 2021
58. Niemann H, Bonnefoy X, Braubach M, Hecht K, Maschke C, Rodrigues C, Robbel N (2006) Noise-induced annoyance and morbidity results from the pan-European LARES study. *Noise Health* 8(31):63–79. <https://doi.org/10.4103/1463-1741.33537>
59. Willich SN, Wegscheider K, Stallmann M, Keil T (2005) Noise burden and the risk of myocardial infarction. *Eur Heart J* 27(3):276–282. <https://doi.org/10.1093/eurheartj/ehi658>
60. Jarup L, Babisch W, Houthuijs D et al (2008) Hypertension and exposure to noise near airports—the HYENA study. *Epidemiology* 116(3):329–333. <https://doi.org/10.1289/ehp.10775>
61. Amundsen AH, Klæboe R, Aasvang GM (2011) The Norwegian façade insulation study: the efficacy of façade insulation in reducing noise annoyance due to road traffic. *J Acous Soc Am* 129(3):1381–1389. <https://doi.org/10.1121/1.3533740>
62. Amundsen AH, Klæboe R, Aasvang GM (2013) Long-term effects of noise reduction measures on noise annoyance and sleep disturbance: the Norwegian facade Insulation study. *J Acous Soc Am* 133(6):3921–3928. <https://doi.org/10.1121/1.4802824>
63. Gidlöf-Gunnarsson A, Öhrström E, Kihlman T (2010) A full-scale intervention example of the quiet side—concept in a residential area exposed to road traffic noise: effects on the perceived sound environment and general noise annoyance. In: 39th International congress on noise control engineering 2010, Lisbon, Portugal, 13–16 June 2010, vol 1, p 2468
64. de Kluizenaar Y, Janssen SA, Vos H, Salomons EM, Zhou H, den Berg FV (2013) Road traffic noise and annoyance: a quantification of the effect of quiet side exposure at dwellings. *Int J Environ Res Public Health* 10(6):2258–2270. <https://doi.org/10.3390/ijerph10062258>
65. United States Environmental Protection Agency (1989) Report to congress on indoor air quality: volume II—assessment and control of indoor air pollution. EPA/400/1-89/001C
66. United States Environmental Protection Agency (1987) Total exposure assessment methodology (team) study summary and analysis, vol 1, final report. EPA/600/6-87/002a
67. Zhang J (2020) Integrating IAQ control strategies to reduce the risk of asymptomatic SARS Cov-2 infections in classrooms and open plan offices. *Sci Technol Built Environ* 26(8):1013–1018. <https://doi.org/10.1080/23744731.2020.1794499>
68. Menezes S (2019) Indoor air quality solutions for commercial buildings. *IOP Conf Ser: Mater Sci Eng* 609(4):042069. <https://doi.org/10.1088/1757-899x/609/4/042069>
69. Steinemann A, Wargocki P, Rsmanchi B (2017) Ten questions concerning green buildings and indoor air quality. *Build Environ* 112:351–358. <https://doi.org/10.1016/j.buildenv.2016.11.010>
70. Lai ACK, Mui KW, Wong LT, Law LY (2009) An evaluation model for indoor environmental quality (IEQ) acceptance in residential buildings. *Energy Build* 41(9):930–936. <https://doi.org/10.1016/j.enbuild.2009.03.016>
71. Deuble MP, de Dear RJ (2012) Green occupants for green buildings: the missing link? *Build Environ* 56:21–27. <https://doi.org/10.1016/j.buildenv.2012.02.029>

72. Altomonte S, Schiavon S (2013) Occupant satisfaction IN LEED and NON-LEED certified buildings. *Build Environ* 68:66–76. <https://doi.org/10.1016/j.buildenv.2013.06.008>
73. Hu M, Simon M, Fix S, Vivino AA, Bernat E (2021) Exploring a sustainable building's impact on occupant mental health and cognitive function in a virtual environment. *Sci Rep* 11 (1):5644. <https://doi.org/10.1038/s41598-021-85210-9>

Analysis of Dominant Influence Factors of the Application of the Incentive Plan Model on the Material Waste



Triongko Agatha Bayuaji and Basuki Anondho

Abstract Incentive plans are increasingly being implemented to align objectives in the implementation of construction projects. Incentives are additional income that is given as an award in the form of monetary/non-monetary so that the parties involved in the construction project are motivated to make every effort to complete the work faster than the agreed time while maintaining the required quality. This research was conducted to know what dominant factors need to be considered in implementing an incentive plan and whether this incentive plan model affects the residual material. This research was conducted by processing primary data in the form of a Likert scale questionnaire. Likert scale 1–5 is used to measure the level of influence of an identified factor on the incentive plan. In the process, this research uses the Factor Analysis Method with a significance level of 5% and is assisted by the application of Statistics Product and Service Solutions (SPSS) or a statistical package for social sciences to test and calculate data. Based on the results of the study obtained three dominant factors that need to be considered in the implementation of the incentive plan.

Keywords Incentive plan · Incentive · Material waste

1 Introduction

The increasing production of waste worldwide is a major issue requiring a management strategy that focuses on a sustainable environment. The construction industry itself is one of the main contributors to this problem because it produces

T. A. Bayuaji (✉) · B. Anondho
Universitas Tarumanagara, 1 Letjen S. Parman Street, Jakarta, Indonesia
e-mail: triongko.325170041@stu.untar.ac.id

B. Anondho
e-mail: basukia@ft.untar.ac.id

large amounts of construction materials and waste [1], which means that material is a problem that can damage the environment. However, many people do not realize it, the use and management of this material is not paid attention to, so there is often a waste of both the excessive use of the material [2]. Judging from the amount of residual material produced is not small. The construction industry in the world produces at least 35% of total solid waste [3] and 10–30% of waste dumps [4].

The resulting effect is of course very pronounced, especially in the cost sector because the remaining material plays an important role in that sector [5]. Not only in the cost sector, but waste storage places are also now filling up very quickly, and landfills for waste materials are scarce [2]. Of course, it will have a huge effect on the environment [6].

Therefore, there must be a solution that can reduce a large amount of construction waste or material waste which continues to be a polemic today. One way that can be used to minimize the remaining material in building construction is to find the main cause.

However, this research will focus on implementing incentive plans in suppressing these problems. Recently, incentive plans are increasingly being implemented to align objectives in the implementation of construction projects [7]. In December 2005, the Hong Kong government designed a construction waste filling scheme to fund incentive plans as well as to promote the reuse and recycling of waste materials in order to reduce the amount of construction waste material [8]. The use of this incentive is also a means of motivation that can encourage workers to work optimally [9]. Incentives are not only used as motivation for the contractor but can also be used to produce alignment with project objectives [10]. Financial incentives use monetary rewards to stimulate increased performance or production as well as psychological incentives, as opposed to financial incentives, are also valid means of generating increased production and or performance [11].

This study conducted a literature survey by applying an incentive plan approach to problems with residual materials that often occur and even have become part of the construction, it is hoped that this approach can reduce the amount of waste material.

1.1 Definition of Waste Material

Waste material is defined as an excess that is indicated either in the form of work or construction material that is left, scattered, or damaged so that it cannot be used again according to its function. Many factors are the source of construction material waste, including design, material procurement, material handling, implementation, residuals and others such as theft [6].

1.2 Definition of Incentive

The definition of incentives is additional income that is given as an award in the form of monetary/non-monetary so that the parties involved in the construction project are motivated to make every effort to complete the work faster than the agreed time while maintaining the quality as required [12].

Mustafa [13] in his book defines incentives as follows: incentives as a means of motivation can be given a set of incentives or incentives that are given intentionally to workers so that there is greater enthusiasm for achievement for the organization. On the other hand, financial incentives are financial rewards given to employees whose production levels exceed predetermined standards.

1.3 Types of Incentives

According to Putra and Hufon [14] argues that basically incentives can be divided into three types, namely: Financial incentives and Non-financial incentives. Financial incentives are incentives in the form of income that are used to meet the needs of life and can be valued in money, including appropriate wages or salaries, profit sharing from companies/agencies, and welfare issues which include health care, recreation, old-age insurance and so on. Meanwhile, non-financial incentives are incentives that are usually psychological rewards. While the forms are, among others: Fostering a sense of pride and pleasure towards employees, giving sympathy and fair treatment to employees, providing opportunities to be promoted, equal opportunities to receive training, security and peace of mind at work, as well as the hope of getting awards, adequate welfare coverage including family medical treatment, old-age benefits, accident insurance and others.

1.4 Initial Identification of Dominant Factors Questionnaire

At this stage, the author summarizes several questions for the questionnaire related to the implementation of the incentive plan model on the remaining material taken from the references to arrange as follows.

2 Methodology

2.1 Preparation of the Questionnaire

At the stage of preparing the questionnaire, what is done is to make problems or questions based on the literature study that has been carried out then summarized and used as questions for the questionnaire, after which the questionnaire is validated by a number of experts. Expert validation is carried out to strengthen the variables in the questionnaire that will be distributed to respondents. The number of experts proposed is 5 (five) people. From the results of expert validation obtained 17 approved variables which are then used as variables in the questionnaire. Respondents who became the target of the questionnaire were the project coordinator, project manager, company owner. Presented on Table 1 are the results of a literature study in the form of factors in the incentive plan.

Table 1 Dominant factors that influence

References	Factors
[8]	Giving insight
[7]	Effective in making project performance better Increase motivation for better performance
[15]	Motivation Performance goals
[16]	Shorten project schedule Budget Project cost
[17]	Project completion with few problems
[18]	Motivation
[1]	Professional ethics Motivation Effective Budget More precise More efficient Good performance Save more waste material Promoting environmentally friendly materials
[12]	Project cost Awards More precise Project cost More efficient More effective

2.2 Distribution of Questionnaires

At the time of distributing the questionnaire, what was done was to distribute the questionnaire to several respondents who worked in the project scope. The questionnaire will be submitted to several respondents, namely the Quantity Surveyor and project manager. The questionnaire will be distributed via social media with the help of Google Form, but some respondents will use paper.

2.3 Distribution of Questionnaire Data Collection

At the time of collecting questionnaire data, what was done was to return to the respondent and ask for the results of the questionnaire.

2.4 Analysis Method

The factor analysis technique is the method used in this research data analysis, with the intention of determining the dominant factor by identifying the relationship between a number of independent factors by conducting a correlation test. Before the factor analysis is carried out, validation is needed to determine whether the data obtained are feasible or not. The validity test technique that will be used is the Pearson correlation, namely by correlating the item score with the total item score for each variable, then significant testing is carried out with criteria using r tables at a significant level of 0.05 with a 2 (two) side test [19]. Then proceed with the reliability test which aims to determine the level of consistency of the data collection tools/instruments used. That is, whether the measuring instrument will get a measurement that remains consistent if the measurement is repeated. The method that is often used in research to measure the Likert scale 1–5 is Cronbach's Alpha. After that, the data were tested for normality to determine whether the data used were normally distributed. One way to detect the normality of the data can be done with the Shapiro Wilk technique. After going through the three tests mentioned earlier, the remaining data and considered valid are then used in factor analysis. In general, the stage of factor analysis is the first to test the correlation between the original variables with the aim of making variable depreciation simpler. Then determine the value of KMO (Kaiser–Meyer–Olkin) and continue to determine the value of Measure of Sampling Adequacy (MSA), namely the feasibility of all observed variables for factor analysis. After all variables are declared eligible for factor analysis, it is continued by extracting factors based on the eigenvalue criteria to get the number of factors formed. Methods that can be used in factor extraction include Principal Component Analysis. After obtaining the number of dominant factor groups formed, factor rotation is carried out in order to obtain a simpler factor

structure for easy interpretation. The last stage of factor analysis is to interpret the results of the factor analysis which can be done by knowing the variables that make up it. The data analysis can be done with the help of the SPSS program.

3 Results and Discussion

3.1 Expert Validation

From the results of expert validation obtained 17 approved variables which are then used as variables in the questionnaire. The variables obtained from the expert validation results can be seen in Table 2. The number of experts proposed is five people.

Table 2 Expert-approved variables

Code	Variable
X1	Professional ethics influences incentive plans for the reduction of waste material
X2	The level of motivation of field workers affects the incentive plan for the reduction of waste materials material
X3	Stakeholder motivation level influences incentive plan for waste material reduction
X4	Incentive plans are affected by effectiveness because this method is considered more effective than providing punitive sanctions for the reduction of waste materials
X5	The efficiency of field workers affects incentive plans for waste material reduction
X6	Good performance of field workers affects incentive plans for waste material reduction
X7	Widespread implementation of incentive plans for building projects will save more waste materials
X8	A project budget influences the incentive plan for waste material reduction
X9	Project costs affect incentive plans for waste material reduction
X11	Achievement of fieldworker performance objectives affects incentive plans for waste material reduction
X12	Insights from field workers influence incentive plans for waste material space
X13	Stakeholder insights influence incentive plans for waste material reduction
X14	Few problems in the project affect the incentive plan for waste material reduction
X15	Improving the quality of field workers affects incentive plans for waste material reduction
X16	The project schedule influences the incentive plan for waste material reduction
X17	Fewer defects that appear on the project affect the incentive plan for the reduction of waste materials
X18	The efficiency of the contractor's work affects the incentive plan for the reduction of waste materials

Table 3 Characteristics of respondents based on position or job title in the project

Position in the project	Number of respondents
Project Manager	5
Project Coordinator	1
Quantity Surveyor	16
Cost Control	1
Director	2
Owner	1
Supervisor	2
Site Manager	2

3.2 Questionnaire Data

Furthermore, questionnaires were distributed to 32 respondents who are project actors who are currently involved in the construction of a construction project using the precast concrete slab method. In this study, researchers managed to collect as many as 30 respondents' responses. The characteristics of the respondent's position in the project are divided into Table 3.

To measure the value of the questionnaire, the Likert measurement technique is used for the measurement scale of the dominant factor that needs to be considered in the application of the incentive planning model listed in Table 4.

3.3 Validity Test, Reliability Test, and Normality Test

The validity test was carried out using the bivariate method. Variables will be declared valid if the value of Pearson correlation or r count on a variable is greater than the value of r product moment from the table. The sample data used in this study was 30 ($N = 30$) and the significance level used was 5%, so by looking at the table of the product-moment r -value, the r -value was 0.361. Then the calculated r is obtained by using SPSS software.

Then perform a reliability test for 13 variables used to determine whether or not a research instrument is reliable by calculating the coefficient value of Cronbach's Alpha. From the analysis, results obtained Cronbach's Alpha value of 0.815 so that the data collection instrument (questionnaire) can be said to be reliable (>0.6). After the reliability test, the normality test was carried out and the results obtained a significance value of 0.200 so that the data can be said to be normally distributed (>0.05).

Table 4 Description of Likert scale

Scale	Information
1	Very unaffected
2	No effect
3	Neutral
4	Take effect
5	Very influential

3.4 Factor Analysis

After testing the validity, reliability, and normality, then a factor analysis was carried out on 13 valid variables. At this stage, the factor analysis method is used because this method can identify the dominant factors and reduce factors to make them more applicable. After doing the factor analysis, it is known that only eight variables can be used as dominant factors in the implementation of the incentive plan. From the results of the initial eigen value, it shows that there are three groups of dominant factors that will be formed, namely factors 1, 2, and 3. The eigen value of each component can be seen in Fig. 1.

With a large variance that can be explained by factor 1 is 45.175%, by factor 2 is 13.1625%, and by factor 3 is 13.0625%. The total of these three factors will be able to explain the variable of 71.4%. After knowing that the maximum number of dominant factor groups that can be formed is three factors, then the determination of each dominant factor group that will be included in the factor 1, factor 2, or factor 3 group is determined in Table 5.

In determining the input variable to a certain factor, it is followed by the correlation between the variables and each group of factors, namely the variable that has the greatest correlation value to the group of factors. Thus, it can be concluded that the group of factors and their dominant factors are: Factor group 1, consisting

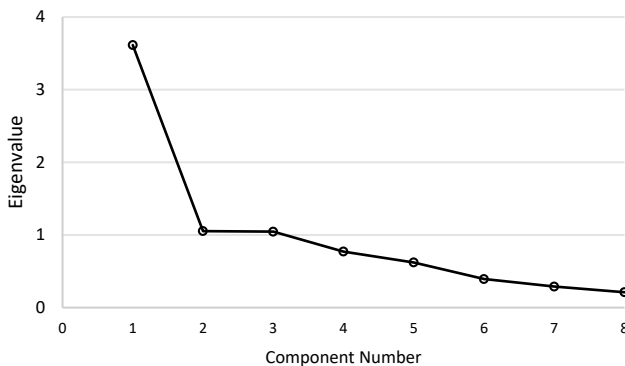


Fig. 1 Scree Plot

Table 5 Result rotated component matrix

Component	1	2	3
X4	0.809	0.173	0.230
X5	0.815	0.327	0.115
X6	0.849	0.051	0.232
X7	0.055	0.875	0.135
X8	0.214	0.616	0.435
X15	0.480	0.670	-0.068
X3	0.084	0.150	0.833
X12	0.286	0.059	0.721

of dominant factors X4, X5, X6. While the factor group 2 consists of the dominant factors X7, X8, and X15. For group 3, factors are arranged on X3 and X12.

4 Conclusions and Suggestions

4.1 Conclusion

The dominant factor group that can be considered in implementing the incentive plan model for the first waste material consists of dominant factors in the form of, Incentive plans are influenced by effectiveness because this method is considered more effective than providing sanctions for reducing waste material, Efficiency of field workers affects incentive plans for waste material reduction. The good performance of the field workers influences the incentive plan for the reduction of waste materials. The second dominant group of factors consists of dominant factors such as Widespread implementation of incentive plans to build projects that will save more waste materials, A project budget that influences incentive plans for waste material reduction, Improved quality of field workers affects incentive plans for waste material reduction. The third group of factors consists of the dominant factor in the form of incentive plans which are influenced by the level of stakeholder motivation influencing the incentive plans for waste material reduction, and the field workers' insights influence the incentive plans for waste material reduction. The first factor is the most dominant factor group among the three factors formed with a value of 45.175%, followed by the second factor with a percentage of 13.1625%, then followed by the third factor with a value of 13.0625%. These three factors can be considered in the application incentive plan model design on waste materials.

4.2 Suggestion

The results of this study can be developed by broadening the perspective, not only from the contractor's point of view but can be viewed from the perspective of the employer (owner) and director broadly. In addition, research can also be carried out using techniques other than factor analysis to obtain the dominant factors. Meanwhile, in terms of respondents, it can also be expanded not only around Jakarta, where it is necessary to expand outside the island of Java. The research influence factors can be made more broadly related to incentive plans.

References

1. Mahpour A, Mortaheb MM (2018) Financial-based incentive plan to reduce construction waste. *J Constr Eng Manag* 144:04018029. [https://doi.org/10.1061/\(asce\)co.1943-7862.0001461](https://doi.org/10.1061/(asce)co.1943-7862.0001461)
2. Gavilan RM, Bernold LE (1994) Source evaluation of solid waste in building construction. *J Constr Eng Manag* 120:536–552. [https://doi.org/10.1061/\(asce\)0733-9364\(1994\)120:3\(536\)](https://doi.org/10.1061/(asce)0733-9364(1994)120:3(536))
3. Llatas C (2011) A model for quantifying construction waste in projects according to the European waste list. *Waste Manage* 31:1261–1276. <https://doi.org/10.1016/j.wasman.2011.01.023>
4. Begum RA, Siwar C, Pereira JJ, Jaafar AH (2009) Attitude and behavioral factors in waste management in the construction industry of Malaysia. *Resour Conserv Recycl* 53:321–328. <https://doi.org/10.1016/j.resconrec.2009.01.005>
5. Aulia NA, Harimurti NKP (2016) Analisis dan evaluasi sisa material konstruksi menggunakan metode pareto dan fishbone diagram (studi kasus pada proyek pembangunan gedung pascasarjana Universitas Islam Malang). *Jurnal Mahasiswa Jurusan Teknik Sipil* 1(2):641–649
6. Devia YP, Unas SEI, Nariswari W (2012) Identifikasi sisa material konstruksi dalam upaya memenuhi bangunan berkelanjutan. *Rekayasa Sipil* 4(3):195–203
7. Tang W, Qiang M, Duffield CF, Young DM, Lu Y (2008) Incentives in the Chinese construction industry. *J Constr Eng Manag* 134:457–467. [https://doi.org/10.1061/\(asce\)0733-9364\(2008\)134:7\(457\)](https://doi.org/10.1061/(asce)0733-9364(2008)134:7(457))
8. Poon CS, Yu AT, Wong A, Yip R (2013) Quantifying the impact of construction waste charging scheme on construction waste management in Hong Kong. *J Constr Eng Manag* 139:466–479. [https://doi.org/10.1061/\(asce\)co.1943-7862.0000631](https://doi.org/10.1061/(asce)co.1943-7862.0000631)
9. Herliana D (2017) Pengaruh insentif terhadap peningkatan kualitas kerja karyawan pada PT Bosowa Berlian Motor (studi kasus pada perusahaan PT Bosowa Berlian Motor). *Economics Bosowa J* 3(7):96–109
10. Bower D, Ashby G, Gerald K, Smyk W (2002) Incentive mechanisms for project success. *J Manag Eng* 18:37–43. [https://doi.org/10.1061/\(asce\)0742-597x\(2002\)18:1\(37\)](https://doi.org/10.1061/(asce)0742-597x(2002)18:1(37))
11. Liska RW, Snell B (1992) Financial incentive programs for average-size construction firm. *J Constr Eng Manag* 118:667–676. [https://doi.org/10.1061/\(asce\)0733-9364\(1992\)118:4\(667\)](https://doi.org/10.1061/(asce)0733-9364(1992)118:4(667))
12. Sarli A, Adianto YLD (2017) Kajian pemberian insentif dalam proyek konstruksi dari persepsi pengguna jasa dan penyedia jasa. *Jurnal Ilmiah Teknik Sipil* 21(1):24–33. <https://doi.org/10.24843/JITS.2017.v21.i01.p04>
13. Mustafa IG (2017) Studi tentang pemberian insentif dalam meningkatkan kinerja pegawai di sekretariat daerah provinsi Kalimantan Timur. *Jurnal Paradigma* 1(3):373–388. <https://doi.org/10.30872/jp.v1i3.315>

14. Putra AP, Hufron M (2017) Pengaruh pemberian insentif terhadap kinerja karyawan di PT Bank Rakyat Indonesia (persero) Tbk. *Jurnal Ilmiah Riset Manajemen* 6(7):136–154
15. Ogwueleka AC, Maritz MJ (2013) A review of incentive issues in the South African construction industry: the prospects and challenges. In: *International conference on construction and real estate management 2013*, Karlsruhe, Germany, 10–11 Oct 2013. <https://doi.org/10.1061/9780784413135.008>
16. Chokor A, El Asmar M, Sai Paladugu B (2017) Quantifying the impact of cost-based incentives on the performance of building projects in the United States. *Pract Period Struct Des Constr* 22:04016024. [https://doi.org/10.1061/\(asce\)sc.1943-5576.0000312](https://doi.org/10.1061/(asce)sc.1943-5576.0000312)
17. Karakhan A, Gambatese J (2018) Hazards and risk in construction and the impact of incentives and rewards on safety outcomes. *Pract Period Struct Des Constr* 23:04018005. [https://doi.org/10.1061/\(asce\)sc.1943-5576.0000359](https://doi.org/10.1061/(asce)sc.1943-5576.0000359)
18. Priyatno D (2018) SPSS: Panduan mudah olah data bagi mahasiswa & umum. ANDI, Yogyakarta
19. Broome J, Perry J (2002) How practitioners set share fractions in target cost contracts. *Int J Project Manage* 20:59–66. [https://doi.org/10.1016/s0263-7863\(00\)00035-1](https://doi.org/10.1016/s0263-7863(00)00035-1)

Accuracy of Schedule Performance Calculation with ES Method and EV Method



Cangga Kristiandi and Basuki Anondho

Abstract The importance of the method to determine the performance of the schedule duration during the project is in planning because it can determine the success or failure of the project because the duration often does not match the predictions due to project uncertainty so that there is no loss. This paper will discuss the accuracy of the schedule performance method between the earned value (EV) method and earned schedule (ES) method. Specifically, this paper aims to determine which schedule performance index (SPI) accuracy is better than the two methods. This paper discusses SPI against time and progress with the aim of knowing the performance of the project schedule over time and the progress of work between the earned value and earned schedule methods based on the average SPI value of the ongoing project and the results of R square ES greater than EV which is close to 1 and the SPI graph The time and work progress shows that the ES method is closer to 1 or closer to the plan than the EV method, so this paper shows that the ES performance estimate is better in assessing schedule performance compared to the EV method.

Keywords Schedule performance · Earned value · Earned schedule · SPI

C. Kristiandi (✉) · B. Anondho (✉)
Universitas Tarumanagara, 1 Letjen S. Parman Street, Jakarta, Indonesia
e-mail: canggakristiandi@yahoo.com

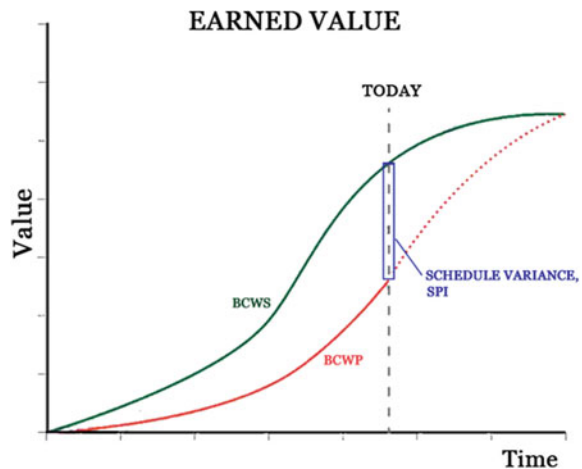
B. Anondho
e-mail: basukia@ft.untar.ac.id

1 Introduction

Planning, cost, and time control are part of the overall construction project management. In addition to the assessment in terms of quality, the achievement of a project can also be assessed in terms of cost and time. The possibility of deviations from the plan in terms of costs and time spent on construction work must be measured on an ongoing basis. Significant cost and time deviations indicate poor project management [1]. The success of the project depends on the timeliness of implementation based on the estimated project duration [2]. The duration of the project often does not match the predictions because it is caused by uncertainty so that the construction schedule can deviate from the original plan [3]. One of the important pieces of information to know is how to increase the use of costs against the budget or against time. In addition, by considering that changes are something that often occurs in the implementation of a construction project, a more integrated method is needed to be able to describe how progress or progress is being made in the field [4]. Traditional cost management only presents two dimensions, namely, a simple relationship between actual costs and planned costs [5].

With traditional cost management, the performance status cannot be known. In Fig. 1, it can be seen that the actual costs are indeed lower, but the fact that the actual costs are lower than this plan does not indicate that the performance that has been carried out has been in accordance with the planned targets. In contrast, the concept of earned value provides a third dimension besides actual costs and planned costs. This third dimension is the amount of physical work that has been completed or called earned value/percent complete [5]. The conventional method or the result value method (EVM), which was developed in 1960, is one of the control methods that quantitatively measures the performance and progress of the project. According to Lipke, EVM is less successful in predicting project completion time because EVM measures scheduling performance, not in terms of time parameters but more

Fig. 1 Earned value elements



in cost parameters [6]. In 2003, Lipke developed a method that is an extension of EVM. This method is known as earned schedule (ES), which was developed to be able to perform scheduling analysis better. In contrast to EVM, ES demonstrates the possibility of describing cost performance in units of time. In other words, ES facilitates time-based analysis of a schedule so that it is easier to understand than EV [7]. After ES was first introduced, a year later, Henderson developed ES to be used to predict project completion duration [8].

1.1 Earned Value Method

As an industry standard defined by the American National Standards Institute (ANSI) EIA-748 (ANSI 1999), EV has been widely accepted as a core performance monitoring, analysis, and forecasting system [9]. Technically, Earned Value uses work progress as an indication of what will happen to the project in the future [10]. The main element in EV analysis is cost, which means that to measure both cost performance and schedule performance, both are cost based. According to Moselhi, by using the Earned Value method, the accuracy of its success in predicting the use of costs until the project completion stage is quite good. However, different results are obtained when EV is used to predict the duration. The prediction accuracy is not satisfactory [11].

Earned Value is a system formed based on three important principles, namely planned value, earned value, and actual cost. These principles are interrelated, therefore, the work process of EV is to assess all aspects simultaneously, not separately. The earned value (EV) method measures information about the position of project progress within a certain period of time and can estimate project progress in the next period using two indicators, namely:

1. BCWP (*Budgeted Cost of Work Performed*) = shows the value of the results from the point of view of the value of the work that has been completed against the planned budget that has been provided to carry out the project (Earned Value). When the ACWP figure is compared with the BCWP, it will show a comparison between the costs incurred for the work carried out with the costs that should have been spent for the work.
2. BCWS (*Budgeted Cost of Work Scheduled*) = plan budget for a work package (Planned value), but compiled and linked to the implementation schedule. So here, there is a combination of costs, schedules, and scope of work where each element of the work has been allocated a cost and schedule that can be used as a benchmark in carrying out the work.

These two parameters indicate that the EV method uses cost indicators in the calculation of project duration predictions [12]. By using the two indicators above, it can be calculated various factors that show progress, various factors that indicate progress and performance of project implementation, such as:

1. Schedule variant
2. Monitor variance changes against standard numbers
3. Productivity and performance index
4. Estimated project completion time.

The formula for finding the time variance is shown in Eq. 1.

$$SV(\text{Schedule Variant}) = BCWP - BCWS \quad (1)$$

A negative number in the variance indicates that the time is late, a zero means that the work is carried out on time, and a positive number means that the work is carried out faster than planned. SV and SPI are used to measure the schedule performance of a project. For example, when a project has a positive SV ($SV > 0$) or an SPI above ($SPI > 1.0$), the project will run ahead of schedule. SPI is also used to generate independent predictions of project duration. The formula for finding the productivity and performance index is shown in Eq. 2.

$$SPI(\text{Schedule Performance Index}) = \frac{BCWP}{BCWS} \quad (2)$$

A number less than one in the SPI indicates that the time is late, the number one means that the work is carried out on time, and a number more than one means the work is carried out faster than planned. By calculating the variance and index as above. It will be seen that the project will be late or ahead of the plan, so the progress of the project for the future needs to be predicted with Eqs. 3 and 4.

$$ECD = \frac{\text{Plan duration} - \text{Actual progress}}{SPI} + \text{Actual progress} \quad (3)$$

$$\frac{\text{Percentage of Delays}}{\text{Schedule Acceleration}} = 100\% - \frac{ECD}{\text{Plan schedule}} \times 100\% \quad (4)$$

Estimation completion date (ECD) is an indicator that can be calculated on a predetermined baseline/milestone so that the values obtained show the progress of time in that period and the progress of the project in terms of time for completion in the future [13]. SPI indicators are more often used for performance appraisal than SV. The SPI value is a weighted value that has no dimensions so that a comparison can be made between the performance of one project with another. In addition, the SPI value provides a relative comparison to the BCWS or Performance Measurement Baseline, which is the basis for assessing project status in terms of time. This is a concept so that deviations (variances) with respect to time can be detected, and delays can be detected earlier so as to extend the life of the project.

1.2 Earned Schedule Method

Earned Schedule Method (ESM) is a method of developing Value Method (EV), which was introduced by Walt Lipke in the spring of 2003, showing the possibility of describing schedule performance in units of time [14]. Earned Schedule (ES) is an analytical technique that solves the EV dilemma. It originates from and is an extension of the EV. No additional data is required to obtain the ES measure; only data from the EV is needed. Unlike the cost-based indicators of EVs, the performance indicators of ES schedules are time-based, making them easier to understand. ES indicators provide status and predictive capabilities for schedules, similar to facilities for costing using EV. Figure 2 shows the concept of the project's s curve.

The theory that has been developed by Lipke is based on the idea to determine the time at which the earned value (EV) should occur, the duration time associated with PMB where the planned value (PV) equals EV is the Earned Schedule. In this method shown in Fig. 2 is to determine the location of the actual time progress (EV curve) against the planned progress that should occur (PV curve) by plotting the EV curve at the actual time to the PV curve. The projection point obtained from the plotting results is the ES value. The actual Time (AT) value or actual time is obtained from the endpoint of the EV curve. The point is projected against the PV curve to get the ES value. However, the ES obtained with this point tend to be less precise. So, it requires empirical calculations. There are two main components in this method, namely the value of C (Planned Duration) and I [14]. Earned Schedule can be calculated with Eq. 5.

$$ES(\text{Earned Schedule}) = C + I \tag{5}$$

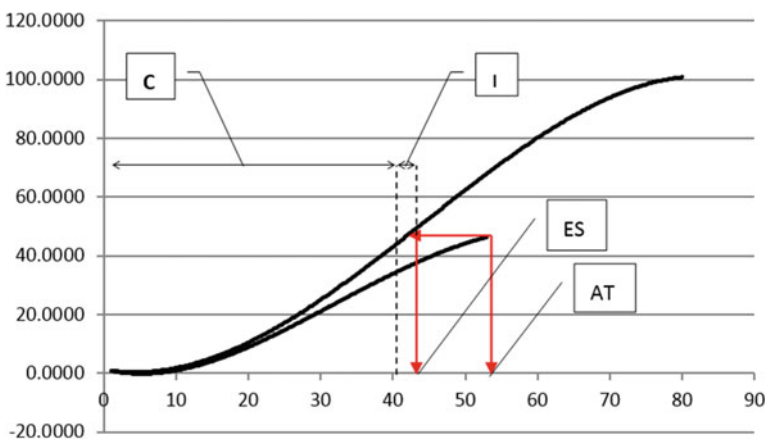


Fig. 2 Earned schedule elements [15]

C: The value of the period is determined by calculating the number of additional times from the basic performance measurement (PMB) that meets the conditions, EV PV.

I: The value of the results of linear interpolation to determine the PMB value at the point under consideration, with Eq. 6.

$$I = \frac{(EV - PVC)}{(PVC + 1 - PVC)} \quad (6)$$

SV (Schedule Variance) presented in Eq. 7 is an indicator of the difference between the time that has been implemented after completing a job (ES) with the actual time (AT).

$$SV(t) = ES - AT \quad (7)$$

SPI (Schedule Performance Index) displayed in Eq. 8 is a factor of performance efficiency in completing work which is shown by comparing the time of work that has been completed (ES) with the actual time (AT). $SPI > 1$; project ahead of plan, $SPI < 1$; project is behind schedule, $SPI = 1$; project according to plan/on time.

$$SPI(t) = \frac{ES}{AT} \quad (8)$$

EAC (Estimate at Completion) calculates the estimated cost and time from the beginning until the project is actually completed as presented in Eq. 9.

$$EAC(t) = AT + \frac{PD - ES}{SPI(t)} \quad (9)$$

Information:

- EV: Earned Value (value received from completing work over a certain period of time).
- PV: Planned Value at the point under review (budget of costs allocated based on a work plan that has been prepared for a certain time).
- PVC + 1: Planned Value at one point after the point under review.
- AT: Actual Time is the actual time of the observed project duration.
- PD: Planned Duration, namely the duration of the project plan from start to finish.

2 Methodology

The methodology that will be used in this paper is to understand the accuracy of schedule performance between EV and ES methods by looking at SPI over time and work progress. SPI is used to see how much accuracy between the methods and the schedule plan. Here are the steps of this research.

2.1 Collect Data

After doing a literature study, working on the earned value and earned schedule requires a plan s curve and an ongoing s curve to find out the duration performance against the planned time in checking the time so that it gets SPI to find out the performance of the ongoing project schedule.

2.2 Tabulation of SPI and SPI(t) Data

After calculating and getting the SPI value, then continued with the tabulation of SPI and SPI(t) and continued with making SPI Graphs that have been averaged to be able to do SPI accuracy, which is better between the Earned Value and Earned Schedule methods on time and work progress. SPI graph uses trend line analysis with the type of trend used is polynomial with data taken based on the average SPI, BCWP, and EV.

2.3 SPI Accuracy

The accuracy of the Schedule Performance Index is based on the average SPI over time, and the work progress between the EV and ES methods will be obtained from the average Schedule Performance Index (SPI) with trend line analysis with the type of trend used is polynomial over time and % of work progress. Comparison of EV and ES is obtained from the accuracy of the actual duration of the project in the estimated success rate.

2.4 Conclusion/Suggestions

Conclusions will be drawn from the average accuracy of the SPI against time and work progress in the form of the estimated success rate. The SPI average is used to

create an SPI graph with a polynomial trend line type to see which R square is larger. With SPI conditions: $SPI > 1$; project ahead of plan, $SPI < 1$; the project is behind schedule, $SPI = 1$; project according to plan/on time at the point of observation.

3 Results and Discussion

3.1 Earned Value (EV)

From Table 1, it can be seen that the SPI EV value for each project to determine deviations from the project schedule performance and the EAC value to predict the final project duration.

3.2 Earned Schedule (ES)

Table 2 is the result of SPI and EAC calculations for the ES method, it can be seen the projected actual time value/ES value, the SPI ES value uses the ES value to see schedule performance deviations and the EAC value to predict the final project duration.

Table 1 SPI and EAC calculation results

Num	Project	Plan duration	BCWS (%)	BCWP (%)	Unit of time	SPI	EAC
1	P1	127	15.27	18.53	Week	1.2135	104.6894
2	P2	40	28.90	30.48	Month	1.0547	37.9423
3	P3	117	9.14	8.51	Week	0.9313	125.6237
4	P4	79	53.61	35.86	Week	0.6689	117.9260
5	P5	63	75.91	82.39	Week	1.0854	58.1063
6	P6	104	14.15	9.25	Week	0.6537	159.0564
7	P7	91	45.23	43.80	Week	0.9684	93.9565

Table 2 SPI(t) and EAC(t) calculation results

Num	Project	Plan duration	Real duration	Unit of Time	ES	SPI	EAC
1	P1	127	42	Week	46.0088	1.0954	115.9345
2	P2	40	19	Month	19.2703	1.0142	39.4390
3	P3	117	33	Week	31.4751	0.9538	122.6682
4	P4	79	53	Week	46.2851	0.8733	90.4610
5	P5	63	56	Week	57.7303	1.0309	61.1117
6	P6	104	37	Week	32.0063	0.8650	120.2263
7	P7	91	55	Week	54.2383	0.9862	92.2780

Table 3 Average SPI EV or SPI ES

Timespan or work progress range by the time	1	2	3	4	5	6	X
<i>Project</i>							
P1	0	1.0293	1.2384	1.8728	2.2739	2.1914	1.9505
P2	1	1	1	1	1	1	1
P3	0	0	0	0.6119	0.7572	0.8224	0.8555
P4	0.447239	0.3354	0.2982	0.2795	0.2683	0.2609	0.2555
P5	0	4.1694	4.7295	4.4822	3.6852	3.2246	3.1832
P6	0	0	0	0	0	0	0
P7	1	1	1	1	1	1.2132	1.148
Average SPI EV or ES	0.349606	1.0763	1.1809	1.3209	1.2835	1.2446	1.199

3.3 Average SPI EV and ES

Average SPI based on time span or range of work progress per unit time. Table 3 is an example of SPI EV and ES table. The average is taken based on previous calculations for or range of work progress per unit of time. Example of the table shown on Table 3 is a table of SPI EV.

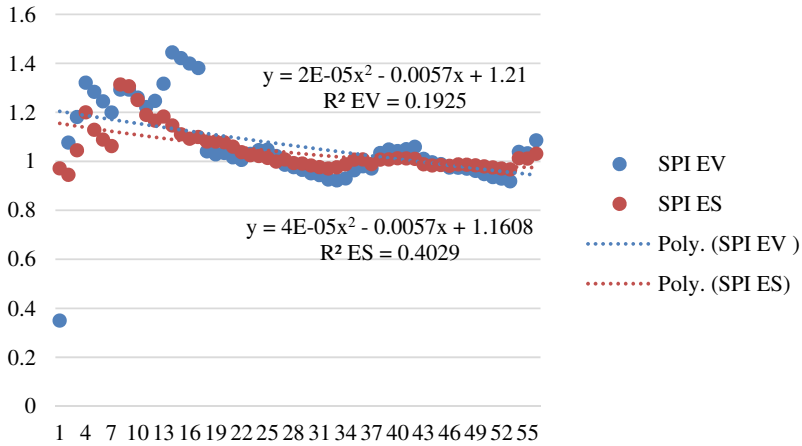


Fig. 3 SPI EV and ES throughout the planning process

3.4 SPI EV and ES Charts Throughout the Planning Progress

The graph points presented on Fig. 3 are derived from the average SPI EV or ES with a range of work progress per unit time. With X-axis units of weeks and Y-axis units of SPI.

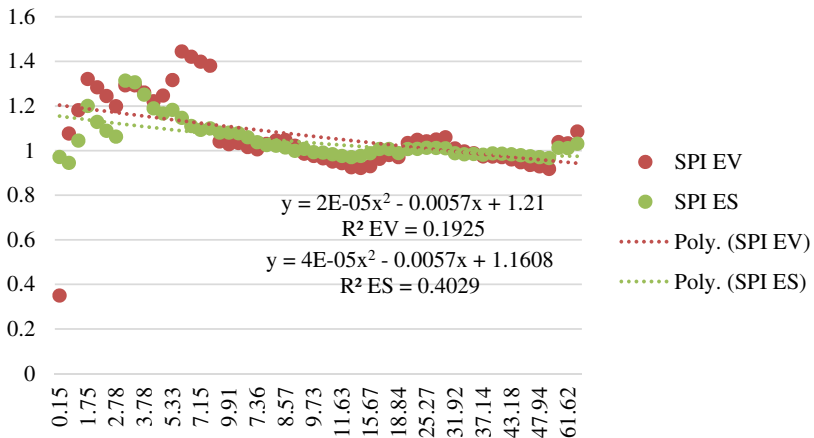


Fig. 4 BCWP, EV and SPI charts throughout the planning progress

3.5 BCWP, EV, and SPI Charts Throughout the Planning Progress

The graph points shown on Fig. 4 are derived from the average SPI EV or ES and the average BCWP per work progress per unit time. With X-axis units of percent work progress and the Y-axis units of SPI.

4 Conclusion and Suggestions

4.1 Conclusion

S curve data collection for ongoing projects can be used to calculate project schedule performance using the EV and ES methods. SPI graph over time and work progress using trend line analysis with the type of trend used is a polynomial with an R square value of 0.1925 with the equation $y = 2E-05x^2 - 0.0057x + 1.21$ for EV and an R square ES value of 0.4029 with the equation $y = 4E-05x^2 - 0.0057x + 1.1608$. The results of R square ES are greater than EV, which is close to 1, and the SPI graph of the ES method is closer to 1 or closer to the planned time than the EV method so that this study shows that the Earned Schedule (ES) schedule performance is better in assessing schedule performance compared to Earned Value (EV) method.

4.2 Suggestions

The following are some suggestions that can be given for the development of further research.

1. The data in this study only focuses on high-rise building construction projects in Jakarta. This limitation can be expanded by analyzing project data other than high-rise buildings, such as housing projects and infrastructure projects, and by expanding the project data collection area outside Jakarta.
2. The comparison variable can be added by several other variables, such as the prediction of the final duration or other variables.

References

1. Ahuja HN, Dozzi SP, Abourizk SM (1994) Project management: techniques in planning and controlling construction projects. John Wiley & Sons Inc., Canada

2. Dursun O, Stoy C (2012) Determinants of construction duration for building projects in Germany. *Eng Constr Archit Manag* 19:444–468. <https://doi.org/10.1108/09699981211237139>
3. Baqerin MH, Shafahi Y, Kashani H (2016) Application of Weibull analysis to evaluate and forecast schedule performance in repetitive projects. *J Constr Eng Manag* 142:04015058. [https://doi.org/10.1061/\(asce\)co.1943-7862.0001040](https://doi.org/10.1061/(asce)co.1943-7862.0001040)
4. Czemplik A (2014) Application of earned value method to progress control of construction projects. *Procedia Eng* 91:424–428. <https://doi.org/10.1016/j.proeng.2014.12.087>
5. Fleming QW, Koppelman JM (1994) The essence of evolution of earned value. *Cost Eng* 36 (11):21
6. Lipke W (2012) Earned schedule contribution to project management. *PM World J* 1(2):1–18
7. Lipke W (2014) Earned schedule-ten years after. *PM World J* 3(1):1–10
8. Henderson K (2005) Earned schedule in action. *Meas News* 8:23–30
9. Project Management Institute (2000) A guide to the project management body of knowledge —2000 edition. Newtown Square, Pennsylvania
10. Bhosekar SK, Vyas G (2012) Cost controlling using earned value analysis in construction industries. *Int J Eng Inno Technol* 1(4):324–332
11. Moselhi O (2011) The use of earned value in forecasting project durations. In: 28th International symposium on automation and robotics in construction, Seoul, Korea, 29 June–2 July 2021. <https://doi.org/10.22260/isarc2011/0129>
12. Vanhoucke M, Andrade P, Salvaterra F, Batselier J (2015) Introduction to earned duration. *Meas News Q Mag Coll Perform Manage*:15–27
13. Husen A (2009) Manajemen proyek. ANDI, Yogyakarta
14. Lipke W, Zwikael O, Henderson K, Anbari F (2009) Prediction of project outcome: the application of statistical methods to earned value management and earned schedule performance indexes. *Int J Project Manage* 27(4):400–407
15. Anondho B, Latief Y, Krishna M (2018) Probabilistic duration calculation based on earned schedule approach. *Int J Civil Eng Technol* 9(5):1121–1127

Analysis of Dominant External Factors on Construction Project Overhead Costs



Hendi Wijaya and Basuki Anondho

Abstract Overhead costs in construction projects are costs that are borne and charged to the contractor to support the work. However, the amount of overhead costs for each project is different and is influenced by external factors such as environmental, socio-cultural, political, and the nature of the project location. Therefore, this study aims to identify the dominant external factors that affect construction project overhead costs and determine the percentage of overhead costs set aside by contractors from the direct costs of construction projects to anticipate the risks posed by overhead costs. In this study, a total of 30 questionnaires were collected from the contractors and a Likert scale of 1–5 was used to measure the level of influence of external factors on construction project overhead costs. Then, the collected data is processed using factor analysis techniques and produces three dominant external factors on construction project overhead costs, including (1) Economics, (2) Law, (3) Social-cultural and the impact of the COVID-19 pandemic. Regarding the percentage of overhead costs on construction projects, the results show that overhead costs on construction projects range from 6 to 10% of direct costs.

Keywords Overhead cost · External factor · Construction project

H. Wijaya (✉) · B. Anondho
Tarumanagara University, 1 Letjen S. Parman Street, Jakarta, Indonesia
e-mail: hendi.325160103@stu.untar.ac.id

B. Anondho
e-mail: basukia@ft.untar.ac.id

1 Introduction

In terms of cost estimation, one of the main parameters in estimating prices in bids is overhead costs [1]. Many contractors take risks and do not take into account the actual overhead costs to win the tender. As a result, this makes the contractor lose money, even go out of business [2].

Overhead costs on construction projects play a significant role and influence the performance of construction companies in maintaining good quality work. Therefore, Overhead costs are costs that cannot be directly related to a product or service and components of construction work but must be incurred by the contractor to support the course of a project [2].

The amount of overhead costs in a project varies and is influenced by external factors of the project because, in general, every construction project must adapt the workplace environment to certain functions, designs, and preferences [3]. Things that become aspects of the project's external factors include the environment, socio-culture, politics, law, and nature.

Therefore, this study aims to identify what external factors are dominant in construction project overhead costs so that it is hoped that in the future, contractors can anticipate the dominant external factors in estimating overhead costs.

2 Literature Review

According to Cilensek, overhead costs in the construction industry are costs that are not part of the actual construction costs but are part of the burden to the contractor to support the project. Overhead costs have also been defined as the case that represents the cost of the work and is almost considered a fixed cost that must be borne by the contractor [4]. In addition, Filicetti in Hesami et al. said overhead costs are independent of the type and product of the project and are costs incurred during the project [5]. Although overhead costs are not the main component in costs, they have an important role for contractors in winning the competition. Therefore, overhead costs must be considered by contractors if they are to obtain competitive margins in a bid. Inaccurate estimates of overhead costs can cause some companies to lose their competitive advantage.

External factors are factors that come from outside the development project. In this study, several references such as journals and books are used to determine the number of external factors that affect overhead costs. The results of the initial identification tabulation for dimensions: political, economy, financial, legal, nature, and environment can be seen in Table 1 and for social, cultural and pandemic are displayed in Table 2.

Table 1 Initial identification of external factors in overhead costs for dimensions: political, economy, financial, legal, nature, and environment

Code	References	Indicator	Dimension
X1	[6, 7]	Changes in laws and regulations by the government	Political
X2	[6, 8]	<i>Political Force Majeure</i>	
X3	[8]	Corruption and bribery	
X4	[8]	Delay in approval of government permits and contracts	
X5	[8, 9]	Inflation and sudden price changes	Economy
X6	[9, 10]	Currency fluctuation	
X7	[10]	Fluctuations in bank interest rates	
X8	[11, 12]	funding from the holding/owner	Financial
X9	[13, 14]	The emergence of difficulties due to Patent Rights	Legal
X10	[13, 14]	The emergence of difficulties due to license	
X11	[13]	The clauses of the contract are unclear	
X12	[13]	Payment method, change order, and claim	
X13	[8, 13]	Warranty and guarantee issues	
X14	[14]	Lawsuits due to breach of contract	
X15	[8]	unexpected site conditions	Nature
X16	[13, 14]	Bad weather	
X17	[9]	Natural disasters	
X18	[6, 8]	Increase in liabilities due to environmental impacts beyond the permitted limits	Environment

Table 2 Initial identification of external factors in overhead costs for dimensions: social and cultural and pandemic

Code	References	Indicator	Dimension
X19	[8]	Criminal act	Social and cultural
X20	[8, 10]	Injustice in tenders	
X21	[8]	Conflict due to differences in culture and traditions at the project site	
X22	[15]	The existence of strict health protocols during the COVID-19 pandemic affects overhead costs	Pandemic
X23	[16]	The decrease in the level of productivity caused by restrictions on the number of workers (social restrictions) during the COVID-19 pandemic affects overhead costs	

3 Research Methodology

3.1 Identification and Validation of Factors

From the results of the literature study, as many as 23 measurement variables and eight dimensions were obtained and used as initial factors. Furthermore, expert validation was carried out aimed at strengthening the indicators used in the questionnaire. This indicator was confirmed by five experts who are people in related fields with a minimum education of undergraduate degree, serving as project managers or similar positions of equal or higher level, and having more than ten years of experience. From expert validation, 21 variables were approved, then these variables were used as variables in the questionnaire.

3.2 Questionnaire Model

In this study, a questionnaire was used as a data collection tool designed to confirm the dominant external factors on construction project overhead costs. The questionnaire consists of 4 parts, including: (1) the introduction of the questionnaire as the introduction of the researcher to the respondents, the definition of overhead costs, and the aims and objectives of the research; (2) General data of respondents in the form of respondent's name, company name, project name, position, education, and work experience; (3) 21 items of questions regarding external project factors that affect overhead costs and additional questions regarding the percentage of overhead costs in a project; (4) Respondents' opinions regarding overhead costs, as well as input and suggestions for the questionnaire. The measurement scale in this questionnaire uses a Likert scale of 1–5 from “very not influential” to “very influential”. The questionnaire items are shown in Table 3.

3.3 Data Collection and Processing

After the questionnaire was designed, the target respondents in this study were the project manager, project coordinator, quantity surveyor, cost control, and other similar or higher positions. Furthermore, the data that has been collected will be processed using factor analysis techniques. However, before doing factor analysis, it is necessary to test the validity, test reliability, and test normality.

A validity test is carried out to determine the extent of the accuracy and accuracy of a measuring instrument in carrying out its measuring function. Measurement of validity is done by comparing the value of r calculations with the value of r product moment in the table with a significance level of 5%. If the value of r count $\geq r$ table, then the data is valid. Then the valid data is continued with the reliability test,

Table 3 Questionnaire items

Code	Indicator	Dimension
X2	<i>Political Force Majeure</i>	Political
X3	Corruption and bribery	
X4	Delay in approval of government permits and contracts	
X5	Inflation and sudden price changes	Economy
X6	Currency fluctuation	
X7	Fluctuations in bank interest rates	
X8	funding from the holding/owner	Financial
X9	The emergence of difficulties due to Patent Rights	Legal
X10	The emergence of difficulties due license	
X11	The clauses of the contract are unclear	
X12	Payment method, change order, and claim	
X14	Lawsuits due to breach of contract	
X15	unexpected site conditions	Nature
X16	Bad weather	
X17	Natural disasters	
X18	Increase in liabilities due to environmental impacts beyond the permitted limits	Environment
X19	Criminal act	Social and cultural
X20	Injustice in tenders	
X21	Conflict due to differences in culture and traditions at the project site	
X22	The existence of strict health protocols during the COVID-19 pandemic affects overhead costs	Pandemic
X23	The decrease in the level of productivity caused by restrictions on the number of workers (social restrictions) during the COVID-19 pandemic affects overhead costs	

which aims to determine the level of consistency of the data collection tools/instruments used. The method that is often used in this research is Alpha Cronbach. If the value of Cronbach’s alpha is less than 0.6, then the data can be said to be less reliable, while 0.7 is acceptable, and above 0.8 is good [17]. Furthermore, valid and reliable data is tested for normality to determine whether the data used is normally distributed or not. The normality test in this study uses the Shapiro–Wilk, where the data can be declared normally distributed if the significance value of the Shapiro Wilk test is greater than 0.05. After going through the three test instruments, then the data are valid, reliable, and normally distributed in factor analysis.

In general, the factor analysis stage is the first to test the correlation between the original variables to simplify variable shrinkage. Then determine the value of KMO (Kaiser–Meyer–Olkin) and continue to determine the value of Measure of Sampling Adequacy (MSA), which is the feasibility of all observed variables for factor analysis. After all, variables are declared eligible for factor analysis, followed by factor extraction based on eigenvalue criteria to obtain the number of factors

formed. Methods that can be used in factor extraction include Principal Component Analysis. After obtaining the number of dominant factor groups formed, factor rotation was carried out to obtain a simpler factor structure to facilitate interpretation. The last stage of factor analysis is to interpret the results of factor analysis which can be done by knowing the variables that compose it. Data analysis was carried out using the Statistical Package for the Social Sciences (SPSS) program.

4 Results

4.1 Questionnaire Data

Furthermore, after going through expert validation, questionnaires were distributed to 34 respondents who are project actors from the project contractor. In this study, researchers managed to collect data of as many as 30 respondents. The characteristics of the position of the respondents in the project are shown in Table 4.

4.2 Validity Test, Reliability Test, and Normality Test

In this study, the validity test was carried out using the bivariate method. The sample data used is 30 ($N = 30$) with a significance level of 5%, where the value of the r product moment in the table is 0.3610. Then the calculated r -value (Pearson correlation) obtained from SPSS is compared with the r table value (product-moment). From the results of the validity test for three iterations, 14 valid variables were obtained. Then, the 14 valid variables were tested for reliability. From the results of the analysis obtained Cronbach's Alpha value of 0.791, which means the value is greater than 0.6, so it can be stated that the data is reliable. Furthermore, after the reliability test was carried out, the normality test was carried out, and the Shapiro Wilk significance value was obtained at 0.749, so it can be said that the data is normally distributed (>0.05).

Table 4 Characteristics of respondents by position or job title in the project

Position/Job title	Number of respondents
Project Manager	8
Project Coordinator	1
Quantity Surveyor	16
Cost Control	1
Director	1
Company Owner	2
Consultant	1
Total	30

Table 5 MSA test results

Variable	Anti-image correlation
X5	0.638
X7	0.666
X10	0.647
X11	0.67
X20	0.761
X21	0.665
X23	0.586

4.3 Factor Analysis

Variables that are valid, reliable, and normally distributed then proceed to the factor analysis stage. In MSA testing on 14 variables, 7 variables have MSA values above 0.5. MSA test results are shown in Table 5.

Then at the factor extraction stage, the extraction value of 7 variables is greater than 0.5. So, it can be said that all the variables studied can be used to explain these factors. From the results of the initial eigenvalues, three groups of dominant factors will be formed, namely factors 1, 2, and 3. The eigenvalue of each component can be seen in Fig. 1.

The variance that can be explained by factor 1 is 36.501%, factor 2 is 17.855%, and factor 3 is 16.682%. The total of these three factors will be able to explain the variables of 71.038%. After knowing the number of dominant factors that can be formed, the next step is to determine the grouping of each dominant factor that will be included in factor 1, factor 2, or factor 3 group by looking at the rotation table of the matrix components in Table 6.

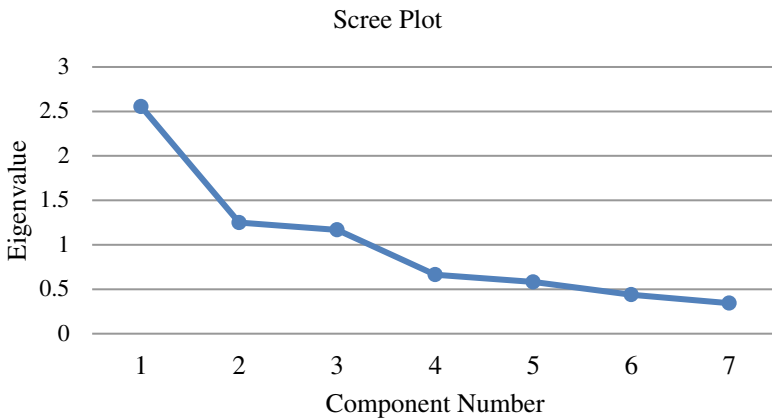


Fig. 1 Scree plot

Table 6 Rotated component matrix

	Rotated component matrix		
	Component		
	1	2	3
X5	0.867	-0.056	0.072
X7	0.782	0.382	0.110
X10	0.372	0.784	-0.078
X11	-0.013	0.832	0.174
X20	0.445	0.206	0.572
X21	-0.122	0.399	0.720
X23	0.145	-0.195	0.801

In determining the input variable to certain factors, it is based on the magnitude of the correlation between the variables and each group of factors formed, namely the variable that has the largest correlation value to the group of factors. Thus, it can be concluded that the group of factors and the dominant factors that compose it, namely: factor group 1 consists of dominant factors X5, X7; Factor group 2 consists of dominant factors X10, X11; Factor group 3 consists of dominant factors X20, X21, X23.

In this study, the researcher also surveyed the range of what percentage of overhead costs were set aside from the direct costs of construction projects to anticipate losses caused by overhead costs. The results of the study are shown in Table 7.

Most of the respondents answered that construction project overhead costs generally ranged from 6 to 10% of the direct costs of construction projects. However, based on the results of interviews with experts, construction project overhead costs are also influenced by the owner of the project. For projects from the government usually have a higher percentage of overhead costs compared to private projects.

Table 7 Percentage of overhead cost

Percentage of overhead cost (%)	Number of respondents
1-5	8
6-10	14
11-15	4
16-20	4
Total	30

5 Conclusions and Suggestions

5.1 Conclusions

Based on the results of the study, it was found that the most dominant external factor was the economy, where inflation and sudden price changes occurred during the construction phase and fluctuations in bank interest rates—then followed by legal factors which include the emergence of difficulties as a result of the company's license, and the unclear articles in the contract. Then, the last dominant external factor is socio-cultural factors which include problems caused by the COVID-19 pandemic, namely the existence of unfair/unfair competition in tenders, conflicts due to differences in culture and traditions at the project site affecting overhead costs, as well as a decrease in productivity levels caused by a reduction in the number of workers due to social restrictions during the COVID-19 pandemic.

In research on the amount of overhead taken on construction projects, most respondents answered 6–10%, and the respondents thought that overhead costs were an important cost and needed to be calculated properly, and the lack of attention to overhead costs could result in significant losses to the company.

5.2 Suggestions

The results of this study can be developed by broadening perspectives, not only from the contractor's point of view but also from the consultant's and owner's point of view. In addition, finding the dominant factor can also be done by using other techniques besides factor analysis. Meanwhile, in terms of influence factors, it can be further expanded, and research can be carried out on the impact of a pandemic such as COVID-19 on overhead costs.

References

1. Lino MLK (2018) Faktor pengaruh estimasi biaya tidak langsung proyek konstruksi. *Jurnal Infrastruktur* 4(1):82–88
2. El-Sawalhi NI, El-Riyati A (2015) An overhead cost assesment for construction projects at Gaza Strip. *Am J Civil Eng* 3(4):95. <https://doi.org/10.11648/j.ajce.20150304.11>
3. Kiew PN, Ismail S, Yusof AM (2013) Key performance indicators in construction quality management system. In: *The second international conference on engineering business management*, Kuala Lumpur, 27–28 Aug 2013
4. Cilensek R (1991) Understanding contractor overhead. *Cost Eng J* 33(12):21
5. Hesami S, Lavasani SA (2014) Identifying and classifying effective factors affecting overhead costs in constructing projects in Iran. *Int J Constr Eng Manage* 3(1):24–41. <https://doi.org/10.5923/j.ijcem.20140301.03>

6. Jaafari A (2001) Management of risks, uncertainties, and opportunities on projects: time for a fundamental shift. *Int J Project Manage* 19:89–101. [https://doi.org/10.1016/s0263-7863\(99\)00047-2](https://doi.org/10.1016/s0263-7863(99)00047-2)
7. Loosemore M, Raftery J, Reilly C, Higgon D (2005) *Risk management in projects* (1st ed). Routledge, London. <https://doi.org/10.4324/9780203963708>
8. El-Sayegh SM (2008) Risk assessment and allocation in the UAE construction industry. *Int J Project Manage* 26:431–438. <https://doi.org/10.1016/j.ijproman.2007.07.004>
9. Ehsan N, Mirza E, Alam M, Ishaque A (2010) Notice of retraction risk management in construction industry. In: 2010 3rd international conference on computer science and information technology, Chengdu, China, 9–11 July 2010, vol 9, p 16–21. <https://doi.org/10.1109/ICCSIT.2010.5564663>
10. Shen LY, Wu GWC, Ng CSK (2001) Risk assessment for construction joint ventures in China. *J Constr Eng Manag* 127(1):76–81
11. Abbasi GY, Abdel-Jabber MS, Abu-Khadejeh A (2005) Risk analysis for the major factors affecting the construction industry in Jordan. *Emirates J Eng Res* 10(1):41–47
12. Ujene AO, Idoro GI, Odesola IA (2013) Contractors perceptions of effects of projects overhead costs on building project performance in South-South of Nigeria. *Civil Eng Dimension* 15(2):102–113. <https://doi.org/10.9744/CED.15.2.102-113>
13. Soeharto I (1999) *Manajemen proyek: Dari konseptual sampai operasional*. Erlangga, Jakarta
14. Project Management Institute (2008) *A guide to the project management body of knowledge* (4th ed). Newtown Square, Pennsylvania
15. Santoso KJ, Wijaya KA, Chandra HP, Ratnawidjaja S (2021) Potret industri konstruksi di Surabaya dalam masa pandemi COVID-19. *Jurnal Dimensi Pratama Teknik Sipil* 10(1):57–64
16. Alsharef A, Banerjee S, Uddin SMJ, Albert A, Jaselkis E (2021) Early impacts of the COVID-19 pandemic on the United States construction industry. *Int J Environ Res Public Health* 18:1559. <https://doi.org/10.3390/ijerph18041559>
17. Priyatno D (2018) *SPSS: Panduan mudah olah data bagi mahasiswa & umum*. ANDI, Yogyakarta

A Competency Model of Thai Small-Medium Enterprise Contractors for Owner Satisfaction in Construction Projects



Grit Ngowtanasuwan 

Abstract For construction projects, service quality involves and relates to the project owners' perception of the service process in terms of activities, interactions, and the attainment of acceptable levels of operation from the construction activities. The competency of contractors includes the personality hidden within them and that can drive them to perform well or meet the criteria set in the construction projects for which they are responsible. The purpose of this study was to formulate a competency model for Thai small and medium enterprise (SME) contractors undertaking construction projects in northeast Thailand in order to influence the satisfaction of project owners by using a structural equation model (SEM). A total of 198 questionnaires that were completed by project owners were analyzed and evaluated to confirm the model. The results found that the competency of contractors comprised three main factors, namely: (1) knowledge, (2) skills, and (3) attributes. Suggestions for strategies to improve the competency of Thai SME contractors are presented and discussed in the conclusions of this research article.

Keywords Competency model · Construction project · Owner satisfaction

1 Introduction

In the service industry as a construction business, the service providers as construction contractors stress the quality of their service to satisfy the customer as the project owners in order to acquire future projects [1]. Such that customer retaining is the most crucial factor in terms of business sustainability. So, this research

G. Ngowtanasuwan (✉)

Faculty of Architecture, Urban Design and Creative Arts, Mahasarakham University, Maha Sarakham 44150, Thailand

e-mail: grit.n@msu.ac.th

extends the author's previous study to investigate the service quality factors of Thai provincial contractors [2], most of which are small enterprises with minimal technology. To survive in the industry, the contractors often ask the following questions: "How can we identify and understand core competencies of our service quality?" "What are competencies that affect the owners' satisfaction and decision to offer the future projects?" "What are strategies to increase our performance?" From such questions, the main objectives of the research are to study and analyze the causal factors and variables related to the competency of Thai SME contractors and project owners' satisfaction in the Thai construction industry. The scope of the study focused on surveys related to perceptions of construction service quality of project owners experienced with contractors on construction projects located in Khon Kaen, Roi Et, Kalasin, and Maha Sarakham, four provinces in the central region of northeast Thailand. The results will help contractors assess the current status, provide guidelines to develop operations in the industry, and present strategies to develop and support the competencies of Thai SME contractors.

2 Literature Review

A contractor is defined by many academicians [3, 4], such as a contractor is a person or company that arranges to supply workers or materials for building or facility construction, performs work on a contractual basis, and provides all of the labor, materials, services, and equipment necessary for a construction project [4]. Although general contractors often employ specialized subcontractors to carry out some or all of the construction, the general contractors are responsible for the quality of all work from all subcontractors [4]. According to the report from Krungsri Research Center [5], from roughly 80,000 construction companies registered for commercial activity in Thailand, 55 are qualified, according to income level, as large-scale companies with 50% of market share, most of which are listed in the stock exchange of Thailand (SET), while the rest are small-medium enterprises (SME) with minimal technology and need to improve their performance and service quality. The concept of competency was initially published by David C. McClelland in 1973 under the title "Testing for Competence Rather than Intelligence" [6]. He defined competency as the personality hidden within an individual that can drive that individual to perform well or meet the criteria set in the job for which they are responsible [7]. Competency comprises the knowledge, skills, and behavior necessary for an individual to be more successful than the general standard, which consists of three main components including (1) knowledge, such as knowledge and understanding of administrative law, (2) skills, such as ICT skills and skills in the field of modern management technology which must be learned, and (3) attributes including desirable behaviors such as curiosity, honesty, and commitment to success [7]. These aspects are deep within the mind and thus are harder to cultivate than knowledge and skills. If they exist, however, they can drive people to have highly effective behaviors. Generally, service quality

is a key to business success in order to sustain the customers and survive in a competitive environment. Garvin [8] stated that service quality comes from understanding the customer's quality perspective and focuses on all factors affecting the customer's awareness of quality varying from different customers. The service quality in the construction business is related to customer perception of the construction process in terms of interactions, activities, dynamic events, operations, and coordination [9]. Quality in the construction industry is defined as an acceptable level of constructing performance attained by meeting or exceeding the requirements of the project owner according to desired specifications. Parasuraman et al. [10, 11] developed a well-known tool for measuring service quality called SERVQUAL, where service quality is defined as the degree of difference between customer expectations and their perception of service done. It is widely used for surveying owner or customer satisfaction in many service industries. SERVQUAL is a tool to demonstrate outcomes and can be used for benchmarking business, consisting of five dimensions: (1) tangible: equipment, physical facilities, and personnel appearance. (2) Reliability: reliable and accurate promise delivery. (3) Responsiveness: customer tending with prompt service. (4) Assurance: employee's knowledge, courtesy, and trustability as well as customer confidence. (5) Empathy: customer's attention to detail [11]. In this research, the researcher used SERVQUAL to measure the initial factors of Thai SME contractor's competency in the construction projects. Whereby customer or owner satisfaction is a measuring of how services and products of a company surpass or lack or meet a customer's expectations [12], and it is defined as the percentage of total customers, or the number of customers, who reported their experience with the services or products of the firms exceeds specified satisfaction goals [12]. In the construction business, the satisfaction of the customer refers to the satisfaction of the project owner. Thus, the criteria for selecting a contractor are mainly based on price, financial capability, the contractor's previous experiences, workmanship, and technical capability with the contractor's competence [12]. Fischgrund and Omachonu [13] examined and presented gaps of the quality in construction projects by referring to the previous studies of Parasuraman et al. [10] in gap analysis of services. The research identified 12 gaps in construction service quality more nuanced than those in the previous studies. One particular interesting gap is the gap between the expectation and the perception of the project owner on construction service quality.

3 Research Methodology

3.1 Factor Identification and Research Hypothesis

The researcher used 22 items within five dimensions of measurements of SERVQUAL as initial information to be factors in the study and conducted a technique of in-depth interviews using related field experts covering certain topics.

The Interviews are designed as a group communication process with experts. This technique is used for detailed discussion and examination of a particular issue and can be repeated continuously until a consensus is reached to confirm the factors and items. Then the researcher summarized the list of all factors and selected a group of experts in three related fields according to their experience, namely experts from educational institutions, a contractor, and a project owner with more than ten years of experience in the Thai construction industry. Each expert carefully considered the identified factors and their implications individually at least three times until a consensus was reached. The researcher improved and modified initial factors and items for the construction service quality suitable to the Thai context adding one item to the list of 22. Once the listed factors were classified and confirmed by the three experts, they were established and available for analysis as outlined in Table 1. To study and explain the competency of Thai SME contractors, the researcher created a research hypothesis (H1): “The competency of Thai SME contractors has a positive effect on owner satisfaction” according to the literature [6–13] mentioned in Sect. 2, particularly SERVQUAL [10, 11].

3.2 *Questionnaire Design*

For data collection, the researcher designed a questionnaire survey to confirm the items and factors that influence the competency of Thai SME contractors for project owners, comprising two parts: (1) demographics of the answerer: answerer’s position, type of project, project delivery type, and project value totally four questions measured by the frequency (percentage) of the answers; (2) project owner’s perceptions and satisfactions totally 26 questions, measured on a 5-level (Likert scale) from “strongly disagree” to “strongly agree”.

The researcher used both reliability and validity tests so that the items in the questionnaire were appropriate for the collection of data. In the validity test, the researcher interviewed three experts in identifying factors to confirm the results. The Experts have reviewed and commented on whether these item lists were accurate representations and ready for measuring the service quality, as well as suggested recommendations that are more appropriate for the research context. The technique was useful in terms of content validity and item clarity. For the reliability test, the researcher used Cronbach’s alpha to check the reliabilities of the questionnaire by conducting a pilot group study with 40 target samples (SME contractors in target areas), tested the 23 items (measured in 5-level Likert scale) by computer statistical software, and found that the Cronbach’s alpha coefficient of 23 items in the project owner’s expectations was 0.93 and that of the project owner’s perceptions was 0.94 respectively; both are higher than 0.7 proving the questionnaire reliable [14].

Table 1 Questionnaire items

Factor	Item
Competency	COM1: Showing readiness to work and sufficient equipment
	COM2: Sufficient labours to finish work
	COM3: Good housekeeping and proper material storage
	COM4: Workmen dress properly in the site operation
	COM5: Details of drawings and documents
	COM6: Keeping their promises
	COM7: Presenting sincerity to solving problems
	COM8: Operating work orderly as required
	COM9: Providing service in accordance with the time promised
	COM10: Away reporting on the progress of work
	COM11: Informing work plan when to the owner the service will be operated and performed
	COM12: Providing quick service for the project owner
	COM13: Willingness to assist and carry the project owner in additional work
	COM14: Workmen behaviors which build confidence to the project owner
	COM15: Assuring the work quality is up to the standard
	COM16: Contractor and workmen politeness
	COM17: Having the knowledge to answer owner inquiries
	COM18: Having the competence to solve problems
	COM19: Understanding specific needs of the project owner
	COM20: Paying attention personally to the project owner
	COM21: Providing and supervising work maintenance services that have been done
	COM22: Organizing tidiness after work
	COM23: Working time is convenient for the project owner
Owner satisfaction	SAT1: I am very satisfied with the construction work performed by this contractor
	SAT2: I think I made the right decision by choosing this contractor
	SAT3: I am very comfortable with this contractor's work

3.3 Data Collection

After designing the questionnaire, the researcher selected a group of the project owners by using a technique of convenience non-probability sampling targeting project owners with experience in hiring contractors at least one project, from Khon Kaen, Roi Et, Kalasin, and Maha Sarakham, four provinces where projects site located in the central region of northeast Thailand. During three months of data collection, the researcher conducted face-to-face and online interviews to explain the details of the questionnaire and ensure that the target group understood the objective and aim of the study. Of the total of 300 questionnaires completed, 102

were discarded due to incomplete and biased responses, and only 198 were recognized as valid and analyzed. Then the researcher develops the model with a statistical technique called structural equation Modeling (SEM) to study the causal factors of the model, including three factors of competency (COM1 to COM 23), and subsequently formulate the effect factors to test the model fit with SEM by including owner satisfaction (SAT1 to SAT3) in the model.

4 Results

4.1 Descriptive Results

The descriptive results and questionnaire items are displayed on Table 2.

Table 2 Questionnaire items

Description	Frequency	Percentage
<i>Respondent's position</i>		
– Project owner	138	69.7
– Project owner representative	60	30.3
<i>Project type</i>		
– House	92	46.5
– Commercial building/ townhouse	34	17.2
– Office building	22	11.1
– Warehouse/factory	24	12.1
– Apartment building	15	7.6
– Others	11	5.6
<i>Project delivery type</i>		
– Design-bid-build	129	65.2
– Design-build	69	34.8
<i>Value of project</i>		
– Less than 1 M Baht	28	14.1
– 1–3 M Baht	75	37.9
– 3–6 M Baht	55	27.8
– 6–10 M Baht	29	14.6
– More than 10 M Baht	11	5.6

4.2 Structural Equation Models

Structural equation modeling (SEM) is a statistical method used to explain the effects or influences among latent variables (factors) on other latent variables in a

model [15]. In this research, the studied model was originated by a statistical technique call Exploratory Factor Analysis (EFA) [16]. Reducing the number of variables to a smaller set of basic summation variables is known as causal factors. EFA was applied by varimax rotation using statistical software. The results showed that Kaiser–Meyer–Olkin (KMO) measure of sampling adequacy = 0.931 (KMO > 0.7) [17, 18]. Bartlett’s test of sphericity had a significant value = 0.001 (less than 0.05) with approx. The 23 variables of competency (COM) were categorized into three groups, with COM I comprising COM1, COM3, COM2, COM4, COM6, COM5, and COM8 (7 items), COM II comprising COM15, COM17, COM18, COM22, COM19, COM16, COM20, COM14, COM7, and COM21 (10 items), and COM III comprising COM12, COM11, COM13, COM10, COM9, and COM23 (6 items). After that, the effect factor (dependent variable), which is owner satisfaction, was added to the model. The model was then analyzed by statistical software. The outputs were not fit in the first analysis. The software output suggested that some variables must be deleted from the study model, including COM4, COM8, COM15, COM16, COM7, COM13, COM9, and COM23. The author acted according to the suggestions and analysis. The outputs showed that the model was fit with Chi-square = 149.5, df = 131, $p = 0.128$ (>0.05), CMIN/df = 1.141 (<3), GFI = 0.895 (>0.85) RMSEA = 0.033 ($0.03 < RMSEA < 0.08$) [15]. Consequently, the research hypothesis (H1) was tested according to the outputs of the model. The results of the test were accepted by a significance level of 0.001 (<0.05) and the regression weight of 0.83, as shown in Fig. 1.

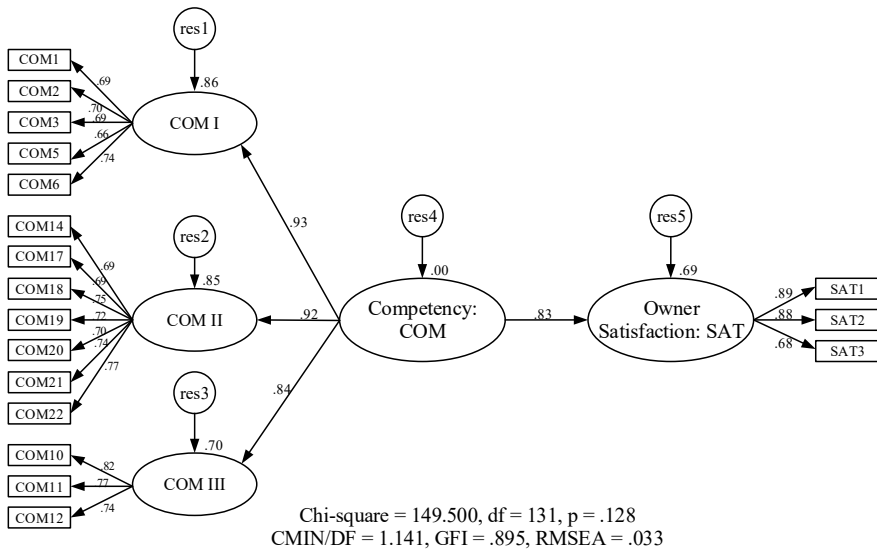


Fig. 1 Structural equation model of Thai SME contractors for owner satisfaction

5 Conclusions

The researcher conducted a factor analysis of the competency of Thai SME contractors for the satisfaction of the owners in construction projects in Thailand. After the project owner with experience in hiring contractors completed a total of 198 questionnaires, the researcher analyzed the questionnaires to confirm the factors. From the factors relating to the competency of Thai SME contractors, the researcher formulated a causal relationship model with the statistical technique SEM and found three competency factors with a positive effect on owner satisfaction: (1) COM I: preparedness of equipment and manpower to start and complete assigned work, good management on material storage, housekeeping and document detailing as well as promise delivery. (2) COM II: worker conduct to gain the project owners’ trust in terms of sufficient knowledge to owners’ inquiries, understanding, and tending owners’ specific needs, problem-solving, after-sales maintenance services, and post-work tidiness. (3) COM III: periodical report of work progress, especially on task schedule with prompt service. According to the competency definition presented by David C. McClelland [6, 7], COM I, COM II, and COM III are defined as attributes, skills, and knowledge, respectively. In order to formulate a competency model to explain Thai SME contractor behaviors for owner satisfaction, the top two highest weight scores of each factor were selected for the model. The completed model is shown in Fig. 2. The competency model of Thai SME contractors could be used as a strategy to improve the service quality of Thai SME contractors to satisfy construction project owners in Thailand, as well as for their business sustainability in the construction industry.

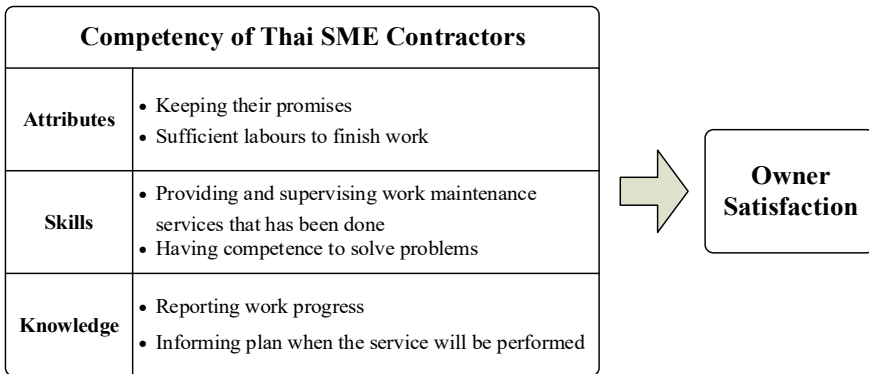


Fig. 2 Competency model of Thai SME contractors

References

1. Arslan G, Kivrak S (2008) Critical factor to company success in the construction industry. *World Acad Sci Eng Technol* 45:43–46
2. Ngowtanasuwan G (2020) Factor analysis of service quality of provincial contractors to owner satisfaction in construction projects in Thailand. *IOP Conf Ser: Mater Sci Eng* 829:012014. <https://doi.org/10.1088/1757-899x/829/1/012014>
3. Cambridge Dictionary (2021) Meaning of contractor in English. <https://dictionary.cambridge.org/dictionary/english/contractor>. Accessed 1 May 2021
4. Wikipedia (2021) Contractor. <https://en.wikipedia.org/wiki/Contractor>. Accessed 1 May 2021
5. Krungsri (2021) ธุรกิจรับเหมาก่อสร้าง. https://www.krungsri.com/bank/getmedia/7fe1e975-13f4-4040-a276-0d40841e504b/IO_Construction_Contractor_190606_TH_EX.aspx. Accessed 1 May 2021
6. McClelland DC (1973) Testing for competence rather than for intelligence. *Am Psychol* 28 (1):1–14. <https://doi.org/10.1037/h0034092>
7. McClelland DC (1998) Identifying competencies with behavioral event interviews. *Psychol Sci* 9:331–339. <https://doi.org/10.1111/1467-9280.00065>
8. Garvin DA (1983) Quality on the line. *Harv Bus Rev* 61:65–73
9. Forsythe P (2008) Modelling customer perceived service quality in housing construction. *Eng Constr Archit Manag* 15(5):485–496. <https://doi.org/10.1108/09699980810902767>
10. Parasuraman A, Zeithaml VA, Berry LL (1985) A conceptual model of service quality and its implications for future research. *J Mark* 49(4):41–50. <https://doi.org/10.2307/1251430>
11. Parasuraman AP, Zeithaml VA, Berry LL (1988) SERVQUAL: a multi-item scale for measuring consumer perceptions of quality. *J Retail* 64:13–40
12. Kärnä S (2004) Analysing customer satisfaction and quality in construction-the case of public and private customers. *Nordic J Surv Real Estate Res* 2. <https://journal.fi/njs/article/view/41488>. Accessed 1 May 2021
13. Fischgrund J, Omachonu V (2014) Quality in construction: identifying the gaps. *Int J Constr Eng Manage* 3(2):65–73. <https://doi.org/10.5923/j.ijcem.20140302.04>
14. Nunnally JC (1978) *Psychometric theory* (2nd). McGraw, New York
15. Byrne BM (2010) *Structural equation modeling with AMOS, basic concepts, applications, and programming*, 2nd edn. Routledge Taylor & Francis Group, New York
16. Norris M, Lecavalier L (2009) Evaluating the use of exploratory factor analysis in developmental disability psychological research. *J Autism Dev Disord* 40(1):8–20. <https://doi.org/10.1007/s10803-009-0816-2>
17. Tabachnik BG, Fidell LS (2001) *Using multivariate statistics*, 4th edn. Allyn & Bacon, Needham, Massachusetts
18. Kaiser HF (1958) The varimax criterion for analytic rotation in factor analysis. *Psychometrika* 23(3):187–200. <https://doi.org/10.1007/bf02289233>